

Susheel Kalia
M.W. Sabaá *Editors*

Polysaccharide Based Graft Copolymers

 Springer

Polysaccharide Based Graft Copolymers

Susheel Kalia • M.W. Saba
Editors

Polysaccharide Based Graft Copolymers

 Springer

Editors

Susheel Kalia
Dept. of Chemistry
Bahra University
Himachal Pradesh
India

M.W. Sabaa
Chemistry Dept.
Faculty of Science
Cairo University
Giza
Egypt

ISBN 978-3-642-36565-2

ISBN 978-3-642-36566-9 (eBook)

DOI 10.1007/978-3-642-36566-9

Springer Heidelberg New York Dordrecht London

Library of Congress Control Number: 2013938957

© Springer-Verlag Berlin Heidelberg 2013

This work is subject to copyright. All rights are reserved by the Publisher, whether the whole or part of the material is concerned, specifically the rights of translation, reprinting, reuse of illustrations, recitation, broadcasting, reproduction on microfilms or in any other physical way, and transmission or information storage and retrieval, electronic adaptation, computer software, or by similar or dissimilar methodology now known or hereafter developed. Exempted from this legal reservation are brief excerpts in connection with reviews or scholarly analysis or material supplied specifically for the purpose of being entered and executed on a computer system, for exclusive use by the purchaser of the work. Duplication of this publication or parts thereof is permitted only under the provisions of the Copyright Law of the Publisher's location, in its current version, and permission for use must always be obtained from Springer. Permissions for use may be obtained through RightsLink at the Copyright Clearance Center. Violations are liable to prosecution under the respective Copyright Law.

The use of general descriptive names, registered names, trademarks, service marks, etc. in this publication does not imply, even in the absence of a specific statement, that such names are exempt from the relevant protective laws and regulations and therefore free for general use.

While the advice and information in this book are believed to be true and accurate at the date of publication, neither the authors nor the editors nor the publisher can accept any legal responsibility for any errors or omissions that may be made. The publisher makes no warranty, express or implied, with respect to the material contained herein.

Printed on acid-free paper

Springer is part of Springer Science+Business Media (www.springer.com)

Preface

Polysaccharides play an important role in the field of science and technology because of their unique properties such as non-toxicity, biodegradability, and availability from renewable resources. Polysaccharide-based graft copolymers have drawn much attention in recent decades because of their controlled biodegradability, shear stability, and high efficiency in various applications. One of the important applications of polysaccharide-based graft copolymers is in biomedical science.

Modification of polysaccharides through graft copolymerization is very versatile to improve the properties of polysaccharides. Polymer grafting is known to improve the characteristic properties of the polymer backbone such as water repellency, thermal stability, flame resistance, dye-ability, and resistance towards acid–base attack, abrasion, etc.

Polysaccharides and their graft copolymers find extensive applications in diversified fields. Applications of modified polysaccharides include drug delivery devices, controlled release of fungicides, selective water absorption from oil–water emulsions, purification of water, etc.

In Chap. 1, methods of grafting and applications of polysaccharide graft copolymers are briefly discussed. Synthesis, properties, and applications of different polysaccharide graft copolymers such as cellulose-g-copolymers, starch-g-copolymers, chitosan-g-copolymers, gum-g-copolymers, and dextran-g-copolymers are reviewed in Chaps. 2–6.

Chapter 7 covers the review on natural backbone-based superabsorbent hydrogels and their classification. The applications of hydrogels in different fields like biomedical, pharmaceuticals, agriculture, and metal ions sorption are also discussed in this chapter. Chapter 8 describes the hyaluronic acid graft copolymers and the chemical strategies employed for their synthesis, characterization procedures, and applications in biomedical and pharmaceutical fields. Chapter 9 deals with the techniques employed for the synthesis of grafted polysaccharides and applications of grafted polysaccharides in controlled/targeted drug delivery.

There is no special book published yet for polysaccharide-based graft copolymers. This book is a single book with contributions from the renowned experts of the area of research. This book covers almost all the topics related to

graft copolymerization; polysaccharides; graft copolymers of cellulose, chitosan, starch, dextran, gum, etc.; and biomedical applications of polysaccharide graft copolymers. Therefore, this book will be in the benefit of society as it covers the essential aspects of “polysaccharide-based graft copolymers.”

Susheel Kalia would like to thank his students, who helped him in the editorial work. Magdy W. Sabaa would like to thank his research team for their continuous help and support.

Finally, we gratefully acknowledge permissions to reproduce copyrighted materials from a number of sources.

The Editors would like to express their gratitude to all contributors of this book, who made excellent contributions.

Solan, India
Giza, Egypt

Susheel Kalia
Magdy W. Sabaa

About the Editors

Dr. Susheel Kalia is Assistant Professor in the Department of Chemistry, Bahra University, Shimla Hills, Solan (H.P.) India. Presently, he is visiting researcher in the department of civil, chemical, environmental and materials engineering at University of Bologna, Italy. After completing his Ph.D. at Punjab Technical University, Jalandhar, India, he began working as Assistant Professor in Singhania University (Rajasthan) and Bahra University (Shimla Hills) where he has been for the past 5 years. Kalia has around 40 research papers in international journals along with 80



publications in national and international conferences and seven book chapters. Kalia's other editorial activities include work as a reviewer and memberships of editorial boards for various international journals. Additionally, he has edited a number of books such as "Handbook of Biopolymers and Their Application," "Cellulose Fibers: Bio- and Nano-Polymer Composites," and "Polymers at Cryogenic Temperatures." He is also a member of a number of professional organizations, including the Asian Polymer Association, Indian Cryogenics Council, the Society for Polymer Science, Indian Society of Analytical Scientists, and the International Association of Advanced Materials. Presently, Kalia's research is in the field of biocomposites, nanocomposites, conducting polymers, cellulose nanofibers, inorganic nanoparticles, hybrid materials, hydrogels, and cryogenics.

Prof. Magdy Sabaa is Emeritus Professor of Polymer Chemistry, at the Faculty of Science, Cairo University, since August 2010. He got his B.Sc. degree in Applied Chemistry in 1971 with grade Distinction and Honor degree from Cairo University. After completing his Ph.D. degree in 1979, in the field of Polymer Chemistry, he was appointed as lecturer of polymer chemistry at the Faculty of science, Cairo University, then assistant professor, and finally as professor of polymer chemistry in 1991. During his scientific career, he attained two postdoctoral fellowships, the first at Prague Institute of Chemical Technology (1981–1982) and the second at Tokyo Institute of Technology (1983–1984).



Moreover, he attained a training course in polymer physics at Trieste, Italy, during April–May 1987. Prof. Sabaa published 86 research articles and one review article in international journals along with 18 publications in proceedings of national and international conferences. He has supervised more than 50 M.Sc. and Ph.D. theses in the field of polymer chemistry. Prof. Sabaa works as a reviewer for various international journals and he is a member in the Arab Society of Material Sciences and in the Egyptian Society of Polymer Science and Technology. Sabaa's research activity is in the field of polymer degradation and stabilization, graft copolymerization, hydrogels and SI-hydrogels, super-absorbing materials, biodegradable polymers, and polymers with antimicrobial activity.

Contents

1 Polymer Grafting: A Versatile Means to Modify the Polysaccharides	1
Susheel Kalia, Magdy W. Sabaa, and Sarita Kango	
2 Cellulose Graft Copolymers: Synthesis, Properties, and Applications	15
Gülten Gürdağ and Shokat Sarmad	
3 Starch-g-Copolymers: Synthesis, Properties and Applications	59
A.N. Jyothi and Antonio J.F. Carvalho	
4 Chitosan-g-Copolymers: Synthesis, Properties, and Applications	111
Magdy W. Sabaa	
5 Gum-g-Copolymers: Synthesis, Properties, and Applications	149
Aiqin Wang and Wenbo Wang	
6 Dextran Graft Copolymers: Synthesis, Properties and Applications	205
Yasuhiko Onishi, Yuki Eshita, and Masaaki Mizuno	
7 Polysaccharide Hydrogels: Synthesis, Characterization, and Applications	271
Jaspreet Kaur Bhatia, Balbir Singh Kaith, and Susheel Kalia	

8 Hyaluronic Acid-g-Copolymers: Synthesis, Properties, and Applications	291
Fabio Salvatore Palumbo, Giovanna Pitarresi, Calogero Fiorica, and Gaetano Giammona	
9 Polysaccharide-Based Graft Copolymers for Biomedical Applications	325
Sagar Pal and Raghunath Das	
Index	347

Chapter 1

Polymer Grafting: A Versatile Means to Modify the Polysaccharides

Susheel Kalia, Magdy W. Sabaa, and Sarita Kango

Abstract The polysaccharides are the most abundant natural organic materials, and polysaccharide-based graft copolymers are of great importance and widely used in the various fields. Natural polysaccharides have received more attention due to their advantages over the synthetic polymers such as non-toxic, biodegradable and low cost. Modification of polysaccharides through graft copolymerisation improves the properties of natural polysaccharides. Grafting is known to improve the characteristic properties of the backbones. Such properties include water repellency, thermal stability, flame resistance, dye ability and resistance towards acid–base attack and abrasion. Graft copolymers play an important role as reinforcing agents in the preparation of green composites. These graft copolymers on subjecting both for composting and soil burial biodegradation studies are found to be biodegradable in nature. Polysaccharides and their graft copolymers find extensive applications in diversified fields. Applications of modified polysaccharides include drug delivery devices, controlled release of fungicides, selective water absorption from oil–water emulsions and purification of water. Methods for the modification of various polysaccharides through graft copolymerisation technique have been reported in this chapter.

Keywords Polysaccharide • Graft copolymers • Radiations • Plasma • Enzymatic grafting

S. Kalia (✉)

Department of Chemistry, Bahra University, Solan 173234, HP, India

e-mail: susheel.kalia@gmail.com

M.W. Sabaa

Faculty of Science, Chemistry Department, Cairo University, Giza, Egypt

e-mail: mwsabaa@hotmail.com

S. Kango

Department of Physics and Materials Science, Jaypee University of Information Technology, Waknaghat 173234, HP, India

1.1 Introduction

In today's world, polymers constitute an important class of materials and are the appropriate substitutes for conventional materials. These materials have been proved to be of industrial importance in diversified fields [1–4]. However, most of the polymers are not able to perform under high temperature and pressure conditions because of which the concept of speciality polymers emerged. Different modification techniques have been developed to enhance the properties of polymeric materials under required conditions [5–8]. Surface morphology of polymers is of great interest, and commercially important products can be developed through the introduction of reactive sites. Such reaction sites are used for the incorporation of properties like hydrophilicity, hydrophobicity and resistance towards acid–base attack along with higher thermal stability [9, 10].

Graft copolymerisation provides a tool in the hands of researchers to incorporate targeted properties in backbones for specialised applications without affecting their biodegradability. It is a technique to hybridise synthetic and natural polymers and assists in fundamental investigation of structure–property relationship. Properties such as melting point, glass transition temperature, solubility, permeability, chemical reactivity and elasticity can be modified through graft copolymerisation as per the specific requirements [11–13]. In recent years, modification of chemical and physical properties of natural polymers and their derivatives through graft copolymerisation has attracted much attention [14–19]. Graft copolymerisation of various vinyl monomers onto different polysaccharides has been reported by various workers. Since polysaccharides occur abundantly in nature, therefore, this class of polymers is of special significance for the scientists. Polysaccharides have wide applications in the field of food, cosmetics and pharmaceuticals [20–24].

In view of the importance of polysaccharides in various fields and their modification through graft copolymerisation for their industrial applications, this chapter deals with the different methods of graft copolymerisation of vinyl monomers onto polysaccharides.

1.2 Polysaccharides

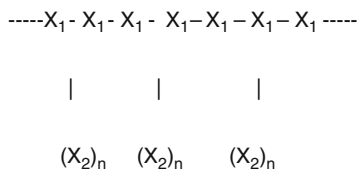
Polysaccharides are polymeric carbohydrate structures which are formed by repeating units joined together by glycoside linkages and contain various degrees of branching. Polysaccharides have a general formula $C_x(H_2O)_y$, where y is usually a large number between 200 and 2,500. Starch and glycogen are storage polysaccharides, whereas cellulose and chitosan act as the structural materials. They provide mechanical strength to plants [25] which make them fit for applications like fibres [26], films [27], adhesives [28], melt-processing plastics [29], hydrogels [30], drug delivery agents [31] and emulsifiers [32]. Polysaccharides are bio-based materials possessing unique combination of functional properties and environmental-friendly features. They are non-toxic, biodegradable and renewable materials. Commercially available products include starch,

cellulose and their derivatives, e.g. cellulose acetate, carboxymethyl cellulose, methyl cellulose, sodium alginate, xanthan gum, dextrin, carrageenin and hydrofluoric acid. Presence of polar functional groups, high molecular weight and relatively rigid backbone are the key features which directly affect the physical and chemical properties of polysaccharides. Polysaccharides are relatively stable at temperature up to about 200 °C for a short period. Due to high interchain cohesive forces, they have high melting and softening temperatures. The stiff backbone makes them brittle and has high degree of crystallinity leading to insolubility in water and common organic solvents.

Hydroxyl groups in the naturally occurring polysaccharides provide the reactive sites for the modification, and materials with new industrial properties can be obtained. Esterification, etherification, urethane formation and cross-linking with polyfunctional reagents are the common reactions employed for the modification of cellulose, chitosan, starch and pectin [33–36]. Cellulose, starch, chitosan, dextrin and guar gum have been most extensively grafted with various vinyl monomers under different reaction conditions [37–45].

1.3 Graft Copolymers

Graft copolymers involve a preformed polymeric backbone and to which are attached other polymeric chains of different chemical nature at several points. Stannett [46] defined graft copolymers as “Graft copolymers consist of a polymer backbone with lateral covalently linked side chains.” Both the backbone and the side-chain polymers can be homopolymers or copolymers. Graft copolymer is a polymer comprising of molecules with one or more blocks of species connected to the main chain as side chains, having constitution or configurational features that differ from those in the main chain [47]. The generalised structure of graft copolymer is shown below, where the monomer (X_2) is incorporated on the backbone of a polymer having building unit (X_1).



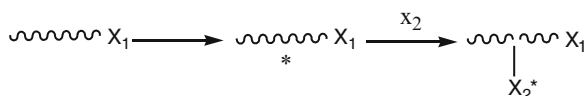
Monomer (X_2) can be grafted as a unitary system or as a binary mixture with other monomer(s). Depending upon the reactivity ratio of two monomers, binary vinyl monomer mixtures can be grafted in a random or in an alternate fashion on the backbone.

1.3.1 Concept of Graft Copolymerisation

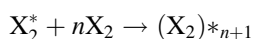
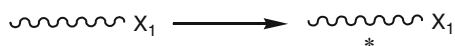
A polymer is called copolymer when the repeating units are of two different monomers. The sequence in which monomers attach themselves depends upon their relative reactivities. Copolymers can be random, alternate, block and graft copolymers. First three types of copolymers differ with respect to sequencing of monomers. In case of random copolymer, monomer units are randomly placed (arranged), whereas monomers are present in an ordered form in case of alternate copolymer. Block copolymer involves the segments of different monomers attached together at terminals. Graft copolymer has a preformed polymer acting as a backbone to which polymeric chains are attached at different sites. Thus, graft copolymer consists of a polymer backbone with lateral covalently linked side chains [46]. The side chains may consist of a single monomer or of binary mixture. The graft copolymerisation involving single monomer usually occurs in a single step, whereas graft copolymerisation in the presence of vinyl monomers binary mixtures may occur with the simultaneous or sequential addition of monomers. When two monomers are added side by side, it is called mosaic grafting. First graft copolymer was synthesised by Alferd and Bandel in 1950 by polymerising vinyl acetate in the presence of styrene and vinylidene chloride [48].

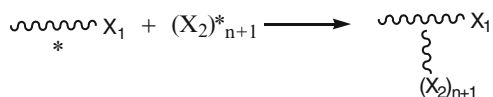
The presence of functional groups on the backbone is the basic requirement for the synthesis of graft copolymers. Graft copolymerisation can be performed in homogeneous as well as in heterogeneous medium depending upon the solubility of monomer and the nature of solvent used for the reaction. Graft copolymerisation proceeds either through “grafting from” or “grafting onto” method.

“Grafting from” method involves the generation of active sites on the polymer backbone which in turn initialises the monomer polymerisation onto backbone and thereby resulting in the formation of graft copolymer as follows:



When a growing polymer chain (X_2) attacks another polymer X_1 , the grafting is said to occur through “grafting onto” method as follows:





“Grafting onto” method results in homogeneity in composition and molecular weights distribution. It provides a technique to incorporate special properties like dye ability, crease resistance, moisture and chemical resistance in the parent backbone polymer [49–51]. Due to these characteristics, a wide variety of natural and synthetic polymers have been modified through graft copolymerisation. Such graft copolymers are called speciality polymers possessing branches of different chain lengths and resulting in desired properties.

1.3.2 Methods of Graft Copolymerisation

Basic principle that lies behind the synthesis of graft copolymerisation is the generation of active sites, in the form of free radicals or a functional group, on the backbone. Polymerisation of monomers onto active sites results in graft copolymerisation. During the last decades, several methods have been suggested for the preparation of graft copolymers by conventional chemical techniques [52, 53]. Creation of an active site on the pre-existing polymeric backbone is the common feature of most methods for the synthesis of graft copolymers. The active site may be either a free-radical or a chemical group which may get involved in an ionic polymerisation or in a condensation process. Polymerisation of an appropriate monomer onto this activated backbone polymer leads to the formation of a graft copolymer. Ionic polymerisation has to be carried out in presence of anhydrous medium and/or in presence of considerable quantity of alkali metal hydroxide. Another disadvantage with the ionic grafting is that low molecular weight graft copolymers are obtained, while in case of free-radical grafting, high molecular weight polymers can be prepared.

1.3.2.1 Chemical Methods

Chemical method of graft copolymerisation involves the use of chemicals which act as initiators to generate active sites on backbone. The use of various redox initiator systems like Lewis acids, strong bases and metal carbonyls has been reported for chemical grafting. Grafting of vinyl monomers onto polymeric backbones has been accomplished by using a range of free radical initiators and redox systems like dibenzoyl peroxide, Azobis(isobutyronitrile) (AIBN), ceric ammonium nitrate, potassium persulphate, potassium permanganate and Fenton’s reagent [54–57]. Researchers are also developing new redox systems for the incorporation of desired properties into backbone. Zahran and Mahmoud [58] investigated the use of potassium peroxydiphosphate–metal ion–cellulose thiocarbonate redox initiator

system for the graft copolymerisation of methyl methacrylate onto cellulosic fabrics.

Atom transfer radical polymerisation (ATRP) is a modern method to generate free-radical sites on dormant chains. In this method, halogen atoms are capped onto inactive sites which are reversibly transferred to metal complexes in lower states. Vlcek et al. [59] reported the controlled grafting of cellulose diacetate with methyl methacrylate and butyl acrylate through ATRP. Tizzotti et al. [60] in a review article reported about ATRP graft copolymerisation of polysaccharides along with other living polymerisation techniques like RAFT and NMP.

1.3.2.2 Radiation-Induced Grafting

Graft copolymerisation involving radiations as an initiating system allows a high degree of control over the number and length of grafted chains. This can be done by careful selection of dose and its rate. This is the most convenient method for the graft copolymerisation. When electromagnetic radiations pass through backbone, it results in the formation of active sites for the reaction. Radiation technique enables to maintain the purity of product as it is free from contamination. It allows to carry out reaction at different depth of backbone which depends upon the penetrating power of the radiation used. Moreover, the molecular weight of polymer formed can be regulated in case of radiation-induced grafting. The unique features of radiation method make it a preferred technique of graft copolymerisation [61, 62].

Low-Energy Radiation-Induced Grafting

Grafting can proceed by the use of either low-energy radiations or high-energy radiations. Irradiation of backbone with low-energy radiations like UV and visible light results in the homolytic fission to generate free radicals on the backbone. Khan et al. [63–66] modified the jute yarn by graft copolymerisation of vinyl monomers using UV radiations. In presence of low-energy radiations, grafting may proceed with or without photo initiator. The graft copolymerisation of poly(ethylene glycol) dimethyl acrylate oligomers onto cotton was investigated under UV radiations using benzophenone as photo initiator. The photo grafting was found to increase the wrinkle resistance of cotton [67].

High-Energy Radiation-Induced Grafting

High-energy radiation like X-rays, gamma rays or accelerated electrons having energy varying between 6.5 and 3.0 MeV has been used for graft copolymerisation of various backbones. Gamma radiations are most commonly used radiations, and Co-60 is the most widely used source of gamma radiations due to its long half-life period of 5.3 years. Cellulose fabric was grafted with divinylbenzene, and the

extent of grafting was found to increase with total gamma radiation dose [68]. Chauhan and co-workers [69] carried out the graft copolymerisation of styrene onto cellulose and studied the effect of some additives on grafting parameters in limited aqueous medium.

Microwave Radiation-Induced Grafting

Microwave radiation is another important energy source and is emerging as an effective tool for graft copolymerisation. Microwave radiations have an advantage of instantaneous in core processing of reactants in homogeneous manner. Microwave radiations can rapidly transfer the energy into bulk of reaction mixture which results in the rapid interaction of the material in the reaction mixture [70]. Polyacrylamide was graft copolymerised onto chitosan under microwave radiations with reaction rate eight times higher than conventional heating [71]. Grafting of ϵ -caprolactone [72] and acrylic acid [73] onto chitosan has been studied under microwave radiations. Grafting of hydroxymethylacrylate onto wool fibres [74], methyl methacrylate onto flax fibres [75], acrylic acid onto Artemisia seed gum [76] and polyacrylamide onto xanthan [77] and guar gum [78] has been reported under microwave radiations. *Cassia siamea* seed gum has been found to undergo graft copolymerisation under microwave radiations without the use of radical initiator [79].

Microwave irradiation significantly reduces the use of toxic solvents, as well as the reaction time for almost all the grafting reactions of interest here, ensuring high yields, product selectivity and clean product formations. Microwave-synthesised polysaccharide copolymers exhibit better properties for commercial exploitation than their conventionally synthesised counterparts [80]. A comparison of advantages of carrying out grafting reactions under microwaves and conventional methods is explained in Fig. 1.1.

Radiation-induced grafting can proceed in three different manners: (a) mutual or direct method, (b) pre-oxidation method and (c) pre-irradiation method. Mutual method involves the simultaneous irradiation of backbone and monomer to generate free radicals. The product formed is a mixture of homopolymer and graft copolymer [81].

Pre-irradiation technique involves the exposure of the polymer backbone to radiations in an inert environment to form free radicals which when treated with monomers result in the graft copolymerisation. Gamma radiation-induced graft copolymerisation of methyl methacrylate onto jute fibres was carried out by the pre-irradiation method in an aqueous medium by using octylphenoxy polyethoxyethanol as an emulsifier. The different factors that influenced the graft copolymer reaction process were investigated [82]. Pre-oxidation method involves the irradiation of polymer in the presence of oxygen. The peroxides and hydroperoxides are formed which in subsequent steps initiate the polymerisation of monomer resulting in the formation of graft copolymers. The rate of formation of peroxide and hydroperoxide is dependent upon the total dose and which in turn influences the rate of grafting [83].

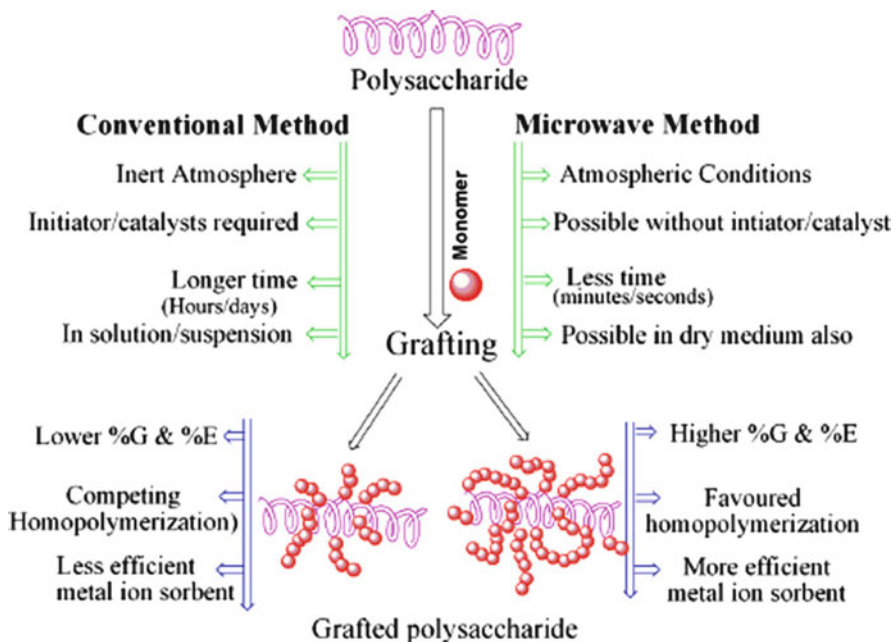


Fig. 1.1 Schematic diagram of microwave-induced grafting of the polysaccharides (adapted from [80])

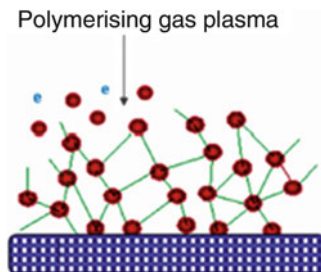
1.3.2.3 Enzymatic Grafting

Enzymatic grafting involves the enzyme as an initiator which initiates chemical grafting onto the polymer backbone. Enzymatic modification has attracted attention due to the requirement of milder reaction conditions and highly specific surface modification resulting in non-destructive transformation of the backbone. Enzymatic grafting onto natural products has been well studied for various industrial applications. A hydrophilic compound chlorogenic acid was grafted onto chitosan in the presence of enzyme tyrosinase to attain the water solubility of chitosan under basic conditions. Tyrosinase converts phenolic substrate into *O*-quinone which can undergo reaction with amino group of chitosan to form graft copolymer [84].

1.3.2.4 Plasma-Initiated Grafting

Surface modification of polymers through plasma polymerisation technique has received increasing interest. Plasma conditions attained through slow discharge offer about the same possibilities as with ionising radiation [85, 86]. The main processes in plasmas are electron-induced excitation, ionisation and dissociation. Thus, the accelerated electrons from the plasma have sufficient energy to induce

Fig. 1.2 Grafting with plasma (adapted from [88])



cleavage of the chemical bonds in the polymeric structure, which forms macromolecular radicals to initiate the graft copolymerisation [87].

Plasma-initiated polymerisation of grafting can be carried out by using polymerising gases and precursors like fluorocarbons, hydrocarbons and silicone-containing monomers (Fig. 1.2). Carrier gas plays important roles in these plasma–surface interactions, and usually inert gas like helium or argon is used as carrier gases [88].

1.4 Applications of Polysaccharide Graft Copolymers

Polysaccharides graft copolymers have got diversified properties and can be used for various applications. Functionalised biopolymers are cost-effective, biodegradable, environment friendly and efficient, and these after graft copolymerisation and cross-linking can be used for sustained release of drugs. Controlled release of fungicides through polysaccharides graft copolymers is the major remedial factor which can occur through diffusion, degradation or a combination of both. Hydrogels are highly selective in nature and can remove saline from petroleum fraction–saline emulsions. Such modified polysaccharides are of great importance in oil industries. Hydrogels have the characteristics to trap the colloidal particles in their folds and force them to settle down at the bottom. Thus, modified polysaccharides play an important role in the removal of colloidal particles from potable water. Since these polysaccharide devices are biodegradable and green in nature, therefore, they are the effective substitutes for synthetic flocculants. Grafting of synthetic polymers onto polysaccharides can further improve their properties like water repellency, acid–base resistance, thermal stability and increased mechanical strength. Moreover, the grafted polysaccharides when used as reinforcing materials for the preparation of biodegradable composites are found to possess better compatibility with the matrix [89, 90].

1.5 Conclusions

Desirable and targeted properties can be imparted to the polysaccharides through polymer grafting in order to meet out the requirement of specialised applications. Polymer grafting is a clean and convenient method for altering the properties of numerous polymer backbones. Polysaccharide-based graft copolymers have got diversified properties and can be used for various applications.

References

1. Ito M, Nagai K (2007) Degradation behaviour and application of recycled PVC sheet made of floor sheet for railway vehicle. *Polym Degrad Stab* 92:1692–1699
2. Makohliso SA, Giovangrandi L, Leonard D, Mathieu HJ, Ilegems M, Aebischer P (1998) Application of teflon thin films for bio-patterning of neural cell adhesion. *Biosens Bioelectron* 13:1227–1235
3. Gao C, Yan D (2004) Hyperbranched polymers: from synthesis to applications. *Prog Polym Sci* 29:183–275
4. Chan HS, Ng SC (1998) Synthesis, characterization and applications of thiophene-based functional polymers. *Prog Polym Sci* 23:1167–1231
5. Goddard JM, Hotchkiss JH (2007) Polymer surface modification for the attachment of bioactive compounds. *Prog Polym Sci* 32:698–725
6. Reisinger JJ, Hllmyer MA (2002) Synthesis of fluorinated polymers by chemical modification. *Prog Polym Sci* 27:971–1005
7. Marcincin A (2002) Modification of fibre forming polymers by additives. *Prog Polym Sci* 27:853–913
8. Muth O, Hirth T, Vogel H (2000) Polymer modification by supercritical impregnation. *J Supercrit Fluids* 17:65–72
9. Lv J, Ma J, HuangFu P, Yang S, Gong Y (2008) Surface modification with both phosphor-ylcholine and stearyl groups to adjust hydrophilicity and hydrophobicity. *Appl Surf Sci* 255:498–501
10. Kalia S, Kaith BS (2008) Mechanical properties of phenolic composites reinforced with flax-g-copolymers prepared under different reaction conditions—a comparative study. *E-J Chem* 5:177–184
11. Fares MM, El-faqeeh AS, Osman ME (2003) Graft copolymerization onto starch—I. Synthesis and optimization of starch grafted with N-tert-butylacrylamide copolymer and its hydrogels. *J Polym Res* 10:119–125
12. Moreira ACE, Oliveira MG, Soares BG (1997) Thermal degradation studies of poly(EVAL-g-methylmethacrylate). *Polym Degrad Stab* 58:181–185
13. Kaith BS, Kalia S (2008) A study of crystallinity of graft copolymers of flax fiber with binary vinyl monomers. *E-Polymers* 2:1–6
14. Meshram MW, Patil VV, Mhaske ST, Thorat BN (2009) Graft copolymers of starch and its application in textiles. *Carbohydr Polym* 75:71–78
15. Kaith BS, Singha AS, Kumar S, Kalia S (2008) Mercerization of flax fiber improves the mechanical properties of fiber- reinforced composites. *Int J Polym Mater* 57:54–72
16. Dhiman PK, Kaur I, Mahajan RK (2008) Synthesis of a cellulose-grafted polymeric support and Its application in the reductions of some carbonyl compounds. *J Appl Polym Sci* 108:99–111
17. El-Sherbiny IM (2009) Synthesis, characterization and metal uptake capacity of a new carboxymethyl chitosan derivative. *Eur Polym J* 45:199–210

18. Wibowo AC, Desai SM, Mohanty AK, Drzal LT, Misra M (2006) A solvent free graft copolymerization of maleic anhydride onto cellulose acetate butyrate bioplastic by reactive extrusion. *Macromol Mater Eng* 291:90–95
19. Kalia S, Kaith BS, Sharma S, Bhardwaj B (2008) Mechanical properties of flax-g-poly(methyl acrylate) reinforced phenolic composites. *Fiber Polym* 9:416–422
20. Levis SR, Deasy PB (2001) Pharmaceutical applications of size reduced grades of surfactant co-processed microcrystalline cellulose. *Int J Pharm* 230:25–33
21. Singh J, Kaur L, McCarthy OJ (2007) Factors influencing the physico-chemical, morphological, thermal and rheological properties of some chemically modified starches for food applications—a review. *Food Hydrocoll* 21:1–22
22. Coviello T, Matricardi P, Marianecchi C, Alhaique F (2007) Polysaccharide hydrogels for modified release formulations. *J Control Release* 119:5–24
23. Mehling T, Smirnova I, Guenther U, Neubert RHH (2009) Polysaccharide-based aerogels as drug carriers. *J Non Cryst Solids* 355:2472–2479
24. Strickland FM (2001) Immune regulation by polysaccharides: implications for skin cancer. *J Photochem Photobiol B* 63:132–140
25. Lapasin R, Prici S (1995) *Rheology of industrial polysaccharides: theory and applications*. Aspen Publishers, New York, NY
26. Pillai C, Paul W, Sharma CP (2009) Chitin and chitosan polymers: chemistry, solubility and fiber formation. *Prog Polym Sci* 34:641–678
27. Bastos DC, Santos AEF, Silva MLV, Simao RA (2009) Hydrophobic corn starch thermoplastic films produced by plasma treatment. *Ultramicroscopy* 109:1089–1093
28. Haag AP, Maier RM, Combie J, Geesey GG (2004) Bacterially derived biopolymers as wood adhesives. *Int J Adhes Adhes* 24:495–502
29. Shi R, Zhang Z, Liu Q, Han Y, Zhang L, Chen D, Tian W (2007) Characterization of citric acid/glycerol co-plasticized thermoplastic starch prepared by melt blending. *Carbohydr Polym* 69:748–755
30. Reis AV, Guilherme MR, Cavalcanti OA, Rubira AF, Muniz EC (2007) Synthesis and characterization of pH-responsive hydrogels based on chemically modified Arabic gum polysaccharide. *Polymer* 47:2023–2029
31. Liu LS, Fishman ML, Hicks KB (2007) Pectin in controlled drug delivery—a review. *Cellulose* 14:15–24
32. Nakauma M, Funamia T, Nodaa S, Ishihara S, Al-Assaf S, Nishinari K, Phillips GO (2008) Comparison of sugar beet pectin, soybean soluble polysaccharide, and gum arabic as food emulsifiers. 1. Effect of concentration, pH, and salts on the emulsifying properties. *Food Hydrocoll* 22:1254–1267
33. Sun RC, Fang JM, Tomkinson J, Hill CAS (1999) Esterification of hemicelluloses from poplar chips in homogenous solution of N, N-dimethylformamide/lithium chloride. *J Wood Chem Technol* 19:287–306
34. Barikani M, Mohammadi M (2007) Synthesis and characterization of starch-modified polyurethane. *Carbohydr Polym* 68:773–780
35. Crini G (2005) Recent developments in polysaccharide-based materials used as adsorbents in wastewater treatment. *Prog Polym Sci* 30:38–70
36. Cunha AG, Gandini A (2010) Turning polysaccharides into hydrophobic materials: a critical review. Part 2. *Cellulose* 17:1045–1065
37. Kaith BS, Kalia S (2008) Graft copolymerization of MMA onto flax under different reaction conditions: a comparative study. *Express Polym Lett* 2:93–100
38. Saikia CN, Ali F (1999) Graft copolymerization of methylmethacrylate onto high α -cellulose pulp extracted from *Hibiscus sabdariffa* and *Gmelina arborea*. *Bioresour Technol* 68:165–171
39. Wan Z, Xiong Z, Ren H, Huang Y, Liu H, Xiong H, Wu Y, Han J (2011) Graft copolymerization of methyl methacrylate onto bamboo cellulose under microwave irradiation. *Carbohydr Polym* 83:264–269

40. Gupta KC, Sahoo S, Khandekar K (2007) Graft copolymerization on to cellulose using binary mixture of monomers. *J Macromol Sci A Pure Appl Chem* 44:707–719
41. Kalia S, Kaith BS (2008) Use of flax-g-poly(MMA) as reinforcing material for enhancement of properties of phenol formaldehyde composites. *Int J Polym Anal Char* 13:341–352
42. Al-Karawi AJM, Al-Daraji AHR (2010) Preparation and using of acrylamide grafted starch as polymer drug carrier. *Carbohydr Polym* 79:769–774
43. Jayakumara R, Prabaharana M, Reisa RL, Mano JF (2005) Graft copolymerized chitosan—present status and applications. *Carbohydr Polym* 62:142–158
44. Onishi Y, Eshita Y, Murashita A, Mizuno M, Yoshida J (2007) Characteristics of DEAE-dextran-MMA graft copolymer as a nonviral gene carrier. *Nanomed Nanotechnol Bio Med* 3:184–191
45. Thimma RT, Reddy NS, Tammishetti S (2003) Synthesis and characterization of guar gum-graft-polyacrylonitrile. *Polym Adv Technol* 14:663–668
46. Stannett V (1981) Grafting. *Radiat Phys Chem* 18:215–222
47. Ring W, Mita I, Jenkins AD, Bikales NM (1985) Source-based nomenclature for copolymers (Recommendations 1985). *Pure Appl Chem* 57:1427–1440
48. Alferey T, Bandel D (1951) Paper presented in 118th American Chemical Society Annual Fall Meeting, through Mark HF. *Rec. Chem. Progr*, vol 12. Chicago, 4 Sept 1950, p 139
49. Kaith BS, Jindal R, Bhatia JK (2011) Morphological and thermal evaluation of soy protein concentrate on graft copolymerization with ethylmethacrylate. *J Appl Polym Sci* 120:2183–2190
50. Basu D, Ak K, Tk M, Banerjee A (1998) Mechanical property studies of poly(methyl methacrylate)-grafted viscose fibres. *J Appl Polym Sci* 69:2585–2591
51. Mehta IK, Misra BN, Chauhan GS (1994) Study of thermal and dyeing behavior of isotactic polypropylene fiber graft copolymerized with acrylate monomers using preirradiation method. *J Appl Polym Sci* 54:1171–1178
52. Battaerd HAJ, Tregear GW (1967) Graft copolymers. Interscience, New York, NY
53. Burlant WJ, Hoffmann AS (1960) Block and graft copolymers. Rheinhold Pub Corp, New York, NY
54. Hsu ST, Pan TC (2007) Adsorption of paraquat using methacrylic acid-modified rice husk. *Bioresour Technol* 98:3617–3621
55. Cho CG, Lee K (2002) Preparation of starch graft copolymer by emulsion polymerization. *Carbohydr Polym* 48:125–130
56. Misra BN, Dogra R (1980) Grafting onto starch. IV. Graft copolymerization of methylmethacrylate by use of AIBN as radical initiator. *J Macromol Sci Chem A* 14:763–770
57. Chiang Wy HC (1996) The improvements in flame retardance and mechanical properties of polypropylene/Fr blends by acrylic acid graft copolymerization. *Eur Polym J* 32:385–390
58. Zahran MK, Mahmoud RI (2003) Peroxydiphosphate–metal ion–cellulose thiocarbonate redox system-induced graft copolymerization of vinyl monomers onto cotton fabric. *J Appl Polym Sci* 87:1879–1889
59. Vlcek P, Janata M, Latalova M, Kriz J, Cadova E, Toman L (2006) Controlled grafting of cellulose diacetate. *Polymer* 47:2587–2595
60. Tizzotti M, Charlot A, Fleury E, Stenzel M, Bernard J (2010) Modification of polysaccharides through controlled/living radical polymerization grafting—towards the generation of high performance hybrids. *Macromol Rapid Commun* 31:1751–1772
61. Kaur I, Misra BN, Gupta A, Chauhan GS (1998) Radiochemical grafting of methacrylonitrile and its binary mixture with methyl acrylate onto gelatin. *Polym Int* 46:275–279
62. Kaith BS, Kalia S (2008) Preparation of microwave radiation induced graft copolymers and their applications as reinforcing material in phenolic composites. *Polym Compos* 29:791–797
63. Khan MA, Shehrzade S, Sarwar M, Chowdhury U, Rahman MM (2001) Effect of pretreatment with UV radiation on physical and mechanical properties of photocured jute yarn with 1,6-hexanediol diacrylate (HDDA). *J Polym Environ* 9:115–124

64. Hassan MM, Islam MR, Khan MA (2002) Effect of additives on the improvement of mechanical and degradable properties of photografted jute yarn with acrylamide. *J Polym Environ* 10:139–145
65. Mamun M, Khan MA, Khan RA, Zaman HU, Saha M, Huque SMF (2010) Preparation of selective ion adsorbent by photo curing with acrylic and phosphoric acid on jute yarn. *Fiber Polym* 11:832–837
66. Zaman HU, Khan MA, Khan RA, Rahman MA, Das LR, Mamun MA (2010) Role of potassium permanganate and urea on the improvement of the mechanical properties of jute polypropylene composites. *Fiber Polym* 11:455–463
67. Jang J, Yoon KC, Ko SW (2001) Durable press finish of cotton via dual curing using UV light and heat. *Fiber Polym* 2:184–189
68. Gobac ST, Vlatkovic M, Meic Z (1979) Gamma radiation-induced graft copolymerization of divinylbenzene onto cellulose fabric. *J Appl Polym Sci* 24:1101–1107
69. Chauhan GS, Mishra BN, Dhiman SK, Guleria LK, Kaur I (2000) Polymers from renewable resources: kinetics of 4-vinyl pyridine radiochemical grafting onto cellulose extracted from pine needles. *Radiat Phys Chem* 58:181–190
70. Deshayes S, Liagre M, Loupy A, Luche JL, Petit A (1999) Microwave activation in phase transfer catalysis. *Tetrahedron* 55:10851–10870
71. Singh V, Tiwari A, Tripathi DN, Sanghi R (2006) Microwave enhanced synthesis of chitosan graft-polyacrylamide. *Polymer* 47:254–260
72. Fang Y, Liu L, Li Y, Chen L (2005) Microwave-assisted graft copolymerization of ϵ -caprolactone onto chitosan via phthaloyl protection method. *Carbohydr Polym* 60:351–356
73. Huacai G, Wan P, Dengke L (2006) Graft copolymerization of chitosan with acrylic acid under microwave irradiation and its water absorbency. *Carbohydr Polym* 66:372–378
74. Xu W, Bao J, Zhang J, Shi M (1996) Microwave irradiation graft copolymerization of hydroxyethyl methacrylate onto wool fabrics. *J Appl Polym Sci* 70:2343–2347
75. Kaith BS, Kalia S (2008) Microwave enhanced synthesis of flax-g-poly(MMA) for use in phenolic composites as reinforcement. *E-J Chem* 5:163–168
76. Zhang J, Zhang S, Yuan K, Wang Y (2007) Graft copolymerization of artemisia seed gum with acrylic acid under microwave and its water absorbency. *Macromol Sci A Pure Appl Chem* 44:881–885
77. Kumar A, Singh K, Ahuja M (2008) Xanthan-g-poly(acrylamide): microwave-assisted synthesis, characterization and in vitro release behaviour. *Carbohydr Polym* 76:261–267
78. Singh V, Tiwari A, Tripathi DN, Sanghi R (2004) Microwave assisted synthesis of guar-g-polyacrylamide. *Carbohydr Polym* 58:1–6
79. Singh V, Tripathi DN (2006) Microwave promoted grafting of acrylonitrile onto cassia siamea seed gum. *J Appl Polym Sci* 101:2384–2390
80. Singh V, Kumar P, Sanghi R (2012) Use of microwave irradiation in the grafting modification of the polysaccharides—a review. *Prog Polym Sci* 37:340–364
81. Chapiro A (1962) *Radiation chemistry of polymeric system*. Wiley Interscience, New York, NY
82. Khan F (2005) Characterization of methyl methacrylate grafting onto preirradiated biodegradable lignocellulose fiber by gamma-radiation. *Macromol Biosci* 5:78–89
83. Daneault C, Kokta BV, Maldae O (1988) Grafting of vinyl monomers onto wood fibres initiated by peroxidation. *Polym Bull* 20:137–141
84. Kumar G, Smith PJ, Payne GF (1999) Enzymatic grafting of a natural product onto chitosan to confer water solubility under basic conditions. *Biotechnol Bioeng* 63:154–165
85. Wenzel A, Yamgishita H, Kitamoto D, Endo A, Haraya K, Nakane T, Hanai N, Matsuda H, Kamuswetz H, Paul D (2000) Effect of preparation condition of photoinduced graft filling polymerized membranes on pervaporation performance. *J Membr Sci* 179:69–77
86. Yamaguchi T, Yamahara S, Nakao S, Kimura S (1994) Preparation of pervaporation membranes for removal of dissolved organics from water by plasma-graft filling polymerization. *J Membr Sci* 95:39–49

87. Bhattacharyaa A, Misra BN (2004) Grafting: a versatile means to modify polymers techniques, factors and applications. *Prog Polym Sci* 29:767–814
88. Kale KH, Desai AN (2011) Atmospheric pressure plasma treatment of textiles using non-polymerizing gases. *Indian J Fiber Text* 36:289–299
89. Kumar K, Kaith BS (2010) Psyllium and acrylic acid based polymeric networks synthesized under the influence of γ -radiations for sustained release of fungicide. *Fiber Polym* 11:147–152
90. Kaith BS, Mittal H, Bhatia JK, Kalia S (2011) Polysaccharide graft copolymers–synthesis, properties and applications. In: Kalia S, Averous L (eds) *Biopolymers: biomedical and environmental applications*. Wiley, Hoboken, NJ

Chapter 2

Cellulose Graft Copolymers: Synthesis, Properties, and Applications

Gülten Gürdağ and Shokat Sarmad

Abstract Grafting of vinyl monomers onto cellulose is an important tool for the modification of cellulose. Depending on the monomer grafted onto cellulose, it gains new properties. The grafting can be performed in heterogeneous or homogeneous medium. In the grafting performed in heterogeneous medium, the reaction is carried out in aqueous medium using a suitable initiator. As initiator, the radiation or chemical initiators such as ceric ammonium nitrate (CAN), various persulfates, azobisisobutyronitrile (AIBN), and Fenton reagent (Fe(II)–H₂O₂) are mostly used. In case of CAN initiator, the grafting should be performed in acidic medium in order to prevent its hydrolysis. In the homogeneous grafting reactions, either a water-soluble cellulose derivative is used in the grafting or cellulose is dissolved in a suitable solvent, and then the grafting is performed. Higher number of grafts per cellulose chain is obtained in homogeneous grafting than those in heterogeneous medium.

Keywords Cellulose • Grafting • Homogeneous medium • Heterogeneous medium • Grafting percentage • Grafting efficiency • Number of grafts per cellulose chain • Ceric ammonium nitrate • Fenton reagent • Persulfates

2.1 Introduction

Cellulose is a naturally occurring polymer, and it is the most abundant and renewable polymer in the world. In addition, it is one of the most promising raw materials due to its abundance, easy availability, and low cost. It is a linear polysaccharide with long chains which consists of β -D-glucopyranose units joined by β -1,4

G. Gürdağ (✉) • S. Sarmad

Faculty of Engineering, Department of Chemical Engineering, Istanbul University, Avcilar 34320, Istanbul, Turkey

e-mail: ggurdag@istanbul.edu.tr; sh_sarmad@yahoo.com

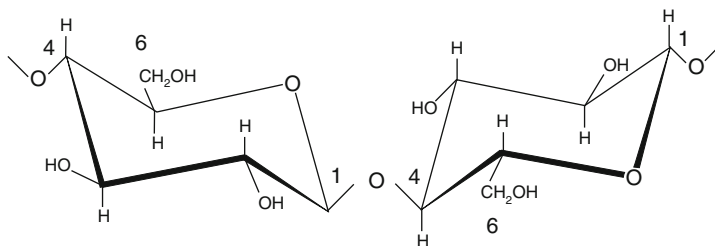


Fig. 2.1 Cellulose formula [4]

glycosidic linkages [1–3]. In one repeating unit of cellulose molecule, there are one methylol and two hydroxyl groups as functional groups [4].

Due to absence of side chains or branching, cellulose chains can exist in an ordered structure. Therefore, cellulose is a semicrystalline polymer, and it contains both crystalline and amorphous phases. Although it is a linear polymer and contains two types of hydroxyl groups, primary hydroxyl in methylol group ($-\text{CH}_2\text{OH}$) at C-6 and secondary hydroxyl groups ($-\text{OH}$) at C-3 and C-4, both of which are hydrophilic, it does not dissolve in water and in common solvents due to strong hydrogen bondings between the cellulose chains. The hydrogen bondings between the cellulose chains and van der Waals forces between the glucose units lead to the formation of crystalline regions in cellulose [5]. In cellulose, there are two types of hydrogen bondings: intramolecular and intermolecular [6]. Intramolecular hydrogen bondings are of two types, i.e., $\text{O}-2-\text{H} \cdots \text{O}-6$ and $-3-\text{H} \cdots \text{O}-5$ links [6]. It can be dissolved in DMSO–PF (dimethyl sulfoxide–paraformaldehyde), LiCl–DMAC (lithium chloride–dimethylacetamide) [7], *N*-methylpyrrolidone–lithium chloride (NMP–LiCl) [7], etc. Cellulose also dissolves in strong concentrated acids such as H_2SO_4 and H_3PO_4 and certain metal complexes such as cuprammonium (cuam) or cupriethylenediamine (cuen) that they break the hydrogen bonds between the cellulose chains.

Cellulose has two crystal forms: cellulose I and cellulose II [4]. In the former, cellulose chains are oriented in parallel conformation, and in the latter, antiparallel one [4] (Fig. 2.1). Cellulose has other polymorphic forms of cellulose III and cellulose IV. According to XRD data [8], the crystallinity of cotton cellulose is 60 % which is in cellulose I form, and the rest is amorphous cellulose. The degree of crystallinity (CrI) of cellulose, namely, the fraction of crystalline content in the cellulose sample, is calculated from XRD patterns by using the peak intensities at $2\theta = 18^\circ$ (I_{am} : intensity due to amorphous portion) and at $2\theta = 22.5^\circ$ (I_{200} : intensity attributed to both amorphous and crystalline phases) [6, 9].

$$\text{CrI} = [(I_{200} - I_{\text{am}})/I_{200}] \times 100 \quad (2.1)$$

Hermans et al. [10] calculated the crystallinity of cellulose (X_c) by another equation given below:

$$X_c = I_c / (I_c + K + I_{\text{am}}) \quad (2.2)$$

where I_c is the intensity of crystalline portions, I_{am} is the intensity of amorphous portions, and K is an empirical constant.

Although the properties of cellulose cannot be modified by conventional copolymerization methods, they can be changed by physical or chemical techniques. The change in the physical structure of cellulose can be performed by swelling it in concentrated (~20 %) NaOH solution and then by regeneration (mercerization) [11]. By this way, cellulose I is irreversibly converted to cellulose II, and the physical properties of cellulose are changed. Mercerization increases the amorphous content, tensile strength, and modulus of cellulose [2, 8], and it makes cellulose more reactive since amorphous regions are more accessible and more reactive than crystalline regions [6]. Chemical properties of cellulose can be changed in three ways:

1. By preparing an ester or ether derivative of cellulose
2. By preparing a cross-linked derivative of cellulose
3. By preparing a graft copolymer of cellulose, namely, a branched derivative of cellulose

2.2 Synthesis of Cellulose Graft Copolymers

Graft copolymerization is a commonly used method for the modification of surfaces of polymers [12, 13], and it is an important tool in order to modify the physical or chemical properties of polymers. During grafting, the side chains are covalently bonded to the main polymer backbone or substrate to form a copolymer with branched structure. Graft copolymers have many different and useful properties different from those which each has alone. Grafting methods can be classified mainly according to grafting medium and the type of initiation mechanisms. Grafting can be performed in a homogeneous or in a heterogeneous medium. Initiation mechanisms can be investigated in three groups:

1. The polymerization of a vinyl monomer in the presence of a polymer in which the propagation reaction is initiated on the polymer backbone by a chain transfer, and the growth of graft chains begin from the active sites on the polymer backbone. This method is called as “grafting from” approach. In that approach [14], the grafting is performed either with a single monomer or with a binary monomer mixture. With single monomer, the grafting usually occurs in a single step, but in the grafting with binary monomer mixture, the reaction is carried out with either the simultaneous or sequential use of the two monomers. In the mosaic grafting, two kinds of monomer are grafted side by side to obtain the required property. This is the origin of bipolar membranes [14].
2. The polymerization of a vinyl monomer in the presence of a polymer with reactive functional end groups. These functional end groups can be activated by means of heat, light, or other ways. This method can be performed by two ways: In “grafting to” approach, a polymer with reactive end groups is reacted

with the functional groups of substrate polymer backbone. In the “grafting through” approach, a macro monomer or a macromer, i.e., a vinyl derivative of cellulose is polymerized with the same or another vinyl monomer [15].

3. The grafting of a monomer onto a polymer backbone by high-energy irradiation. The radiation grafting can be performed by direct/mutual method in which the monomer and the polymer (graft substrate) is irradiated together simultaneously to create the radicals which are starting the polymerization or by preirradiation/indirect grafting in which the monomer is contacted with the polymer backbone irradiated alone before.

Depending on the chemical structure of the monomer grafted onto cellulose, graft copolymers gain new properties such as water absorption [16], improved elasticity, hydrophilic or hydrophobic character, ion-exchange [17–23] and dye-adsorption capabilities [19, 24], heat resistance [16, 25–28], thermosensitivity [29, 30], pH sensitivity [31], antibacterial effect [32], resistance to microbiological attack, etc. [33, 34]. While the internal grafting changes the dyeing behavior of cellulose fibers, surface grafting improves the abrasion resistance [7]. In order to obtain a cellulose graft copolymer with high water or moisture absorbency, hydrophilic monomers such as acrylic acid (AA), acrylamide (AAm), 2-acrylamido-methylpropane sulfonic acid (AASO₃H), etc. should be grafted onto cellulose. In order to improve the compatibility and adhesion of hydrophilic cellulose fibers to the components of hydrophobic composites, hydrophobic monomers such as methyl methacrylate, styrene, acrylonitrile, butadiene, isobutyl vinyl ether, and vinyl acetate should be grafted onto the surface of cellulose [35–38].

The synthesis of cellulose graft copolymers are different from that of the completely synthetic graft copolymers since cellulose does not dissolve in common solvents, and the grafting takes place in a heterogeneous medium. Therefore, the physical structure and the state of aggregation play an important role in the grafting reaction if it is performed in heterogeneous medium. In the grafting in a heterogeneous medium, cellulose exists in dispersed form in an aqueous medium. It is known that in the grafting onto cellulose under heterogeneous conditions, the reaction proceeds only in the amorphous regions of cellulose [39–42]. For that reason, unpurified graft product is not homogeneous, and it consists of cellulose graft copolymer, ungrafted cellulose, and homopolymer [35, 43]. In addition, chain degradation of cellulose backbone takes place during the creation of free radicals in heterogeneous grafting. Another drawback of the heterogeneous grafting is nonuniformity of graft chain lengths, namely, the formation of short and very long graft chains or high molecular weight distribution of graft chains. Strong hydrogen bonds between the cellulose chains hinder grafting when vinyl monomers are used without an appropriate swelling agent, such as water [44]. In heterogeneous grafting reactions [45], grafting percentage decreases with the increase in crystallinity and intermolecular hydrogen bondings in cellulose. As the swelling power of the solvent or the amount of the swelling agent increases, the rate of diffusion of monomer and, in turn, the rate of grafting increases [44, 45]. However, the swelling agent also affects the rate of termination of the graft copolymerization [44]. In the

case of the grafting in a homogeneous medium in which the cellulose dissolves molecularly, it is known that all the cellulose chains participate in grafting reaction [41, 46]. By performing the grafting reaction using soluble cellulose derivatives in a homogeneous medium, the extent and frequency of grafting and the molecular weight of graft chains and homopolymer can be controlled better, the formation of by product homopolymer is minimized, the homogeneity of graft product or uniform distribution of graft chains can be ensured, etc. [35, 47]. In addition, in homogeneous grafting, the molecular weight of graft chains is similar to that of homopolymer occurring simultaneously with the graft copolymer [48]. The grafting reactions in homogeneous medium can be performed by using a soluble cellulose derivative (mostly water-soluble cellulose derivative) such as hydroxyethyl cellulose (HEC), carboxymethyl cellulose sodium salt (CMCNa) [49, 50], carboxymethyl cellulose (CMC) [51], methyl cellulose (MC) [52, 53], cellulose acetate [54], and ethyl cellulose [42, 46] or dissolving the cellulose in a suitable solvent pair such as *N,N*-dimethylacetamide/LiCl system [43], dimethyl sulfoxide–paraformaldehyde (DMSO–PF) system [39–41, 55] and using carboxymethyl cellulose by xanthate method [56]. In another group of homogeneous grafting works, the reaction is performed in two steps. In the first step, a derivative of cellulose is prepared, and then the product of the first step is reacted with the monomer in the second step. For example, Bianchi et al. [7, 43] prepared a cellulose derivative, such as cellulose acrylate or cellulose methacrylate, by reacting cellulose dissolved in DMAc-LiCl with acryloyl chloride and methacryloyl chloride (MACl), respectively, and then they grafted the acrylonitrile (AN) or methyl methacrylate (MMA) onto acrylate or methacrylate derivative of cellulose in homogeneous medium, respectively. In another work, Wang et al. [57] grafted poly(caprolactone monoacrylate) (PCLA) with isocyanate end groups (NCO) (NCO-PCLA) onto cellulose diacetate (CDA) in homogeneous medium of acetone. Lin et al. [58] grafted acrylic acid (AA) onto cellulose dissolved in an ionic liquid (IL) of 1-*N*-butyl-3-methylimidazolium chloride (BMIMCl) by microwave irradiation in a short irradiation duration such as 3 min. ILs which are organic salts are good solvents [59] and good reaction media for cellulose. They are environmental friendly alternatives to volatile organic compounds (VOC) due to their nonvolatility, nonflammability, thermal stability, chemically inertness, and recyclability [60]. Due to their high ionic conductivities and polarizability properties, they absorb microwave irradiation, and as a consequence they provide high heating rates and shorten the reaction duration [58]. Zhu et al. [61] grafted poly(*p*-dioxanone) (PDO) onto ethyl cellulose (EC) by ring-opening polymerization with a tin-2-ethylhexanoate ($\text{Sn}(\text{Oct})_2$) as catalyst in bulk at 120 °C. In the grafting of PDO onto EC in homogeneous medium by $\text{Sn}(\text{Oct})_2$ catalyst, it was not necessary to add any solvent in reaction mixture [61] due to well solubility of EC in PDO. In the grafting methods summarized above, the grafting is performed mostly by creation of free-radical sites on the cellulose backbone either by chemical means or by irradiation. The growth of side chains from vinyl monomers is initiated from these radical sites on the cellulose backbone. However, these techniques have some drawbacks as stated above. More advanced, controlled/living polymerization

methods such as atom-transfer radical polymerization (ATRP) (or metal-catalyzed living-radical polymerization) [30, 31, 60, 62–67], nitroxide-mediated polymerization (NMP) [68], and reversible addition-fragmentation chain transfer (RAFT) [69–72] polymerization are promising methods for the synthesis of well-defined graft polymers with sophisticated architectures such as comb and star polymers, copolymers with the same length of graft chains (low polydispersity/or narrow molecular weight distribution for graft chains), homogeneous grafting frequency, and no homopolymer formation. The main advantage of ATRP is resulting from the relatively low radical concentration in grafting medium which suppresses the termination in comparison to propagation reaction [73–75]. Hiltunen et al. [76] prepared cellulose-graft-polyacrylamide and cellulose-graft-poly(*N,N*-dimethylacrylamide) copolymers by single-electron transfer living radical polymerization (SET-LRP) in DMSO solution. In the first step of grafting, they [76] synthesized cellulose macroinitiators by direct acylation of cellulose with 2-bromoisobutyryl bromide (BiB) in LiCl/DMAc (dimethylacetamide). Then, the grafting of acrylamide (AAm) or *N,N*-dimethylacrylamide (DMAAm) onto cellulose macroinitiator was performed in LiCl/DMAc solvent pair under nitrogen atmosphere using CuCl/PMDETA (*N,N,N',N',N'*-pentamethyldiethylenetriamine) as catalyst.

A detailed list about the grafting reactions performed in homogeneous or heterogeneous media was given in Table 2.1.

2.2.1 *Initiators Used in the Preparation of Cellulose Graft Copolymers*

It is known that the type of initiator has an important effect on the grafting, and it determines the grafting percentage depending on the monomer to be grafted. In the grafting of vinyl monomers onto cellulose or cellulose derivatives, the initiation can be performed by chemical initiators or by (ir)radiation. The grafting of non-vinyl monomers is performed by reaction of monomer with the reactive functional groups of the cellulose. As chemical initiators, redox initiators such as ceric (IV) ion (ceric ammonium nitrate: $(\text{NH}_4)_2\text{Ce}(\text{NO}_3)_6$ (CAN) [77] or cerium (IV) sulfate [21], ceric ammonium sulfate (CAS) [49, 50], iron(II)–hydrogen peroxide (Fe^{2+} – H_2O_2 : Fenton reagent), cobalt (III) acetylacetonate complex salts [45], Co(II)–potassium monopersulfate [78], and sodium sulfite–ammonium persulfate [51], and free radical generators such as azobisisobutyronitrile ($\text{C}_8\text{H}_{12}\text{N}_4$: AIBN) [79], potassium persulfate ($\text{K}_2\text{S}_2\text{O}_8$: KPS) [42, 46, 52, 80–82], ammonium persulfate ($(\text{NH}_4)_2\text{S}_2\text{O}_8$: APS) [42, 46, 53], and benzoyl peroxide ($\text{C}_{14}\text{H}_{10}\text{O}_4$: BPO) [42, 46] can be used. The grafting is also performed by radiation [54, 83] or microwave irradiation [54, 58, 84]. Redox initiator systems can be used at low temperatures, and they react only with the amorphous region of cellulose because the latter are more reactive than the crystalline phase.

Table 2.1 Grafting onto cellulose and its derivatives performed in homogeneous or heterogeneous media

Graft substrate	Monomer	Initiator	Reaction medium	References
Grafting in homogeneous medium				
Cellulose	Methyl methacrylate	Cellulose chloroacetate (macroinitiator)	1-Butyl-3-methylimidazolium chloride	[60]
Cellulose	<i>N</i> -isopropylacrylamide	6-O-bromoisobutyryl-2,3-di-O-methyl cellulose (macroinitiator)	Dimethylacetamide/lithium chloride	[30]
Ethyl cellulose	2-Hydroxyethyl methacrylate	EC, 2-Bromoisobutyryl bromide (macroinitiator)	Methanol	[67]
Carboxymethyl cellulose	Styrene	Bulk polymerization	Tetrahydrofuran	[68]
Cellulose	Styrene, methyl methacrylate, methacrylamide, and acryloylmorpholine	Cellulose chloroacetate (macroinitiator)	Dimethyl formamide	[66]
Cellulose	<i>p</i> -dioxanone	Tin 2-ethyl-hexanoate (catalyst)	1-Butyl-3-methylimidazolium chloride	[110]
Cellulose	Styrene	Azobisisobutyronitrile	Toluene	[35]
Cellulose	Methyl methacrylate and styrene	Cellulose 2-bromoisobutyrylate (macroinitiator)	1-Allyl-3-methylimidazolium chloride	[112]
Cellulose filter paper	Acrylonitrile	Gamma rays of ⁶⁰ Co	Dimethyl formamide	[141]
Carboxymethyl/cellulose	Acrylamide	Sodium bisulfate/ammonium persulfate	Sulfate acid-potassium dichromate	[56]
Ethyl cellulose	2-(diethylamino) ethyl methacrylate	Cellulose 2-bromoisobutyrylate (macroinitiator)	Dimethyl formamide	[31]
Ethyl cellulose	Methyl methacrylate	Ammonium persulfate, potassium persulfate, and benzoyl peroxide	Benzene/DMSO	[42]
Methacrylate-modified cellulose	Methyl methacrylate	Azobisisobutyronitrile	Dimethylacetamide/lithium chloride	[7]
Ethyl cellulose	Azobenzene-containing polymethacrylates	Ethyl cellulose based macroinitiator	Anisole	[113]

(continued)

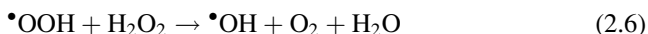
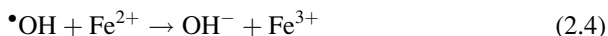
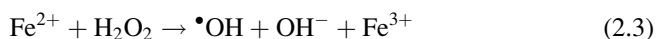
Table 2.1 (continued)

Graft substrate	Monomer	Initiator	Reaction medium	References
Ethyl cellulose	Acrylamide	Ammonium persulfate, potassium persulfate, and benzoyl peroxide	Dimethyl sulfoxide/toluene	[46]
Cellulose	Acrylamide and poly(<i>N,N</i> -dimethylacrylamide)	2-Bromoisobutyl bromide (macroinitiator)	LiCl/dimethylacetamide	[76]
Cellulose	Acrylic acid	Ammonium persulfate	1-Butyl-3-methylimidazolium chloride	[58]
Cellulose	Acrylonitrile and methyl methacrylate	Ammonium persulfate, Azobisisobutyronitrile	Dimethylsulfoxide–paraformaldehyde	[40]
Cellulose	Acrylonitrile and methyl methacrylate	Ammonium persulfate, azobisisobutyronitrile	Dimethylsulfoxide–paraformaldehyde	[41]
Cellulose	Acrylonitrile	Azobisisobutyronitrile	<i>N,N</i> -dimethylacetamide/LiCl	[43]
Cellulose diacetate	Caprolactone monoacrylate	Dibutyltin dilaurate (catalyst)	Acetone	[57]
Cellulose	Methyl acrylate	Ammonium persulfate, Azobisisobutyronitrile, benzoyl peroxide	Dimethylsulfoxide–paraformaldehyde	[39]
Cellulose acetate	Styrene and acrylamide	Gamma rays of ⁶⁰ Co	Water, methanol, ethanol, isopropanol, and <i>t</i> -butanol	[54]
Mixture of carboxymethylcellulose and its sodium salt with hydroxyethylcellulose	<i>N</i> -vinyl-2-pyrrolidone	Ceric ammonium sulfate	Aqueous	[49, 50]
Carboxymethyl cellulose	Acrylamide	Ammonium persulfate and sodium sulfite	Aqueous	[51]
Methyl cellulose	Acrylamide	Potassium persulfate	Water	[52]
Cellulose	2-Hydroxyethyl methacrylate	Ammonium persulfate, potassium persulfate, azobisisobutyronitrile	Dimethylsulfoxide–paraformaldehyde	[55]
Grafting in heterogeneous medium				
Cellulose	Acrylamide and ethyl acrylate	Ceric ammonium nitrate	Aqueous	[100]
Wood pulp	Acrylamide	Ceric ammonium nitrate	Acidic	[98]

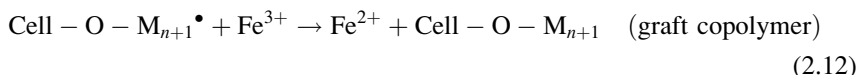
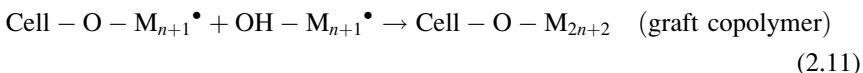
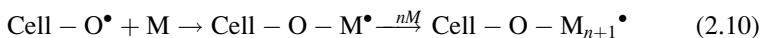
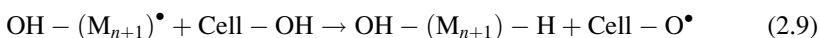
Cassia tora gum	Acrylonitrile	Ceric ammonium nitrate–nitric acid	Aqueous	[95]
Tamarind kernel powder	Acrylamide	Ceric ammonium nitrate–nitric acid	Aqueous	[124]
Stone ground wood	Methyl methacrylate	Fe ²⁺ /H ₂ O ₂	Distilled water	[90]
Carboxymethyl cellulose	Methyl acrylate	Ammonium persulfate	Aqueous	[53]
Cotton fibers	Acrylic acid, methacrylic acid and acrylamide	Potassium persulfate	Aqueous	[80]
Cotton cellulose	Allyl–dimethylhydantoin	Potassium persulfate	Aqueous	[81]
Henequen cellulose microfibrils	Acrylic acid	Potassium persulfate	Water	[105]
Cotton cellulose	Acrylamide	Potassium monopersulfate	Acetic acid, formic acid, and methanol	[78]
Cellulose	Acrylic acid	Ceric ammonium nitrate	Aqueous	[44]
Cellulose	Acrylic acid	Xanthone, 2-chloroanthraquinone and hydrogen peroxide (photoinitiator)	Aqueous Water	[106]
Cellulose	<i>N</i> -isopropylacrylamide	Ammonium cerium(IV) nitrate	Aqueous	[29]
Cellulose fibers	Acrylonitrile	Azobisisobutyronitrile	Bulk polymerization	[79]
Cellulose	4-Vinyl pyridine	Gamma rays of ⁶⁰ Co	Water	[114]
Cellulose	Ethyl acrylate	Fe ²⁺ /H ₂ O ₂	Aqueous	[89]
Cellulose fluff pulp	Acrylic acid, acrylonitrile	Ceric ammonium nitrate	Aqueous	[109]
Cellulose	Acrylamide–methyl acrylate	Ceric ammonium nitrate	Aqueous	[103]
Ethyl cellulose	<i>p</i> -dioxanone	Tin 2-ethyl-hexanoate (catalyst)	Bulk polymerization	[61]
Cellulose	<i>N</i> -vinyl pyrrolidone	Cobalt acetylacetonate	Aqueous	[45]
Cellulose	4-Vinyl pyridine	Ceric ammonium nitrate	Aqueous	[96]
Hollocellulose	Acrylic acid	Ceric ion	Aqueous	[77]
Cellulose fiber	Acrylic and methacrylic acid	Gamma rays of ⁶⁰ Co	Water	[83]
Cellulose	Vinyl acetate	Fe ²⁺ /H ₂ O ₂	Aqueous	[85]
Cellulose	Acrylamide	Cerium sulfate	Water	[21]
Cellulose	<i>N</i> -isopropylacrylamide and methyl acrylate	Potassium persulfate and ceric ammonium nitrate	Aqueous	[84]

2.2.1.1 Fe(II)–H₂O₂

Iron (II)–hydrogen peroxide system (Fenton reagent) is a cheap and easy available redox initiator, and the grafting with that initiator may be carried out in low temperatures [85]. The mechanism for the creation of $\bullet\text{OH}$ radicals by one electron transfer by the reaction of Fe(II) ion with hydrogen peroxide was proposed for the first time by Haber and Weiss [86, 87], and it was given in Eqs. (2.3)–(2.6) below:

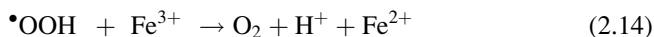


The hydrogen peroxide molecules react with ferrous (Fe^{2+}) ions, and thus, ferric (Fe^{3+}) ions and primary hydroxyl radicals are created. Then, the primary hydroxyl radicals abstract a hydrogen atom from cellulose resulting in a secondary cellulose radical, and the grafting is initiated from these hydrogen-abstracted sites on the cellulose backbone, or the hydroxyl radicals react with monomer to produce homopolymer. Merz and Waters [88] suggested for the first time that the hydroxyl radicals ($\bullet\text{OH}$) created in reaction (2.3) can be used for the grafting of vinyl monomers onto cellulose. The grafting of vinyl acetate onto cellulose by Fenton reagent was proposed to occur by the following mechanism given in Eqs. (2.7)–(2.12) [85];



The grafting yield or the grafting percentage is dependent on the molar ratio of $\text{Fe}^{2+}/\text{H}_2\text{O}_2$. As seen in Eq. (2.12), Fe^{3+} ion, which is created in Eq. (2.3), leads to the

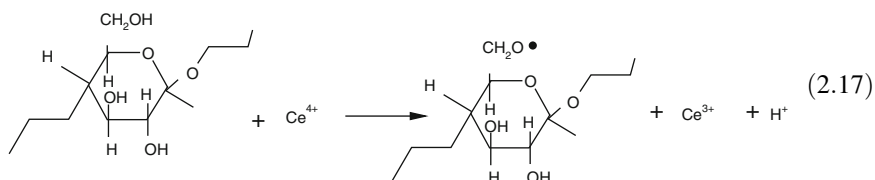
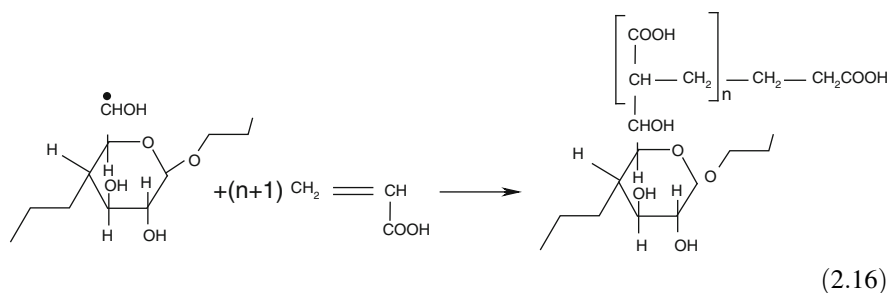
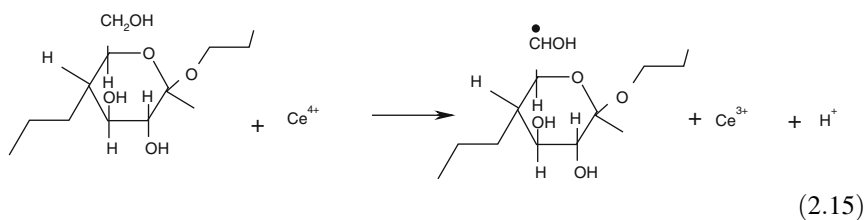
termination of growing side chain on cellulose, and it negatively affects the grafting. When the molar ratio of $\text{Fe}^{2+}/\text{H}_2\text{O}_2$ is higher than 1, some of the $\cdot\text{OH}$ radicals that are created in Eq. (2.3) are consumed by Fe^{2+} ions [Eq. (2.4)], and Fe^{3+} ions affecting the grafting adversely are introduced to the reaction system. Both lead to decrease in the grafting percentage. When the molar ratio of $\text{Fe}^{2+}/\text{H}_2\text{O}_2$ is lower than 1, namely, the concentration of H_2O_2 is higher than optimum value, $\cdot\text{OH}$ radicals are also consumed in the reactions given below [89]:



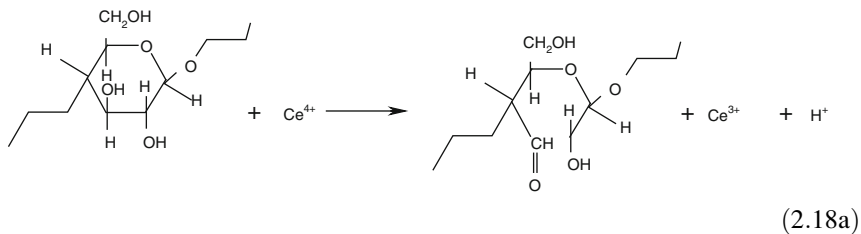
H_2O_2 alone does not lead to the formation of radicals, and it can only create the radicals together with metal impurities which are considered as reducing agent. In the grafting of ethyl acrylate onto the cellulose by Fenton reagent at 30 °C, the optimum value for the molar ratio of $\text{Fe}^{2+}/\text{H}_2\text{O}_2$ was found to be 1.04:1, and the maximum amount of vinyl acetate (12 % grafting) was grafted at that ratio [85]. In order to avoid the negative effect of Fe^{3+} ions on the grafting, the grafting has been carried out in the presence of some complexing agents with Fe^{3+} ions such as ascorbic acid, potassium fluoride (KF), and ethylenediaminetetraacetic acid (EDTA) [85, 89]. In order to minimize the formation of homopolymer and the wastage of primary hydroxyl ($\cdot\text{OH}$) radicals by Fe^{3+} ions, Huang et al. [90] adsorbed Fe^{2+} ions on the lignocellulose by contacting it with an Fe^{2+} salt solution in a given time period (15 min) and separated the Fe^{2+} ion-adsorbed cellulose from the solution containing excess Fe^{2+} ions by filtration. Then, they grafted methyl methacrylate (MMA) onto that Fe^{2+} salt pretreated-lignocellulose.

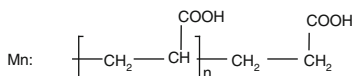
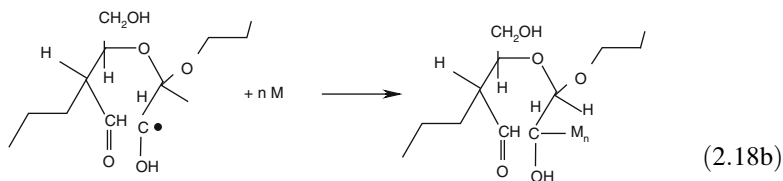
2.2.1.2 Ceric Ion

Among the various types of redox initiators, ceric ion offers many advantages because of its high grafting efficiency and lower amount of homopolymer formation [91]. When Ce^{4+} salts such as cerium sulfate or cerium ammonium nitrate (CAN) is used as initiator in the grafting of vinyl monomers onto cellulose, at first a ceric ion–cellulose complex occurs, and then it decomposes to cerous (Ce^{3+}) ion, and cellulose radicals created by hydrogen abstraction from cellulose [85, 92]. Thus, the initiation sites for grafting are created on the cellulose backbone. The presence of radicals on the cellulose backbone has been confirmed by electron spin resonance (ESR) measurements [93]. The probable positions for grafting to occur are given in equations below [92, 94]. The radical formation on the cellulose backbone may occur either on the carbon (C-6) or oxygen atom of methylol ($-\text{CH}_2\text{OH}$) group [Eqs. (2.15)–(2.17)] [92].

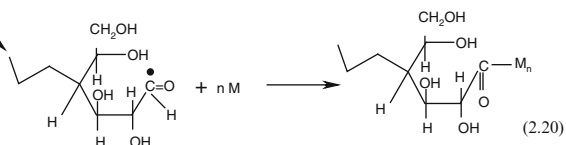
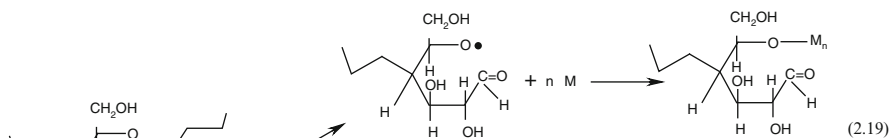


According to Gaylord [94], the grafting may also initiate on C-2 carbon by the ring opening of cellulose backbone [Eqs. (2.18a) and (2.18b)].

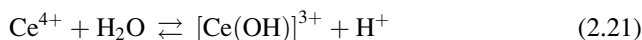




Consistent with the finding of Gaylord [94], Sharma et al. [95] proposed that the grafting occurs mainly at the C2–C3 glycol unit, and to a lesser amount at the C6-hydroxyl in the grafting of acrylonitrile onto cassia tora gum which is a common herbaceous annual weed growing in India. The following mechanism was also reported to be a probable mechanism for the grafting by Ce^{4+} ion [94]:



Although Ce^{4+} is an efficient initiator for the grafting of vinyl monomers onto cellulose, it requires the use of an acid together in order to create initiation sites (radicals) on graft substrate since the ceric ion undergoes hydrolysis in neutral medium [96] through $\text{Ce}(\text{OH})^{3+}$ finally to $[\text{Ce}-\text{O}-\text{Ce}]^{6+}$ ion which has no or low activity [95] for the creation of radicals via the reactions as shown below:



In the absence of acid, no grafting on wool was determined most probably because $[\text{Ce}-\text{O}-\text{Ce}]^{6+}$, which is the hydrolysis product of Ce^{4+} ions, could not form a complex with wool [97]. Since the grafting efficiency of Ce^{4+} ion in neutral medium is low [98], it is used together with an acid, mostly nitric acid (HNO_3). In order to reduce the formation of homopolymer accompanying the grafting, the reaction has been carried out in the absence of the excess of ceric ions.

For that reason, ceric ion solution has been contacted with cellulose in acidic medium for a predetermined time duration, and ceric ions are adsorbed on the cellulose, and then the excess of ceric ions in the mixture (non-adsorbed ceric ions) are removed from the ceric ion-adsorbed cellulose by filtration [98–100]. The rate of disappearance of ceric ions during the grafting of binary monomers (acrylamide and ethyl acrylate) onto cellulose [101] was found to be very high in the initial 1-h period of grafting, and the disappearance of ceric ions was attributed to their consumption for the creation of active sites on cellulose. After that initial 1-h period, no significant change in the concentration of ceric ions has been observed [101].

2.2.1.3 Persulfates

When $K_2S_2O_8/CoSO_4$ system was used as redox initiator [80], at first the primary radicals, $SO_4^{\bullet-}$ and $\bullet OH$, are generated by the decomposition of $K_2S_2O_8$ in the presence of $CoSO_4$, and then these primary $SO_4^{\bullet-}$ and $\bullet OH$ radicals abstract a hydrogen atom from cellulose backbone and create the secondary C- or O-centered cellulose radicals. The growth of graft chains carries on these hydrogen-abstracted active sites [53]. The possible reaction mechanism by a persulfate initiator in the presence of a metal ion (Co(II)) was given in Fig. 2.2 [80].

Potassium persulfate (KPS) is the best radical initiator for hydrogen abstraction [81], and it is cheap and soluble in water. In the investigation of the grafting site via oxidative hydrogen abstraction by potassium persulfate without monomer, the carbon atoms of C3 and C4 on saccharide ring are reported to be probable grafting sites [81]. The radical formation of cellulose backbone by KPS was confirmed by both scanning electron microprobe and elemental analyses [81].

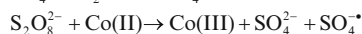
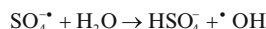
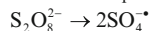
2.3 Characterization of Cellulose Graft Copolymers

After grafting of various vinyl monomers onto linear-chained cellulose backbone, a branched cellulose copolymer is obtained. The physical and chemical properties of a cellulose graft copolymer depend on the kind and amount of monomer grafted onto cellulose, the length of graft chains, the frequency of grafting or the number of grafts per one cellulose chain, etc. After grafting reaction in a heterogenous medium, the cellulose graft copolymer is purified by completely removing the homopolymer from grafting mixture generally by extraction with a suitable solvent. In case of homogeneous grafting performed with soluble cellulose derivatives or dissolving the cellulose in a suitable solvent pair, the graft copolymer is purified by precipitation. Then, it is mainly characterized by the parameters such as grafting percentage (GP %), grafting efficiency (GE %), and the number of grafts per cellulose chain (N_g). The grafting percentage can be determined simply by gravimetry or volumetry [44] if the monomer has suitable functional group such as carboxyl groups. In the volumetric method, the functional groups (carboxyl groups)

Fig. 2.2 The mechanism for graft polymerization of vinyl monomers onto cotton fibers by $K_2S_2O_8/CoSO_4$ redox system [80]

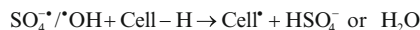
Initiation

1. Creation of primary radicals



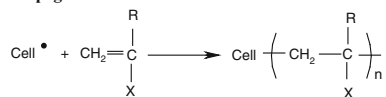
$SO_4^{\bullet -}$ and $\bullet OH$ are primary radicals.

2. Creation of secondary radicalic sites on the cellulose (Cell) backbone



$Cell^{\bullet}$ is secondary radical.

Propagation and termination



$R = H, X = COOH, COOCH_3, CONH_2, OCOCH_3$

of graft copolymer are titrated with a base solution [44]. The grafting percentage can also be determined by elemental analysis. Thus, the grafting percentage in cellulose-graft-polyacrylamide copolymer can be determined by nitrogen (N) content since only polyacrylamide contains nitrogen, but cellulose does not. Besides these main grafting parameters, other parameters such as monomer conversion % and cellulose conversion % have also been determined.

2.3.1 Grafting Percentage and Grafting Efficiency

The grafting percentage (GP) indicates the increase in weight of original cellulose subjected to grafting with a monomer and is calculated generally by the following equation:

$$\begin{aligned} \text{Grafting percentage (GP) (\%)} &= \frac{\text{Weight of polymer grafted}}{\text{Initial weight of backbone}} \times 100 \\ &= \frac{W_1 - W_0}{W_0} \times 100 \end{aligned} \quad (2.23)$$

where W_1 and W_0 are the weights of the cellulose graft copolymer and the original cellulose, respectively. GP (%) defined above has also been defined as apparent graft yield (GY %) which is a weight ratio of grafted polymer to original cellulose [100].

Grafting efficiency (GE) shows the fraction of monomer grafted onto cellulose among the amount of monomer converted to graft polymer plus the homopolymer, in other words, the fraction of polymer which is grafted to cellulose in total polymer, and it is calculated by the equation given below:

Grafting Efficiency (GE) (%)

$$\begin{aligned}
 &= \frac{\text{Weight of polymer grafted}}{\text{Weight of polymer grafted} + \text{Weight of homopolymer}} \times 100 \\
 &= [W_1 - W_0] / [W_1 - W_0 + W_2] \times 100
 \end{aligned}
 \tag{2.24}$$

where W_1 , W_0 , and W_2 are the weights of the cellulose graft copolymer, the original cellulose, and the homopolymer, respectively. The weight of homopolymer (W_2) can be calculated by subtracting the amount of grafted polymer plus the amount of unreacted monomer from the initial amount of monomer. The amount of monomer remaining without reacting after grafting can be determined by volumetric method (bromide–bromate method) [102] or by spectrophotometric methods.

Naturally, the GP (%) and GE (%) values given above are apparent or crude values, and they do not indicate the true values since they are calculated for the mixture consisting of true graft copolymer and the non-grafted cellulose. In some papers [100], the true values, for example, true grafting percentage (GP_T %) which is the weight ratio of grafted polymer to true-grafted polymer, have also been determined after separating the non-grafted cellulose from the apparent cellulose graft copolymer.

2.3.2 Molecular Weight of Grafted Polymer Chains and the Frequency of Grafting

The molecular weight of graft chains is determined generally by viscometric method [39–41, 76, 101], by gel permeation chromatography (GPC) [30], and by $^1\text{H-NMR}$ spectroscopy after separating the graft chains from the graft copolymer, i.e., by hydrolyzing the cellulose backbone of graft copolymer using 72 % H_2SO_4 [100]. Grafting frequency (G_F) is defined as the number of grafted polymer chains (N_g) per chain of cellulose [39, 101, 103].

Number of grafts per cellulose chain (\bar{N}_g) :

$$\frac{\text{Molecular weight of cellulose}}{\text{Molecular weight of graft copolymer}} \times \frac{\text{Grafting percentage}}{100} \tag{2.25}$$

When the grafting process occurs mainly on the surface of the cellulose backbone, in other words the grafting is performed in heterogeneous medium, the number of grafted polymer chains per cellulose chain is in the range of unity, and it rarely exceeds the unity [104]. In addition, the molecular weight of graft chains may be in the order of 10^5 [7]. Nishioka and Kosai [41] reported that in homogeneous grafting carried out in dimethyl sulfoxide–paraformaldehyde (DMSO–PF)

binary solvent system with AIBN initiator, the number of grafts per cellulose chain was 1.3. In the grafting of methyl methacrylate (MMA) onto methacrylate-modified cellulose in homogeneous medium (DMAc-LiCl) [7], the number of grafts per cellulose chain was found to be about 6 at both 60 and 70 °C.

2.3.3 Water Absorption Capacity

When hydrophilic or ionic monomers such as acrylamide (AAm), acrylic acid (AA), or 2-acrylamido-methyl propane sulfonic acid (AASO₃H) or their binary mixture are grafted onto cellulose, the cellulose gains hydrophilic character, and the copolymer will absorb high amount of water depending on ionization degree of graft chains, grafting percentage, length of graft chains, and ionic strength of swelling medium. For example, the water absorption capacity of poly(acrylic acid) (PAA)-grafted cellulose microfibrils was found to be three times higher than that of original cellulose microfibrils [105]. The water absorption capacity of cellulose graft copolymers is determined by the following equation [44, 99, 106]:

$$\begin{aligned} & \text{Water absorption capacity (gH}_2\text{O/g copolymer)} \\ &= \frac{\text{Weight of swollen copolymer (}W_s\text{)} - \text{Weight of dry copolymer (}W_d\text{)}}{\text{Weight of dry copolymer (}W_d\text{)}} \end{aligned} \quad (2.26)$$

2.3.4 Mechanical Properties

Grafting changes the mechanical properties of substrate polymer. The mechanical properties of acrylonitrile-grafted hemp varied with the amount of grafting [79], and the grafting led little degradation effect on the mechanical properties. It has been reported that grafting of isocyanate-terminated poly(caprolactone monoacrylate) (NCO-PCLA) onto cellulose diacetate (CDA) backbone broke intermolecular hydrogen bonds and increased the elongation of the graft copolymers (PCLA-g-CDA) [57]. The amount of elongation increased with the increase in grafting percentage. The introduction of flexible PCLA segments to CDA by grafting improved the tenacity of the graft copolymers too [57]. The grafting of vinyl monomers onto amine-treated cotton fibers has been found to improve the moisture sorption ability, and it had little impact on the mechanical properties [80].

2.3.5 Biodegradability

Depending on the monomer grafted onto cellulose, the copolymer gains biodegradability. Wang et al. [57] grafted isocyanate-terminated poly(caprolactone

monoacrylate) (NCO-PCLA) onto cellulose diacetate (CDA) and determined from the soil burial tests and active sludge tests that graft copolymers have good biodegradability in natural conditions.

2.3.6 Confirmation of Grafting

The proof of grafting can be checked by various methods such as swelling, thermal (by DTA/TGA) and mechanical property measurements, FTIR, DSC, XRD, NMR, SEM, and XPS.

Grafting has been confirmed mostly by FTIR analysis which is performed by ATR or KBr technique. While ATR technique gives information about the changes due to grafting in the surface of graft copolymer [107], KBr technique indicates the changes occurred both inside and in the surface of graft product [4]. The band in the FTIR spectrum of graft product, which is not present in the spectrum of graft substrate, is the proof of grafting if substrate has no FTIR band at the same wave number. In the case of a graft copolymer consisting of a vinyl monomer such as acrylamide or acrylic acid and cellulose, FTIR band assigned to the stretching vibration of carbonyl ($\nu_{C=O}$) is generally used for the confirmation of grafting. An example for the characteristic band positions and assignments used in the characterization of various graft products by FTIR was listed in Table 2.2 with their references.

The grafting also leads to changes in the thermal properties. As known, the original cellulose has no glass transition temperature (T_g) and melting temperature (T_m) due to strong inter- and intramolecular hydrogen bondings [108]. For that reason, depending on structure the polymer grafted and the lengths of graft chains, a slight deviation in baseline in the DSC curve of graft copolymer will be a good indicator for both the presence of a T_g due to the graft side chains on the cellulose backbone and for the proof of grafting. For example, Zhe et al. [53] determined in the grafting of methyl acrylate onto carboxymethyl cellulose (CMC) that while CMC does not display any transition between -40 and 60 °C, poly(methyl acrylate)-grafted CMC and poly(methyl acrylate) have T_g 's at 19.2 and 13.75 °C, respectively. Wang et al. [57] reported that the grafting of poly(caprolactone monoacrylate) (PCLA) onto isocyanate-terminated cellulose diacetate (CDA) decreased the flow temperatures of graft copolymers in comparison to that of CDA, and the processibility of CDA-g-PCLA copolymers was easier than that of original CDA. The introduction of PNIPAM onto cellulose backbone by grafting increased the T_g of graft copolymer [30]. Thermal degradation or stability of cellulose can also change with grafting. Dahou et al. [109] reported that the thermal stability of cellulose-g-PAN or cellulose-g-PAA is higher than that of ungrafted cellulose. A similar improvement in the thermal stability observed by grafting was determined for polyacrylamide-grafted carboxymethyl cellulose [51] and *N*-isopropylacrylamide- and methyl acrylate-grafted cellulose [84], poly(acrylic acid)-grafted cellulose microfiber [105], cellulose-graft-poly(*N,N*-

Table 2.2 The characteristic band positions and assignments used in the characterization of various graft products by FTIR

Wave number, cm ⁻¹	Peak assignment	References
Original cellulose		
3,570–3,460	Intramolecular OH bending	[130]
3,460	Intramolecular OH bending	[131]
3,418–3,250	Intermolecular OH bending	[130]
3,346	Intermolecular OH bending	[131]
3,400–2,750	–OH stretching	[56]
3,100–3,500	–OH vibration	[105]
3,400	–OH	[8, 50, 57]
3,471	–OH stretching	[114]
3,413	–OH stretching	[132]
1,640	H–O–H intermolecular stretching	[105]
1,645	OH bending	[114]
1,648–1,620	OH bending (absorbed water)	[130]
1,640	OH bending (absorbed water)	[131]
2,920–2,848	Symmetrical CH ₂ stretching	[130]
2,908	Symmetrical CH ₂ stretching	[131]
2,902	C–H stretching	[96]
2,854	–CH ₂ -symmetric stretching	[53]
2,927	C–H stretching	[114]
2,901	C–H stretching	[132]
2,904–2,891	Stretching of the C–H bond in –CH ₂ group	[105]
2,983	C–H stretching	[50]
2,903	C–H stretching	[96]
1,430–1,376	C–H deformation	[96]
1,384–1,360	C–H deformation	[130]
1,370	C–H deformation	[131]
1,740	C=O stretching vibration	[130]
1,745	C=O stretching vibration	[131]
1,750	C=O stretching vibration	[60]
1,655	C=O stretching vibration	[56]
1,745	C=O stretching vibration	[31]
1,747	C=O stretching vibration	[35]
1,750	C=O stretching vibration	[66]
1,175–1,160	Assym. C–O–C bridge stretching	[130]
1,175	Assym. C–O–C bridge stretching	[131]
1,150	Assym. C–O–C stretching	[109]
1,165	C–O–C stretching	[114]
1,138–1,124	Assym. C–O–C bridge	[130]
1,130	Assym. C–O–C bridge	[131]
1,300–1,000	C–O stretching	[132]
1,221	C–O stretching	[56]
1,280 and 1,185	C–O stretching	[35]
1,375–1,030	C–O stretching	[96]
667–706	C=C out-of-plane ring bending	[132]
1,653	Double bond stretching in alkenes	[132]
905–880	Assym. out-of-phase ring	[130]

(continued)

Table 2.2 (continued)

Wave number, cm ⁻¹	Peak assignment	References
896	Stretch C ₁ –O–C ₄	[131]
694	Out-of-plane C–H bending	[35]
Cellulose graft copolymer		
1,660	C=O stretching, <i>N</i> -vinylpyrrolidone	[133]
1,735	C=O stretching, glycidyl methacrylate	[134]
1,670	C=O stretching, acrylamide	[134]
1,617	C=O stretching, acrylic acid	[134]
1,718	C=O stretching, acrylic acid	[135]
1,738	C=O stretching, <i>O</i> -butyryl chitosan	[107]
1,700	C=O stretching, acrylonitrile/methacrylic acid	[132]
1,750	C=O stretching, poly(methyl methacrylate)	[60]
1,676	Carbamide group of acrylamide, acrylamide–methyl acrylate	[103]
1,783	Ester carbonyl of methacrylate, acrylamide–methyl acrylate	[103]
790	C–Cl stretching, poly(methyl methacrylate)	[60]
3,400–2,750	O–H stretching, acrylamide	[56]
3,164 and 3,047	N–H stretching, acrylamide	[56]
1,665	C=O, Acrylamide	[56]
1,406	C–N, Acrylamide	[56]
1,221	C–O, Acrylamide	[56]
1,731	C=O, 2-(diethylamino) ethyl methacrylate	[31]
3,476	–OH, 2-(diethylamino) ethyl methacrylate	[31]
3,043	=C–H heteroaromatic group, poly(4-vinyl pyridine)	[96]
1,352	C=C, poly(4-vinyl pyridine)	[96]
1,521	C=C, poly(4-vinyl pyridine)	[96]
1,644	C=C, poly(4-vinyl pyridine)	[96]
1,352	C=N, poly(4-vinyl pyridine)	[96]
1,521	C=N, poly(4-vinyl pyridine)	[96]
1,644	C=N, poly(4-vinyl pyridine)	[96]
1,176–1,031	C–O, poly(4-vinyl pyridine)	[96]
1,660	Amide I (C=O), acrylamide	[98]
1,600	Amide II (N–H), acrylamide	[98]
1,700	Assym. stretching of carboxylate anion, acrylamide	[98]
1,560	Symm. stretching of carboxylate anion, acrylamide	[98]
3,430	–OH, methyl acrylate	[53]
1,120	C–O stretching, methyl acrylate	[53]
1,639	–COO– bending, methyl acrylate	[53]
2,854	–CH ₂ symm. stretching, methyl acrylate	[53]
1,740	C=O, methyl methacrylate	[42]
1,727	C–O, poly(acrylic acid)	[105, 136]
1,725	C=O, acrylic acid	[58]
1,262	C–O, acrylic acid	[58]
890–1,160	Polysaccharide	[135]
2,243	C–N stretching, acrylonitrile	[43]
1,259	COOH, acrylic acid	[135]
1,270	C=O stretching of saturated ester, glycidyl methacrylate	[138]
1,270	C(=O)–O stretching of unsaturated ester, glycidyl methacrylate	[138]

(continued)

Table 2.2 (continued)

Wave number, cm ⁻¹	Peak assignment	References
800	C–O–C assym. stretching of unsaturated ester, glycidyl methacrylate	[138]
1,655	C=N stretching overlapped with C=O, acrylonitrile/methacrylic acid	[132]
2,238	C≡N, acrylonitrile	[137, 139]
2,241	C≡N, acrylonitrile	[134]
2,243	C≡N, acrylonitrile	[132]
2,273	NCO, poly(caprolactone monocrylate)	[57]
1,583	Amide N–H, poly(caprolactone monocrylate)	[57]
~1,735	C=O stretching vibration of ester group, acrylic acid and acrylonitrile	[109]
2,240	–CN vibration of nitrile group, acrylonitrile	[109]
1,710	C=O stretching, acrylic acid	[109]
1,758–1,704	Carbonyl groups, allyl-dimethylhydantion	[81]
3,444	O–H group, polyacrylamide	[51]
1,625	Carboxyl group, polyacrylamide	[51]
1,068	CH–O–CH ₂ , polyacrylamide	[51]
695	Deformation vibration of –CH–, polystyrene	[35]
700	Cellulose-g-polystyrene, polystyrene	[140]
1,665	C=O in the amide group, methacrylamide	[66]
3,200	N–H in NH ₂ group, methacrylamide	[66]
1,640	C=O in the amide group, acryloylmorpholine	[66]
1,735	C=O in the ester group, methyl methacrylate	[66]
3,190	N–H stretching vibration, polyacrylamide and poly(<i>N,N</i> -dimethylacrylamide)	[76]
1,650	Amide I, polyacrylamide and poly(<i>N,N</i> -dimethylacrylamide)	[76]
1,610	Amide II, polyacrylamide and poly(<i>N,N</i> -dimethylacrylamide)	[76]
1,623–1,597	C=N stretching, poly(4-vinyl pyridine)	[114]
1,416 and 1,552	C=C stretching, poly(4-vinyl pyridine)	[114]
3,185	OH stretching, poly(4-vinyl pyridine)	[114]
1,638–1,641	C=N, poly(4-vinyl pyridine)	[114]
1,513 and 1,455	Phenyl ring, poly(4-vinyl pyridine)	[114]
1,719 and 1,751	C=O stretching of the five-member anhydride ring, poly(4-vinyl pyridine)	[114]

dimethylacrylamide) [76], NIPAM-grafted-cellulose derivatives [30], and polyacrylamide-grafted cellulose [103]. Wojnárovits et al. [4] claim that although the grafting does not change basically the XRD pattern of cellulose, it dilutes the cellulose fraction and crystalline fraction of cellulose in graft copolymer. Therefore, the intensity of the characteristic peak due to crystalline structure of cellulose decreases, and the intensity of the peak attributed to the amorphous phase becomes more apparent. Although the claim of Wojnárovits et al. [4] is reasonable, chain scission in cellulose occurs during the grafting due to the oxidative effect of initiator. Similar to the finding of Wojnárovits et al. [4], we [110] have observed

on the grafting of acrylic acid on the cellulose that cellulose chains shorten during grafting as can be seen in the SEM pictures in Fig. 2.3. In addition, the change in molecular weight can also occur due to dissolution of cellulose in a suitable solvent or solvent pair when the grafting is performed in homogeneous medium. For that reason, a different XRD pattern can be expected after grafting.

Zhu et al. [111] reported that native cellulose shows two characteristic diffraction peaks at $2\theta = 15.7$ and 22.5° assigned to the diffraction patterns of cellulose I. They also investigated the XRD pattern of regenerated cellulose after dissolving the cellulose in an ionic liquid and then coagulating it with water. They observed that regenerated cellulose exhibits diffraction patterns for cellulose II at $2\theta = 20.3^\circ$ and 21.2° [111]. So, they concluded that the crystallization of cellulose was affected not only by grafting but also by its dissolution and precipitation. The confirmation of grafting can also be performed by the analyses of ^{13}C NMR and ^1H NMR spectra of graft copolymers and ungrafted substrate [31, 42, 43, 57, 60, 61, 76, 111–113]. SEM pictures of both graft copolymers and ungrafted cellulose may confirm the grafting of monomer [58, 109, 111, 114] too.

2.4 Effect of Reaction Conditions on the Grafting Parameters and Properties of Cellulose Graft Copolymers

The factors affecting the grafting can be listed as the nature of the backbone, the pretreatment of cellulose substrate with initiator or a swelling agent, the type of monomer (hydrophilic or hydrophobic) and the presence of comonomer, the type of solvent or grafting medium (homogeneous/heterogeneous), the type and the concentration of the initiator, the presence of additives, temperature, the grafting duration, the presence or absence of oxygen during grafting, etc. [16, 44, 98–100]. A detailed list of optimum grafting conditions was given in Table 2.3.

2.4.1 Pretreatment of Cellulose Before Grafting

When the grafting onto cellulose is carried out in a heterogeneous medium, the accessibility of cellulose by the initiator and the vinyl monomer is an important parameter determining the grafting yield or the grafting percentage. Although cellulose is a linear polymer, the presence of crystalline regions and the strong intermolecular hydrogen bondings decrease its accessibility or reactivity for the grafting reaction. However, in water, the intercrystalline swelling of cellulose occurs mainly on its accessible or amorphous regions, and it enhances the grafting efficiency. It is known that the grafting occurs preferably on the amorphous regions of cellulose due to high reactivity and accessibility of these regions. The grafting efficiency can be increased by increasing the ratio of cellulose/monomer either by

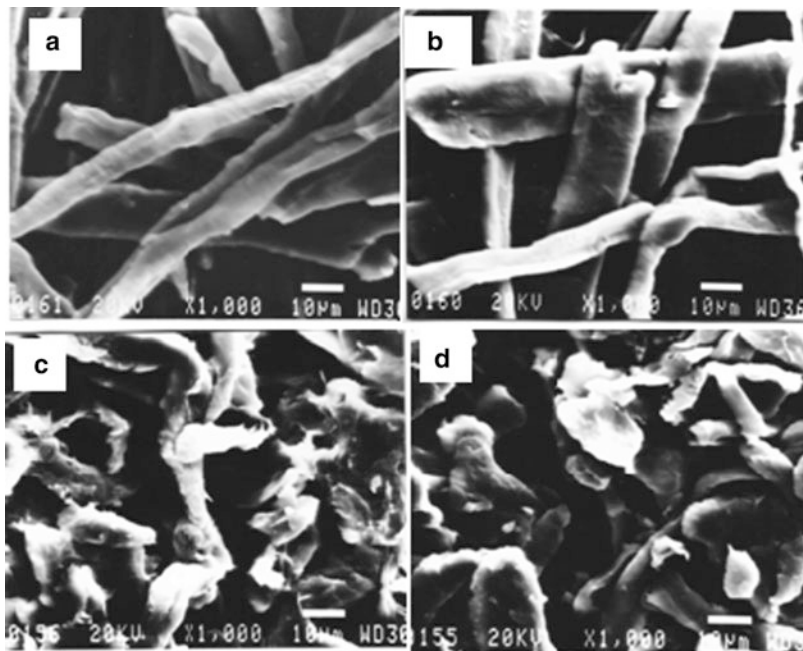


Fig. 2.3 SEM pictures of (a) original cellulose, (b) cellulose-graft-PAA with low grafting %, (c) Na salt of cellulose-graft-PAA with high grafting %, and (d) cellulose-graft-PAA with high grafting % [110]

swelling the cellulose before the reaction or by performing the grafting reaction in a medium in which cellulose swells [99]. Namely, the accessibility or reactivity of cellulose for grafting can be enhanced by decreasing its crystallinity or by increasing the content of amorphous phase since the grafting occurs mainly on the amorphous regions [16, 24]. Therefore, Okieimen [22] and Stannet et al. [115–117] decrystallized the poly(acrylic acid)-grafted cellophane and rayon by treating them with 70 wt% $ZnCl_2$ solution in order to enhance the water absorption capacity of graft products. They determined that the decrystallization of graft copolymer with $ZnCl_2$ solution alone was not enough to increase its water absorbency, and it should be performed by the solutions of both $ZnCl_2$ and NaOH. Fernandez et al. [100] grafted vinyl acetate and methyl acrylate onto the cotton mercerized with 20 % NaOH solution. They carried out the grafting reaction by using two types of cellulose: In the first one, they contacted mercerized or non-pretreated cellulose with ceric ion solution, and then they removed the excess of ceric ions by filtration. In the second, they grafted vinyl monomers onto mercerized or non-pretreated cellulose without any treatment by ceric ions. They [100] determined that the grafting frequency and molecular weight of graft chains are higher in the case of the removal of excess ceric ions. In addition, they found that the ceric ion consumption with mercerized cotton is slightly higher [100]. Gürdağ et al. [99] investigated the effect of pretreatment of cellulose on the grafting of acrylic acid by

Table 2.3 The optimum reaction conditions at which the maximum grafting was obtained in some works

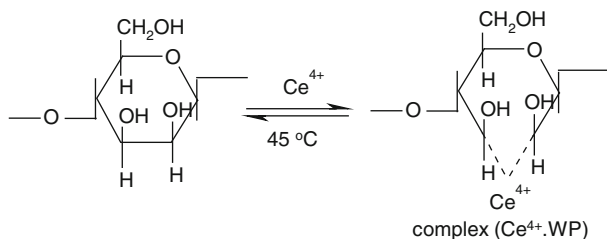
Monomer and its optimum concentration (M)	Max. grafting percentage (%)	Initiator and its concentration	Reaction conditions (temp. and medium)	References
N-vinyl pyrrolidone/ 30.0×10^{-3} mol dm ⁻³	~200	Cobalt acetylacetonate/ 10×10^{-5} mol dm ⁻³	Aqueous/50 °C	[45]
Acrylamide/ $2.5 \text{ g} \cdot 100 \text{ cm}^{-3}$	~300	Ammonium persulfate/ $0.4 \text{ g} \cdot 100 \text{ cm}^{-3}$	Dimethylsulfoxide-toluene/50 °C	[46]
Acrylamide/ $1 \text{ g} \cdot 100 \text{ cm}^{-3}$	400	Potassium persulfate/ $0.4 \text{ g} \cdot 100 \text{ cm}^{-3}$	Dimethylsulfoxide-toluene/50 °C	[46]
Acrylamide	BPO is an unsuitable initiator	Benzoyl peroxide	Dimethylsulfoxide-toluene/50 °C	[46]
4-vinyl pyridine/ 0.927 mol/L	585	Ceric ammonium nitrate/ 0.018 mol L^{-1}	Aqueous/45 °C	[96]
Acrylonitrile/ 0.42 mol	211.57	Ceric ammonium nitrate/ 0.02 mol	Aqueous/30 °C	[95]
2-hydroxyethyl methacrylate/ 10 g in 100 g DMSO	~120	Ammonium persulfate/ 0.4 g	Dimethylsulfoxide-paraformaldehyde/ 40 °C	[55]
2-hydroxyethyl methacrylate/ 10 g in 100 g DMSO	KPS is an unsuitable initiator	Potassium persulfate/ 0.4 g	Dimethylsulfoxide-paraformaldehyde/ 50 °C	[55]
2-hydroxyethyl methacrylate/ 10 g in 100 g DMSO	n.a. (not available)	Azobisisobutyronitrile/ 0.4 g	Dimethylsulfoxide-paraformaldehyde/ 60 °C	[55]
Acrylamide/ 0.099 mol	229.68	Ceric ammonium nitrate/ 0.035 mol	Aqueous/30 °C	[124]
Methyl acrylate/ 40 ml	700	Ammonium persulfate/ 1.50 mg	Aqueous/70 °C	[53]
Methyl methacrylate/ 8 g in 100 cm^{-3}	~140	Ammonium persulfate/ $0.2 \text{ g}/100 \text{ cm}^{-3}$	Benzene/DMSO/50 °C	[42]
Methyl methacrylate/ 16 g in 100 cm^{-3}	~140	Potassium persulfate/ $0.2 \text{ g}/100 \text{ cm}^{-3}$	Benzene/DMSO/50 °C	[42]
Methyl methacrylate	BPO is an unsuitable initiator	Benzoyl peroxide	Benzene/DMSO/50 °C	[42]
Acrylic acid/ 2 (g/g CE)	~98	Ammonium persulfate/ 0.05 (g/g CE)	1-Butyl-3-methylimidazolium chloride/60 °C	[58]
Acrylonitrile/ 4 g in 100 g DMSO solution	~90	Ammonium persulfate/ 0.8 g in 100 g DMSO solution	Dimethylsulfoxide-paraformaldehyde/ 40 °C	[40]
Methyl methacrylate/ 4 g in 100 g DMSO solution	50	Ammonium persulfate/ 0.2 g in 100 g DMSO solution	Dimethylsulfoxide-paraformaldehyde/ 40 °C	[40]
Acrylonitrile	AIBN is an unsuitable initiator	Azobisisobutyronitrile	Dimethylsulfoxide-paraformaldehyde/ 60 °C	[40]

Methyl methacrylate/4 g in 100 g DMSO solution	50	Azobisisobutyronitrile/0.08 g in 100 g DMSO solution	Dimethylsulfoxide-paraformaldehyde/ 60 °C	[40]
Acrylonitrile/4 g in 100 g DMSO solution	90	Ammonium persulfate/0.8 g in 100 g DMSO solution	Dimethylsulfoxide-paraformaldehyde/ 40 °C	[41]
Methyl methacrylate/4 g in 100 g DMSO solution	50	Ammonium persulfate/0.2 g in 100 g DMSO solution	Dimethylsulfoxide-paraformaldehyde/ 40 °C	[41]
Acrylonitrile	AIBN is an unsuitable initiator	Azobisisobutyronitrile	Dimethylsulfoxide-paraformaldehyde	[41]
Methyl methacrylate/4 g in 100 g DMSO solution	50	Azobisisobutyronitrile/0.08 g in 100 g DMSO solution	Dimethylsulfoxide-paraformaldehyde/ 60 °C	[41]
Methyl acrylate/4 g in 100 g DMSO solution	40	Ammonium persulfate/0.4 g in 100 g DMSO solution	Dimethylsulfoxide-paraformaldehyde/ 40 °C	[39]
Methyl acrylate/4 g in 100 g DMSO solution	n.a. (not available)	Azobisisobutyronitrile/0.08 g in 100 g DMSO solution	Dimethylsulfoxide-paraformaldehyde/ 60 °C	[39]
Methyl acrylate / 4 g in 100 g DMSO solution	BPO is an unsuitable initiator	Benzoyl peroxide	Dimethylsulfoxide-paraformaldehyde/ 40 °C	[39]

ceric ammonium nitrate–nitric acid (CAN–HNO₃) initiator system onto cellulose. For that aim, they [99] pretreated the cellulose before grafting reactions with either 2 or 20 wt% NaOH solutions for 24 or 2 h, respectively. As another pretreatment for cellulose, they heated it in distilled water or in aqueous nitric acid (2.5×10^{-3} M) solution at 55 °C in order to enhance the accessibility of cellulose by the initiator and the monomer. In addition, they also carried out the grafting reaction by ceric ion-pretreated and non-pretreated cellulose in order to determine how the excess of initiator affects the grafting percentage and homopolymer formation and determined that in the presence of excess ceric ions, higher grafting percentages were obtained. In the presence of excess ceric ions, higher grafting percentages were obtained with the cellulose which is swelled in aqueous nitric acid than that swelled in water. When the excess of ceric ions were removed by filtration and the grafting was carried out with ceric ion-pretreated cellulose, swelling of cellulose in water resulted in higher amount of grafting than that in acid solution. The same authors [99] also determined that the pretreatment of cellulose with dilute or concentrated NaOH solutions made no improvement on the grafting percentages of copolymers; on the contrary grafting values decreased due to treatment with NaOH. Kim and Mun [98] treated wood pulp (WP) with CAN in 0.24 M nitric acid solution and removed the excess of Ce⁴⁺ ions by filtration from the WP. Then, they grafted acrylamide onto Ce⁴⁺-pretreated WP. They [98] determined that the rate of grafting of acrylamide onto Ce⁴⁺-pretreated WP is higher than that onto non-pretreated WP, and the grafting yield increased with the concentration of Ce⁴⁺ in the pretreatment solution from 1×10^{-3} M to 2×10^{-3} M, but its further increase to 5×10^{-3} and 10×10^{-3} M decreased the amount of grafting. In addition, the graft copolymers prepared by Ce⁴⁺-pretreated WP displayed higher water and saline absorbency than those with non-pretreated WP due to uniformity of grafting with former cellulose substrate [98] (Fig. 2.4).

Ouajai et al. [79] grafted acrylonitrile onto modified natural cellulose fibers (hemp: *Cannabis sativa*) by using AIBN as initiator. With this aim, they modified natural cellulose fibers (hemp: *Cannabis sativa*) by first acetone extraction in order to remove wax and lignin and then by pretreatment with the solutions of NaOH at various concentrations (3, 5, 8, 10, 12, 15, and 20 wt/vol%). They [79] determined from the WA-XRD data that the treatment with NaOH at high concentrations (10–20 wt/vol%) led to transformation of cellulose fibers from cellulose I to cellulose II structure. The formation of amorphous cellulose and cellulose II by mercerization (namely, by NaOH treatment) in the structure of fibers was also confirmed by crystallinity index calculated by the FTIR analyses. In addition, no crystalline transformation in AN-grafted cellulose fibers was determined due to grafting [79]. Various methods such as ozonation/oxidation and pretreatment with alkali, amine, or water have been tried to enhance the reactivity of cellulose for modification reactions [24, 117]. In these methods, the enhancement in accessibility is based on the depolymerization as well as decrystallization of cellulose. The treatment of cellulose with amines leads to swelling and decrystallization of cellulose; thus, the reactivity and properties of amine-treated cellulose changes [118–120]. Mondal et al. [80] investigated the grafting of water-soluble monomers

(I) Pretreatment with Ce^{4+} ion:



(II) grafting of acrylamide (AAm)

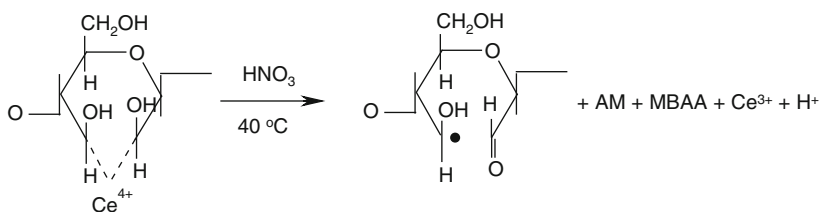


Fig. 2.4 The formation of complex (Ce^{4+} .WP) between Ce^{4+} ions and wood pulp (WP) (I) and the grafting of acrylamide (AM) onto Ce^{4+} .WP (ceric ion-adsorbed WP) (II) [98]

such as acrylic acid (AA), methacrylic acid (MAA), and acrylamide (AM) and water-insoluble monomers such as methacrylate (MA), methyl methacrylate (MMA), and vinyl acetate (VAc) on the amine-treated cotton fiber using potassium persulfate (KPS) and $CoSO_4$ as initiator system. Ethylenediamine (EDA), 1,2-propanediamine (PDA), and diethylenetriamine (DTA) have been used as the pretreatment agent by Mondal et al. [80]. Treatment of cotton fibers with amines, ethylenediamine (EDA) in particular, decreased the crystallinity and tensile strength of the cotton fibers and improved the moisture sorption. Depending on the amine used for treatment, the following decreases (given in parenthesis) in the crystallinity was determined: EDA (51.4 %), DTA (67.7 %), PDA (68.7), EA (82.9 %), and water (84 %). While in the grafting of water-soluble monomers, amine treatment of cellulose fibers gave higher grafting yields than water treatment; lower amount of grafting was obtained with water-insoluble monomers. The grafting of vinyl monomers onto amine-treated cotton fibers has improved the moisture sorption ability [80]. Toledano-Thompson et al. [105] modified henequen cellulosic microfibers (CM) by the reaction with an epoxide containing a terminal double bond [105], and then, they grafted the poly(acrylic acid) (PAA) onto the cellulosic fibers with terminal double bond. They determined that the water sorption capacity of cellulosic fibers with 21 wt% PAA grafting increased up to three times [105].

2.4.2 Effect of the Kind and Concentration of the Monomer

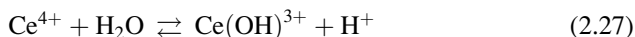
The kind and the concentration of monomer are also important parameters as well as graft substrate and the grafting medium. The graft yield or grafting percentage depend on various properties of monomers such as polarity and steric nature, the power of swelling for graft substrate [14], and reactivity ratios and the presence or absence of synergistic effects between the comonomers in case of the grafting of binary monomer mixture as well as the concentration of monomer. Bhattacharya et al. [121] reported that the grafting of substituted acrylamides such as acrylamide (AAm), methylacrylamide (MAAm), and *N,N*-dimethylacrylamide (DMAAm) onto cellulose acetate occurs in the order $\text{AAm} > \text{MAAm} > \text{DMAAm}$. The low grafting efficiency of MAAm was attributed to the decrease in the mobility of monomer due to the presence of methyl group and also to the stability of polymer radical. The polymeric radicals that occur from AAm and MAAm are secondary and tertiary in structure, respectively, and secondary radicals are more reactive than the tertiary ones. The extent of grafting with DMAAm was found to be the least among the monomers investigated due to steric inhibition of methyl groups [121]. Similar findings were also determined for the grafting of acrylates such as methyl acrylate (MA), ethyl acrylate (EA), butyl acrylate (BA), and methyl methacrylate (MMA) onto cellulose with Ce^{4+} initiator [122, 123]. The grafting order was found to be $\text{MA} > \text{EA} > \text{BA} > \text{MMA}$ due to steric and polar effects as well as stability of polymer radical. Mondal et al. [80] investigated the grafting of the water-soluble and water-insoluble monomers onto cellulose pretreated by heating in water using $\text{K}_2\text{S}_2\text{O}_8$ (KPS)/ CoSO_4 redox initiator at 60°C and reported that the graft yields or grafting percentages of water-insoluble monomers are higher than those of water-soluble ones. They explained this finding by the difference in the affinity of monomers towards the cellulose and the grafting. Dahou et al. [109] grafted acrylic acid (AA) and acrylonitrile (AN) monomers onto cellulose by CAN-HNO_3 initiator separately, and they have found that the grafting percentage of AN was 12–20 % higher than that of AA. Gupta and Khandekar [103] investigated the grafting of binary monomer mixture of acrylamide (AAm) and methacrylate (MA) onto cellulose using CAN-HNO_3 ($7.5 \times 10^{-3} \text{ M} - 6 \times 10^{-3} \text{ M}$) initiator system at 25°C . They determined that the grafting of binary mixture onto cellulose takes place by a second-order reaction according to the monomer concentration, and the presence of acrylamide in the binary monomer mixture increased the graft yields because of its synergistic effect. The same synergistic effect of acrylamide was also observed by the same authors in the grafting of the binary mixture of acrylamide (AAm) and ethyl acrylate (EA) onto cellulose by CAN-HNO_3 initiator system ($6 \times 10^{-3} \text{ M} - 6 \times 10^{-2} \text{ M}$) at 25°C [101]. The activation energies (E_a) in the grafting of AAm-MA and AAm-EA onto cellulose by CAN-HNO_3 initiator by a second-order reaction were found to be 6.96 kJ mol^{-1} [103] and 5.57 kJ mol^{-1} [101], respectively. However, in the graft copolymerization of acrylic acid (AA) onto cellulose by using the same initiator (CAN-HNO_3) system, the overall activation energy (E_a) for the first-order reaction between 30 and 90°C was found to be

2.3 kcal mol⁻¹ [44]. Gupta and Sahoo [45] investigated the grafting of *N*-vinyl pyrrolidone (NVP) onto cellulose with the initiator of Co(III) acetylacetonate (Co(acac)₃)–HClO₄ complex between 40 and 60 °C and found that the activation energy of (*E*_a) for grafting of NVP onto cellulose was 22.7 kJ mol⁻¹. The synergistic effect of comonomer was observed by Gürdağ et al. [99] in the grafting of AASO₃H and AA onto cellulose using CAN–HNO₃ (4 × 10⁻³ M – 7.5 × 10⁻³ M) as initiator system at 30 °C. The presence of 10 mol% AASO₃H in the binary monomer mixture led to twice increase in grafting percentage in comparison to the grafting of AA alone. In the grafting reactions, normally, the increase in the monomer concentration increases the grafting percentage and grafting efficiency up a certain value independent from the kind of initiator, monomer, and the medium of grafting (homogeneous/heterogeneous) [41, 46, 55, 89, 95, 96, 98, 101, 103, 124]. Further increases in monomer concentration beyond the optimum value decrease the grafting percentage and grafting values since the homopolymer formation dominates over the grafting, although the optimum monomer concentration differs for each grafting reaction depending on the kind of monomer and substrate, and the reaction conditions.

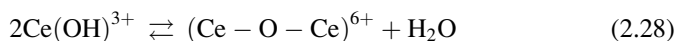
2.4.3 Effect of the Kind and Concentration of Initiator

Except the radiation technique, all chemical grafting reactions require an initiator, and its nature, concentration, solubility, as well as radical creation mechanism affect the grafting [14]. Various kinds of initiators have been used for grafting reactions: (Fe²⁺–H₂O₂), azobisisobutyronitrile (AIBN), K₂S₂O₈, Ce⁴⁺, etc. Grafting percentage can be increased either by increasing the number of grafts (grafting frequency) per substrate chain or by increasing the molecular weight of grafted chains at constant number of graft. It is apparent that the initiator concentration affects both the number of grafts per cellulose chain and the molecular weights of graft chains. Radicalic sites may also be created on cellulose by some transition metals such as Ce⁴⁺, Co³⁺, V⁵⁺, and Cr⁶⁺ [14]. The redox potential of the metal ion determines its grafting ability. In general, metal ions with low oxidation potential provides higher grafting efficiency [14]. The number of active sites created on the cellulose backbone depends on the initiator concentration, namely, the ratio of initiator/cellulose. Gupta and Sahoo [45] observed in the grafting of NVP onto cellulose with Co(acac)₃–HClO₄ initiator at the concentrations of (2 × 10⁻⁵ – 20 × 10⁻⁵) – 2.5 × 10⁻³ M, respectively, that the amount of grafted NVP and the conversion of cellulose to graft copolymer increased up to 15 × 10⁻⁵ M Co (acac)₃, but beyond this concentration they decreased. While the number of grafts per cellulose chains increased from 1.23 × 10⁻⁶ to 5.5 × 10⁻⁶ with the increase of Co(acac)₃ concentration from 2 to 20 × 10⁻⁵ M, number average molecular weights (Mn) of graft chains decreased from 105 × 10³ to 56 × 10³. The similar finding, first the increase in grafting with the initiator and then the decrease with further increase of initiator, observed for Co(acac)₃–HClO₄ initiator was also

determined in the grafting reactions performed by the initiators CAN–HNO₃ [95, 96, 101, 103, 124], ceric ammonium sulfate [49], persulfates [39, 40, 52], and KHSO₃–CoSO₄ [78]. In the grafting of AAm–MA onto cellulose by CAN–HNO₃ initiator system, Gupta and Khandekar [103] determined that the disappearance rate of Ce⁴⁺ ions did not change with the variation of monomer concentration from 0.1 to 0.5 M and concluded from this finding that the Ce⁴⁺ ions do not directly create active radicals on the monomers. The high efficiency of grafting with Ce⁴⁺ ions was attributed to the creation of active radicals by CAN initiator preferentially on the cellulose backbone than the monomers [92, 101, 125]. In addition, they [101] observed that true grafting percentage (G_T %) increased with the increase in Ce⁴⁺ concentration from 1.5×10^{-3} M to 7.5×10^{-3} M, but the higher concentrations of CAN than 7.5×10^{-3} M led to decrease in G_T % due to hydrolysis of CAN and being the hydrolysis product inactive for the creation of active sites in the absence of sufficient amount of nitric acid (HNO₃). They [101] have also determined that the rate of grafting of these comonomers onto cellulose is dependent on the square root of CAN concentration [103]. The similar findings were observed for the grafting of EA and AAm onto cellulose by CAN–HNO₃. Kim and Mun [98] investigated the effect of the concentration of CAN in the solution pretreated with wood pulp (WP) on the grafting of AAm in the presence of BAAM as cross-linker. They [98] determined that grafting percentage increases with the increase in CAN concentration of the solution pretreated with WP from 1×10^{-3} to 2×10^{-3} M because the number of grafting sites on the cellulose backbone increases. The further increase in the concentration of CAN solution to 5×10^{-3} and 10×10^{-3} M decreased the grafting percentage. The similar relationship was also determined between the water absorbency of AAm-grafted Ce⁴⁺·WP and the concentration of CAN in the pretreatment solution [98]. The maximum amount of water absorption (2,700 g/g) was observed for the copolymer with grafting percentage of ca. 240 % which was prepared from Ce⁴⁺·WP treated with 5×10^{-3} M CAN solution before the grafting. The water absorbency of AAm-grafted Ce⁴⁺·WP is very high, but it should be taken into consideration that the grafting was performed in the presence of cross-linker (the opinion of Gürdağ). Although the authors [98] have reported that they extracted the ungrafted homopolymer PAAm by successive washings of graft product with the mixture 70 % isopropanol–water, it cannot be completely removed from the reaction mixture since the grafting was performed in the presence of cross-linker MBAAM, and the cross-linked homopolymer will not be extracted by any solvent (the opinion of Gürdağ). The increase in CAN concentration leads to decrease in grafting yield, but the increase in homopolymer formation [96]. CAN prefers to form complex with cellulose over the monomer [96]. However, at higher concentrations of CAN, Ce⁴⁺ ions form complex with the monomer in addition to that with cellulose, and homopolymer formation can also occur. The termination of growing polymer radicals is also accelerated with Ce⁴⁺ concentration, and it leads to the decrease in grafting yield. When CAN was used as initiator, the acid, mostly HNO₃, has an important effect on the efficiency of initiator for grafting. As known, the reaction of CAN with aqueous HNO₃ occurs as written below:



As known, ceric ion in CAN exists as the species of Ce^{4+} , $\text{Ce}(\text{OH})^{3+}$, and $(\text{Ce}-\text{O}-\text{Ce})^{6+}$ in its aqueous solution. It was reported that the efficiency of Ce^{4+} and $\text{Ce}(\text{OH})^{3+}$ species to form radicalic sites on cellulose backbone is higher than that of $(\text{Ce}-\text{O}-\text{Ce})^{6+}$ since the size of the former is smaller than that of the latter [124] and the former is more mobile than the latter. Goya et al. [124] also reported that at high acid concentrations, Ce^{4+} and $\text{Ce}(\text{OH})^{3+}$ species affects the grafting adversely, namely, the termination reaction dominates over the propagation. A possible explanation for this adverse effect of high acid concentration on the grafting may be the difficulty in hydrogen abstraction from graft substrate (opinion of Gürdağ). The concentration of these species depends on the amount of acid present in the medium. At high nitric acid concentrations, the equilibrium reaction (2.27) shifts to the left and ceric ions in CAN occur in the form of Ce^{4+} which are responsible for the creation of active radicals preferably on the cellulose than monomer. In the case of low acid concentrations, the equilibrium shifts to the right, and the formation of high amount of $\text{Ce}(\text{OH})^{3+}$ led to the formation of considerable amount of $(\text{Ce}-\text{O}-\text{Ce})^{6+}$ which is not active for the creation of radicalic sites.



For that reason, CAN or another ceric salt should be used together with an acid. Dhiman et al. [96] found that the increase in the concentration of HNO_3 from 0.3 M to 0.5 M led to ca. 20 % increase in grafting percentage of 4-VP onto cellulose by CAN initiator, and further increase in HNO_3 concentration resulted in ca. 10 % decrease in grafting percentage. The decrease in grafting with the increase in acid concentration beyond the optimum value was attributed to the effect of excess H^+ ions as free-radical terminator [96]. Ibrahim et al. [49, 50] investigated the effects of reaction parameters on the water absorbency of graft products in the grafting of NVP onto CMCNa/HEC in homogeneous medium using ceric ammonium sulfate (CAS) as initiator. They determined that the increase in Ce^{4+} concentration from 0.02 % to 0.2 % reduced the water absorption capacity of graft product from 209 g/g to 131 g/g. They explained this finding so that higher initiator concentrations lead to the increase in grafting frequency, namely, a graft product with high amount of short graft chains occurs. As known, the increase in polymer chain ends does not contribute to the water absorption capacity [49, 50]. Therefore, the water absorption capacity of NVP-grafted CMCNa/HEC decreased with the initiator CAS. Misra et al. [89] investigated the effect of complexing agent such as KF, ascorbic acid, and EDTA on the grafting of ethyl acrylate (EA) onto cellulose by Fenton reagent ($\text{Fe}^{2+}-\text{H}_2\text{O}_2$). In order to avoid the negative effect of Fe^{3+} ions on the grafting, namely, the wastage of $\cdot\text{OH}$ radicals by reaction with Fe^{3+} ions, the grafting was carried out in the presence of some complexing agents with Fe^{3+} ions such as ascorbic acid, potassium fluoride (KF), and ethylenediaminetetraacetic acid (EDTA) [85, 89]. At low concentration (81×10^{-4} M), KF gave highest amount

of grafting among the complexing agents, but its increase to 166×10^{-4} M reduced the grafting of EA significantly [89]. The similar behavior was observed for the grafting of VAc under the same conditions. KF makes complex with Fe^{3+} ions and favors the grafting. The decrease in grafting percentage with KF attributed to the oxidation of KF to elemental fluorine (F) which reacts with vinyl monomer giving as an addition product, and it leads to decrease in grafting. Both EDTA and ascorbic acid reduced the grafting of both EA [89] and vinyl acetate (VAc) [85] at all concentrations investigated. Huang et al. [90] grafted MMA onto stone ground-wood by Fenton reagent and determined that graft yield increased with the molar ratio of Fe^{2+} - H_2O_2 up to 0.085, and after that concentration, the graft yield decreased slightly. They concluded that only a low molar ratio of Fe^{2+} - H_2O_2 is enough to succeed the grafting [90]. The similar trend (first increase and then decrease) for the grafting with the concentration of various persulfates such as KPS [52, 80], and APS [39–41, 53] was observed for AIBN [41] and BPO [39] too. The radicals created by the redox initiators on cellulose backbone are short-lived and temperature sensitive [126]. Abdel-Razik [46] investigated the effects of various redox initiators, APS, KPS, and BPO, in the grafting of AAm onto ethyl cellulose (EC) in dimethylsulfoxide (DMSO)/toluene solution. He [46] determined that APS is a suitable initiator for grafting of AAm onto EC because it leads no degradation in EC chains [46]. He also determined that the increase in APS concentration led to decrease in grafting parameters such as grafting percentage or grafting yield due to termination of primary radicals, but the use of KPS in the same reaction increased the same grafting parameters. The opposite effects of the concentration of redox initiators APS and KPS on the grafting were attributed to the difference in the decomposition rates of initiators [55]. In the same paper, it was also determined that BPO (benzoyl peroxide) is not a suitable initiator since it leads to degradation of EC, and for that reason, BPO gave considerably lower grafting yield and efficiency in comparison to APS and KPS. Bardhan et al. [52] reported that maximum grafting efficiency was obtained at KPS concentration of 3.7×10^{-4} M in the grafting of acrylamide onto methyl cellulose in aqueous solution, and both the grafting percentage and the grafting efficiency decreased with the initiator concentration at all monomer/substrate ratios (1:1–2.5:1). The similar effect of APS, KPS, and BPO with that observed in the grafting of AAm onto EC in previous work [46] was also observed in the grafting of methyl methacrylate (MMA) onto EC in benzene/DMSO (1:1) solution [42]. He performed the grafting in the 1:1 mixture of DMSO and a solvent such as chloroform, toluene, and benzene, using two different initiators, APS and KPS, and determined that grafting yield was dependent on dielectric constant of the solvent, namely, the highest yield was observed for the solvent with highest dielectric constant. The order of solvents was found to be chloroform > toluene > benzene with respect to their contribution to increase in grafting yield. The increase in grafting with increasing initiator concentration up to an optimum value takes place due to increase in radical sites created on the graft substrate. The further increase in KPS concentration beyond the optimum value results in the decrease in grafting % due to terminations of both the growing graft polymer chains and primary

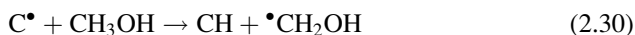
radicals by the excess amount of radicals present [53]. Nishioka and Kosai [41] investigated the grafting of two monomers AN and MMA separately onto cellulose in DMSO/PF system (in homogeneous medium) using two types of initiators: APS and BPO. It is known that DMSO/PF system is a non-degrading solvent for cellulose [41]. The nature of the initiator has an important effect on the grafting. AIBN is known to show resonance stabilization, but no such resonance exists in the peroxide initiators [41]. For that reason, they reported that higher grafting yield is obtained with APS, 87.3 % for AN and 52 % for MMA, in comparison to those with AIBN, i.e., 10 % for AN and 48 % for MMA. The number of grafts per cellulose chain by APS and AIBN initiator were found to be 3.9 and 0.5 for AN and 3.4 and 1.3 for MMA monomers. They [41] suggested from the results that grafting occurred in higher parts of cellulose chain in homogeneous medium than heterogeneous medium in which the number of grafts per cellulose chain rarely exceed the unity. They also found that the grafting onto cellulose hardly proceeded with AN–AIBN system, but appreciably in MMA–AIBN system. The solution of cellulose in DMSO/PF had a high viscosity, and the maximum amount of cellulose which could be dissolved in DMSO/PF solution was 4 wt% [41]. At 2 wt% cellulose concentrations in DMSO/PF solvent, the optimum molar ratios of monomer/initiator ($[M]/[I]$) were found to be 22 and 46 for AN and MMA, respectively. Nishioka et al. [39] investigated the grafting of methyl acrylate (MA) onto cellulose in homogeneous (DMSO/PF) medium and determined that grafting proceeded with APS (the highest number of grafts per cellulose chain was 1.5), but hardly at all with BPO and AIBN initiators. In addition, BPO was found to be unsuitable as initiator for the grafting of MA onto cellulose in homogeneous medium because it led to degradation of cellulose chains [39]. It is known that while redox initiators and radiation lead to the oxidative degradation of cellulose in the absence of monomer [127–129], the degradation of cellulose is minimized in the presence of monomer [24]. Nishioka et al. [55] investigated the grafting of 2-hydroxyethyl methacrylate (HEMA) onto cellulose in DMSO/PF system using various initiators, APS, KPS, and AIBN. They [55] determined that the grafting hardly proceeded with AIBN initiator similar to their previous works [39–41], and KPS is not a suitable initiator for the grafting of HEMA in this system since it led to degradation of cellulose. The maximum rate of propagation in the grafting of MMA onto EC in benzene/DMSO solvent system was determined depending on the kind of initiator [42] and found to be $0.2 \times 10^{-2} \text{ min}^{-1}$ and $0.08 \times 10^{-2} \text{ min}^{-1}$ for APS and KPS, respectively. For that reason, higher grafting yield was obtained with APS than KPS [42].

2.4.4 Effect of Solvent

The reaction medium or solvent has also an effect on the grafting yield or percentage in the grafting reactions. Jun et al. [142] investigated the effect of solvent such as alcohols and acetone in the grafting of *N*-isopropylacrylamide (NIPAM) onto

cotton cellulose preirradiated in air by ^{60}Co - γ -rays using mixture of water and alcohols such as methanol, ethanol, propanol, or acetone. They reported that in the grafting in solvent mixture of water and ethanol, propanol, isopropanol, and acetone, the grafting decreased continuously from pure water to pure organic solvents, where the grafting yields were almost zero. They concluded that the alcohols had different degrees of inhibiting effects on the grafting of NIPAM, but acetone was inert. The alcohols are good swelling agents for cellulose [142]. However, they also play role as chain transfer agent during polymerization reaction. In the case of methanol as cosolvent, the size of methanol is small, and its effect as chain transfer agent is lower than that of its swelling power for cellulose at low concentrations. At high methanol concentrations, its chain transfer role becomes higher than that of swelling power, and it affects the swelling adversely. Since the molecular sizes of ethanol, propanol, and isopropanol are high, their swelling power for cellulose were lower in comparison to their chain transfer properties, and they led to decrease in grafting. Abdel-Razik [42] investigated the effect of solvent (benzene, toluene, and chloroform) in homogeneous grafting of MMA onto ethyl cellulose in solvent/DMSO (1:1 v/v) solvent system with two persulfate initiator, APS and KPS. In the grafting with APS and KPS initiators, the highest grafting yields 84.5 % and 44 %, respectively, were observed in chloroform. It was concluded that grafting was correlated with the dielectric constant of solvent used, and their increasing effect on grafting yield was found in the order chloroform > toluene > benzene [42].

The efficiency of grafting in a solution will depend upon the competition between the relative reactivity of monomer and solvent for the radicals created on the graft substrate as shown in the equations below [54]:



where C^{\bullet} represents the radicalic site created on the graft substrate and X the monomer styrene or acrylamide. The rate constant for hydrogen abstraction is known to be in the order isopropanol > ethanol > methanol > *t*-butanol [54]. When reaction (2.29) is dominant over reaction (2.30), a graft copolymer will be obtained, but in case of the domination of reaction (2.30) over the reaction (2.29), the radical on the graft substrate abstracts one hydrogen atom from alcohol, and produces $\bullet\text{CH}_2\text{OH}$ radicals, leading to the formation of a homopolymer rather than a graft product. It was determined that in grafting of styrene onto cellulose acetate, reaction (2.29) is faster; but reaction (2.30) is faster in the grafting of the acrylamide [54]. Therefore, alcohols are suitable solvents for the grafting of styrene onto cellulose acetate, but not for the acrylamide. The addition of water in alcohol system increased the extent of grafting of acrylamide, but it suppressed the grafting of styrene due to decrease in the solubility of styrene in aqueous alcohol [123].

2.4.5 Effect of Temperature

The temperature is one of the important reaction parameters determining the grafting kinetics. Generally, the grafting yield or percentage first increase with temperature up to a certain value, and then it decreases for persulfates [39, 41, 42, 46, 53]. Similar results have also been reported in the literature for Ce^{4+} initiator [41, 97, 99, 104, 125]. For example, Nishioka et al. [39, 40] found in the grafting in homogeneous medium by persulfate initiators that with the increase in temperature, the molecular weight of graft chains decreased, but the number of grafts increased up to a certain amount, and then leveled off. The optimum temperature for highest grafting depends on the initiator used. In the grafting of HEMA onto cellulose in DMSO/PF solvent system using various initiators, Nishioka et al. [55] determined that the optimum temperatures are 40 °C for APS, 50 °C for KPS, and 60 °C for both AIBN and BPO. In the grafting of AA onto cellulose in heterogeneous medium by CAN–HNO₃ initiator [44], nearly the same grafting percentages were obtained at 30, 50, and 70 °C, but three to four times lower grafting percentages were obtained at 90 °C than those at former temperatures. The graft copolymer prepared at 30 °C had highest water absorption capacity probably due to difference in their grafting frequencies and graft lengths. Therefore, the optimum grafting temperature was determined as 30 °C for the grafting of AA onto cellulose by CAN–HNO₃ initiator [44]. It was also determined that the rate constants for the disappearance of AA during the grafting increased from 0.018 min⁻¹ to 0.033 min⁻¹ with the increase in temperature from 30 to 90 °C [44], and the increase in temperature favored the formation of homopolymer poly(acrylic acid) (PAA). The decreasing effect of increasing temperature from 30 to 90 °C on the water absorbency of graft copolymer was also observed in the Ce^{4+} -initiated grafting of NVP onto CMCNa/HEC [49, 50], and the maximum water absorption was displayed by the graft copolymer which was prepared at 30 °C. With the increase in temperature, a graft copolymer with shorter graft chains will be obtained, and the number of polymer chain end will increase. Since the polymer ends with short length in the graft copolymer do not positively contribute to the swelling, the increase in grafting temperature affects negatively the water absorption capacity of graft copolymer.

2.5 Applications of Cellulose Graft Copolymers

The applications of cellulose graft copolymers change with the structure of polymer grafted on cellulose. For example, cellulose graft copolymers with poly(acrylic acid), *N*-vinyl-2-pyrrolidone or polyacrylamide grafts which are hydrophilic in structure, have high water absorption capacity [44, 49]. For that reason, they could be used as body fluid absorbent in medical applications [105]. For example, the water and saline absorbencies of polyacrylamide-grafted Ce^{4+} -treated wood

pulp were found to be 2,500–2,700 g/g and 40–60 g/g, respectively [98]. The grafting of water-soluble vinyl monomers onto amine-treated cotton fiber gave a graft copolymer with enhanced moisture sorption ability that can be used in fabrics, such as underwear and athletic wear [80]. Cellulose graft copolymers synthesized in DMSO–PF solvent system has been used as permselective membranes [143, 144]. Cellulose-thiocarbamate-g-PAN had high antimicrobial activity. Matahwa et al. [84] reported that *N*-isopropyl acrylamide and methyl acrylate-grafted cellulose as template in the crystallization of CaCO₃ has better nucleating property than cellulose. In addition, the cellulose graft copolymers obtained by grafting of vinyl monomers with functional groups such as acrylamide [21], acrylic acid [58, 145–147], acrylonitrile, and 2-acrylamidomethylpropane sulfonic acid [145] have been used in the adsorption of hazardous contaminants such as heavy metal ions or dyes [66] from aqueous solutions [148, 149]. The product of poly(4-vinyl pyridine)-grafted cellulose with sodium borohydride has been used as reducing agents for various carbonyl compound such as benzaldehyde, cyclohexanone, crotonaldehyde, acetone, and furfural [96]. Wang et al. [31] reported that pH-responsive poly(2-diethylamino) ethyl methacrylate grafted-ethyl cellulose (EC-g-PDEAEMA) synthesized by ATRP can be used in the pH-responsive release of rifampicin (RIF). In addition, another graft product obtained by ATRP, which is graft copolymer of ethyl cellulose with azobenzene-containing polymethacrylates [113], was reported to be used in the some applications such as sensors and optical materials. In recent years, cellulose graft copolymers with thermosensitive graft chains such as poly(*N*-isopropylacrylamide or poly(*N,N*-diethylacrylamide) have been used in the removal of heavy metal ions from aqueous solutions by temperature swing adsorption (TSA) which is different from the removal of metal ions by complexation or ion exchange [29, 30, 150–154].

2.6 Conclusion

Cellulose graft copolymers can be prepared in homogeneous or in heterogeneous medium. Grafting can be confirmed by gravimetry, volumetric method (a simple acid–base titration), or spectroscopic methods such as FTIR, NMR, and SEM. Cellulose gains hydrophilic or hydrophobic character depending on the monomer grafted. Therefore, cellulose graft copolymers have many applications. Among them, heavy metal and dye removal from aqueous solutions are the most prominent ones. In the grafting reactions performed in homogeneous medium, the grafting can be controlled better, and higher number of grafts per cellulose chain is obtained. By these methods such as RAFT and ATRP methods, tailor-made copolymers such as comb- or brush-type cellulose graft copolymers can be synthesized. The applications of these special polymers will be studied more in the near future.

References

1. Bikales NM, Segal L (1971) Cellulose and cellulose derivatives. Wiley Interscience, New York, NY
2. Qin C, Soykeabkaew N, Xiuyuan N, Peijs T (2008) The effect of fiber volume fraction and mercerization on the properties of all-cellulose composites. *Carbohydr Polym* 71:458–467
3. Gurgel LVA, Junior OK, Gil RPDF, Gil LF (2008) Adsorption of Cu(II), Cd(II), and Pb(II) from aqueous single metal solutions by cellulose and mercerized cellulose chemically modified with succinic anhydride. *Biores Technol* 99:3077–3083
4. Wojnárovits L, Földváry CM, Takács E (2010) Radiation-induced grafting of cellulose for adsorption of hazardous water pollutants: a review. *Radiat Phys Chem* 79:848–862
5. Bansal P, Hall M, Realf MJ, Lee JH, Bommarius AS (2010) Multivariate statistical analysis of X-ray data from cellulose: A new method to determine degree of crystallinity and predict hydrolysis rates. *Biores Technol* 101:4461–4471
6. Inagaki T, Siesler HW, Mitsui K, Tsuchikawa S (2010) Difference of the crystal structure of cellulose in wood after hydrothermal and aging degradation: a NIR spectroscopy and XRD study. *Biomacromolecules* 11:2300–2305
7. Bianchi E, Bonazza A, Marsano E, Russo S (2000) Free radical grafting onto cellulose in homogeneous conditions. 2. Modified cellulose–methyl methacrylate system. *Carbohydr Polym* 41:47–53
8. Takács E, Wojnárovits L, Földváry C, Hargittai P, Borsa J, Sajó I (2000) Effect of combined gamma-irradiation and alkali treatment on cotton-cellulose. *Radiat Phys Chem* 57:399–403
9. Segal L, Creely JJ, Martin AE Jr, Conrad CM (1959) An empirical method for estimating the degree of crystallinity of native cellulose using the X-ray diffractometer. *Textile Res J* 29:786–794
10. Hermans PH, Weidinger A (1948) Quantitative X-ray investigations on the crystallinity of cellulose fibers. *J Appl Phys* 19:491–506
11. El Seoud OA, Fidale LC, Ruiz N, D’Almeida MLO, Frollini E (2008) Cellulose swelling by protic solvents: which properties of the biopolymer and the solvent matter? *Cellulose* 15:371–392
12. Dworjany PA, Fields B, Garnett JL (1989) Effects of various additives on accelerated grafting and curing reactions initiated by UV and ionizing-radiation. *ACS Symp Ser* 381:112–131
13. Khan F (2004) Photoinduced graft-copolymer synthesis and characterization of methacrylic acid onto natural biodegradable lignocellulose fiber. *Biomacromolecules* 5:1078–1088
14. Bhattacharya A, Misra BN (2004) Grafting: a versatile means to modify polymers techniques, factors and applications. *Prog Polym Sci* 29:767–814
15. Roy D, Semsarilar M, Guthrie JT, Perrier S (2009) Cellulose modification by polymer grafting: a review. *Chem Soc Rev* 38:2046–2064
16. Stannett VT, Doane VM, Fanta G (1984) Absorbency. Elsevier, Amsterdam
17. Richards GN, White EF (1964) Graft polymerization on cellulosic materials. Part I. Cation-exchange membranes from paper and acrylic acid. *J Polym Sci* 4:1251–1260
18. Jayme G, Hebbel GW (1971) Comparison of the influence of graft polymerization and polymer impregnation on the properties of pulps and papers. *Das Papier* 25:113–119
19. Waly A, Abdel-Mohdy FA, Aly AS, Hebeish A (1998) Synthesis and characterization of cellulose ion exchanger. II. Pilot scale and utilization in dye-heavy metal removal. *J Appl Polym Sci* 68:2151–2157
20. Beker ÜG, Güner FS, Dizman M, Erciyas T (1999) Heavy metal removal by ion exchanger based on hydroxyethyl cellulose. *J Appl Polym Sci* 74:3501–3506
21. Biçak N, Sherrington DC, Senkal BF (1999) Graft copolymer of acrylamide onto cellulose as mercury selective sorbent. *React Funct Polym* 41:69–76
22. Okieimen EF (1987) Studies on the graft copolymerization of cellulosic materials. *Eur Polym J* 23:319–322

23. Chauhan GS, Mahajan S, Guleria KL (2000) Polymers from renewable resources: sorption of Cu^{2+} ions by cellulose graft copolymers. *Desalination* 130:85–88
24. Hebeish A, Guthrie JT (1981) *The chemistry and technology of cellulosic copolymers*. Springer, New York, NY
25. Samal BB, Sahu S, Chinara BB, Nanda S, Otta PK, Mohapatro LM, Mohanty TR, Ray AR, Singh KC (1988) Grafting of vinyl monomers onto sisal fiber in aqueous solution. *J Polym Sci Part A Polym Chem* 26:3159–3166
26. Misra M, Mohanty AK, Singh BC (1987) A study on grafting of methyl methacrylate onto jute fiber ($\text{S}_2\text{O}_8^{2-}$ -thiourea redox system). *J Appl Polym Sci* 33:2809–2819
27. Huque MM, Habibuddowla MD, Mahmood AJ, Mian AJ (1980) Graft-copolymerization onto jute fiber—ceric ion-initiated graft-copolymerization of methyl-methacrylate. *J Polym Sci Polym Chem Ed* 18:1447–1458
28. Das HK, Nayak NC, Singh BC (1991) Effect of toluene on the kinetics of Ce(IV) -ion-initiated grafting of methyl-methacrylate onto chemically modified jute fibers. *J Macromol Sci Chem* A28:297–309
29. Xie J, Hsieh YL (2003) Thermosensitive poly(*n*-isopropylacrylamide) hydrogels bonded on cellulose supports. *J Appl Polym Sci* 89:999–1006
30. Ifuku S, Kadla J (2008) Preparation of a thermosensitive highly regioselective cellulose/*n*-isopropylacrylamide copolymer through atom transfer radical polymerization. *Biomacromolecules* 9:3308–3313
31. Wang D, Tan J, Kang H, Ma L, Jin X, Liu R, Huang Y (2011) Synthesis, self-assembly and drug release behaviors of pH-responsive copolymers ethyl cellulose-graft-PDEAEMA through ATRP. *Carbohydr Polym* 84:195–202
32. Lee SB, Koepsel RR, Morley SW, Matyjaszewski K, Sun Y, Russell AJ (2004) Permanent, nonleaching antibacterial surfaces. I. Synthesis by atom transfer radical polymerization. *Biomacromolecules* 5:877–882
33. McDowall DJ, Gupta BS, Stannett VT (1984) Grafting of vinyl monomers to cellulose by ceric ion inhibition. *Prog Polym Sci* 10:1–50
34. Saikia CN, Ali F (1999) Graft copolymerization of methyl methacrylate onto high α -cellulose pulp extracted from *Hibiscus sabdariffa* and *Gmelina arborea*. *Bioresour Technol* 68:165–171
35. Roy D, Guthrie JT, Perrier S (2005) Graft polymerization: grafting poly(styrene) from cellulose via reversible addition-fragmentation chain transfer (RAFT) polymerization. *Macromolecules* 38:10363–10372
36. Zhang LM, Chen LQ (2002) Water-soluble grafted polysaccharides containing sulfobetaine groups: Synthesis and characterization of graft copolymers of hydroxyethyl cellulose with 3-dimethyl(methacryloyloxyethyl)ammonium propane sulfonate. *J Appl Polym Sci* 83:2755–2761
37. Tsubokawa N, Iida T, Takayama T (2000) Modification of cellulose powder surface by grafting of polymers with controlled molecular weight and narrow molecular weight distribution. *J Appl Polym Sci* 75:515–522
38. Narayan R, Biermann CJ, Hunt MO, Horn DP (1989) *In adhesives from renewable resources*. American Chemical Society, Washington, DC
39. Nishioka N, Minami K, Kosai K (1983) Homogeneous graft copolymerization of vinyl monomers onto cellulose in a dimethyl sulfoxide-paraformaldehyde solvent system III. Methyl acrylate. *Polym J* 15:591–596
40. Nishioka N, Matsumoto K, Kosai K (1983) Homogeneous graft copolymerization of vinyl monomers onto cellulose in a dimethyl sulfoxide-paraformaldehyde solvent system II. Characterization of graft copolymers. *Polym J* 15:153–158
41. Nishioka N, Kosai K (1981) Homogeneous graft copolymerization of vinyl monomers onto cellulose in a dimethyl sulfoxide-paraformaldehyde solvent system I. Acrylonitrile and methyl methacrylate. *Polym J* 13:1125–1133
42. Abdel-Razik EA (1997) Aspects of thermal graft copolymerization of methyl methacrylate onto ethyl cellulose in homogeneous media. *Polym Plast Technol Eng* 36:891–903

43. Bianchi E, Marsano E, Ricco L, Russo S (1998) Free radical grafting onto cellulose in homogeneous conditions I. Modified cellulose–acrylonitrile system. *Carbohydr Polym* 36:313–318
44. Gürdağ G, Yaşar M, Gürkaynak MA (1997) Graft copolymerization of acrylic acid on cellulose: reaction kinetics of copolymerization. *J Appl Polym Sci* 66:929–934
45. Gupta KC, Sahoo S (2001) Co(III) Acetylacetonate-complex-initiated grafting of N-vinyl pyrrolidone on cellulose in aqueous media. *J Appl Polym Sci* 81:2286–2296
46. Abdel-Razik EA (1990) Homogeneous graft copolymerization of acrylamide onto ethylcellulose. *Polymer* 31:1739–1744
47. Diamantoglou M, Kunding EF (1995) Cellulose and cellulose derivatives: physico-chemical aspects and industrial applications. Woodhead, Cambridge
48. Hebeish A, Guthrie JT (1981) Grafting by chemical activation of cellulose, and nature of substrate. Springer, New York, NY
49. Ibrahim MM, Flefel EM, El-Zawawy WK (2002) Cellulose membranes grafted with vinyl monomers in a homogeneous system. *Polym Adv Technol* 13:548–557
50. Ibrahim MM, Flefel EM, El-Zawawy WK (2002) Cellulose membranes grafted with vinyl monomers in homogeneous system. *J Appl Polym Sci* 84:2629–2638
51. Yang F, Li G, He YG, Ren FX, Wang JX (2009) Synthesis, characterization, and applied properties of carboxymethyl cellulose and polyacrylamide graft copolymer. *Carbohydr Polym* 78:95–99
52. Bardhan K, Mukhopadhyay S, Chatterjee SR (1977) Grafting of acrylamide onto methyl cellulose by persulfate ion. *J Polym Sci: Polym Chem Ed* 15:141–148
53. Zhe C, Xiaoyan L, Xuegang L (2011) Study on the synthesise of thermoplastic carboxymethyl cellulose with graft copolymerization. doi:10.1109/CDCIEM.2011.135
54. Bhattacharyya SN, Maldas D (1982) Radiation-Induced graft copolymerization of mixtures of styrene and acrylamide onto cellulose acetate. I. Effect of solvents. *J Polym Sci: Polym Chem Ed* 20:939–950
55. Nishioka N, Matsumoto Y, Yumen T, Monmae K, Kosai K (1986) Homogeneous graft copolymerization of vinyl monomers onto cellulose in a dimethyl sulfoxide-paraformaldehyde solvent system IV. 2-hydroxyethyl methacrylate. *Polym J* 18:323–330
56. El-Hady BA, Ibrahim MM (2004) Graft copolymerization of acrylamide onto carboxymethylcellulose with the xanthate method. *J Appl Polym Sci* 93:271–278
57. Wang D, Xuan Y, Huang Y, Shen J (2003) Synthesis and properties of graft copolymer of cellulose diacetate with poly(caprolactone monoacrylate). *J Appl Polym Sci* 89:85–90
58. Lin CX, Zhan HU, Liu MH, Fu SU, Huang LH (2010) Rapid homogeneous preparation of cellulose graft copolymer in BMIMCL under microwave irradiation. *J Appl Polym Sci* 118:399–404
59. Swatloski RP, Spear SK, Holbrey JD (2002) Dissolution of cellulose with ionic liquids. *J Am Chem Soc* 124:4974–4975
60. Chun-xiang L, Huai-yu Z, Ming-hua L, Shi-yu F, Jia-jun Z (2009) Preparation of cellulose graft poly(methyl methacrylate) copolymers by atom transfer radical polymerization in an ionic liquid. *Carbohydr Polym* 78:432–438
61. Zhu J, Dong XT, Wang XL, Wang YZ (2010) Preparation and properties of a novel biodegradable ethyl cellulose grafting copolymer with poly(p-dioxanone) side-chains. *Carbohydr Polym* 80:350–359
62. Carlmark A, Malmström E (2003) ATRP grafting from cellulose fibers to create block-copolymer grafts. *Biomacromolecules* 4:1740–1745
63. Carlmark A, Malmström E (2002) Atom transfer radical polymerization from cellulose fibers at ambient temperature. *J Am Chem Soc* 124:900–901
64. Ikeda I, Higuchi T, Maeda Y (2002) Synthesis of cellulosic graft copolymers by atom transfer radical polymerization. *Sen'i Gakkaishi* 58:308–313
65. Zhou Q, Greffe L, Baumann MJ, Malmström E, Teeri TT, Brumer H (2005) Use of xyloglucan as a molecular anchor for the elaboration of polymers from cellulose surfaces: a general route for the design of biocomposites. *Macromolecules* 38:3547–3549

66. Coskun M, Temuz MM (2005) Grafting studies onto cellulose by atom-transfer radical polymerization. *Polym Int* 54:342–347
67. Kang H, Liu W, Liu R, Huang Y (2008) A novel, amphiphilic ethyl cellulose grafting copolymer with poly(2-hydroxyethyl methacrylate) side chains and its micellization. *Macromol Chem Phys* 209:424–430
68. Daly WH, Evenson TS, Iacono TS, Jones RW (2001) Recent developments in cellulose grafting chemistry utilizing barton ester intermediates and nitroxide mediation. *Macromol Symp* 174:155–163
69. Quinn JF, Chaplin RP, Davis TP (2002) Facile synthesis of comb, star, and graft polymers via reversible addition–fragmentation chain transfer (RAFT) polymerization. *J Polym Sci Part A: Polym Chem* 40:2956–2966
70. Barner L (2003) Surface grafting via the reversible addition–fragmentation chain-transfer (RAFT) process: from polypropylene beads to core–shell microspheres. *Aust J Chem* 56:1091–1091
71. Perrier S, Takolpuckdee P, Westwood J, Lewis DM (2004) Versatile chain transfer agents for reversible addition fragmentation chain transfer (RAFT) polymerization to synthesize functional polymeric architectures. *Macromolecules* 37:2709–2717
72. Takolpuckdee P (2005) Chain transfer agents for RAFT polymerization: molecules to design functionalized polymers. *Aust J Chem* 58:66–66
73. Matyjaszewski K (1998) Radical nature of cu-catalyzed controlled radical polymerizations (atom transfer radical polymerization). *Macromolecules* 31:4710–4717
74. Patten TE, Matyjaszewski K (1999) Copper(I)-catalyzed atom transfer radical polymerization. *Acc Chem Res* 32:895–903
75. Xia JH, Matyjaszewski K (1999) Controlled/“living” radical polymerization. Atom transfer radical polymerization catalyzed by copper(I) and picolyamine complexes. *Macromolecules* 32:2434–2437
76. Hiltunen MS, Raula J, Maunu SL (2011) Tailoring of water-soluble cellulose-gcopolymers in homogeneous medium using single-electron-transfer living radical polymerization. *Polym Int* 60:1370–1379
77. Okieimen EF, Ebhoaye JE (1986) Grafting acrylic acid monomer on cellulosic materials. *J Macromol Chem* A23:349–353
78. Sahoo PK, Samantaray HS, Samal RK (1986) Graft copolymerization with new class of acidic peroxy salts as initiators. I. Grafting of acrylamide onto cotton-cellulose using potassium monopersulfate, catalyzed by Co(II). *J Appl Polym Sci* 32:5693–5703
79. Ouajai S, Hodzic A, Shanks RA (2004) Morphological and grafting modification of natural cellulose fibers. *J Appl Polym Sci* 94:2456–2465
80. Ibrahim MD, Mondal H, Uraki Y, Ubukata M, Itoyama K (2008) Graft polymerization of vinyl monomers onto cotton fibres pretreated with amines. *Cellulose* 15:581–592
81. Liu S, Sun G (2008) Radical graft functional modification of cellulose with allyl monomers: Chemistry and structure characterization. *Carbohydr Polym* 71:614–625
82. Mukhopadhyay S, Prasad J, Chatterjee SR (1975) Grafting of acrylic acid onto methylcellulose. *Makromol Chem* 176:1–7
83. Zahran AH, Williams JL, Stannett VT (1980) Radiation grafting of acrylic and methacrylic acid to cellulose fibers to impart high water sorbency. *J Appl Polym Sci* 25:535–542
84. Matahwa H, Ramiah V, Jarrett WL, McLeary JB, Sanderson RD (2007) Microwave assisted graft copolymerization of n-isopropyl acrylamide and methyl acrylate on cellulose: solid state NMR analysis and CaCO₃ crystallization. *Macromol Symp* 255:50–56
85. Misra BN, Dogra R, Kaur I, Jassal JK (1979) Grafting onto cellulose. IV. Effect of complexing agents on Fenton’s reagent (Fe²⁺–H₂O₂)-initiated grafting of poly(vinyl acetate). *J Polym Sci: Polym Chem Ed* 17:1861–1863
86. Haber F, Weiss J (1932) Über die Katalyse des Hydroperoxydes. *Naturwissenschaften* 20:948–950

87. Haber F, Weiss J (1934) The catalytic decomposition of hydrogen peroxide by iron salts. *Proc R Soc A* 147:332–351
88. Merz JH, Waters WA (1949) Some oxidations involving the free hydroxyl radical. *J Chem Soc S15–S25*. doi:10.1039/JR9490000S15
89. Misra BN, Dogra R, Mehta IK (1980) Grafting onto cellulose. V. Effect of complexing agents on Fenton's reagent (Fe^{2+} – H_2O_2)-initiated grafting of poly(ethyl acrylate). *J Polym Sci: Polym Chem Ed* 18:749–752
90. Huang Y, Zhao B, Zheng C, He S, Gao J (1992) Graft copolymerization of methyl methacrylate on stone ground wood using the H_2O_2 – Fe^{2+} method. *J Appl Polym Sci* 45:71–77
91. Hon DNS (1982) Graft copolymerization of lignocellulosic fibers. ACS Symposium Series, Washington, DC
92. Mino G, Kaizerman S (1958) A new method for the preparation of graft copolymers. Polymerization initiated by ceric ion redox systems. *J Polym Sci* 31:242–243
93. Bains MS (1972) Inorganic redox systems in graft polymerization onto cellulosic materials. *J Polym Sci Part C: Polym Symp* 37:125–151
94. Gaylord N (1972) A proposed new mechanism for catalyzed and uncatalyzed graft polymerization onto cellulose. *J Polym Sci* 37:153–172
95. Sharma BR, Kumar V, Soni PL (2003) Graft copolymerization of acrylonitrile onto Cassia tora gum with ceric ammonium nitrate–nitric acid as a redox initiator. *J Appl Polym Sci* 90:129–136
96. Dhiman PK, Kaur I, Mahajan RK (2008) Synthesis of a cellulose-grafted polymeric support and its application in the reductions of some carbonyl compounds. *J Appl Polym Sci* 108:99–111
97. Fanta GF, Burr RC, Doane WM (1987) Graft polymerization of acrylonitrile onto wheat straw. *J Appl Polym Sci* 33:899–906
98. Kim BS, Mun SP (2009) Effect of Ce^{4+} pretreatment on swelling properties of cellulosic superabsorbents. *Polym Adv Technol* 20:899–906
99. Gürdağ G, Güçlü G, Özgümüş S (2001) Graft copolymerization of acrylic acid onto cellulose: effects of pretreatments and crosslinking agent. *J Appl Polym Sci* 80:2267–2272
100. Fernandez MJ, Casinos I, Guzman GM (1990) Grafting of a vinyl acetate/methyl acrylate mixture onto cellulose. Effect of temperature and nature of substrate. *Makromol Chem* 191:1287–1299
101. Gupta KC, Khandekar K (2006) Ceric(IV) ion-induced graft copolymerization of acrylamide and ethyl acrylate onto cellulose. *Polym Int* 55:139–150
102. Snell FD, Etre LC (1973) *Encyclopedia of industrial chemical analysis*. Wiley Interscience, New York, NY
103. Gupta KC, Khandekar K (2002) Graft copolymerization of acrylamide–methylacrylate comonomers onto cellulose using ceric ammonium nitrate. *J Appl Polym Sci* 86:2631–2642
104. Ogiwara Y, Ogiwara Y, Kubota H (1968) Studies of the initiation mechanism of ferric ion–hydrogen peroxide systems in graft copolymerization on cellulose. *J Appl Polym Sci* 12:2575–2584
105. Toledano-Thompson T, Loría-Bastarrachea MI, Aguilar-Vega MJ (2005) Characterization of henequen cellulose microfibrils treated with an epoxide and grafted with poly(acrylic acid). *Carbohydr Polym* 62:67–73
106. Kubota H, Fukushima Y, Kuwabara S (1997) Factors affecting liquid-phase photografting of acrylic acid on cellulose and its derivatives. *Eur Polym J* 33:67–71
107. Mao C, Qiu YZ, Sang HB, Mei H, Zhu AP, Shen J, Lin SC (2004) Various approaches to modify biomaterial surfaces for improving hemocompatibility. *Adv Colloid Interface Sci* 110:5–17
108. Hatakeyama T, Nakamura K (1982) Studies on heat capacity of cellulose and lignin by differential scanning calorimetry. *Polymer* 23:1801–1804
109. Dahoua W, Ghemati D, Oudia A, Aliouche D (2010) Preparation and biological characterization of cellulose graft copolymers. *Biochem Eng J* 48:187–194

110. Cavus S, Gurdag G, Yasar M, Gurkaynak MA (2003) Competitive removal of Pb^{2+} , Cu^{2+} , Cd^{2+} by cellulose graft copolymer. *Polym Prep* 44:714–715
111. Zhu J, Wang WT, Wang XL, Li B, Wanga YZ (2009) Green synthesis of a novel biodegradable copolymer base on cellulose and poly(p-dioxanone) in ionic liquid. *Carbohydr Polym* 76:139–144
112. Meng T, Gao X, Zhang J, Yuan J, Zhang Y, He J (2009) Graft copolymers prepared by atom transfer radical polymerization (ATRP) from cellulose. *Polymer* 50:447–454
113. Tang X, Gao L, Fan X, Zhou Q (2007) Controlled grafting of ethyl cellulose with azobenzene-containing polymethacrylates via atom transfer radical polymerization. *J Polym Sci: Part A: Polym Chem* 45:1653–1660
114. Chauhan GS, Singh B, Dhiman SK (2004) Functionalization of poly(4-vinyl pyridine) grafted cellulose by quaternization reactions and a study on the properties of postquaternized copolymers. *J Appl Polym Sci* 91:2454–2464
115. Williams JL, Stannet VT (1979) Highly water-absorptive cellulose by postdecrystallization. *J Appl Polym Sci* 23:1265–1268
116. Williams JL, Stannet VT (1977) Method of increasing the water absorption of cellulose-containing materials. US Patent 4,036,588
117. Ibrahim AA, Nada AMA (1985) Grafting of acrylamide onto cotton linters. *Acta Polym* 36:342–343
118. Davis WE, Barry AJ, Peterson FC, King AJ (1943) X-ray studies of reactions of cellulose in aqueous systems. II. Interaction of cellulose and primary amines. *J Am Chem Soc* 65:1294–1299
119. Venkataraman A, Subramanian DR, Manjunath BR (1979) A comparative study of the swelling action of monoamines and diamines on cotton cellulose. *Indian J Textile Res* 4:106–110
120. Klemm D, Philipp B, Heinze T, Heinze U, Wagenknecht W (1998) Interaction of cellulose with aliphatic mono- and diamines. In: *Comprehensive cellulose chemistry–functionalization of cellulose*. Wiley-VCH, Weinheim
121. Bhattacharya A, Das A, De A (1998) Structural influence on grafting of acrylamide based monomers on cellulose acetate. *Ind J Chem Tech* 5:135–138
122. Varma DS, Narashinan V (1972) Thermal behavior of graft copolymers of cotton cellulose and acrylate monomers. *J Appl Polym Sci* 16:3325–3339
123. Varma DS, Narashinan V (1975) Grafting of formaldehyde-crosslinked and cyanoethylated cotton cellulose with acrylate monomers. *J Appl Polym Sci* 19:29–36
124. Goyal P, Kumar V, Sharma P (2008) Graft copolymerization of acrylamide onto tamarind kernel powder in the presence of ceric ion. *J Appl Polym Sci* 108:3696–3701
125. Mansour OY, Nagaty A (1985) Grafting of synthetic polymers to natural polymers by chemical processes. *Prog Polym Sci* 11:91–165
126. Arthur JC, Hinojosa O, Banis MS (1968) ESR study of reactions of cellulose with $\cdot OH$ generated by Fe^{+2}/H_2O_2 . *J Appl Polym Sci* 12:1411–1421
127. Arthur JC (1970) Cellulose graft copolymers. *J Macromol Sci Chem* A4:1057–1065
128. Dilli S, Garnett JL (1967) Radiation induced reactions with cellulose III. Kinetics of styrene copolymerisation in methanol. *J Appl Polym Sci* 11:859–870
129. Yasukawa T, Sasaki Y, Murukami K (1973) Kinetics of radiation induced grafting reactions II. Cellulose acetate-styrene systems. *J Polym Sci Polym Chem* 11:2547–2556
130. Kokot S, Stewart S (1995) An exploratory-study of mercerized cotton fabrics by DRIFT spectroscopy and chemometrics. *Text Res J* 65:643–651
131. Takács E, Wojnárovits L, Földváry CS, Hargittai P, Borsa J, Sajó I (2001) Radiation activation of cotton-cellulose prior to alkali treatment. *Res Chem Intermed* 27:837–845
132. Othman SH, Sohah MA, Ghoneim MM (2009) The effects of hazardous ions adsorption on the morphological and chemical properties of reactive cloth filter. *Radiat Phys Chem* 78:976–985
133. Takács E, Mirzadeh H, Wojnárovits L, Borsa J, Mirzataheri M, Benke N (2007) Comparison of simultaneous and pre-irradiation grafting of N-vinylpyrrolidone to cotton-cellulose. *Nucl Instrum Meth Phys Res B* 265:217–220

134. Chauhan GS, Guleria L, Sharma R (2005) Synthesis, characterization and metal sorption studies of graft copolymers of cellulose and glycidyl methacrylate and some comonomers. *Cellulose* 12:97–110
135. Abdel-Aal SE, Gad YH, Dessouki AM (2006) The use of wood pulp and radiation-modified starch in wastewater treatment. *J Appl Polym Sci* 99:2460–2469
136. Kondo T, Sawatari CA (1996) Fourier transform infrared spectroscopic analysis of the character of hydrogen bonds in amorphous cellulose. *Polymer* 37:393–399
137. Lepoutre P, Hui SH, Robertson AA (1973) The water absorbency of hydrolyzed polyacrylonitrile-grafted cellulose fibers. *J Appl Polym Sci* 17:3143–3156
138. Andreozzi L, Castelvetro V, Ciardelli G, Corsi L, Faetti M, Fatarella E, Zulli F (2005) Free radical generation upon plasma treatment of cotton fibers and their initiation efficiency in surface-graft polymerization. *J Colloid Interf Sci* 289:455–465
139. Hegazy ESA, Kamal H, Khalifa NA, Mahmoud GA (2001) Separation and extraction of some heavy and toxic metal ions from their wastes by grafted membranes. *J Appl Polym Sci* 81:849–860
140. Imrisova D, Maryska S (1968) Study of radiation-induced graft polymerization of vinyl monomers to cellulose by infrared spectroscopy. II. Cellulose–polystyrene copolymers. *J Appl Polym Sci* 12:2007–2011
141. Badawy SM, Dessouki AM, Nizam El-Din HM (2001) Direct pyrolysis mass spectrometry of acrylonitrile–cellulose graft copolymer prepared by radiation-induced graft polymerization in presence of styrene as homopolymer suppressor. *Radiat Phys Chem* 61:143–148
142. Jun L, Jun L, Min Y, Hongfei H (2001) Solvent effect on grafting polymerization of NIPAAm onto cotton cellulose via γ -preirradiation method. *Radiat Phys Chem* 60:625–628
143. Nishioka N, Watase K, Arimura K, Kosai K, Uno M (1984) Permeability through cellulose membranes grafted with vinyl monomers in a homogeneous system. 1. Diffusive permeability through acrylonitrile grafted cellulose membranes. *Polym J* 16:867–875
144. Nishioka N, Yoshimi S, Iwaguchi T, Kosai K (1984) Permeability through cellulose membranes grafted with vinyl monomers in homogeneous system. 2. States of water in acrylonitrile grafted cellulose membranes. *Polym J* 16:877–885
145. Güçlü G, Gürdağ G, Özgümüş S (2003) Competitive removal of heavy metal ions by cellulose graft copolymers. *J Appl Polym Sci* 90:2034–2039
146. Çavuş S, Gürdağ G, Yaşar M, Güçlü K, Gürkaynak MA (2006) The competitive heavy metal removal by hydroxyethyl cellulose-g-poly(acrylic acid) copolymer and its sodium salt: The effect of copper content on the adsorption capacity. *Polym Bull* 57:445–456
147. Wen OH, Kuroda SI, Kubota H (2001) Temperature-responsive character of acrylic acid and *N*-isopropylacrylamide binary monomers-grafted celluloses. *Eur Polym J* 37:807–813
148. O’Connell DW, Birkinshaw C, O’Dwyer TF (2006) A modified cellulose adsorbent for the removal of nickel(II) from aqueous solutions. *J Chem Technol Biotechnol* 81:1820–1828
149. Liu S, Sun G (2008) Radical graft functional modification of cellulose with allyl monomers: chemistry and structure characterization. *Carbohydr Polym* 71:614–625
150. Esen E, Ozbas Z, Kasgoz H, Gurdag G (2011) Thermoresponsive cellulose-g-N,N'-diethyl acrylamide copolymers. *Curr Opin Biotechnol* 22(1):S61–S62. doi:10.1016/j.copbio.2011.05.173
151. Gupta KC (2009) Thermoresponsive cellulose by ATRP graft copolymerization of comonomers. Abstracts of Papers of American Chemical Society 237: 384-poly.
152. Csoka G, Marton S, Gelencser A, Klebovich I (2005) Thermoresponsive properties of different cellulose derivatives. *Eur J Pharm Sci* 25:S74–S75
153. Bokias G, Mylonas Y, Staikos G, Bumbu GG, Vasile C (2001) Synthesis and aqueous solution properties of novel thermoresponsive graft copolymers based on a carboxymethyl-cellulose backbone. *Macromolecules* 34:4958–4964
154. Li YX, Liu RG, Liu WY, Kang HL, Wu M, Huang Y (2008) Synthesis, self-assembly, and thermosensitive properties of ethyl cellulose-g-p(PEGMA) amphiphilic copolymers. *J Polym Sci Part A: Polym Chem* 46:6907–6915

Chapter 3

Starch-g-Copolymers: Synthesis, Properties and Applications

A.N. Jyothi and Antonio J.F. Carvalho

Abstract Starch is one of the cheapest and most abundant natural carbohydrate biopolymers and is compatible with hydrocolloids and other water-soluble polymers. Therefore, it can be an effective component in multifunctional systems. To impart end use specific properties, starch is often modified. Chemical modification of starch by grafting various monomers onto it has been found attractive to impart desirable properties to starch without sacrificing its biological nature. Graft copolymerisation is one way to introduce biodegradability and improved properties to a polymer. Usually graft copolymerisation reactions are carried out by free radical initiated polymerisation reaction and in the literature different types of initiating systems are reported. Depending upon the type of monomers and the conditions employed the properties of the starch-graft-copolymers vary to a large extent. In this chapter, the various techniques used for the synthesis of starch-graft-copolymers, their properties and possible end uses are discussed in detail.

Keywords Starch-graft-copolymers • Free radical initiation • Grafting percentage • FTIR • Thermogravimetry • Superabsorbent polymers • Water treatment industry • Flocculation

A.N. Jyothi (✉)

Division of Crop Utilization, Central Tuber Crops Research Institute, Sreekariyam,
Thiruvananthapuram, Kerala, India
e-mail: sreejyothi_in@yahoo.com

A.J.F. Carvalho

Departamento de Engenharia de Materiais, Escola de Engenharia de São Carlos, Universidade de São Paulo – SMM/EESC/USP, Av. Trabalhador São-carlense, 400, Caixa-Postal: 359, 13566-590 São Carlos, SP, Brazil
e-mail: toni@sc.usp.br

3.1 Introduction

Starch is a carbohydrate of high natural abundance next to cellulose [1] and chitin [2]. It is the most common constituent of human diet, where it accounts for the major share of energy required for the sustenance of life. It is widely distributed in the form of tiny granules as the major reserve carbohydrate in stems, roots, grains and fruits of all forms of green leafed plants. Cereal grains, such as corn, wheat, sorghum, and tubers and roots, such as potato, tapioca, arrowroot, etc., are some of the commercial sources of starch for industrial exploitation.

Starch granules are heterogeneous in nature consisting of crystalline as well as amorphous regions. Amylose forms the amorphous region in starch. It is a linear polymer of glucose with α -1,4 linkages. Amylopectin molecule is the crystalline component in the granules, with the short branched chains forming local organisations. It is a polymer which contains 20–25 glucose units on average, a highly branched polymer consisting of relatively short branches of α -D-(1–4)-glucopyranose that are interlinked by α -D-(1–6)-glycosidic linkages. The proportions of amylose and amylopectin range from about 10–20 % amylose and 80–90 % amylopectin depending on the source [3]. Starch is hydrophilic and the available hydroxyl groups on the starch chains potentially exhibit reactivity specific for alcohols [4]. Starch exhibits a wide range of functional properties, and it is probably the most commonly used hydrocolloid.

Among the chemical modifications of starch, grafting of vinyl monomers onto it seems to be promising modification to impart desirable properties [5]. Graft copolymerisation is a free radical reaction, where starch upon treatment with initiators yields free radical sites on the glucan backbone which act as micro-initiators in the presence of synthetic monomers to yield polymer grafts of high molecular weight [5]. Graft copolymerisation imparts increased hydrophilicity, hydrophobicity or polyelectrolyte nature to starch depending on the reagent and conditions used.

3.2 Synthesis of Graft Copolymers from Starch

In starch-graft-copolymers, the side chains of a given monomer are attached to the main chain of starch. Acrylic/vinyl monomers are usually used for grafting onto starch, which include acrylic acid, acrylamide, acrylonitrile, methacrylic acid, methacrylamide, methacrylonitrile, vinyl acetate, etc. The copolymers are synthesised by the polymerisation reaction of starch with the monomers in the presence of a free radical initiator. Two types of free radical initiating systems are used. The first type is chemical initiation through use of chemical reagents such as peroxy or azo compounds. Examples of these are hydrogen peroxide, sodium, potassium and ammonium peroxodisulphate, di-tert-butyl peroxide, etc. Redox initiator systems, in which said free radical initiators are used together with a

reducing agent, are suitable as initiators. Examples of reducing agents are sodium sulphite, sodium pyrosulphite, sodium hydrogen sulphite, sodium dithionite, sodium formaldehyde sulfoxylate and ascorbic acid. In addition the free radical initiators can also be combined with heavy metal salts, such as cerium(IV), manganese or iron salts, to give a suitable redox system. Ternary initiator systems consisting of free radical initiator, reducing agent and heavy metal salt are furthermore suitable.

The second type of initiation is free radical initiation by irradiation with electron beam, UV-, γ -rays or microwaves. There are many reports on the synthesis and characterisation of starch-graft-copolymers using various free radical initiation systems [6–13].

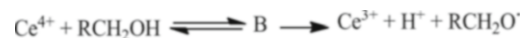
3.2.1 *Initiation by Ceric Ion*

Ceric salts [Ce(IV)] such as the ceric nitrate and ceric sulphate are widely used as free radical initiators in the graft copolymerisation of starch. The oxidation–reduction produces cerous [Ce(III)] ions and transient free radical species capable of initiating vinyl polymerisation. The mechanism of the initiation reaction can be written generally as follows (Scheme 3.1).

The most important feature of the oxidation with ceric ion is that it proceeds via single electron transfer with the formation of free radicals on the reducing agent [14]. Thus, if the reducing agent is a polymeric substrate such as starch, cellulose or polyvinyl alcohol, and the oxidation is carried out in the presence of vinyl monomer, the free radical produced on the substrate molecule initiates polymerisation to produce a graft copolymer. This method of grafting yields substantially pure graft copolymers since the free radicals are produced exclusively on the backbone. Another advantage of this method is that it proceeds in a quite facile manner even at ambient temperature [14].

A study on the Ce(IV) consumption in the graft copolymerisation of methacrylonitrile/*n*-alkyl (methyl, ethyl and butyl) methacrylate mixtures was carried out [15]. Ce(IV) consumption increased with increasing mole fraction of the methacrylate in the monomer feed and with increasing the *n*-alkyl group length of the methacrylate. The molecular weight distribution of the copolymers was obtained through gel-permeation chromatography.

Carr et al. [16] employed continuous reactive twin-screw extrusion for the graft copolymerisation of cationic methacrylate, acrylamide and acrylonitrile monomers onto starch for rapidly and efficiently producing starch-g-copolymers. Ceric ammonium nitrate was used as the initiator, and levels of temperature, screw speed, starch concentration and CAN addition on extrusion process were studied. Starch-graft-poly(acrylonitrile)-copolymers with high conversion of monomer to polymer (74–78 %) and high synthetic polymer add-on (42–44 %) were achieved within a reaction period of 7 min.



Where, B represents the ceric complex.

Scheme 3.1 Mechanism of free radical initiation by ceric ions

The grafting of acrylic acid (AA) onto granular maize starch was carried by ceric ion initiation [6, 7]. The effect of grafting parameters has been studied in terms of % GE and %add-on. The optimum conditions obtained for the grafting of AA onto 2 g of granular maize starch were AA = 0.2775 mol/L, CAN = 0.004 mol/L, time = 240 min, temperature = 35 °C and material-to-liquor ratio = 1:10.

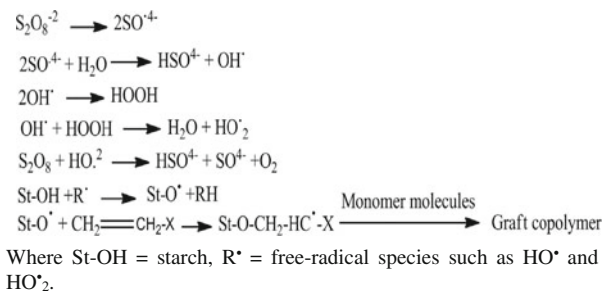
Grafting of *N*-tert-butyl acrylamide (BAM) onto starch in aqueous medium initiated by ceric ammonium nitrate ion has been studied [17]. The optimum conditions obtained for maximum percent grafting efficiency (%GE) and grafting yield (%GY) during the grafting of BAM on 1.0 g starch were [BAM] = 0.020 mol/L, [CAN] = 0.91×10^{-3} mol/L, temperature = 30 °C and time = 240 min. As the concentration of CAN initiator increases, the %GE first increases up to [CAN] = 0.91×10^{-3} mol/L, and then it is reduced slowly from [CAN] = 1.82×10^{-3} to 3.65×10^{-3} mol/L. Ceric ammonium nitrate-initiated polymerisation of acrylonitrile onto spherocrystals formed in slowly cooled solutions of jet-cooked corn starch yielded graft copolymers containing higher percentages of grafted poly (acrylonitrile) than comparable polymers prepared from granular corn starch [18].

Graft copolymerisation of low-density polyethylene (LDPE) onto starch was carried out with glucose–cerium(IV) redox initiator in an aqueous sulphuric acid medium. The graft yield was influenced by various parameters like reaction time, temperature and concentrations of acid, glucose, polyethylene, starch and initiator. A maximum graft yield of 85.66 % was obtained at temperature of 50 °C [19]. On increasing the temperature beyond 60 °C, the interactions of PE macroradicals with Ce(IV) ions destroyed the activity of the initiating species and hence decreased the graft yields.

Jyothi et al. [20] synthesised highly water-absorbing graft copolymers of cassava starch by polymerisation with poly(acrylamide) in the presence of ceric ion initiator. The optimum values of parameters predicted through response surface methodology were 20 g acrylamide/10 g dry starch, 3.29 g/L ceric ammonium nitrate, 180 min reaction duration and 45 °C temperature which resulted in products with a % grafting of 190.03.

Ceric ammonium ion initiation was used for the synthesis of graft copolymers of starch and acrylonitrile in aqueous solution by varying the monomer and initiator concentrations [21]. The results showed that the grafting ratio reached the maximum value of 4.32 % at 3 M ceric ion concentration which indicates the reduction equivalent of the polymer backbone. The decrease in grafting ratio at 4 M ceric ion concentration was attributed to the solubility limitation of the starch and also to the termination of the growing grafted chains in the presence of excess of ceric ions.

In general, a critical concentration of ceric ion exists up to which the grafting efficiency (%GE) and the percentage grafting increase and decrease thereafter [5]. The initial increase in %GE can be attributed to the increasing number of free



Scheme 3.2 Mechanism of graft copolymerisation reaction of starch with vinyl monomers in presence of persulphate as free radical initiator

radical sites on the starch backbone at which the monomer can be grafted. However, the decrease in %GE at higher concentration of CAN may be attributed to the termination of the growing grafted chains by excess ceric ions [22], and also primary radical termination, i.e. the reaction of the free radicals on the starch backbone with excess of ceric ions to produce oxidised starch which is incapable of initiating polymerisation.

3.2.2 Initiation by Persulphates

Potassium or ammonium persulphate system was found to be an efficient redox initiator in the graft copolymerisation of starch in aqueous medium. When an aqueous solution of persulphate is heated, it decomposes to produce sulphate ion radical along with other radical species [23–25]. The mechanism of reaction is represented below (Scheme 3.2).

Using potassium persulphate as the radical initiator, a series of starch-graft-copolymers of vinyl monomers, such as acrylamide, acrylonitrile, acrylic acid and methacrylic acid, have been prepared, and their properties have been studied [24]. Taghizadeh and Mafakhery [25] studied the mechanism and kinetics of graft polymerisation of acrylonitrile (AN) onto starch in aqueous solution using potassium persulphate (I) redox system. The percentage of grafting and the rate of grafting were dependent on the concentration of I, AN, starch and starch/water as well as reaction time and temperature. From the kinetic studies, the expressions for rate of graft polymerisation (R_g) and rate of homopolymerisation (R_h) were obtained as $R_g = k[\text{AN}]^{1.185} \cdot [\text{I}]^{0.499} \cdot [\text{Starch}]^{0.497}$ and $R_h = k[\text{AN}]^{1.359} \cdot [\text{I}]^{0.436}$, respectively.

The allyl-modified maize starch was copolymerised with methacrylic acid and a combination of methacrylic acid and acrylamide at 50 and 70 °C with potassium persulphate as initiator [26]. Mustafa and Samarkandy [27] synthesised new thickeners for printing cotton fabrics with reactive dyes based on graft copolymers of methacrylonitrile onto pregelled starch [27]. Potassium monopersulphate in the

presence of ferrous ion redox pair was used as initiator and the appropriate conditions obtained were initiator concentration 0.004 mmol/L, ferrous ion concentration 0.005 mmol/L, sulphuric acid 0.002 mmol/L, methacrylonitrile 50 % based on weight of the substrate, material liquor ratio 1:2.5, reaction time 60 min and temperature 40 °C.

Semi-interpenetrating polymer network (IPN) hydrogels composed of starch and random copolymer of poly(acrylamide-*co*-sodium methacrylate) [poly(AAm-*co*-NMA)] were prepared by polymerising an aqueous solution of acrylamide (AAm) and sodium methacrylate (NMA) using ammonium persulphate (APS)/*N,N,N',N'*-tetramethylethylenediamine (TMEDA) as redox initiating system in the presence of a crosslinker and starch solution [28]. Biodegradable superabsorbent polymers were synthesised by graft copolymerisation of acrylamide (AM)/itaconic acid (IA) onto cassava starch via a redox initiator system of ammonium persulphate (APS) and *N,N,N',N'*-tetramethylethylenediamine (TEMED), in the presence of *N,N'*-methylenebisacrylamide (*N*-MBA) as cross-linking agent, sodium bicarbonate as foaming agent and a triblock copolymer of polyoxyethylene/polyoxypropylene/polyoxyethylene as a foam stabiliser [12]. The optimal ratio of AM:IA giving the highest water absorption could be due to copolymerisation reactions via the charge transfer complex from a donor (oxidant) to an acceptor (reductant), i.e. from the electron-rich AM to the electron-poor IA [11].

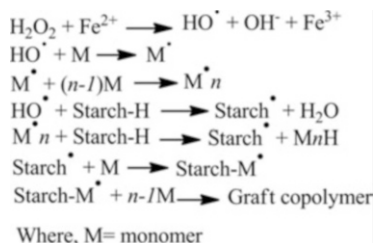
A patent reports the use of ammonium peroxodisulphate free radical initiator in the preparation of cationic starch-graft-copolymers composed of the monomers 20–80 % by weight of acrylamide, methacrylamide or mixtures thereof, 3–20 % by weight of a cationic vinyl monomer, 0.005–1.5 % by weight of a cross-linking agent, 0–10 % by weight of a non-ionic or anionic vinyl monomer and a grafting base and 15–70 % by weight of starch or starch derivative [29].

The graft copolymerisation of mixed grafting monomers such as vinyl acetate and butyl acrylate onto corn starch has been investigated using ammonium persulphate as initiator [30]. By single-factor tests, the optimum graft copolymerisation conditions with higher grafting efficiency and grafting percent ratio correspond to the reaction time of 3 h, reaction temperature of 65 °C, initiator concentration of 9.7×10^{-3} mol/L, mixed grafting monomers concentration of 1.0 mol/L and volume ratio of vinyl acetate to butyl acrylate of 5:5. An amphoteric starch-graft-poly(acrylamide) was prepared by inverse emulsion polymerisation using ammonium persulphate and urea as redox initiator, subsequent hydrolysis reaction and Mannich reaction [31].

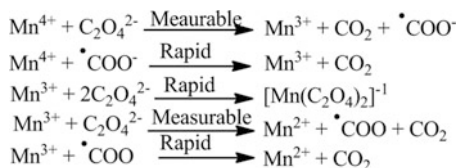
3.2.3 Fe^{2+} -Hydrogen Peroxide Initiation

As in the other systems, in the case of Fe^{2+} - H_2O_2 system also, formation of radical sites on the backbone polymer is involved [32]. The possible steps in the grafting process are (Scheme 3.3).

Scheme 3.3 Graft copolymerisation reaction of starch in presence of Fe^{2+} -hydrogen peroxide system



Scheme 3.4 Formation of carboxyl radical ions by potassium permanganate-oxalic acid system



Methacrylamide was successfully grafted onto starch using benzoyl peroxide as a radical initiator in aqueous medium [33]. The optimum initiator concentration was 2.0×10^{-3} mol/L. The graft copolymerisation of styrene (ST) and methyl methacrylate (MMA)/butyl acrylate (BA) onto starch was carried chemically using ferrous ion-peroxide redox system [34]. The grafting was performed at 60°C and the monomer ratios of ST/MMA and ST/BA were varied with their % composition as 80/20, 50/50 and 20/80 parts by weight.

3.2.4 Manganese Initiation

Potassium permanganate-acid system (Mn^{4+}) and manganic pyrophosphate (Mn^{3+}) have been employed for graft polymerisation of vinyl monomers onto starch. Starch is generally immersed in KMnO_4 solution to deposit MnO_2 on it. In the presence of acid, formation of primary radical species occurs as a result of the action of the acid on the deposited MnO_2 [35]. Hence, different primary radical species are created depending on the type and nature of the acid used. The initiation has been explained using different acids as follows.

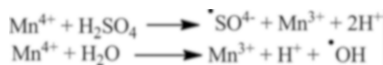
In the case of oxalic acid, the carboxyl radical ions constitute the primary radical species and are possibly formed as given below (Scheme 3.4).

In the presence of sulphuric acid, sulphate ion is oxidised by fresh MnO_2 to produce the sulphate ion radical, which acts as the primary radical species. Other free radical species, namely, the hydroxyl radical, may also be formed (Scheme 3.5).

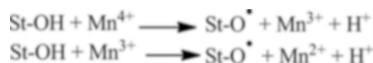
Starch macroradicals may also be formed by direct attack of Mn^{4+} or Mn^{3+} ions on starch molecule via abstraction of hydrogen atom (Scheme 3.6).

In the presence of vinyl monomer, the starch macroradical is added to the double bond of the vinyl monomer, resulting in a covalent bond between the monomer and starch and the creation of free radical on the monomer. Subsequent addition of

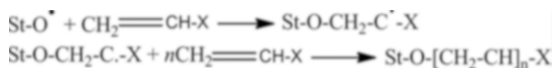
Scheme 3.5 Formation of sulphate ion radical and hydroxyl radical in potassium permanganate–sulphuric acid system



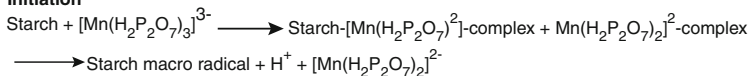
Scheme 3.6 Starch macroradical formation by Mn^{4+} and Mn^{3+} ions



Scheme 3.7 Grafting reaction of starch with vinyl monomers



Initiation



Propagation



Termination



Scheme 3.8 Mechanism of grafting of starch with manganic pyrophosphate initiator

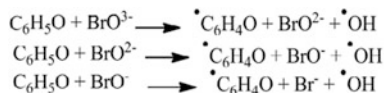
monomer molecules to the initiated chain propagates the grafting onto starch as shown below (Scheme 3.7).

Termination of the growing grafted chain may occur via coupling, disproportionation, reaction with the initiator and/or chain transfer.

The mechanism of grafting with manganic pyrophosphate initiator is represented as follows [36] (Scheme 3.8)

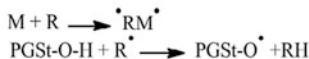
Graft polymerisation of AA onto rice starch using potassium permanganate/acid (citric, tartaric, oxalic and hydrochloric acid) was investigated [37]. The dependence of the MnO_2 amount deposited was related directly to the KMnO_4 solution. The graft yield increased by increasing the concentration of acid to a certain concentration beyond which grafting levelled off. The emulsion polymerisation of styrene onto starch was investigated using manganic pyrophosphate $[\text{Mn}(\text{H}_2\text{P}_2\text{O}_7)_3]^{3-}$ as the initiator and hexadecyl trimethyl ammonium bromide as the emulsifier [38, 39].

The initiating ability of the potassium permanganate in the graft copolymerisation of acrylonitrile onto corn starch was studied [40]. The results indicate that the grafting parameters, such as concentrations of potassium permanganate, acrylonitrile, starch and catalyst acids, all have significant effects on the graft copolymerisation and the components of the graft copolymers. The grafting efficiency was maximum at a temperature of 40 °C. The preheat treatment and pre-oxidation of starch, as well as the adding sequence of the reactants, influenced the



Where, R = $\cdot\text{C}_6\text{H}_4\text{O}$, Br^\cdot and $\cdot\text{OH}$

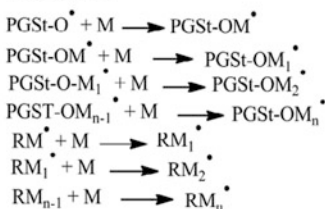
Initiation



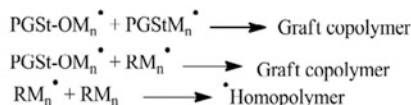
Where, PGSt-O-H = Pregelled starch, M = Monomer, R = Free radical, PGSt-O^\cdot = Pregelled starch

macro radical

Propagation



Termination



Scheme 3.9 Reaction scheme of grafting of starch with vinyl monomers in bromate/cyclohexanone redox system

graft copolymerisation, which explains that oxidation degree of starch decides the grafting ability. The graft mechanism of acrylonitrile onto starch under the initiation of potassium permanganate was investigated [41]. The relationships of the grafting rate and the concentrations of potassium permanganate, acrylonitrile and starch, as well as the reaction temperature, were established.

3.2.5 Initiation by Bromate/Cyclohexanone Redox System

Bromate/cyclohexanone redox system was investigated as a novel initiator for graft copolymerisation of *N*-vinyl formamide onto pregelled starch [42]. It is assumed that in the presence of sulphuric acid, during the oxidation of cyclohexanone by bromate ion, the free radicals like $\cdot\text{C}_6\text{H}_4\text{O}$, $\cdot\text{OH}$ and Br^\cdot are produced. These radicals abstract hydrogen atom from pregelled starch molecules producing pregelled starch macroradical. The monomer molecules, which are in the close vicinity of reaction sites, accept starch macroradicals, resulting in chain initiation and thereby themselves become free radical donor to neighbouring molecules leading to the propagation. These grafted chains are terminated by coupling to

give graft copolymer. The following reaction scheme was proposed on the basis of experimental results [42] (Scheme 3.9).

The optimum conditions for grafting of *N*-vinyl formamide onto pregelled starch were *N*-vinyl formamide 50 % based on weight of substrate, cyclohexanone 15 mmol/L, bromate ion, 30 mmol/L, liquor ratio 10, pH 6, time 120 min and temperature 40 °C [42].

3.2.6 Initiation by Irradiation

Employing high-energy γ -radiation is an efficient method for initiating radical graft polymerisation onto polysaccharides [43]. It was reported that although the radiation-based grafting is cleaner and more efficient in this regard than chemical initiation methods, they are harder to handle under technical conditions. Hence, research reports available for the synthesis of graft copolymers using radiation initiation system are few.

Gamma-rays were used as initiator for the graft copolymerisation of acrylamide and/or acrylic acid onto cassava starch and the effect of various parameters such as monomer–starch ratio, total dose of gamma rays (kGy), dose rate (kGy/h) and acrylamide–acrylic acid ratio and the addition of nitric acid and maleic acid as the additives were studied [44]. The porosity of the saponified starch-graft-copolymers prepared by the acrylamide/acrylic acid ratios of 70:30 and 50:50 was much higher than the porosity of copolymers in terms of fine networks.

Cassava starch-g-poly(acrylic acid) copolymers were prepared by a simultaneous irradiation technique with γ -ray irradiation from a ^{60}Co source [45]. The graft copolymer was prepared using γ -ray irradiation at a dose rate of 2 kGy/h to a total dose of 10 kGy, and a ratio of acrylic acid to cassava starch of 1:1. The resulting graft copolymer contained 2.7 % homopolymer, 24.9 % add-on, 40 % conversion, 90 % grafting efficiency and 33.2 % grafting ratio. Graft copolymerisation of acrylonitrile onto maize starch by a simultaneous irradiation technique using gamma-rays as the initiator was studied with regard to the monomer-to-maize starch ratio and total dose (kGy) [46].

Potato starch-graft-poly(acrylonitrile) could be efficiently synthesised using small concentration of ammonium peroxydisulphate (0.0014 M) in aqueous medium under microwave irradiation [47]. Maximum grafting ratio and efficiency of 225 % and 98 %, respectively, were obtained at 0.17 M acrylonitrile, 0.0014 M $(\text{NH}_4)_2\text{S}_2\text{O}_8$, 0.1 g potato starch and 70 s microwave exposure at a power of 1,200 W keeping total reaction volume fixed at 25 mL. The temperature of the reaction mixture just after the microwave exposure was 98 °C.

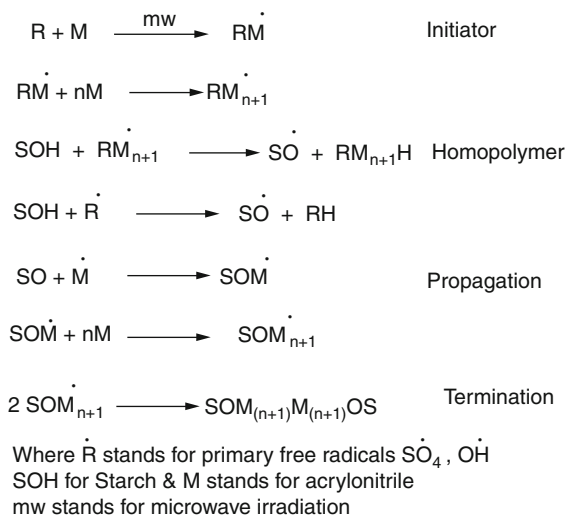
Microwaves are reported to have the special effect of lowering of Gibbs energy of activation of the reactions [48]. Along with this effect, the dielectric heating of the reaction medium causes quick decomposition of peroxydisulphate into sulphate ion radicals as shown below (Schemes 3.10 and 3.11).

The primary radicals $\text{SO}_4^{\cdot-}$ and OH^{\cdot} initiate the vinyl polymerisation as the vinyl polymerisation is reported to be faster than the H abstraction from the

Scheme 3.10
Decomposition of peroxydisulphate into sulphate ion radicals by microwave heating



Scheme 3.11 Mechanism of grafting reaction of starch with acrylonitrile by microwave irradiation



polysaccharide starch backbone [49]. The macroradical (SO^{\cdot}) may be generated by abstraction of H by the growing vinyl polymer radical, which may add onto the vinyl monomer (M) generating new radical SOM^{\cdot} and this chain will grow till it combines with other such chains to give the graft copolymer.

3.2.7 Other Initiating Systems

Besides the major grafting processes described above, several other initiating systems and methods for synthesising starch-graft-copolymers are reported. Pregelled starch has been graft copolymerised with methacrylamide as a reactive monomer using vanadium mercaptosuccinic acid redox pair as an initiation system [50].

Starch was reacted with acrylamide in water in the presence of horseradish peroxidase (HRP) catalyst/ H_2O_2 /2,4 pentane dione in water and acetate buffer at 30 °C temperature and pH 7.0 to give starch–poly(acrylamide) graft copolymers [51]. It is postulated that peroxide activated HRP oxidises PDO to a free radical which then abstracts a proton from starch backbone to give carbonyl radicals which in turn initiates the grafting reaction and copolymerisation. Extrusion technique was also reported for grafting reactions of starch for grafting [52–55].

3.3 Characterisation of Starch-g-Copolymers

3.3.1 Grafting Parameters

The compositional parameters of starch-graft-copolymers are usually expressed on a weight basis [56–58]. The terms generally used are percentage grafting, grafting efficiency, % add-on, grafting ratio, etc. Grafting efficiency and add-on/grafting (%) are the most important parameters that completely describe the copolymer system. The various equations can be expressed as follows:

$$\text{Add-on or grafting (\%)} = (\text{Weight of grafted polymer} / \text{Weight of copolymer sample}) \times 100$$

$$\begin{aligned} \text{Grafting efficiency (\%)} &= (\text{Weight of grafted polymer} / \text{Weight of grafted polymer plus homopolymer}) \times 100 \text{ or} \\ &= (\text{Weight of grafted polymer} / \text{Weight of monomer used}) \times 100 \end{aligned}$$

$$\text{Grafting ratio (\%)} = (\text{Weight of grafted polymer} / \text{Weight of starch}) \times 100$$

$$\begin{aligned} \text{Monomer conversion (\%)} &= (\text{Total weight of polymer produced} \\ &\quad \text{(i.e., grafted plus homopolymer)} / \\ &\quad \text{Weight of monomer used}) \times 100 \end{aligned}$$

$$\begin{aligned} \text{Homopolymer (\%)} &= \text{Weight of homopolymer} / \text{Total weight of polymer produced} \\ &\quad \text{(i.e., grafted polymer plus homopolymer)} \times 100 \text{ or} \\ &= (\text{Weight of homopolymer} / \text{Weight of monomer charged}) \times 100 \end{aligned}$$

The percent grafting ratio (Gr) is reported as the ratio of the weight of the grafted polymer to the weight of the starch multiplied by 100 [59]. The percentage conversion is taken as the ratio of the weight of the grafted polymer to the weight of the monomer.

$$\text{Gr\%} = (\text{weight of grafted polymer} / \text{weight of starch}) \times 100/1$$

$$\% \text{Conversion} = (\text{weight of grafted polymer} / \text{weight of monomer}) \times 100/1$$

According to Shogren et al. [51], conversion, graft content and grafting efficiency of grafted starch containing acrylamide groups (AAm) were calculated from the nitrogen content as follows:

$$\text{Conversion} : W_{\text{tq}} \times 100 \times N_{\text{q}} / 19.72 / \text{weight of AAm}$$

$$\text{Graft content} : 100 \times N_{\text{ext}} / 19.72$$

$$\text{Graft efficiency} : f \times N_{\text{ext}} / N_{\text{q}}$$

where W_{tq} = product weight after removal of AAm by extraction with ethanol, N_q = nitrogen content after removal of AAm by extraction with ethanol, N_{ext} = nitrogen content after removal of homopolymer PAAm by extraction with 30 % ethanol, f = insoluble weight fraction as $\% 100 \times W_{tinsoluble}/W_{soluble} + W_{tinsoluble}$ and 19.72 % is the nitrogen content of acrylamide (AAm).

Grafting efficiency is based on the polymerised monomer, i.e. the ratio of insoluble PAAm to total PAAm.

3.3.2 Acrylamide/Acrylic Acid Content in Grafted Copolymers

Bhuniya et al. [26] reported the methods for the determination of percentage acrylamide, acrylic acid or methacrylic acid content in the starch-graft-copolymers. The acrylamide content can be calculated from the nitrogen content. The nitrogen content was quantitatively determined by elemental analysis, and the acrylamide content was calculated as follows:

$$\text{Acrylamide, \%} = (71.08 \times y)/14.006$$

where 71.08 is the molecular weight of acrylamide, y is the percentage of nitrogen present in the hydrogel and 14.006 is the atomic weight of nitrogen.

The acrylic/methacrylic acid contents can be estimated from the carboxyl content. The carboxylic group content in the hydrogels was determined by the sodium bicarbonate–sodium chloride method and with the following equations [26]:

$$\text{Carboxylic group per 100 g of hydrogel, } y = (V_2 - V_1) \times M \times 100/W$$

$$\text{Acrylic acid content, \%} = (72.06 \times y)/45$$

$$\text{Methacrylic acid content, \%} = (86 \times y)/45$$

where W is the weight of sample, and 50 mL of 0.01 M NaCO_3 – NaCl solution was added for neutralisation to W g of sample; V_2 is the volume of HCl required to neutralise 50 mL of 0.01 M Na_2CO_3 – NaCl solution; V_1 is the volume of HCl required to neutralise excess 0.01 M Na_2CO_3 – NaCl solution; M is the molarity of the HCl solution; and 45 is the molecular weight of the carboxylic group (COOH).

3.3.3 Molecular Weight and Frequency of Grafts

Grafted polymer is generally separated from the starch backbone by the acid hydrolysis technique [14]. In the acid hydrolysis technique, the graft copolymer is hydrolysed with 1 N HCl solution. Enzymatic hydrolysis is employed for the acrylamide-grafted copolymers, since refluxing acid greatly altered the molecular

weights of grafted branches [60]. The separated grafts are purified and the average molecular weight is determined by GPC, osmometry or intrinsic viscosity methods [17, 54]. The frequency of anhydroglucose units (AGU) per graft is calculated as follows:

$$\begin{aligned} \text{AGU/Graft} &= M_n \text{ of grafted polymer} \\ &\times (\text{Wt\% of starch in graft copolymer/Wt\% of grafted polymer}) \\ &\times (1/162) \end{aligned}$$

where M_n is the number average molecular weight, 162 is the molecular weight of the AGU repeating unit and wt% of starch + wt% of grafted polymer is 100.

Molecular weights of poly(acrylonitrile) grafted onto spherocrystals formed in slowly cooled solutions of jet-cooked corn starch-grafted spherocrystals were higher by about a factor of six than the PAN molecular weight in grafted granular corn starch [18].

Molecular weight of polyacrylonitrile (PAN) in the grafted starch was determined from apparent viscosity (ν) [40]. The purified starch-g-PAN copolymer was hydrolysed in 1 mol/L HCL solution at 105–110 °C for 24 h to get the grafted side chains. The solution viscosity of the grafted chains was determined with an Ubbelohde viscometer at 50 °C with dimethyl sulphoxide as solvent, and the molecular weight was consequently calculated according to the Mark–Houwink equation:

$$[\eta] = KM_v^\alpha$$

where $K = 2.83 \times 10^{-4}$ and $\alpha = 0.758$.

Molecular weight of starch-g-butyl(acrylamide) copolymer was determined by acid hydrolysis and viscosity measurement of the separated PBAM branches [17]. Starch on acid hydrolysis is converted into glucose units, which are soluble in water, and does not precipitate with methanol. The viscosity average molecular weight (M_v) of the separated branches of PBAM was determined from the relation: $[\eta] = 2.56 \times 10^{-4} M_v^{0.74}$ using 0.03 g/mL in THF solvent at 30 °C [61]. The average molecular weight of all side chains of PBAM was in the range of 105.

Physically cross-linked starch-g-PVA hydrogels with controllable grafted branch length were prepared [62]. The molecular weight of PVAc was tailored using the chain transfer reaction. The grafted PVA was separated from starch by acid hydrolysis and the intrinsic viscosity ($[\eta]$, mL/g) of PVA was measured using an Ubbelohde viscometer at 30 °C. Then the viscosity average molecular weight (M_v) could be calculated according to the formula $[\eta] = K \times M_v^\alpha$ (coefficients K and α were 6.65×10^{-2} mL/g and 0.64, respectively). The viscosity average molecular weight of grafted PVA could be 7.2×10^4 , 1.6×10^4 and 1.3×10^4 when no chain transfer agents, 11.79 mol/L of methanol or 4.38 mol/L of ethyl alcohol, were added, respectively.

3.3.4 Evidence for Grafting

The confirmation of grafting reaction is mainly obtained by infrared spectroscopy and in a few cases by ^{13}C -NMR spectroscopy [14].

3.3.4.1 FTIR Spectroscopy

Fourier transform infrared (FTIR) spectroscopy has been used extensively for the confirmation of graft copolymer formation [38, 63–66]. The appearance of the characteristic bands of starch and the grafted polymer in the spectrum is taken as the evidence for grafting [8, 11–13, 56, 67]. The percentage of poly(ACN) graft chains in starch-g-poly(ACN) copolymer was determined quantitatively by IR spectrometry, taking the 855 cm^{-1} characteristic absorption frequency as the internal standard peak and the $2,245\text{ cm}^{-1}$ characteristic absorption frequency as the quantitative analysis peaks.

Grafting of acrylamide onto cassava starch was confirmed by comparing the FTIR spectra of the native cassava starch with those of the grafted starches [12, 20]. The IR spectra of cassava starch display the O–H stretching absorption in the region of $3,550\text{--}3,200\text{ cm}^{-1}$ (broad, s), the C–H stretching at $2,930\text{ cm}^{-1}$ (m) and the wave numbers of $1,158, 1,081$ and $1,015\text{ cm}^{-1}$ (s) for the C–O–C stretching (a triplet peak of starch). The IR spectra of cassava starch display the O–H stretching absorption in the region of $3,390\text{ cm}^{-1}$, the C–H stretching at $2,932\text{ cm}^{-1}$, C=O stretching at $1,647.7\text{ cm}^{-1}$ and the triplet band for the C–O–C stretching absorption at $1,159, 1,084$ and $1,013\text{ cm}^{-1}$ (Fig. 3.1). Additionally, the peaks found at $3,400, 1,650$ and $1,600\text{ cm}^{-1}$ indicate the N–H stretching, the C=O stretching and N–H bending of the amide bands, respectively, which are characteristics of the $-\text{CONH}_2$ group present in the acrylamide. The peak at $1,411\text{ cm}^{-1}$ is for the $-\text{C}-\text{N}$ stretching and $765\text{--}710\text{ cm}^{-1}$ for the weak band N–H out of plane bending. These are also typical absorption bands of the amide.

Gao et al. [40] reported the existence of a characteristic absorption of PAN at $2,245\text{ cm}^{-1}$, which confirms the graft copolymer starch-g-PAN. Singh et al. [47] reported that the IR spectrum of microwave-synthesised starch-graft-PAN has absorption peaks at $2,242\text{--}2,245\text{ cm}^{-1}$ ($-\text{CN}$ stretching) and $1,453\text{ cm}^{-1}$ (CH_2 deformation vibration), which could be attributed to grafted PAN chains at starch backbone.

The FTIR spectra of cassava starch-graft-poly(acrylonitrile) copolymer showed the existence of a moderate peak at $2,240\text{ cm}^{-1}$ (Fig. 3.2), which is an evidence of grafting [21]. This absorption band arises from the stretching vibration mode of the nitrile groups. There is also a small characteristic peak at $2,340\text{ cm}^{-1}$ which is a $-\text{C}\equiv\text{N}-$ peak, an intermediate from the hydrolysis to carboxylic group. Most of the other peaks are related to the starch backbone.

Infrared spectroscopy was carried out to characterise the chemical structure of semi-IPNs of starch and poly(acrylamide-*co*-sodium methacrylate) [28]. In the IR

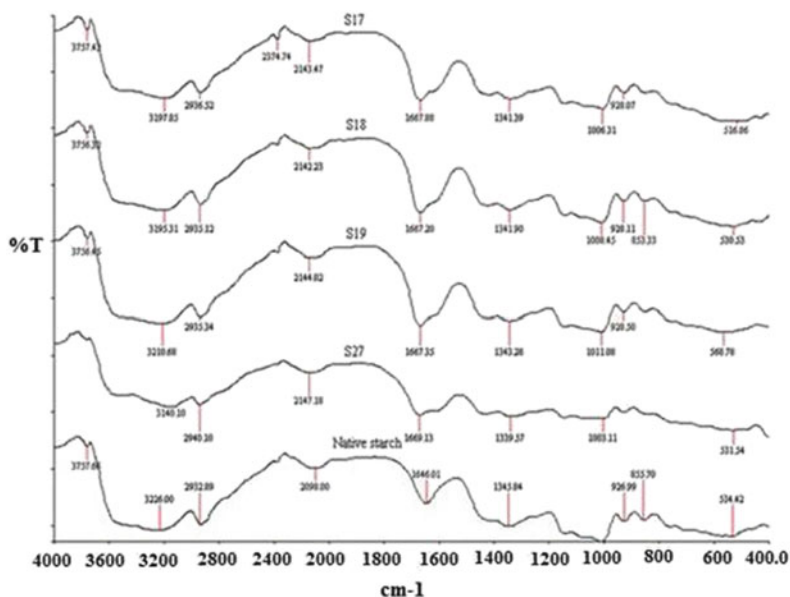


Fig. 3.1 FTIR spectra of native cassava starch and starch-graft-poly(acrylamide) [20]

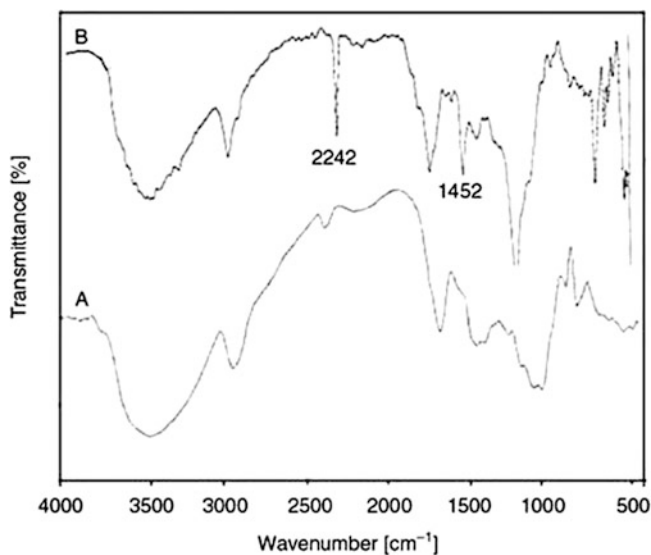


Fig. 3.2 IR spectra of starch (A) and starch-graftpoly(acrylonitrile) [21]

spectra (Fig. 3.3), the peaks observed between 3,580 and 3,050 cm^{-1} correspond to hydrogen bonded O–H and N–H stretching of acrylamide/starch/MBA units, the peaks at 1,683 cm^{-1} correspond to the C=O of the acrylate unit of sodium

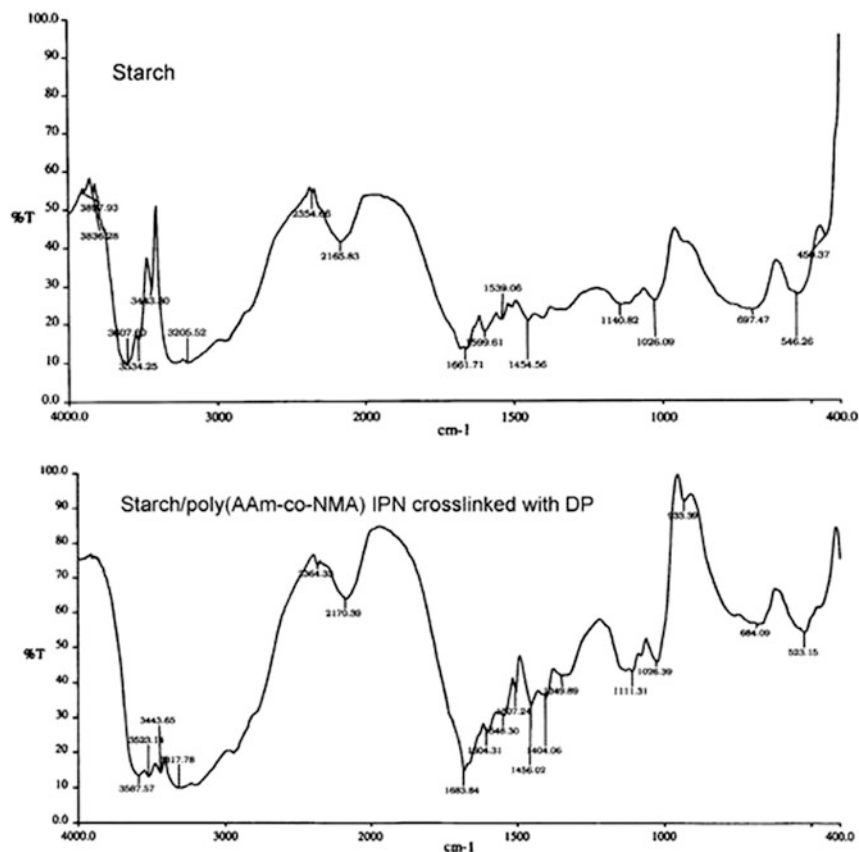


Fig. 3.3 IR spectra of the starch and starch/poly(AAm-co-NMA) semi-IPN hydrogel [28]

methacrylate/crosslinker, $1,670\text{ cm}^{-1}$ corresponds to the C=O group of acrylamide/MBA units and $1,140\text{ cm}^{-1}$ corresponds to C–O–C stretching peaks of ester groups.

FTIR spectra of the pure starch, homopolymer of polymethacrylamide, and 63.1 % polymethacrylamide-grafted starch showed the characteristic absorption of starch at $3,000\text{--}3,800\text{ cm}^{-1}$, due to the OH stretching band and also the N–H stretching band at $3,200\text{--}3,385\text{ cm}^{-1}$, CO amide peaks at $1,666\text{ cm}^{-1}$ and CN resonance peaks at $1,602\text{ cm}^{-1}$ coming from the grafted poly(methacrylamide), and not in pure starch [33].

FTIR technique cannot be applied for the confirmation of grafting to those copolymers for which the bands merge such as starch-g-poly(acrylamide), starch-g-poly(*N*-methylol acrylamide) and the like. In such cases, acid hydrolysis method is used to confirm graft copolymer formation [56]. During acid hydrolysis, starch hydrolyses, and the grafted chains are isolated. Generally, 1 N HCl is preferred to hydrolyse selectively starch without affecting the grafts. The purified isolated chains are identified and confirmed from IR spectroscopy.

3.3.4.2 Morphology of Starch-g-Copolymers

The surface morphology of the starch-graft-copolymers is investigated using scanning electron microscopy (SEM). SEM is the right technique used for direct observation of microstructure of spherulites of size in the range between 0.1 and 10 μm like maize starch granules [5]. The electron micrographs of pure starch samples clearly exhibit granular structure. A change in contour of the granules on grafting and the thick polymeric coating on their surface, was obviously of grafted poly(methacrylonitrile).

Scanning electron micrographs of starch-graft-poly(potassium acrylate-*co*-acrylamide) showed that the polymer is composed of fine particles [67]. Holes existed between these fine particles, so water can be absorbed easily by the resin because it had a higher specific surface area. Scanning electron microscopic study of the morphology of the surface of pure starch and starch-graft-poly(butyl acrylamide) with a %G of 33 revealed that the grafting process did not alter the granular nature of starch, but it made it more compact and it participated in the orientation of the surface by making some cubic granules [17]. This confirms that grafting process makes individual starch granules remain intact and the grafted synthetic polymer chains surround and agglomerate individual granules of starch forming impact and block-like structures.

SEM micrographs showed that the granular structure of starch was not maintained after graft copolymerisation and grafting is essentially a surface phenomenon [33]. After 28.6 % grafting, the granule surface was covered with poly(methacrylamide) and, finally, grafting process altered and destroyed the granular structure of starch. Also, the grafted chains surrounded and attached to the starch surface.

SEM micrographs have indicated planar but non-uniform surface structures with virgin polyethylene (PE) [19]. But starch-g-poly(ethylene) samples showed neither planar nor uniform surface (Fig. 3.4). With increase in percentage of grafting, the planarity and uniformity of the surface have decreased.

The microstructural cross-sectional features of starch/poly(acrylamide-*co*-sodium methacrylate) semi-IPN cross-linked with different methylene *bis*-acrylamide (MBA) concentrations determined with SEM revealed that hydrogel networks density improved enormously as MBA concentration increased (Fig. 3.5) [28]. At higher concentration of MBA crosslinker (Fig. 3.5b, c), the observed cross-linked densities are very high for these semi-IPNs and thereby lower the swelling capacity of the IPNs.

Jyothi et al. [20] studied the morphology of cassava starch-graft-poly(acrylamide) with different levels of grafting (Fig. 3.6). They observed that in the SEM micrographs of the grafted starch with a %G of 31.91, the spherical granules of the native starch (Fig. 3.6a) have been replaced by chunky and partial granule structures, which appeared like embedded in a continuous mass (Fig. 3.6b). For the grafted starch with the highest level of grafting (%G = 174.82), there was

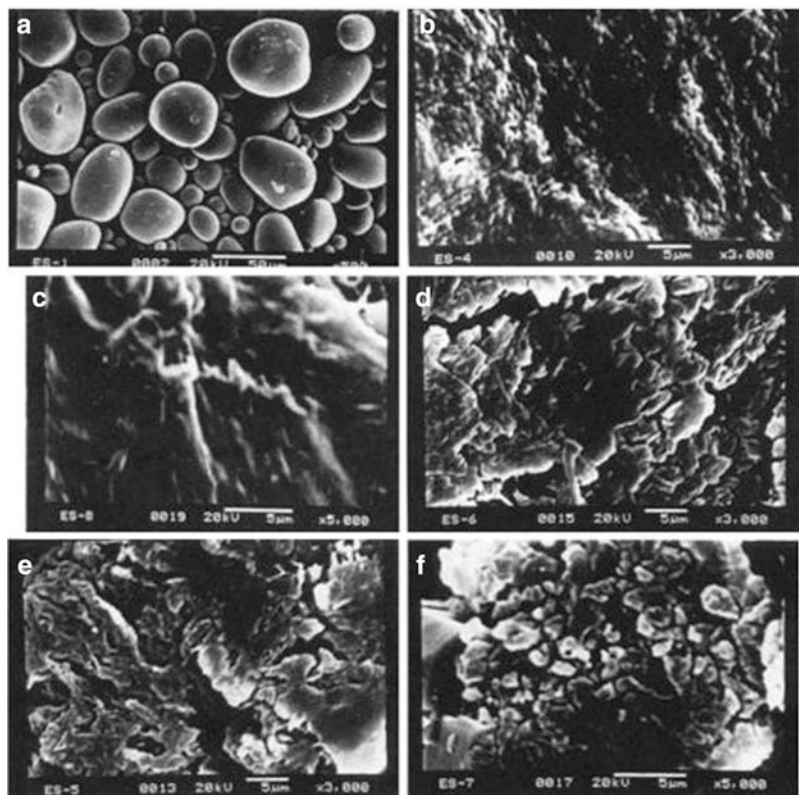


Fig. 3.4 Scanning electron micrographs of (a) pure starch, (b) Virgin LDPE, (c) PE-g-starch (46.83 %), (d) PE-g-starch (61.5 %), (e) PE-g-starch (76.7 %) and (f) PE-g-starch (80.68 %) [19]

complete disappearance of the granular structure and the surface appeared non-uniform and non-planar (Fig. 3.6c).

3.3.4.3 Crystallinity of Starch-Graft-Copolymers: X-ray Diffraction Analysis

X-ray diffraction analysis is a very useful and powerful analytical technique for understanding the crystallinity of polymers. In the case of starch-graft-copolymers, the crystallinity as well as the type of XRD pattern of the starch was found to be altered by grafting reaction. The percentage of crystallinity is determined by using the formula as given below [68]:

$$X_c(\%) = (A_c/A_a + A_c) \times 100$$

where A_c = area of crystalline phase, A_a = area of amorphous phase and X_c = percentage of crystallinity.

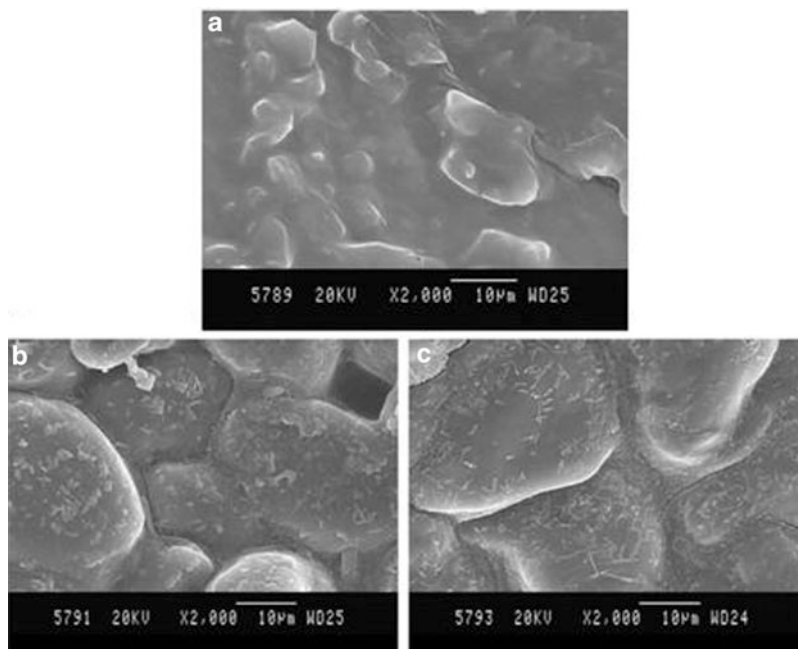


Fig. 3.5 Scanning electron micrographs of semi-IPN hydrogels prepared with (a) 0.013 mM, (b) 0.052 mM and (c) 0.097 mM of MBA [28]

The grafting of acrylic acid (AA) onto granular maize starch in aqueous medium initiated by ceric ion has been studied [6, 7]. XRD showed that the crystallinity of starch decreased owing to grafting.

Starch granules are semicrystalline in nature. The crystallinity is essentially due to amylopectin fraction. The areas of crystallinity comprise about 20–25 % of the total volume of the starch granule [5]. The wide angle X-ray diffraction pattern of pure granular maize starch comprises four more or less sharp peaks with low counts merely up to 800 between 2θ values of 10–30°, which on drying and grafting appears to have compressed into a broad smoothed peak, thereby altering the crystallinity of pure granular starch. Therefore, along with the amorphous region, crystalline region of the granular starch is also involved in grafting.

There were five peaks around 19.798 on the XRD pattern of starch, while only two peaks exhibited near 16.938 on that of starch-g-PVA [62]. The XRD profiles suggested that both starch and starch-g-PVA were semicrystalline (Fig. 3.7). It could be calculated that the crystallinity of starch and starch-g-PVA was approximately 8.03 % and 7.74 %, respectively.

The XRD pattern of pure starch shows four crystal peaks, indicating low crystallinity, but after the starch was grafted with methacrylamide (176.3 % grafting), the four crystal peaks were merged into a smooth peak, suggesting that the crystal phase was also involved [33]. The crystalline region increases on

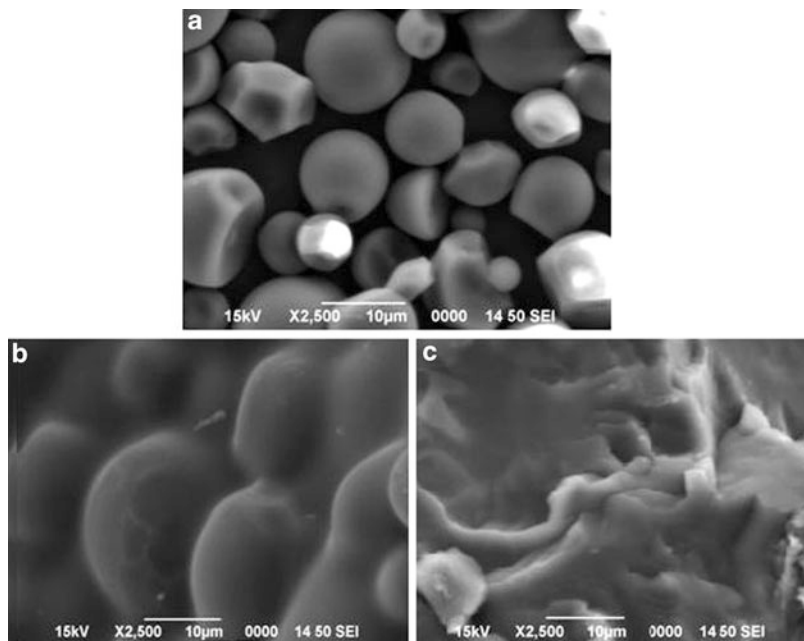


Fig. 3.6 Scanning electron micrographs of (a) native cassava starch, (b) starch-g-poly(AM) (%G = 31.91) and (c) starch-g-poly(AM) (%G = 174.82) [20]

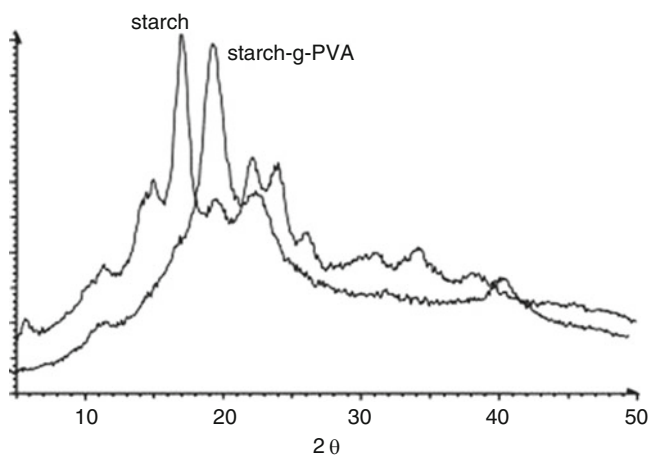


Fig. 3.7 XRD profiles of starch and starch-g-PVA [62]

grafting of homopolymer (PEMA) onto starch with crosslinker, sodium acrylate (SA) and additive, sodium silicate (SS) [69]. Although starch and SS are semicrystalline, XRD studies showed that St-g-PEMA/SS was more crystalline and porous

in nature and this could be the reason for the high water absorption capacity of starch-g-ethyl methacrylate/sodium acrylate/sodium silicate.

X-ray diffractograms of virgin low-density polyethylene (LDPE) and starch-graft-LDPE samples have shown that there was a decrease in percent crystallinity with the increase in percent graft yields of starch from 61.5 % to 80.68 % [19]. This was attributed to the formation of cross-links by starch molecules on the backbone of PE. It was also envisaged that, in addition to the decrease in percent crystallinity of PE, there was trapped amorphous starch between the PE chains, which also had contributed towards the decrease in crystallinity of the modified PE. The decrease in crystallinity of PE has been due to the disruption of crystallites and the dilution of inherent crystallinity of PE [68]. Singh et al. [13] reported that microwave-accelerated grafting of potato starch with acrylamide resulted in loss of crystallinity of the starch and showed halos typical for amorphous polymers in the XRD patterns.

Comparison of XRD of starch, poly(acrylonitrile) (PAN) and starch-graft-PAN was used to confirm grafting reaction [47]. XRD spectra of the grafted starch showed increased crystallinity in the region of $2\theta = 28\text{--}32^\circ$ due to the presence of PAN grafts on starch backbone, while peak at $2\theta = 18^\circ$ originally present in the starch has been significantly reduced after grafting (Fig. 3.8). The XRD patterns of graft copolymers of mixed monomers vinyl acetate and butyl acrylate onto corn starch showed that there were several dispersion peaks; therefore, the graft copolymerisation was the concomitant structure of a little crystalline state and amorphous state [30].

Jyothi et al. [20] have done the powder X-ray diffraction analysis of native cassava starch as well as starch-graft-poly(acrylamide) and observed that native cassava starch showed C_A -type X-ray diffraction pattern with major peaks at diffraction angles, $2\theta = 14.932^\circ$ ($d = 5.928$), 17.141° ($d = 5.169$), 18.058° ($d = 4.908$), 22.989° ($d = 3.866$) and 23.408° ($d = 3.797$). The graft copolymers showed decreased peak intensity in comparison to native starch, which indicates reduction in crystallinity, and with an increase in percentage graft yield, there was a decrease in crystallinity.

The X-ray diffraction analysis of amylopectin-rich starch grafted with polyethers revealed that the diffractograms of the amylopectin used for grafting presented A-type pattern, whereas the peaks disappeared after the grafting reaction, indicating a predominantly amorphous state.

3.3.4.4 NMR Spectra of Graft Copolymers

Cassava starch was chemically modified by radiation grafting with acrylic acid to obtain cassava starch-graft-poly(acrylic acid), which was further modified by esterification and etherification with poly(ethylene glycol) 4000 and propylene oxide, respectively [45], and the product was characterised by NMR spectroscopy. The hydroxypropyl groups on cassava starch were etherified with propylene oxide. The presence of a peak at a chemical shift of 19.96 ppm is indicative of the presence

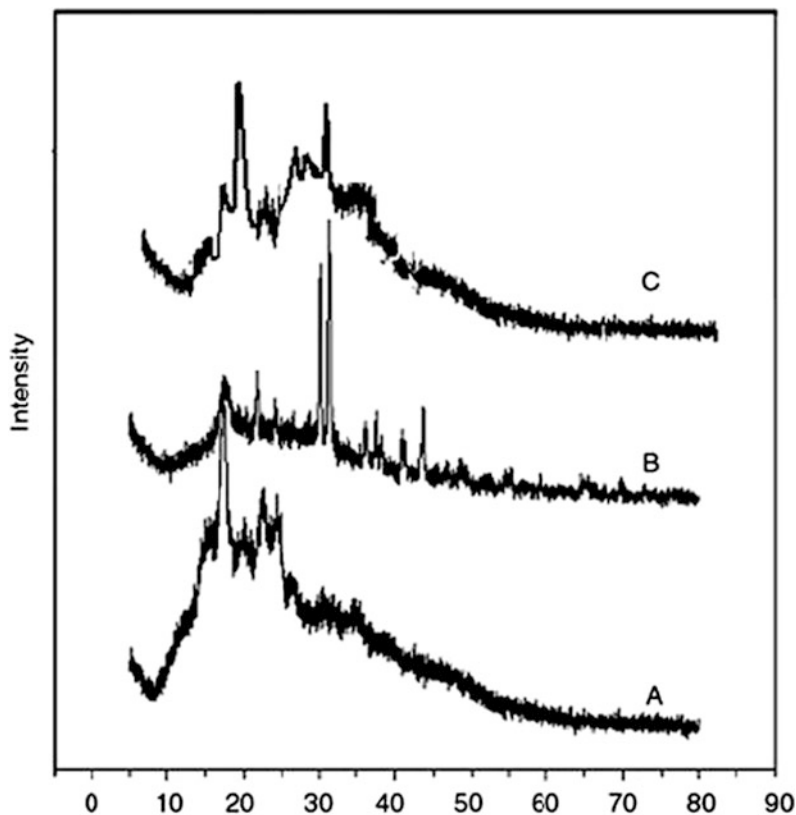


Fig. 3.8 X-ray diffraction pattern of (A) starch, (B) starch-graft-poly(acrylonitrile) and (C) poly(acrylonitrile) [47]

of hydroxypropyl groups on the modified starch. The chemical shift at 52 ppm indicates the presence of C–O– on PEG 4000 chains. Furthermore, the occurrence of a distinct peak at 1.2 ppm in the ^1H -NMR spectrum was attributed to protons of hydroxypropyl groups on the modified starch.

The domain structure of samples containing a series of starch/poly(sodium acrylate)-grafted superabsorbents, pure starch, pure poly(sodium acrylate) and blend of starch/poly(sodium acrylate) has been studied by high-resolution solid-state ^{13}C NMR spectroscopy at room temperature [70]. The result showed that the crystallinity of starch decreases greatly in the grafted and blended samples. The values of ^1H spin–lattice relaxation time in rotating frame $T_{1\rho}$ and ^1H spin–lattice relaxation time T_1 shows that starch and poly(sodium acrylate) components in both grafted and blended samples have good compatibility in nanometre scale. In the ^{13}C cross-polarisation/magic-angle-spinning (CP/MAS) spectra, the chemical shift of the carbonyl group of poly(sodium acrylate) depends on the composition of the grafting samples, which indicated that starch and poly(sodium acrylate)

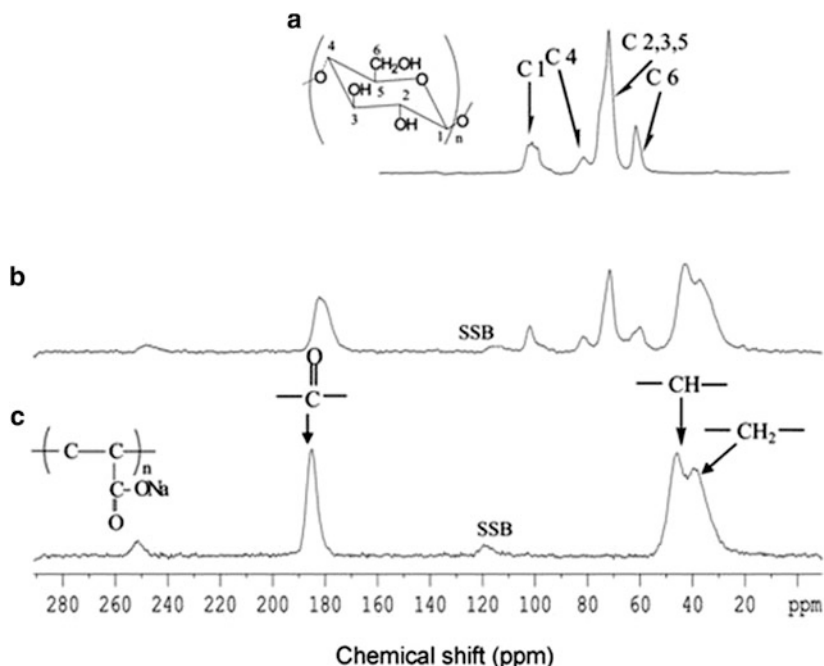


Fig. 3.9 ^{13}C CP/MAS spectra of the samples: (a) pure starch, (b) starch-g-poly(sodium acrylate) and (c) poly(sodium acrylate) [71]

components of the grafting samples exhibit better compatibility with each other than that of blended samples at molecular level.

Figure 3.9 shows the ^{13}C CP/MAS NMR spectra of pure starch (sample S), poly(sodium acrylate) (sample P) and starch-g-poly(sodium acrylate) (sample G-S30) at 25 °C. In Fig. 3.9a, the peaks at 94–104 ppm and 59–62 ppm are identified as C1 and C6 of pure starch, respectively, and the peak at 72 ppm is identified as C2, C3 and C5 overlapping lines. In Fig. 3.9c, the carbonyl carbon signal of pure poly(sodium acrylate) appears at about 180 ppm, and the peaks at 34 ppm and 44 ppm are identified as CH_2 and CH resonances, respectively. In Fig. 3.9b, the spectrum of starch-g-poly(sodium acrylate) shows combined feature of pure starch (Fig. 3.9a) and pure poly(sodium acrylate) (Fig. 3.9c). However, several significant chemical shifts of starch can be observed, which were attributed to the graft reaction between starch molecules and sodium acrylate monomers. A new shoulder peak appears on C6 peak of starch, indicating that a part of hydroxyl groups of C6 participated in graft reaction. The peaks at about 101 and 103 ppm of C1 belong to B-type crystal feature peaks of starch [71], and the peak at 102.5 ppm of C1 shows the existence of amorphous phase of starch [72, 73]. Comparing Fig. 3.9a with Fig. 3.9b, it is clear that graft copolymerisation of starch and sodium acrylate reduces the crystallinity of starch.

In order to investigate the difference of compounds structure before and after graft copolymerisation, the ^{13}C CP/MAS NMR spectra of the blend of starch/poly(sodium acrylate) and starch-g-poly(sodium acrylate) were analysed [70]. The peak at 180 ppm, which is linked to the carbonyl carbon of poly(sodium acrylate) component, shifts obviously to higher field with increasing starch contents in grafted copolymer (spectra for sample G-S40, G-S30, G-S20 and G-S15). This shift of the carbonyl carbon resonance is attributed to intermolecular hydrogen bonding between the hydroxyl groups of starch and the carbonyl groups in poly(sodium acrylate) component [74, 75].

3.4 Properties of Starch-g-Copolymers

Graft copolymerisation significantly alters the solution properties of starch. The viscosity, gelling characteristics and solution rheology, e.g. degree of pseudo plasticity, ion compatibility, etc., can be drastically altered through graft copolymerisation reaction [76]. High viscosity, thermal stability, biodegradability, good film forming properties and water absorption capacity are some of the properties shown by the graft copolymers of starch.

3.4.1 Water-Absorbing Property

Starch-graft-copolymers can be either water soluble [e.g. starch-g-poly(acrylamide)] or water insoluble [e.g. starch-g-poly(acrylonitrile)]. Copolymers of starch with hydrophobic grafts such as starch-g-poly(acrylonitrile) cannot be dispersed in water, but remain as grainy solids, even after prolonged heating. But these form smooth dispersions/or dissolve in solvents such as DMSO, DMF, etc. However, copolymers with water-soluble grafts swell in water at room temperature. These either dissolve or disperse to give smooth pastes when heated in water.

In general, the graft copolymers prepared from gelatinised starch, rather than granular starch, show very high water absorbency. Among the vinyl monomers, ACN, AM and AA have been frequently employed as the grafting monomer to obtain superabsorbents. Starch-graft superabsorbents have been prepared by graft copolymerising either with poly(ACN) and saponifying the resulting copolymer or with trimethyl aminoethyl acrylate chloride and methylene bis-acrylamide as cross-linking agent [77]. The water absorbency was found to decrease with an increase in the cross-link density. Alkali saponified starch-graft-copolymers can absorb more than several times of their weight of water and can act as superabsorbents.

Lu et al. [67] reported the synthesis of a superabsorbent/starch-graft-poly(potassium acrylate-co-acrylamide) by inverse suspension polymerisation. Surface cross-linking of the SAP particles significantly improves swelling capacity under pressure because the particle structure does not change. Here, special crosslinkers may be

necessary in order to obtain high swelling capacities under pressure. The percentage absorption capacity of the hydrogels of copolymers of mixtures of methacrylic acid and acrylamide onto allyl-modified maize starch was determined with distilled water and 0.9 % NaCl solution [26]. The highest percentage of absorption, 6,500 %, was achieved for the developed hydrogel containing allyl starch and acrylic monomer in a 1.7:1 w/w ratio and acrylic monomer, namely, methacrylic acid and acrylamide in a 3.2:1 w/w ratio.

The swelling of hydrogel depends on the carboxylic group content of the hydrogel product and ionic strength of the absorbing medium. Addition of some salts to the polymer solution leads to network contraction [67]. Because the repulsive carboxylate group on the polymeric chain was shielded by the bound cation, the osmotic pressure difference between the gel network and the external solution decreased. Therefore, the polyelectrolyte component in the gel cannot imbibe as much salt water as pure water. The swelling capacity of the copolymer gel is also found to depend on the pH. The water absorbency was low in a strongly acidic region, because the carboxylate side chains of the potassium acrylate in the gel became the carboxylic group, thus decreasing the charge density of anions on the network. However, the water absorbency increased with increase in pH value when its value was lower than pH 8.0. The reason is that the anions of base-hydrolysed acrylamide and the carboxylate group inside the network will increase with an increase of the pH. The water absorbency decreased with a further increase of pH value over 8.0 [67]. This is primarily due to the decrease of the osmotic pressure difference between the gel and external solution.

To develop starch-based hydrogels with greater starch content than synthetic components, synthesis of allyl starch and consequent grafting of the allyl starch were reported [26]. The highest percentage absorption capacity obtained was 6,500 % for the sample which contains allyl starch and acrylic monomer in the ratio 1.7:1 w/w and methacrylic acid and acrylamide in the ratio 3.2:1 w/w.

The swelling ratio (SR) of starch-g-PVA hydrogel increased with the increase of the molecular weight of grafted PVA [62]. The SR of starch-g-PVA hydrogel slightly decreased with increasing the number of freeze/thaw cycles, due to more physical cross-linking forming as a result of PVA crystallisation. The water uptake and moisture retainment values of starch-graft-copolymers were investigated by Çelik [33].

The swelling and diffusion characteristics of semi-interpenetrating polymer network (IPN) hydrogels composed of starch and random copolymer of poly (acrylamide-co-sodium methacrylate) were evaluated for different semi-IPN hydrogels prepared under various formulations [28]. The hydrogel networks density improved enormously as the crosslinker (methylene bis-acrylamide) concentration increased. The equilibrium swelling ratio (Seq) increased very slightly from 58.21 to 58.70 g/g, when the starch content increased from 0.25 to 0.50 g, but considerable increase in Seq value (68.23 g/g) was noticed when the starch content was 0.75 g. The percentage of hydrophilic character in graft copolymer increases with increasing chain of pendant poly(*N*-vinyl formamide) onto pregelled starch, thereby increasing swelling capability of graft copolymer [42]. The swelling of starch-g-

poly(acrylamide) was 39 g/g while the starch-g-poly(acrylamide-*co*-itaconic acid) with the IA content of 0.02–0.15 % mole gave the water swelling value in the range of 70–390 g/g [12].

The solubility of starch-graft-copolymers synthesised from *n*-alkyl acrylates and methacrylates (where alkyl = methyl, ethyl, butyl), *N*-methylol acrylamide, methacrylic acid and the like in various polar and non-polar solvents was found to be negligible [14]. Starch gelatinises in water at around 70 °C. However, the graft copolymers do not gelatinise even after heating at 100 °C, which further confirms the cross-linking of starch-graft-copolymers.

The solubility % of poly(*N*-vinyl formamide)-pregelled starch-graft-copolymer increases by increasing the graft yield up to a certain value and then decreases [78]. Lower solubility % is observed with the grafted samples having graft yield higher than 44.2 %. This can be explained as follows: (a) introduction of (*N*-vinyl-formamide) group as a hydrophilic groups into the molecular structure of pregelled starch up to 44.2 % leads to a decrease in hydrogen bonding between pregelled starch molecules which increases solubility %, and (b) further increase in the degree of grafting of poly(*N*-vinyl formamide)-pregelled starch-graft-copolymer leads to an increase in the molecular weight of the starch which adversely affects the solubility % of the grafted pregelled starch [79, 80].

3.4.2 Thermal Properties

3.4.2.1 Melting and Glass Transition Temperature

The two most important thermal transitions exhibited by polymers are the glass transition temperature, T_g , and the crystalline melting temperature, T_m . The glass point is the temperature at which amorphous polymer becomes elastomeric and flexible as the temperature is raised. The crystalline melting point is that point when the crystalline component loses coherence and long-range order. Since most polymers are rarely completely crystalline owing to chain entanglements, most crystalline polymers will show both a T_g and a T_m . The thermogram can be obtained using differential scanning calorimetry (DSC) technique. It is a very accurate way of evaluating the thermal properties of polymers, and it needs only a few milligrams of the polymer for analysis.

In the case of substances like starch which contains amorphous as well as crystalline regions, the midpoint of transition in the DSC curve is taken as the glass transition temperature. At this point majority of the molecules undergo phase transition. Glass transition temperature of starch-graft-copolymers are usually lower than native starch, since the monomer when grafted to starch acts as internal plasticisers and lower the T_g , making it easier for micro- or macro-level changes to occur.

The DSC thermograms of starch, virgin PE and PE-g-starch have shown that both area and intensity of the peaks have decreased significantly with increase in the

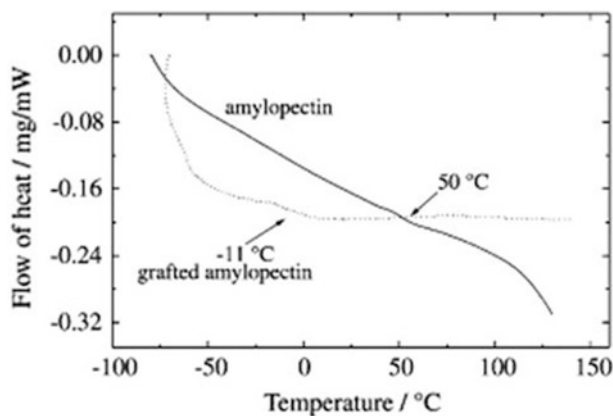


Fig. 3.10 DSC curves of pure and amylopectin-rich starch grafted with poly(propylene oxide) diisocyanate [81]

extent of grafting onto PE [19]. The heat of fusion has also decreased considerably with increase in the degree of grafting, which has indicated that grafted PE is less stable in comparison with the virgin PE. DSC studies of amylopectin-rich starch samples grafted with poly(propylene oxide) was carried out [81]. The DSC curves of the pure and grafted amylopectins showed that the glass transition temperature for pure amylopectin was about 50 °C and after grafting reaction T_g value dropped to -11 °C (Fig. 3.10). This T_g in grafted samples, which is lower than room temperature, is a highly relevant factor for the potential application of this material as solid electrolytes, since low T_g allows for greater chain mobility and, hence, improves solvation and ion conduction. The presence of a second endotherm in the DSC curves around 250 °C for the copolymers synthesised from acrylamide was reported earlier and this was attributed to the fusion of the crystallites [82].

The thermal transition and crystallisation of starch-g-poly(1,4-dioxan-2-one) copolymers were studied by means of DSC [83]. It was found that the graft structures of copolymers have obvious effects on the thermal and crystallisation behaviours. Because there were more defect sites in the crystalline phase originating from the short grafted chains of poly(1,4-dioxan-2-one) (PPDO), the crystal structure of the copolymers was much less perfect than that of PPDO.

3.4.2.2 ThermoGravimetric Analysis of Starch-Graft-Polymers

The grafting of vinyl monomers alters the thermal stability of starch and in most cases enhances it [13]. The thermal stability of graft copolymer can be compared at the onset temperature of decomposition and the percentage of weight loss for different stages of the decomposition. Pure starch shows a two-step characteristic thermogram, wherein the major weight loss (75 %) takes place in the second step within the temperature range of 233–368 °C; the temperature for a maximum

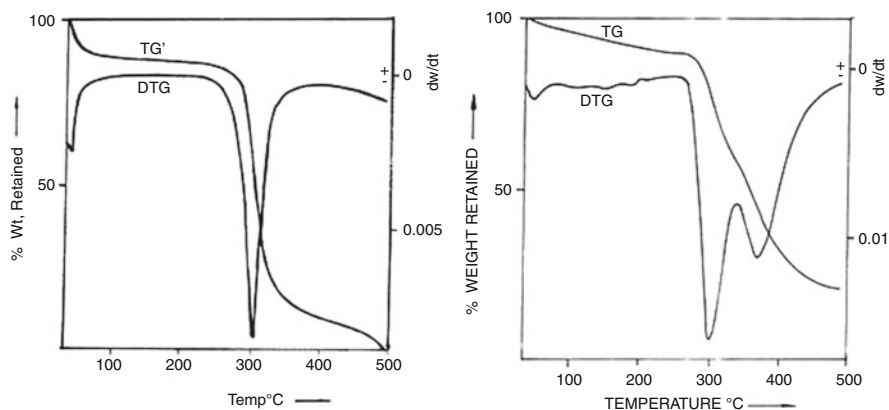


Fig. 3.11 Primary thermogram and derivatogram for (a) pure granular maize starch and (b) grafted starch with %G = 97.3 [82]

decomposition was 308 °C [82]. Athawale and Lele studied the thermal properties of native starch and graft copolymers of starch with poly(methacrylonitrile) (PMAN). Pure starch showed a characteristic three-step thermogram in thermogravimetric analysis (Fig. 3.11). The initial slight loss in weight was due to evaporation of absorbed moisture. The rapid decomposition occurred in the second stage resulting in the major weight loss of 76 %. The grafting of methacrylonitrile onto starch does not significantly alter the thermal stability of starch and the derivatogram exhibits the temperature for maximum decomposition for this stage as 309 °C. The final stage of decomposition was due to formation and evaporation of some volatile compounds and resulted in about 11 % weight loss. Poly(methacrylonitrile) shows two-stage decomposition pattern, the first stage (30–107 °C) was due to dehydration showing about 9 % weight loss, while about 53 % weight loss occurred in the second stage of decomposition in the temperature range of 259–492 °C. The char yield of 38 % was obtained at 496 °C. The third stage of decomposition was quite significant for the grafted samples with high % grafting and decomposed rather slowly up to 496 °C.

TGA/DTA thermograms of poly(ethylene) PE and PE-g-starch were obtained and the grafted membranes have shown multistep degradation of PE backbone and grafted starch [84].

Cassava starch was stable up to 275 °C. The maximum decomposition rate appeared at 375 °C [45]. For cassava starch-graft-poly(acrylic acid), which was further modified by esterification and etherification with poly(ethylene glycol) 4000 and propylene oxide, respectively, there were two stages of decomposition. The first was starch moiety decomposition, and the second was poly(acrylic acid) moiety decomposition. Then second decomposition stage started above 400 °C and ended at about 550 °C, giving an ash residue.

For LDPE, the curve was stable up to 350 °C and reached maximum decomposition at 505 °C. After blending with various contents of modified starch, the

decomposition onset temperature of plastic composite sheets was lower than for LDPE sheets (at about 300 °C). This was attributed to the decomposition of the modified starch composition. This observation suggests that the starch or modified starch blended LDPE plastics consume less thermal energy to start a decomposition process. It also implies that this type of blended material degrades easily in modified starch or starch [45].

The results of thermogravimetric analysis (TGA) technique employed to characterise the thermal properties of the obtained graft copolymers revealed that the percentage of the weight loss at the decomposition temperatures of starch, itaconic acid and acrylamide presented in the starch-g-poly[acrylamide-*co*-(itaconic acid)] thermograms. The weight loss can be used to calculate the grafting characteristics expressed as the percentages of add-on and grafting ratio [12].

Fares et al. [17] also reported a three different stage decomposition for starch in the thermograms with a major weight loss of 69 %, where the major weight loss occurred at the second stage within the temperature range of 263–336 °C at $T_{\max} = 316$ °C (Fig. 3.12). Poly(butylacrylamide) (BAM) homopolymer also showed three decomposition stages with major weight loss within the temperature range of 300–367 °C at $T_{\max} = 348$ °C. Starch-g-BAM copolymer shows two characteristic peaks within the temperature range of 263–332 °C and 332–400 °C with T_{\max} at 316 and 343 °C, respectively. The second and the third steps referred to starch and PBAM, respectively, providing clear evidence on grafting of PBAM chains onto starch. Up to 400 °C the total weight losses of starch and PBAM were 84.5 % and 67 %, respectively, whereas the total weight loss of starch-g-BAM copolymer was 72 %. Thus it was concluded that grafting of synthetic polymer which has higher degradation temperature (i.e. PBAM) onto natural polymer which has lower degradation temperature (i.e. starch) can lead to the formation more thermally stable copolymer (i.e. starch-g-BAM) than pure starch.

TGA thermograms showed that the thermal stability of starch increased as a result of grafting [33]. The thermal behaviour of starch, poly(ethyl methacrylate) (PEMA), St-g-PEMA and St-g-PEMA/sodium silicate (SS) were studied at room temperature at (28 ± 2 °C) by comparing their thermogram curves [69]. From the curves the temperature of decomposition (TD) was found to be 210 °C for starch, 230 °C for PEMA and 285 °C for St-g-PEMA/SS. As the sample St-g-PEMA/SS decomposes at high temperature so it has high thermal stability than other mentioned samples.

The thermal behaviour of pure starch, 7.7 % and 63.1 % poly(methacrylamide)-grafted starch, respectively, was studied by Celik [33]. The initial weight loss in pure and poly(methacrylamide)-grafted starch up to 100 °C was due to the loss of the absorbed moisture. The weight loss of pure starch started at 290 °C and reached a value of 91.39 % at 600 °C. The weight loss of 7.7 % and 63.1 % poly(methacrylamide)-grafted starch reached a value of 88.72 % and 82.95 % at 600 °C, respectively. At higher graft yield values, the decomposition temperature of poly(methacrylamide)-grafted starches was observed to increase. Thus, it was concluded that grafting of poly(methacrylamide) onto starch can lead to the formation of a more thermally stable copolymer than pure starch.

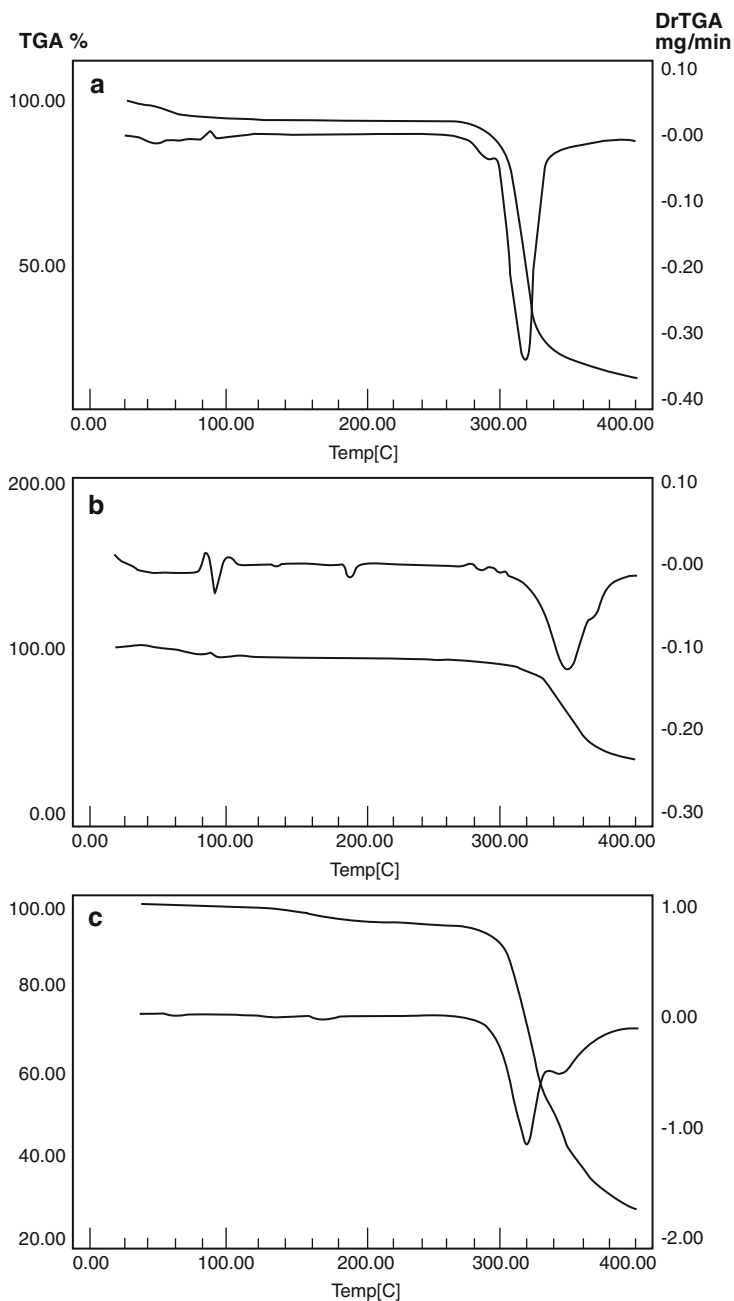


Fig. 3.12 TGA and differential TGA profiles of (a) pure starch; (b) pure PBAM; (c) starch-g-BAM copolymer (%GE = 33.0) [17]

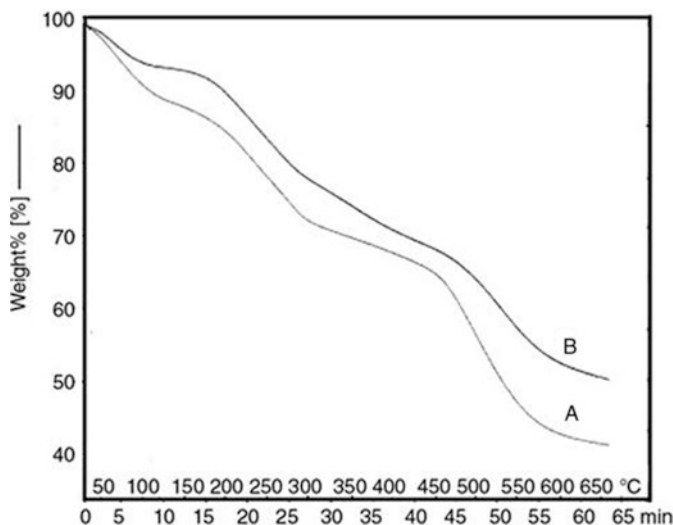


Fig. 3.13 TGA of (A) starch and (B) starch-graft-poly(acrylonitrile) [47]

Thermogravimetric analysis of starch and microwave-synthesised starch-graft-poly(acrylonitrile) showed that grafted starch was more thermally stable than the pure starch [47]. Up to 650 °C, 49 % loss in total weight was observed for grafted starch in comparison to 58 % weight loss in starch (Fig. 3.13). TG and DTA curves of graft copolymers of mixed monomers vinyl acetate and butyl acrylate onto corn starch confirmed the occurrence of graft copolymerisation, and showed that the thermal stability of starch copolymer was better than that of pure corn starch [30]. Thermal stability of cassava starch was reported to increase by grafting poly (acrylamide) onto it [85].

3.4.3 Biodegradability

Hydrogels prepared from only synthetic monomers are not expected to be biodegradable. Degradation is a desirable requirement of hydrogels. Glycosidic linkages in the polysaccharide chain are degradable by microorganisms and hydrolytic enzymes. Alpha amylase (1,4 - α -D-glucan glucohydrolase) is a well-known enzyme that hydrolyses (1 \rightarrow 4) linkages between α -D-glucopyranosyl residues in an endo action. Hydrolysis occurs in a random fashion at any (1 \rightarrow 4) linkage within the polysaccharide chain to rapidly reduce the molecular size of starch and the viscosity of starch solutions. Hence, attempts were obvious to prepare starch-based hydrogels in the last three decades [86]. Biodegradability of hydrogels of allyl starch, graft-copolymerised with methacrylic acid and acrylamide, was compared with starch under accelerated enzymatic conditions. After 6 h of enzyme

treatment, only 12 % starch remained intact in the case of pure starch, whereas in the case of hydrogels of grafted starch, it was 28 % and biodegradation of the hydrogel followed the same first-order kinetics as pure starch [26]. On degradation of starch with enzyme, the attached synthetic polymeric components with the degraded fraction also became water soluble.

A comparative biodegradation study of starch, PEMA [poly(ethyl methacrylate)] and starch-g-ethyl methacrylate/sodium silicate (St-g-PEMA/SS) was carried out by three different methods mentioned as follows: degradation in activated sludge, soil burial test and degradation by *Bacillus cereus* in culture medium [69]. It was found that St-g-PEMA/SS showed accelerated rate of degradation (by weight loss). But starch showed less amount of weight loss and there was very negligible amount of weight loss found in case of PEMA. As St-g-PEMA/SS has more netlike space than others, it holds up more water than others, as a result of which it is more biodegradable. In soil burial test, there was very low increase in the rate of weight loss in PEMA, for its hydrophobic nature. But in case of starch, there was slow rate of degradation up to 28 days and then gradually up to 1 year some improvement in weight loss was found. For St-g-PEMA/SS, as it is a superporous material and having networks in it, it can hold up more water which helps microorganisms to grow easily. From the experiment it was confirmed that St-g-PEMA/SS degraded at a faster rate than PEMA and starch by *B. cereus*.

3.5 Applications of Starch-Graft-Copolymers

Starch-graft-copolymers find various applications in industry as flocculants, in wastewater treatment for heavy metal ion removal, as mulch films, in oil drilling, in biodegradable polymers and in superabsorbents. Acrylamide-based water-soluble graft copolymers are applied in numerous areas such as the petroleum and paper industries, in environmental protection and as biomaterials [87, 88]. Starch-graft-copolymers are also used in the manufacture of moulded plastics, ion-exchange resins and plastic films and in cosmetics.

3.5.1 Application as Ion-Exchange Resins and Flocculating Agents in Water Treatment Industry

In the present scenario of industrialisation and problems related to industrial wastewater treatment, managing world's water resources has become more complex than ever. Wastewater is comprised of approximately 99 % water. Suspended solids, which make up the remaining 1 %, contain soluble and insoluble substances such as nitrates, phosphorous and heavy metals present in varying concentrations, and bacteria, viruses and other microorganisms. Heavy metals such as Pb(II), Cu

(II), Hg(II), Ag(I) and Cr(VI) from industrial effluents, due to their high toxic effect on living organisms, are highly harmful to human health and to ecological systems.

Most of the water-soluble polymers in the water treatment industry are presently based on acrylamide and the demand for acrylamide polymers is on rise [89, 90]. Chemical precipitation, reverse osmosis, electrodialysis, solvent extraction and ion exchange are some of the methods used for removal of heavy metals from all kinds of wastewater. However these are relatively expensive, and therefore, there is research interest in using alternative low-cost and effective methods for water treatment. Adsorption of heavy metal ions on water-insoluble stationary phases such as functionalised polymers, silica and activated carbon with chelating groups has been a widely investigated topic. Recently, adsorbents based on natural products and their derivatives deserved particular attention. Natural polysaccharides such as starch, gums, glues, alginate, etc. function as bridging flocculants. It has been established that by grafting polyacrylamide branches on polysaccharides, the dangling grafted chains have easy approachability to the contaminants. Among the grafted guar gum, xanthan gum, carboxy methyl cellulose and starch, grafted starch flocculates better. As starch-g-polyacrylamide has fewer and longer branches, it provides better flocculating performance. Starch-g-polyacrylamide copolymers are useful as flocculants for clays and coal refuse slurries.

Enhanced functionality can be imparted to starch by grafting suitable acrylic polymers onto it which will allow it to be more effective in flocculation, dispersion and other applications such as retention aids in paper, dry strength additives, etc. [76]. Polyelectrolyte side chains can be introduced onto suitable substrates by either grafting an ion-containing monomer or a suitable monomer which can then be transformed to an electrolyte by a simple chemical reaction. An example of the latter is where methyl methacrylate or acrylonitrile can be grafted onto starch and then transformed by alkaline hydrolysis to acrylic acid or methacrylic acid grafts. Vinyl pyridine or dimethyl aminoethyl methacrylate can be grafted and then subsequently quaternised [76]. The grafted amylopectin is found to be a suitable flocculant for various kinds of industrial effluents. Many researchers have carried out work on starch-based flocculants [91–94]. Synthesis and applications of graft copolymers of polyacrylamide onto natural polymer like CMC [95], guar gum [96, 97], xanthan gum [98], starch [95] and amylose [99]. Among the graft copolymers with various polysaccharides, starch-g-polyacrylamide was the best in performance [100]. Karmakar [99] studied the flocculation and rheological studies of starch-g-polyacrylamide and amylose-g-polyacrylamide and starch-g-polyacrylamide was found to be the better in performance. When the performance of amylopectin-g-polyacrylamide was investigated by Rath and Singh [101], it was found to perform better than any other graft copolymers and various commercial flocculants.

Hydrolysed starch-graft-poly acrylonitrile (HSPAN) functions as ion exchangers and useful in heavy metal removal from waste waters [102]. It can be potentially used for treatment of sewage sludge for dehydration and solidifying waste and also to absorb heavy metal ions such as Cr^{3+} and Co^{2+} . The potential of the graft copolymers of pregelled starch–methacrylamide for heavy metal ion removal was

assessed through measurements of critical properties such as removal of different heavy metal ions as well as durability [50]. The amount of heavy metal ions removed was higher at higher levels of grafting. The poly(methacrylamide)-pregelled starch-graft-copolymers were more effective in removing Hg^{+2} than all other metal ions in question and follow the order: $\text{Hg}^{+2} > \text{Cu}^{+2} > \text{Zn}^{+2} > \text{Ni}^{+2} > \text{Co}^{+2} > \text{Cd}^{+2} > \text{Pb}^{+2}$.

An investigation was undertaken regarding the adsorption behaviours of copper (II) and lead(II) ions from aqueous solutions by cross-linked starch-graft-copolymers with aminoethyl groups, which were synthesised by grafting 2-aminoethyl methacrylate onto cross-linked starch [103]. The dynamic adsorption method was utilised to evaluate absorbability of graft copolymer under various parameters such as metal ion concentration, adsorption time, grafting percentage and adsorption temperature. The adsorption time reaching equilibrium for Cu(II) and Pb(II) was found to be 2 h and 1 h, respectively. The adsorption capacity increases with the increasing graft percentage and metal ions concentration. For the starch-graft-copolymer with grafting percentage of 75.5 %, when the metal ions concentration was about 5.0 mmol/L, the saturation adsorption capacity of Cu(II) and Pb(II) is 21.05 mg/g and 144.08 mg/g (dry weight), respectively, and its desorption percentage is about 95 %.

Eight levels of poly(*N*-vinyl formamide)-cross-linked pregelled starch-graft-copolymers (graft yields in the range 11.5–55.3 %) were used for removing different heavy metal ions from their solutions at a concentration of about 200 ppm [42]. The different heavy metal ions used were Cu^{+2} , Pb^{+2} , Cd^{+2} and Hg^{+2} . The residual amount of heavy metal ions removed is governed by the %graft yield as well as the nature of metal ion used (Fig. 3.14). So, when the graft yield increased from 11.5 to 55.3 % the residual removal of heavy metal increased irrespective of the nature of metal ion used. It was also observed that poly(*N*-vinyl formamide)-cross-linked pregelled starch-graft-copolymers were more effective in removing Hg^{+2} than the other metal ions and followed the order: $\text{Hg}^{+2} > \text{Cd}^{+2} > \text{Pb}^{+2} > \text{Cu}^{+2}$. The relative atomic size, ability for metal ion to interact with the polymer, metal ion charge density and reactivity of the metal ion affect the adsorption behaviour.

An investigation was carried out to study the adsorption of basic violet 7, basic blue 3, direct yellow 50 and acid red 37 from aqueous solutions by the water-insoluble modified starch containing amidoxime groups and rice straw. The effects of initial pH of the solution, pollutant concentration and treatment time on the adsorption were studied and it was found that the maximum adsorption was at 1:2 (starch/acrylonitrile) at irradiation dose 30 kGy [46].

By grafting flexible poly(acrylic acid) chains onto the polysaccharide backbone, it is possible to develop efficient and shear stable polymers for water treatment in industrial effluents and mineral processing. In the flocculation of bauxite red mud suspensions, starch-g-poly(acrylic acid) can be effectively used. A synergetically acting new flocculant was synthesised by graft copolymerisation of corn starch acrylamide and sodium xanthate using epichlorohydrin as cross-linking agent and CAN as polymerisation initiator which exhibits excellent flocculation and capacity

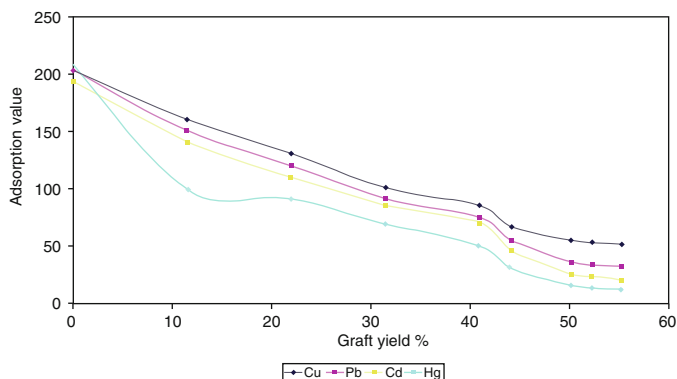


Fig. 3.14 The relation between changing the extent of grafting on the adsorption % of different heavy metal ions in removal [42]

to trap heavy metal ions [104]. An amphoteric starch-graft-polyacrylamide (S-g-PAM) was prepared by inverse emulsion polymerisation, subsequent hydrolysis reaction and Mannich reaction and evaluated for flocculation efficiency. The application test showed that the results of treatment of several kinds of industrial wastewater by amphoteric S-g-PAM were better than those treated with cationic polyacrylamide (PAM), hydrolytic PAM and amphoteric PAM [31].

The reason for better flocculating power of the graft copolymers over the linear polymers may be explained by Singh et al. [105] as follows: essentially polymer bridging occurs because segments of a polymer chain absorb on different particles, thus linking the particles together. For effective bridging to occur there must be sufficient chain lengths, which extend far enough from the particle surface to attach to other particles. In case of linear polymers, the polymer segments attached to the surface project into the solution as tails, or form part of loops [106]. Thus they can form bridges between the colloidal particles to form flocs (Fig. 3.15). But for the graft copolymers, the grafted chains can easily bind the colloidal particles through bridging to form flocs and hence act as more effective flocculating agents. Since in amylopectin-g-polyacrylamide the polyacrylamide branches are grafted on backbone as well as on amylopectin branches, this provides better approachability of grafted polyacrylamide branches to contaminants.

3.5.2 Application in Biodegradable Plastics and Films

Another important area of application of grafted starches is in biodegradable plastics. Man-made synthetic polymers such as PCL, PLA, PHB and PHBV are used in a wide array of applications such as food packaging, films, fibres, tubing, pipes and like. Many objects in daily use from packing, wrapping and building materials include half of all polymers synthesised. Graft copolymerisation of starch

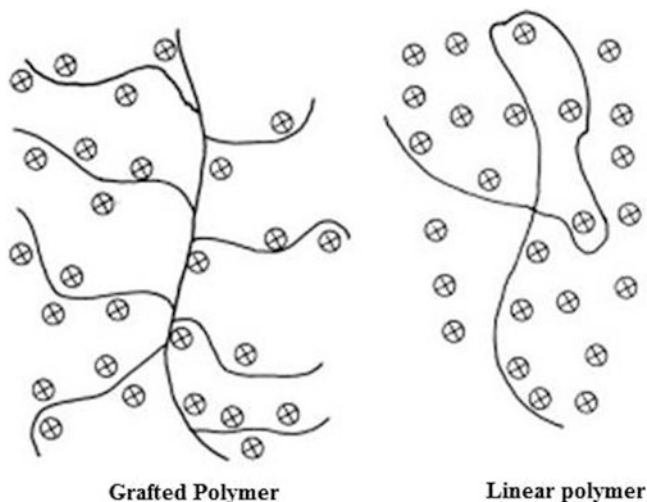


Fig. 3.15 Approachability of grafted and linear polymers to the particles in an effluent [106]

with acrylate esters, methacrylate esters and styrene results in thermoplastic grafts and these are used in the preparation of starch-filled plastics because hydrophobic grafted branches will make a graft copolymer more compatible with the plastic matrix than unmodified starch. Plastics filled with the graft copolymers were easily attacked by the common soil microorganisms and these plastics also exhibit higher tensile strength and better appearance than those filled with unmodified starch. One of the most promising polymer for this type of use is starch-g-poly(methyl methacrylate-*co*-acrylonitrile). Extrusion processing of granular starch-g-poly(methyl acrylate) yields tough, leathery, translucent plastics, which maintain their integrity when immersed in water for prolonged period of time.

Starch-graft-poly(acrylonitrile) and starch-graft-polymethacrylate can be extruded for use as expanded packaging material or foamed protective packaging material that can replace traditional expanded “polystyrene peanuts” [107]. Such starch-based loose fills contain a variety of biodegradable polymers and additives that will improve resiliency and compressibility and aid in processing. Low shear conditions during extrusion produce loose fills that are both brittle and heavy, regardless of the type of starch used. The process of the disordering of amylose and amylopectin chains through the melting of crystallites taking place during heating of starch with limited amounts of water is called “destructured starch” [108]. The latter is useful in the development of extrusion-blown films from starch and poly(ethylene *co*-acrylic acid) graft copolymers. As much as 50 % of the weight of starch can be incorporated into such composites, yet still retain acceptable properties.

The use of such biodegradable films for agricultural mulching controls weeds conserves soil moisture and heat for early cropping, and reduces nutrient leaching. As the starch portion is utilised by the organism, the available surface area of the

degraded copolymer is increased, which in turn enhances further microbial and oxidative degradations [109]. Halley et al. [110] have developed starch-based plastics for use as biodegradable mulch films based on low-cost starch-based biodegradable polymers blended with higher cost, higher performance polyester polymers. These films showed good strength, water resistance and biodegradability. Maharana and Singh [19] have successfully developed and characterised biodegradable polyethylene by graft copolymerisation of starch and tested the biodegradability.

3.5.3 Application as Superabsorbent Polymers

Superabsorbent polymers (SAPs) are unique group of materials that can absorb over a hundred times their weight in liquids and the absorbed liquid can be released slowly when put in dry air to maintain the moisture of the environment. Superabsorbents were first developed by the United States Department of Agriculture in the late 1960s (<http://www.nexant.com>). Early commercial versions of SAPs were called “superslurpers” which were in the form of starch/acrylonitrile/acrylamide-based polymers.

Application of superabsorbent hydrogels is vast which involves use in agriculture, control delivery systems and perfumes, soft contact lenses, artificial lenses, artificial vitreous and materials used in plastic surgery. Disposable diapers and sanitary napkins use hydrogel as superabsorbent polymer. The SAP hydrogels with the ability to absorb urine and blood are used in hygiene products such as in baby diapers and feminine incontinence products, and they account for most of the commercial SAP use. Over the next decade, worldwide SAP demand is forecast to exhibit growth of 3.6 % per year. This is a result of rising demand for disposable diapers, primarily in countries with rising disposable incomes and low current penetration rates of SAPs.

There are two primary types of superabsorbent polymers: starch-graft-polymers and those based on cross-linked polyacrylates. Mostly, they are cross-linked copolymer of acrylates and acrylic acid and grafted starch–acrylic acid polymer that are prepared by reverse suspension and emulsion polymerisation, aqueous solution polymerisation and starch graft polymerisation. Alkaline hydrolysis of starch-graft-polyacrylonitrile (SPAN) led to the first commercial SAP. The product, HSPAN, was developed in the 1970s at the Northern Regional Research Laboratory of the US Department of Agriculture and patents were licensed to General Mills Inc. among others [111]. It finds a number of agriculture applications. It can be used as seed coating to increase the rate of germination by absorbing and holding the water on seed surface. It is required in small amounts and the recommended quantity is about 1 lb/100 lb of seed [102]. It can be applied as a gel slurry to the root zone of plants before transplanting to prevent roots from drying, to reduce wilting and thereby to improve the plant survival. Another area of application of HSPAN is as a soil additive to improve the water holding capacity for different

types of soils. In agriculture and horticulture, it is being used as plant growth medium to improve the water retaining property of sandy soil and promotes more efficient germination of seeds and plant growth [112]. It can be used as tackifier in hydro-mulching along with aqueous slurry of straw, wood fibres or similar materials.

The water absorption of the saponified cassava starch-graft-poly(acrylamide) and/or poly(acrylic acid) in salt and buffer solutions of different ionic strengths was also measured, from which the superabsorbent properties are found to be pH sensitive [44]. The starch-graft-copolymers of acrylamide and acrylic acid give higher water absorption than the starch-graft-copolymers of either acrylamide or acrylic acid alone. The porosity of the saponified starch-graft-copolymers prepared by the acrylamide/acrylic acid ratios of 70:30 and 50:50 was much higher than the porosity of copolymers in terms of fine networks. Ionic strength and multi-oxidation states of the saline and buffer solutions markedly decreased the water absorption of the saponified cassava starch-grafted superabsorbent polymers.

Polymer-grafted sago starch has been further modified by reacting with hydroxylamine to obtain derivatives having the property of high water absorption (192 g water/g material at 31 % starch in the absorbent) [113]. Such products are useful in feminine napkins, disposable diapers, water blocking tapes, medicine and agriculture, where water absorbency or water retention is important. Because of higher equilibrium water content of these IPN hydrogels, they are promoted as novel biomaterials in biomedical/pharmaceutical technology or as moisture maintenance materials in agriculture/horticulture fields.

Lu et al. [67] showed that the superabsorbent/starch-graft-poly(potassium acrylate-co-acrylamide) synthesised by inverse suspension polymerisation has a good compressive strength and keeps the shape of particles after absorbing water. After mixing with soil it does not become sticky, and the loose structure can better retain air. It is fit to retain water in soil.

Methods of production and application of a superabsorbent based on starch-graft-copolymers, having particle sizes useful for agricultural applications, have been disclosed by Doane and Doane [114]. The superabsorbent applied to field crops provided excellent anti-crusting properties, increased seed germination and stand, increased crop growth, increased yields and reduced water requirements [114].

Superabsorbents comprising the graft polymer of acrylonitrile and AMPS onto starch were prepared using a manganic pyrophosphate redox initiation system [115]. The addition of AMPS results in a gradual saponification time decrease for the graft polymer and then the total synthesis time decrease of superabsorbents. The effect of KOH volume, KOH concentration and saponification temperature on the water absorbency of superabsorbent was investigated using response surface methodology (RSM). The maximum response at the optimal saponification conditions can be obtained. The water absorbency was 1,345 g/g dry superabsorbent, using the following saponification conditions: KOH volume 203.7 mL, KOH concentration 0.51 mol/L and saponification temperature 92.6 °C. The shortest saponification time is 17 min, and then the total synthesis time of superabsorbents is 2.5 h.

A new superabsorbent composite polymer (SAP) has been prepared by graft copolymerisation reaction using starch, ethyl methacrylate (EMA), benzoyl peroxide (BPO) as initiator and sodium acrylate as cross-linking agent [69]. The composite doped with sodium silicate exhibits higher water absorbency as the silicate can well disperse in the water and enter into the network structure of the composite, thereby increasing the porosity of the composite. Sodium acrylate plays an important role as the crosslinker forming a network structure of the superabsorbent composite.

Talaat et al. [116] reported a new process design features of a multi-component fertilising starch acrylic SAP with relevant techno-economic indicators. After preparation of hydrolysed starch-g-polyacrylonitrile (HSPAN) superabsorbent with N content of 2.1 %, the authors simply produced a fertilising base as a mixture composed of 65–70 % corn starch, 28–33 % urea and 2 % of other ingredients as conventional salts. The product (ESRF) was prepared via sequential addition and mixing of the ingredients followed by controlled drying and size reduction procedures, and it contained certain amounts of N (14 %), P (5.6 mg/g), K (9 mg/g) and Zn (0.65 mg/g). A fertilising slow release blend (HESRF) was developed by appropriate mixing of HSPAN and ESRF (ratio 1:5). A plant with a capacity of 10 metric tons/day is estimated to produce HESRF product with an approximate price of 770\$/ton.

The new process design features of a multi-component fertilising high swelling hydrogel were reported by Talaat et al. [116]. The hydrogel was prepared in two steps including grafting of starch with acrylonitrile followed by saponification of the produced graft. Preliminary agricultural experiments using in house pots showed an excess of seed/grain yield for faba and wheat crops by about 80 % and 116 %, respectively, as compared to the normal fertilising treatment. Slow release experiments manifested characteristics of slow release pattern for the developed fertilising blend (HESRF) and HSG component seems to regulate zinc and potassium release probably through ion-exchange component. The prepared fertilising base (ESRF) contained 65–70 % starch, 28–33 % urea and 2 % of other ingredients (zinc, potassium and phosphorous). Preliminary cost estimates were conducted for a small-scale industrial production facility (10 ton/day). The estimated cost of HESRF is about 770\$/ton. A suspension of starch-based SAP particles was combined with a liquid fertiliser solution to use as fertiliser for soil amendments [117].

3.5.4 Oilfield Applications

An important area of application of water-soluble starch-graft-copolymers is in oil drilling. To promote the utilisation of starch in oilfield the grafting of various vinyl monomers onto starch substrate has been a subject of extensive investigation. Graft copolymers having starch as the central chain with grafted side chains of acrylamide or acrylamide–acrylic acid are employed in preparing highly viscous aqueous solutions that are particularly useful in oil recovery from subterranean wells. Zhang

Table 3.1 Role of different grafted starches in oilfield applications [118]

Grafted starch	Application
Starch-g-poly(acrylamide)	1. Controlling filtrate loss for drilling muds 2. Increasing viscosity of drilling muds 3. Modifying viscosity in displacement fluids for enhanced oil recovery (EOR)
Oxidised starch-g-poly(acrylamide)	Modifying viscosity in displacement fluids for EOR
Soluble starch-g-poly(acrylamide)	Modifying viscosity in displacement fluids for EOR
Starch-g-poly(sulphomethylated acrylamide)	1. Controlling filtrate loss for drilling muds 2. Increasing viscosity of drilling muds
Pregelatinised starch-g-poly (acrylonitrile)	Reducing filtrate loss for drilling muds
Starch-graft-copolymer with cationic allyl monomer	Inhibiting hydration of clay and shale
Starch-graft-copolymer with acrylamide and vinyl alcohol	1. Controlling filtrate loss for drilling muds 2. Increasing viscosity of drilling muds

[118] reviewed the applications of starch and their derivatives in oilfield applications in China. The role of these polymers in oil drilling is multifaceted depending on the properties (Table 3.1). Most of the starch-graft-copolymers have better resistance to temperature and shear rate than hydrolysed poly(acrylamide) and have potential application in enhanced oil recovery.

Water-soluble starch-graft-copolymers are mainly used for controlling filtrate loss for drilling muds, modifying viscosity in displacement fluids and inhibiting the hydration of clay and shale [119, 120]. It was found that grafted starch could provide more effective shale inhibition than anionic or non-ionic modified starches, showing potential as a shale- or clay-hydration inhibitor for oilfields. Acrylamide is the widely used monomer for this application. Grafting of shear degradable poly (acrylamide) onto the rigid starch backbone provides fairly shear stable systems. Monomers such as acrylamide and vinyl alcohol have been grafted onto starch substrate resulting in non-ionic grafted starches having possible use as drilling mud additives. A copolymer was synthesised by graft copolymerisation of starch with acrylamide and 2-acrylamido-2-methylpropanesulfoacid for oil recovery enhancement [121]. When using 0.2 % of the grafted starch [S-g-P(AM-co-AMPS)] as the flooding agent, a higher enhanced oil recovery rate was obtained than with hydrolytic polyacrylamide (HPAM).

Starch-grafted polyacrylamide copolymers were prepared and their rheological properties, either in water or in water-based muds, were investigated Eutamene et al. [122]. Compared to the non-modified starch, starch-grafted polyacrylamide copolymers behaved as shear-thinning and salt resistant, and their rheological properties are stable with time. The grafted starches as prepared above were also added to water-based mud and the rheological properties of the resulting muds were determined under oil-well conditions. Grafted starches, having high AM contents, were more efficient in decreasing the filtrate volume, and increasing the plastic viscosity of the muds, when compared to PAC-L, a modified cellulosic polymer used in the filtration control of most water-based muds.

3.5.5 *Application as Textile Sizing Agents and Thickeners*

Other fields of application include textile/cotton yarn sizing [123], thickener for aqueous systems, thickener for printing cotton fabrics with reactive dyes [27] and to increase the dry tensile strength of paper hand sheets prepared without clay filler. Saponified starch-g-poly(vinyl acetate) can be used as a sizing agent for cotton, rayon and polyester yarns.

Characterisations of the poly(*N*-vinyl formamide)-pregelled starch-graft-copolymers with respect to swelling capacity, solubility %, metal ion uptake and suitability as a sizing agent for cotton textiles were investigated [42]. The starch-graft-copolymers and original pregelled starch was applied to light cotton fabrics to see their suitability for temporary improvement of the physico-mechanical properties of cotton textiles. Fabric samples sized with poly(*N*-vinyl formamide)-pregelled starch-graft-copolymers acquire tensile strength, elongation at break and abrasion resistance, which exceeds that of fabric sized with original pregelled starch. Fabric samples sized with grafted starch-graft-copolymers having different graft yields ranging from about 11.5 to 55.3 % showed higher tensile strength and abrasion resistance by increasing the graft yields within the range studied, while on the other hand, elongation at break was approximately unaltered.

3.5.6 *Graft Copolymers in Medical Applications*

Hydrolysed starch-graft-acrylic acid when used as micro-hydrogel in surgical dressing helps to maintain a relatively constant temperature on application to skin [124]. Yamamoto et al. [125] have described the manufacture of a wound dressing comprising of (1) a supporting layer, (2) a water absorbable or swellable layer consisting of starch-graft-acrylic acid copolymer and (3) a separable layer. The dressing acts as barrier for microorganisms. A transdermal therapeutic system with excellent storage stability and capacity to control the release rate of drugs contained the hydrogels as one of its essential component. It consists of a rubbery adhesive and microcapsule containing a water-soluble wall material, encapsulating drugs and a water-absorbing resin powder such as starch grafted with poly(acrylic acid) as core material [126].

A silicone polymer-grafted starch microparticle system was developed that was efficacious both orally and intranasally [127]. Unlike most other microparticle systems, this system does not appear to retard the release of antigen or to protect antigen from degradation. The results indicate that a unique physiochemical relationship occurs between protein antigen and silicone in a starch matrix that facilitates the mucosal immunogenicity of antigen. This leads to predominance of Th2 antibody response. This microparticle system may be advantageous for the delivery of small quantities of antigen, especially intranasally, and may be useful for the induction of oral tolerance.

Non-irritant bioadhesive drug release systems based on starch–acrylic acid graft copolymers were developed for buccal application [128]. The release rate of theophylline depended on the ratio of starch to acrylic acid and on the presence of cations in the graft copolymers, but was practically not affected by the pH of the dissolution medium nor by the type of starch used (corn, rice or potato). The release behaviour of the graft copolymers was found to be non-Fickian, suggesting that the release was controlled by a combination of tablet erosion and the diffusion of the drug from the swollen matrix. Incorporation of divalent cations into the graft copolymers led to a significant decrease in swelling erosion of the tablets as well as a substantial retardation of drug release. Highest work of adhesion was obtained with graft copolymers containing calcium ions as well as longer time of adhesion on dog's gingival.

Two anti-inflammatory model drugs, 5-aminosalicylic acid (5-ASA) and salicylic acid (SA), were entrapped in the nanogels prepared by freeze drying the hydrogel of poly(methacrylic acid) grafted onto carboxymethyl starch and the *in vitro* release profiles were established separately in both enzyme-free simulated gastric and intestinal fluids (SGF and SIF, respectively) [129]. The drug release was found to be faster in SIF. The drug release profiles indicate that amount of drug release depends on their degree of swelling, and cross-linking. The size and the nature of the incorporated drug were reported to play a very important role in determining the efficiency of its release from the carrier and an increase in the molecular size of the drug or PBDs reduces the drug release rate

Nowadays, graft copolymers are being used as an interesting option when developing a direct compression excipient for controlled release matrix tablets. Polysaccharide-based graft copolymers are of great importance to develop various stimuli-dependent controlled release systems [43]. A series of acrylic monomers–starch-graft-copolymers were prepared by ceric ion initiation method by varying the amount of monomers viz. acrylic acid (AA), methacrylic acid (MA) and methyl methacrylate (MMA) [130]. The release rate of paracetamol as a model drug from these graft copolymers as well as their blends was studied at two different pH 1.2 and 7.4 spectrophotometrically. The release of paracetamol in phosphate buffer solution at pH 1.2 was insignificant in the first 3 h for St-g-PAA- and St-g-PMA-graft copolymers, which was attributed to the matrix compaction and stabilisation through hydrogen bonding at lower pH. At pH 7.4, the release rate was seen to decrease with increase in add-on. The tablet containing poly(methyl methacrylate) (PMMA) did not disintegrate at the end of 30–32 h, which was attributed to the hydrophobic nature of PMMA. The study indicated that starch-graft-copolymers be used as excipients in colon-targeting matrices.

Graft copolymers of ethyl methacrylate (EMA) on waxy maize starch (MS) and hydroxypropyl starch (MHS) were synthesised by free radical polymerisation and alternatively dried in a vacuum oven (OD) or freeze dried (FD) [131]. The graft copolymers present mainly a hydrophobic character and lead to more amorphous materials with larger particle size and lower apparent density and water content than carbohydrates (MS, MHS). Tablets obtained from graft copolymers showed higher crushing strength and disintegration time than tablets obtained from raw

starches. This behaviour suggests that these copolymers could be used as excipients in matrix tablets obtained by direct compression and with a potential use in controlled release. It was observed that physical blends of starch-graft-copolymers offer good controlled release of drugs, as well as of proteins and present suitable properties for use as hydrophilic matrices for colon-specific drug delivery [132].

Large numbers of carboxylic functional groups were introduced onto CMS by grafting with polymethacrylic acid (PMAA) [133]. Free radical graft copolymerisation was carried out at 70 °C, bis-acrylamide as a cross-linking agent and persulphate as an initiator. Equilibrium swelling studies were carried out in enzyme-free simulated gastric and intestinal fluids (SGF and SIF, respectively). The drug release was found to be faster in SIF. The drug release profiles indicate that amount of drug release depends on their degree of swelling, and cross-linking.

Well-defined polysaccharides-graft-poly(p-dioxanone) (SAn-PPDO) copolymers were successfully synthesised via the ring-opening polymerisation of p-dioxanone (PDO) with an acetylated starch (SA) initiator and a Sn(Oct)₂ catalyst in bulk [134]. The in vitro degradation results showed that the introduction of SA segments into the backbone chains of the copolymers led to an enhancement of the degradation rate, and the degradation rate of SAn-PPDO increased with increase of SA wt%. Microspheres with an average volume diameter of 20 µm, which will have potential applications in controlled release of drugs, were successfully prepared by using these new copolymers.

3.5.7 *Miscellaneous Applications*

Starch-graft-copolymers with tailor made properties find potential applications in various other fields also. Graft copolymers such as HSPAN can be used as a dehydrating agent for organic solvents such as ethanol–gasoline mixtures and aqueous solutions of polymers such as proteins. It has potential application as an agar substitute in tissue culture procedures. Film prepared from HSPAN can be used as composite membranes for molecular separations.

Starch-based wood adhesive was prepared by emulsion synthesis of graft copolymers of mixed monomers viz., vinyl acetate and butyl acrylate onto corn starch with superior property and low cost [30]. The adhesive is white or cream white emulsion paste and has excellent emulsive properties and high temperature stability. All properties of starch-based wood adhesive can meet the national standard HG/T2727-95 of polyvinyl acetate wood adhesive, and the compressive shear strength outdistances the national standard especially Wu et al. [30].

Starch-g-polymer can be used as an effective compatibiliser for starch-based blends [11, 135, 136]. PCL and PLA are chemically bonded onto starch and can be used directly as thermoplastics or compatibiliser. The graft-copolymers, starch-g-PCL and starch-g-PLA, can be completely biodegraded under natural conditions and exhibit improved mechanical performances. To introduce PCL or PLA

segments onto starch, the ring-opening graft polymerisation of ϵ -caprolactone or L-lactide with starch is carried out [137–140].

3.6 Conclusions

Starch is found to be a very good substrate for copolymerisation with other monomers to develop products with properties suited for specific applications. Starch-graft-copolymers are synthesised by the grafting reaction of vinyl monomers onto starch by free radical initiated polymerisation reaction. Ceric ammonium nitrate is the commonly used free radical initiator. Other systems like potassium or ammonium persulphate, potassium permanganate–acid system, Fe^{2+} –hydrogen peroxide, bromate/cyclohexanone redox system, etc., are reported for initiation. Irradiation by microwaves or γ -rays is another mode of free radical initiation for grafting reaction. Starch-graft-copolymers are characterised by determining percentage grafting or % add-on and structural characterisation using various instrumental techniques like FTIR, SEM, XRD, DSC and TG. Starch-g-copolymers find potential application as flocculants, in wastewater treatment for heavy metal ion removal, as mulch films, in oil drilling, in biodegradable polymers and in superabsorbents. These are also gaining increasing importance in the manufacture of moulded plastics, ion-exchange resins and plastic films and in cosmetics.

References

1. Tharanathan RN (1995) Polysaccharide gums of industrial importance—a review. *J Sci Ind Res* 54:512–523
2. Tharanathan RN (1995) Starch—the polysaccharide of high abundance and usefulness. *J Sci Ind Res* 54:452–458
3. Ramesh M, Mitchell JR, Harding SE (1999) Amylose content of rice starch. *Starch/Stärke* 51:311–313
4. Tomasik P, Schilling CH (2004) Chemical modification of starch. *Adv Carbohydr Chem Biochem* 59:175–403
5. Athawale VD, Lele V (2000) Synthesis and characterization of graft copolymers of maize starch and methacrylonitrile. *Carbohydr Polym* 41:407–416
6. Athawale VD, Lele V (1998) Graft copolymerization onto starch. 3: grafting of acrylamide using ceric ion initiation and preparation of its hydrogels. *Starch/Stärke* 50:426–431
7. Athawale VD, Lele V (1998) Graft copolymerization onto starch. II. Grafting of acrylic acid and preparation of its hydrogels. *Carbohydr Polym* 35(1–2):21–27
8. Athawale VD, Rathi SC, Lele V (1998) Graft copolymerization onto maize starch. I. Grafting of methacrylamide using ceric ammonium nitrate as initiator. *Eur Polym J* 34(2):159
9. Khalil MI, Bayazeed A, Farag S, Hebeish A (1987) Chemical modification of starch via reaction with acrylamide. *Starch/Stärke* 39:311–318
10. Varma K, Singh OP, Sandle NK (1983) Graft-copolymerization of starch with acrylamide, 1. *Angew Makromol Chem* 119:183–192

11. Kiatkamjornwong S, Mongkolsawat K, Sonsuk M (2002) Synthesis and property characterization of cassava starch grafted poly[acrylamide-co-(maleic acid)] superabsorbent via γ -irradiation. *Polymer* 43:3915–3924
12. Lanthong P, Nuisin R, Kiatkamjornwong S (2006) Graft copolymerization, characterization and degradation of cassava starch-g-acrylamide/itaconic acid superabsorbents. *Carbohydr Polym* 66:229–245
13. Singh V, Tiwari A, Pandey S, Singh SK (2006) Microwave-accelerated synthesis and characterization of potato starch-g-poly(acrylamide). *Starch/Stärke* 58:536–543
14. Athawale VD, Rathi SC (1999) Graft polymerization: starch as a model substrate. *J Macromol Sci Rev Macromol Chem Phys* 39(3):445–480
15. Vázquez B, Goñi I, Gurruchaga M, Areízaga J, Valero M, Guzmán GM (1992) Ceric ion consumption in graft copolymerization of methacrylonitrile/methacrylate mixtures onto amylo maize. *Die Makromolekulare Chemie* 193(9):2189–2198
16. Carr ME, Kim S, Yoon KJ, Stanley KD (1992) Graft polymerization of cationic methacrylate, acrylamide, and acrylonitrile monomers onto starch by reactive extrusion. *Cereal Chem* 69:70–75
17. Fares MM, El-faqeeh AS, Osman ME (2003) Graft copolymerization onto starch–I. Synthesis and optimization of starch grafted with N-tert-butylacrylamide copolymer and its hydrogels. *J Polym Res* 10(2):119–125
18. Fanta GF, Felker FC, Shogren RL (2004) Graft polymerization of acrylonitrile onto spherocrystals formed from jet cooked cornstarch. *Carbohydr Polym* 56:77–84
19. Maharana T, Singh BC (2006) Synthesis and characterization of biodegradable polyethylene by graft copolymerization of starch using glucose-Ce(IV) redox system. *J Appl Polym Sci* 100:3229–3239
20. Jyothi AN, Sajeev MS, Moorthy SN, Sreekumar J (2010) Effect of graft-copolymerization with poly(acrylamide) on the thermal and rheological properties of cassava starch. *J Appl Polym Sci* 116(1):337–346
21. Ikhuria EU, Folyan AS, Okieimen FE (2010) Studies in the graft copolymerization of acrylonitrile onto cassava starch by ceric ion induced initiation. *Int J Biotechnol Mol Biol Res* 1(1):10–14
22. Shukla JS, Sharma GK (1987) Graft copolymerization of methyl methacrylate onto wool initiated by ceric ammonium nitrate-thioglycolic acid redox couple in presence of air. *J Polym Sci A Polym Chem* 25:595–605
23. Bhattacharyya SN, Maldas D (1984) Graft copolymerization onto cellulose. *Prog Polym Sci* 10:171–270
24. Hebeish A, El Alfy E, Bayazeed A (1988) Synthesis of vinyl polymer-starch composites to serve as size base materials. *Starch/Stärke* 40:191–196
25. Taghizadeh MT, Mafakheri S (2001) Kinetics and mechanism of graft polymerization of acrylonitrile onto starch initiated with potassium persulfate. *J Sci I R Iran* 12(4):333–338
26. Bhuniya SP, Rahman MDS, Satyanand AJ, Gharia MM, Dave AM (2003) Novel route to synthesis of allyl starch and biodegradable hydrogel by copolymerizing allyl-modified starch with methacrylic acid and acrylamide. *J Polym Sci A Polym Chem* 41:1650–1658
27. Mostafa KM, Samarkandy AR (2004) Synthesis of new thickener based on carbohydrate polymers for printing cotton fabrics with reactive dyes. *J Biol Sci* 4(3):334–341
28. Keshava Murthy PS, Mohan Y M, Sreeramulu J, Mohana Raju K (2006) Semi-IPNs of starch and poly(acrylamide-co-sodium methacrylate): preparation, swelling and diffusion characteristics evaluation. *React Funct Polym* 66:1482–1493
29. Bernd H, Bernd T, Thomas H, Bernhard J (2004) Cationic starch graft copolymers and novel process for the preparation of cationic starch graft copolymers. US Patent 20040170596
30. Wu YB, Lv CF, Han MN (2009) Synthesis and performance study of polybasic starch graft copolymerization function materials. In: Yin Y, Wang X (eds) *Advanced materials research*, vol 79–82., pp 43–46

31. Song H, Wu D, Zhang R-Q, Qiao L-Y, Zhang S-H, Lin S, Ye J (2009) Synthesis and application of amphoteric starch graft polymer. *Carbohydr Polym* 78(2):253–257
32. Brockway CE, Moser KB (1963) Grafting of poly(methyl methacrylate) to granular corn starch. *J Polym Sci A* 1:1025
33. Celik M (2006) Preparation and characterization of starch-g-polymethacrylamide copolymers. *J Polym Res* 13:427–432
34. Meshrama MW, Patila VV, Mhaskeb ST, Thorat BN (2009) Graft copolymers of starch and its application in textiles. *Carbohydr Polym* 75(1):71–78
35. Khalil MI, Mostafa KM, Hebeish A (1990) Synthesis of poly(methacrylic acid-) starch graft copolymers using Mn-IV-acid system. *Starch/Stärke* 42:107–111
36. Mehrotra R, Ranby B (1977) Graft copolymerization onto starch. I. Complexes of Mn^{3+} as initiators. *J Appl Polym Sci* 21(6):1647–1654
37. Mostafa KM (1995) Graft polymerization of acrylic acid onto starch using potassium permanganate acid (redox system). *J Appl Polym Sci* 56(2):263–269
38. Zhang C, Bao L, Tong Z (1994) Gaofenzi Cailiao Kexue Yu Gongcheng 10(1): 33
39. Zhang C, Bao L, Tong Z (1995) *Chem Abstr* 112:11235u
40. Gao J, Yu J, Wang W, Chang L, Tian R (1998) Graft copolymerization of starch-AN initiated by potassium permanganate. *J Appl Polym Sci* 68:1965–1972
41. Zhang L, Gao J, Tian R, Yu J, Wang W (2003) Graft mechanism of acrylonitrile onto starch by potassium permanganate. *J Appl Polym Sci* 88(1):146–152
42. Mostafa KM, Samarkandy AR, El-Sanabary AA (2009) Synthesis and characterization of poly (N-vinyl formamide)-pregelled starch-graft copolymer. *J Polym Res* (online). doi:10.1007/s10965-009-9370-z
43. Maiti S, Ranjit S, Sa B (2010) Polysaccharide-based graft copolymers in controlled drug delivery. *Int J Pharm Tech Res* 2(2):1350–1358
44. Kiatkamjornwong S, Chomsaksakul W, Sonsuk M (2000) Radiation modification of water absorption of cassava starch by acrylic acid/acrylamide. *Radiat Phys Chem* 59(4):413–427
45. Kiatkamjornwong S, Thakeow P, Sonsuk M (2001) Chemical modification of cassava starch for degradable polyethylene sheets. *Polym Degrad Stab* 73:363–375
46. Abdel-Aal SE, Gad YH, Dessouki AM (2006) Use of rice straw and radiation-modified maize starch/acrylonitrile in the treatment of wastewater. *J Hazard Mater* 129(1–3):204–215
47. Singh V, Tiwari A, Pandey S, Singh SK (2007) Peroxydisulfate initiated synthesis of potato starch-graft-poly(acrylonitrile) under microwave irradiation. *Express Polym Lett* 1(1):51–58
48. Galema SA (1997) Microwave chemistry. *Chem Soc Rev* 26:233–238
49. Singh V, Tiwari A, Sanghi R (2005) Studies on $K_2S_2O_8$ /ascorbic acid initiated synthesis of Ipomoea dasyperma seed gum-g-poly(acrylonitrile): a potential industrial gum. *J Appl Polym Sci* 98:1652–1662
50. Mostafa KM, Samerkandy AR, El-Sanabay AA (2007) Modification of carbohydrate polymers part 2: grafting of methacrylamide onto pregelled starch using vanadium-mercapto-succinic acid redox pair acrylamide based graft copolymers. *J Appl Sci Res* 3(8):681–689
51. Shogren RL, Willett JL, Biswas A (2009) HRP-mediated synthesis of starch-polyacrylamide graft copolymers. *Carbohydr Polym* 75:189–191
52. Finkenstadt VL, Willett JL (2005) Reactive extrusion of starch-polyacrylamide graft copolymers: effects of monomer/starch ratio and moisture content. *Macromol Chem Phys* 206:1648–1652
53. Frost K, Kaminski D, Shanks R (2009) Extrusion grafting of starch with reactive dyes to form sheets with reduced retrogradation. In: 33rd annual condensed matter and materials meeting. Wagga, NSW, Australia, 4–6 Feb. <http://www.aip.org.au/Wagga>
54. Willett JL, Finkenstadt VL (2006) Reactive extrusion of starch-polyacrylamide graft copolymers using various starches. *J Polym Environ* 14:125–129
55. Willett JL, Finkenstadt VL (2003) Preparation of starch-graft-polyacrylamide copolymers by reactive extrusion. *Polym Eng Sci* 43:1666

56. Athawale VD, Rathi SC (1996) Graft polymerisation of N-methylol acrylamide onto starch using Ce^{4+} as initiator. *J Polym Mater* 13:335
57. Patil DR, Fanta GF (1993) Graft copolymerization of starch with methyl acrylate: an examination of reaction variables. *J Appl Polym Sci* 47(10):1765–1772
58. Vera-Pacheco M, Vazquez-Torres H, Canche-Escamilla G (1993) Preparation and characterization of hydrogels obtained by grafting of acrylonitrile onto cassava starch by ceric ion initiation. *J Appl Polym Sci* 47:53–59
59. Jideonwo A, Okieimen FE (2000) Graft copolymerization of methylacrylate onto gum Arabic, Niger. *J Appl Sci* 18:109–114
60. Fanta GF, Burr RC, Doane WM, Russell CR (1971) Influence of starch granule swelling on graft copolymer compositions. A comparison of monomers. *J Appl Polym Chem* 15:2651–2660
61. Brandrup J, Immergut EH (1966) *Polymer handbook*. Wiley, New York, NY
62. Xiao C, Yang M (2006) Controlled preparation of physical cross-linked starch-g-PVA hydrogel. *Carbohydr Polym* 64:37–40
63. Gao J, Tian R, Yu J, Duan M (1994) Graft copolymers of methyl methacrylate onto canna starch using manganic pyrophosphate as an initiator. *J Appl Polym Sci* 53(8):1091–1102
64. Trimmell D, Fanta GF, Salch JH (1996) Graft polymerization of methyl acrylate onto granular starch: comparison of the Fe^{+2}/H_2O_2 and ceric initiating systems. *J Appl Polym Sci* 60(3):285–292
65. Vazquez B, Goni I, Gurruchaga M, Valero M, Guzman GM (1992) *J Polym Sci A Polym Chem* 30(8):1541
66. Yao KJ, Tang YB (1992) Synthesis of starch-g-poly(acrylamide-co-sodium allyl sulfonate) and its application of flocculation to Kaolin suspension. *J Appl Polym Sci* 45(2):349–353
67. Lu S, Duan M, Lin S (2003) Synthesis of superabsorbent starch-graft-poly(potassium-acrylate-co-acrylamide) and its properties. *J Appl Polym Sci* 88:1536–1542
68. Gupta B, Anjum N (2003) Preparation of ion-exchange membranes by hydrolysis of radiation-grafted polyethylene-g-polyacrylamide membranes. *J Appl Polym Sci* 90:149
69. Sahoo PK, Rana PK (2006) Synthesis and biodegradability of starch-g-ethyl methacrylate/sodium acrylate/sodium silicate superabsorbing composite. *J Mater Sci* 41:6470–6475
70. Zhang Q, Xu K, P W (2008) Study on structure and molecular dynamics of starch/poly (sodium acrylate)-grafted superabsorbent by ^{13}C solid state NMR. *Fiber Polym* 9(3):271–275
71. Veregin RP, Fyfe CA, Marchessault RH, Taylor MG (1986) Characterization of the crystalline A and B starch polymorphs and investigation of starch crystallization by high-resolution carbon-13 CP/MAS NMR. *Macromolecules* 19:1030–1034
72. Cheetham NWH, Leping T (1998) Solid state NMR studies on the structural and conformational properties of natural maize starches. *Carbohydr Polym* 36:285–292
73. Paris M, Bizot H, Emery J, Buzare JY, Buleon A (2001) NMR local range investigations in amorphous starchy substrates I. Structural heterogeneity probed by (^{13}C) CP-MAS NMR. *Int J Biol Macromol* 29:127–136
74. Chen Q, Kurosu H, Ma L, Matsuo M (2002) Elongation-induced phase separation of poly (vinyl alcohol)/poly(acrylic-acid) blends as studied by ^{13}C CP/MAS NMR and wide-angle X-ray diffraction. *Polymer* 43:1203–1206
75. Miyoshi T, Takegoshi K, Hikichi K (1996) High-resolution solid-state ^{13}C nuclear magnetic resonance study of a polymer complex: poly(methacrylic acid)/poly(ethylene oxide). *Polymer* 37:11–18
76. Tripathy T, De RB (2006) Flocculation: a new way to treat the waste water. *J Phys Sci* 10:93–127
77. Castle D, Richard A, Audebert RJ (1990) Swelling of anionic and cationic starch-based superabsorbents in water and saline solution. *J Appl Polym Sci* 39(1):11–29
78. Mostafa KM, El-Sanabary AA (1997) Carboxyl containing starch and hydrolyzed starch derivatives as size base materials for cotton textiles. *Polym Degrad Stab* 55(2):181–184

79. Cheng Y, Brown KM, Prudhome RK (2002) Preparation and characterization of molecular weight fractions of guar galactomannans using acid and enzymatic hydrolysis. *Int J Biol Macromol* 31:29–35
80. Picout DR, Murphy SBR, Errington N, Harding SE (2001) Pressure cell assisted solution characterization of polysaccharides.1. Guar gum. *Biomacromolecules* 2:1301–1309
81. Dragunski DC, Pawlicka A, Carlos S (2001) Preparation and characterization of starch grafted with toluene poly(propylene oxide) diisocyanate. *Mater Res* 4(2):77–81, 1516-1439
82. Athawale VD, Lele V (2000) Thermal studies on granular maize starch and its graft copolymers with vinyl monomers. *Starch/Stärke* 52:205–213
83. Wang XL, Yang KK, Wang YZ, Chen DQ, Chen SC (2004) Crystallization and morphology of starch-g-poly(1,4-dioxan-2-one) copolymers. *Polymer* 45:7961–7968
84. Gupta B, Anjum N (2001) Development of membranes by radiation grafting of acrylamide into polyethylene films: characterization and thermal investigations. *J Appl Polym Sci* 82:2629
85. Jyothi AN, Sreekumar J, Moorthy SN (2010) Response surface methodology for the optimization and characterization of cassava starch-graft-poly(acrylamide). *Starch/Stärke* 62:18–27
86. Kennedy JF, Cabral JMS, Sa-Correia I, White CA (1987) Starch biomass: a chemical feedstock for enzyme and fermentation process. In: Galliard T (ed) *Starch: properties and potential*, vol 13. Wiley, New York, NY, p 123
87. Abraham J, Pillai VNR (1996) Membrane-encapsulated controlled-release urea fertilizers based on acrylamide copolymers. *J Appl Polym Sci* 60:2347–2351
88. Renken A, Hunkeler D (1999) Effect of the surfactant blend composition on the properties of polymerizing acrylamide-based inverse-emulsions: characterization by small-angle neutron scattering and quasi-elastic light scattering. *Polymer* 40:3545–3554
89. Goin J (1991) Water soluble polymers. CEH Marketing research report 582.0000 D-E. August, SRI International
90. Hunkeler D, Hernandez-Barajas J (1996) A concise review of the influence of synthesis and technological factors on the structure and properties of polyacrylamides. In: *Industrial water soluble polymers*. ACS symposium series, p 11–27
91. Karmakar GP, Singh RP (1996) Synthesis and application of polymeric flocculants for the treatment of paper mill effluents. In: *Advances in Chemical Engineering*, Allied Publishers, New Delhi, p 201
92. Karmakar GP, Singh RP (1996) Synthesis and characterisation of starch-g-acrylamide copolymers for improved oil recovery. In: *International Symposium on Oilfield Chemistry*, Houston, Texas, 18–21 February 1997
93. Karmakar NC, Sastry BS, Singh RP (2002) Flocculation of chromite ore fines suspension using polysaccharide based graft copolymers. *Bull Mater Sci* 25(6):477–478
94. Sharma BR, Dhuldhoya NC, Merchant UC (2006) Flocculants – an ecofriendly approach. *J Polym Environ* 14:196–202
95. Deshmukh SR, Singh RP (1986) Drag reduction characteristics of graft copolymers of xanthan gum and polyacrylamide. *J Appl Polym Sci* 32:6163
96. Fanta GF, Burr RC, Russel CR, Rist RE (1970) Graft copolymers of starch and poly (2-hydroxy-3-methacryloxy propyl trimethyl ammonium chloride) preparation and testing as flocculating agents. *J Appl Polym Sci* 14:2601
97. Fanta GF, Burr RC, Russell CR, Rist CE (1970) Graft copolymers of starch and poly (2-hydroxy-3-methacryloxypropyltrimethylammonium chloride): preparation and testing as flocculating agents. *J Appl Polym Sci* 14:2601–2607
98. Deshmukh SR (1986) Turbulent drag reduction effectiveness, shear stability and biodegradability of graft copolymers. Ph.D. Thesis, IIT, Kharagpur, India
99. Karmakar GP (1994) Flocculation and rheological properties of grafted polysaccharides. Ph.D. Thesis, IIT, Kharagpur, India

100. Fanta GF, Burr RC, Doane WM, Russel CR (1972) Graft copolymers of starch with mixtures of acrylamide and the nitric acid salt of dimethyl aminomethyl methacrylate. *J Appl Polym Sci* 16:2835
101. Rath SK, Singh RP (1997) Flocculation characteristics of grafted and un grafted starch, amylose, and amylopectin. *J Appl Polym Sci* 66(9):1721–1729
102. Fanta GF, Doane WM (1986) Grafted starches. In: Wurzburg OB (ed) *Modified starches: properties and uses*. CRC, Boca Raton, FL, pp 149–178
103. Kuilin D, Na J, Yaqin Z, Dawei Y, Duanmin H (2006) Adsorption behaviors of copper (II) and lead (II) ions by crosslinked starch graft copolymer with aminoethyl group. *Chem J Internet* 8(11):68
104. Hao X, Chang Q, Duan L, Zhang Y (2007) Synergetically acting new flocculants on the basis of starch-graft-poly(acrylamide)-co-sodium xanthate. *Starch/Stärke* 59:251–257
105. Singh RP, Tripathy T, Karmakar GP, Rath SK, Karmakar NC, Pandey SR, Kannan K, Jain SK, Lan NT (2000) Novel biodegradable flocculants based on polysaccharides. *Curr Sci* 78 (7):798–803
106. Dickinson E, Eriksson L (1991) Particle flocculation by adsorbing polymers. *Adv Colloid Interface Sci* 34:1–29
107. Riaz MN (1999) Processing biodegradable packaging materials from starches using extrusion technology. *Cereal Food World* 44:705–709
108. Shogren RL, Fanta GF, Doane WM (1993) Development of starch based plastics—a reexamination of selected polymer systems in historical perspective. *Starch/Stärke* 45:276–280
109. Saroja N, Shamala TR, Tharanathan RN (2000) Biodegradation of starch-g-polyacrylonitrile, a packaging material, by *Bacillus cereus*. *Process Biochem* 36(1–2):119–125
110. Halley P, Rutgers R, Coombs S, Kettels J, Gralton J, Christie G, Jenkins M, Beh H, Griffin K, Jayasekara R, Lonergan G (2001) Developing biodegradable mulch films from starch-based polymers. *Starch/Stärke* 53:362–367
111. Buchholz FL, Peppas NA (1994) *Superabsorbent polymers science and technology*. American Chemical Society, Washington, DC
112. Toyama M (1990) *Chemistry* 45(2):108–110, Japanese
113. Lutfor MR, Sidik WYWMZ, Ab Rahman MZ, Mansoor A, Jelas H (2001) Preparation and swelling of polymeric absorbent containing hydroxamic acid group from polymer grafted sago starch. *Carbohydr Polym* 45:95–100
114. Doane SW, Doane WM (2004) Starch graft copolymers and methods of making and using starch graft copolymers for agriculture. WO/2004/033536
115. Qunyi T, Ganwei Z (2005) Rapid synthesis of a superabsorbent from a saponified starch and acrylonitrile/AMPS graft copolymers. *Carbohydr Polym* 62:74–79
116. Talaat HA, Sorour MH, Aboulmour AG, Shaalan HF, Ahmed EM, Awad AM, Ahmed MA (2008) Development of a multi-component fertilizing hydrogel with relevant techno-economic indicators. *Am Eurasian J Agric Environ Sci* 3(5):764–770
117. Savich MH, Olson GS, Clark EW (2009) WO/2009/014824
118. Zhang L (2001) A review of starches and their derivatives for oilfield applications in China. *Starch/Stärke* 53(9):401–440
119. Yao KJ, Wang M (1987) Synthesis of starch-g-polyacrylamide for oil field drilling treatments. *Oilfield Chem* 4:175–179
120. Guo JA (1996) Synthesis and performance of heat-resistant and salt tolerant filtrate loss reducer based on grafted starch. *Oilfield Chem* 13:169–171
121. Song H, Zhang SF, Ma XC, Wang DZ, Yang JZ (2007) Synthesis and application of starch-graft-poly(AM-co-AMPS) by using a complex initiation system of CS-APS. *Carbohydr Polym* 69(1):189–195
122. Eutamene M, Benbakhti A, Khodja M, Jada A (2009) Preparation and aqueous properties of starch-grafted polyacrylamide copolymers. *Starch/Stärke* 61(2):81–91

123. Mostfa KM, Morsy MS (2004) Tailoring a new sizing agent via structural modification of pregelated starch molecules, Part 1: carboxymethylation and grafting. *Starch/Stärke* 56: 254–261
124. Kuraray Co Ltd. (1982) Japan Patent 82 47,339. Abstr. 97(1982) 44362b
125. Yamamoto K, Watanabe T, Yamamoto T (1994) Japan Patent 06,00,201. Abstr. 120 (1944) 173553g
126. Mori M (1997) Release controlled transdermal therapeutic system. US Patent 569577
127. McDermott MR, Heritage PL, Bartzoka V, Brook MA (1998) Polymer-grafted starch microparticles for oral and nasal immunization. *Immunol Cell Biol* 76:256–262
128. Geresh S, Gdalevsky GY, Gilboa I, Voorspoels J, Remon JP, Kost J (2004) Bioadhesive grafted starch copolymers as platforms for peroral drug delivery: a study of theophylline release. *J Control Release* 94:391–399
129. Saboktakin MR, Maharramov A, Ramazanov MA (2007) Modification of carboxymethyl starch as nano carriers for oral drug delivery. *Nat Sci* 5(3):67
130. Shaikh MM, Lonikar SV (2009) Starch–acrylics graft copolymers and blends: synthesis, characterization, and applications as matrix for drug delivery. *J Appl Polym Sci* 114 (5):2893–2900
131. Marinich JA, Ferrero C, Jiménez-Castellanos MR (2009) Graft copolymers of ethyl methacrylate on waxy maize starch derivatives as novel excipients for matrix tablets: physicochemical and technological characterisation. *Eur J Pharm Biopharm* 72(1):138–147
132. Silva I, Gurruchaga M, Goñi I (2009) Physical blends of starch graft copolymers as matrices for colon targeting drug delivery systems. *Carbohydr Polym* 76:593–601
133. Saboktakin MR, Maharramov A, Ramazanov MA (2009) pH-sensitive starch hydrogels via free radical graft copolymerization, synthesis and properties. *Carbohydr Polym* 77 (3):634–638
134. Lu F, Wang X-L, Chen S-C, Yang K-K, Wang Y-Z (2009) An efficient approach to synthesize polysaccharides-graft-poly(p-dioxanone) copolymers as potential drug carriers. *J Polym Sci A Polym Chem* 47:5344–5353
135. Chen L, Qiu XY, Xie ZG, Hong ZK, Sun JR, Chen XS, Jing XB (2006) Poly(L-lactide)/starch blends compatibilized with poly(L-lactide)-g-starch copolymer. *Carbohydr Polym* 65:75–80
136. Choi E-J, Kim C-H, Park J-K (1999) Structure-property relationship in PCL/starch blend compatibilized with starch-g-PCL copolymer. *J Polym Sci B Polym Phys* 37:2430–2438
137. Chen L, Xie ZG, Zhuang XL, Chen XS, Jing XB (2008) Controlled release of urea encapsulated by starch-g-poly(L-lactide). *Carbohydr Polym* 72:342–348
138. Choi E-J, Kim C-H, Park J-K (1999) Synthesis and characterization of starch-g-polycaprolactone copolymer. *Macromolecules* 32:7402–7408
139. Dubois P, Krishnan M, Narayan R (1999) Aliphatic polyester grafted starch-like polysaccharides by ring-opening polymerization. *Polymer* 40:3091–3100
140. Xu Q, Kennedy JF, Liu LJ (2008) An ionic liquid as reaction media in the ring opening graft polymerization of ϵ -caprolactone onto starch granules. *Carbohydr Polym* 72:113–121

Chapter 4

Chitosan-g-Copolymers: Synthesis, Properties, and Applications

Magdy W. Sabaa

Abstract Chitosan (Ch), which is the result of the alkaline hydrolysis of the naturally occurring chitin biopolymer, is considered to be one of the highly versatile polymeric materials due to its active functional groups ($-\text{NH}_2$ and $-\text{OH}$ groups), biocompatibility, biodegradability, and nontoxic property. Preparation, analysis, and general properties of Ch and its derivatives have been reported in this chapter. Moreover, chemical modification of Ch by direct reactions on its active functional groups and by grafting technique has been discussed in details. Characterization of Ch and its carboxymethyl derivative (CMCh) grafted by various functionalized polymers has been carried out using spectral and thermal analyses, X-ray diffraction, and scanning electron microscopy. Various fields of applications of Ch and CMCh as superabsorbent materials, metal ions adsorption, ion exchangers, as well as in pharmaceutical and biomedical areas have been also discussed.

Keywords Chitosan • Carboxymethyl chitosan • Grafting technique • Superabsorbent materials • Metal uptake • Drug delivery systems

4.1 Introduction

Chitosan (Ch) is a *N*-deacetylated derivative of chitin, which is a structural polysaccharide [1] commonly found in nature, though this *N*-deacetylation is almost never complete [2, 3]. Actually, the name “chitin” and “chitosan” corresponds to a family of polymer varying in acetyl content. Therefore, the degree of acetylation determines whether the biopolymer is chitin or chitosan. Ch is a linear hydrophilic polysaccharide that has received much attention in biological field. It is a copolymer composed of glucosamine and *N*-acetyl glucosamine [4]. The physical

M.W. Sabaa (✉)

Faculty of Science, Chemistry Department, Cairo University, Giza, Egypt
e-mail: mwsabaa@hotmail.com

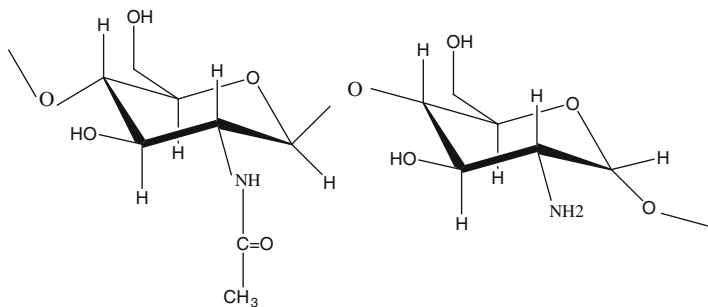


Fig. 4.1 Chemical structure of chitosan

properties of Ch depend on a number of parameters such as the molecular weight, degree of deacetylation (DD), and sequence of the amino and the acetamido groups. It is an attractive biocompatible, biodegradable, and nontoxic natural biopolymer that exhibits excellent film forming ability [5]. Ch is poly [β -(1-4)-2-amino-2-deoxy-D-glucopyranose] and its idealized structure is represented in Fig. 4.1.

4.2 Chitosan

4.2.1 Synthesis of Chitosan

Shrimp shells were cleaned and dried under sunlight before grinding into small pieces. The shrimp shell chips were then immersed in 1 M HCl for 2 days with occasional stirring. The product was washed with distilled water until becoming neutral and then soaked in a 4 wt% NaOH solution at 80–90 °C for 4 h. After the NaOH solution was decanted, the chips were washed again with distilled water until they became neutral and then heated with 50 wt% NaOH solution in an autoclave at 110 °C for 1 h. The Ch product was washed with distilled water until becoming neutral and dried in an air oven at 60 °C for 24 h [6].

4.2.2 Properties of Chitosan

Ch has many properties that classified it as one of the most important modified natural polymer due to its biodegradability, its biocompatibility, its nontoxic nature, and its metal uptake capacity [7]. The presence of amino group in C₂ position of Ch provides major functionality toward biotechnological needs in food applications, in drug carriers, etc. Ch-based polymeric materials can be formed into fibers, films, gels, sponges, beads, or nanoparticles [8]. Moreover, Ch was proved to have broad-spectrum antifungal activity toward a variety of fungi [9], in addition to its ability to represent the core of a new generation of drug and vaccine delivery systems [10].

4.2.2.1 Solubility in Inorganic and Organic Acids

Ch is soluble in dilute inorganic acids like HCl and it dissolves in aqueous solutions of organic acids as acetic, formic, and citric, resulting in viscous solutions [11].

4.2.2.2 Solubility in Organic Solvents

Ch is insoluble in organic solvent [12] such as THF, pyridine, petroleum ether, trichloromethane, dichloromethane, and cyclohexane, but poorly soluble in polar solvents like DMSO and DMF. Solubility of Ch in organic solvents increases by introducing long chain of acyl group into Ch.

Ch is a brittle material and has the ability to absorb a quantity of moisture. Due to the strong inter- and intramolecular H-bonding, Ch is insoluble in water, but it dissolves in aqueous solutions of aliphatic organic acids like formic, acetic, and citric acids. Moreover, it is soluble in some dilute inorganic acids like HCl, HI, HNO₃, and HClO₄ [11].

Ch has, besides the hydroxyl groups, a very reactive amino group at C₂ which is highly useful as ion exchangers [13] and in the preparation of a great number of Ch derivatives [14]. Moreover, Ch derivatives soluble in neutral and in basic media in addition to its aqueous acid solutions are considered as useful biomaterials [15], for example, as antibacterial agents [16] and for drug delivery systems [17].

Ch is well known for its capability as a sorbent material for metal ions [18, 19], which depends on the concentration of its amino group [20, 21]. Due to its cationic properties, Ch offers good opportunities to take advantages of electron interaction with a variety of compounds and incorporate specific properties into the material [22].

4.3 Analysis of Chitosan

Analysis of Ch is carried out in order to characterize the material. Such characterization includes the determination of amino groups (i.e., the degree of deacetylation, DD).

4.3.1 Determination of the Amino Group Content

4.3.1.1 Acid–Base Titration Method

This method was first proposed by Broussignac [23], where Ch is dissolved in a known excess amount of acid and the solution is then titrated against NaOH

potentiometrically. This gives a titration curve with two inflection points, the difference between the two along the x abscissa ($a - b$) corresponding to the amount of acid required to protonate the amino group, and thus, the amino group concentration is determined according to the following equation:

$$\% \text{NH}_2 = \frac{6.1(a - b)F}{W}$$

where F is the molarity of NaOH solution and W is the weight of the sample in grams.

This technique has been used by a number of workers, but its precision has been questioned by Domard and Rinaudo [24] because of the tendency toward precipitation of the Ch in the neutralization pH range. These workers reported an improved technique in which the Ch is progressively titrated with HCl, while the conductivity is monitored to determine the stoichiometry of the interaction. This procedure gave an equivalent weight of 16 ± 1 for the amino group of the Ch sample. Prior to this, Moore [25] examined a back-titration method in which a sample is steeped in a known excess of 0.5 M HCl, in which Ch is insoluble, followed by titration of aliquots of the supernatant liquor.

4.3.1.2 Colloidal Titration Method

The colloidal titration technique was developed by Hirai et al. [26] as a method for analyzing polyelectrolyte. Ch was dissolved in an aqueous solution of acetic acid and titrated with polyvinyl potassium sulfate solution using toluidine blue as an indicator. The end point is determined by the color change from blue to reddish purple.

4.4 Chemical Modifications of Chitosan

Ch is a versatile molecule, which contains, besides the primary and secondary hydroxyl groups, the highly active amino group at C_2 . This in addition to a slight ratio of the remaining non-hydrolyzed acetamido group. Due to the high activity of functional groups present in Ch, it can be easily subjected to chemical modifications without disturbing its degree of polymerization [27]. Figure 4.2 represents the various functional groups in Ch.

The chemical modifications are designed to change solid viscosity gelling tendency, hydrophilic character, affinity toward metals and dyes, and moisture content and to introduce ionic character. The modifications may involve controlled degradation of Ch chains or the introduction of chemical groups not normally present.

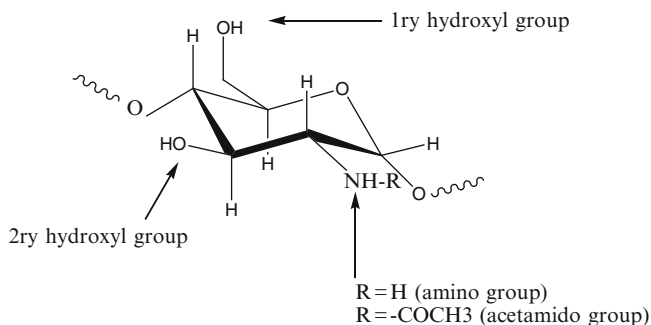


Fig. 4.2 Various functional groups in chitosan (adapted from [27], Elsevier publisher)

The introduction of different chemical groups may be carried out through inorganic esters such as nitrate, phosphate, and sulfate or by organic esters such as acyl derivatives or by etherification such as carboxyalkyl group.

4.4.1 Inorganic Esters

4.4.1.1 Chitosan Nitrate

Wolfrom et al. [28] examined the preparation of Ch nitrate and perchlorate salts. There are two routes; in the first, Ch was dissolved in conc. HNO_3 , while in the second, it was suspended in 1:1:1.3 mixture of glacial acetic acid/acetic anhydride/conc. nitric acid for about 5.5 h at $\leq 5^\circ\text{C}$. The products from both processes were very similar. In the first route, Ch nitrate has a DS (ONO_2) value of 1.65. It was converted to Ch nitrate with *O*-nitrate content unchanged by addition of dilute alkali to a solution of the salt in 50 vol% aqueous acetone. In the second route, Ch nitrate was converted to the perchlorate salt by suspending it in glacial acetic acid containing perchloric acid.

4.4.1.2 Chitosan Phosphate

Reaction of Ch with phosphorous acid and formaldehyde sequentially or simultaneously in aqueous acidic medium provides water-soluble *N*-mono- and di-phosphonic methylene Ch [29]. The structure of Ch phosphorylation products and the degree of substitution depend on the reactants ratio and reaction conditions especially reaction time [30, 31].

The introduction of a hydrophobic alkyl chain onto the free amino groups of *N*-methylene phosphonic Ch by a reductive amine reaction leads to a new amphiphilic Ch derivatives with potential to act as a surfactant. *N*-lauryl-*N*-methylene phosphonic Ch is one of such surfactant reported [32]. Karrer et al. [33] were the

first to attempt the phosphorylation of Ch. They treated Ch with 15 parts pyridine and 5 parts phosphorous oxychloride at 40 °C for 5 h, the obtained product was found to contain 24 % phosphorous. Hackman [34] was unable to obtain phosphorylated derivatives of chitin using the above method. However, interest in phosphate esters of Ch has increased, because of its metal ion capabilities. Such preparation is based on a method for preparing cellulose phosphates, through heating with mixtures of phosphoric acid and urea by an impregnation backing sequence [35] and modified by using inert liquid as the reaction medium [36]. Both DMF [37] and toluene [38] have been used as the inert reaction medium for the preparation of chitin and Ch phosphate.

4.4.1.3 Chitosan Sulfate

Ch sulfates represent a very important family of derivatives of Ch which can improve the biological activities [27]. Various methods which involve combinations of sulfating agents and the reaction media have been used for the sulfation of Ch. For sulfation of Ch or its derivatives, various reagents being used including concentrated sulfuric acid [39], oleum [40], sulfur trioxide, sulfur trioxide/pyridine [41], sulfur trioxide/trimethylamine [42], sulfur trioxide/sulfur dioxide, chlorosulfonic acid/sulfuric acid, and the most commonly used chlorosulfonic acid [43] in homogeneous or heterogeneous conditions in different media as DMF, DMF–dichloroacetic acid, THF, and formic acid [44] at different temperature ranges or under microwave irradiation [45].

There are two methods for the selective 6-*O*-sulfation of Ch that have been developed. The first [46] involves the use of a 2:1 mixture of 95 wt% H₂SO₄ and 98 wt% ClSO₃H at 0.4 °C. The reaction time was about 1 h and the product is isolated by precipitation. The product can be characterized by conductometric titration, IR spectrum, and ¹³C-NMR spectroscopy. The DS value was found to be 0.95–1.0 and sulfation takes place at the C(6) OH group. The spectrum in D₂O solution was compared with that for a low-molecular weight Ch (DP ~ 30), and it shows that the signals for C(1)–C(5) of Ch 6-*O*-sulfate were shifted by relatively small amounts compared with their positions in the spectrum for the Ch oligomer; the C(6) signal is shifted significantly downfield (~6.2 ppm). The more or less complete absence of any C(1) signal attributed to reducing end groups indicates that the sulfation reaction did not involve hydrolysis of the polymer chain.

4.4.2 Organic Esters

4.4.2.1 *N*-Acyl Derivatives of Chitosan

N-acyl derivatives of Ch can be easily obtained by using acyl chlorides and anhydrides. In a general way, acylation reactions take place frequently in media

as aqueous acetic acid/methanol, pyridine, pyridine/chloroform, trichloroacetic acid/dichloroethane, ethanol/methanol, methanol/formamide, or DMA–LiCl [47]. Due to the fairly different reactivity of the two hydroxyl groups (at C₃ and C₆) and the amino group (at C₂) of the repeating unit of Ch, acylation can be controlled at the expected sites, that is, on either amino [48], hydroxyls [49], or on both groups [50].

N-acylation may be prepared by a number of ways, not all of which are applicable to the preparation of all *N*-acyl derivatives. The simplest procedure is the reaction between a carboxylic acid and Ch to produce *N*-formyl Ch by heating a solution of Ch in 100 % HCOOH acid at 90 °C with gradual addition of pyridine [51], while Aiba [52] proceeds *N*-acetylation of Ch in 20 wt% acetic acid. This latter method was much slower and the extent of *N*-acetylation being about 50 % after 300 h at 80 °C.

The most common reagents for *N*-acylation of Ch are the acyl anhydrides and may be used under heterogeneous and homogeneous conditions, principally the latter. *N*-acylation [53] under heterogeneous conditions has been studied using three systems: they were (a) acetic anhydride–glacial acetic acid and HClO₄ acid; (b) acetic anhydride at room temperature for 120 h followed by refluxing in acetic anhydride for 2 h; (c) acetic anhydride–methanol at room temperature. Of these, the last method was found to be the most efficacious. Acid chlorides have been found to have little application in the selective *N*-acylation of Ch because of their high reactivity. Kurita et al. [54] attempted *N*-acetylated water-soluble Ch, but only a very limited amount of *N*-acetylation was obtained, and this is due to the steric arrangement of the Ch molecules at the liquid interface limiting the accessibility of the amino groups to the acetyl chloride molecules.

4.4.2.2 *O*-Acyl Derivatives of Chitosan

Introducing a hydrophobic moiety with an ester linkage into Ch has two benefits: (1) hydrophobic groups contribute organosolubility and (2) the ester linkage is hydrolyzed by enzymes such as lipase. Moreover, the glycoside linkage of Ch derivatives is also degraded by glycosidase. Therefore, Ch derivatives with *O*-acyl groups are designed as biodegradable coating materials. The successful preparation of *N,O*-acyl Ch in methyl sulfonic acid (MeSO₃H) as solvent was performed [49]. The preparation of *O,O*-didecanoyl Ch, *O*-succinyl Ch was also reported through protected *N*-phthaloyl Ch as an intermediate [55]. This method, however, needs several steps as the protection of the amino group by phthaloylation, *O*-acylation, and finally removal of protecting group by suitable method as by using hydrazine hydrate.

Another method for the protection of the amino group is through the formation of Schiff's base, followed by *O*-acetylation using acetic anhydride–pyridine to prevent acid hydrolysis of the Schiff's base [56]. The protection of the amino groups is necessary in this case due to the high reactivity of the amino groups as compared with the hydroxyl groups. Using a Ch sample, it was found that with

Schiff's bases formed with aliphatic aldehydes, *O*-acetylation proceeded rapidly, provided that the aldehyde contained three or more C atoms, but the complete *O*-acetylation was not achieved owing to the hydrolysis of the Schiff's base [57]. However Schiff's base derivatives formed with aromatic aldehydes show little tendency to hydrolyze under the conditions used in the *O*-acetylation step, and di-*O*-acetyl-*N*-arylidene Ch is readily obtained. Some of the important examples of modified Ch and their fields of applications are reported in details in the work of Mourya and Inamdar [27].

4.4.2.3 Cross-Linking of Chitosan

Gupta and Jabrail [58] have prepared the glutaraldehyde cross-linked Ch microspheres by dissolving Ch in acetic acid and, after that, transferring the solution into methanolic solution of NaOH to form Ch microspheres. The microspheres were then transferred to a solution of glutaraldehyde for cross-linking. Coelho et al. [59], on the other hand, have prepared Ch microspheres by the phase inversion method. For the preparation of the microspheres, powdered Ch was dissolved in acetic acid solution to produce a viscous solution. The resulting Ch solution was then pumped through a nozzle into a precipitation bath consisting of 2.0 mol L⁻¹ NaOH. The neutralization of the acetic acid by the alkali solution results in the precipitation of Ch with the formation of gel microspheres. The microspheres were washed with distilled water to neutralize their pH. Cross-linking of Ch microspheres was achieved using epichlorohydrin as cross-linking agent in the presence of NaOH solution.

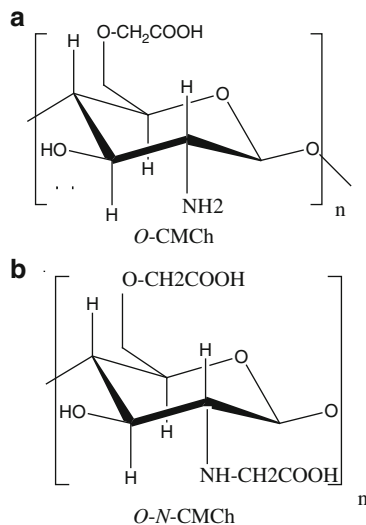
Yisong and coworkers [60] cast Ch solutions containing glutaraldehyde. The solvent was allowed to evaporate under infrared light, where cross-linking occurred. The swelling of the membranes was measured by comparing the surface area before and after immersion in water at 25 °C. The swelling was found to decrease with an increase in cross-linking agent. Ch microspheres were prepared through cross-linking of Ch with glutaraldehyde [61]. Ch is cross-linked with epichlorohydrin, followed by heating with alkali to give an anion exchange resin [62].

4.4.2.4 Carboxymethylation of Chitosan

Chemical modification of Ch by introducing carboxymethyl groups to improve some of its physical properties such as water insolubility (soluble in 1 % acetic acid), where carboxymethyl chitosan (CMCh) is water soluble and has improved chemical properties as being able to form salts with heavy metal ions and not only by chelation through amino or hydroxyl groups as in the case of Ch.

There are two types of CMCh, *O*-CMCh and *O,N*-CMCh, as represented in Fig. 4.3 [63].

Fig. 4.3 Types of carboxymethyl chitosan (a) *O*-carboxymethyl chitosan and (b) *O,N*-carboxymethyl chitosan



The production of *O*-CMCh and *O,N*-CMCh depends on the reaction conditions as illustrated in Scheme 4.1.

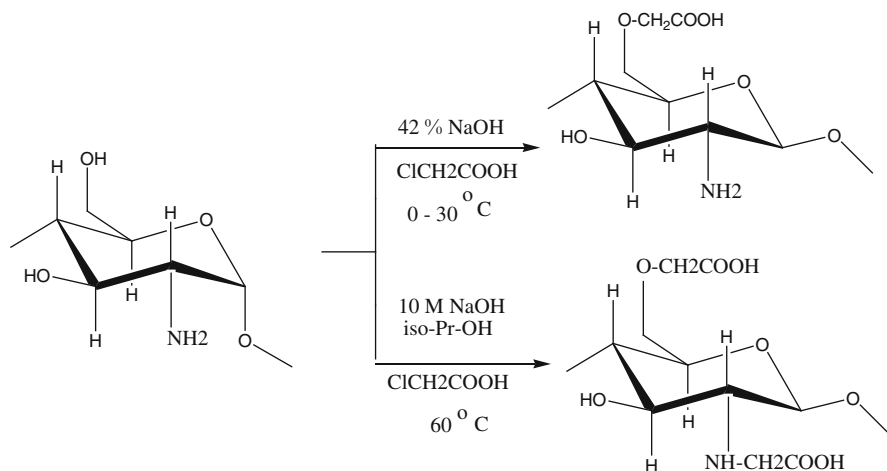
Preparation of *O*-Carboxymethyl Chitosan

Okimasu [64] prepared CMCh, obtaining the product either as sodium salt with the amino group present in the free base form or as the hydrochloride salt of the amine with the carboxymethyl groups present in the free acid form. The sensitivity to added electrolyte increased with the increase in the extent of carboxymethylation.

The *O*-alkylation of Ch in which the amino group is protected by Schiff's base formation has been studied by Plisko and coworkers [65, 66]. In this case, *N*-salicylidene Ch was treated with monochloroacetic acid in the presence of an alkali and a diluent, such as isopropyl alcohol or xylene, to give *O*-carboxymethyl-*N*-salicylidene Ch which was converted to *O*-CMCh by hydrolysis of the Schiff's base under acidic conditions. Other procedures obtaining the product by using two different techniques either microwave [67] or thermal [68] technique.

Microwave Technique

Ge and Luo [67] prepared CMCh in aqueous solution under microwave irradiation by treating firstly the Ch with NaOH solution and then adding the required amount of chloroacetic acid. The product is then precipitated in acetone as white powder.



Scheme 4.1 Synthesis of *O*-CMCh and *O-N*-CMCh

Thermal Technique

CMCh has been prepared by Joshi and Sinha [68] by thermal treatment (55 °C), a mixture of Ch dissolved in NaOH in the presence of isopropanol with chloroacetic acid. The product was then obtained by precipitation from ethanol (80 %).

Determination of Degree of Substitution of *O*-CMCh

Elemental Analyses [69]

The degree of substitution (DS) of *O*-CMCh was calculated using the DD value, C%, and N% of the sample's elemental analyses using the following equation:

$$DS\% = [7/12 \times (C\%/N\%) + DD - 4] \times 100$$

where (DD) is the degree of deacetylation of Ch.

Potentiometric Titration Method

The degree of substitution was determined by dissolving CMCh in distilled water, and the solution was adjusted to pH < 2 by adding hydrochloric acid. Then, the CMCh solution was titrated with aqueous NaOH and the pH value of the solution was simultaneously recorded. The amount of aqueous NaOH was determined by the second-order differential method [67].

The degree of substitution (DS) can be calculated using the following equation:

$$DS = \frac{161 \times A}{m_{\text{CMCh}} - 58 \times A}$$

$$A = V_{\text{NaOH}} \times C_{\text{NaOH}}$$

where V_{NaOH} and C_{NaOH} are the volume and molarity of aqueous NaOH, respectively; m_{CMCh} is the mass of CMCh (g); and 161 and 58 are the respective molecular weights of glucosamine (chitosan skeleton unit) and the carboxymethyl group.

4.4.3 Modification of Chitosan by Grafting Technique

Ch has prospective applications in many fields such as biomedicine, wastewater treatment, functional membranes, and flocculation. However, Ch can only be soluble in few dilute acid solutions, which limits its wide applications. Recently, it has been a growing interest in chemical modification of Ch to improve its solubility and widen its applications [70]. Among various methods, graft copolymerization is most attractive because it is a useful technique for modifying the chemical and physical properties of natural polymers. Ch bears two types of reactive groups that can be grafted: firstly, the free amino groups resulted from the hydrolysis of the deacetylated units at C₂ and, secondly, the hydroxyl groups at C₃ and C₆ carbons on acetylated or deacetylated units. Grafting of Ch allows the formation of functional derivatives by covalent binding of a molecule, the graft, onto the Ch backbone [71]. Free radical initiating method may be considered in terms of physical method or chemical method:

4.4.3.1 Physical Methods

Physical initiation includes irradiation [72], gamma rays, or an electron beam, producing the free radical sites at the breakpoints. If this application is done in the presence of a vinyl or an acrylate monomer, copolymerization is initiated and graft copolymer is produced, attached to the Ch at the site of the free radical formation. Irradiation can be applied to a mixture of the Ch and the monomer which will yield some homopolymers but will also provide for the reaction short-lived free radicals. Low temperature, low moisture content, and the absence of oxygen will favor increased stability of the free radicals. Free radicals can be generated by complicated mechanisms when organic substrates are subjected to high-energy radiation, such as γ -radiation. The mechanism of radical production has the following characteristics: radicals are produced by means of electron abstraction to form radical cations, typically radical formation is concentrated along the path of the incident radiation beam, and radical generation is fairly unselective. Although it appears to have a number of disadvantages in terms of

its lack of specificity, it is a convenient method because there are no “synthetic” steps to be formed. Thus, it is often used for the initiation of vinyl polymerization by both radical (predominantly) and ionic mechanisms.

Ch has been graft copolymerized with various monomers by means of γ -radiation where the substrates are exposed to γ -radiation, creating macroradicals that when in the presence of vinyl or acrylate monomers lead to graft copolymerization. Wang et al. [72] graft copolymerized acrylamide (AM) onto Ch by means of γ -radiation. The graft copolymerization was carried out at 20–25 °C. The graft copolymer obtained was characterized by various techniques including FTIR spectroscopy, X-ray diffraction, and thermogravimetric analysis. Effects of acetic acid concentration (which is the medium for dissolving Ch), total irradiation dose, dose rate, and monomer concentration on the grafting percentage were investigated. Flocculation experiment results demonstrated that the graft copolymer produced was significantly superior to Ch and polyacrylamide (PAM).

Pengfei et al. [73] graft copolymerized styrene onto Ch using ^{60}Co γ -radiation. The solvent composition has a marked effect on the degree of grafting. The graft yield increased with the increase in absorbed dose. At the same dose, the graft yield of styrene on Ch was higher than that on chitin. The grafting reaction was promoted in the presence of methanol, and oxygen delayed the grafting reaction but did not inhibit it completely.

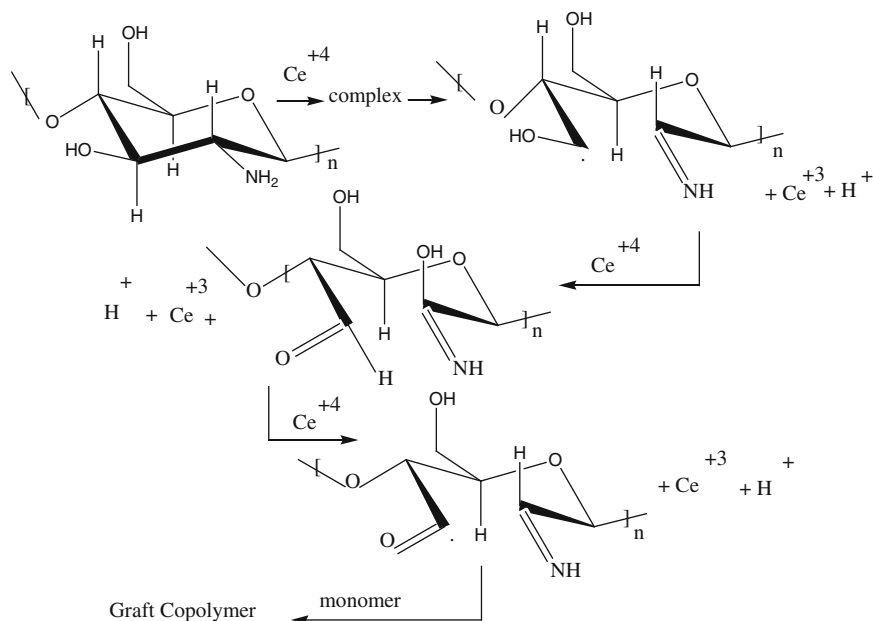
4.4.3.2 Chemical Methods

Various Radical Induced Methods

Chemical method means the grafting can proceed along two major pathways, via free radical and ionic mechanisms. In the chemical process, the role of initiator is very important as it determines the path of the grafting process. The most used method of chemical initiation of vinyl graft copolymerization onto Ch is the reaction of Ch with ceric (IV) ions [74], $\text{H}_2\text{O}_2/\text{Fe}^{2+}$ [75], or Fe^{2+} /persulfate [76] as redox systems. In these systems, free radicals are produced from the initiators and transferred to the substrate to react with monomer to form the graft copolymers. In general, one can consider the generation of free radicals by indirect or direct methods.

Ceric Ion-Induced Grafting

Cerium in its tetravalent state is a versatile oxidizing agent used most frequently in the graft copolymerization of vinyl monomers onto cellulose and starch [77, 78]. It forms a redox pair with the anhydro glucose units of the polysaccharide to yield the macroradicals under slightly acidic conditions. As with cellulose and starch, the ceric ion had been a useful initiation method for graft copolymerizing of chitin and Ch with typical vinyl monomers due to the similarities in the chemical structures of these polysaccharides [79–83]. The mechanism of initiation for Ch is believed to



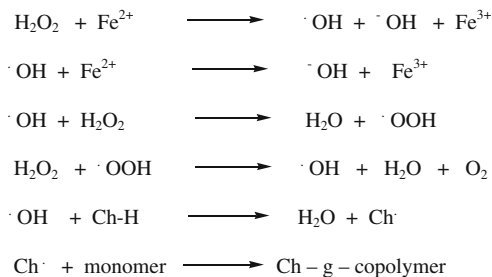
Scheme 4.2 Proposed reaction mechanism for macroradical production on the chitosan backbone using ceric ion initiator

begin with a complex formation of Ce^{4+} with the primary amine and the hydroxyl groups at the C-2 and C-3 positions, respectively. The radicals responsible for the initiation of grafted copolymer chains using vinyl monomer are produced from the complex dissociation. A typical mechanism for the chemical initiation by cerium ammonium nitrate for the graft copolymerization of vinyl and acrylate monomers onto Ch is represented in Scheme 4.2.

Fenton's Reagent

Fenton's reagent is a typical redox initiator used frequently for the initiation of graft copolymerization of various monomers onto chitin and chitosan [84]. The reagent involves a redox reaction between the ferrous ions (usually ferrous sulfate) and hydrogen peroxide. This interaction leads to the formation of a single hydroxyl radical which initiate the graft copolymerization through abstraction of a hydrogen atom from the hydroxyl groups of the glycosidic ring of the chitin or Ch (usually from the primary alcohol at C₆). Although hydrogen peroxide can be used alone as effective initiator for the copolymerization, there are reasons why reducing agent like ferrous ions is preferable to be used. Firstly, a higher yield of radicals is produced at lower temperature in the presence of redox initiator, and secondly, the chelating properties of Ch with the metal ions promote the formation of $\cdot OH$ radicals in the vicinity of the Ch chains thus lower the opportunity for

Scheme 4.3 Radical formation by means of Fenton's reagent in an aqueous environment



homopolymer formation. Methyl methacrylate (MMA) was graft copolymerized onto Ch with grafting percentage of 400–500 % in the presence of Fenton's reagent with a homopolymer yield in the range of 20–30 % [75].

A schematic presentation for the graft copolymerization in the presence of Fe(II)/H₂O₂ redox initiator is illustrated in Scheme 4.3.

Persulfate-Induced Grafting

Ch has been graft copolymerized with vinyl monomers using potassium persulfate (KPS) as initiator. When an aqueous solution of KPS is heated, it decomposes to yield sulfate radical with other free radicals species [85] (Scheme 4.4).

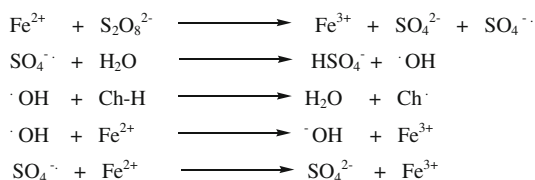
An interesting reaction mechanism with Ch/persulfate system has been proposed by Wang et al. [86], where chitosan's free amino group reacts directly with the persulfate to yield R-NH, OSO₃H, and SO₄²⁻. In the work of Yazdani-Pedram et al. [87, 88], KPS was used to graft Ch by vinyl pyrrolidone and both methyl acrylate (MA) and MMA. They compare the use of KPS alone and in the presence of various reducing agents in the initiation process [88].

Modification of Ch by grafting of vinyl butyrate was carried out in homogeneous phase using KPS as redox initiator and 1.5 % acetic acid as solvent. The grafted product is insoluble in common organic solvents as well as in dilute organic and inorganic acids. The maximum grafting percentage (%G) and grafting efficiency (GE%) values obtained under these conditions were 359 % and 94 %, respectively. Moreover, the thermal property measurements (DSC measurements) have proved the higher thermal stability of the grafted Ch as compared with the ungrafted one [89].

Ch as a biopolymer was chemically modified by grafting polyacrylamide (PAM) in a homogeneous phase by using KPS as redox initiator system in the presence of *N,N*-methylene-bis-acrylamide as a cross-linking agent. The percentage of grafting was found to depend on the various reaction conditions. At optimized combinations of the reaction variables, a GE of 88 % and a G% of 220 % were attained. When grafting of AM onto Ch was achieved in the absence of the cross-linker, the obtained grafted product was slightly soluble, while in the presence of the cross-linker, it is completely insoluble giving a typical polymeric hydrogel [90].

Graft copolymerization of 2-hydroxyethyl acrylate (HEA) onto Ch using ammonium persulfate (APS) as a redox initiator was carried out in aqueous solution. HEA

Scheme 4.4 Mechanism for macroradical formation on the backbone of chitosan by means of ferrous ion-persulfate redox system in aqueous media



was successfully grafted onto Ch up to 300 % in homogeneous phase under inert atmosphere. It was possible to control the grafting parameters by varying the reaction conditions. The polymerization rate was found to be more sensitive to the concentration of the monomer than to the concentration of the initiator. The grafted samples are soluble in water and at alkaline pH, describing an enhanced hydrophilic character as compared with the parent acetylated Ch [91].

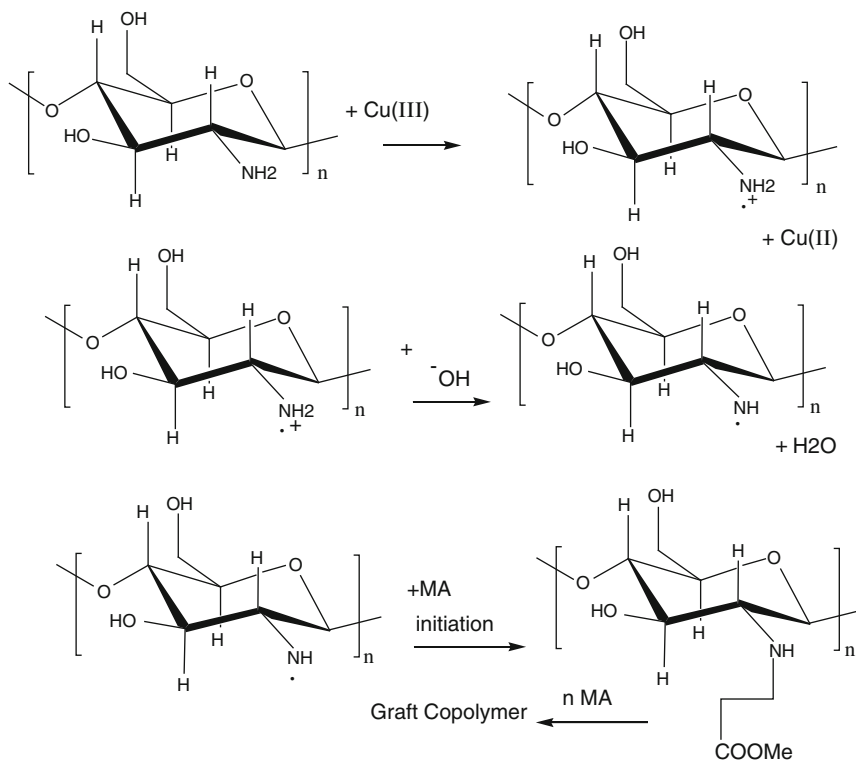
Novel Redox Initiators

A novel redox system, potassium diperiodatocuprate (III)-Ch [92], was employed to initiate the graft copolymerization of methyl acrylate (MA) onto Ch in alkaline aqueous solution. Cu(III) was used as an oxidant and Ch as a reductant in this redox system. Cu(III) was an efficient as well as a cheap initiation system, and the initiation mechanism of grafting reaction proceeds according to Scheme 4.5.

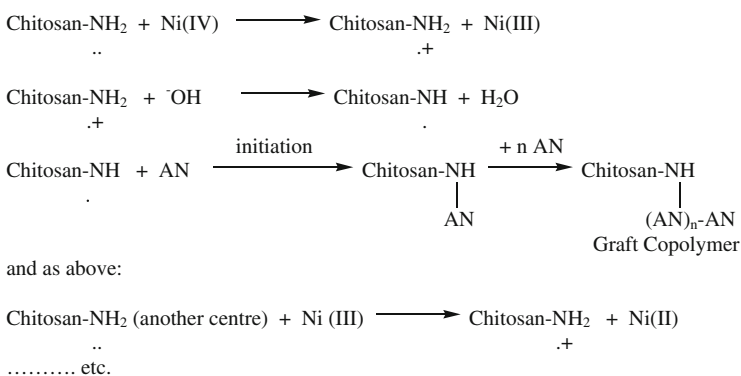
Another novel redox system, potassium diperiodatonickelate (IV)-Ch, was employed to initiate the graft copolymerization of acrylonitrile (AN) onto Ch. A two-step electron-transfer mechanism is proposed to explain the formation of radicals and the initiation [93]. The authors proposed that Ni(IV) may react with amino group in Ch to originate macroradicals first and then initiate AN grafting copolymer. The initiation mechanism [93, 94] is represented in Scheme 4.6.

Ch displays several advantages among other poly cations including cost-effectiveness, biocompatibility, biodegradability, and low cytotoxicity [95]. Modification of Ch through grafting with biodegradable hydrophobic polymers has been reported by several research groups as, for example, grafting of Ch with polycaprolactone [96–98], with polylactide [99–101], or with aliphatic polyesters [102]. Because of the insolubility of Ch in common organic solvents, the conjugation of water-insoluble polymers onto Ch backbone always takes several reaction steps [96–98]. *N*-phthaloyl Ch was frequently used as an organo-soluble precursor for modifying Ch in common organic solvents [103]. Stoichiometric sulfate Ch complex (SChC) which was soluble in common organic solvents was adopted as an intermediate. Regioselective conjugation of polycaprolactone (PCL) onto SChC could be achieved through condensation reaction between isocyanate-terminated PCL and hydroxyl groups of Ch. The grafting level of PCL could be modulated by varying PCL/SChC weight ratio.

However, Preparation of *N*-phthaloyl Ch and the subsequent deprotection process were very tedious and time-consuming. In addition, it was reported that the Ch backbone was subjected to significant breakdown during the protection/deprotection processes due to the harsh reaction conditions [104].



Scheme 4.5 Initiation mechanism of grafting using potassium diperiodatocuprate (III)



Scheme 4.6 Initiation mechanism of grafting using potassium diperiodatonickelate (IV)

Cai et al. [105] synthesized Ch-*O*-poly(ϵ -caprolactone) (Ch-*O*-PCL) with well-defined structure under very mild conditions. By adopting sodium dodecyl sulfate–Ch complex (SCHC) as an organo-soluble intermediate [106], PCL could

be facilely conjugated to the hydroxyl groups of Ch without the need for chemically protecting amino groups.

4.5 Characterization of Chitosan-g-Copolymers

Characterization of grafted copolymers is usually done through spectral and thermal analyses, X-ray diffraction, and morphological studies.

4.5.1 Spectral Analyses

FTIR spectroscopy is a common tool used by many authors [89, 107–111] to characterize the prepared copolymers and acts as a proof for the grafting process. In addition, if it is done quantitatively, it can be considered as an additional proof for the grafting yield. For example, Li et al. [107] characterized the prepared Ch-graft-poly(ethyleneimine) (Ch-g-PEI) by FTIR, Fig. 4.4. They found that new peaks appeared at 1,468, 1,412, and 814 cm^{-1} as a result of grafting which are attributed to the absorption of $-\text{CH}_2-\text{CH}_2-\text{NH}$ -moiety. This result gave a strong evidence for the grafting process.

Graft copolymer of Ch with poly[rosin-(2-acryloyloxy)ethyl ester] (Ch-g-PRAEE) has been synthesized and characterized using FTIR spectroscopy by Duan et al. [108], Fig. 4.5. In the spectrum (Fig. 4.5b) of Ch-g-PRAEE copolymer, in addition to the characteristic peaks of Ch (Fig. 4.5a), some new peaks appeared. The peaks at 1,728, 1,105, and 1,248 cm^{-1} were attributed to the C=O, $-\text{C}-\text{O}-$ and $-\text{O}-\text{C}-$ ester functional groups from grafted PRAEE, respectively; the CH_2 peak from grafted PRAEE appeared at 1,456 cm^{-1} . Also, C=O and $-\text{NH}$ -peaks in the amide groups were shifted toward lower wave numbers, that is, from 1,652 and 1,597 cm^{-1} to 1,631 and 1,525 cm^{-1} , respectively. From the IR spectra, it is confirmed that the Ch-g-PRAEE copolymer was successfully synthesized.

Li et al. [107] used $^1\text{H-NMR}$ spectroscopy as a fine tool to prove and characterize the grafting of poly(ethylenimine) with a disulfide linkage onto Ch (Ch-g-PEI). The $^1\text{H-NMR}$ spectra of the Ch derivatives are represented in Fig. 4.6. The proton peaks of $-\text{CH}_2\text{CH}_2\text{S}-$ appeared at 2.8–2.95 and 2.5–2.6 ppm in the spectrum of the intermediate Ch-SS-COOH (Fig. 4.6b), indicating that 3,3'-dithiodipropionic acid was grafted to the Ch chain. The PEI grafting degree per glucosamine unit was determined by comparing the $^1\text{H-NMR}$ signal integrals from $-\text{CH}_2$ protons of PEI, which should subtract the absorption areas of $-\text{CH}_2\text{CH}_2\text{S}-$, with integrals of the Ch backbone proton signals.

Liu et al. [112] used the ring-opening polymerization technique for the graft copolymerization of *p*-dioxanone (PDO) onto Ch (Ch-g-PDO), and its chemical structure was determined by $^1\text{H-NMR}$. Comparing the $^1\text{H-NMR}$ spectrum of Ch

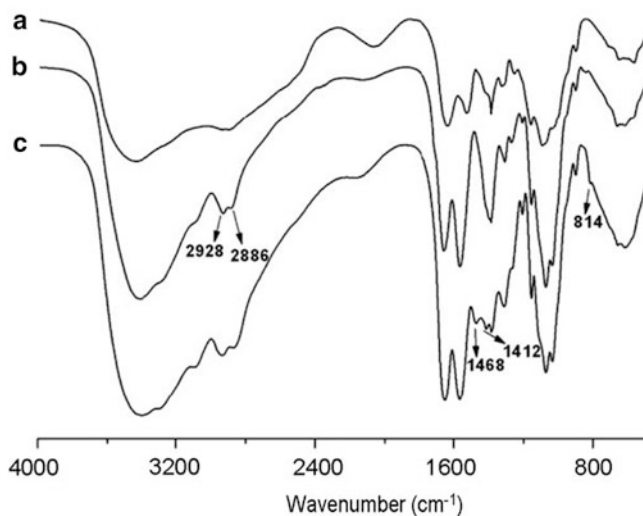


Fig. 4.4 FTIR spectra of (a) Ch, (b) Ch-SS-COOH, and (c) Ch-g-PEI (adapted from [107], Elsevier publisher)

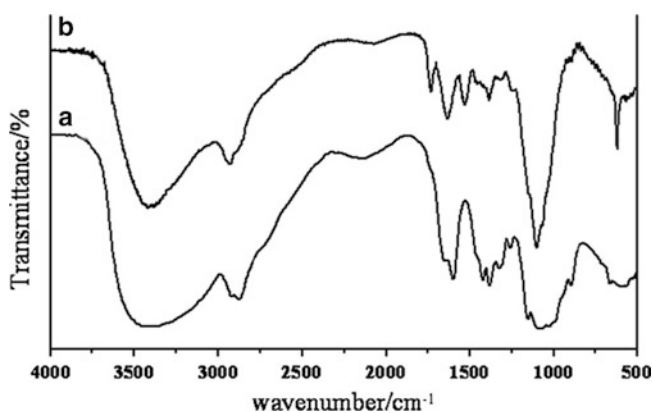


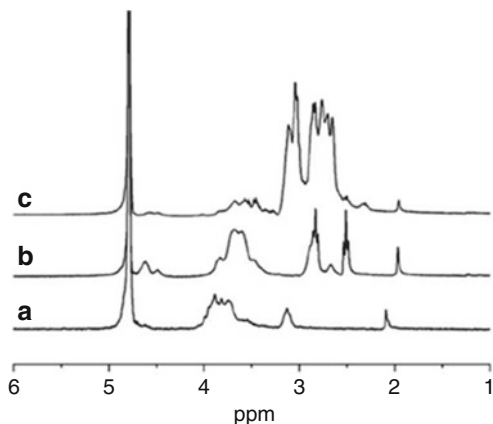
Fig. 4.5 FTIR spectra of (a) Ch and (b) Ch-g-PRAEE (adapted from [108], Elsevier publisher)

[113, 114] and that of graft copolymer showed some new proton signals at 4.16, 3.70, and 4.22 ppm assigned to the different methylene groups of PPDO side chains.

4.5.2 X-Ray Diffraction Analysis

X-ray powder diffraction analysis (XRD) is another useful method used by several authors [115–117] to demonstrate the structure of graft copolymers in solid state.

Fig. 4.6 $^1\text{H-NMR}$ spectra of (a) Ch, (b) Ch-SS-COOH, and (c) Ch-g-PEI in D_2O (adapted from [107], Elsevier publisher)



Ch-based copolymers with binary grafts of hydrophobic polycaprolactone and hydrophilic poly(ethylene glycol) (Ch-g-PCL and PEG) were synthesized by Liu et al. [115] and characterized by X-ray diffraction analysis. The results indicate the disappearance of signal at $2\theta = 12^\circ$ belonging to polysaccharide sequences of Ch indicated that the introduction of PEG or PCL branches suppressed the crystallization of Ch. Similar results were obtained in the work of EIKhholy et al. when Ch was grafted with poly(acryloyl cyanoacetohydrazide) [117].

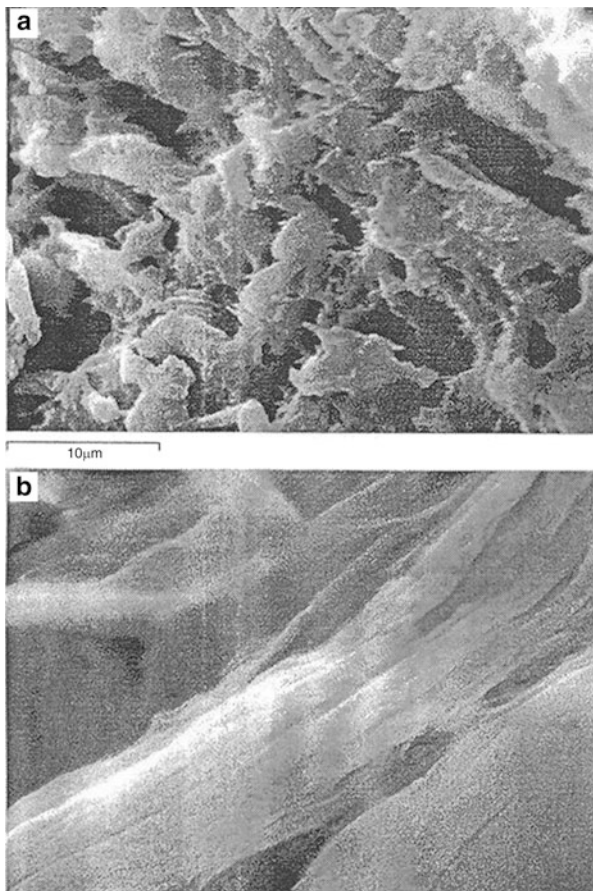
4.5.3 Scanning Electron Micrograph

Several authors have considered the scanning electron micrograph (SEM) as a useful tool for proving the grafting process. Thus, any change in the morphological structure of the pure Ch is a direct evidence that grafting had occurred [89, 108–110, 118]. For instance, Mum et al. [118] have characterized the graft copolymerization of 2-hydroxyethyl acrylate (HEA) onto Ch by SEM. The results are represented in Fig. 4.7. The Ch particles typically present a porous morphology (Fig. 4.7a), while a nonporous fibrous structure was observed for the Ch-g-PHEA copolymer with percent graft near 100 % (Fig. 4.7b).

4.5.4 Thermal Analyses

Thermal analyses (TGA and, DSC) are considered by many investigators [108–111, 119] as powerful tools to prove the grafting copolymerization process from one side and to characterize the thermal stability (or instability) of the resulting graft copolymers as compared with the native matrix. Thus, for example, in the work of Duan et al. [108], the degradation process and thermal stability of Ch and

Fig. 4.7 SEM images of the top view of (a) Ch and (b) Ch-g-PHEA at 3,000 \times magnification (adapted from [118], Elsevier publisher)



Ch-g-poly[rosin-(2-acryloyloxy)ethyl ester] (Ch-g-PRAEE) copolymer were evaluated through thermogravimetric analysis (TGA) experiments, and the results are shown in Fig. 4.8. The figure clearly showed that three consecutive weight loss steps were observed in the Ch (curve a) and Ch-g-PRAEE copolymer (curve b). For the TGA curve of Ch, the first stage showed a loss of absorbed and bounded water of 6.3 wt% at 55–191 °C, indicating its hygroscopic nature; the second weight loss occurred in the range 230–327 °C which corresponded to the scission of the ether linkage in the Ch backbone, while the third stage showed a weight loss in the range of 327–703 °C, which is responsible for the thermal decomposition of glucosamine residue. However, the Ch-g-PRAEE copolymer (curve b) had different course of the thermal degradation compared to Ch. The first stage showed that a loss of absorbed water started in the range between 30 and 153 °C; the second stage was from 196 to 328 °C which corresponded to the scission of the ether linkage in the Ch backbone. The third stage was from 400 to 470 °C, which is contributed to the thermal decomposition of PRAEE side chains. The onset temperature of both

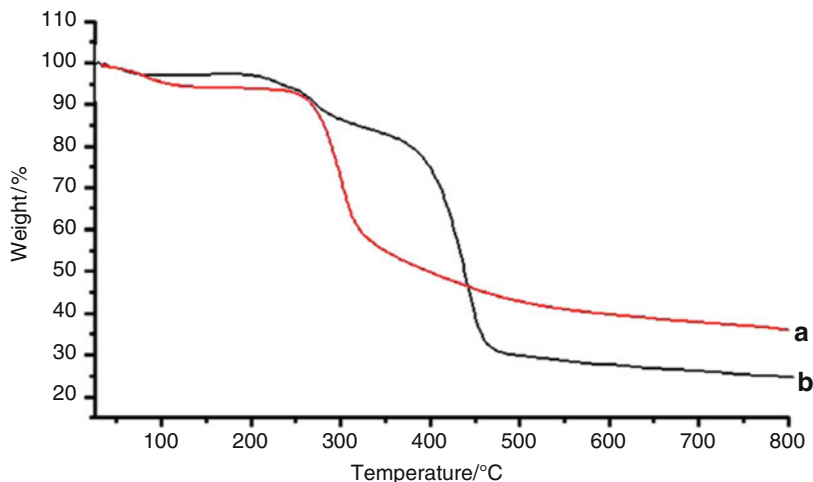


Fig. 4.8 TGA thermograms of (a) Ch and (b) Ch-g-PRAEE copolymer (adapted from [108], Elsevier publisher)

the dehydration and the thermal degradation of the grafted copolymer was lower than the native Ch, that is, the thermal stability of Ch decreased slightly after graft copolymerization. This is because more hydroxyl and amino groups exist in the Ch structure, and consequently, the crystalline regions are easily formed compared to the graft copolymer. Increase in the crystallinity of the polymer is beyond its relatively higher thermal stability.

Akgün et al. [89] graft copolymerized poly(vinyl butyrate) onto Ch. Characterization of the graft copolymers was done by differential scanning calorimetry (DSC). The results revealed a difference in thermal stability between Ch and its grafted product. The thermal property of Ch-g-poly(vinyl butyrate) was more stable than that of the ungrafted Ch. El-Sherbiny and Smith [120] graft copolymerized polyethylene glycol (PEG) onto *N*-phthaloyl Ch (NPHCh). The prepared copolymer was confirmed by studying its thermal characteristics in comparison with PEG-COOH and NPHCh starting materials. The results indicated that the DSC thermogram of PEG-COOH showed an endothermic peak at around 65 °C which corresponds to its melting process. The same endothermic peak appeared also in the thermogram of the copolymer (PEG-g-NPHCh) at around 58 °C due to the melting of the grafted PEG side chains which gave a good evidence for the grafting process. Moreover, the copolymer showed an exotherm at 231 °C which was ascribed to the decomposition of the graft copolymer.

4.6 Applications of Chitosan and Modified Chitosan

4.6.1 As Superabsorbent Materials

Yu et al. [121] have synthesized a novel superabsorbent polymer by graft copolymerization of sodium acrylate and 1-vinyl-2-pyrrolidone onto the chain of *N-O*-CMCh. They found that the water absorption properties of the superabsorbent polymer are greatly affected by the reaction temperature and time as well as by the ratios of the reagents including the amounts of the cross-linking agent, the initiator, the monomer, the molar ratio of the two monomers, and the volume of the water in the reaction system. Superabsorbent polymers are defined as polymers with a network structure and an appropriate degree of cross-linking [122] which can absorb a large amount of water. Ch-based superabsorbent polymers could be prepared by graft copolymerization with vinyl monomers along the Ch chains and cross-linking [123]. Because of its very good biocompatibility and antibacterial property, Ch-based superabsorbent polymers are expected to be widely used in many applications [124] such as medical materials, sanitary materials, controlled release devices, and matrices for enzyme immobilization. The same was found to be true for CMCh [125].

Graft copolymerization of acrylonitrile (AN) and its amidoxime derivative onto Ch and CMCh has been investigated by Sabaa et al. [109, 110]. The obtained results clearly showed the great improvement of the water uptake behavior of Ch in basic medium, as both the grafted Ch and its corresponding amidoxime derivative swell more than the parent ungrafted polymer and that the swell ability increased only for the amidoxime derivative in neutral medium more than the parent Ch. While in the case of CMCh [110], the results indicated that the parent polymer had the greatest ability to swell in different pH values in comparison to the different graft copolymers and their amidoxime derivatives. Huacai et al. [111] synthesized a superabsorbent Ch resin by a graft copolymerization reaction of Ch with the partially neutralized acrylic acid under microwave radiation. Under the optimum conditions, they attained a grafting degree and a grafting efficiency equal to 0.896 and 0.865, respectively, which approached the ones obtained by the traditional heating method. However, the reaction rate under this microwave irradiation method was increased by eight times that obtained by the conventional method, and the resin can absorb water 704 times its own dry weight, which indicates that the prepared resin can be considered as an effective superabsorbent material.

4.6.2 As Metals Ions Adsorption and as Ion Exchangers

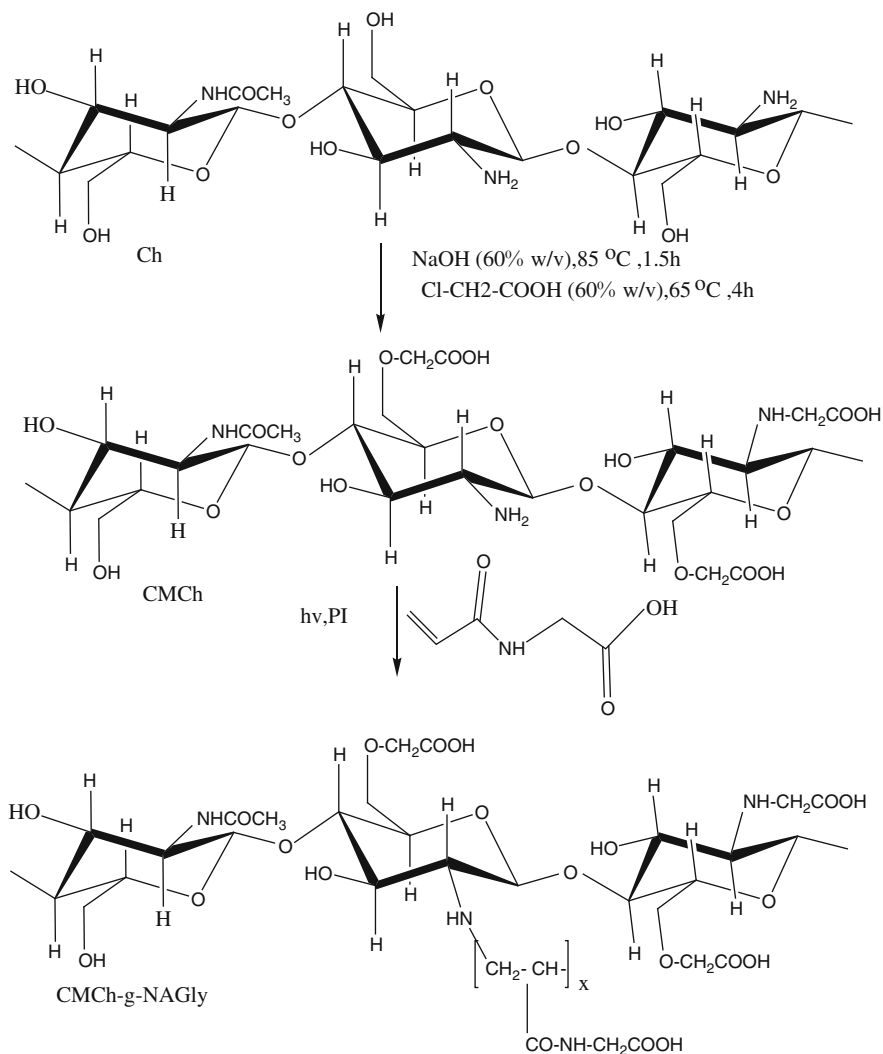
Environmental contamination is a serious problem that is related to possible serious consequences, including heavy metals contamination of water from various sources. The traditional methods for heavy metals removal from wastewater

involve filtration, flocculation, activated charcoal, and ion exchange resins, which are expensive and can result in toxic exposures of the workers involved. Recently, due to its chelating capacity for cations, low price, rich resources, and environmental kindness, Ch has been developed as one of the most popular adsorbents for the removal of metal ions from aqueous solution and is widely used in water treatment applications [126, 127]. The capacity of Ch to complex metallic ions is one of its most important potentialities. However, the adsorption ability of Ch has not been realized to a satisfying level. Many chemical modifications of Ch have been made to improve the cation adsorption capacities. For example, carboxymethylation was prepared and regarded as a simple and effective process to facilitate the adsorption ability of Ch with heavy metals [128, 129]. Farag and Kareem [130] reported that the adsorption capacities of Pb^{2+} ions increased with increasing the degree of substitution of CMCh at the range of 0.8–1.5 mmol g^{-1} sample and that the formation of cross-linking between the amino group and aldehyde group improved the adsorption capacity up to maximum before a decrease. In addition, Sousa et al. [131] chemically modified Ch with ethylene sulfide under solvent-free conditions to give the higher capacity for cations removal from aqueous solution. Emara et al. [132] synthesized two modified Ch polymers by reaction of Ch with cinnamoyl chloride (Ch-Cin) and cinnamoyl isothiocyanate (Ch-ThioCin). The metal uptake capacity of the two polymers was measured at different pH values. The results indicated that the order of the overall rate constant K_a for Ch-Cin was $Fe(III) > Cr(III) > Cu(II)$, while for Ch-ThioCin, it was $Fe(III) > Cu(II) > Cr(III)$.

Jiang and his group [133] have prepared poly(sodium 4-styrenesulfonate) (PSS)-grafted Ch by nitroxide-mediated polymerization (NMP) of sodium 4-styrenesulfonate in the presence of Ch-4-hydroxy-2,2,6,6-tetramethyl piperidine-1-oxyl (4-hydroxy-TEMPO) macro initiator. The results indicated that the Ch-g-PSS could be used as ion exchanger for the environment protection and that the ion exchanging property of Ch-g-PSS could be controlled by adjusting the PSS graft content.

The results obtained by Sabaa and his group [109] showed that the amount of metal ions uptake (Ni^{2+} and Co^{2+}) by Ch is highly increased by grafting with polyacrylonitrile (PAN) and that this increase is highly pronounced when the nitrile groups in the grafted samples were converted into the more polar amidoxime groups. The results also indicated that CMCh-g-PAN, on the other hand, adsorb less metal ions (Ni^{2+} , Co^{2+} , Cd^{2+} , and Cu^{2+}) from aqueous solutions than the parent CMCh, while their amidoxime derivatives adsorb more metal ions than both the graft copolymers and CMCh [110].

The influence of pH on zinc ion binding ability of both Ch and Ch-grafted PMMA (Ch-g-PMMA) was investigated by Muzzarelli [134] and was found to be higher at alkaline pH (pH 8 for Ch and pH 10 for Ch-g-PMMA). In addition, the results obtained by Singh and his group [135] have proved that the zinc ions binding capacity of Ch is markedly increased by the presence of PMMA grafts, which provide additional metal binding sites. Since hydroxyl groups of Ch are highly hydrated and are known not to be adsorption sites, the amino groups of Ch and the ester groups at grafted sites are the sites responsible for metal ion adsorption. Since at the acidic pH the amino groups remain protonated and are not free for binding,



Scheme 4.7 Preparation of CMCh and CMCh-g-NAGly (adapted from [136], Elsevier publisher)

better adsorption is observed at alkaline pH. However, it was shown that at pH > 8 for Ch and >10 for graft copolymer, the adsorption decreases.

El-Sherbiny [136] graft copolymerized *N*-acryloylglycine (NAGly) onto CMCh using 2,2-dimethoxy-2-phenyl acetophenone as photo initiator under nitrogen atmosphere in aqueous solution. A preliminary study was then carried out to evaluate the capacity of the prepared new graft copolymer to uptake copper ions from aqueous systems. The obtained results showed that this system may be extended to be used for metal ions uptake and treatment of wastewater. Scheme 4.7 represents the preparation of CMCh as well as the preparation of the grafted copolymer.

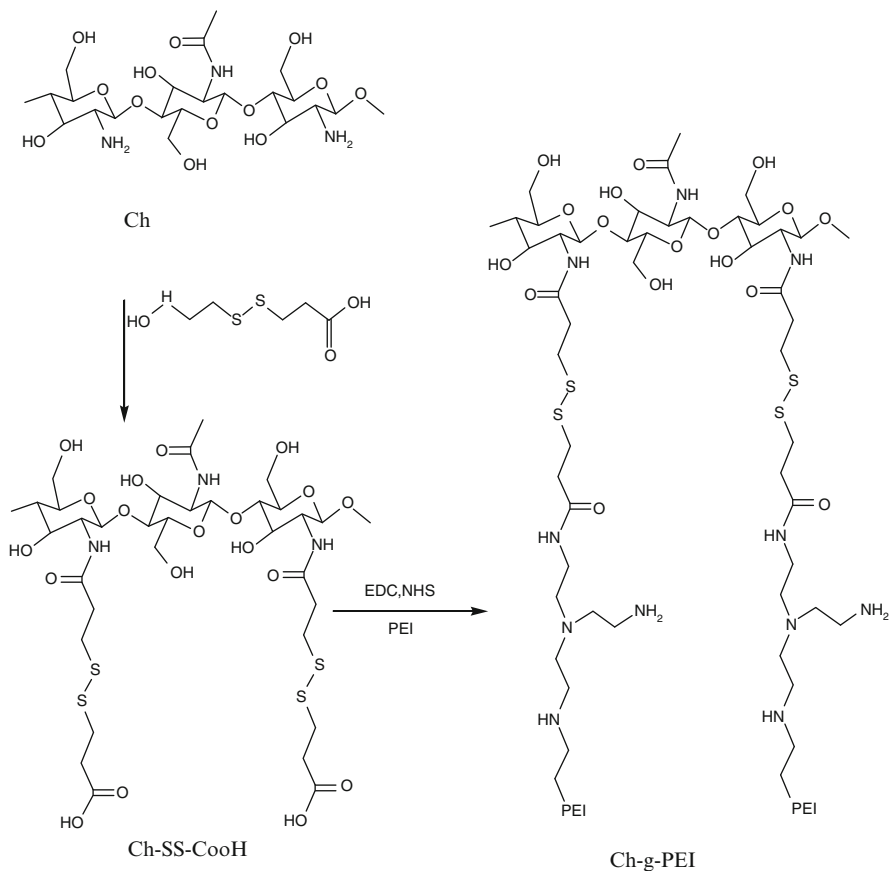
4.6.3 *In Pharmaceuticals and Biomedicals Field*

A novel copolymer of Ch-g-poly(*p*-dioxanone) (Ch-g-PDO) was synthesized by Liu et al. [112] in bulk by ring-opening polymerization of *p*-dioxanone (PDO) initiated by the hydroxyl group or amino group of Ch using stannous octanoate (SnOct₂) as catalyst. The feed ratio of Ch to PDO had great influence on the degree of substitution (DS) and the degree of polymerization (DP) of the copolymer. The in vitro release behavior of ibuprofen (IBU) indicated that the copolymers seem to be a promising vehicle for controlling delivery drugs.

In recent years, nonviral cationic vectors have been applied to protect the DNA from degradation based on the condensation of negatively charged DNA into compact particles essentially by electrostatic interactions [137, 138]. To improve the safety of gene transfer vectors, the materials used for preparing cationic polymers must be biocompatible and biodegradable [139], with high stability and favorable biocompatibility [95]. Ch was first applied in the effort of gene delivery [140] and widely acknowledged as one of the most attractive cationic vectors [141]. However, the transfection efficiency of Ch poly plexes are poor, and among all those efforts to solve this problem, direct grafting of Ch with poly(ethylenimine) (PEI) was considered to be one of the most prominent methods [142–144]. With a substantial increased charge density [145, 146], the modified Ch polymer creates a hydrophilic exterior that reduces interactions of the cationic vector with plasma proteins and erythrocytes. The transfection efficiency may depend on several factors, such as the chemical composition of the synthetic polymer and the nanoparticle size of the complex [147]. The conjugation mechanism and grafting ratios of PEI are two influential factors contributing to the obtained properties of Ch-g-PEI [148].

A novel Ch-g-PEI copolymer with bio-cleavage disulfide linkages between Ch chains and PEI grafts was synthesized, characterized, and examined as a potential nonviral gene vector [107]. The obtained results showed that the bio-reducible Ch-g-PEI copolymer could be used as a promising nonviral gene carrier due to its excellent properties. Scheme 4.8 represents the synthesis of Ch-g-PEI copolymer with the disulfide linkage between Ch and PEI.

Duan and his coworkers [108] have studied the graft copolymerization of rosin-(2-acryloyloxy) ethyl ester (RAEE) onto Ch, with the aim to examine the prepared copolymer as carrier for fenoprofen calcium, and their controlled release behavior in artificial intestinal juice. They came to the conclusion that the rate of release of fenoprofen calcium from the carrier of Ch-g-PRAEE copolymer becomes very slower than that of Ch in artificial intestinal juice. A promising approach for sustained pulmonary drug delivery system has been achieved by the work of El-Sherbiny et al. [149]. In their study, poly(D,L-lactic-co-glycolic acid) (PLGA) nanoparticles encapsulated in amphiphilic Ch-g-PEG copolymer-based hydrogel microspheres were developed and evaluated as a new potential carrier system for sustained pulmonary delivery of curcumin.



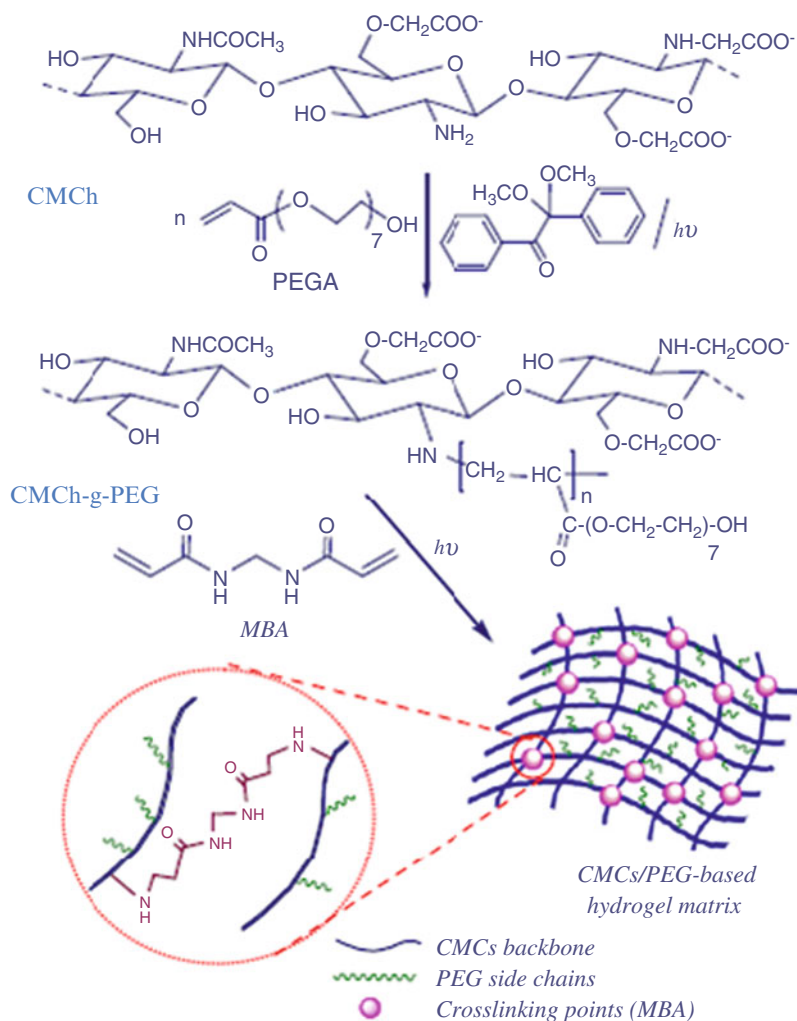
Scheme 4.8 Synthesis of Ch-g-PEI (adapted from [107], Elsevier publisher)

Three different acyl thiourea derivatives of Ch were synthesized by Zhong et al. [150], and their antimicrobial behaviors compared with native Ch against four species of bacteria (*Escherichia coli*, *Pseudomonas aeruginosa*, *Staphylococcus aureus*, and *Sarcina*) and four crop-threatening pathogenic fungi (*Alternaria solani*, *Fusarium oxysporum* f. sp. *vasinfectum*, *Colletotrichum gloeosporioides* (Penz.) Saec, and *Phyllisticta zingiberi*) were investigated. The results indicated that the antimicrobial activities of the acyl thiourea derivatives are much better than that of the parent Ch. Moreover, all of the acyl thiourea derivatives had a significant inhibitory effect on the fungi in concentrations of 50–500 $\mu\text{g mL}^{-1}$. The antifungal activities of the chloroacetyl thiourea derivatives of Ch are noticeably higher than the acetyl and benzoyl thiourea derivatives. The degree of grafting of the acyl thiourea group in the derivatives was related to antifungal activity; higher substitution resulted in stronger antifungal activity.

The Ch graft poly(*p*-dioxanone) copolymer (Ch-g-PDO) was prepared by Wang and his group [151] starting from *N*-phthaloyl-chitosan (PHCh) [103]. PHCh is soluble in organic solvents, such as DMF and DMSO, due to the presence of the phthaloyl protecting group which prevents formation of inter- and intramolecular hydrogen bonds as present in Ch. It could then be reacted with the previously prepared reactive poly(1,4-dioxane-2-one) tolylene-isocyanate (PPDO-NCO), in DMF homogeneous solution, allowing grafting of PPDO onto the Ch backbone, in a similar manner as described for the grafting of PPDO onto starch [152]. Finally, deprotection of the *N*-phthaloyl protecting group was carried out in the presence of hydrazine in order to regenerate the free amino group. The length of PPDO graft chains can be controlled easily by using the prepolymers of PPDO with different molecular weights. The copolymers were used as drug carriers for sinomenine (7,8-didehydro-4-hydroxy-3,7-dimethoxy-17-methyl-9a,13a,14a-morphinan-6-one), and these exhibited a significant controlled drug-releasing behavior whether in artificial gastric juice or in neutral phosphate buffer solution [151].

CMCh was graft copolymerized with poly(ethylene glycol) in the presence of 2,2-dimethoxy-2-phenyl acetophenone (DMPA) as photo initiator [153]. The resulting copolymer was cross-linked via methylene bis-acrylamide as a cross-linking agent to develop pH-responsive hydrogel matrices. The swelling characteristics and the *in vitro* release profiles of 5-fluorouracil (5-FU), as a model drug, from the hydrogels were investigated. The results revealed that the hydrogel matrices developed in this study can be customized to act as good candidates in drug delivery systems. Scheme 4.9 represents the synthesis of CMCh-g-PEG and its hydrogel matrix.

Due to its nontoxicity and high biocompatibility, Ch has been formulated as films, beads, microspheres, and nanoparticles in the pharmaceutical and biomedical fields [154, 155]. Ch could adhere to the mucosal surface and transiently open the tight junction between epithelial cells. It has been reported that Ch can enhance the penetration of macromolecules across the intestinal and nasal barriers [156]. The reason beyond the investigation of Ch as drug delivery systems for genes and proteins was because of the positively charged Ch which can be easily connected with negatively charged DNAs and proteins [157, 158]. However, there are some limitations for Ch to be applied in pharmaceutical and biomedical fields. This is because Ch is only soluble in acidic medium due to the protonation of the free amino groups in its polymeric chains. In neutral and physiological environments, Ch will lose charge and precipitate from solution, which indicates that it does not seem to be a suitable carrier for DNA and protein drugs. To improve the water solubility of Ch, several derivatives of Ch have been studied. For example, the modifications of Ch by quaternization of the amino groups have been extensively reported. *N*-trimethyl chitosan chloride (TMC) is a quaternized derivative of Ch, and it has been studied and described by several research groups [159, 160] for its absorption-enhancing effect. It was concluded that the potential use of TMC, in neutral and physiological environments could contribute significantly to the delivery of hydrophilic compounds such as protein and gene drugs. Although quaternized derivative of Ch does possess outstanding properties for



Scheme 4.9 CMCh-g-PEG and its hydrogel matrix (adapted from [153], Elsevier publisher)

pharmaceutical and biomedical applications, those applications which involve blood-contact problems such as hemolysis, thrombosis, and embolization limit its use [161]. Many cationic polymers have been found to be toxic and it has been suggested that this toxicity comes from their effect on the plasma membranes [162]. Other possible toxic mechanisms are due to their interaction with negatively charged cell components and proteins [163]. Quaternized derivative of Ch possesses high positive charge, which can be easily contacted with negatively charged blood corpuscles, resulting in hemolysis and toxicity.

To overcome these problems, PEG was selected to modify Ch derivatives because of its recognized biocompatibility and ability to reduce the interaction

between cationic polymers and cell membranes [161]. PEG is a kind of hydrophilic flexible, nonionic, and biodegradable polymer. PEG-coated nanoparticles have been found to be of great potential in therapeutic application for controlled release of drugs and site-specific drug delivery [164–166]. In addition, hydrophilic PEG could form a hydrated outer shell, which can protect the nanoparticles from being quickly uptaken by the reticuloendothelial system (RES) [167], extend the half-lives of drugs, and change the tissue bio-distribution of drugs.

Some novel thiosemicarbazone-Ch derivatives were prepared and characterized for their antifungus activity by Qin et al. [168]. The results indicated that the thiosemicarbazone-Ch derivatives possessed great antifungal activity against *S. solani*, *R. solani*, *A. solani*, and *P. asparagi*. On the other hand, Sabaa and his group [119] graft copolymerized poly(*N*-vinyl imidazole) onto CMCh and tested the prepared copolymer for its antimicrobial activity. The results indicated that the grafted products have improved the antimicrobial activity of CMCh against *S. aureus* and *E. coli* bacteria and against *F. oxysporum* and *A. fumigatus* fungi.

4.7 Conclusions

Chitosan, the *N*-deacetylated product of the naturally occurring chitin, is a cheap and nontoxic material, in addition to its biocompatibility and biodegradability. Ch possesses two active functional groups, the amino and the hydroxyl groups, which make it easy to be chemically modified to give desirable products for diverse applications. Modification of Ch can be done by direct interaction with the mentioned functional groups through esterification, carboxymethylation, acylation, Schiff's bases reactions, etc. or through grafting with vinyl or acrylate polymers. Recently, the increasing importance and interest in chemical modification of Ch by graft copolymerization became a demand to improve its solubility and widen its applications. Thermal analyses, scanning electron microscopy, X-ray diffraction, and spectral analyses are considered to be useful tools for the proof of grafting. The physical and chemical properties of Ch are greatly altered with the type of modification. Ch-grafted copolymers find wide applications as superabsorbent materials, in metal uptakes, and as ion exchangers, in swelling properties and in forming hydrogel materials, as well as in pharmaceuticals and in drug delivery systems.

References

1. Pillai CKS, Paul W, Sharma CP (2009) Chitin and chitosan polymers: chemistry, solubility and fiber formation. *Prog Polym Sci* 34(7):641–678
2. Khor E (2002) Chitin: a biomaterial in waiting. *Curr Opin Solid State Mater Sci* 6(4):313–317
3. Van Luyen D, Dm H (1996) In: Salamone J (ed) *Polymeric materials encyclopedia*, vol 2. CRC, Boca Raton, FL, p 1208

4. Roja G, Floores JA, Rodriguez A, Ly M, Maldonado H (2005) Adsorption of chromium onto cross-linked chitosan. *Sep Purif Technol* 44:31–36
5. Peniche C, Argüelles-Monal W, Peniche H, Acosta N (2003) Chitosan: an attractive biocompatible polymer for microencapsulation. *Macromol Biosci* 3(10):511–520
6. Thanpicha T, Sirivat A, Jamieson AM, Rujiravanit R (2006) Preparation and characterization of polyaniline/chitosan blend film. *Carbohydr Polym* 64(4):560–568
7. Varma AJ, Deshpande SV, Kennedy JF (2004) Metal complexation by chitosan and its derivatives: a review. *Carbohydr Polym* 55:77–93
8. Dutta PK, Tripathi S, Mehrotra CK, Dutta J (2009) Perspectives for chitosan based antimicrobial films in food applications. *Food Chem* 114:1173–1182
9. Bautista-Bānos S, Hermàdez-Lauzardo AN, Velàzquez-del Valle HG, Hermàdez-López M, Ait Barka E, Bosquez-Holina B et al (2006) Chitosan as a potential natural compound to control pre and postharvest diseases of horticultural commodities. *Crop Prot* 25:108–118
10. Kato Y, Onishi H, Hachida Y (2003) Application of chitin and chitosan derivatives in the pharmaceutical field. *Curr Pharm Biotechnol* 4:303–309
11. Rinaudo M (2006) Chitin and chitosan: properties and applications. *Prog Polym Sci* 31:603–632
12. Ma G, Yang D, Kennedy JF, Nie J (2009) Synthesize and characterization of organic-soluble acylated chitosan. *Carbohydr Polym* 75(3):390–394
13. Muzzarelli RAA, Rochetti R (1974) The determination of vanadium in sea water by hot graphite atomic absorption spectrometry on chitosan after separation from salt. *Anal Chim Acta* 70:283–289
14. Xia YQ, Cuo TY, Song MD, Zhang BH, Zhang BL (2006) Selective separation of quercetin by molecular imprinting using chitosan beads as functional matrix. *React Funct Polym* 66:1734–1740
15. Sashiwa H, Aiba S (2004) Chemically modified chitin and chitosan as biomaterials. *Prog Polym Sci* 29:887–908
16. Xie WM, Xu PX, Wang W, Liu Q (2002) Preparation and antimicrobial activity of a water-soluble chitosan derivative. *Carbohydr Polym* 50(1):35–40
17. Qu X, Wirsén A, Albertsson A (1999) Synthesis and characterization of pH-sensitive hydrogels based on chitosan and D, L-Lactic acid. *J Appl Polym Sci* 74:3193–3202
18. Guibal E, Touraud E, Roussy J (2005) The use of silver-coated ceramic beads for sterilization of *Sphingomonas* sp. in drinking mineral water. *World J Microbiol Biotechnol* 21(6–7):913–920
19. Li N, Bai R, Liu C (2005) Enhanced and selective adsorption of mercury ions on chitosan beads grafted with polyarylamide via surface-initiated atom transfer radical polymerization. *Langmuir* 21(25):11780–11787
20. Xiaohui W, Yumin Du, Fei H, Hui L, Lihong F (2005) Abstract of papers. In: 22nd 9th ACS national meeting, San Diego, CA, USA, 13–17 March
21. Ju-Young Y, Hee-lack C, Tae S II, Young-Moo K, Wha-Jung K, Doo-Kyung M (2005) *J Ind Eng Chem* 11(6):957–963
22. Lacroix M, Le Thien C (2005) Edible films and coatings from non-starch polysaccharides. In: Han JH (ed) *Innovations in food packagings*. Elsevier, Amsterdam, pp 338–361
23. Broussignac P (1968) *Chem Ind Geniechim* 99:1242
24. Domard A, Rinaudo M (1983) Preparation and characterization of fully deacetylated chitosan. *Int J Biol Macromol* 5(1):49–52
25. Moore GK (1978) Ph.D. Thesis (CNA), Trent Polytechnic, UK
26. Hirai A, Odani H, Nakajima A (1991) Determination of degree of deacetylation of chitosan by ^1H NMR spectroscopy. *Polym Bull* 26:87–94
27. Mourya VK, Inamdar NN (2008) Chitosan-modifications and applications opportunities galore. *React Funct Polym* 68:1013
28. Wolfrom ML, Maher GG, Chaney A (1957) Chitosan nitrate. *J Org Chem* 23:1990

29. Heras A, Rodrigues NM, Ramos VM, Agullo E (2001) N-methylene phosphonic chitosan: a novel soluble derivative. *Carbohydr Polym* 44:1–8
30. Ramos VM, Rodrigues NM, Dyaza MF, Rodrigues MS, Heras A, Agullo E (2003) N-methylene phosphonic chitosan. Effect of preparation methods on its properties. *Carbohydr Polym* 52:39–46
31. Matevosyan GL, Yukha YS, Zavlin PM (2003) Phosphorylation of chitosan. *Russ J Gen Chem* 73:1725–1728
32. Ramos VM, Rodrigues NM, Rodrigues MS, Heras A, Agullo E (2003) Modified chitosan carrying phosphonic and alkyl groups. *Carbohydr Polym* 51:425–429
33. Karrer P, Loenig H, Usteri E (1943) Zur Kenntnis blutgerinnungshemmender polysaccharide-poly-schwefelsäure-ester und ähnlicher verbindungen. *Helv Chim Acta* 26:1296
34. Hackman RH (1954) Studies on Chitin I: enzymic degradation of chitin and chitin esters. *Aust J Biol Sci* 7:168–178
35. Coppick S, Hall WP (1947) In: Little RW (ed), Reinhold, New York, p 179
36. Katsuura K, Mizuno H (1966) Flame proofing of cotton fabrics with urea and phosphoric acid in organic solvent. *Sen-i Gakkishi* 22(11):510–514
37. Sakaguchi T, Horikoshi T, Nakajima A (1981) Adsorption of uranium by chitin phosphate and chitosan phosphate. *Agric Biol Chem* 45(10):2191–2195
38. Laszkiewicz B (1985) Thermal properties of chitin ammonophosphates and their complexes with methanol. *J Therm Anal Calorim* 30(4):889–894
39. Nagasawa K, Tohira Y, Inoue Y, Tanoura N (1971) Reaction between carbohydrates and sulfuric acid: part I. Depolymerization and sulfation of polysaccharides by sulfuric acid. *Carbohydr Res* 18:95–102
40. Vikhoreva G, Bannikova G, Stolbushkina P, Panov A, Drozd N, Makarov V, Varlamov V, Galbraikh L (2005) Preparation and anticoagulant activity of a low-molecular-weight sulfated chitosan. *Carbohydr Polym* 62:327–332
41. Gamzazade A, Sklyar A, Nasibov S, Sushkov I, Shashkov A, Knirel Y (1997) Structural features of sulfated chitosans. *Carbohydr Polym* 34(1):113–116
42. Je JY, Park PJ, Kim SK (2005) Protly endopeptidase inhibitory activity of chitosan sulfates with different degree of deacetylation. *Carbohydr Polym* 60(4):553–556
43. Zhang C, Ping Q, Zhang H, Shen J (2003) Preparation of N-alkyl-O-sulfate chitosan derivatives and micellar solubilization of taxol. *Carbohydr Polym* 54(2):137–141
44. Xing R, Liu S, Yu H, Guo Z, Li Z, Li P (2005) Preparation of high-molecular weight and high-sulfate content chitosans and their potential antioxidant activity in vitro. *Carbohydr Polym* 61(2):148–154
45. Xing R, Liu S, Yu H, Zhang Q, Li Z, Li P (2004) Preparation of low-molecular-weight and high-sulfate-content chitosans under microwave radiation and their potential antioxidant activity in vitro. *Carbohydr Res* 339(5):2515–2519
46. Naggi AM, Torri G, Compagnoni T, Casu B (1986) In: Muzzarelli RAA, Jeuniaux C, Goody GW (eds) *Chitin in nature and technology*. Plenum, New York, NY, p 371
47. Shigemasa Y, Usui H, Morimoto M, Saimoto H, Okamoto Y, Minami S, Sashiwa H (1999) Chemical modification of chitin and chitosan 1: preparation of partially deacetylated chitin derivatives via a ring-opening reaction with cyclic acid anhydride in lithium chloride/N, N-dimethyl acetamide. *Carbohydr Polym* 39(3):237–243
48. Tien C, Lacroix M, Ispas-Szabo MMA (2003) N-Acetylated chitosan: hydrophobic matrices for controlled drug release. *J Control Release* 93:1–3
49. Sashiwa H, Kawasaki N, Nakayama A, Muraki E, Yamamoto N, Zhu H, Nagano H, Omura Y, Saimot H, Shigemasa Y, Aiba S (2002) Chemical modification of chitosan. 13. Synthesis of organosoluble, palladium adsorbable and biodegradable chitosan derivatives towards the chemical plating on plastics. *Biomacromolecules* 3:1120–1125
50. Wu Y, Seo T, Maeda S, Sasaki T, Irie S, Sakurai K (2005) Circular dichroism induced by the helical conformations of acylated chitosan derivatives bearing cinnamate chromophores. *J Polym Sci B Polym Phys* 43:1354–1364

51. Hoffmann-La-Roche F and CO (1957) UK Patent 777: 204
52. Aiba S (1986) Studies on chitosan: 1. Determination of the degree of N-acetylation of chitosan by ultraviolet spectrophotometry and gel permeation chromatography. *Int J Biol Macromol* 8(3):173–176
53. Moore GK, Roberts GAF (1981) Reaction of chitosan: 2. Preparation and reactivity of N-acyl derivatives of chitosan. *Int J Biol Macromol* 3:292–296
54. Kurita K, Sannan T, Iwakura Y (1977) Studies on chitin, 3. Preparation of pure chitin, poly (N-acetyl-D-glucosamine) from the water soluble chitin. *Die Makromol Chem* 178:2595–2602
55. Zhang C, Ping Q, Zhang H, Shen J (2003) Synthesis and characterization of water soluble O-succinyl-chitosan. *Eur Polym J* 39:1629–1634
56. Moore GK, Roberts GAF (1982) Reactions of chitosan: 4. Preparation of organosoluble derivatives of chitosan. *Int J Biol Macromol* 4:246–249
57. Moore GK, Roberts GAF (1981) Reactions of chitosan: 3. Preparation and reactivity of Schiff's base derivatives of chitosan. *Int J Biol Macromol* 3:337–341
58. Gupta KC, Jabrail FH (2007) Glutaraldehyde cross-linked chitosan microspheres for controlled released of centchroman. *Carbohydr Res* 342(15):2244–2252
59. Coelho TC, Laus RR, Mangrich AS, deFávere VT, Laranjeira CM (2007) Effect of heparin coating on epichlorohydrin cross-linked chitosan microspheres on the adsorption of copper (II) ions. *React Funct Polym* 67:468–475
60. Yisong Y, Wenjun L, Tongyin Y (1990) *Polym Commun* 31:319–321
61. Jamella SR, Jayakrishnan A (1995) Glutaraldehyde cross-linked chitosan microspheres as a long acting biodegradable drug delivery vehicle: studies on the *in vitro* release of mitoxantrone and *in vivo* degradation of microspheres in rat muscle. *Biomaterials* 16 (10):769–775
62. Noguchi J (1963) (Asachi Chemical Industry Co., Ltd.) *Japan* 24, 400 (65), Oct 25, Appl. May 17, 3 pp
63. Lim S. “PhD thesis 2002” Faculty of North Carolina State University. “Synthesis of a fiber-reactive chitosan derivative and its application to fabrics an antimicrobial finish and a dyeing-improving agent.” (Under the direction of Sameul Mack Hudson).
64. Okimasu S (1958) *Nippon Nogei Kagaku Kaishi* 32:383
65. Plisko EA, Nud'ga LA, Danilov SN (1972) USSR Patent 325: 234
66. Nud'ga LA, Plisko EA, Danilov SN (1963) *Zhur Obsch Khim* 43:2752
67. Ge H, Luo D (2005) Preparation of carboxymethyl chitosan in aqueous solution under microwave irradiation. *Carbohydr Res* 340(7):1351–1356
68. Joshi JM, Sinha VK (2006) Graft copolymerization of 2-hydroxyethyl methacrylate onto carboxymethyl chitosan using CAN as an initiator. *Polym J* 47(6):2198–2204
69. Wu YG, Chan WL, Szeto YUS (2003) Preparation of O-carboxymethyl chitosan and their effect on color yield of acid dyes on silk. *J Appl Polym Sci* 90(9):2500–2502
70. Sugimoto M, Morimoto M, Sashiwa H (1998) Preparation and characterization of water-soluble chitin and chitosan derivatives. *Carbohydr Polym* 36(1):49–59
71. Jayakumar R, Prabakaran M, Reis RL, Mano JF (2005) Graft copolymerized chitosan—present status and applications. *Carbohydr Polym* 62:142–158
72. Wang J, Chen Y, Zhang S, Yu H (2008) A chitosan-based flocculant prepared with gamma-irradiation-induced grafting. *Bioresour Technol* 99:3397–3402
73. Pengfei L, Maolin Z, Jilan W (2001) Study on radiation-induced grafting of styrene onto chitin and chitosan. *Radiat Phys Chem* 61(2):149–153
74. Mino G, Kaizerman S (1958) A new method for the preparation of graft copolymers. Polymerization initiated by ceric ion redox systems. *J Polym Sci* 31(122):242–243
75. Lagos A, Reyes J (1988) Grafting onto chitosan: 1. Graft copolymerization of methylmethacrylate onto chitosan with Fenton's reagent (Fe^{2+} - H_2O_2) as a redox initiator. *Polym Sci A Polym Chem* 26:985–991

76. Kataoka S, Ando T (1981) Molecular weight regulation in radical polymerization of methacrylic acid by chitosan. *Kobunshi Ronbunshu* 38(11):797–799
77. Athawale VD, Rathi SC (1999) Graft polymerization: starch as a model substrate. *J Macromol Sci Rev Macromol Chem Phys* C39(3):445–480
78. Berlin Ad A, Kislenco VN (1992) Kinetics and mechanism of radical graft polymerization of monomers onto polysaccharides. *Prog Polym Sci* 17:765–825
79. Pourjavada A, Mahdavinia GR, Zohuriaan-Mehr MJ (2003) Modified chitosan. II. H-ChitoPAN, a novel pH-responsive supersorbent hydrogel. *J Appl Polym Sci* 90:3115–3121
80. Pourjavadi A, Zohuriaan-Mehr MJ, Mahdavinia GR (2004) Modified chitosan. III. Superabsorbency, salt- and pH-sensitivity of smart ampholytic hydrogels from chitosan-g-PAN. *Polym Adv Technol* 15(4):173–180
81. Mahdavinia GR, Pourjavadi A, Hosseinzadeh H, Zohuriaan MJ (2004) Modified chitosan. 4. Superabsorbent hydrogels from poly(acrylamide—co-acrylic acid) grafted chitosan with salt- and pH-responsiveness properties. *Eur Polym J* 40:1399
82. Jenkins DW, Hudson SM (2001) Review of vinyl graft copolymerization featuring recent advances towards controlled radical-based reactions and illustrated with chitin/chitosan trunk polymers. *Chem Rev* 101(11):3245–3274
83. Pourjavadi A, Mahdavinia GR, Zohuriaan-Mehr MJ, Omidian H (2003) Modified chitosan. I. Optimized cerium ammonium nitrate-induced synthesis of chitosan-g-polyacrylonitrile. *J Appl Polym Sci* 88(8):2048–2054
84. Yazdani-Pedram M, Lagos A, Retuert J, Guerrero R, Riquelme P (1995) On the modification of chitosan through grafting. *J Macromol Sci Pure Appl Chem* A32(5):1037–1047
85. Kataoka S, Ando T (1984) Radical polymerization of acrylic acid in the presence of chitosan. *Kobunshi Ronbunshu* 41(9):519–524
86. Wang Y, Jingxinan Y, Kunyuan Q (1994) Studies of graft copolymerization onto chitosan. *Acta Polymerica Sinica* 2:188
87. Yazdani-Pedram M, Retuert J (1997) Homogeneous grafting reaction of vinyl pyrrolidone onto chitosan. *J Appl Polym Sci* 63(10):1321–1326
88. Retuert J, Yazdani-Pedram M (1993) Cocatalyst effect in potassium persulfate initiated grafting onto chitosan. *Polym Bull* 31(5):559–562
89. Akgün S, Ekici G, Mutlu N, Besirli N, Hazer B (2007) Synthesis and properties of chitosan—modified poly(vinyl butyrate). *J Polym Res* 14:215–221
90. Yazdani-Pedram M, Lagos A, Retuert PJ (2002) Study of the effect of reaction variables on grafting of polyacrylamide onto chitosan. *Polym Bull* 48:93–98
91. Mun GA, Nurkeeva ZS, Dergunov SA, Nam IK, Maimakov TP, Shaikhutdinov EM, Lee SC, Park K (2008) Studies on graft copolymerization of 2-hydroxyethyl acrylate onto chitosan. *React Funct Polym* 68:389–395
92. Zohuriaan-Mehr MJ (2005) Advances in chitin and chitosan modification through graft copolymerization: a comprehensive review. *Iran Polym J* 14(3):235–265
93. Liu YH, Shang YJ, Li WP, Wang Z, Deng KL (2000) Study on the kinetics of acrylonitrile polymerization initiated by diperiodatonickelate (IV) periodate complex. *Acta Polymerica Sinica* 2:235–238
94. Liu YH, Li WP, Deng KL (2001) Graft copolymerization of methyl acrylate onto nylon1010 initiated by potassium diperiodatonickelate (IV). *J Appl Polym Sci* 82(11):2636–2640
95. Ravi Kumar MNV, Muzzarelli RAA, Muzzarelli C, Sashiwa H, Domb AJ (2004) Chitosan chemistry and pharmaceutical perspectives. *Chem Rev* 104(12):6017–6084
96. Liu L, Wang YS, Shen XF, Fang YE (2005) Preparation of chitosan-g-polycaprolactone copolymers through ring-opening polymerization of ϵ -caprolactone onto phthaloyl-protected chitosan. *Biopolymers* 78(4):163–170
97. Guan XP, Quan DP, Shuai XT, Liao KR, Mai KC (2007) Chitosan-graft poly(ϵ -caprolactone)s: an optimized chemical approach leading to a controllable structure and enhanced properties. *J Polym Sci A Polym Chem* 45(12):2556–2568

98. Liu L, Chen LX, Fang YE (2006) Self-catalysis of phthaloylchitosan for graft copolymerization of ϵ -caprolactone with chitosan. *Macromol Rapid Commun* 27(23):1988–1994
99. Wu Y, Zheng YL, Yang WL, Wang CC, Hu JH, Fu SK (2005) Synthesis and characterization of a novel amphiphilic chitosan-poly(lactide) graft copolymer. *Carbohydr Polym* 59(2):165–171
100. Skotak M, Leonov AP, Larsen G, Noriega S, Subramanian A (2008) Biocompatible and biodegradable ultrafine fibrillar scaffold materials for tissue engineering by facile grafting of L-lactide onto chitosan. *Biomacromolecules* 9(7):1902–1908
101. Feng H, Dong CM (2006) Preparation, characterization, and self-assembled properties of biodegradable chitosan-poly(L-lactide) hybrid amphiphiles. *Biomacromolecules* 7(11):3069–3075
102. Fujioka M, Okada H, Kusaka Y, Nishiyama S, Noguchi H, Ishii S et al (2004) enzymatic synthesis of chitin- and chitosan-graft-aliphatic polyesters. *Macromol Rapid Commun* 25(20):1776–1780
103. Kurita K, Ikeda H, Yoshida Y, Shimojoh M, Harata M (2002) Chemosselective protection of the amino groups of chitosan by controlled phthaloylation: facile preparation of a precursor useful for chemical modifications. *Biomacromolecules* 3(1):1–4
104. Makuška R, Goročovceva N (2006) Regioselective grafting of poly(ethylene glycol) onto chitosan through C-6 position of glucosamine units. *Carbohydr Polym* 64(2):319–327
105. Cai G, Jiang H, Chen Z, Tu K, Wang L, Zhu K (2009) Synthesis, characterization and self assemble behavior of chitosan-O-poly(ϵ -caprolactone). *Eur Polym J* 45:1674–1680
106. Cai GQ, Jiang HL, Tu KH, Wang LQ, Zhu KJ (2009) A facile route for regioselective conjugation of organo-soluble polymers onto chitosan. *Macromol Biosci* 9(3):256–261
107. Li Z, Guo J, Zhang J, Zhao Y, Lv L, Ding C, Zhang X (2010) Chitosan-graft-polyethylenimine with improved properties as a potential gene vector. *Carbohydr Polym* 80(1):254–259
108. Duan W, Chen C, Jiang L, Li GH (2008) Preparation and characterization of the graft copolymer of chitosan with poly[rosin-(2-acryloyloxy)ethyl ester]. *Carbohydr Polym* 73(4):582–586
109. Mohamed RR, Sabaa MW (2010) Graft copolymerization of acrylonitrile and its amidoxime derivative onto chitosan. *J Appl Polym Sci* 116:413–421
110. Sabaa MW, Mohamed NA, Ali R, Abd El Latif SM (2010) Chemically induced graft copolymerization of acrylonitrile onto carboxymethyl chitosan and its modification to amidoxime derivative. *Polym Plast Technol Eng* 49:1055–1064
111. Huacai G, Wan P, Dengke L (2006) Graft copolymerization of chitosan with acrylic acid under microwave irradiation and its water absorbency. *Carbohydr Polym* 66:372–378
112. Liu G, Zhai Y, Wang X, Wang W, Pan Y, Dong X, Wang Y (2008) Preparation, characterization, and in vitro drug release behavior of biodegradable chitosan-graft-poly(1,4-dioxan-2-one) copolymer. *Carbohydr Polym* 74(4):862–867
113. Detchprohm S, Aoi K, Okada M (2001) Synthesis of a novel chitin derivative having oligo(ϵ -caprolactone) side chains in aqueous reaction media. *Macromol Chem Phys* 202:3560–3570
114. Zhong Z, Kimura Y, Takahashi M, Yamane H (2000) Characterization of chemical and solid state structures of acylated chitosans. *Polymer* 41:899–906
115. Liu L, Xu X, Guo S, Han W (2009) Synthesis and self-assembly of chitosan-based copolymer with a pair of hydrophobic/hydrophilic grafts of polycaprolactone and poly(ethylene glycol). *Carbohydr Polym* 75:401–407
116. Kang H, Cai Y, Liu P (2006) Synthesis, characterization and thermal sensitivity of chitosan-based graft copolymers. *Carbohydr Res* 341:2851–2857
117. ElKhholy SS, Khalil KD, Elsabee MZ (2011) Grafting of acryloyl cyanoacetohydrazide onto chitosan. *J Polym Res* 18:459–467
118. Mum GA, Nurkeeva ZS, Dergunov SA, Nam IK, Maimakov TP, Shaikhutdinov EM, Lee SC, Park K (2008) Studies on graft copolymerization of 2-hydroxyethyl acrylate onto chitosan. *React Funct Polym* 68:389–395

119. Sabaa MW, Mohamed NA, Mohamed RR, Khalil NM, Abd El Latif MS (2010) Synthesis, characterization and antimicrobial activity of poly (N-vinylimidazole) grafted carboxymethyl chitosan. *Carbohydr Polym* 79:998–1005
120. El-Sherbiny IM, Smyth HDC (2010) Biodegradable nano-micro carrier systems for sustained pulmonary drug delivery: (I) self-assembled nanoparticles encapsulated in respirable/swellable semi-IPN microspheres. *Int J Pharm* 395:132–141
121. Yu C, Yun-fei L, Hui-min T, Jian-xin J (2009) Synthesis and characterization of a novel superabsorbent polymer of N, O-carboxymethyl chitosan graft copolymerized with vinyl monomers. *Carbohydr Polym* 75:287–292
122. Omidian H, Rocca JC, Park K (2005) Advances in superporous hydrogels. *J Control Release* 102:3–12
123. Liu JH, Wang Q, Wang AQ (2007) Synthesis and characterization of chitosan-g-poly(acrylic acid)sodium humate superabsorbent. *Carbohydr Polym* 70:166–173
124. Sun LP, Du YM, Shi XW, Chen X, Yang JH, Xu YM (2006) A new approach to chemically modified carboxymethyl chitosan and study of its moisture-absorption and moisture-retention abilities. *J Appl Polym Sci* 102:1303–1309
125. Pang HT, Cheng XG, Park HJ, Cha DS, Kennedy JF (2007) Preparation and rheological properties of deoxycholate-chitosan and carboxymethyl chitosan in aqueous systems. *Carbohydr Polym* 69:419–425
126. Babel S, Kurniawan TA (2003) Low-cost adsorbents for heavy metals uptake from contaminated water: a review. *J Hazard Mater* 97(1–3):219–243
127. Guibal E (2004) Interaction of metal ions with chitosan-based sorbents: a review. *Sep Purif Technol* 38(1):43–74
128. Chen XG, Park HJ (2003) Chemical characteristics of O-carboxymethyl chitosans related to the preparation conditions. *Carbohydr Polym* 53(4):355–359
129. Hon DNS, Tang LG (2000) Chelation of chitosan derivatives with zinc ions. I. O, N-carboxymethyl chitosan. *J Appl Polym Sci* 77(10):2246–2253
130. Farag S, Kareem SSA (2009) Different natural biomasses for lead cation removal. *Carbohydr Polym* 78(2):263–267
131. Sousa KS, Silva EC, Airoidi C (2009) Ethylenesulfide as a useful agent for incorporation into the biopolymer chitosan in a solvent-free reaction for use in cation removal. *Carbohydr Res* 344(13):1716–1723
132. Emará AAA, Tawab MA, El-ghamry MA, Elsabee MZ (2011) Metal uptake by chitosan derivatives and structure studies of the polymer metal complex. *Carbohydr Polym* 83:192–202
133. Jiang J, Hua D, Jiang J, Tang J, Zhu X (2010) Synthesis and property of poly(sodium 4-styrenesulfonate) grafted chitosan by nitroxide-mediated polymerization with chitosan-TEMPO macroinitiator. *Carbohydr Polym* 81:358–364
134. Muzzarelli RAA (1973) Analytical application of chitin and chitosan. In: Belcher R, Freiser H (eds) *Natural chelating polymers; alginic acid, chitin and chitosan*. Pergamon Press, New York, NY, pp 177–227
135. Singh V, Tripathi DN, Tiwari A, Sanghi R (2006) Microwave synthesized chitosan-graft-poly (methylmethacrylate): an efficient Zn^{+} ion binder. *Carbohydr Polym* 65(1):35–41
136. El-Sherbiny IM (2009) Synthesis, characterization and metal uptake capacity of a new carboxymethyl chitosan derivative. *Eur Polym J* 45:199–210
137. Mintzer MA, Simanek EE (2009) Nonviral vectors for gene delivery. *Chem Rev* 109:259–302
138. Nguyen DN, Green JJ, Chan JM, Langer R, Anderson DC (2009) Polymeric materials for gene delivery and DNA vaccination. *Adv Mater* 21(16):847–867
139. Hussain SM, Braydich-Stolle LK, Schrand AM, Murdock RC, Yu KO, Mattie DM et al (2009) Toxicity evaluation for safe use of nanomaterials: recent achievements and technical challenges. *Adv Mater* 21(16):1549–1559

140. Mumper RJ, Wang J, Claspell JM, Rolland AP (1995) Novel polymeric condensing carriers for gene delivery. In: Proceedings of the international symposium on controlled release of bioactive materials, vol 22, p 178
141. Liu WG, Yao KD (2002) Chitosan and its derivatives—a promising non-viral vector for gene transfection. *J Control Release* 83(1):1–11
142. Jiang HL, Kim YK, Arote R, Nah JW, Cho MH, Choi YJ et al (2007) Chitosan-graft-polyethylenimine as a gene carrier. *J Control Release* 117(2):273–280
143. Lu B, Xu XD, Zhuo RX, Cheng SX, Zhuo RX (2008) Low molecular weight polyethylenimine grafted N-maleated chitosan for gene delivery: properties and in vitro transfection studies. *Biomacromolecules* 9:2594
144. Wong K, Sun G, Zhang X, Dai H, Liu Y, He C, Leong KW (2006) PEI-g-chitosan, a novel gene delivery system with transfection efficiency comparable to polyethylenimine in vitro and after liver administration in vivo. *Bioconjug Chem* 17(1):152–158
145. Kunath K, Von Harpe A, Fischer D, Petersen H, Bickel U, Voigt K, Kissel T (2003) Low-molecular-weight polyethylenimine as a non-viral vector for DNA delivery: comparison of physicochemical properties, transfection efficiency and in vivo distribution with high-molecular-weight polyethylenimine. *J Control Release* 89(1):113–125
146. Neu M, Fischer D, Kissel T (2005) Recent advances in rational gene transfer vector design based on poly(ethylene imine) and its derivatives. *J Gene Med* 79(8):992–1009
147. Jeong JH, Kim SW, Park TG (2007) Molecular design of functional polymers for gene therapy. *Prog Polym Sci* 32(11):1239–1274
148. Kircheis R, Wightman L, Wagner E (2001) Design and gene delivery activity of modified polyethylenimines. *Adv Drug Deliv Rev* 53(3):341–358
149. El-Sherbiny IM, Smyth HDC (2012) Controlled release pulmonary administration of curcumin using swellable biocompatible microparticles. *Mol Pharm* 9:269–280
150. Zhong Z, Xing R, Liu S, Wang L, Cai S, Li P (2008) Synthesis of acyl thiourea derivatives of chitosan and their antimicrobial activities in vitro. *Carbohydr Res* 343(3):566–570
151. Wang X, Huang Y, Zhu J, Pan Y, He R, Wang Y (2009) Chitosan-graft poly(p-dioxanone) copolymers: preparation, characterization, and properties. *Carbohydr Res* 344(6):801–807
152. He R, Wang X, Wang Y, Yang K, Zeng J, Ding S (2006) A study on grafting poly(1,4-dioxan-2-one) onto starch via 2,4-toluene diisocyanate. *Carbohydr Polym* 65(1):28–34
153. El-Sherbiny IM, Smyth HDC (2010) Poly(ethylene glycol)-carboxymethyl chitosan-based pH-responsive hydrogels: photo-induced synthesis, characterization, swelling, and in vitro evaluation as potential drug carriers. *Carbohydr Res* 345(14):2004–2012
154. Calvo P, Remunan-lopez C, Vila-Jato JL, Alonso MJ (1997) Novel hydrophilic chitosan-polyethylene oxide nanoparticles as protein carriers. *J Appl Polym Sci* 63:125–132
155. Giunchedi P, Genta B, Muzzarelli RAA, Conte U (1998) Preparation and characterization of ampicillin loaded methylpyrrolidinone and chitosan microspheres. *Biomaterials* 19:157–161
156. Borchard G, Lueben HL, De Boer GA, Verhoef JC, Lehr CM, Junginger HE (1996) The potential of mucoadhesive polymers in enhancing intestinal peptide drug absorption. III. Effects of chitosan-glutamate and carbomer on epithelial tight junctions in vitro. *J Control Release* 39(2–3):131–138
157. Richardson SCW, Kolbe HVJ, Duncan R (1999) Potential of low molecular mass chitosan as a DNA delivery system: biocompatibility, body distribution and ability to complex and protect DNA. *Int J Pharm* 178:231–243
158. Janes KA, Calvo P, Alonso MJ (2001) Polysaccharide colloidal particles as delivery systems for macromolecules. *Adv Drug Deliv Rev* 47:83–97
159. Thanou MM, Kotze AF, Scharringhausen T, Lueben HL, De Boer AG, Verhoef JC et al (2000) Effect of degree of quaternization of N-trimethyl chitosan chloride for enhanced transport of hydrophilic compounds across intestinal Caco-2 cell monolayers. *J Control Release* 64(1–2):15–25

160. Xu YM, Du YM, Huang RH, Gao LP (2003) Preparation and modification of N-(2-hydroxyl) propyl-3-trimethyl ammonium chitosan chloride nanoparticle as a protein carrier. *Biomaterials* 24:5015–5022
161. Amiji MM (1997) Synthesis of anionic poly(ethylene glycol) derivative for chitosan surface modification in blood-contacting applications. *Carbohydr Polym* 32(3–4):193–199
162. Choksakulnimitr S, Masuda S, Tokuda H, Takakura Y, Hashida M (1995) In vitro cytotoxicity of macromolecules in different cell culture systems. *J Control Release* 34(3):233–241
163. Fischer D, Li Y, Ahlemeyer B, Krieglstein J, Kissel T (2003) In vitro cytotoxicity testing of polycations: influence of polymer structure on cell viability and hemolysis. *Biomaterials* 24:1121–1131
164. Gref R, Minamitake Y, Perracchia MT, Trubetsky V, Torchilin V, Langer R (1994) Biodegradable long-circulating polymeric nanospheres. *Science* 263:1600–1603
165. Peracchia MT, Gref R, Minamitake Y, Domb A, Lotan N, Langer R (1997) PEG-coated nanoparticles from amphiphilic diblock and multiblock copolymer: investigate of their encapsulation and release characteristics. *J Control Release* 46(3):223–231
166. Quellec P, Gref R, Perrin L, Dellacherie E, Sommer F, Verbavatz JM et al (1998) Protein encapsulation within polyethylene glycol-coated nanospheres. I. Physicochemical characterization. *J Biomed Mater Res* 42:45–54
167. Hu Y, Jiang XQ, Ding Y, Zhang LY, Yang CZ, Zhang JF et al (2003) Preparation and drug release behaviors of nimodipine-loaded poly(caprolactone)-poly(ethylene oxide)-polylactide amphiphilic copolymer nanoparticles. *Biomaterials* 24:2395–2404
168. Qin Y, Xing R, Liu S, Li K, Meng X, Li R, Cui J, Li B, Li P (2012) Novel thiosemicarbazone chitosan derivatives: preparation, characterization, and antifungal activity. *Carbohydr Polym* 87:2664–2670
169. Mohamed RR, Seoudi RS, Sabaa MW (2012) Synthesis and characterization of antibacterial semi-interpenetrating carboxymethyl chitosan/poly(acrylonitrile) hydrogels. *Cellulose* 19(3):947–958

Chapter 5

Gum-g-Copolymers: Synthesis, Properties, and Applications

Aiqin Wang and Wenbo Wang

Abstract With the increasing concerns on environmental problems, the petroleum-based synthetic polymers gradually highlight their disadvantages and threats to the modern world from the perspective of energy source, resource, and environment. So the naturally renewable polymers have received great developments by virtue of their unique environmental and commercial advantages. The commonly cognitive natural polymers are mainly cellulose, starch, and chitosan, which were intensively researched and got extensive applications in food, fine chemicals, soft-tissue and pharmaceutical engineering, biomedical engineering, artificial sensors, etc. as a substitution of synthetic polymers. But these natural polymers fail to meet all requirements in modern industrial application because their boundedness in structure, solubility, colloidal properties, machinability, and so on. Gums have showed variety of structure and property due to their abundant sources and have gained enormous attention as new families of natural polymers. The original forms of gums have excellent suspension, viscosity, rheological properties, stimuli responsivity, flocculation, and adsorption performance besides the common renewable, biodegradable, nontoxic, and biocompatible characteristics. The usability can be further enhanced through the simple derivatization or graft copolymerization, and the drawbacks of gums such as poor rotting resistance can be improved. Compared with conventional derivatization reaction, graft copolymerization is especially important and effective because it can introduce various functional groups and increase the molecular weight of polymers. The graft copolymerization of gums with various monomers can enhance the intrinsic properties and can also bring new properties that raw gums do not have. The gum-g-copolymers usually

A. Wang (✉) • W. Wang

Center for Eco-material and Green Chemistry, Lanzhou Institute of Chemical Physics,
Chinese Academy of Science, 18#, Tianshui middle road, Lanzhou, 730000,

People's Republic of China

e-mail: aqwang@licp.cas.cn; boywenbo@126.com

showed better thermo- and degradation-resistant properties, high-viscous and shear-resistant properties, stimuli-responsive properties, electric properties, etc. and have been widely applied in many areas, such as drilling additives, flocculating agent, drug delivery carriers, adsorption of toxic heavy metals and dyes, water-saving materials, sand-binding materials, daily chemicals, thickener, electrical biomaterials, and macromolecular surfactants. Thus, this chapter detailedly introduced the types, structure, and derivatives of gums; the synthesis method of graft copolymer; the properties of graft copolymer; and their application domains.

Keywords Gum • Graft copolymers • Biopolymers • Initiator • Modification • Synthesis • Applications

Abbreviations

AG	Acacia gum
AMPS	2-Acrylamido-2-methyl-1-propane sulfonic acid
APS	Ammonium persulfate
CAN	Cerium(IV) ammonium nitrate
CAS	Ceric ammonium sulfate
CG	Cashew gum
CGG	Cationic guar gum
CHPTAC	3-Chloro-2-hydroxypropyltrimethylammonium chloride
CRSG	Cassia reticulata seed gum
CTG	Cassia tora gum
DDMC	Diallyldimethylammonium chloride
FET	Final decomposition temperature
GG	Guar gum
GGT	Gum ghatti
H ₂ O ₂	Hydrogen peroxide
IDSG	<i>Ipomoea dasyperma</i> seed gum
IHSG	<i>Ipomoea hederacea</i> seed gum
IPSG	<i>Ipomoea palmata</i> seed gum
<i>k</i> -CGN	<i>k</i> -Carrageenan
KG	Konjac gum
KGM	Konjac glucomannan
KPS	Potassium persulfate
LBG	Locust bean gum
LGSG	<i>Leucaena glauca</i> seed gum
MW	Microwave
P4V	Poly(4-vinylpyridine)
PAA	Poly(acrylic acid)
PACA	Poly(2-acrylamidoglycolic acid)
PAM	Poly(acrylamide)

PAN	Poly(acrylonitrile)
PANI	Poly(aniline)
PCMGG	Partially carboxymethylated guar gum
PDAM	Poly(<i>N,N</i> -dimethylacrylamide)
PEA	Poly(ethylacrylate)
PEMA	Poly(ethyl methacrylate)
PEO	Poly(ethylene oxide)
PGMA	Poly(glycidyl methacrylate)
PIA	Poly(itaconic acid)
PMA	Poly(methacrylic acid)
PMAD	Poly(methacrylamide)
PMMA	Poly(methyl methacrylate)
PNVF	Poly(<i>N</i> -vinyl formamide)
PNVP	Poly(<i>N</i> -vinyl-2-pyrrolidone)
PPO	Poly(propylene oxide)
PSY	Psyllium
SA	Sodium alginate
SD	Sodium disulfite
TGG	Tragacanth gum
TK	Tamarind kernel
UV	Ultraviolet
XG	Xanthan gum
XGC	Xyloglucan

5.1 Introduction

Gums are important families of natural polymers derived from the seeds or tubers of plants and seaweed and are one of the most fast developed environmentally friendly polymers [1–3]. The different sources of gums endow them with different molecular structure and properties, but their common advantages such as renewable, biodegradable, nontoxic, biocompatibility, etc. make them found extensive applications as a commercial polymer in many areas such as thickening agent [4, 5], suspending agents [6], coagulant [7], drilling additives [8, 9], textile and dyeing [10], food [11], pharmaceuticals [12], cosmetic [13], matrix of nanomaterials [14], and papermaking [15]. However, the performance and applicability of raw gums are still limited due to their fixed structure and functional groups as well as the poor resistance to enzyme corrosion. Thus, many efforts have been engaged to develop the derivatives of gums by their reaction with active modification agents for introducing various or more functional groups [i.e., $-\text{NH}_2$, $-\text{COOH}$, $-\text{NH}_4^+\text{Cl}^-$, $-\text{SO}_3^{2-}$, $-\text{OC}_2\text{H}_5$, $-\text{OCH}_3$, $-\text{CH}=\text{CH}_2$, $-\text{C}=\text{O}(\text{NH}_2)$]. The introduction of new functional groups changed the charges, aggregation state

of molecular chains, hydrophilic–hydrophobic capability, complexing capacity, stimuli-responsive ability, and rheological behavior of gums, and so the application domain of gums was greatly extended. But, the derivatization of gum can only improve the properties to a finite degree because the number of introduced functional groups is less and the molecular weight of gum fails to be increased by the simple modification with small molecules. Graft polymerization is anticipated to be a quite promising technique for modifying the properties of a polymer, and the modification of natural polymer materials by graft copolymerization offers the opportunity to tailor their physical and chemical properties, functionalize biopolymers to impart desirable properties onto them, and combine the advantages of both natural and synthetic polymers [16–19]. Several grafting modification techniques have been reported, involving with “grafting-from” (growth of polymer chains from initiating sites on the polysaccharide backbone) and “grafting-to” methods (coupling of preformed polymer chains to the polysaccharide) [20]. “Grafting-from” is the most common procedure with the initiating sites generated by various chemical or high-energy irradiation methods. Different from the derivative modification by active small molecules, the graft reaction may introduce polymer chains with large amounts of functional groups to form a “brush-like” structure around the main chains. Correspondingly, the properties of gums, such as flocculation efficiency, complexing, stimuli-responsive, viscosity, controlled biodegradation, and shear resistance characteristics, were greatly changed by the new functional groups for extending the application domains of gums [21–23]. The results of graft polymerization are to improve the intrinsic properties of gums or bring gums with new properties. For example, *Cassia javahikai* seed gum is a better coagulant, but the graft of PAM chains onto the gum can further enhance its coagulant properties [24]. The graft of PAN onto *Ipomoea seed* gum may clearly enhance its viscosity (the maximum value reaches 10.56 folds of the gum) and stability [25]. The AG does not have conducting capability, but the graft of PANI results in good processability along with the electrical conductivity, and used to develop biopolymer-based electronic materials for the environmental favorable technologies [26]. By virtue of the excellent intrinsic properties and the adjustable character of the structure and properties of gums, their graft copolymers play vital role in almost each chemical industrial field, especially in wastewater treatment, controlled release of agricultural chemicals or pharmaceuticals, petroleum industry, papermaking, daily chemicals, dyeing, thickener, smart materials and biomaterials, etc.

The properties of a gum-g-copolymer are highly dependent on the intrinsic structure and nature of gums, the sort of grafted monomer, grafting ratio, and efficiency. Over the past decades, researchers devoted many efforts to explore the graft mechanism, the structure-activity relation of graft copolymer, and the key influence factors of graft ratio and efficiency, and greater progress was made. So, the introduction about the types, structure, and derivatives of gums, the synthesis method, properties, and applications of gum-g-copolymer will be attractive.

5.2 Sorts, Structures, and Properties of Natural Gums

To understand the sorts, structure, and properties of gums is essential to develop their new derivatives or graft copolymers because the charge and polarity of functional groups, the molecular weight, and the viscosity of gum solution may affect the reaction activity and modification efficiency. According to the difference of the functional groups attached on the macromolecular chains, the gums are mainly sorted as nonionic and anionic gums, and their properties are different due to the discrepant structure.

5.2.1 Nonionic Gums

Most of natural gums are neutral polysaccharides with numerous hydroxyl groups and without charges. These hydroxyl groups are distributed in both main chains and side chains and form hydrogen bonding with each other. These bonding interactions among molecular chains render the gums higher viscosity, and so they are widely used as food additives or industrial thickening agents. However, the raw nonionic gums have no charge and cannot be ionized, and so they are usually used in the form of derivatives or graft copolymers for extending the application domains. The commonly concerned and representative nonionic gums are guar gum, locust bean gum (LBG), cassia gum, konjac glucomannan (KGM), *Ipomoea* seed gum, and so on.

5.2.1.1 Guar Gum

Guar gum (GG) is a nonionic edible carbohydrate polymer derived from the seeds of *Cyamopsis tetragonolobus* [1, 2, 27]. GG is consisted of a straight chain of mannose units joined by β -D-(1–4) linkages having α -D-galactopyranose units attached to this linear chain by (1–6) linkages, with a galactose-to-mannose ratio of about 1:2 (Fig. 5.1). GG could dissolve in cold water to form a highly viscous solution even at very low concentration and is one of the highly efficient water-thickening agents, dispersion agents, and water binders used in industry fields such as mining, textile and dyeing, explosive, papermaking, and drilling muds for petroleum industry, food, controlled drug release, etc. [28–32]. The viscosity of GG solution increases when heated for shorter periods of time, but decreases for longer periods of time. Also, the viscosity of such a solution is not very stable and is difficult to be controlled because of its drawback like easier susceptibility of microbial attack, which restricts its application and the gum is rarely used in its natural form [33, 34]. So, the derivative products are the main usage style of GG, and the direct derivatization and graft copolymerization of GG represent the main modification methods, which results in the retention of intrinsic properties and the introduction of desirable properties [22, 35–37].

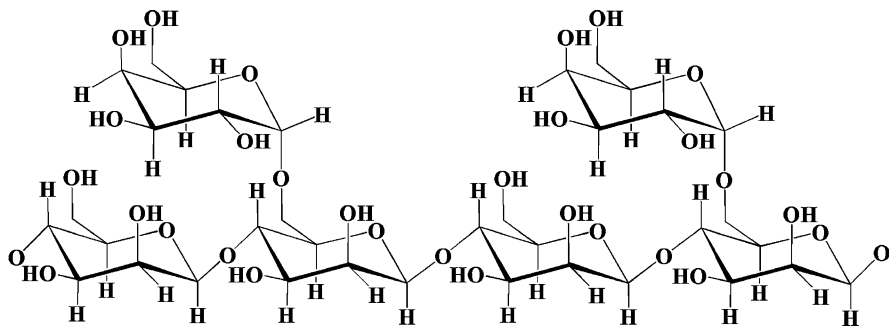


Fig. 5.1 Structure unit of guar gum [38]

The purification of guar gum is the basis of developing its derivatives and graft copolymers as well as studying the corresponding mechanism. Singh groups [39] reported a purification method of gum as follows: the 2.5 % (w/v) solution of GG was prepared by continuous stirring for 12 h at 60 °C and then precipitated with a standard barium hydroxide solution. The formed complex was separated and taken in 1 M acetic acid and stirred for 8 h and precipitated with ethanol. After washed with 70 %, 80 %, 90 %, and 95 % ethanol, the sample was purified by dialysis and filtration through 0.45 μm Millipore membranes (Millipore, Milford, MA).

5.2.1.2 Locust Bean Gum

LBG is a commercially available water-soluble β -1,4-polysaccharide obtained from the seed of the carob tree (*Ceratonia siliqua L.*) and is a galactomannan consisting of a mannose backbone with single side chain galactose units (Fig. 5.2) [40–42]. It can dissolve in water at 85 °C to form a viscous solution with the pH values of 5.4–7.0, and the solution can further form gel by adding sodium tetraborate. LBG is also soluble in LiCl-DMSO solutions. The viscosity is stable in the pH range of 3.5–9.0 and is not affected by Ca^{2+} and Mg^{2+} ions. But the acid or oxidizer will make the LBG salting out and reduce the viscosity. LBG can be used as emulsifier, thickener, stabilizer, and gelling agent [43, 44]. It can create a cream form, and so usually used for cream structure nature and usually used for dairy products and ice cream, jams, jellies, and cream cheese to improve the smear performance.

The typical preparation method of LBG is as follows: the endosperm of the legume beans was crushed after being roasted, and then extracted with hot water to remove the insoluble matters. After the extraction solution was concentrated, 95 % ethanol solution was added and the white floc was obtained. The solid was separated, dried, and smashed to obtain the product.

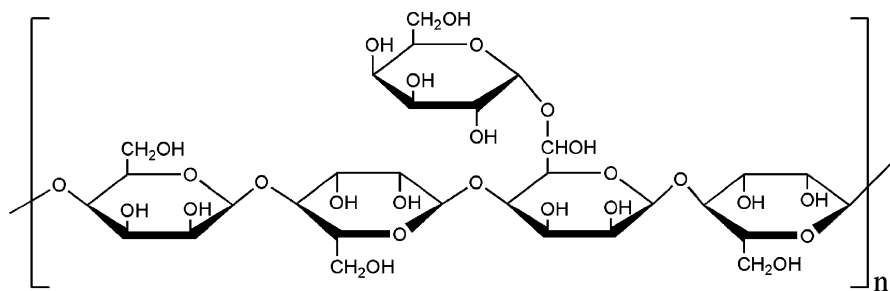


Fig. 5.2 Chemical structure of locust bean gum

5.2.1.3 Cassia Gum

Cassia is a common annual plant grown in tropical countries and is abundantly available in India. The plants of genus *cassia* are known to possess medicinal value and are a good source of mucilages, flavonoids, anthraquinones, and polysaccharides [45, 46]. *C. javahikai* (N.O. leguminosae) is a tree cultivated in gardens as ornamental plant. The seed gum of *C. javahikai* was investigated extensively for its potential as a coagulant in textile wastewater treatment [24, 35]. *Cassia* gum is a nonionic water soluble galactomannan isolated from endosperm of the *C. javahikai* seeds, with a molar ratio of galactose to mannose, 1:2. Seed gum has a branched structure consisting of a linear chain of β -(1 \rightarrow 4)-linked mannopyranosyl units with D-galactose side chains attached through α -(1 \rightarrow 6) linkage to the main chain [47]. It is very similar with LBG and GG in structure and chemical characteristics. Cinnamon gum is suitable to form gel with other colloid production and show potential applications in foods as a thickener, emulsifier, foam stabilizer, and insurance agent [48, 49]. The usage amount is the same as LBG and GG. *Cassia* gum is a yellowish gray powder-like substance with a unique fruit-like flavor, which can dissolve in cold water to form a colloid solution and form a hydrocolloid after boiling. The pH value of 5 % solution is 6.5–7.5.

Cassia gum was isolated by extracting the dried crushed seeds with light petroleum and ethanol to defat and decolorize, respectively. Then, the seed was extracted with 1 % aqueous acetic acid and the solution was added slowly to large excess of ethanol. The crude gum was collected, washed with ethanol, and dried (yield 3.2 g/100 g). The crude gum was purified through the method similar with the GG [50].

5.2.1.4 Konjac Glucomannan

KGM is a type of neutral heteropolysaccharide extracted from tubers of *Amorphophallus konjac* C. Koch. Chemically, KGM has β -(1 \rightarrow 4)-linked D-mannose and D-glucose units in a molar ratio of 1.6:1 as the main chain, with branches joined through C-3 of the D-glucosyl and D-mannosyl residues and a low number of

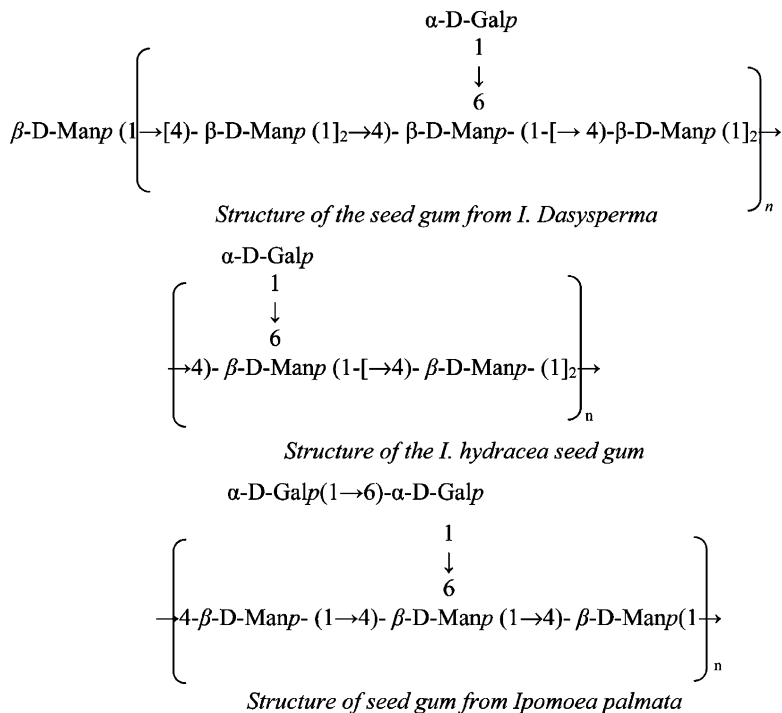


Fig. 5.3 Structure of *Ipomoea* seed gums [25]

acetyl groups (approximately one acetyl group per 17 residues) at the C-6 position [51–54]. It has the characteristics of low cost, high viscosity, excellent film-forming ability, good biocompatibility and biodegradability, as well as gel-forming properties, and KGM and its derivatives have been used widely in various fields, such as food and food additives, and the pharmaceutical, biotechnology and fine chemical industries [55].

5.2.1.5 *Ipomoea* Seed Gums

Seed gum from *Ipomoea* plants is a nonionic water-soluble galactomannan with a branched side chains like GG (Fig. 5.1). The ratio of the galactose to mannose and degree of branching is found to vary from species to species and was 1:6, 1:3, and 2:3 for *Ipomoea dasysperma*, *Ipomoea hederacea*, and *Ipomoea palmata*, respectively (Fig. 5.3) [25, 56]. The seed gum was isolated from endosperm of the seeds and has a branched structure consisting of a linear chain of β -(1–4)-linked mannopyranosyl units with D-galactose side chains attached through α -(1–6) linkage to the main chain, a fundamental structural pattern found in other seed galactomannans like GG, carob gum, and LBG commercial gums, and the solution of gum showed similar behavior to the GG and was found to be stable over a wide

range of pH [39, 57]. The seed gum can be isolated by the following procedure: dried crushed seeds were extracted successively with light petroleum and ethanol to defat and decolorize, respectively, then extracted with 1 % aqueous acetic acid and extract was added slowly, with stirring to large excess of ethanol. The crude gum was collected, washed with ethanol, and dried (yield 2.3 g/100 g) [39]. The seed gum can be purified by barium complexing method [58].

5.2.2 Anionic Gums

A sort of gum contains anionic functional groups, such as $-\text{COOH}$, $-\text{SO}_3^{2-}$, etc. attached on its backbone and carries negative charges. Different from the nonionic gum without charges, the negatively charged functional groups of anionic gums may bring better hydrophilicity, complexing capability to cations, responsive behaviors to external stimulus, and higher reactive activity resulting from the polar functional groups. Thus, the anionic gums were also developed as valuable commercial polymer materials and found more expensive application in chemical and industrial fields. Xanthan gum, *k*-carrageenan, psyllium, alginate, and acacia gum are the representative sorts.

5.2.2.1 Xanthan Gum

Xanthan gum (XG) is an extracellular heteropolysaccharide of *Xanthomonas campestris*. Structural unit of xanthan gum consists of β -(1-4)-D-glucopyranose glucan (as cellulose) backbone with side chains of β -(3-1)- α -linked D-mannopyranose-(2-1)- β -D-glucuronic acid-(4-1)- β -D-mannopyranose on alternating residues (Fig. 5.4) [59, 60]. It was the first fermentative biopolymer product based on corn sugar and has attained commercial status. It can be used in food and pharmaceutical industry because of the properties like thickening, emulsion stabilization, water binding, suspending, and oil recovery [61-64]. Beside these usages, it has a drawback: it is susceptible to microbial attack, which limits its use. Modification of XG by graft copolymerization technique allows one to chemically change the polysaccharide chain by introducing polymer chain that configures different structural characteristics to the initial polymer.

5.2.2.2 *k*-Carrageenan (Also Called as Antlers Gum)

k-Carrageenan is one of the nontoxic linear sulfated polysaccharides that are obtained commercially by alkaline extraction of certain species of red seaweeds (algae). The structure of *k*-carrageenan is made up of α -(1-4) D-galactose-4-sulfate and β -(1-3) 3,6-anhydro-D-galactose (Fig. 5.5) [65-67]. It is widely used as a thickening, gelling, and stabilizing agent in food industry [68] as well as has applications in pharmaceutical [69] and biotechnology sectors [70]. *k*-Carrageenan

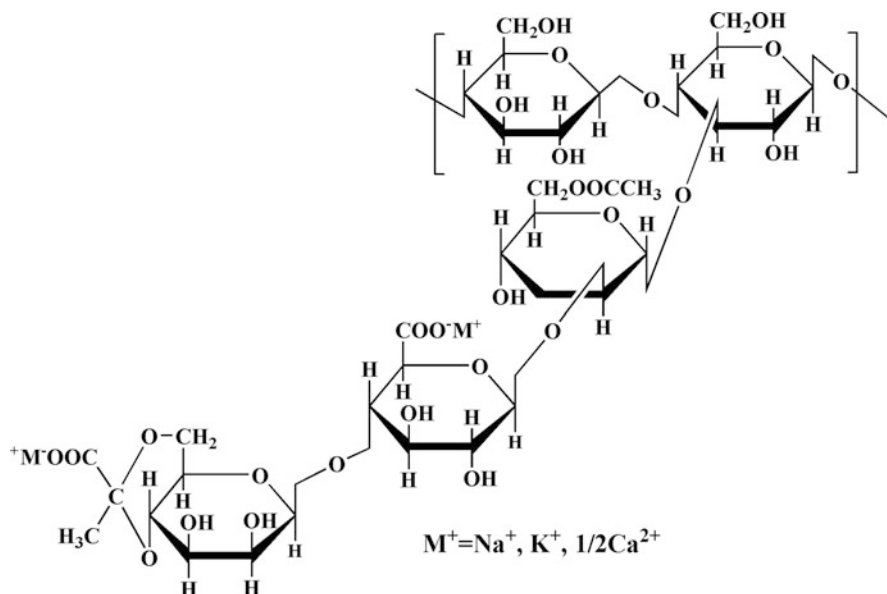


Fig. 5.4 Chemical structure of xanthan gum [60]

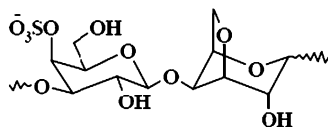


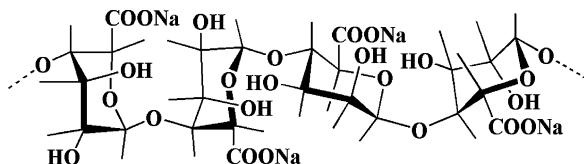
Fig. 5.5 Repeating disaccharide units of kappa-carrageenan (κC) [73]

has also been subjected to play an important role as free radical scavengers in vitro and antioxidants for prevention of oxidative damage in living organisms [71, 72]. Although *k*-carrageenan has wide application range, it suffers from certain drawback like biodegradability, which limits its use considerably. The presence of hydrophilic sulfate groups endows *k*-carrageenan with higher reactive activity, ionization tendency, and less sensitivity to salt solution [73].

5.2.2.3 Alginate

Alginate is an anionic linear polysaccharide extracted from the cell walls of brown algae or produced by bacteria, and so it is a renewable, water soluble, odorless, nontoxic, and biodegradable natural polymer. Alginate is a linear copolymer with homopolymeric blocks of (1–4)-linked β -D-mannuronate (M), and its C-5 epimer α -L-guluronate (G) residues, respectively, covalently linked together in different sequences or blocks. The monomers can appear in homopolymeric blocks of consecutive G-residues (G-blocks), consecutive M-residues (M-blocks), or alternating

Fig. 5.6 Chemical structure of sodium alginate [77]



M and G-residues (MG-blocks) [74]. Due to the existence of $-\text{COOH}$ or $-\text{COO}^-$ groups, alginate is capable of absorbing 200–300 times its own weight in water to form a viscous solution, and it is widely used as thickening agent, emulsifier, sizing agents, and stabilizing agent of dye printing. The molecular chains of alginate could be modified by ionic cross-linking [75], grafting copolymerization [76, 77] to derive new hydrogel materials. It shows great application potentials in drug delivery carriers, especially for the target delivery of gastrointestinal tract drug. Chemical structure of sodium alginate is shown in Fig. 5.6 [77].

5.2.2.4 Acacia Gum

Acacia gum (AG) is a water-soluble chemically modified natural gum which is susceptible to easy biodegradation [78, 79]. AG is a complex arabinogalactan which contains a small proportion of proteinaceous materials and has been classified as arabinogalactan–protein complex [80]. Due to the existence of acacia acid (X-COOH) in the gum, the AG can be ascribed as an anionic gum. The gum is composed of D-galactose, L-arabinose, L-rhamnose, D-glucuronic acid, and 4-O-methyl-D-glucuronic acid [81]. It can easily dissolve in water to form viscous, weakly acidic solution (the solubility reaches 50 %), but does not dissolve in ethanol and most organic solvents. AG can be used as thickening agent, suspending agent, and stability agent and enjoys a wide range of applications in industries such as paper, textiles, pharmaceuticals, drink, and food. It has been reported that inorganic salt complexes of AG can behave as a superionic electrical conductor [82]. AG was produced from *Acacia senegal* or the cut flow effusion of stem and branch of tree *A. seyal*. After removing the impurities, the effusion was dried and smashed to form AG. The former is brittle than the latter. The AG can be used in the form of raw gum, derivatives, and graft copolymers.

5.3 Derivatives of Natural Gums

As described above, the intrinsic structure and properties of nonionic, anionic, and cationic gums make them found extensive application in various areas, but the raw gum also emerges some drawbacks and cannot meet all application requirements for some special purpose. Thus, the modification of gums with acrive small molecules was conducted because the derivatives can not only bring the favorable properties due to the introduction of functional groups, but also keep the intrinsic advantages of gums to the greatest degree [83]. And so the chemical modification

always plays a dominant role to improve gums and open prospects for extending the application of raw gums. Generally, the chemical functionalization of gums mainly includes the esterification, etherification, and cross-linking reactions of hydroxyl groups.

5.3.1 *Carboxyl Derivatives*

The reactive $-OH$ functional groups of gum endow it with great potentials to be modified to meet various applications. In the presence of reactive carboxyl or carboxymethyl reagents (i.e., chloroacetic acid, maleic anhydride, and succinic anhydride), the $-OH$ groups of gum may occur nucleophilic substitution reaction with the $HOOC \cdot \cdot Cl$ or $(C=O)O(C=O)$ groups to form an ether or ester under the alkali condition [84]. The reaction can introduce $-COOH$ or $-COONa$ groups on the macromolecular backbone and transform a nonionic gum into an anionic gum. For one thing, the hydratability and solubility of gum was clearly improved due to the introduction of strong hydrophilic $-COOH$ or $-COONa$ groups; for another, the $-COOH$ groups make gum having responsive capability to external stimuli such as pH value, electrolytes, or electronic field, which extended its application domain in biomedical or sensor fields. For instance, the carboxymethyl derivative of cashew gum has negative charges, and can form physical complex with the cationic polymer such as chitosan. The complex can generate insoluble cross-linked materials that can swell and realize the intelligent delivery and release of drugs [85]. The substitution degree of gum may be controlled by adjusting the reaction condition and recipe, and it determined the usage properties of the derivatives. Usually, the gum was partially carboxymethylated by controlling the reaction prescription and only a part of $-OH$ groups were reacted. The residual active $-OH$ groups can still graft with various monomers or react with other modifier to form derivatives with various groups (Fig. 5.7).

5.3.2 *Hydroxyethyl Derivatives*

Like cellulose, the hydroxyethyl derivatives of gum have better solubility and thermal stability in solution, good dispersibility in water, and high compatibility with anionic, cationic, and nonionic surfactants. So, they show more extensive application in many industrial sectors such as oil recovery, fabric printing, fracture fluids, food system, paints, mineral industry, and personal care [86]. The hydroxyethyl derivatives of gum could be prepared from natural gum via an irreversible nucleophilic substitution, and the derivatives show better colloid properties than the raw gums [87–89]. The chemical and functional properties of gum are mainly dependent on the distribution of molecular weight, the amount of hydroxyethyl substituents, the pattern of substitution, and the distribution of substituents.

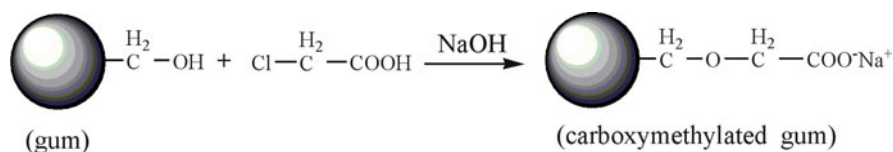


Fig. 5.7 Carboxymethyl modification of gum

5.3.3 Vinyl-Functioned Derivatives

Many gums show poor reactive activity, and so it is difficult to derive new materials by the direct graft reaction with vinyl monomers. The modification of such gums by highly active small molecules with both vinyl groups and reactive end functional groups (i.e., acyl chloride and epoxy groups) may introduce reactive vinyl groups on the gum backbone. The vinyl-functionalized gum was denoted as macromonomers, which can graft with vinyl monomers to form a grafting copolymer with cross-linker network structure. The most frequently used modifying agent is glycidyl methacrylate (GMA), acrylic acid, acryloyl chloride, and maleic anhydride. Thus far, the vinyl-functionalized arabic gum [90], guar gum [91], cashew gum [92], xanthan gum [93], and pectin [94] were prepared under basic condition. At basic condition, the nucleophilic substitution reaction occurred. The $-\text{OH}$ groups of gums tend to lose hydrogen under basic condition and generate some negative electrical property, which can attack the carbon atom in epoxy or the carbon atom connected with ester groups to form vinyl-functionalized gum (Figs. 5.8 and 5.9). At acidic condition, the oxygen atom in epoxy group may be protonated, which makes the nucleophilic occurring more easily [95]. The suggested pH values are in the range of 8–10 (basic condition) and 3.5–3.8 (acidic condition).

Desbrieres groups [93] also prepared vinyl-functionalized xanthan gum by esterification reaction of $-\text{OH}$ groups with acrylic acid and by nucleophilic reaction with acryloyl chloride and maleic anhydride under different reaction conditions.

5.3.4 Cationic Derivatives

The cationic derivatives of gum have positive charges due to the introduction of cationic functional groups such as amino, ammonium, imino, sulfonium, or quaternary phosphonium groups. The cationic modification of gum is usually an etherification process, and the modifier is a reactive molecule with the end $\text{R}-\text{Cl}$ or R -epoxy as well as the cationic functional groups. Specifically, the $\text{R}-\text{Cl}$ or R -epoxy active groups may react with $-\text{OH}$ groups to form ether, and the cationic groups were simultaneously introduced. The existence of these substituents and numerous hydroxyl groups in their structure may allow the establishment of different types of interactions with the anionic matters including anionic drugs, anionic dyes, and numerous negatively charged particles and can be used as

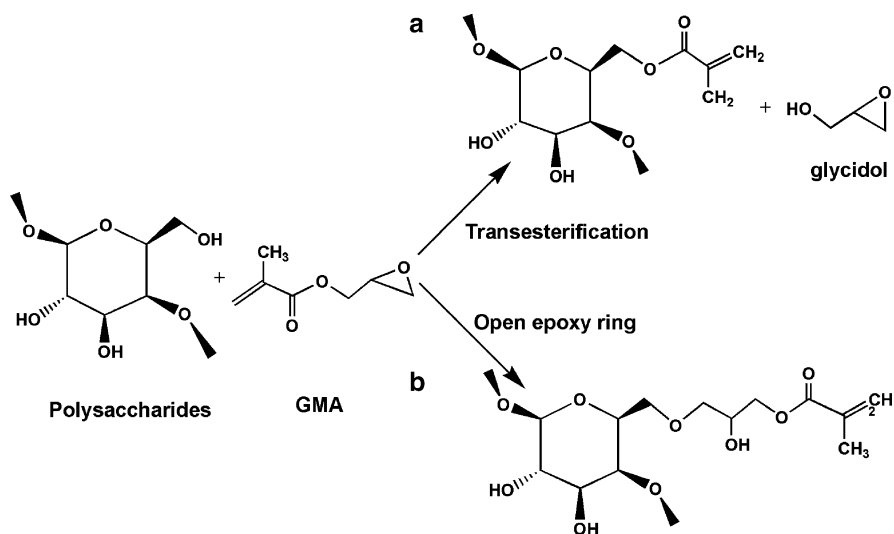


Fig. 5.8 The feasible pathways of modification of polysaccharides with GMA: (a) transesterification and (b) open epoxy ring mechanism [92]

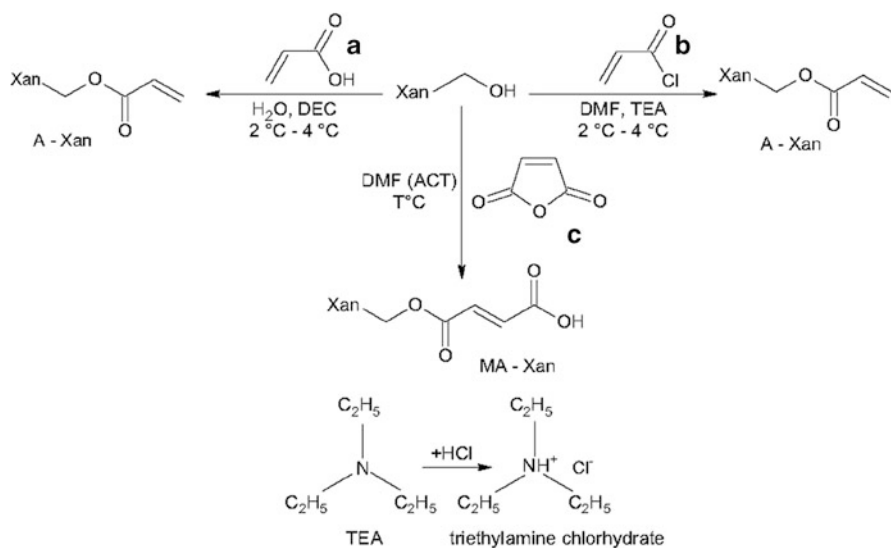


Fig. 5.9 Strategies for modification of xanthan: (a) acrylic acid, (b) acryloyl chloride, and (c) maleic anhydride [93]

effective carriers, filter aid agents, cationic flocculant, and additives of fine chemicals [96, 97]. Compared with the natural cationic polysaccharide chitosan, the ionization degree of cationic derivatives of gum is almost independent of pH owing to the presence of cationic substituents that cannot be protonated. Currently,

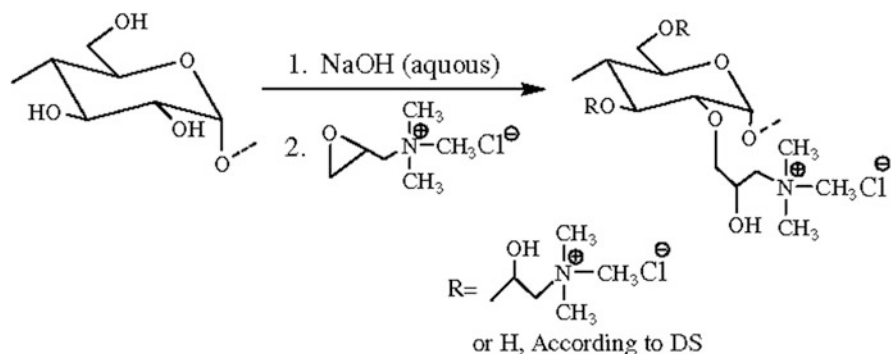


Fig. 5.10 Cationic derivatization mechanism of guar gum [99]

the quaternary ammonium derivatives of gum were focused, and the most common used modifier is 3-chloro-2-hydroxypropyltrimethylammonium chloride (CHPTAC) [98, 99]. The quaternization of gum using CHPTAC as an etherifying agent under the catalytic action of NaOH may undergo several reaction steps (Fig. 5.10). Under the action of strong alkali, the $-\text{OH}$ groups may generate O^- with stronger nucleophilic capability, which may attack the $\text{R}-\text{Cl}$ end of CHPTAC and form $-\text{C}-\text{O}-\text{C}$ ether. The $-\text{NH}_4^+ \text{Cl}^-$ group was also simultaneously introduced and the gums carried some positive charges.

5.3.5 Amphoteric Derivatives

Amphoteric natural polymer contains both anionic and cationic substituents on its structure, which exhibits distinct properties in contrast to the individual anionic or cationic polymer and receives extensive applications in fine chemicals, papermaking, dyeing, and package materials [100–102]. The common methods to prepare amphoteric derivatives of gum include the following: (1) simultaneously modifying gum with anionic and cationic modifiers [103] and (2) modifying gum with an amphoteric modifier [104]. The former was frequently used because it is simple, but the content of anionic and cationic groups of resultant derivative is difficult to be controlled. The latter is relatively complex because it needs to design an amphoteric modifier, but the ratio of anionic and cationic ions can be controlled at 1:1. Xiong et al. [104] synthesized an amphoteric modifier *N*-(3-chloro-2-hydroxypropyl)-*N*-(carboxymethyl)-*N,N*-dimethylammonium-hydroxide (CCDH) and used for modifying guar gum to obtain an amphoteric guar gum with the positive–negative charge ratio of 1:1.

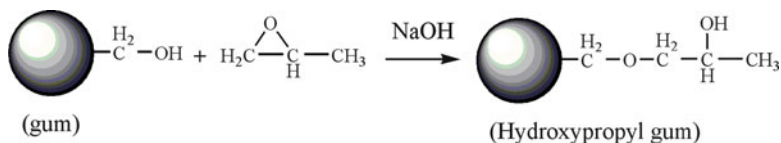


Fig. 5.11 Preparation procedure of hydroxypropyl gum

5.3.6 Hydrophobic Derivatives

The natural gums are mainly hydrophilic and soluble in aqueous medium, but it cannot meet the requirements for the application in organic solvent system. Other polysaccharide (i.e., starch, cellulose, chitosan) may form hydrophobic derivatives by introducing short chain hydrocarbon substituents through etherification reaction and show solubility in organic solvents. Similarly, the reactive groups of gum may be etherized by RO-X, pHO-X (X = Cl or Br) to produce the derivatives with hydrophilic and hydrophobic characters. The hydrophobic modification of gums can form hydrophilic-hydrophobic gums with the characteristics similar to surfactants and can form a micelle in solution. For instance, the modification of gum under alkaline catalyst may form hydroxypropyl gum [105], which could trigger and accelerate the sol-gel transition of tetraethoxy-silicone in water and induce rapid formation of homogeneous gel matrix without the addition of any organic solvents or catalysts, and can modulate the gel strength of the silica matrix by the amount of hydroxypropyl gum (Fig. 5.11) [106]. The substitution and the average length of the hydroxypropyl substituents usually affect the properties of products [107].

5.4 Synthesis of Gum-g-Copolymers

5.4.1 Gum-g-Copolymers via Conventional Radical Grafting Methods

The conventional grafting method of gum was involved with the direct grafting reaction and the ring-opening reaction of macromolecular chains of gum. The direct grafting reaction usually occurred on the -OH groups of gum by a radical polymerization reaction process, and the used initiators are usually thermal initiator or redox initiator. In this process, the radicals were generated from the decomposition of thermal initiator (i.e., ammonium persulfate, sodium persulfate, potassium persulfate, azodiisobutyronitrile) or the oxide-redox action of redox initiation pairs (i.e., H₂O₂/Fe²⁺, K₂S₂O₄/Fe²⁺, K₂S₂O₄/ascorbic acid, benzoyl peroxide/dimethylaniline). The formed anionic radicals may strip down the H atom of -OH groups and initiate the macromolecular chains of gums to generate macro-radicals, and these radical reactive sites may initiate the vinyl groups of monomers to process the chain propagation.

Comparatively, the most commonly used initiation system is redox system because activation energy for the redox initiation is quite low and it can initiate the reaction under ambient condition, and the reaction rate is faster and the energy consumption is low [108]. The type and activity of initiator usually decide the grafting reaction efficiency and rate, and the development of new initiator has long been the subject of great interests. Because of the different types of oxidants and reductants, the formation mechanism of free radicals in redox system is distinct, and the sorts of redox initiators are important factor to decide the graft efficiency. Figure 5.12 depicts the most frequently used redox initiation system and depicts the reaction and formation mechanism of radicals [34, 58, 59, 62, 67, 109–123]. For instance, in the $\text{KHSO}_5/\text{Fe}^{2+}$ redox system, the divalent Fe^{2+} may lose one electron under the action of oxidant KHSO_5 to form Fe^{3+} , and simultaneously the S–O or O–H bonds of KHSO_5 were broken to form $-\text{OH}^\bullet$ and $-\text{SO}_4^{\bullet-}$ radicals. In the potassium chromate/malonic acid initiation system, the CrO_4^{2-} ions may transform with H_2CrO_4 each other at acidic condition. The oxidant H_2CrO_4 may react with reductant $\text{CH}_2(\text{COOH})_2$ to form Cr^{4+} midbody with higher activity. The Cr^{4+} may capture the active H atom of $\text{CH}_2(\text{COOH})_2$ (the strong electron withdrawing capability of $-\text{COOH}$ render the conjoint $-\text{CH}_2-$ higher reactivity) to form $^\bullet\text{CH}(\text{COOH})_2$ radicals, and the Cr^{4+} ion was reduced as Cr^{3+} ion. In a word, the formation process of radicals is an electron transport process induced by a redox reaction.

As discussed above, although the formation mechanism of radicals for various initiation systems is different, the radicals have the same effect when they initiate the gum to perform a graft reaction and form a graft copolymer. Figure 5.13 gives the typical grafting mechanism of vinyl monomers onto gum backbone. Firstly, the primary radicals were generated by the decomposition of thermal initiator or the reaction of redox initiators (Fig. 5.12). These radicals striped down the hydrogen atoms of the $-\text{OH}$ groups on gum chains to form macro-radicals. After added vinyl monomers, the active radical sites on gum chains may initiate vinyl groups of the monomers to process chain propagation. This is a typical “graft from” reaction. In the grafting process, the type and activity of initiators, the concentration, viscosity and activity of gum solution, the concentration of monomers, the reaction temperature, and time may greatly affect the graft ratio and efficiency. Table 5.1 shows the different gum-g-copolymers prepared by using various redox initiator systems as well as the grafting efficiency.

Besides the direct grafting reaction of $-\text{OH}$ groups, the saccharide ring of gum may be opened. Typically, when the initiator is multivalent metal ions such as Ce^{4+} ion, the metal ions may interact with the C2–C3 glycol and the C6 hydroxyl of the anhydro-D-glucose unit of saccharide ring to form a gum– Ce^{4+} complex [134]. The Ce^{4+} ion in the complex can then be reduced as Ce^{3+} ion with the release of a proton and a subsequent formation of a free radical on the backbone of gum. These free radicals could then react with the end vinyl groups of monomer to initiate graft copolymerization (Fig. 5.14) [135]. Termination of the graft copolymer was carried out through the

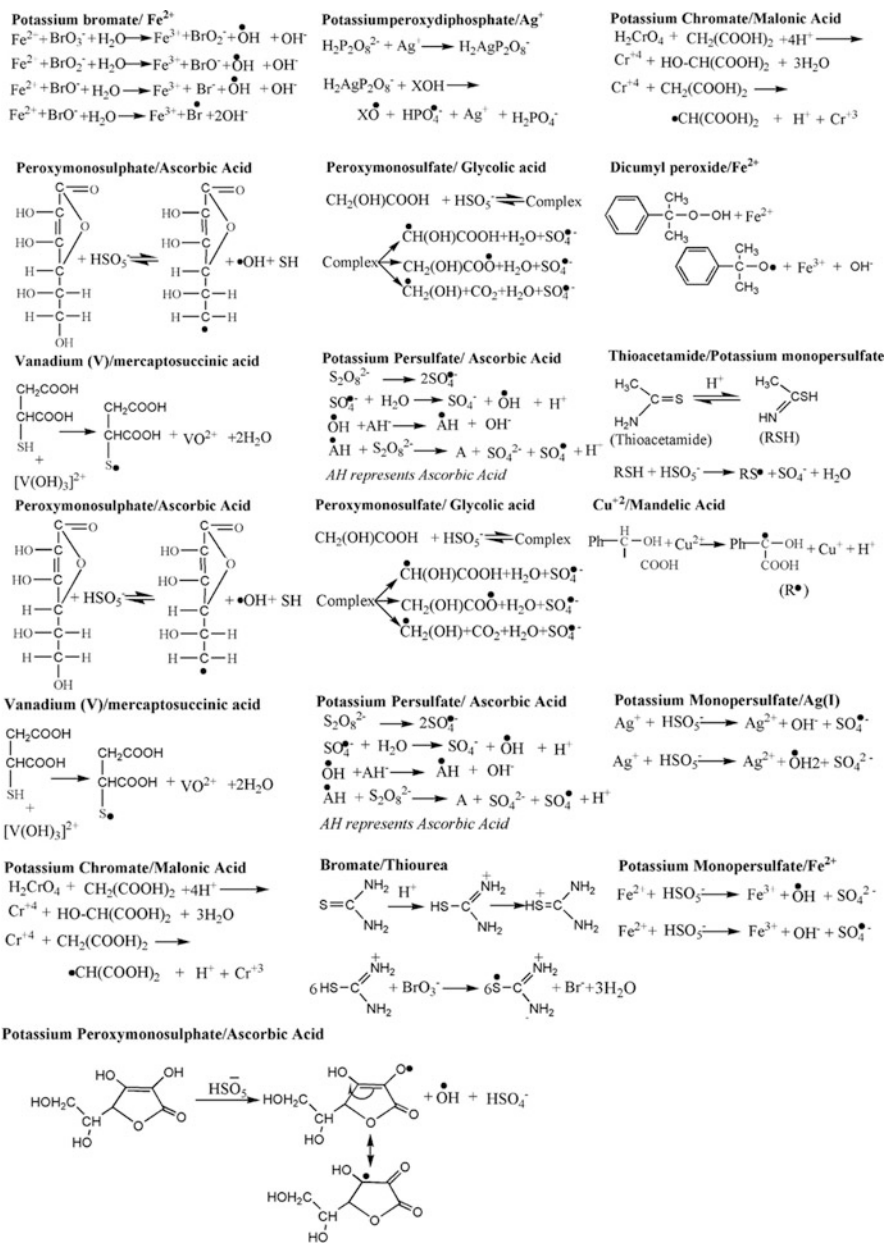
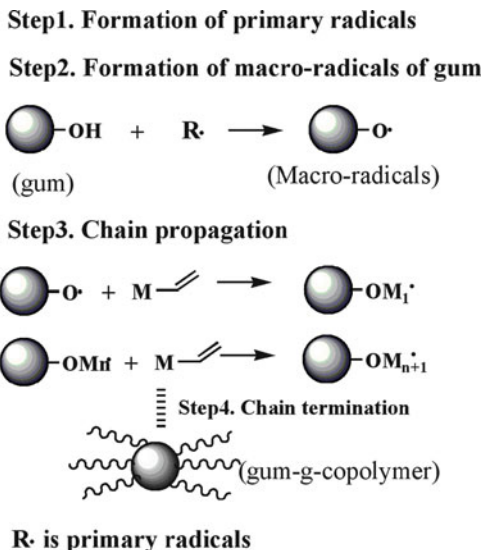


Fig. 5.12 Illustration of the conventional redox initiation systems [34, 58, 59, 62, 67, 109–123]

combination of radicals [135, 136]. In this system, the pH value of reaction system is important to the initiation efficiency of Ce^{4+} ion [78]. In contrast to the persulfate initiators or peroxide initiator, the Ce^{3+} initiators usually have higher grafting

Fig. 5.13 The common mechanism for the graft copolymerization of gum



efficiency. Compared with other transition metal ions (i.e., Fe^{3+} , Cu^{2+} , Co^{3+} , Cr^{6+}) [137, 138], the Ce^{4+} ion has the advantage that it produces a minimum amount of homopolymer [139, 140]. The representative graft-copolymer synthesized by the initiation of Ce^{4+} ions is listed in Table 5.2. Despite the Ce^{4+} ion initiator shows better efficiency, but it is not industrially feasible due to the undesirable toxicity and the higher cost.

5.4.2 Gum-g-Copolymers via Macromonomer Radical Methods

For the gum with lower reactive activity, its modification for forming a macromonomer-like structure is essential and becomes an effective approach to prepare gum-g-copolymer. The synthesis of macromonomers is the key factors affecting the grafting reaction and the properties of product. For general free radical graft reaction, the vinyl-functionalized gums were usually considered as a macromonomer because it contains many active vinyl groups that are similar with vinyl monomers. Desbrieres et al. [93] synthesized a vinyl-functionalized xanthan gum and used as a macromonomer to prepare new graft polymer. Tiwari et al. [157] modified guar gum with GMA to obtain guar gum-methacrylate (GG-MA) macromonomers and then polymerize them to form a hydrogel material. Guilherme et al. [92] synthesized cashew gum-based macromonomers with vinyl groups and used to react with vinyl monomer acrylamide. The monomer acrylamide was reacted with the vinyl groups of gum to form a graft copolymer, and the molecular chains of gum were connected with each other by the polymerization of monomers to form a network structure. The grafting and cross-linking reaction was simultaneously conducted.

Table 5.1 Examples of gum-g-copolymers formed by direct grafting reaction

Initiation system	Gum-g-copolymers	GE% ^a	GR% ^b	References
H ₂ O ₂	GG-g-PMMA	61.50	–	[109]
KMnO ₄ /oxalic acid	GG-g-PAM	29.00	102.80	[124]
Potassium bromate/thiomalic acid	GG-g-PAM	81.00	–	[110]
KPS/ascorbic acid	GG-g-PAN	76.00	123.00	[111]
Cu ²⁺ /mandelic acid	GG-g-PAM	93.70	129.77	[112]
Peroxydiphosphate/silver(I)	GG-g-PAA	87.00	1237.83	[125]
Peroxydiphosphate/metabisulphite	GG-g-PAM	97.70	277.80	[126]
Potassium chromate/malonic acid	GG-g-PMAD	88.30	151.20	[113]
Potassiummonopersulfate/thioacetamide	GG-g-P4V	75.80	504.29	[127]
KPS	GG-g-PMA	24.20	241.60	[114]
Bromate/ascorbic acid	GG-g-PNVF	96.90	358.70	[128]
Vanadium (V)/mercaptosuccinic acid	GG-g-PAA	63.60	160.40	[115]
Peroxymonosulfate/ascorbic acid	GG-g-P4V	52.90	560.90	[34]
Cu ²⁺ /Na ₂ S ₂ O ₅	GG-g-PAM	25.35	60.0	[129]
KPS/ferrous ammonium sulfate	GG-g-PNVP	77.90	168.00	[130]
Peroxymonosulfate/glycolic acid	GG-g-PNVP	76.92	200.00	[116]
Peroxymonosulfate/thiourea	PCMGG-g-PACA	70.60	292.80	[117]
H ₂ O ₂	LGSg-g-PAN	100.00	167.60	[131]
KPS/ascorbic acid	IDSG-g-PAN	97.20	360.00	[58]
KPS/ascorbic acid	IDSG-g-PAN	–	80.00	[25]
KPS/ascorbic acid	IHSG-g-PAN	–	124.00	[25]
KPS/ascorbic acid	IPSG-g-PAN	–	149.00	[25]
Potassium monopersulfate/Fe ²⁺	XG-g-PAA	–	192.30	[118]
Potassium bromate/Fe ²⁺	XG-g-PAM	84.90	145.60	[119]
Fe ²⁺ /H ₂ O ₂	XG-g-PMA	93.33	168.00	[62]
Bromate/thiourea redox	XG-g-PAMPS	–	160.00	[59]
Potassium monopersulfate/Ag(I)	XG-g-PNVF	97.59	324.00	[120]
Potassium bromate/ascorbic acid	XG-g-PAMPS	–	433.00	[121]
Potassium peroxydiphosphate/Ag ⁺	XG-g-PNVP	78.90	300.00	[122]
Peroxymonosulfate/ascorbic acid	XG-g-P4V	87.80	400.00	[123]
Peroxymonosulfate/glycolic acid	<i>k</i> -CGN-g-PDAM	81.30	509.90	[67]
KPS	CG-g-PAM	96.30	144.40	[132]
APS	AG-g-PAM	73.50	459.00	[133]

^aGraft efficiency^bGraft ratio

5.4.3 Gum-g-Copolymers via High-Energy Initiation Grafting Method

The synthesis of gum-g-copolymers by conventional chemical initiation methods was described above. These methods were intensively developed and used to derive numerous graft polymer materials. However, these methods are highly depended on the chemical initiator and can only be used for the liquid-phase reaction. For one thing, the usage of chemical initiators may inevitably introduce undesirable

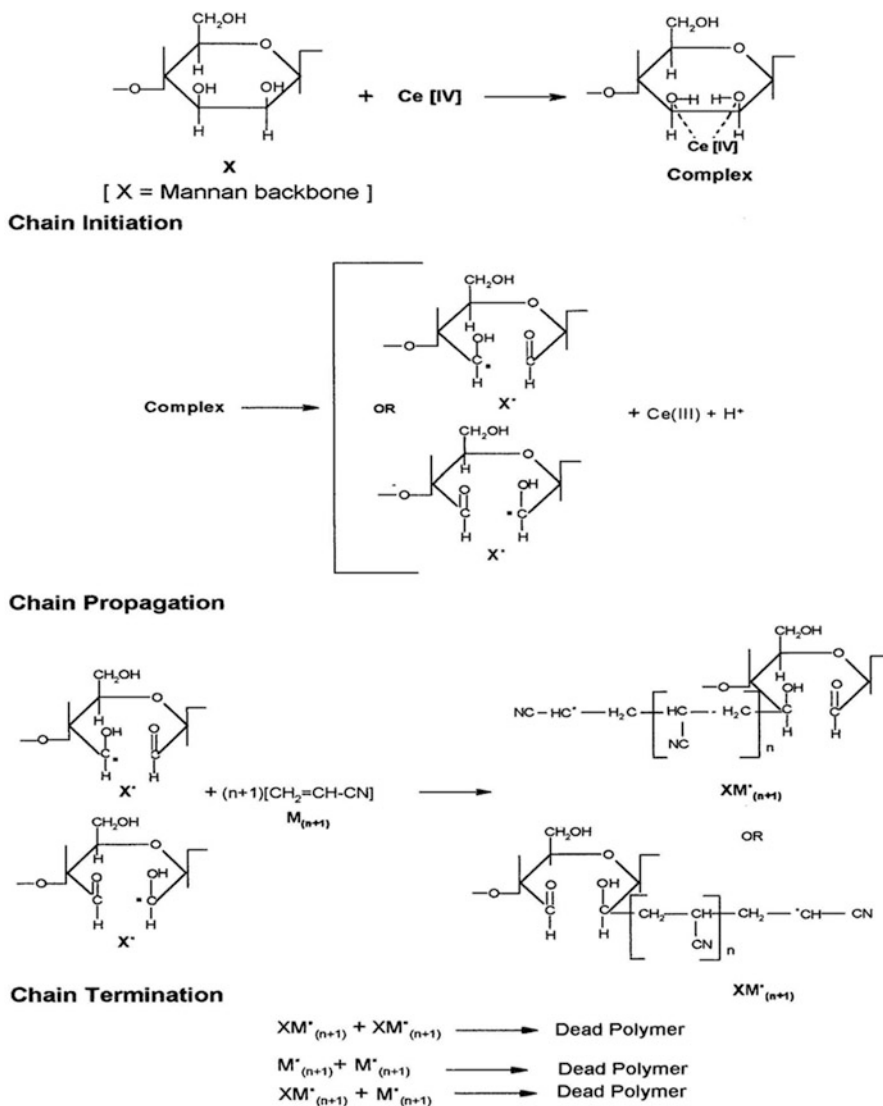


Fig. 5.14 Grafting mechanism of AN onto cassia tora gum initiated with CAN [135]

chemical matters, which affected the safety of graft copolymer in many application fields, especially in food, daily chemicals, and drug carrier areas; for another, the grafting reaction in solution may increase the cost and generate secondary pollution, and the conventional method is not suitable to treat solid sample. Thus, the high-energy initiation technologies have recently received increasing concerns because they are simple and can be done in both solution and dry medium.

Table 5.2 Examples of gum-g-copolymers formed by Ce⁴⁺-initiated reaction

Initiation system	Graft copolymer	GE%	GR%	References
CAS/dextrose	GG-g-PMMA	65.34	–	[141]
CAN	GG-g-PAN	94.00	295.00	[142]
CAS	AG-g-PMMA	82.45	–	[78]
CAN	PCMGG-g-PAN	98.50	291.75	[143]
CAS	CGG-g-PAM	98.20	–	[144]
CAS	AG-g-PEMA	86.64	1629.00	[145]
CAS	CGG-g-PAM	95.00	1200.00	[146]
CAN	TGG-g-PAN	–	543.00	[147]
CAS/SD	CRSG-g-PAM	91.20	142.60	[148]
CAN	TK-g-PAM	93.66	231.45	[149]
CAN	<i>k</i> -CGN-g-PAN	95.00	125.00	[150]
CAN	SA-g-PIA	87.87	635.28	[151]
CAN	KG-g-PAM	98.60	–	[152]
CAN	TK-g-PAN	64.00	86.00	[153]
CAN	GG-g-PGMA	–	730.00	[154]
CAN/MW	GGT-g-PAM	168.6	843.00	[155]
CAN	CTG-g-PAN	98.50	211.57	[135]
CAN	XGC-g-PMMA	94.78	84.70	[156]

5.4.3.1 Microwave-Assisted Grafting Copolymerization

As an efficient thermal energy, microwave (MW) irradiation technology is becoming the standard and high-efficient synthesis technique in various fields of chemistry or engineering [158, 159]. Microwaves generate electromagnetic radiation in the frequency of 300 MHz to 300 GHz, and the energy can be rapidly transferred in the bulk of the reaction mixture. Usage of microwave initiation for preparing the grafting copolymers of polysaccharides has recently been developed [158, 160–162]. By comparison with conventional method, the relatively higher yields and grafting efficiency could be achieved within a very short time with no or little addition of any radical initiators or catalyst, and the extent of grafting could be adjusted by controlling the microwave conditions [163–166]. Microwave radiations cause “selective excitation” of the polar bonds only, which in turn leads to their rupture/cleavage. This cleavage of bonds creates many free radical sites on the polymer backbone. The “C–C” sequence of the backbone polymer remains unaltered by the microwave radiation since it is relatively nonpolar [167]. Figure 5.15 depicts the graft polymerization mechanism initiated by individual microwave and based on free radical mechanism. Typically, the polar O–H bond can easily be broken under the action of microwave radiation, while the C–C bond (practically nonpolar) has not been affected. The cleavage of the O–H bonds leads to the formation of free radical “active” sites on the backbone of gum. These active sites can react with vinyl monomers to achieve the growth of chains, and the graft copolymer could be formed [167–169].

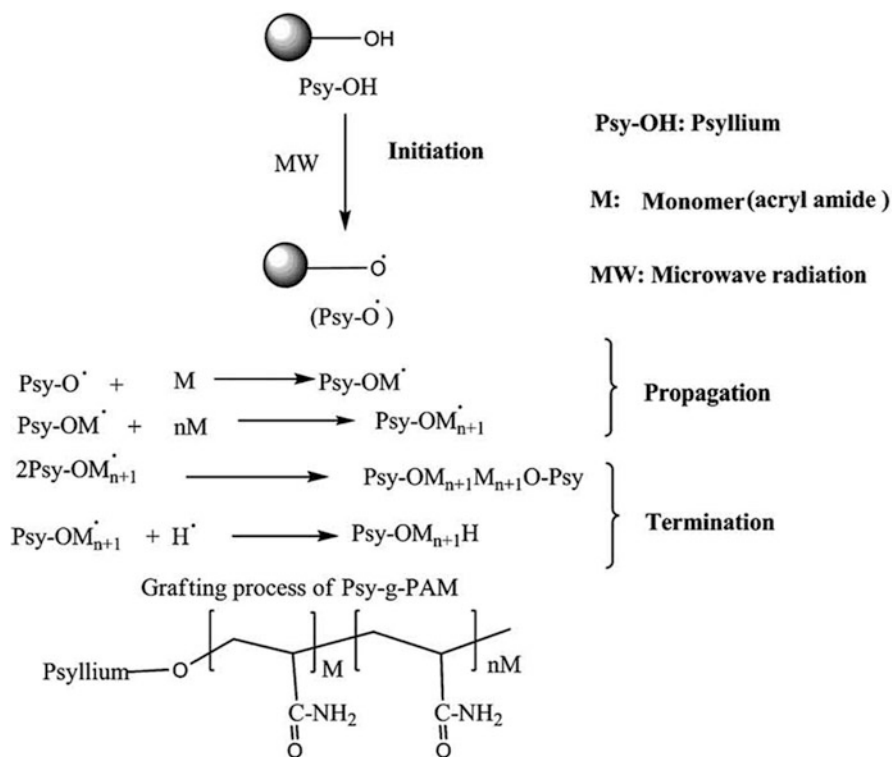


Fig. 5.15 Mechanism for “microwave-initiated synthesis of PSY-g-PAM” [167]

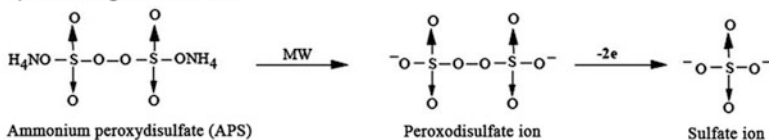
The microwave-assisted graft copolymerization in the presence of little (or catalytic amount of) chemical initiator is another important reaction styles [26, 162, 163, 166, 170]. The main initiator is persulfate and ceric salts. The primary radical can be formed more effectively under the action of microwave, and the graft efficiency can be improved to a certain degree. The active radicals formed on the hydroxyl groups of gum may react with vinyl monomers (i.e., acrylic acid, acrylamide, acrylonitrile, 4-vinylpyridine) or non-vinyl monomers (i.e., aniline) to form graft polymers. Figure 5.16 shows the graft mechanism of aniline onto the AG using APS and MW as the associated initiation approach. The radical initiator APS was decomposed under microwave radiation to form a sulfate ion radical, and then the radical stripped down the H atom of the -OH groups of gum to generate a macroradical. The macroradical may react with the active PANI chains [26] to form the graft copolymer.

5.4.3.2 Radiation-Initiated Grafting Copolymerization

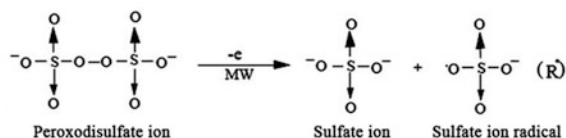
Gamma ray is electromagnetic radiation of high frequency and therefore energy. Gamma rays are ionizing radiation and are classically produced by the decay from high-energy states of atomic nuclei (gamma decay) but also in many other ways.

Step1: Generation of primary radicals

1) Oxidizing action of APS



2) APS act as initiator



Step2: Polymerization of aniline to form polyaniline ion radical

Step3: Graft of PANI onto acacia gum

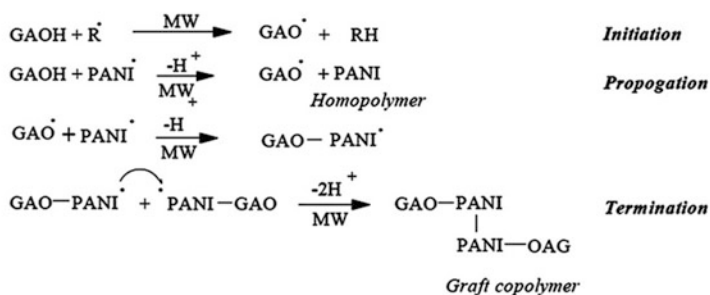


Fig. 5.16 The grafting mechanism of AG with aniline initiated by MW and APS [26]

Recently, gamma irradiation-initiated graft polymerization was developed as a preferred method for commercial synthesis and exhibits a great potential to synthesize the graft copolymers by virtue of its higher efficiency, low cost, and convenient to modify polymer [171, 172]. The utilization of gamma irradiation for the synthesis of gum-g-copolymers has been intensively concerned. For example, Lokhande et al. [173] and Biswal et al. [174] prepared guar gum-g-copolymer by using γ -radiation as the initiation approach. It was found that ideal graft efficiency was obtained, and the graft efficiency is dependent on the dose of radiation. The increase of radiation dose can enhance the graft ratio and decrease the content of homopolymers, but the viscosity or molecular weight was decreased due to the depolymerization effect of radiation to gum. Besides, the graft copolymer of other gums such as XG [175] and KG [54] was reported. However, the problems associated with radiation initiation involve lack of distinction between the different bonds of the backbone polymer because there is always a strong probability of radiation damage (radiolysis) to the gum backbone, and undesirable breakage of bonds may occur under the action of strong radiation [176]. In addition, this method

has required a complex instrument and equipment and exists with safety problem resulting from the radiation. This limited the extensive application of radiation technology in the synthesis of gum-g-copolymer. Figure 5.17 depicts the graft mechanism of the PSY-g-PAA initiated by gamma-radiation [177]. The $-OH$ groups of arabinoxylan on PSY chains act as active sites for the graft copolymerization reaction, and the formed radical sites may initiate the monomers to form grafted side chains.

5.4.3.3 UV Radiation-Initiated Grafting Copolymerization

Due to the advantages of low operation cost and mild reaction conditions, UV has been extensively applied for surface graft polymerization with the aid of a photo-initiator or photosensitizer, such as benzophenone (BP) [178, 179]. UV radiation is usually used for the purpose of surficial grafting [178], and various surface functional groups were grafted on the substrate surface by UV irradiation with various sources [180]. In the process of grafting reaction in solution, UV radiation has usually been used along with a photo-initiator. For example, the graft copolymer of PCGG with methyl acrylate was synthesized by using ultraviolet radiation (generated by a 125-W medium-pressure mercury lamp) as an assisted initiation approach and CAN as a photo-initiator [181]. The UV-initiation method shows higher graft ratio and graft efficiency than that without UV-initiation [181].

5.4.3.4 Electron Beam-Initiated Grafting Copolymerization

High-energy electron beams have usually been used to graft vinyl monomers to solid-state natural polymers in order to make plastic composite materials and modify the properties of solid surface [182–184]. The product prepared by high-energy electron beams can be free from impurities such as chemical residues from initiators for no or less catalysts or additives are needed to initiate the reaction in radiation processing, and the degree of cross-linking and grafting can be controlled by the change of radiation dose [185]. For the graft reaction of natural polymers to form a dispersible or soluble graft copolymer, only less works were made [186, 187], and this greatly extended the application domain of electron beam. Different from conventional initiation method, the electron beam may break the C–C bonds of gum chains and degrade the gum at room temperature to a predetermined molecular weight and polydispersity, and so the viscosity, flow property, suspending, and stability of gum-g-copolymers can be controlled. In addition, the impurities in the final product were reduced. For example, the vinyl monomer may be grafted onto the XG or GG chains when they are exposed to a high-energy electron beam irradiation. In this process, GG with molecular weight of 2,000,000 Da can be depolymerized to a lower preselected molecular weight that is about 700,000 or 500,000 or 300,000 Da, and this provides possibility that the molecular weight of graft-copolymer is lower than the original gum [187].

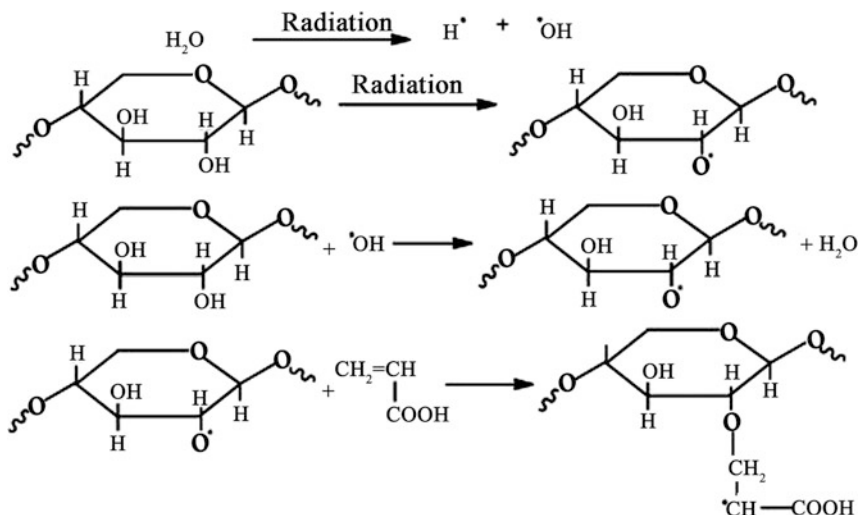


Fig. 5.17 The mechanism of gamma-radiation-initiated graft copolymerization [177]

5.4.4 Synthesis of Gum-g-Copolymers by Click Chemistry

Click chemistry, called as dynamic combinatorial chemistry, is a new synthetic concept proposed by chemist K. B. Sharpless in 2001. The characteristic of click chemistry is to rapidly synthesize various molecules by the montage of small molecular units, and this method emphasizes the synthesis pathways based on the construction of C–X–C bonds. The representative reaction is the copper-catalyzed azide-alkyne Huisgen cycloaddition and was usually used in the development of drugs and biomedical materials [188]. For gum-g-copolymers, the conventional synthesis methods are not quantitative and are sensitive to the molecular weight of the polysaccharide, and the gum may be degraded under some harsh reaction conditions and the yield is low. Thus, the click chemistry, a “graft to” approach, provided a new pathway to prepare special graft copolymers. For example, the thermo-responsive bio-hybrid grafted copolymers GG-g-(PEO-co-PPO) were prepared in aqueous medium by copper-catalyzed 1,3-dipolar Huisgen cycloaddition, and the structure and composition is tunable [189]. The detail synthesis procedure is depicted in Fig. 5.18. Typically, guar gum was firstly alkyne functionalized through the reaction of guar gum with propargyl bromide under basic condition using isopropanol as the solvents. Similarly, the methanesulfonyl chloride and triethylamine may react with α -butoxy- ω -hydroxy-PEO-co-PPO to generate α -butoxy- ω -azido-poly[(ethylene oxide)-co-(propylene oxide)] (ω -N₃-PEO-co-PPO) grafted chains. The alkyne-functionalized guar gum may react with ω -N₃-PEO-co-PPO under action of the catalysis copper(II) sulfate and ascorbate to form GG-g-(PEO-co-PPO) polymer. Using the similar method, the guar gum-based graft copolymer was also prepared by this workgroups [189, 190].

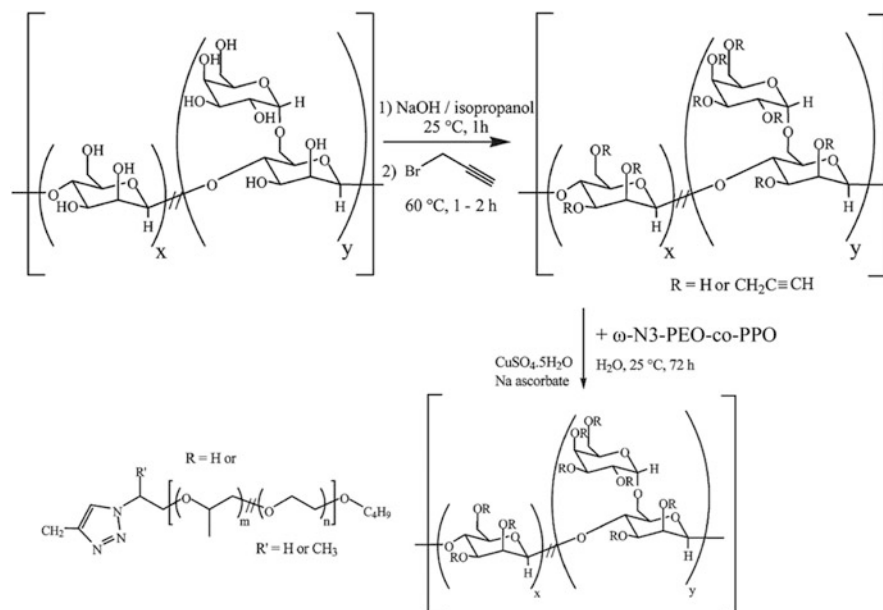


Fig. 5.18 Synthesis mechanism of GG-g-(PEO-co-PPO) copolymer by click chemistry [189]

5.4.5 Atom Transfer Radical Grafting Copolymerization

Atom transfer radical polymerization (ATRP) is a new type of active polymerization reaction. Active radical polymerization is one of the most active research areas in polymer science, and ATRP reaction is an effective way to achieve the controlled/living polymerization. The character of ATRP is to use alkyl halide as initiator, and to use the style of transition metal catalyst or degradation chain transfer effectively inhibits double-base termination reaction of radicals. ATRP can also be applied to both nonpolar and polar monomer and can be used to prepare polymer with various, controlled, and clear structures [191]. With the development of ATRP technology, it is possible to synthesize a gum-g-copolymer for some special application. For example, Rannard workgroups [40] have synthesized a series of locust bean gum-graft-copolymers by a “graft to” method using ambient aqueous ATRP. The reaction mechanism was depicted in Fig. 5.19. Typically, the hydroxyl groups of 2-bromoisobutyric acid (**2**, BIBA) or its acid bromide may react with the coupling agent 1,1'-carbonyl diimidazole (**3**, CDI) to produce a tertiary bromide capable of initiation. The CDI solution was added dropwise at ambient temperature to **2** to form the acid imidazolide. Once the reaction was completed, **4** was added to the LBG solution and then reacted for certain time. After being precipitated with methanol and subsequent methanol washings and Soxhlet extractions, the macroinitiator, **5**, was generated. The macroinitiator may further react with the vinyl-monomers to form a series of graft copolymers with controlled graft ratio. A similar mechanism for other polysaccharides was also proposed [192].

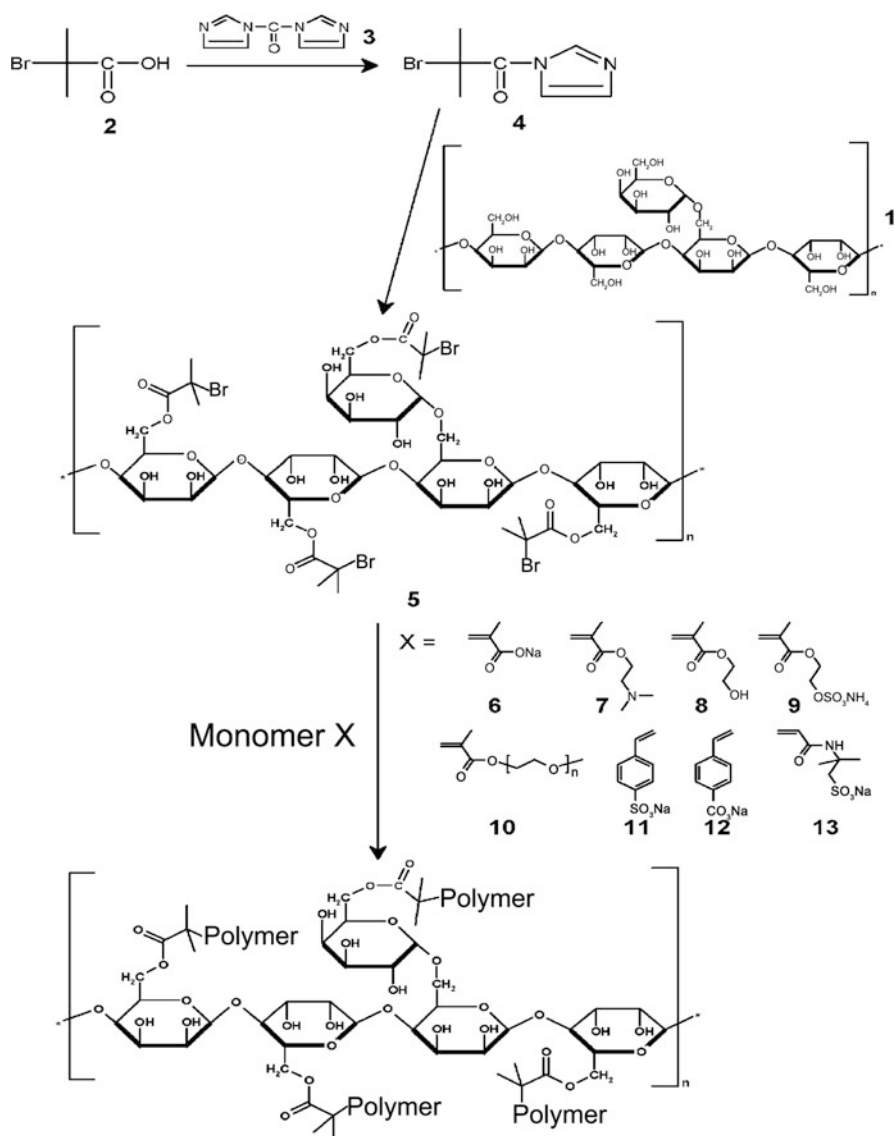


Fig. 5.19 ATRP reaction mechanism of locust bean gum-graft-copolymers. **1** is locust bean gum; **2** is 2-bromoisobutyric acid (BIBA); **3** is 1,1'-carbonyl diimidazole (CDI); **4** is acid imidazolide; **5** is water-soluble macroinitiator; **6** is sodium methacrylate (NaMA); **7** is 2-dimethylaminoethyl methacrylate (DMAEMA); **8** is 2-hydroxyethyl methacrylate (HEMA); **9** is 2-(sulfoxy)ethyl methacrylate (SEM); **10** is monomethoxy poly-(ethylene glycol methacrylate) (PEGMA); **11** is 4-styrene sulfonic acid sodium salt (SSA); **12** is 4-vinyl-benzoic acid sodium salt (VBA); **13** is 2-acrylamido-2-methyl-1-propanesulfonic acid sodium salt (AMPS) [40]

5.5 Evidence of Grafting Copolymerization

5.5.1 Infrared Spectra

Infrared spectroscopy is an important approach to identify the characteristic groups and prove the existence of a special chemical group. For the gum-g-copolymer, the FTIR spectra can be used as the evidence of forming a graft polymer. Typically, the spectrum of the gum-g-copolymer shows a set of strong absorption bands which is absent in the spectrum of raw gum, and the new characteristic bands are ascribed to the polymerization of monomers. The position of absorption bands is decided by the type of functional groups of monomers. The grafted product was usually washed by large amount of water and then soaked or extracted with ethanol (or methanol, acetone, etc.) to remove the unreacted gum and the formed homopolymers. After these treatments, the interference can be suppressed and the FTIR spectra are convincing and can be as an evidence for graft copolymers. For instance, Biswal et al. [174] proved the acrylamide was grafted onto guar gum backbone by FTIR spectra. The appearance of absorption bands of gum at $1,670$ and $1,635\text{ cm}^{-1}$ (amide-I (C=O stretching) and amide-II (N-H bending)) indicated the graft of poly(acrylamide) chains onto the guar gum backbone. Another approach to prove the graft reaction by FTIR spectra is to remove the gum backbone through chemical reaction and to determine the FTIR spectra of the residual moiety. For example, Chowdhury et al. [78] hydrolyzed AG by acid in the grafted polymers and then determined the FTIR spectra of residues. Results indicate that the FTIR spectra of the residues are identical with the spectra of PMMA, but are different from the FTIR spectra of graft copolymer. It proved the occurrence of graft reaction between AG and MMA.

5.5.2 Thermogravimetric and Differential Scanning Calorimetric Analysis

Thermal analysis is also a conventional method to provide an evidence for graft reaction. Besides the gum backbone, the grafted polymer chains may generate various interactions with each other (such as condensation and cyclizing reaction) to affect the thermal behavior during the process of thermal decomposition [116, 120, 121]. So, different grafted monomers (or functional groups) and graft efficiency may cause different thermal stability of the corresponding graft copolymers. However, it is true that the thermal stability and endothermic–exothermic behaviors of graft copolymer are clearly better than the matrix gum due to the increase of molecular weight and number of functional groups. The raw gum may rapidly thermal decompose by a one-step process, but the graft copolymer enhances the thermal decomposition temperature and usually exhibited 2–4 steps thermal decomposition. For example, the graft

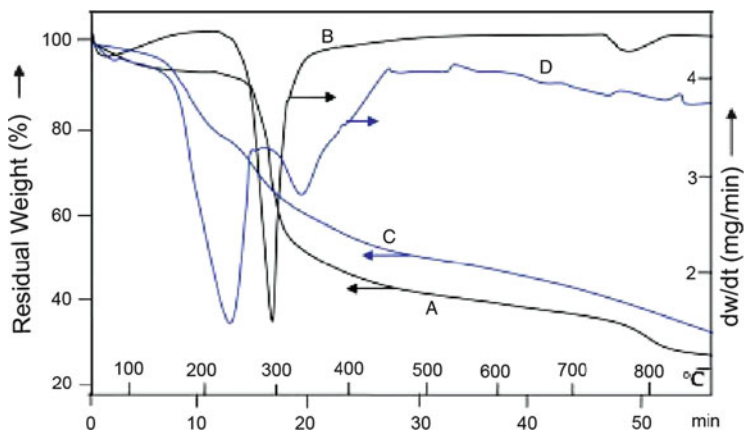


Fig. 5.20 TG (A) and DTG (B) curves of XG; TG (C) and DTG (D) curves of XG-g-PMA [62]

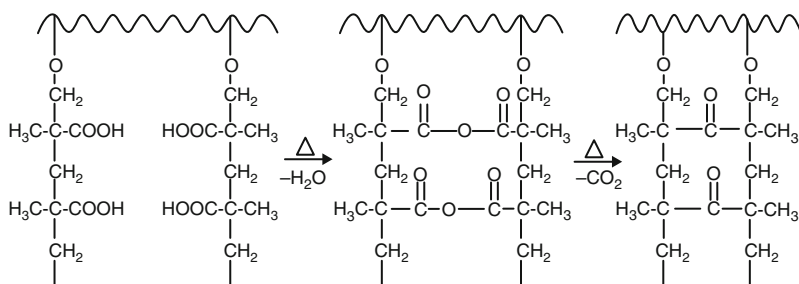


Fig. 5.21 Schematic representation of degradation of XG-g-PMA [62]

copolymer of XG with methacrylic acid shows different thermal behaviors from XG (Fig. 5.20) [62].

XG shows a single step thermal degradation process started at about 232 °C, and nearly 45 % weight loss occurred between 200 and 310 °C, and the final decomposition temperature (FDT) is 316 °C. The 60 % of XG was degraded at 600 °C. The weight loss rate of graft copolymer increased with increasing the temperature up to 250 °C, and two T_{\max} are obtained at 243.9 and 343.58 °C. The FDT is 452 °C, which is much higher than XG. The weight loss in the range of 150–250 °C is due to the formation of anhydride with elimination of H_2O molecule from the two neighboring carboxylic group of the grafted chains. The second T_{\max} is attributed to the decarboxylation of the anhydrides formed earlier (Fig. 5.21). The change of thermal behaviors confirmed the formation of grafted copolymer.

Differential scanning calorimetric analysis (DSC) is a useful technique to explain the formation of graft copolymers. The endothermic or exothermic peaks of the gum could be changed after grafting reaction due to the increased interaction between the main chains of gum and the grafted polymer chains.

5.5.3 *UV-Vis Spectra*

UV-vis spectra are simple and accurate approach to identify the existence of aromatic groups. In the families of gum-g-copolymers, many used monomers (such as styrene, aniline, sodium 4-vinylbenzenesulphonate) have benzene rings, and so the corresponding graft copolymers possess aromatic characteristic. Thus, UV-vis spectra were developed as an effective approach to prove the graft of these monomers onto the gum backbone. The the grafting copolymers of gum with aniline has focused much attention because it can introduce electrical properties into gum. In the UV-vis spectra of AG-g-PANI polymer [26], AG showed a broad absorption band at 298 nm due to the presence of arabinogalactan components in the AG. Furthermore, the characteristic peaks of both arabinogalactan components and PANI were observed in the graft copolymer, and it confirmed the grafting of PANI onto AG backbone. In addition, UV-vis spectra are effective for a hydrogel based on graft-copolymer of gum. Wang et al. [193] introduce styrene in the GG-g-PAA/muscovite hydrogel system and the properties were obviously improved. In the UV-vis spectra of the swollen gel, the E band absorption of phenyl rings was observed, but it is absent in the spectra of sample without addition of styrene. This proved styrene participates in graft copolymerization. The UV-vis spectra are suitable for solution, solid, film, and gel.

5.5.4 *Elemental Analysis*

Elemental analysis is an identification method based on the difference of elements between gum backbone and graft copolymers in a type or content of special elements. The main characteristic elements are N and S. The monomers containing N elements (i.e., acrylamide, *N*-vinyl-2-pyrrolidone, aniline, *N*-isopropylacrylamide, 4-vinylpyridine) or containing S elements (i.e., 2-acrylamido-2-methyl propane sulfonic acid, sodium 4-vinylbenzenesulphonate) were grafted to the gum backbone; the elemental analysis may show the change of contents of N or S elements (for the gums containing N or S elements) or the appearance of N or S elements in the graft copolymer (for the gums without N or S elements). This provides direct evidence that these elements were grafted onto the gum backbone [132, 152, 155]. According to the change of elemental contents, the graft amount of monomers may also be roughly calculated, and this is also the advantages of elemental analysis method.

5.5.5 *NMR Analysis*

The ^1H -NMR and ^{13}C -NMR analyses are accurate approach to identify the molecular structure. By comparing with the change of special groups before and after grafting reaction, the occurrence of graft copolymerization reaction can be

confirmed. In the literature [58], the $^1\text{H-NMR}$ of the pure gum showed a peak at δ 4.65 (s) for anomeric protons and at δ 3.5–3.9 (m) and 2.05–2.06 (d) due to sugar protons, while the gum-g-copolymer showed an additional peak at δ 2.5 (due to protons of methylene groups at grafted chains of PAN on the guar gum backbone), indicating the presence of PAN in the graft copolymer and the grafting reaction occurred.

5.6 Properties of Gum-g-Copolymers

5.6.1 *Thermo- and Degradation-Resistance Properties*

Thermal stability is important to the application of a polymer material. The raw gums are mainly saccharides-type carbohydrate backbone, and so they can be easily thermally decomposed and carbonized. The graft copolymerization of gum can introduce new polymer chains and functional groups. The polymer chains may increase the molecular weight of gum, and the functional groups may form a cross-linking or cyclization structure to delay the thermal degradation. For instance, the value for ΔH in case of xyloglucan is found to be 258.5 J/g, but the xyloglucan-g-PMMA increased this value to 265.8 J/g. An endothermic peak is observed at 132.5 °C in XG-g-PMMA and another exothermic peak above 227 °C. This supports that the grafting of PMMA onto xyloglucan improved the thermal stability [156].

Similarly, the degradation-resistance capability can be improved by the graft copolymerization. Samui et al. [145] improved the degradation-resistance properties of acacia gum by grafting ethyl methacrylate onto its molecular chains. The acacia gum may be biodegraded about 37.5 % after 150 days, but the graft copolymer only degraded 5.4 % and the degradation degree can be controlled by the grafting ratio.

5.6.2 *Viscous and Rheological Properties*

The grafting reaction of gum may alter its molecular weight and charge and thus affect the viscosity of graft copolymers. The viscosity of graft copolymer is closely related to the graft ratio and graft efficiency which is mainly decided by the type and concentrations of gums, structure and concentration of monomers, initiation efficiency, and so on. Singh workgroups [25] investigated the effect of structure of *Ipomoea* seed gums on the graft efficiency and viscosity. It was concluded that the extent of grafting was dependent on the galactose-to-mannose ratio and the degree of the branching in the galactomannans. After grafting with acrylonitrile, the viscosity of gum was clearly enhanced from 3.87 cP to 40.9 cP (galactose-to-

mannose ratio, 1:6), 47.1 to 168.5 cP (galactose-to-mannose ratio, 1:2), and 129.6 to 193 cP (galactose-to-mannose ratio, 1:1.5). In addition, the graft of acrylonitrile obviously enhanced the stability of viscosity. The viscosity of raw gum decreased from 3.87 cP to 2 cP (galactose-to-mannose ratio, 1:6), 129.6 to 1.9 cP (galactose-to-mannose ratio, 1:2), and 47.1 to 2.54 cP (galactose-to-mannose ratio, 1:1.5) after 254 h, but the graft copolymers have no change of viscosity. The absolute viscosity of cashew gum-g-acrylamide at 2.5 % concentration (w/v) up to 33 and 3.3 times of the CG and PAM values, respectively [132].

5.6.3 Complexing Capacity

The nonionic gum may complex with metal ions by the $-C-OH$ groups, and the anionic gum may complex with ions through $-COOH$ or $-SO_3^{2-}$ groups. However, most of the natural gum has poor complexing capacity to metal ions because of the lack of functional groups with strong chelating capability. As described above, the simple graft of gum with functional monomers such as AMPS, AA, AM, AN, *N*-vinyl-2-pyrrolidone, 4-vinylpyridine, etc. may introduce numerous chelating groups (i.e., $-COOH$, $-COO^-$, $-C=O(NH_2)$, $-CN$, $-SO_3^{2-}$) in the gum backbone. Based on this, the gum was changed as a “bush” with numerous “hand,” and it can easily fetch metal ions from aqueous medium with a higher adsorption amount. The main mechanism is the chelating action of functional groups with metal ions. Because the functional groups are mainly from the grafted chains, the type of gum backbone has only small influence on the complexing capacity, and it mainly takes a supporting action. The adsorption capacity is related with the grafting ratio, molecular weight of graft copolymer, and the type of functional groups.

5.6.4 Mechanical Property

The mechanical property of polymer materials is mainly derived from the strength of molecular chains and the interaction among chains. The graft copolymers have usually higher molecular weight than raw gum and have branched graft chains and the functional groups that can easily generate hydrogen-bonding or ionic interaction. Thus, the mechanical property can be adjusted by controlling the graft ratio and the type functional groups. For example, Samui et al. [145] prepared the AG-g-PHEMA copolymer and compared its mechanical properties with that of AG. It was concluded that the tensile strength (N/mm^2) and elongation at break (%) were enhanced by 140 % and 650 %, respectively, in contrast to raw AG. The improvement of mechanical properties is extremely favorable to prepare high-strength film materials.

5.6.5 Flocculating and Decoloring Properties

The flocculating or decoloring mechanism of a flocculating agent is to change the electric potential of the suspended matter or dyes in water body through the interaction of flocculating agent having positive or negative charges with these matters and then make the suspended matter precipitating [194–196]. Due to the molecular weight and molecular charges, some gums have intrinsic flocculating and decoloring properties. After moderate modification, these properties can be enhanced, but the usage properties are still not satisfactory due to the limited charges. The graft copolymerization of gum may introduce numerous functional groups and increase the molecular weight and so can greatly enhance the flocculating or decoloring effect [144]. The type (positive or negative) and number of charges on the chains of gum can be controlled by the grafting technology, and so the graft-copolymer can be designed to be suitable for various water bodies. For instance, the introduction of $-\text{COO}^-$ may increase the flocculating and decoloring capability to positively charged particle or dyes, and the introduction of NH_4^+Cl^- may enhance the flocculating and decoloring capability to negatively charged particle or dyes.

5.6.6 Amphiphilic Properties

Most of the gums are hydrophilic and water-swellaable polymers. The graft copolymerization of gum with hydrophobic monomer may introduce moderate hydrophobic groups and make the gum having amphiphilic properties. The hydrophilic or hydrophobic capability can be controlled by the selection of functional groups and the graft ratio [197].

5.6.7 Electrical Property

Generally, the raw gums have usually no electrical properties due to their structure characteristics, but the graft copolymers of gums may generate electric conduction. The electric characteristics are mainly derived from the grafted chains and are dependent on the type and graft efficiency of monomers, and the commonly used monomer is aniline. Polyaniline (PANI) is considered as one of the most promising conducting polymer materials [198], but the synthesized PANI has low molecular weight and mechanical strength, poor solubility in common solvents, and infusibility at traditional melt-processing temperatures, which limited its application in the fabrication of electronic devices [199–202]. The graft of PANI with gum may not only improve the mechanical strength of graft copolymer but also endow the gum with electrical properties, and so the desirable hybrid properties of biopolymer and

PANI can be obtained. Tiwari et al. [203] prepared an electrical conducting guar gum-based polymer through the graft copolymerization reaction of guar gum with aniline using APS as the initiator. The features of gum were kept and an electrical conductivity of 1.6×10^{-2} S/cm was reached at room temperature. This work group also synthesized AG-g-PANI copolymer, and its cyclic voltammogram showed three anodic peaks at 0.20 V, 0.58 V, and 0.64 V along with two cathodic peaks at 0.50 V and 0.40 V, and the electrical conductivity is dependent on the ratio of aniline to AG, temperature, and pH value. Besides, the other monomer such as pyrrole was also grafted onto biopolymer collagen and shows better electrical properties [204, 205], but rare research is regarded on its graft reaction with gum.

5.6.8 Stimuli-Responsive Property

Many natural gums, such as PSY and XG, have stimuli-responsive capability when it suffers external stimuli such as pH value and electrolyte because they have functional groups $-\text{COOH}$ or $-\text{SO}_3^{2-}$. The responsive mechanism is the transform between $-\text{COOH}$ and $-\text{COO}^-$ groups with the change of external pH values. When the pH value is lower (acidic condition), the $-\text{COO}^-$ was changed as $-\text{COOH}$ groups, and the gum may generate volume change and a responsive behavior occurred. Based on these characters, many stimuli-responsive materials were designed, such as cross-linked XG [206, 207], PSY [208], CG [209], and SA [210]. But the stimuli-responsive capacity is weak because of the limited functional groups. The graft copolymerization of gum may introduce various types and numbers of functional groups, and the intrinsic responsive property can be enhanced or new responsive properties were introduced. For example, the introduction of temperature-sensitive groups such as isopropyl acrylamide, dimethyl formamide may bring the gum with temperature-responsive properties.

5.7 Applications of Gum-g-Copolymers

Graft copolymerization of gums with vinyl monomers or other functional monomers may introduce new groups on the gum backbone to form a comb-type structure or form a three-dimensional network structure by adding slight cross-linker. The introduced groups or branch chains on the gum backbone may alter its charges, mobility, flexibility, hydrophilic or hydrophobic properties, molecular weight, and so on, and thus, the colloidal properties, complexing capacity for metal ions, and water absorbing were obviously improved, or the new function derived from the grafted chains was presented.

5.7.1 *Drilling Additives*

With the increasing concerns on the environmental impact of oil-based drilling fluids in oil-field applications, the water-based drilling additive systems have been extensively used as shale inhibition, viscosity building, and filtration control for enhancing oil recovery [211, 212]. As the most important environmentally friendly polymers, the modified natural polymers show great potentials in oil-field application due to their renewable, low cost, nontoxicity, and biodegradability [213]. Currently, the modified cellulose such as carboxymethylcellulose, polyanionic cellulose, and cellulose graft copolymers was mainly focused and frequently used. Recently, with the increasing concerns on plant gum, gum-based polymers begin to be concerned because they have excellent viscosity and can be easily modified to form new materials. XG or its graft polymer was considered as a potential drilling additive because it has anionic characteristic with side-chain structure, higher molecular weight, excellent viscosity, good shear stability, and salt-resistance capability [214, 215].

5.7.2 *Thickener*

Currently, the commercial thickeners mainly include four categories: inorganic thickeners, cellulose, polyacrylate, and associative polyurethane thickener. The cellulose thickener has long usage history and various types, such as methylcellulose, carboxymethyl cellulose, hydroxyethyl cellulose, and hydroxypropyl methyl cellulose. With the progress of modern industry, the development of novel thicker with higher thickening efficiency and nontoxic characteristic becomes the subject of great interest. As described above, the aqueous solution of almost all the gums has gained great viscosity due to the interactions between polymer chains, and so gums are the important thickener in manufacture, distribution, storage, and consumption of water-based products, particularly formulations of surface coatings, drugs, cosmetics, and foods [216, 217]. Compared with the raw gums, the gum-g-copolymer usually showed higher viscosity due to the change of molecular weight, chain-chain interaction, and structure charges. Nickzare et al. modified acacia gum by its graft copolymerization with acrylic monomers for a thickening purpose, and it was found that the thickening properties were highly improved to form non-Newtonian fluids in water at concentrations below 2 % [218].

5.7.3 *Adsorption of Toxic Heavy Metals*

As discussed above, the gum-g-copolymer has strong complexing capability, and so it showed great prospect in the adsorption of toxic heavy metals. Sharma and Lalita [130] prepared GG-g-PNVP polymer and used for the sorption of Fe^{2+} and Cr^{6+} ions. It was found that the adsorption amount increased with increasing percent

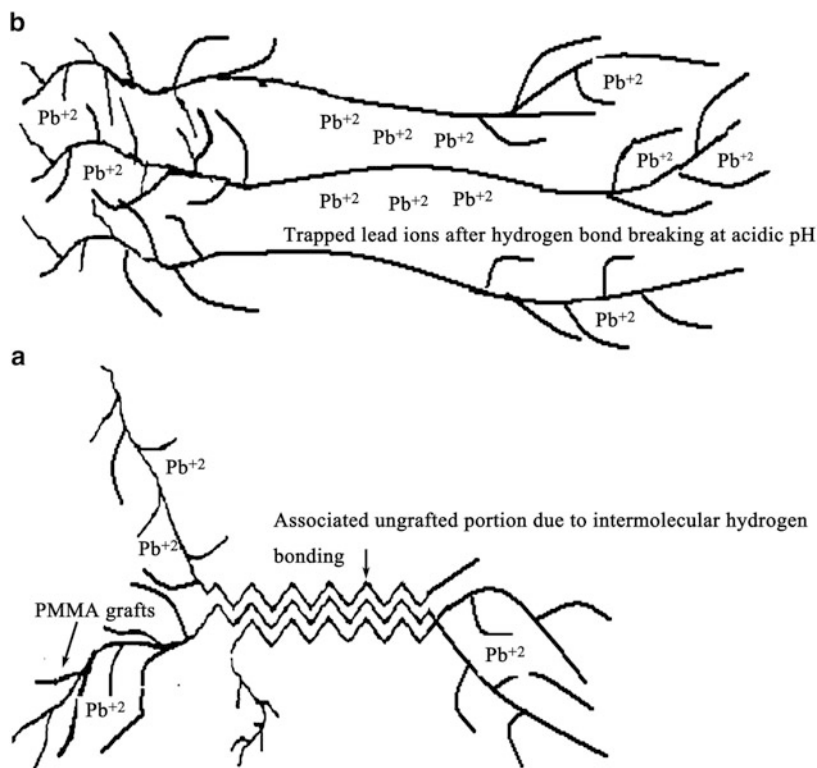


Fig. 5.22 Model for interaction between the Pb(II) and graft copolymer: (A) at normal pH, (B) at highly acidic pH [219]

grafting. Srivastava and Behari [116] synthesized GG-g-PNVP and evaluated its adsorption on heavy metal ions Cu^{2+} , Ni^{2+} , Zn^{2+} , Pb^{2+} , and Hg^{2+} ; it was concluded that the graft copolymers enhanced the adsorption amount by 279.4 % (Cu^{2+}), 240.7 % (Ni^{2+}), 207.1 % (Zn^{2+}), 367.2 % (Pb^{2+}), and 433.3 % (Hg^{2+}) in contrast to GG. Behari and coworkers [59] prepared XG-g-PAMPS graft copolymer, and its adsorption capacity on Cu^{2+} , Pb^{2+} , Ni^{2+} , Zn^{2+} , and Hg^{2+} ions was enhanced by 382.2 %, 353.9 %, 356.8 %, 292.0 %, and 262.3 %, respectively, and the retention capability was improved. The adsorption capacity is proportional to the graft ratio. The grafting ratio may be controlled by altering the graft reaction condition and the dosage of monomers, and the type of gum has obvious effect on it. For a gum with low reaction activity such as cashew gum or higher viscosity, the grafting ratio usually is low. By controlling the graft parameter, the solubility of the graft copolymer was decreased, and this is favorable to its application for wastewater treatment [138]. The GG-g-PEA graft copolymers shows ideal adsorption properties to Cd^{2+} ions than guar gum [165], and the adsorption capability can be adjusted by the grafting ratio. Singh et al. also proved the *Cassia grandis* seed gum-graft-poly(methylmethacrylate) has stronger combination action with the Pb(II) ions than the gum (Fig. 5.22) [219].

In the process of graft reaction, if the cross-linker was introduced, the cross-linked three-dimensional network structure can be formed, and the resultant adsorbents show better adsorption capability [130].

5.7.4 Flocculating Agent

Flocculating agent is important in the fields of wastewater treatment. The frequently used flocculating agents are inorganic polyhydroxyl metal salts (i.e., poly(aluminum sulfate), poly(ferric sulfate), poly(aluminum silicate), poly(ferric silicate), poly(aluminum phosphate), poly(iron phosphate), poly(silicic ferric sulfate) (PFSS), poly(phosphorus aluminum chloride) and synthetic polymers (i.e., poly(acrylamide), poly(sodium acrylate), poly(2-methyl acryloxyethyl trimethyl ammonium chloride), and poly(diallyldimethylammonium chloride)). These flocculating agents have found extensive application, but they are not eco-friendly. With the increasing attention on the safety of materials, natural polymer-based flocculating was focused. Many gums, such as xanthan gum, *C. javahikai* seed gum, etc. have intrinsic flocculating properties, and so they gained wide application in wastewater treatment as a commercial polymer material, and were honored as the green materials in twenty-first century. However, the flocculating properties of raw gums are limited due to their finite charges, functional groups, and molecular weight. Also, the fungus resistance ability of raw gums is low. Thus, the gum-g-copolymers show great application prospect as a flocculating agent because they combined the advantages of synthetic polymers and natural gum. For example, Sanghi groups [24] synthesized *C. javahikai* seed gum-g-polyacrylamide and used as coagulant for the removal of dyes from wastewater. The graft copolymer shows better coagulant effect than the raw gums. The graft of poly(acrylamide) onto the gum ghatti may decrease the turbidity from 200 NTU to about 45 NTU, but the raw gum can only decrease it to about 160 NTU [155]. The flocculating efficiency is increased with enhancing the graft ratio. The coagulants based on psyllium [167], tamarind kernel polysaccharide [220], *Ipomoea* seed gums [221], tamarind kernel polysaccharide, sodium alginate [222], *C. javahikai* seed gum [24], cationic guar gum [96], etc. have been developed.

5.7.5 Pitch Control Agents in Papermaking Industry

Papermaking plays an important role in modern chemical industries. The key process of papermaking is pulping. The aggregation and deposition of hydrophobic wood resins in the papermaking process has a problem for the pulp and paper industry. The sticky wood resins tend to deposit on the surface and result in downtime of the paper machine. The traditional alum is futile at neutral and alkaline pH when it was used as a pitch control agent. Thus, the water-soluble cationic

polymers have received great attention because they can act as bridging agents, attaching the wood resin particles onto papermaking fibers besides neutralizing the anionic matters. The commonly used cationic polymers are synthetic homopolymer or block copolymer based on petroleum monomers, which is not environmental friendly [223]. The natural polymer may resolve the environmental problem resulting from synthetic polymers, but it is hardly to reach an ideal effect. The graft copolymer of natural polymers with cationic monomers may integrate the advantages of natural polymers and synthetic polymers, especially was used as a pitch control agent. For example, the GG-g-P(AM-co-DDMC) was synthesized; it was proved that the graft copolymer is a good fixative as well as a good colloidal stabilizer with the combination of properties shared only by high molar mass P(AM-co-DDMC) and GG. And the wood pitch fixative properties of the graft-copolymer are effective over the entire pH range as compared to the other fixatives evaluated [224].

5.7.6 Macromolecular Surfactants

As known, most of the chemical surfactants such as cetyltrimethyl ammonium bromide, sodium dodecyl sulfate, and dodecyltrimethylammonium bromide are toxic and extremely harmful to the environment, but they are indispensable in modern industry. Thus, to seek for a substitution of chemical surfactants, the natural polymers, such as cellulose, starch, and gums were introduced. The surfactants are usually composed of hydrophobic end and hydrophilic chain end. Because the gum is usually hydrophilic, the moderate hydrophobic modification of gum may form a surfactant-like structure. For example, Daly groups [197] synthesized a graft copolymer of guar gum with polyalkoxyalkyleneamide. The introduction of hydrophobic monomers provides a facile approach to introduce hydrophobic region on the gum chains, and the hydrophobic degree can be controlled by adjusting grafting conditions. The graft copolymer has water-soluble characteristic, but can form micelle structure in water or oil (Fig. 5.23), and can be used for the emulsion polymerization or the others. Currently, the corresponding research is less, but it shows great application prospect in the modern industrial fields.

5.7.7 Electrical Biomaterials

Conducting biopolymer hybrids are widely adoptable materials for the fabrication of artificial nerves and muscles, sensors and actuators, blood vessels, etc. [225, 226]. For biomedical application, the safety and durability of materials are extremely important, and so the biopolymer-based materials are attractive and promising. Compared with other material derived from natural polymers, the graft copolymers of biopolymers with PANI have controlled electrical

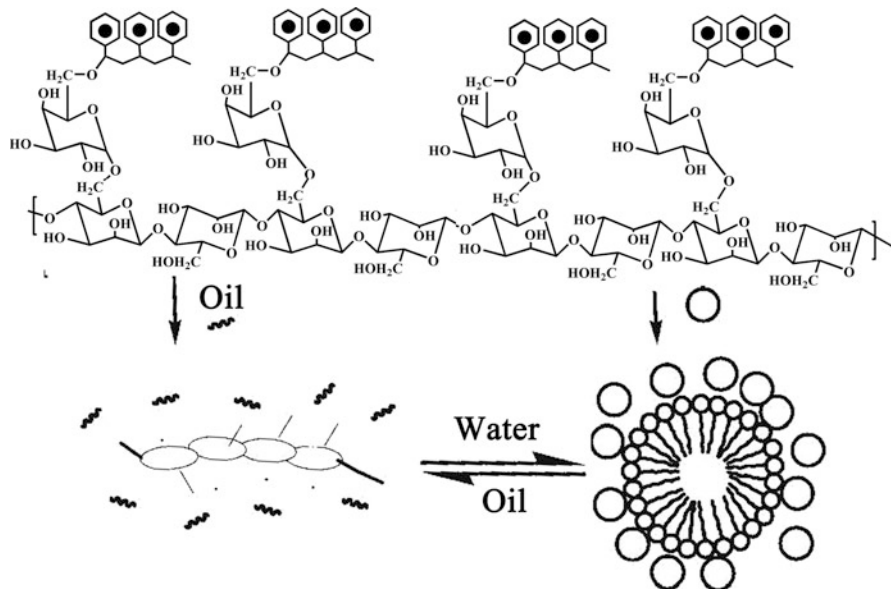


Fig. 5.23 Introduction of hydrophobic grafts may facilitate reversible micelle formation [197]

conductivity, good adhesion properties, high mechanical strength, and sandwich properties of component polymers [227–229]. Tiwari workgroups [227, 230, 231] developed the graft copolymer of AG with PANI, studied its electrical properties, and evaluated the application prospect of the graft copolymer in semiconductor, biomaterial for the fabrication of various sensor field. In addition, the conductive graft polymer of guar gum [203] was developed and evaluated for its practical application.

5.7.8 Drug Delivery Carriers

Natural gums have been used as drug delivery carrier for the controlled release of oral drug by virtue of their non-toxic, biodegradable, and biocompatible advantages. The gums were made as nanoparticles, beads, or tablet to load, deliver, and release the target drugs [232, 233], and the usage of gums fully resolved the safety problem of drug delivery carriers. For reducing the by-side effect of drugs resulting from the improper release and enhancing the efficiency of drugs, the smart drug carriers with ideal loading capability were highly concerned. The smart characteristics of carriers are mainly their responsive capability to external stimuli such as pH, temperature, electrolyte, electrical field, and photo. The nonionic gum has no responsive ability to external stimuli due to the absence of functional groups. The anionic gums (i.e., XG, PSY, *k*-CGN) may response to pH, electrical field, and

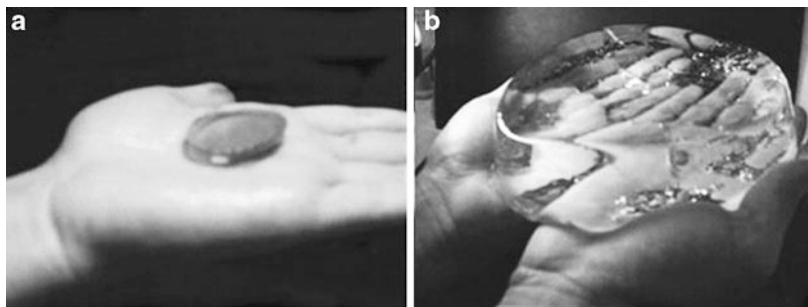


Fig. 5.24 Digital photo of superabsorbent hydrogel before (a) and after (b) swelling [238]

electrolytes because of the existence of functional $-\text{COOH}$ or $-\text{SO}_3^{2-}$ groups in their structure, and they have been developed as pH-sensitive drug carriers [234–236]. However, the loading efficiency of natural gums on drugs is lower and can only be used for pH- and saline-sensitive carriers. Thus, the gum-g-copolymers exhibit greater advantages as drug delivery carriers because the introduction of more functional groups enhance the loading of drug and responsive functionality. Toti et al. synthesized AG-g-PAM copolymer and used as a delivery tablet of two antihypertensive drugs diltiazem hydrochloride and nifedipine [133]. The graft of PAM chains may prolong the release time to 6 and 14 h for diltiazem hydrochloride and nifedipine, respectively. The graft of *N*-isopropylacrylamide onto guar gum makes it sensitive to temperature [129], which can be used to deliver and control the release of drug by the change of temperature.

5.7.9 Superabsorbent Materials

Superabsorbent materials are moderately cross-linked hydrophilic polymer materials with three-dimensional network structure and water-swellaable characteristics (Fig. 5.24) [237, 238]. Traditional superabsorbent materials are mainly synthetic polymers based on petroleum monomers, which cannot be biodegraded and are easy to induce secondary pollution [239]. So the biopolymer-based superabsorbents have attracted great attention in recent years. The raw natural polymer or its derivative has relatively lower water uptake capability, and so the developed superabsorbents are mainly graft copolymers of biopolymers. Grafting of hydrophilic monomer on the gum backbone usually introduces many hydrophilic graft chains, which can enhance the water-holding capability of gums. The graft copolymer can be directly used in soil to improve the water-retention capability, but its water-absorption and retention capability is poor. Thus, the utilization of gum-g-copolymer as water-saving materials (named as superabsorbent) usually involved with the fabrication of three-dimensional network structure by the addition of cross-linker. In the preparation process of superabsorbent, the graft reaction and cross-linking reaction simultaneously occurred. In the presence

of initiator, the hydrophilic monomers (i.e., acrylic acid, acrylamide, AMPS, acrylonitrile) may graft onto the gum backbone to form a chain structure. In the process of chain propagation, the cross-linker with double end vinyl groups may react with the radical on the graft chains and connect these chains to form a network structure. When the superabsorbent was contacted with water, the hydrophilic groups can be ionized and form an osmotic difference between interior network and external solution. The water molecules may penetrate into the network by diffusion or hydrogen-bonding attractive action and hold in the network structure. When the swollen superabsorbent was placed in a dry condition, the water molecules absorbed can release slowly to reach a water-saving effect. The superabsorbent product was mainly applied in agriculture, physiologic hygiene livings, drug delivery, and fine chemicals. Among most of these applications, the safety and biodegradability of materials are highly concerned, and correspondingly the research on gum-g-copolymers-type superabsorbent has been focused. Thus far, the superabsorbent based on the graft copolymer of GG [77, 240–243], XG [244], artemisia seed gum [245], PSY [246], tara gum [247], cashew gum [92, 248], AG [249], gum ghatti [250], and *k*-carrageenan [251–253] has been developed and applied.

5.7.10 *Sand-Binding Materials*

With the aggravation of global aridity and desertation of lands, the ecological recovery of sand lands becomes exigent. The mobility of sands increases the difficulty of planting in sandy land, and the fixation of sand is the key. It is expected that the sand binder can not only fix the mobile sand but can also retain and hold water. The traditional sand-bonding materials are mainly petroleum-based synthetic polymer. Although it has better corrosion-resistance properties, it is expensive and nonbiodegradable. Gums are hydrophilic natural polymer with viscosity and water-holding capability and have shown greater potentials as environmental friendly ecological recovery materials [254, 255]. The usage efficiency of such materials is dependent on the viscosity and water-absorbing capability. The natural gums have relatively better viscosity and water-swelling capability, but they are easily attacked by bacterial and the water-absorbing capability is limited. As a result, the binding capability and water-holding capability is poor when it was used for longer period of time. Therefore, the gum-g-copolymer was widely developed as sand-binding materials because it overcomes the drawbacks of both petroleum-based polymers and natural gums. The incorporation of more hydrophilic groups also improved the water-absorbing and retention properties.

5.7.11 *Micro-reactor of Preparing Nanomaterials*

With the boost of application field of nanomaterials, the synthesis method of nanomaterials tends to be diverse. As a formation template of nanomaterials (called as micro-reactor of nanomaterials), the gum-g-copolymer shows great potential due

to the various molecular structure and functional groups. The gum-based micro-reactor was usually used as two forms: the direct usage of gum-g-copolymer and the construction of a three-dimensional network structure based on graft copolymer. Abdel-Halim groups [256] prepared GG-g-PAM graft copolymer and used for the synthesis of Ag nanoparticles through the reduction of silver nitrate at pH 12.5. It was confirmed that the graft copolymer contributes to form a nanoparticle with better dispersion, small particle size, and narrow particle distribution. This provides possibility of using gum-g-copolymer to synthesize various nanoparticles with desirable morphology and property.

5.8 Conclusions

The increasing global resource and environment crisis continuously propels the development of eco-friendly materials as a succedaneum of petroleum-based products. The naturally occurring raw materials have recently raised a research upsurge owing to their unique “green” characteristics, and considerable efforts have been engaged. On the one hand, the new natural polymers were explored; on the other hand, the chemical or material researchers devoted to modify or utilize these polymers to derive new eco-friendly materials with desirable applicability. Gum is one of the rapidly developed natural polymers by virtue of its abundance, biodegradability, processibility, and structural diversity, and so the gums play irreplaceable role in modern industry. With the extension of application domains, the drawbacks of raw gum were increasingly highlighted, and the modification and derivatization of gum especially significant, and becomes the hot research subject. The derivatization of gum may tailor the properties of gum by introducing additional functional groups, and the application domains were greatly deepened. But the general derivatization can only introduce limited number of functional groups, and the congenital drawbacks of gums such as poor fungus resistance and heat-resistance capability have no evident improvement. Therefore, graft copolymerization of gum shows its advantages over general derivatization because it can improve the properties to a great degree or bring additional properties in the premise of keeping the intrinsic superiorities. The structure and properties of the graft copolymers could be easily tailored, and so the applications of gum were greatly extended. The influence factors of graft reaction are complex, and the exploration of the optimal reaction condition suitable for various gums and monomers is concerned. Thus, based on the latest efforts to the graft copolymerization of gum, this chapter demonstrated the sorts, structure, and sources of gums; the derivatives of gums; as well as the synthesis, properties, and applications of representative gum-g-copolymers. The development of new graft copolymer will provide a new approach for the utilization of gums. In addition, the work has also paved the way for enhancing the commercial importance and values of gums.

Acknowledgment This work is supported by the National Natural Science Foundation of China (Nos. 51003112 and 21107116).

References

1. Whistler RL, BeMiller JN (1993) Industrial gums: polysaccharides and their derivatives, 3rd edn. Academic, San Diego, CA
2. Amjad Z (1998) Water soluble polymers solution properties and applications. Kluwer Academic Publishers, Boston, MA
3. Phillips GO, Williams PA (2000) Handbook of hydrocolloids. Woodhead Publishing, Cambridge
4. Koocheki A, Mortazavi SA, Shahidi F, Razavi SMA, Taherian AR (2009) Rheological properties of mucilage extracted from *Alyssum homolocarpum* seed as a new source of thickening agent. *J Food Eng* 91:490–496
5. Ibrahim NA, Abo-Shosha MH, Allam EA, El-Zairy EM (2010) New thickening agents based on tamarind seed gum and karaya gum polysaccharides. *Carbohydr Polym* 81:402–408
6. Mahmud HS, Oyi AR, Allagh T (2009) Evaluation of the suspending properties of khya senegalensis gum in paracetamol suspensions. *Niger J Pharm Sci* 8:128–134
7. Al-Hamadani YAJ, Yusoff MS, Umar M, Bashir MJK, Nordin Adlan M (2011) Application of psyllium husk as coagulant and coagulant aid in semi-aerobic landfill leachate treatment. *J Hazard Mater* 190:582–587
8. Hamed SB, Belhadri M (2009) Rheological properties of biopolymers drilling fluids. *J Petrol Sci Eng* 67:84–90
9. Khalil M, Jan BM (2012) Herschel-Bulkley rheological parameters of a novel environmentally friendly lightweight biopolymer drilling fluid from xanthan gum and starch. *J Appl Polym Sci* 124:595–606
10. Gong HH, Liu MZ, Zhang B, Cui DP, Gao CM, Ni BL, Chen JC (2011) Synthesis of oxidized guar gum by dry method and its application in reactive dye printing. *Int J Biol Macromol* 49:1083–1091
11. Nakauma M, Funami T, Noda S, Ishihara S, Al-Assaf S, Nishinari K, Phillips GO (2008) Comparison of sugar beet pectin, soybean soluble polysaccharide, and gum arabic as food emulsifiers. 1. Effect of concentration, pH, and salts on the emulsifying properties. *Food Hydrocolloid* 22:1254–1267
12. Jian HL, Zhu LW, Zhang WM, Sun DF, Jiang JX (2012) Galactomannan (from *Gleditsia sinensis* Lam.) and xanthan gum matrix tablets for controlled delivery of theophylline: in vitro drug release and swelling behavior. *Carbohydr Polym* 87:2176–2182
13. Fabre B, Florini-Puybaret C (2011) Cosmetic composition containing a locust bean gum hydrolysate. US Patent No. US2011/0256087A1
14. Sundar S, Kundu J, Kundu SC (2010) Biopolymeric nanoparticles. *Sci Technol Adv Mater* 11:014104, 13 pp
15. Yu TJ, Wu BC, Tang BH, Lu YH (2011) Study on the application of guar gum in papermaking wet end (*Chinese*). *Paper Chem* 23:44–47
16. Battaerd HAJ, Treglar GW (1967) Graft copolymers. Wiley, New York, NY
17. Jenkins D, Hudson S (2001) Review of vinyl graft copolymerization featuring recent advances toward controlled radical-based reactions and illustrated with chitin/chitosan trunk polymers. *Chem Rev* 101:3245–3273
18. Roy D, Semsarilar M, Guthrie JT, Perrier S (2009) Cellulose modification by polymer grafting: a review. *Chem Soc Rev* 38:2046–2064
19. Kalia S, Kaith BS, Kaur I (2011) Cellulose fibers: bio- and nano-polymer composites-green chemistry and technology. Springer, Berlin
20. Bhattacharya A, Rawlins JW, Ray P (2009) Polymer grafting and crosslinking. Wiley, Hoboken, NJ
21. Singh RP (1995) In: Mark JE, Fai TJ (eds) Polymers and other advanced materials: emerging technologies and business opportunities. Plenum, New York, NY

22. Singh RP, Karmakar GP, Rath SK, Karmakar NC, Tripathy T, Panda J, Kanan K, Jain SK, Lan NT (2000) Biodegradable drag reducing agents and flocculants based on polysaccharides: materials and applications. *Polym Eng Sci* 40:46–60
23. Singh RP, Karmakar GP, Rath SK, Karmakar NC, Tripathy T, Pandey SR, Kanan K, Jain SK, Lan NT (2000) Novel biodegradable flocculants based on polysaccharides. *Curr Sci* 78:798–803
24. Sanghi R, Bhattacharya B, Singh V (2006) Use of *Cassia javahikai* seed gum and gum-g-polyacrylamide as coagulant aid for the decolorization of textile dye solutions. *Bioresour Technol* 97:1259–1264
25. Singh V, Tiwari A, Tripathy DN, Sanghi R (2005) Poly(acrylonitrile) grafted *Ipomoea seed*-gums: a renewable reservoir to industrial gums. *Biomacromolecules* 6:453–456
26. Tiwari A, Singh V (2008) Microwave-induced synthesis of electrical conducting gum acacia-graft-polyaniline. *Carbohydr Polym* 74:427–434
27. Whistler RL (1969) The encyclopedia of polymer science and technology, vol 11. Wiley, New York, Ny, p 416
28. Prado BM, Kim S, Ozen BF, Mauer LT (2005) Differentiation of carbohydrate gums and mixtures using fourier transform infrared spectroscopy and chemometrics. *J Agric Food Chem* 53:2823–2829
29. Turk SŠ, Schneider R (2000) Printing properties of a high substituted guar gum and its mixture with alginate. *Dyes Pigm* 47:269–275
30. Krishnaiah YSR, Karthikeyan RS, Gouri Sankar V, Satyanarayana V (2002) Three-layer guar gum matrix tablet formulations for oral controlled delivery of highly soluble trimetazidine dihydrochloride. *J Control Release* 81:45–56
31. Wong D, Larabee S, Clifford K, Tremblay J, Friend DR (1997) USP dissolution apparatus III (reciprocating cylinder) for screening of guar-based colonic delivery formulations. *J Control Release* 47:173–179
32. Singh V, Kumaril P, Pandey S, Narayan T (2009) Removal of chromium (VI) using poly (methylacrylate) functionalized guar gum. *Bioresour Technol* 100(6):1977–1982
33. Deshmukh SR, Chaturvedi PN, Singh RP (1985) The turbulent drag reduction by graft copolymers of guar gum and polyacrylamide. *J Appl Polym Sci* 30:4013–4018
34. Srivastava A, Tripathy J, Mishra MM, Behari K (2007) Modification of guar gum through grafting of 4-vinyl pyridine using potassium peroxymonosulphate/ascorbic acid redox pair. *J Appl Polym Sci* 106:1353–1358
35. Sanghi R, Bhattacharya B, Singh V (2002) *Cassia angustifolia* seed gum as an effective natural coagulant for decolourisation of dye solutions. *Green Chem* 4:252–254
36. Sullad AG, Manjeshwar LS, Aminabhavi TM (2010) Novel pH-sensitive hydrogels prepared from the blends of poly(vinyl alcohol) with acrylic acid-graft-guar gum matrixes for isoniazid delivery. *Ind Eng Chem Res* 49:7323–7329
37. Yadav M, Mishra DK, Behari K (2011) Synthesis of partially hydrolyzed graft copolymer (H-partially carboxymethylated guar gum-g-methacrylic acid): a superabsorbing material. *Carbohydr Polym* 85:29–36
38. Wang WB, Wang AQ (2009) Synthesis, swelling behaviors, and slow-release characteristics of a guar gum-g-poly(sodium acrylate)/sodium humate superabsorbent. *J Appl Polym Sci* 112:2102–2111
39. Singh V, Srivastava V, Pandey M, Sethi R, Sanghi R (2003) *Ipomoea turpethum* seeds: a potential source of commercial gum. *Carbohydr Polym* 51:357–359
40. Rannard SP, Rogers SH, Hunter R (2007) Synthesis of well-defined Locust Bean Gum-graft-copolymers using ambient aqueous atom transfer radical polymerisation. *Chem Commun* 362–364
41. Dakiaa PA, Bleckerb C, Roberta C, Watheleta B, Paquot M (2008) Composition and physicochemical properties of locustbeangum extracted from whole seeds by acid or water dehulling pre-treatment. *Food Hydrocolloid* 22:807–818

42. Simões J, Nunesb FM, Dominguesa MR, Coimbra MA (2011) Demonstration of the presence of acetylation and arabinose branching as structural features of locustbeangum galactomannans. *Carbohydr Polym* 86:1476–1483
43. Hefnawy HTM, Ramadan MF (2011) Physicochemical characteristics of soy protein isolate and fenugreek gum dispersed systems. *J Food Sci Technol* 48:371–377
44. Saha D, Bhattacharya S (2010) Hydrocolloids as thickening and gelling agents in food: a critical review. *J Food Sci Technol* 47:587–597
45. Somchit MN, Reezal I, Elysha Nur I, Mutali AR (2003) In vitro antimicrobial activity of ethanol and water extracts of *Cassia alata*. *J Ethnopharmacol* 84:1–4
46. Singh V, Srivastava A, Tiwari A (2009) Structural elucidation, modification and characterization of seedgum from *Cassia javahikai* seeds: anon-traditional source of industrial gums. *Int J Biol Macromol* 45:293–297
47. Yamada H, Nagai T, Cyong JC, Tomoda YO, Shimizu N, Shimada Y (1985) Relationship between chemical structure and anti-complementary activity of plant polysaccharides. *Carbohydr Res* 144(15):101–111
48. Mann AS, Jain NK, Kharya MD (2007) Evaluation of the suspending properties of *Cassia tora* mucilage on sulphadimidine suspension. *Asian J Exp Sci* 21:63–67
49. Williams PA, Sworn G (2007) Handbook of industrial water soluble polymers, Chapter 2. Natural thickeners. Wiley, New York, NY
50. Bajpai UDN, Jain A, Rai S (1990) Grafting of polyacrylamide on to guar gum using $K_2S_2O_8$ ascorbic acid redox system. *J Appl Polym Sci* 39:2187–2204
51. Kato K, Matsuda K (1969) Studies on the chemical structure of konjac mannan. *Agric Biol Chem* 33:1446–1453
52. Maeda M, Shimahara H, Sugiyama N (1980) Detailed examination of the branched structure of *konjac glucomannan*. *Agric Biol Chem* 44:245–252
53. Katsuraya K, Okuyama K, Hatanaka K, Oshima R, Satoc T, Matsuzakic K (2003) Constitution of konjacglucomannan: chemical analysis and ^{13}C NMR spectroscopy. *Carbohydr Polym* 53(2):183–189
54. Xu ZL, Yang YH, Jiang YM, Sun YM, Shen YD, Pang J (2008) Synthesis and characterization of konjac glucomannan-graft-polyacrylamide via γ -irradiation. *Molecules* 13:490–500
55. Zhang YQ, Xie BJ, Gan X (2005) Advance in the applications of konjac glucomannan and its derivatives. *Carbohydr Polym* 60:27–31
56. Singh V, Gupta PC (2000) In: Proceeding of the international symposium on trends in medicinal chemistry and biocatalysis, New Delhi, p 76
57. Arthur MG, Emil NA, James KS (1973) In: Whistler RL (ed) Industrial gums, 2nd edn. Academic, New York, NY
58. Singh V, Tiwari A, Sanghi R (2005) Studies on $K_2S_2O_8$ /ascorbic acid initiated synthesis of ipomoea dasysperma seed gum-g-poly(acrylonitrile): a potential industrial gum. *J Appl Polym Sci* 98:1652–1662
59. Srivastava A, Behari K (2007) Synthesis and study of metal ion sorption capacity of xanthan gum-g-2-acrylamido-2-methyl-1-propane sulphonic acid. *J Appl Polym Sci* 104:470–478
60. Adhikary P, Singh RP (2004) Synthesis, characterization, and flocculation characteristics of hydrolyzed and unhydrolyzed polyacrylamide grafted xanthan gum. *J Appl Polym Sci* 94:1411–1419
61. Kang KS, Cottrell I (1979) In: Pepler HJ, Perlman D (eds) Microbial technology, vol 1, 2nd edn. Academic, New York, NY, p 417
62. Kumar R, Srivastava A, Behari K (2007) Graft copolymerization of methacrylic acid onto xanthan Gum by Fe^{2+}/H_2O_2 redox initiator. *J Appl Polym Sci* 105:1922–1929
63. Sandvick EI, Merker JM (1977) In: Sandford P, Laskin A (eds) Extra cellular microbial polysaccharides, ACS symposium series No. 45. American Chemical Society, Washington, DC, p 242
64. Kadajji VG, Betageri GV (2011) Water soluble polymers for pharmaceutical applications. *Polymers* 3:1972–2009

65. Harding SE, Day K, Dhami R, Lowe PM (1997) Further observation on the size, shape and hydration of kappa-carrageenan in dilute solution. *Carbohydr Polym* 32:81–87
66. Thanh TTT, Yuguchi Y, Mimura M, Yasunaga H, Takano R, Urkawa H (2002) Molecular characteristics and gelling properties of carrageenan family, 1: preparation of novel carrageenans and their dilute solution properties. *Macromol Chem Phys* 203:15–23
67. Mishra DK, Tripathy J, Behari K (2008) Synthesis of graft copolymer (k-carrageenan-g-N, N-dimethylacrylamide) and studies of metal ion uptake, swelling capacity and flocculation properties. *Carbohydr Polym* 71:524–534
68. Clark AH, Ross-Murphy SB (1987) Mechanical and structural properties of biopolymers gels. *Adv Polym Sci* 83:60–184
69. Guo JH, Skinner GW, Harcum WW, Barnum PE (1999) Investigating the fundamental effects of binder on pharmaceutical tablet performance. *Drug Dev Ind Pharm* 25:1129–1135
70. De Ruiter GA, Rudolph B (1997) Carrageenan biotechnology. *Trends Food Sci Technol* 8 (12):389–395
71. Zhang QB, Li N, Liu XG, Zhao ZQ, Li ZE, Xu ZH (2004) The structure of a sulfated galactan from *Porphyra haitanensis* and its in vivo antioxidant activity. *Carbohydr Res* 339:105–111
72. Zhang QB, Yu PZ, Li ZE, Zhang H, Xu ZH, Li PC (2003) Antioxidant activities of sulfated polysaccharide fractions from *Porphyra haitanensis*. *J Appl Phycol* 15:305–310
73. Hosseinzadeh H, Sadeghzadeh M, Babazadeh M (2011) Preparation and properties of carrageenan-g-poly(acrylic acid)/bentonite superabsorbent composite. *J Biomater Nanobiotechnol* 2:311–317
74. Yang JS, Xie YJ, He W (2011) Research progress on chemical modification of alginate: a review. *Carbohydr Polym* 84:33–39
75. Jay SM, Saltzman WM (2009) Controlled delivery of VEGF via modulation of alginate microparticle ionic crosslinking. *J Control Release* 134:26–34
76. Wong TW (2011) Alginate graft copolymers and alginate-co-excipient physical mixture in oral drug delivery. *J Pharm Pharmacol* 63:1497–1512
77. Wang WB, Wang AQ (2010) Synthesis and swelling properties of pH-sensitive semi-IPN superabsorbent hydrogels based on sodium alginate-g-poly(sodium acrylate) and polyvinylpyrrolidone. *Carbohydr Polym* 80(4):1028–1036
78. Chowdhury P, Samui S, Kundu T, Saha B (2004) Synthesis and characterization of poly(methyl methacrylate) grafted from acacia gum. *J Chin Chem Soc* 51:97–101
79. Williams PA, Phillips GO (2009) Gum arabic. In: Phillips GO, Williams PA (eds) *Handbook of hydrocolloids*. Woodhead, Cambridge, pp 252–273
80. Islam AM, Phillips GO, Sijivo A, Snowden MJ, Williams PA (1997) A review in recent developments on the regulatory, structural and functional aspects of gum arabic. *Food Hydrocolloid* 11:493–505
81. Sanchez C, Renard D, Robert P, Schmitt C, Lefebvre J (2002) Structure and rheological properties of acacia gum dispersions. *Food Hydrocolloid* 16:257–267
82. Mallik H, Gupta N, Sarkar A (2002) Anisotropic electrical conduction in gum Arabic—a biopolymer. *Mater Sci Eng C* 20:215–218
83. Zhang LM, Zhou JF, Hui PS (2005) A comparative study on viscosity behavior of water-soluble chemically modified guar gum derivatives with different functional lateral groups. *J Sci Food Agric* 85:2638–2644
84. Dodi G, Hritcu D, Popa MI (2011) Carboxymethylation of guar gum: synthesis and characterization. *Cell Chem Technol* 45:171–176
85. Magalhães GA Jr, Santos CMW, Silva DA, Maciel JS, Feitosa JPA, Paula HCB, de Paul RCM (2009) Microspheres of chitosan/carboxymethyl cashew gum (CH/CMCG): effect of chitosan molar mass and CMCG degree of substitution on the swelling and BSA release. *Carbohydr Polym* 77:217–222
86. Seaman JK (1980) In: Davidson RL (ed) *Handbook of water-soluble gums and resins*. McGraw-Hill, New York, NY

87. Prabhanjan H, Gharia MM, Srivastava HC (1989) Guar gum derivatives. Part I: preparation and properties. *Carbohydr Polym* 11(4):279–292
88. Lapasin R, Priel S, Tracanelli P (1991) Rheology of hydroxyethyl guar gum derivatives. *Carbohydr Polym* 14(4):411–427
89. Patel SP, Ranjan G, Patel VS (1987) Rheological properties of guar gum and hydroxyethyl guar gum in aqueous solution. *Int J Biol Macromol* 9(6):314–320
90. Reis AV, Guilherme MR, Cavalcanti OA, Rubira AF, Muniz EC (2006) Synthesis and characterization of pH-responsive hydrogels based on chemically modified Arabic gum polysaccharide. *Polymer* 47:2023–2029
91. Shenoy MA, D'Melo DJ (2010) Synthesis and characterization of acryloyloxy guar gum. *J Appl Polym Sci* 117:148–154
92. Guilherme MR, Reis AV, Takahashi SH, Rubira AF, Feitosa JPA, Muniz EC (2005) Synthesis of a novel superabsorbent hydrogel by copolymerization of acrylamide and cashew gum modified with glycidyl methacrylate. *Carbohydr Polym* 61:464–471
93. Hamcerencu M, Desbrieres J, Popa M, Khoukh A, Riess G (2007) New unsaturated derivatives of xanthan gum: synthesis and characterization. *Polymer* 48:1921–1929
94. Guilherme MR, Moia TA, Reis AV, Paulino AT, Rubira AF, Mattoso LHC, Muniz EC, Tambourgi EB (2009) Synthesis and water absorption transport mechanism of a pH-sensitive polymer network structured on vinyl-functionalized pectin. *Biomacromolecules* 10:190–196
95. Reis AV, Fajardo AR, Schuquel ITA, Guilherme MR, Vidotti GJ, Rubira AF, Muniz EC (2009) Reaction of glycidyl methacrylate at the hydroxyl and carboxylic groups of poly(vinyl alcohol) and poly(acrylic acid): is this reaction mechanism still unclear? *J Org Chem* 74:3750–3757
96. Singh RP, Pal S, Mal D (2006) A high performance flocculating agent and viscosifiers based on cationic guar gum. *Macromol Symp* 242:227–234
97. Oberstar HE, Westman MA (1977) Conditioning shampoo composition containing a cationic derivative of a natural gum (such as guar) as the active conditioning ingredient. US Patent No. 4061602
98. Huang YH, Yu HQ, Xiao CB (2007) pH-sensitive cationic guar gum/poly (acrylic acid) polyelectrolyte hydrogels: swelling and in vitro drug release. *Carbohydr Polym* 69:774–783
99. Huang YH, Lu J, Xiao CB (2007) Thermal and mechanical properties of cationic guar gum/poly(acrylic acid) hydrogel membranes. *Polym Degrad Stab* 92:1072–1081
100. Chowdhary MS, Cottrell IW (1999) Method for preparation of amphoteric guar gum derivatives. EP Appl. No. 0943627
101. Benninga H (1969) Cationic and anionic substituted polysaccharides and process for preparing same. US Patent No. 3467647
102. Liu XL, Cao CY, Peng JJ (2010) Study on half-dry preparation of amphoteric guar gum and its application in papermaking as strength aid. In: *Research progress in paper industry and biorefinery (4th ISETPP)*. 1-3:1780–1784
103. Wang XH, Cui YC, Li DL (2004) Application of amphoteric sesbania gum to treatment wastewater from printing and drying. *Technol Water Treat (Chinese)* 30(6):369–371
104. Xiong Y, Hu ZY (2007) Synthesis of zwitterionic guar gum. *Chemical Industry Times (Chinese)* 21(1):37–39
105. Lapasin R, Lorenzi LD, Priel S, Torriano G (1995) Flow properties of hydroxypropyl guar gum and its long-chain hydrophobic derivatives. *Carbohydr Polym* 28:195–202
106. Wang GH, Zhang LM (2007) Manipulating formation and drug-release behavior of new sol–gel silica matrix by hydroxypropyl guar gum. *J Phys Chem B* 111(36):10665–10670
107. Ho FFL, Kohler RR, Ward GA (1972) Determination of molar substitution and degree of substitution of hydroxypropyl cellulose by nuclear magnetic resonance spectrometry. *Anal Chem* 44(1):178–181
108. Odian G (1981) *Principles of polymerization*, 2nd edn. Wiley, New York, NY
109. Raval DK, Patel RG, Patel VS (1988) Grafting of methyl methacrylate onto gum gum by hydrogen peroxide initiation. *J Appl Polym Sci* 35:2201–2209

110. Bajpai UDN, Jain A (1993) Grafting of polyacrylamide on to guar gum with the redox system potassium bromate/thiomalic acid. *Polym Int* 31:1–7
111. Bajpai UDN, Mishra V, Rai S (1993) Grafting of poly (acrylonitrile) onto guar gum using potassium persulfate/ascorbic acid redox initiating system. *J Appl Polym Sci* 47:717–722
112. Behari KUNJ, Taunk KAVITA, Tripathi MALA (1999) Cu^{+2} /mandelic acid redox pair initiated graft copolymerization acrylamide onto guar gum. *J Appl Polym Sci* 71:739–745
113. Behari K, Kumar R, Tripathi M, Pandey PK (2001) Graft copolymerization of methacrylamide onto guar gum using a potassium chromate/malonic acid redox pair. *Macromol Chem Phys* 202:1873–1877
114. Mundargi RC, Agnihotri SA, Patil SA, Aminabhavi TM (2006) Graft copolymerization of methacrylic acid onto guar gum, using potassium persulfate as an initiator. *J Appl Polym Sci* 101:618–623
115. Pandey PK, Srivastava A, Tripathy J, Behari K (2006) Graft copolymerization of acrylic acid onto guar gum initiated by vanadium (V)–mercaptosuccinic acid redox pair. *Carbohydr Polym* 65:414–420
116. Srivastava A, Behari K (2006) Synthesis and characterization of graft copolymer (guar gum-g-N-vinyl-2-pyrrolidone) and investigation of metal ion sorption and swelling behavior. *J Appl Polym Sci* 100:2480–2489
117. Sand A, Yadav M, Mishra MM, Tripathy J, Behari K (2011) Studies on graft copolymerization of 2-acrylamidoglycolic acid on to partially carboxymethylated guar gum and physico-chemical properties. *Carbohydr Polym* 83:14–21
118. Pandey PK, Banerjee J, Taunk K, Behari K (2003) Graft copolymerization of acrylic acid onto xanthum gum using a potassium monopersulfate/ Fe^{2+} redox pair. *J Appl Polym Sci* 89:1341–1346
119. Pandey BPK, Kumar R, Taunk K (2001) Graft copolymerization of acrylamide onto xanthan gum. *Carbohydr Polym* 46:185–189
120. Banerjee J, Srivastava A, Srivastava A, Behari K (2006) Synthesis and characterization of xanthan Gum-g-N-vinyl formamide with a potassium monopersulfate/Ag(I) system. *J Appl Polym Sci* 101:1637–1645
121. Srivastava A, Behari K (2009) Modification of natural polymer via free radical graft copolymerization of 2-acrylamido-2-methyl-1-propane sulfonic acid in aqueous media and study of swelling and metal ion sorption behavior. *J Appl Polym Sci* 114:1426–1434
122. Srivastava A, Mishra DK, Tripathy J, Behari K (2009) One pot synthesis of xanthan gum-g-N-vinyl-2-pyrrolidone and study of their metal ion sorption behavior and water swelling property. *J Appl Polym Sci* 111:2872–2880
123. Kumar R, Srivastava A, Behari K (2009) Synthesis and characterization of polysaccharide based graft copolymer by using potassium peroxymonosulphate/ascorbic acid as an efficient redox initiator in inert atmosphere. *J Appl Polym Sci* 112:1407–1415
124. Bajpai UDN, Rai S (1988) Grafting of acrylamide onto guar gum using KMnO_4 /oxalic acid redox system. *J Appl Polym Sci* 35:1169–1182
125. Taunk K, Behari K (2000) Graft copolymerization of acrylic acid onto guar gum. *J Appl Polym Sci* 77:39–44
126. Behari K, Tripathi M, Taunk K, Kumar R (2000) Studies of graft copolymerization of acrylamide onto guar gum using peroxydiphosphate–metabisulphite redox pair. *Polym Int* 49:153–157
127. Taunk K, Behari K (2002) Studies on graft copolymerization of 4-vinylpyridine onto guar gum. *J Appl Polym Sci* 84:2380–2385
128. Behari K, Banerjee J, Srivastava A, Mishra DK (2005) Studies on graft copolymerization of N-vinyl formamide onto guar gum initiated by bromate/ascorbic acid redox pair. *Indian J Chem Technol* 12:664–670
129. Bajpai UDN, Jain A, Bajpai AK (1990) Grafting of acrylamide onto guar gum with the redox system $\text{Cu}^{2+}/\text{Na}_2\text{S}_2\text{O}_5$. *Acta Polym Sin* 41:577–581

130. Sharma RK, Lalita (2011) Synthesis and characterization of graft copolymers of N-Vinyl-2-Pyrrolidone onto guar gum for sorption of Fe^{2+} and Cr^{6+} ions. *Carbohydr Polym* 83:1929–1936
131. Raval DK, Patel MV, Patel RG, Patel VS (1991) Perspective study of vinyl grafting onto leucaena glauca seed gum and guar gum by hydrogen peroxide Initiation. *Starch/Stärke* 43:483–487
132. da Silva DA, de Paula RCM, Feitosa JPA (2007) Graft copolymerisation of acrylamide onto cashew gum. *Eur Polym J* 43:2620–2629
133. Toti US, Soppimath KS, Mallikarjuna NN, Aminabhavi TM (2004) Acrylamide-grafted-acacia gum polymer matrix tablets as erosion-controlled drug delivery systems. *J Appl Polym Sci* 93:2245–2253
134. Pottenger CR, Johnson DC (1970) Mechanism of cerium (IV) oxidation of glucose and cellulose. *J Polym Sci A1 Polym Chem* 8:301–318
135. Sharma BR, Kumar V, Soni PL (2003) Graft copolymerization of acrylonitrile onto Cassia tora gum with ceric ammonium nitrate–nitric acid as a redox initiator. *J Appl Polym Sci* 90:129–136
136. Yoshida T, Hattori K, Sawada Y, Choi Y, Uryu T (1996) Graft copolymerization of methyl methacrylate onto curdlan. *J Polym Sci A Polym Chem* 34:3053–3060
137. Duan ML, Garica FG, Pinto MR, Soares BG (2002) Grafting of polymethyl methacrylate from poly(ethylene-co-vinylacetate) copolymer using atom transfer radical polymerization. *Eur Polym J* 38:759–769
138. Mark HF, Bikales NM, Overberger C, Menges G (1987) *Encyclopedia of polymer science and engineering*, vol 7, 2nd edn. Wiley, New York, NY
139. Chowdhury P (1998) Graft copolymerization of ethyl methacrylate onto polyvinyl alcohol using ceric ion initiator. *Indian J Chem Technol* 5:346–350
140. Chowdhury P, Pal CM (1999) Graft copolymerization of methyl acrylate onto polyvinyl alcohol using Ce(IV) initiator. *Eur Polym J* 35:2207–2213
141. Chowdhury P, Samui S, Kundu T, Nandi MM (2001) Graft polymerization of methyl methacrylate onto guar gum with ceric ammonium sulfate/dextrose redox pair. *J Appl Polym Sci* 82:3520–3525
142. Thimma RT, Reddy NS, Tammishetti S (2003) Synthesis and characterization of guar gum-graft-polyacrylonitrile. *Polym Adv Technol* 14:663–668
143. Trivedi JH, Kalia K, Patel NK, Trivedi HC (2005) Ceric-induced grafting of acrylonitrile onto sodium salt of partially carboxymethylated guar gum. *Carbohydr Polym* 60:117–125
144. Wan XF, Li YM, Wang XJ, Chen SL, Gu XY (2007) Synthesis of cationic guar gum-graft-polyacrylamide at low temperature and its flocculating properties. *Eur Polym J* 43:3655–3661
145. Samui S, Ghosh AK, Ali MA, Chowdhury P (2007) Synthesis, characterization and kinetic studies of PEMA grafted acacia gum. *Indian J Chem Technol* 14:126–133
146. Wan XF, Li YM, Wang XJ, Wang YX, Song LL (2007) Ceric ion-induced graft copolymerization of acrylamide on cationic guar gum at low temperature. *J Appl Polym Sci* 104:3715–3722
147. Mohamadnia Z, Zohuriaan-Mehr MJ, Kabiri K, Razavi-Nouri M (2008) Tragacanth gum-graft-polyacrylonitrile: synthesis, characterization and hydrolysis. *J Polym Res* 15:173–180
148. Singh V, Tiwari A, Singh SP, Kumari P, Tiwari S (2008) Ceric ammonium sulfate/sodium disulfite initiated grafting of acrylamide on to cassia reticulata seed gum. *J Appl Polym Sci* 110:1477–1484
149. Goyal P, Kumar V, Sharma P (2008) Graft copolymerization of acrylamide onto tamarind kernel powder in the presence of ceric ion. *J Appl Polym Sci* 108:3696–3701
150. Hosseinzadeh H (2009) Ceric-initiated free radical graft copolymerization of acrylonitrile onto kappa carrageenan. *J Appl Polym Sci* 114:404–412
151. Işıkkan N, Kurşun F, İnal M (2009) Graft copolymerization of itaconic acid onto sodium alginate using ceric ammonium nitrate as initiator. *J Appl Polym Sci* 114:40–48

152. Xie CX, Feng YJ, Cao WP, Teng H, Li JF, Lu ZY (2009) Novel biodegradable flocculating agents prepared by grafting polyacrylamide to konjac. *J Appl Polym Sci* 111:2527–2536
153. Goyal P, Kumar V, Sharma P (2009) Graft copolymerization onto tamarind kernel powder: ceric(IV)-initiated graft copolymerization of acrylonitrile. *J Appl Polym Sci* 114:377–386
154. Wang CX, Qiu B (2011) Graft copolymerization of glycidyl methacrylate onto guar gum (Chinese). *New Chem Mater* 39(6):112–114
155. Rani P, Sen G, Mishra S, Jha U (2012) Microwave assisted synthesis of polyacrylamide grafted gum ghatti and its application as flocculant. *Carbohydr Polym* 89:275–281
156. Mishra A, Malhotra AV (2012) Graft copolymers of xyloglucan and methyl methacrylate. *Carbohydr Polym* 87:1899–1904
157. Tiwari A, Grailler JJ, Pilla S, Steeber DA, Gong SQ (2009) Biodegradable hydrogels based on novel photopolymerizable guar gum–methacrylate macromonomers for in situ fabrication of tissue engineering scaffolds. *Acta Biomater* 5:3441–3452
158. Kumar R, Setia A, Mahadevan N (2012) Grafting modification of the polysaccharide by the use of microwave irradiation—a review. *Int J Recent Adv Pharm Res* 2(2):45–53
159. Singh V, Kumara P, Sanghi R (2012) Use of microwave irradiation in the grafting modification of the polysaccharides—a review. *Prog Polym Sci* 37:340–364
160. Singh V, Tiwari A, Tripathi DN, Sanghi R (2004) Grafting of polyacrylonitrile onto guar gum under microwave irradiation. *J Appl Polym Sci* 92:1569–1575
161. Kaith BS, Jindal R, Jana AK, Maiti M (2009) Characterization and evaluation of methyl methacrylate-acetylated *Saccharum spontaneum* L. graft copolymers prepared under microwave. *Carbohydr Polym* 78:987–996
162. Kumar A, Singh K, Ahuja M (2009) Xanthan-g-poly(acrylamide): microwave-assisted synthesis, characterization and in vitro release behavior. *Carbohydr Polym* 76:261–267
163. Singh V, Tiwari A, Tripathi DN, Sanghi R (2004) Microwave assisted synthesis of guar-g-poly-acrylamide. *Carbohydr Polym* 58:1–6
164. Singh V, Premalata C, Tiwari A, Sharma AK (2007) Alumina supported synthesis of Cassia marginata gum-g-poly(acrylonitrile) under microwave irradiation. *Polym Adv Technol* 18:379–385
165. Singh V, Sharma AK, Maurya S (2009) Efficient cadmium(II) removal from aqueous solution using microwave synthesized guar gum-graft-poly(ethylacrylate). *Ind Eng Chem Res* 48:4688–4696
166. Malik S, Ahuja M (2011) Gum kondagogu-g-poly (acrylamide): microwave-assisted synthesis, characterisation and release behaviour. *Carbohydr Polym* 86:177–184
167. Sen G, Mishra S, Rani GU, Rani P, Prasad R (2012) Microwave initiated synthesis of polyacrylamide grafted Psyllium and its application as a flocculant. *Int J Biol Macromol* 50:369–375
168. Sena G, Mishra S, Jha U, Pal S (2010) Microwave initiated synthesis of polyacrylamide grafted guar gum (GG-g-PAM)—characterizations and application as matrix for controlled release of 5-amino salicylic acid. *Int J Biol Macromol* 47:164–170
169. Singh V, Kumari PL, Tiwari A, Pandey S (2010) Alumina-supported microwave synthesis of *cassia marginata* seed gum-graft-polyacrylamide. *J Appl Polym Sci* 117:3630–3638
170. Pal S, Ghorai S, Dash MK, Ghosh S, Udayabhanu G (2011) Flocculation properties of polyacrylamide grafted carboxymethyl guar gum (CMG-g-PAM) synthesised by conventional and microwave assisted method. *J Hazard Mater* 192:1580–1588
171. Gupta B, Scherer G (1994) Proton exchange membranes by radiation-induced graft copolymerization of monomers into Teflon-FEP films. *Chimia* 48:127–137
172. Xu Z, Sun Y, Yang Y, Ding J, Pang J (2007) Effect of γ -irradiation on some physicochemical properties of konjac glucomannan. *Carbohydr Polym* 70:444–450
173. Lokhande HT, Varadarajan PV, Nachane ND (1993) Gamma-radiation induced grafting of acrylonitrile onto guar gum: Influence of reaction conditions on the properties of the grafted and saponified products. *J Appl Polym Sci* 48:495–503

174. Biswal J, Kumar V, Bhardwaj YK, Goel NK, Dubey KA, Chaudhari CV, Sabharwal S (2007) Radiation-induced grafting of acrylamide onto guar gum in aqueous medium: synthesis and characterization of grafted polymer guar-g-acrylamide. *Radiat Phys Chem* 76:1624–1630
175. Li YF, Ha YM, Tao LR, Li YJ, Wang F (2011) Preparation of xanthan gum-g-N-vinylpyrrolidone by radiation and adsorption property of phenol and polyphenol. *Adv Mater Res* 236–238:2694–2700
176. Sommers CH (2004) Recent advances in food irradiation. ACS, Philadelphia, PA
177. Kumar K, Kaith BS, Jindal R, Mittal H (2012) Gamma-radiation initiated synthesis of Psyllium and acrylic acid-based polymeric networks for selective absorption of water from different oil–water emulsions. *J Appl Polym Sci* 124:4969–4977
178. Odian G (2002) Principles of polymerization, 3rd edn. Wiley, New York, NY
179. Shanmugaraj AM, Kim JK, Ryu SH (2006) Modification of rubber surface by UV surface grafting. *Appl Surf Sci* 252(16):5714–5722
180. Ma H, Davis RH, Bowman CN (2001) Principal factors affecting sequential photoinduced graft polymerization. *Polymer* 42:8333–8338
181. Thaker MD, Trivedi HC (2005) Ultraviolet-radiation-induced graft copolymerization of methyl acrylate onto the sodium salt of partially carboxymethylated guar gum. *J Appl Polym Sci* 97:1977–1986
182. Yamagishi H, Saito K, Furusaki S, Sugo T, Hosoi F, Okamoto J (1993) Molecular weight distribution of methyl methacrylate grafted onto a microfiltration membrane by radiation-induced graft polymerization. *J Memb Sci* 85:71–80
183. Ruckert D, Cazaux F, Coqueret X (1999) Electron-beam processing of destructureized allylurea–starch blends: immobilization of plasticizer by grafting. *J Appl Polym Sci* 73:409–417
184. Olivier A, Cazaux F, Coqueret X (2001) Compatibilization of starch–allylurea blends by electron beam irradiation: spectroscopic monitoring and assessment of grafting efficiency. *Biomacromolecules* 2:1260–1266
185. Mesquita AC, Mori MN, Andrade e Silva LG (2004) Polymerization of vinyl acetate in bulk and emulsion by gamma irradiation. *Radiat Phys Chem* 71:253–256
186. Fan JC, Chen J, Yang LM, Lin H, Cao FQ (2009) Preparation of dual-sensitive graft copolymer hydrogel based on N-maleoyl-chitosan and poly(N-isopropylacrylamide) by electron beam radiation. *Bull Mater Sci* 32:521–526
187. Liu LZ, Priou C (2010) Grafting polymerization of guar and other polysaccharides by electron beams. US Patent No. 7838667 B2
188. Kolb HC, Finn MG, Sharpless KB (2001) Click chemistry: diverse chemical function from a few good reactions. *Angew Chem Int Ed* 40:2004–2021
189. Tizzotti M, Creuzet C, Labeau MP, Hamaide T, Boisson F, Drockenmuller E, Charlot A, Fleury E (2010) Synthesis of temperature responsive biohybrid guar-based grafted copolymers by click chemistry. *Macromolecules* 43:6843–6852
190. Tizzotti M, Labeau MP, Hamaide T, Drockenmuller E, Charlot AL, Fleury E (2010) Synthesis of thermosensitive guar-based hydrogels with tunable physico-chemical properties by click chemistry. *J Polym Sci A Polym Chem* 48:2733–2742
191. Matyjaszewski K, Xia JH (2001) Atom transfer radical polymerization. *Chem Rev* 101:2921–2990
192. Bontempo D, Masci G, Leonardis PD, Mannina L, Capitani D, Crescenzi V (2006) Versatile grafting of polysaccharides in homogeneous mild conditions by using atom transfer radical polymerization. *Biomacromolecules* 7:2154–2161
193. Wang WB, Kang YR, Wang AQ (2010) Synthesis, characterization and swelling properties of the guar gum-g-poly(sodium acrylate-co-styrene)/muscovite superabsorbent composites. *Sci Technol Adv Mater* 11(2):025006
194. Biggs S, Habgood M, Jameson GJ, Yan YD (2000) Aggregate structures formed via a bridging flocculation mechanism. *Chem Eng J* 80:13–22

195. Negro C, Fuente E, Blanco A, Tijero J (2005) Flocculation mechanism induced by phenolic resin/PEO and floc properties. *AIChE J* 51:1022–1031
196. Chen L, Chen DH, Wu CL (2003) A new approach for the flocculation mechanism of chitosan. *J Polym Environ* 11:87–92
197. Bahamdan A, Daly WH (2007) Hydrophobic guar gum derivatives prepared by controlled grafting processes. *Polym Adv Technol* 18:652–659
198. Skotheim TA, Elsenbaumer RL, Reynolds JR (1997) *Handbook of conducting polymers*, 2nd edn. Dekker, New York, NY
199. Gang L, Freund MS (1997) New approach for the controlled cross-linking of polyaniline: synthesis and characterization. *Macromolecules* 30:5660–5665
200. Trivedi DC, Dhawan SK, Trivedi DC, Dhawan SK (1993) Antistatic applications of conducting polyaniline. *Polym Adv Technol* 4:335–340
201. Zhang X, Goux WJ, Manohar SK (2004) Synthesis of polyaniline nanofibers by “nanofiber seeding”. *J Am Chem Soc* 126:4502–4503
202. Li XG, Feng QL, Huang MR (2006) Facile synthesis and optimization of conductive copolymer nanoparticles and nanocomposite films from aniline with sulfodiphenylamine. *Chem Eur J* 12:1349–1359
203. Tiwari A, Singh SP (2008) Synthesis and characterization of biopolymer-based electrical conducting graft copolymers. *J Appl Polym Sci* 108:1169–1177
204. Li HC, Khor E (1994) Interaction of collagen with polypyrrole in the production of hybrid materials. *Polym Int* 35:53–59
205. Li HC, Khor E (1995) A collagen-polypyrrole hybrid: influence of 3-butanedisulfonate substitution. *Macromol Chem Phys* 196:1801–1812
206. Bejenariu A, Popa M, Dulong V, Picton L, Cerf DL (2009) Trisodium trimetaphosphate crosslinked xanthan networks: synthesis, swelling, loading and releasing behaviour. *Polym Bull* 62:525–538
207. Ray S, Maiti S, Sa B (2008) Preliminary investigation on the development of diltiazem resin complex loaded carboxymethyl xanthan beads. *AAPS PharmSciTech* 9:295–301
208. Singh B, Chauhan N (2009) Modification of psyllium polysaccharides for use in oral insulin delivery. *Food Hydrocolloid* 23:928–935
209. Silva DA, Feitosa JPA, Maciea JS, Paula HCB, de Paul RCM (2006) Characterization of crosslinked cashew gum derivatives. *Carbohydr Polym* 66:16–26
210. George M, Abraham TE (2007) pH sensitive alginate–guar gum hydrogel for the controlled delivery of protein drugs. *Int J Pharm* 335:123–129
211. Davies JM, Addy JM, Blackman RA, Blanchard JR, Ferbrache JE, Moore DC, Somerville HJ, Whitehead A (1984) Environmentaleffects of the use of oil-baseddrillingmuds in the NorthSea. *Mar Pollut Bull* 15:363–370
212. Zhang LM, Tan YB, Li ZM (2000) Multifunctional characteristics of new carboxymethyl-cellulose-based graft copolymers for oilfield drilling. *J Appl Polym Sci* 77:195–201
213. Zhang LM, Tan YB, Li ZM (2001) New water-soluble ampholytic polysaccharides for oilfield drilling treatment: a preliminary study. *Carbohydr Polym* 44:255–260
214. Reddy BR, Eoff LS, Whitfill DL, Wilson JM et al (2002) Methods of consolidating formations or forming chemical casing or both while drilling. US Patent No. US6702044B2
215. Rosalam S, England R (2006) Review of xanthan gum production from unmodified starches by *Xanthomonas compestris* sp. *Enzyme Microb Technol* 39:197–207
216. Glicksman M, Sand RE (1973) Arabic gum. In: Whistler RL, BeMiller JN (eds) *Industrial gums: polysaccharides and their derivatives*. Academic, New York, NY
217. Yassen EI, Herald TJ, Aramouni FM, Alavi S (2005) Rheological properties of selected gum solutions. *Food Res Int* 38:111–119
218. Nickzare M, Zohuriaan-Mehr MJ, Yousefi AA, Ershad-Langroudi A (2009) Novel acrylic-modified acacia gum thickener: preparation, characterization and rheological properties. *Starch/Stärke* 61:188–198

219. Singh V, Tiwari S, Sharma AK, Sanghi R (2007) Removal of lead from aqueous solutions using *Cassia grandis* seed gum-graft-poly(methylmethacrylate). *J Colloid Interface Sci* 316:224–232
220. Ghosh S, Sen G, Jha U, Pal S (2010) Novel biodegradable polymeric flocculant based on polyacrylamide-grafted tamarind kernel polysaccharide. *Bioresour Technol* 101:9638–9644
221. Sanghi R, Bhattacharya B, Singh V (2007) Seed gum polysaccharides and their grafted copolymers for the effective coagulation of textile dye solutions. *React Funct Polym* 67:495–502
222. Pal S, Sen G, Ghosh S, Singhc RP (2012) High performance polymeric flocculants based on modified polysaccharides—microwave assisted synthesis. *Carbohydr Polym* 87:336–342
223. McLean D, Agarwal V, Stack K, Horne J, Richardson D (2011) Synthesis of guar gum-graft-poly(acrylamide-co-diallyldimethylammonium chloride) and its application in the pulp and paper industry. *Bioresources* 6(4):4168–4180
224. McLean D, Agarwal V, Stack K, Richardson D (2011) Use of a new novel grafted guar gum-copolymer as a pitch fixative [online]. In: 65th Appita annual conference and exhibition, Rotorua New Zealand 10–13 April 2011: Conference technical papers. Carlton, Vic.: Appita Inc., pp 65–69
225. Xu XH, Ren GL, Cheng J, Liu Q, Li DG, Chen Q (2006) Layer by layer self-assembly immobilization of glucose oxidase onto chitosan-graft-polyaniline polymers. *J Mater Sci* 41:3147–3149
226. Spinks GM, Shin SR, Wallace GG, Whitten PG, Kim IY, Kim SI, Kim SJ (2007) A novel “dual mode” actuation in chitosan/polyaniline/carbon nanotube fibers. *Sens Actuators B Chem* 121:616–621
227. Tiwari A (2007) Gum Arabic-graft-polyaniline: an electrically active redox biomaterial for sensor applications. *J Macromol Sci A Pure Appl Chem* 44:735–745
228. Shin SR, Park SJ, Yoon SG, Spinks GM, Kim SI, Kim SJ (2005) Synthesis of conducting polyaniline in semi-IPN based on chitosan. *Synth Met* 154:213–216
229. Kim SJ, Shin SR, Spinks GM, Kim IY, Kim SI (2005) Synthesis and characteristics of a semi-interpenetrating polymer network based on chitosan/polyaniline under different pH conditions. *J Appl Polym Sci* 96:867–873
230. Tiwari A, Sen V, Dhakate SR, Mishra AP, Singh V (2008) Synthesis, characterization, and hoping transport properties of HCl doped conducting biopolymer-co-polyaniline zwitterion hybrids. *Polym Adv Technol* 19:909–914
231. Tiwari A (2008) Synthesis and characterization of pH switching electrical conducting biopolymer hybrids for sensor applications. *J Polym Res* 15:337–342
232. Philip AK, Philip B (2010) Colon targeted drug delivery systems: a review on primary and novel approaches. *Oman Med J* 25(2):79–87
233. Prabaharan M (2011) Prospective of guar gum and its derivatives as controlled drug delivery systems. *Int J Biol Macromol* 49(2):117–124
234. Kulkarni RV, Sa B (2008) Evaluation of pH-sensitivity and drug release characteristics of (polyacrylamide-grafted-xanthan)–carboxymethyl cellulose-based pH-sensitive interpenetrating network hydrogel beads. *Drug Dev Ind Pharm* 34:1406–1414
235. Singh B, Chauhan GS, Kumar S, Chauhan N (2007) Synthesis, characterization and swelling responses of pH-sensitive psyllium and polyacrylamide based hydrogels for the use in drug delivery (I). *Carbohydr Polym* 67:190–200
236. Chen J, Liu MZ, Chen S (2009) Synthesis and characterization of thermo- and pH-sensitive kappa-carrageenan-g-poly(methacrylic acid)/poly(N, N-diethylacrylamide) semi-IPN hydrogel. *Mater Chem Phys* 115:339–346
237. Wang AQ, Wang WB (2009) Superabsorbent materials. *Kirk-Othmer Encyclopedia of Chemical Technology*. doi: 10.1002/0471238961.supewang.a01
238. Guilherme MR, Reis AV, Paulino AT, Fajardo AR, Muniz EC, Tambourgi EB (2007) Superabsorbent hydrogel based on modified polysaccharide for removal of Pb²⁺ and Cu²⁺ from water with excellent performance. *J Appl Polym Sci* 105:2903–2909

239. Kiatkamjornwong S, Mongkolsawat K, Sonsuk M (2002) Synthesis and property characterization of cassava starch grafted poly[acrylamide-co-(maleic acid)] superabsorbent via γ -irradiation. *Polymer* 43:3915–3924
240. Wang WB, Wang AQ (2010) Nanocomposite of carboxymethyl cellulose and attapulgite as a novel pH-sensitive superabsorbent: synthesis, characterization and properties. *Carbohydr Polym* 82:83–91
241. Shi XN, Wang WB, Wang AQ (2011) Synthesis, characterization and swelling behaviors of guar gum-g-poly(sodium acrylate-co-styrene)/vermiculite superabsorbent composites. *J Compos Mater* 45:2189–2198
242. Fujioka R, Tanaka Y, Yoshimura T (2009) Synthesis and properties of superabsorbent hydrogels based on guar gum and succinic anhydride. *J Appl Polym Sci* 114:612–616
243. Wang WB, Wang AQ (2009) Preparation, characterization and properties of superabsorbent nanocomposites based on natural guar gum and modified rectorite. *Carbohydr Polym* 77:891–897
244. Li ZJ, Li MJ, Zhu XF, Hao MD, Wang HF, Miao ZC, Zhang CW (2010) Study on xanthan Gum-based superabsorbent resin prepared by graft modification. *Fine Chem (Chinese)* 27:16–25
245. Zhang J, Zhang ST, Yuan K, Wang YP (2007) Graft copolymerization of artemisia seed gum with acrylic acid under microwave and its water absorbency. *J Macromol Sci A Pure Appl Chem* 44:881–885
246. An JK, Wang WB, Wang AQ (2010) Preparation and swelling properties of a pH-sensitive superabsorbent hydrogel based on psyllium gum. *Starch/Stärke* 62:501–507
247. Abd Alla SG, Sen M, El-Naggar AWM (2012) Swelling and mechanical properties of superabsorbent hydrogels based on Tara gum/acrylic acid synthesized by gamma radiation. *Carbohydr Polym* 89(2):478–485
248. Guilherme MR, Campese GM, Radovanovic E, Rubira AF, Feitosa JPA, Muniz EC (2005) Morphology and water affinity of superabsorbent hydrogels composed of methacrylated cashew gum and acrylamide with good mechanical properties. *Polymer* 46:7867–7873
249. Favaro SL, de Oliveira F, Reis AV, Guilherme MR, Muniz EC, Tambourgi EB (2008) Superabsorbent hydrogel composed of covalently crosslinked gum arabic with fast swelling dynamics. *J Appl Polym Sci* 107:1500–1506
250. Kaith BS, Jindal R, Mittal H (2010) Superabsorbent hydrogels from poly(acrylamide-co-acrylonitrile) grafted Gum ghatti with salt, pH and temperature responsive properties. *Der Chemica Sinica* 1(2):92–103
251. Pourjavadi A, Harzandi AM, Hosseinzadeh H (2004) Modified carrageenan 3. Synthesis of a novel polysaccharide-based superabsorbent hydrogel via graft copolymerization of acrylic acid onto kappa-carrageenan in air. *Eur Polym J* 40:1363–1370
252. Salimi H, Pourjavadi A, Seidi F, Jahromi PE, Soleyman R (2010) New smart carrageenan-based superabsorbent hydrogel hybrid: investigation of swelling rate and environmental responsiveness. *J Appl Polym Sci* 117:3228–3238
253. Abd El-Mohdy HL, Abd El-Rehim HA (2009) Radiation synthesis of kappa-carrageenan/acrylamide graft copolymers as superabsorbents and their possible applications. *J Polym Res* 16:63–72
254. Ademoh NA, Abdullahi AT (2010) Determination of optimal binding properties of grade I Nigerian acacia species for foundry moulding sand. *Middle-East J Sci Res* 5(5):402–406
255. Jordan WA (1966) Gum gel compositions and compositions and processes for their production. US Patent No. 3265631
256. Abdel-Halim ES, El-Rafie MH, Al-Deyab SS (2011) Polyacrylamide/guar gum graft copolymer for preparation of silver nanoparticles. *Carbohydr Polym* 85:692–697

Chapter 6

Dextran Graft Copolymers: Synthesis, Properties and Applications

Yasuhiko Onishi, Yuki Eshita, and Masaaki Mizuno

Abstract A graft polymer of methyl methacrylate (MMA) on dextran was prepared using ceric ammonium nitrate (CAN). The properties of these graft copolymers are very interesting because of their amphiphilic microseparated domain. The solubility, infrared absorption spectrum and thermal behavior of the graft copolymer were investigated. It was found that an extruded film of the copolymer not only shows better water wettability and water absorbing power than PMMA but also exhibits thrombo-resistance and can be formed into a transparent contact lens with an affinity for tears and blood. A transparent dextran-matrix copolymer (DMC) has also been newly prepared that consists of a polyelectrolyte complex between cationic dextran and unsaturated acids with compounds of vinyl. This material has been used for hard contact lenses and intraocular lenses. A stable latex of 2-diethylaminoethyl (DEAE)-dextran-MMA graft copolymer (DDMC) has been developed for non-viral gene delivery vectors that are autoclavable at 121 °C for 15 min. Transfection activity was determined using the X-gal staining method, and DDMC samples showed at least 5–10 times higher transfection activity than the starting DEAE-dextran hydrochloride. DDMC has been also confirmed as having a high facility for protection against DNase degradation. The resistance of B16F10 melanoma cells to paclitaxel was confirmed using survival curve analysis. A DDMC/paclitaxel complex showed superior anticancer activity to paclitaxel alone. The rate of mortality of the cells was determined using Michaelis–Menten equations, as the complex promoted an allosteric supramolecular reaction to tubulin. Our results show that the DDMC/

Y. Onishi (✉)
Ryuju Science Co. Ltd, Seto 489-0842, Japan
e-mail: yasu-onishi@ryuju-science.com

Y. Eshita
Department of Infectious Diseases, Faculty of Medicine, Oita University, Oita 879-5593, Japan

M. Mizuno
The Center for Advanced Medicine and Clinical Research, Nagoya University Hospital, 65
Tsurumai-cho, Showa-ku, Nagoya, Aichi 466-8560, Japan

paclitaxel complex was not extensively degraded in cells and achieved good efficacy as an intact supramolecular anticancer agent.

Keywords Dextran • Contact lens • MMA • Matrix copolymer • Non-viral gene delivery • Transfection • DNA • Intracellular transport • Cancer • Drug delivery systems (DDS) • Supramolecular facilities • Melanoma cells • Nanoparticles • DEAE-dextran-MMA copolymer/paclitaxel complex • Cancer • Paclitaxel • Graft copolymer • DEAE-dextran

6.1 Introduction

Recently, there have been many attempts at modifying starch and cellulose to use them in graft polymerizations of vinyl compounds. Since graft polymerization of acrylamide onto poly(vinyl alcohol) (PVA) in the presence of Ce^{4+} salts was reported by Mino and Kaizerman [1], many attempts have been made to graft polymerize vinyl compounds onto polysaccharides [2, 3]. Most reports in this field were concerned with water-insoluble polysaccharides, and some reports have been concerned with water-soluble polysaccharides [4, 5].

Due to their hydrophilic–hydrophobic microphase-separated structure, these copolymers should be useful as biocompatible materials, such as used in contact lenses, artificial blood vessels, artificial bone [6–8], transfection and drug delivery systems (DDS). With this in mind, we previously reported graft polymerization of methyl methacrylate (MMA) on dextran using ceric ammonium nitrate (CAN) and the characteristic properties of the resulting copolymer [7]. The influence of initiator concentration, monomer concentration and backbone polymer concentration on the polymerization were investigated [9].

Effects of the backbone polymer molecular weight on these graft copolymerization are very important for polymer design [10, 11], but there are few published reports because of difficulty in measuring precisely the molecular weight of a backbone polymer. However, the weight-average molecular weight (M_w) of dextran can be measured precisely by using the relationship between M_w and intrinsic viscosity $[\eta]$ (in units of deciliters per gram; $dl\ g^{-1}$) in aqueous solution.

In the previous paper [7], the contributions of molecular weight of dextran to both the graft polymerization and characteristic properties of the resulting copolymers were studied.

A stable and soapless latex of DEAE-dextran-MMA graft copolymer (DDMC) has been developed for non-viral gene delivery vectors. Transfection activity was determined with a HEK293cell line in culture conditions with serum using the X-gal staining method. A high transfection activity was confirmed for DDMC samples that was at least 5–10 times that for the starting DEAE-dextran hydrochloride.

In vivo gene delivery has allowed the study of gene expression through insertion of foreign genes or alteration of existing genes. However, some dangerous adverse effects remain associated with the use of viral vectors. Non-viral gene delivery

vectors can be a key technology in circumventing the immunogenicity inherent in viral-mediated gene transfer.

DEAE-dextran has been used as a non-viral gene delivery vector [12, 13]. However, cationic polysaccharides such as DEAE-dextran may not be superior to viral vectors regarding transfection efficiency. For safety and a high transfection efficiency, many endeavors have been made in the field of non-viral gene delivery vectors [14–16]. In particular, DEAE-dextran was investigated for increasing the transfection efficiency and several good conditions were found for a human macrophage [17]. Due to its cationic properties, DEAE-dextran has strong adsorbing properties with DNA or RNA and was found to change its adsorbing power for nucleic acids with pH and ionic strength [18, 19]. The dextran-MMA graft copolymer is known to have a hydrophilic–hydrophobic microseparated-domain and has a good affinity for cell membranes [7]. This previous paper described a novel graft copolymer composed of a cationic derivative of dextran and an vinyl monomer with efficacy as a non-viral gene delivery vector.. DDMC was obtained by graft-polymerizing MMA onto DEAE-dextran, in water, using ceric ammonium nitrate(CAN) to obtain a stable latex of DDMC [20] that is very effective for non-viral gene delivery [21–23].

Recently, a complex of DDMC/PTX obtained by including paclitaxel (PTX) as guest in DDMC as host was prepared as nanoparticles of 200–300 nm size. These nanoparticles are considered to be very useful for delivery of the anticancer agent to malignant melanoma cells because they promote an allosteric supramolecular reaction to tubulin that is different to the reaction to paclitaxel alone. The resistance of B16F10 melanoma cells to paclitaxel was confirmed using survival curve analysis. On the other hand, there was no resistance of melanoma cells to the DDMC/PTX complex and the melanoma cells reached apoptosis, depending on amount of the paclitaxel in the DDMC/PTX complex.

Of note, the DDMC/PTX complex is not considered to be degraded in cells, and represents the efficacy as an intact supramolecular such as artificial enzymes having substrate-selectivity. These results have never been reported and will be very helpful in overcoming cancer diseases.

6.2 Dextran-MMA Graft Copolymers

A graft copolymer of dextran-MMA has been prepared using ceric ammonium nitrate. The solubility, infrared (IR) absorption spectrum and thermal behavior of the graft copolymer have been studied and compared with those of dextran and poly(methyl methacrylate) (PMMA) alone. It was found that a hot-pressed film of the copolymer not only shows better water wettability and water absorbing power than PMMA but also exhibits thrombo-resistance and can be shaped into a transparent contact lens having an affinity for tears and blood. High resolution scanning electron microscopy (SEM) shows that the surface of the contact lens has a microheterogeneous structure consisting of phase-separated grains of about 0.2 μm in size that are distributed uniformly, as shown in Fig. 6.1.

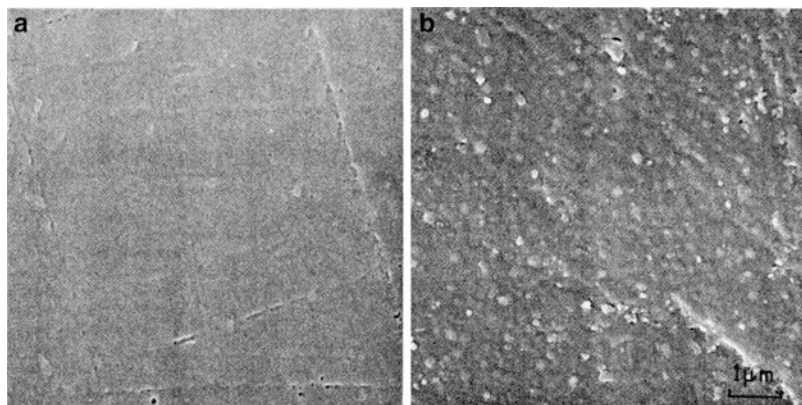


Fig. 6.1 High resolution SEM images of lenses made with PMMA (a) and dextran-MMA graft copolymer (b)

6.2.1 Polymerization Procedure

6.2.1.1 Grafting of MMA onto Dextran and Separation of Grafted PMMA

Dextran (average molecular weight 61,000; Meito Sangyo Co. Ltd) dissolved in water and MMA was placed in a reaction vessel. After nitrogen was bubbled through the solution, grafting was initiated by ceric ammonium nitrate (CAN) solution (0.012 mol) in nitric acid (0.1 N). The mixture was reacted with stirring for the time needed to obtain various grafting compositions. Subsequently, an aqueous solution of hydroquinone (0.1%) was added to terminate the reaction. The polymerization product was precipitated in methanol, washed through with hot water, filtered and dried in vacuum. A purified dextran-MMA copolymer was extracted from the crude copolymer using acetone.

Separation of the grafted PMMA was carried out as follows. The dextran-MMA copolymer was heated at 30 °C for 2 h in 72% sulfuric acid and then boiled for 40 min after the addition of water until the concentration of sulfuric acid became 2%. The undissolved solids (polymer) were filtered, washed with water and dissolved in acetone, re-precipitated with methanol and dried in vacuum.

The molecular weight (M_w) of the grafted PMMA chain obtained above was calculated from the intrinsic viscosity measured in acetone at 25 °C using equation [24]: $[\eta] = 0.96 \times 10^{-4} M_w^{0.69}$

The relationship between the grafting (%)¹ of dextran-MMA copolymers and the reaction time is shown in Fig. 6.2. The grafting increases almost linearly in the range of reaction time <30 min and then an equilibrium is reached. At the same time, we have found that the grafting increases with decreasing molecular weight of dextran (the backbone polymer).

¹ Grafting (%) = (weight of monomer grafted/weight of dextran in the copolymer) × 100

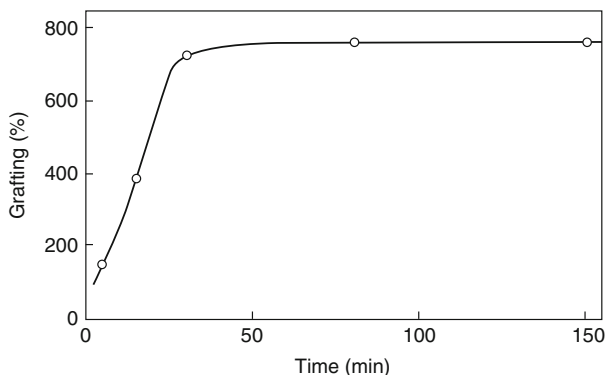


Fig. 6.2 The relationship between the grafting (%) of dextran-MMA copolymers and the reaction time. Polymerization conditions: dextran (M_w 61,000) 8 g, water 220 mL, initiator concentration 30×10^{-4} mol/L, 0.1 N HNO_3 60 mL, MMA 60 mL, temperature 25 °C

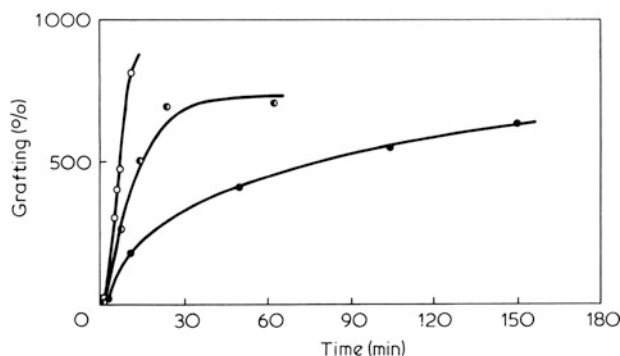


Fig. 6.3 Grafting (%) versus reaction time. Backbone polymer dextran: *open circles* D1, M_w 9,000; *half-filled circles* D2, M_w 61,000; *filled circles* D3, M_w 196,000

6.2.1.2 Grafting and Graft Polymerization

In Figs. 6.3 and 6.4, the relation of the grafting (%)¹ and the graft polymerization (%)² to reaction time are illustrated for dextran samples D1 of M_w 9,000, D2 of M_w 61,000 and D3 of M_w 196,000.

Graft polymerization of a vinyl monomer with polysaccharides under a redox-system initiates from the *cis*-1,2-glycol function at the ends of the saccharides in preference to other mechanisms [16, 25] and polymerization of a simple MMA initiated by CAN is almost negligible [26].

² Graft polymerization (%) = (weight of monomer grafted/weight of total monomer) \times 100

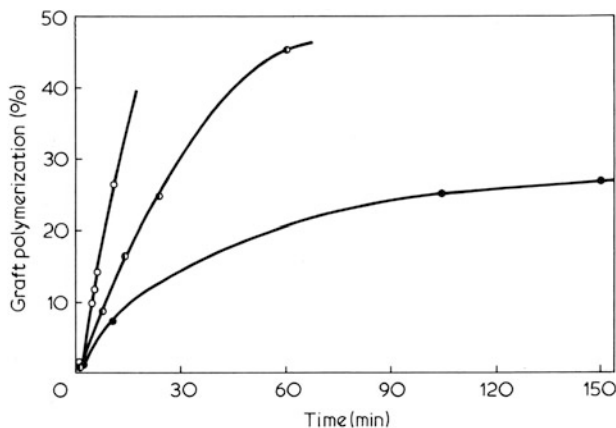
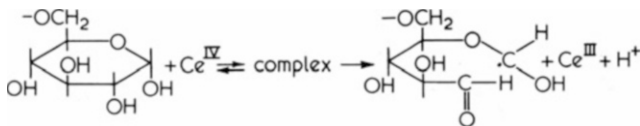


Fig. 6.4 Grafting polymerization (%) versus reaction time. Backbone polymer dextran: *open circles* D1, M_w 9,000; *half-filled circles* D2, M_w 61,000; *filled circles* D3, M_w 196,000

Figure 6.3 shows that grafting (%) increased rapidly at the beginning of the reaction when D1 sample (M_w 9,000) was one of the reactants, but only gradually with D2 or D3. Graft polymerization (%) plotted against time for the purpose of obtaining the rate of graft polymerization produces a similar profile (Fig. 6.4). The results can be explained in terms of the diffusion control by the increase in viscosity of the reaction solution due to augmentation of dextran molecular weight [9, 27]. It is suggested that the lower the molecular weight of dextran, the greater the number of reactive functions per unit weight. This accords with the interpretation of other graft polymerizations proposed by Wallace et al. [5] that polymerization is initiated mainly by the breakdown of coordination complexes of ceric ions with 1,2-glycol groups on the ends of the dextran chains. There are three such functional glycol neighbours in a terminal pyranose ring, so that three different modes of ring cleavage are possible. Homolytic bond fission between C1 and C2 may be most preferable, considering both the *cis*-orientation of the two hydroxyl groups [28] and the powerful electron-withdrawal ability for either oxygen.

The polymerization is initiated by a ceric ion–alcohol redox system by way of an intermediate complex [9].



6.2.2 Rate of Consumption of Ce^{4+}

Reaction rates were determined by following the absorbance of the reaction solution (Hitachi model 101 spectrophotometer). The composition of the solution ($[\text{Ce}^{4+}] = 2 \times 10^{-3}$ M, [dextran] = 2%, $[\text{HNO}_3] = 0.017$ N) was similar to that

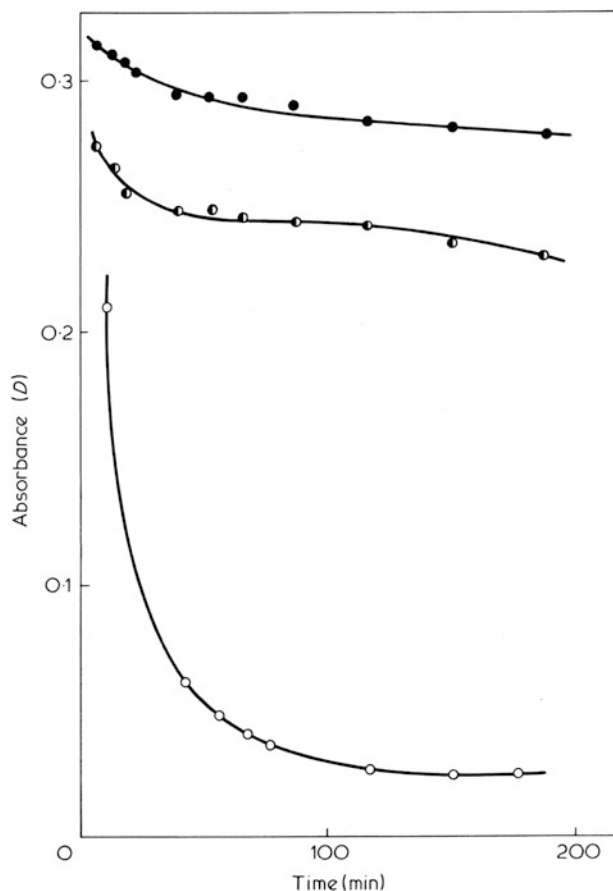


Fig. 6.5 The absorbance variation of dextran solution oxidized by Ce^{4+} with time. Backbone polymer dextran: *open circles* D1, M_w 9,000; *half-filled circles* D2, M_w 61,000; *filled circles* D3, M_w 196,000

under the polymerization conditions. Absorbance was measured at 25 °C in a 0.5×1 cm spectrophotometer cell. Reaction solutions were purged with nitrogen before mixing. The wavelength at which absorbance was followed, 380 nm, was chosen to give a reasonably large initial absorbance.

6.2.2.1 Rate of Consumption of Ce^{4+} by Dextran

Figure 6.5 shows the absorbance variation of dextran solution oxidized by Ce^{4+} with time. The overall kinetic constant (k') of consumption of Ce^{4+} by dextran was calculated from the initial slopes of the logarithm of absorbance versus time [29] as good pseudo-first order kinetics [cf. Eq. (6.19)] were observed during the initial

reaction time. The value of k' obtained was $6.5 \times 10^{-4} \text{ s}^{-1}$ with dextran D1, $5.0 \times 10^{-5} \text{ s}^{-1}$ with D2 and $3.2 \times 10^{-4} \text{ s}^{-1}$ with D3. The molecular weight of these dextrans oxidized by Ce^{4+} and that of each starting dextran were the same. The order for the rates of consumption of Ce^{4+} by dextran was $\text{D1} > \text{D2} > \text{D3}$. Thus, for lower molecular weights, the rate of oxidation increases moderately. The result is consistent with that for grafting (%) (cf. Fig. 6.5).

From the above results, it was concluded that graft polymerization proceeds under the influence of the molecular weight of the backbone polymer dextran.

6.2.3 Polymerization Kinetics

6.2.3.1 Theory

Ceric ions complex reversibly with alcohols and glycols. The disproportionation of the complexes is the rate-determining step of the reaction [29–31]. Mino and Kaizerman have also shown that the oxidation–reduction proceeds via free radicals, which are capable of initiating vinyl polymerization [1]. The elementary reactions considered from experiment are as follows:

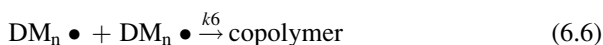
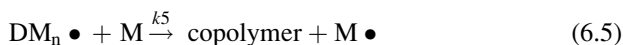
Initiation

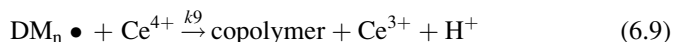
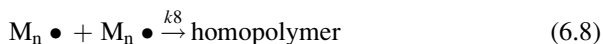


Propagation



Termination





where D, Ce^{4+} and M are the concentrations of dextran, tetravalent cerium and MMA, respectively.

From Eq. (6.1):

$$\text{Complex} = K[D][Ce^{4+}] = [Ce^{4+}]_T K[D]/(1 + K[D]) \quad (6.10)$$

where $[Ce^{4+}]_T$ is the total tetravalent cerium concentration and K is the equilibrium constant. From Eqs. (6.1), (6.2) and (6.3), the rate of formation of free radicals in dextran becomes:

$$d[D\bullet]/dt = k1 K[D][Ce^{4+}] - (k2 + k3)[D\bullet][M] \quad (6.11)$$

At the steady state, its rate change is zero or $d[D\bullet]/dt = 0$.

Then:

$$[D\bullet] = k1 K[D][Ce^{4+}]/(k2 + k3)[M] \quad (6.12)$$

From Eqs. (6.2), (6.5), (6.6), (6.7) and (6.9), the rate of formation of $[DM^*]$ becomes:

$$d[DM\bullet]/dt = k2[D\bullet][M] - [DM\bullet](k5[M] + k6[DM\bullet] + k7[M\bullet] + k9 \times [Ce^{4+}]) \quad (6.13)$$

Substituting Eq. (6.12) in Eq. (6.13) to eliminate $[D^*]$, we obtain the steady-state approximation:

$$[DM\bullet] = k1k2K[D][Ce^{4+}]/(k2 + k3)(k5[M] + k6[DM\bullet] + k7[M\bullet] + k9 \times [Ce^{4+}]) \quad (6.14)$$

As the propagation reaction is shown by Eq. (6.4), the rate of propagation is given by:

$$d[M]/dt = k4[DM\bullet][M] \quad (6.15)$$

Thus:

$$\begin{aligned} d[M]/dt = & k_1 k_2 k_4 K [D][Ce^{4+}][M]/(k_2 + k_3)(k_5[M] + k_6[DM\bullet] + k_7 \\ & \times [M\bullet] + k_9[Ce^{4+}]) \end{aligned} \quad (6.16)$$

If the termination step is presented mainly by Eq. (6.5), the termination would be predominantly by chain transfer of the polymeric radical to monomer as:

$$k_5[M] \gg k_6[DM\bullet] + k_7[M\bullet] + k_9[Ce^{4+}] \quad (6.17)$$

Equation (6.16) becomes:

$$-d[M]/dt = k_1 k_2 k_4 K [D][Ce^{4+}][M]/(k_2 + k_3)(k_5) \quad (6.18)$$

In the presence of excess substrate, the disappearance rate of $[Ce^{4+}]_T$ shows pseudo-first order with respect to the total Ce^{4+} concentration.

$$d[Ce^{4+}]_T/dt = k'[Ce^{4+}]_T \quad (6.19)$$

where:

$$k' = k_1 K [D]/(1 + K[D]) \quad (6.20)$$

As the experiment gave $k't \ll 1$, by rearranging and integrating equations (6.18) and (6.19), and assuming that $[D]$ is constant, we obtain:

$$[M] - [M_0] = -k_1 k_2 k_4 / k_5 (k_2 + k_3) (1 + K[D]) \bullet [Ce_0^{4+}]_T [D] t \quad (6.21)$$

or:

$$\psi = -100 k_1 k_2 k_4 / k_5 (k_2 + k_3) (1 + K[D]) [M_0] \bullet [Ce_0^{4+}]_T [D] t \quad (6.22)$$

where $[M_0]$, $[Ce_0^{4+}]_T$, and ψ are the initial concentration of MMA, total ceric ion and graft polymerization (%), respectively. If a plot of ψ versus t gives a straight line, the termination must be caused by Eq. (6.5).

In the case of bimolecular termination, as in Eq. (6.6), assuming that:

$$k_6[DM\bullet] \gg k_5[M] + k_7[M\bullet] + k_9[Ce^{4+}] \quad (6.23)$$

Equation (6.16) becomes:

$$d[M]/dt = (k_1 k_2 k_4^2 K [D][Ce^{4+}]/(k_2 + k_3)(k_6))^{1/2} [M] \quad (6.24)$$

By rearranging and integrating equations (6.10), (6.19) and (6.24), we obtain:

$$\ln(100 - \psi) = -\frac{(k_1 k_2 k_4^2 (1 + K[D])[D][\text{Ce}^{4+}]_T / (k_2 + k_3)(k_6))^{1/2} t}{+ 4.6} \quad (6.25)$$

If the termination is caused by bimolecular termination as in Eq. (6.6), a plot of $\ln(100 - \psi)$ versus t must give a straight line.

If a termination step can be shown as in Eq. (6.7), the termination would be caused by bimolecular termination between the graft polymeric radical and the homo-polymeric radical. Assuming that:

$$k_7[\text{M}\bullet] \gg k_5[\text{M}] + k_6[\text{DM}\bullet] + k_9[\text{Ce}^{4+}] \quad (6.26)$$

Equation (6.16) becomes:

$$-d[\text{M}]/dt = k_1 k_2 k_4 K[D][\text{Ce}^{4+}][\text{M}] / (k_2 + k_3) k_7[\text{M}\bullet] \quad (6.27)$$

with the formation rate of monomeric and homopolymeric radical, we obtain:

$$d[\text{M}]/dt = k_3[\text{D}\bullet][\text{M}] - k_8[\text{M}\bullet][\text{M}\bullet] - k_7[\text{DM}\bullet][\text{M}\bullet] \quad (6.28)$$

Because of their high concentration, we may not assume that $[\text{M}^*]$ reaches a steady state in the experiment within a short time. Assuming $k_2 < k_3$, $[\text{M}^*]^2 \ll 1$, and $k't \ll 1$, by integrating and rearranging Eq. (6.28) we obtain:

$$[\text{M}\bullet] = k_1 K (k_3 - k_2) / (k_2 + k_3) \bullet [D][\text{Ce}^{4+}] t \quad (6.29)$$

Substituting Eq. (6.29) in Eq. (6.27) and integrating, we obtain:

$$\ln([\text{M}]/[\text{M}_0]) = -k_2 k_4 / k_7 (k_3 - k_2) \bullet \ln t + 2.3 k_2 k_4 / k_7 (k_3 - k_2) + 4.6 \quad (6.30)$$

or:

$$\ln(100 - \psi) = -k_2 k_4 / k_7 (k_3 - k_2) \bullet \ln t + 2.3 k_2 k_4 / k_7 (k_3 - k_2) + 4.6 \quad (6.31)$$

If termination is caused by bimolecular collision between the graft polymeric radical and homopolymeric radical, a plot of $\ln(100 - \psi)$ versus $\ln t$ must yield a straight line of slope $-k_2 k_4 / k_7 (k_3 - k_2)$.

If the termination step can be written as in Eq. (6.9), the termination would be predominantly by redox reaction of the polymeric radical with ceric ion. We may ignore other terminations. Thus:

$$k_9[\text{Ce}^{4+}] \gg k_5[\text{M}] + k_6[\text{DM}\bullet] + k_7[\text{M}\bullet] \quad (6.32)$$

Equation (6.16) becomes:

$$-d[M]/dt = k_1 k_2 k_4 K[D][M]/(k_2 + k_3)k_9 \quad (6.33)$$

As the concentration of uncomplexed alcohol in dextran is large, we can assume that $[D]$ is constant. By rearranging and integrating Eq. (6.33):

$$\ln(100 - \psi) = -k_1 k_2 k_4 K[D]t/(k_2 + k_3)k_9 + 4.6 \quad (6.34)$$

If $\ln(100 - \psi)$ becomes a linear function of time (t), the termination may be represented by Eq. (6.9).

6.2.4 Effects of the Molecular Weight of Dextran

Effects of the weight-average molecular weight (M_w) of dextran on its graft copolymerization with MMA, initiated by CAN, have been investigated. The results indicate that grafting (%), graft polymerization (%) (ψ), the overall rate constant (k') for consumption of Ce^{4+} and number of branch PMMA chains are influenced significantly by the M_w of the backbone polymer dextran. The number of branch PMMA chains per dextran molecule was 0.05–0.30 for dextran of M_w 9,000 (D1), 0.35–0.55 for M_w 61,000 (D2) and 0.8–1.6 for M_w 196,000 (D3), respectively. The relationship between the rate of graft polymerization and M_w was expressed by the equation: $R_{pg} = -A(\log M_w) + B$. Another linear relationship was obtained between $\ln(100 - \psi)$ and reaction time (t) for both D1 and D2 samples or $\ln t$ for D3. Detailed kinetic analysis has been done on the basis of the latter relationship. Mechanical properties were also studied on the molded sample plates of these copolymers.

6.2.4.1 Grafting (%) and Molecular Weight of Branch PMMA

Curves of grafting (%) versus M_w of the branch PMMA are illustrated in Fig. 6.6 for samples D1, D2 and D3. The M_w of the branch PMMA increases the higher the M_w of the backbone polymer dextran at fixed grafting (%). The M_w of branch PMMA and initial dextran balance one another. This suggests that the growth of the branch PMMA progresses on the backbone polymer dextrans and that, under conditions where MMA monomer is coiled round the surface of a dextran molecule, the polymerization proceeds along the random coil formed by large dextran molecules. The number of branch PMMA chains per dextran molecule on these copolymers, derived from Fig. 6.6, was 0.05–0.30 for D1, 0.35–0.55 for D2 and 0.8–1.6 for D3.³

³ The number of branch PMMA chains per dextran molecule = (molecular weight of dextran / molecular weight of branch PMMA) \times grafting (%) / 100

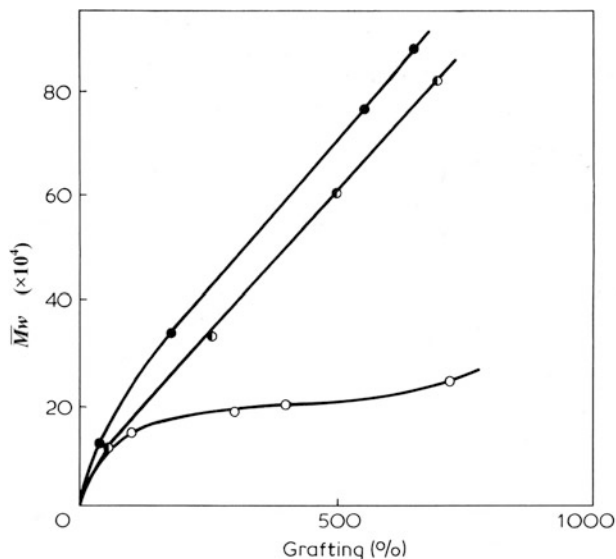


Fig. 6.6 Curves of grafting (%) versus weight-average molecular weight of the branch PMMA. Backbone polymer dextran: *open circles* D1, M_w 9,000; *half-filled circles* D2, M_w 61,000; *filled circles* D3, M_w 196,000

The results show that the number of these branch PMMA chains grows with increased grafting (%) and dextran M_w , and that the structures of these copolymers are different from one another.

Figures 6.7 and 6.8 illustrate that, with samples D1 and D2, the plot of $\ln(100 - \psi)$ versus t gives a straight line with intersection at 4.6. This indicates that termination is presented by Eqs. (6.6) or (6.9), i.e., normal termination (by mutual collision of the graft polymeric radical) or oxidative termination (with Ce^{4+}). For sample D3, the plot of $\ln(100 - \psi)$ versus $\ln t$ yields a straight line of slope 0.1 and intersection $(4.6 + 0.23)$ (Fig. 6.9). It is deduced from this linear relationship that the termination should be presented by Eq. (6.7), i.e., bimolecular termination between the graft polymeric radical and homopolymeric radical (or monomer radical).

The copolymer from D3 should be composed of one dextran molecule and one molecule of branch PMMA on average (1:1), because the calculated number (0.8–1.6) from Fig. 6.6 should be about 1 on consideration of molecular basis. This composition must be consistent with the mechanism of termination [Eq. (6.7)].

For sample D2, the polymerization may not be finished by bimolecular termination of branch PMMA, judging from the relations shown in Figs. 6.3 and 6.6. The number of branch PMMA chains was calculated as 0.35–0.55. On the molecular level, the result indicates that one molecule of branch PMMA might be grafted onto two molecules of dextran, crosslinked by non-growing PMMA (on average 1:2). In addition to the initiation at the reduced terminal glucose group of D2, polymerization would occur at another glucose unit [25] in higher dextrans like D2.

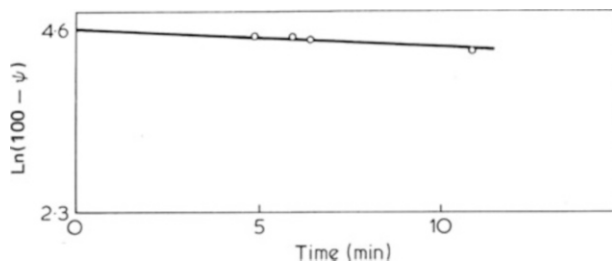


Fig. 6.7 Plot of $\ln(100 - \psi)$ versus time (t) for dextran D1 (M_w 9,000), where ψ is grafting polymerization (%)

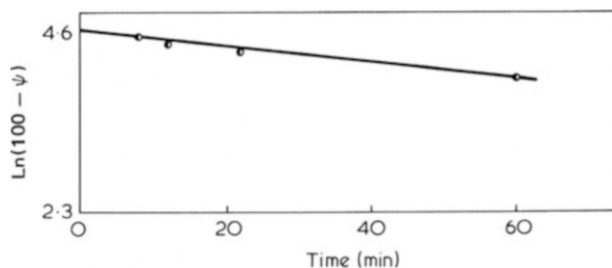


Fig. 6.8 Plot of $\ln(100 - \psi)$ versus time (t) for dextran D2 (M_w 61,000), where ψ is grafting polymerization (%)

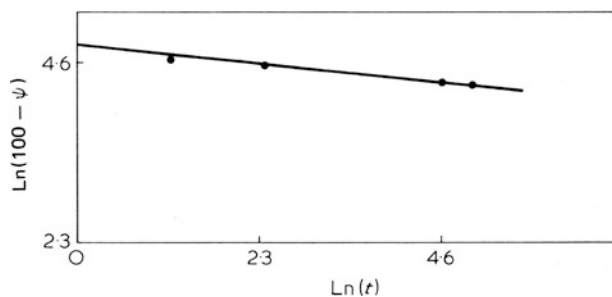


Fig. 6.9 Plot of $\ln(100 - \psi)$ versus time $\ln(t)$ for dextran D3 (M_w 196,000), where ψ is grafting polymerization (%)

In Fig. 6.6, it can be seen that the M_w of branch PMMA from sample D1 increases gradually with grafting (%), in contrast to D2 and D3. With D1, some molecules of the starting dextran D1 would be easily crosslinked by intermediation of MMA at the beginning of the reaction. Propagation of the branch PMMA would occur on the crosslinked dextrans produced. Finally, polymerization would terminate by the above bimolecular process. Although there are uncertainties in detail, the mechanism can be deduced mainly from the experimental results for D1.

6.2.4.2 Effect of Backbone Polymer Dextran Molecular Weight on Rate of Graft Polymerization

The plot of rate of graft polymerization (R_{pg}) versus $\log M_w$ yielded a straight line. The result shows that R_{pg} was a linear function of $\log M_w$. The relation obtained can be expressed as the following equation:

$$R_{pg} = -A(\log M_w) + B \quad (6.35)$$

where R_{pg} is the initial rate obtained at $t = 0$ from the slope of Fig. 6.4; the relationship between graft polymerization (%) and time, and A and B are constant.

Equation (6.35) shows that the number of reactive functions per unit weight decreases with an increase in molecular weight of backbone polymer; however, the increase in M_w affects the termination step negatively because of increases in viscosity.

6.2.5 Characterization of Dextran-MMA Grafted Copolymers

6.2.5.1 Isolation of PMMA from Graft Composition and Measurement of Degree of Polymerization

Hydrolysis of the dextran substrate is required for analysis of the copolymer product to allow M_w determinations of the grafted PMMA chain. The hydrolysis conditions were the same used as by Ite [2]. The graft copolymer was heated at 30 °C for 2 h in 72% H₂SO₄. Boiling for 40 min followed. The solid collected by filtration was dissolved in acetone and filtered. Methanol was then added to the resulting filtrate to form a precipitate, which was dried in a vacuum drier at 40–50 °C. The isolated purified PMMA was dissolved in acetone, and its intrinsic viscosity was measured using an Ostwald viscometer at 25 °C. Its molecular weight was calculated by using the following equation: $[\eta] = 0.96 \times 10^{-4} M_w^{0.69}$

where $[\eta]$ is the intrinsic viscosity (dl g⁻¹) and M_w is the weight-average molecular weight of PMMA.

6.2.5.2 Methods of Material Tests

A 1-mm thick sheet sample was shaped at 200 °C to 80 kg cm⁻² gauge by a press (26 tons; TOHO Press Co. Ltd.). The sheet was subjected to the following tests:

- (a) *Tensile strength* (kg cm⁻²). A rectangular specimen with a width of 12.7 mm was used. Tensile strength was measured using an Autograph IM500 (Shimadzu Seisakusyo Ltd.). The testing speed was 5 mm min⁻¹, the testing temperature was 23 °C, and the inter-chuck distance was maintained at 50 mm.

- (b) *Contact angle*. A contact angle meter was used (Kyowa Kagaku Company). A water drop (about 0.02 mL) was prepared by a microsyringe and brought into contact with the surface of the sample. At 30 s after contact, the water drop was photographed, and h and x (shown in the following equation) were measured. The contact angle (θ) was calculated from the following equation:

$$\theta = 2 \tan^{-1} h/x$$

where x is the radius of the contact area between the water drop and the sample plate and h is the height of the water drop in contact with the sample plate. Measurements were taken at 20 °C.

- (c) *Water absorption (%)*. A 25 × 7.5 mm sample was dried for 24 h in air at 50 °C, and then allowed to cool. After weighing, the sample was placed in distilled water at room temperature for 24 h. The sample was removed from the water, wiped lightly with a cloth and its weight measured again. The water absorption (%) was determined by weight difference.

6.2.5.3 Material Tests and Water Absorption of the Resulting Copolymer

The plate of this copolymer, produced by a heat and press molding method, was used to test water absorbing power. Water absorption reduced with increased grafting (%) and decreased M_w of the backbone polymer dextran at a fixed grafting (%). Perhaps, this water absorbing power depends on the water absorbing capacity of its dextran parts.

The tensile strength of these copolymers grew with increases in grafting (%) for each different M_w of backbone polymer dextran. Though a systematic effect of the dextran M_w on this was not observed, it was shown that the mechanical fragility of the dextran was reinforced by PMMA grafted on dextran. The copolymer with the backbone polymer dextran of M_w 61,000 (D2) had the highest tensile strength. The relation between elongation and grafting (%) was similar to the above relation. The copolymer with the backbone polymer dextran of M_w 61,000 (D2) was superior to others with regard to elongation.

The contact angle of these copolymers was lower than for PMMA, but a systematic effect of grafting (%) and the backbone polymer dextran M_w was not observed.

6.2.5.4 Characteristic Properties of Dextran-MMA Graft Copolymers

Table 6.1 shows the solubility of dextran-MMA graft copolymer with a grafting of 700 % in water, acetone and various other solvents compared with those of the starting material dextran and the side chain PMMA. The graft copolymer was not only insoluble in water, acetone, pyridine, tetrahydrofuran and benzene, but also in dimethylsulfoxide, a common excellent solvent for dextran and PMMA.

Table 6.1 Solubilities of dextran-MMA graft copolymer, dextran and PMMA

Solvent	Copolymer	Dextran	PMMA
Water	Insoluble	Soluble	Insoluble
Acetone	Swelling	Insoluble	Soluble
Pyridine	Insoluble	Swelling	Insoluble
Benzene	Insoluble	Insoluble	Soluble
Tetrahydrofuran	Insoluble	Insoluble	Soluble
Methanol	Insoluble	Insoluble	Insoluble
Dimethyl sulfoxide	Insoluble	Soluble	Soluble

Table 6.2 Material tests for dextran-MMA graft copolymer and PMMA

Parameter	Dextran-MMA	PMMA
Tensile strength (kgf/cm ²)	420	500
Bending strength (kgf/mm ²)	10.1	8.6
Vicat softening temperature (°C)	99	92
Water absorbing capacity (%)	0.8	0.2
Contact angle (°)	61	71
Rockwell hardness (M scale)	81	83

Grafting (%) = (weight of MMA graft polymerized/weight of dextran in the copolymer) × 100

Furthermore, the copolymer remained unchanged in appearance and insoluble after heating in boiling water for 1 h.

From the above results, it seems reasonable to conclude that the dextran-MMA copolymer is in part crosslinked with graft PMMA. The plate consisting of dextran-MMA graft copolymer was transparent, whereas that of a polymer blend dextran and PMMA, molded in hot press in the same way, became turbid. Table 6.2 shows the results of material tests for the dextran-MMA graft copolymer, for which the grafting was 700%, and for the chain PMMA. The tensile strength of the graft copolymer decreased about 16 % compared with that of PMMA, but there were no significant differences between the graft copolymer and PMMA in the bending strength, the Vicat softening temperature or the Rockwell hardness. The water absorbing capacity of the graft copolymer was four times greater than that of PMMA and the contact angle of the former was fairly small compared with that of PMMA.

6.2.5.5 Characteristic Properties of Dextran-MMA Graft Copolymers Depending on M_w

Water absorption reduced with increased grafting (%) and decreased M_w of the backbone polymer dextran at a fixed grafting (%). It may be that this water absorbing capacity depends on that of its dextran parts. The tensile strength of these copolymers grew with increases in grafting (%) for each different M_w of backbone polymer dextran. Although a systematic effect of the dextran M_w on this was not observed, it was shown that the mechanical fragility of the dextran was reinforced by PMMA grafted on dextran. Table 6.3 shows that the copolymer with the backbone polymer dextran of M_w 61,000 (D2) has superior tensile strength.

Table 6.3 Properties of copolymers having different molecular weight

Sample	Tensile strength (kgf/cm ⁻²)	Elongation	Contact angle (°)	Water absorption (%)	Grafting (%)
1 ^a	80	0.54	66	1.4	650
2 ^a	90	0.52	65	2.6	550
3 ^a	86	0.42	65	7.0	175
4 ^b	410	3.00	68	0.9	690
5 ^b	390	2.64	65	1.6	500
6 ^b	365	2.20	65	2.5	260
7 ^c	293	2.20	69	1.2	720
8 ^c	270	1.66	68	1.5	400
9 ^c	266	1.50	68	1.6	300
PMMA ^d	507	3.90	72	0.8	–

^aBackbone polymer dextran D3 (M_w 196,000)

^bD2 (M_w 61,000)

^cD1 (M_w 9,000)

^dSample isolated from copolymer

The relation between elongation and grafting (%) was similar to the above relation. The copolymer with the backbone polymer dextran of M_w 61,000 (D2) was superior to others with regard to elongation.

The contact angle of these copolymers was lower than for PMMA, but a systematic effect of grafting (%) and the backbone polymer dextran M_w was not observed.

6.2.5.6 Characteristic Properties of Dextran-MMA Graft Copolymers for Biomaterials

Figure 6.10 shows the IR absorption spectra of dextran-MMA copolymer, the starting material dextran and side chain PMMA. The spectrum of the copolymer has some characteristic absorption bands, e.g., the bands at around 3,410 cm⁻¹, 1,725 cm⁻¹ and 1,000–1,150 cm⁻¹ are due to O–H stretching vibrations of dextran, the carbonyl group of PMMA and the pyranose ring of dextran, respectively. Comparison of this spectrum with those of dextran and PMMA shows that the spectrum of dextran alone has no absorption band at 1,720 cm⁻¹ due to the stretching vibration of C=O, and that the spectrum of PMMA alone has no absorption band at around 3,410 cm⁻¹.

Figure 6.11 shows DSC (differential scanning calorimetry) curves for the dextran-MMA copolymer, having grafting of 230 %, and for the starting material dextran and the side chain PMMA. The glass transition temperature (T_g), which appears as a step or a small kink in the DSC curve, is observed near 199 and 127 °C for the copolymer and PMMA, respectively. For dextran, a broad and strong endothermic peak (similar to the thermal features of starch having α -linkages [32]) is observed in the range 50–200 °C (peak temperature at 120 °C) and the complicated decomposition of the dextran occurs at temperatures above 220 °C. For the copolymer, the endothermic peak relating to the molecular constitution of

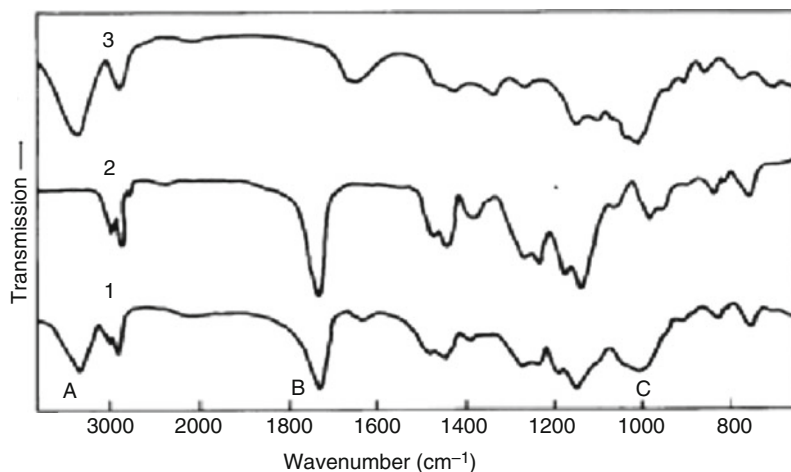


Fig. 6.10 The infrared absorption spectra of dextran-MMA copolymer (1), the starting material dextran (3) and the side chain PMMA (2). A indicates the $3,410\text{ cm}^{-1}$ band due to O–H stretching vibrations of dextran; B $1,725\text{ cm}^{-1}$ band due to the carbonyl group of PMMA; and C $1,000\text{--}1,150\text{ cm}^{-1}$ band due to the pyranose ring of dextran

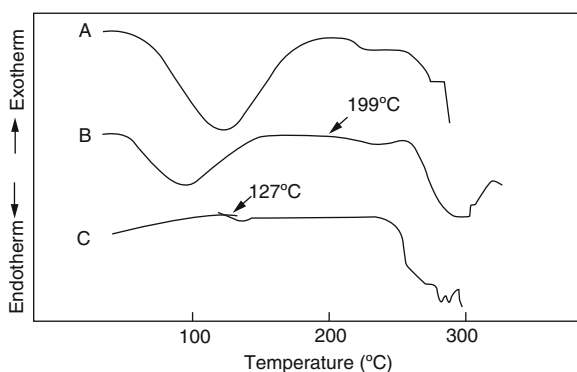


Fig. 6.11 DSC curves for the dextran-MMA copolymer, having grafting of 230 % (B), and for the starting material dextran (A) and the side chain PMMA (C). The shoulders at 127 and 199 °C indicate the T_g .

dextran appears in the range 50 to 160 °C (peak 94 °C). Figure 6.12 shows the value of T_g obtained for copolymers having different percentages of grafting, where the molecular weight of the dextran used was constant (M_w 61,000). T_g values decreased linearly with an increase in the grafting, which corresponds to the increase in the M_w of side chain, PMMA. The T_g of the sample having grafting of 1,050 % is close to the value of T_g (115 °C) for isotactic PMMA [33]. This fact indicates that the reaction product consisting of dextran and MMA is not an aggregate mixture of dextran and PMMA, but a copolymer of dextran and PMMA. In the preparation of plates or vessels made of the graft copolymer by a hot press molded technique, it should clearly be preferable to change the molding temperature according to the grafting.

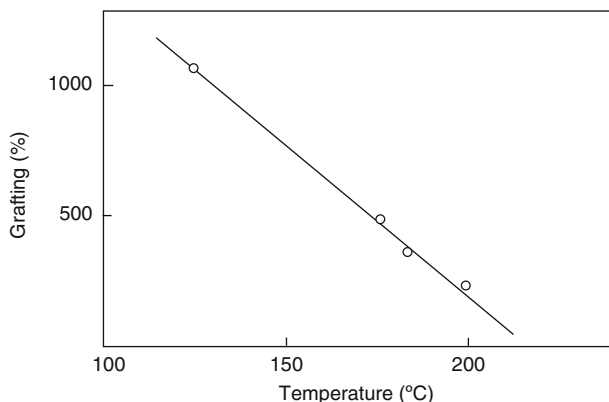


Fig. 6.12 The value of T_g (circles) obtained for copolymers having different percentages of grafting

Figure 6.13 shows the comparison of thrombus formation curves for dextran-MMA copolymer lens, silicate glass and PMMA lens in a blood clotting test, where the percentage of thrombus formed is normalized so that the saturated values for glass, which has been used as a standard material, becomes 100 %. In the case of the dextran-MMA copolymer lens, a firm clot of blood was rarely formed in tests up to 10 min after calcium chloride solution was added to ACD blood (blood containing the anticoagulant acid-citrate-dextrose). In addition, the maximum amount of thrombus formed was about 60 % of that for PMMA. It also became evident that the PMMA lens enhances the coagulation of ACD blood. It can therefore be said from this experiment that the dextran-MMA copolymer lens has an anti-thrombogenic character, whereas the PMMA lens exhibits a promotive thrombogenic character.

When considering the compositional similarity of tears and plasma, the above results and the physical characters of the graft copolymers (given in Table 6.2) suggest that the graft copolymer provides a contact lens that may be worn by persons who suffer from discomfort such as bloodshot eyes, burning feelings in the eyes and blurred vision when provided with conventional contact lenses, mainly caused by MMA resin. It was confirmed that contact lenses produced with the graft copolymer of dextran and MMA gave no irritation to the eye. High resolution scanning electron micrographs of the surfaces of contact lens produced with PMMA and the dextran-MMA graft copolymer are shown in Fig. 6.1. There are remarkable differences in the microstructure although polished traces (slanting stripes) can be seen to be present on the surfaces and are especially clear for the PMMA sample shown in Fig. 6.1a. The PMMA lens appears to be continuous with a smooth surface, whereas dextran-MMA graft copolymer lenses give rise to coarse surfaces and have a microphase-separated structure (as shown in Fig. 6.1b), similar to the phase-separated structure in oxide glasses [34]. Since the microphase grains (average size $\sim 0.2 \mu\text{m}$) shown in Fig. 6.1b are dissolved in acetone, it is presumed that they consist mainly of PMMA components.

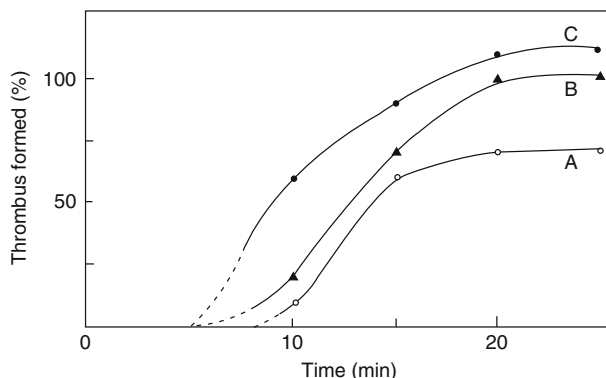


Fig. 6.13 Comparison of thrombus formation curves for DM lens (A), silicate glass (B) and PMMA lens (C) in a blood clotting test

It is known that the surface unevenness of samples and/or their microheterogeneity (0.1–2.0 μm) bring satisfactory results for the application of graft copolymers such as PVA-MMA and PVA-acrylonitrile as biocompatible materials [6]. The dextran-MMA graft copolymer lens has a good affinity for tear as well as blood compared with the PMMA contact lens. Therefore, it is clear that the surface microheterogeneous structure of the dextran-MMA graft copolymer lens as well as the water-soluble properties of dextran play a major role in the compatibility with tears and blood.

It seems reasonable to conclude from the present study that the graft copolymer of dextran and MMA is a biological plastic having biocompatibility.

6.3 Dextran-Matrix Copolymer

A transparent dextran-matrix copolymer (DMC) has recently been prepared that is composed of both a polyelectrolyte complex (PEC) between cationic dextran and unsaturated acids and vinyl compounds. The PEC used as a matrix is expected to be biocompatible and be able to transport O_2 . We confirmed that the DMC has good biocompatibilities for a human eye, with good tear-wettability, and has a good O_2 transport ability, as indicated by its O_2 permeability (DK value⁴). From electron probe microanalysis (EPMA) and SEM observation, it is confirmed that the surface of DMC has a microphase-separated structure formed by both the PEC of DEAE-dextran-poly(MA) (PMA) and PMMA.

⁴ Oxygen permeability coefficient $P = D \cdot S (\times 10 - 11 \text{ ml}(\text{O}_2) \text{ cm}/\text{cm}^2 \cdot \text{s} \cdot \text{mmHg})$

6.3.1 *Intraocular Lenses and Hard Contact Lenses*

The most embarrassing problem related to GPHCL (gas-permeable hard contact lens) for clinical eye doctors is the clouding of its surface during wearing (such as shown in Fig. 6.14) owing to its lack of biocompatibility for tears.

We have developed dextran-MMA copolymers for IOL (intraocular lens) and HCL (hard contact lens) having a hydrophilic–hydrophobic microseparated-domain [7–9].

Matrix polymerization was first reported by Kargin et al. [35] and matrix polymerization between cationic matrix and unsaturated acid has been reported in the case of poly(ethylene imine)/acrylic acid [36–38]. We have newly prepared a transparent dextran matrix copolymer that is composed of both a PEC between cationic dextran and unsaturated acids and vinyl compounds. It is expected to have a regular hydrophilic–hydrophobic microseparated domain. The PEC used as a matrix is expected to be a material having biocompatibility and the ability to transport O_2 [39]. We also think that this matrix copolymer can have good biocompatibility because it not only has a hydrophilic–hydrophobic microseparated domain structure (from the hydrophilic PEC and the hydrophobic vinyl compound), but also an electric charge distribution of localized polyions. For a biomembrane such as a cell membrane, Singer and Nicolson proposed the “fluid mosaic model”, which is composed of a lipid binary molecule membrane having a hydrophilic–hydrophobic microseparated domain, containing proteins and polysaccharides chains on the surface of the protein [40] as shown in Fig. 6.15.

As mentioned above, the matrix copolymer can be considered as a model substance for the component of this biomembrane.

For antibody reaction by the immune system, the recognition of antibody is made by the polysaccharide chains on the surface of the protein. From this viewpoint, a matrix copolymer using a biocompatible polysaccharide such as the dextran used for plasma expanders (e.g., Dextran 70) is not expected to produce an antibody response in vivo.

6.3.2 *Preparation of DMC*

DMC has been prepared to be bulk-polymerized by reacting the basic type of DEAE [(2-diethyl-aminoethyl)-dextran] dissolved in a methacrylic acid (MA) with methyl methacrylate (MMA) using azobisisobutyronitrile (AIBN) as initiator.

Chemicals. DEAE-dextran having 5 % of nitrogen content, obtained by Shotten-Baumann reaction between dextran 500 (M_w 500,000) and 2-diethyl-aminoethyl-chloride in an alkali solution, was used after purification by acetone–NaCl–water sedimentation. MA and MMA were purified from first grade reagents by distillation under a reduced pressure.

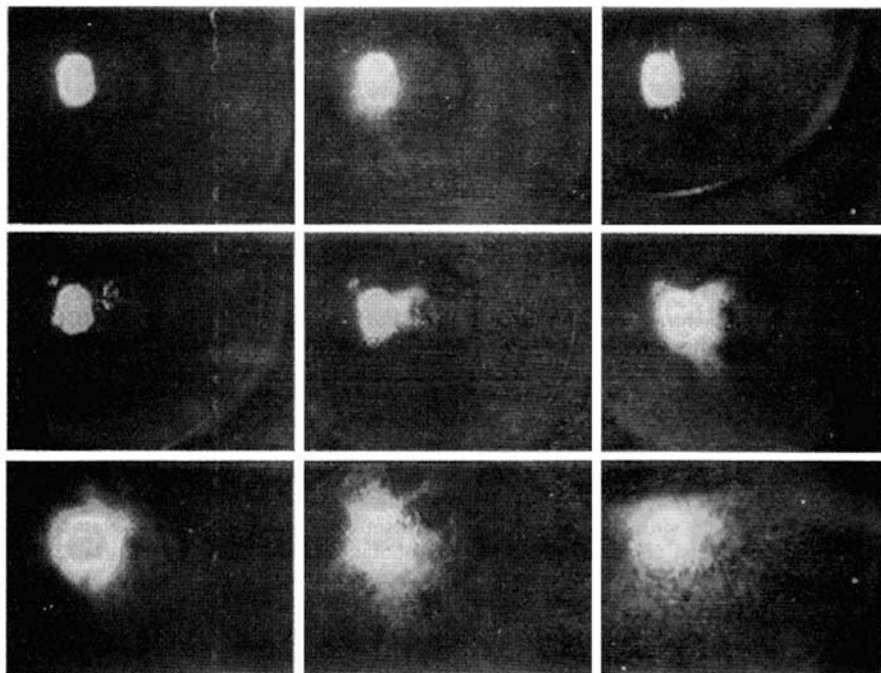


Fig. 6.14 Observation of the surface of a gas-permeable hard contact lens. Cloudiness appeared on the surrounding of the light source and its cloudiness increased and expanded with time. The maximum was reached in 1–1.5 min. This cloudiness revealed the fact that the tears dry up when the eye is open

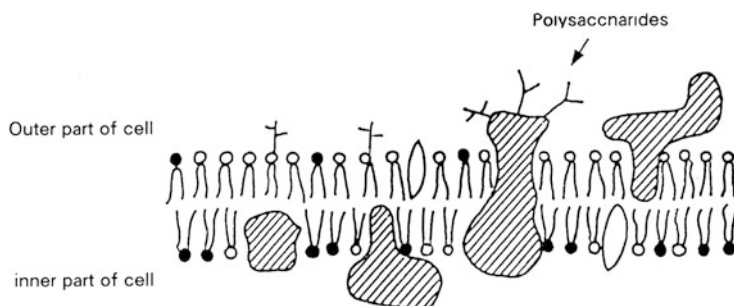


Fig. 6.15 Fluid mosaic model of Singer and Nicolson [40]

DMC preparation. DMC was prepared to be bulk-polymerized by reacting the basic type of DEAE dissolved in MA with MMA using AIBN as initiator. DMC bulk-polymerized was cut into small pieces, and then purified using *n*-hexane using a Soxhlet extractor.

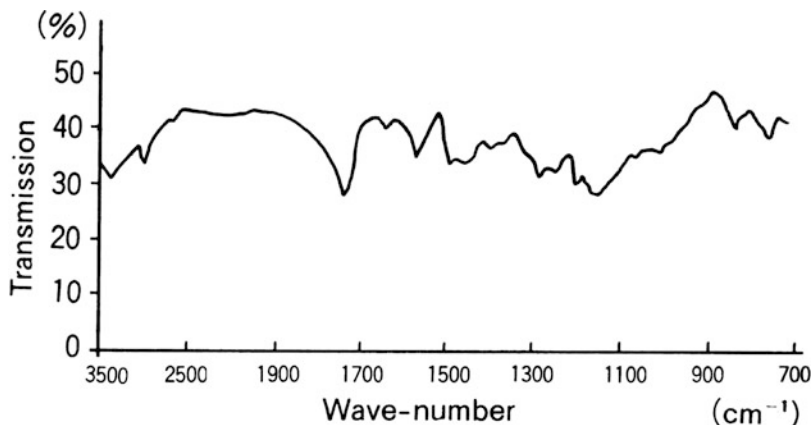


Fig. 6.16 IR spectra of DMC having a ratio of 1:3:36 for DEAE-dextran/MA/MMA

6.3.3 Characterization of DMC

6.3.3.1 Measurement of IR Absorption Spectra and Thermal Analysis

IR measurements on DMC, PMMA and dextran were carried out by the KBr powder method. Differential scanning calorimetry (DSC) was run on ~10 mg of powder sample packed into aluminum pans at $10\text{ }^{\circ}\text{C min}^{-1}$ heating rate. DMC was prepared by bulk-polymerization by reacting the basic type of DEAE-dextran dissolved in MA with MMA using AIBN as initiator.

Figure 6.16 shows the IR spectra of DMC having a ratio of 1:3:36 of DEAE-dextran/MA/MMA. There are bands at around $2,650\text{ cm}^{-1}$ and $1,720\text{ cm}^{-1}$ owing to DEAE-dextran and the C=O of PMMA and PMA, respectively. There was no appearance of the band at around $1,630\text{ cm}^{-1}$ attributed to the double bond of PMMA and PMA monomers, showing that they are polymerized.

6.3.3.2 Solubility and Material Tests

The solubility of a powder sample in water and several organic solvents were investigated at room temperature.

Table 6.4 shows the solubility of DMC with a ratio of 1:3:36 of DEAE-dextran/MA/MMA in water, acetone and various other solvents compared with the solubilities of the starting material DEAE-dextran, PA and PMMA. From this result, it is confirmed that the resulting matrix copolymer is not a mixture but a copolymer because DMC is insoluble in acetone, which is a good solvent for PMMA and PMA.

Table 6.4 Solubility of DMC with a ratio 1:3:36 of DEAE-dextran/MA/MMA in water, acetone and various other solvents

Solvent	DMC	DEAE-dextran ^a	PMA	PMMA
Water	Insoluble	Insoluble	Insoluble	Insoluble
Acetone	Insoluble	Soluble	Soluble	Soluble
Pyridine	Insoluble	Soluble	Swelling	Insoluble
Benzene	Insoluble	Insoluble	Soluble	Soluble
Tetrahydrofuran	Insoluble	Insoluble	Soluble	Soluble
Methanol	Insoluble	Insoluble	Insoluble	Insoluble
DMSO	Insoluble	Soluble	Soluble	Soluble

^aBase type

6.3.3.3 Material Tests and Physical Properties

Material tests and physical property tests were carried out as follows:

- Bending strength.* Both ends of a sample 3 cm in width and 10 cm in length were supported in a longitudinal direction on a supporting stand with a span of 5 cm. The load exerted at the center of the sample at breakage or at maximum load was measured.
- Vicat softening point.* The measurement was made under a load of 5 kg at heating rate of 50 °C/h.
- Rockwell hardness.* The measurement was made with the M scale described in ASTM D785-62.
- Water absorption.* The difference in weight of samples before and after being immersed in distilled water at 37 °C for 24 h was measured.

The DMC samples have a high oxygen permeability, as shown by examples such as the 1:3:36 form of DEAE-dextran/MA/MMA as well as shell crosslinked PVP-MMA copolymer of 30 % water content (see Table 6.5).

It is interesting that a polymer having a hydrophilic domain has a high oxygen permeability (DK value⁴) in a dry state due to its electrolyte structure. We can understand that the mechanism of oxygen permeability for this DMC depends not on its diffusion coefficient D but on its solubility coefficient S because of the long time needed to reach steady state at measuring. From the mechanism of oxygen permeability for this DMC, the thin lens of DMC can be expected to have a superior oxygen permeability.

Table 6.6 shows the physical properties of DMC having a ratio of 1:3:36 of DEAE-dextran/MA/MMA. DMC shows a superior bending modulus compared with PMMA, because the crosslinking points in DMC increase with the ratio of both polyanion and polycation to the total.

Polyelectrolyte complexes (PEC) are usually non-transparent, but DMC is a transparent material having a refractive index of 1.49 for the sample of ratio 1:3:36 (DEAE-dextran/MA/MMA).

Table 6.5 Oxygen permeability of dextran matrix copolymer and PMMA

Sample	Oxygen permeability (DK value ^a)
DMC	4.80
PMMA	2.87

^a($\times 10^{-11}$ mL(O₂) cm/cm² s mmHg)

Table 6.6 Physical properties of dextran matrix copolymer (DMC) and PMMA

Parameter	DMC	PMMA
Bending strength (kgf/mm ²)	11.8	8.6
Vicat softening temperature (°C)	93	92
Water absorbing capacity (%)	9.0	0.2
Rockwell hardness (M scale)	85	83
Refractive index	1.49	–

The DMC sample that possess the ratio of 1:3:36 of DEAE-dextran/MA/MMA has been passed for the Japan Standard of Hard Contact Lenses. The superior properties of transparency can be applied for optical fields such as HCL and IOL.

6.3.3.4 Electron Probe Microanalysis and SEM Observation

Electron probe microanalysis of nitrogen distribution of DMC was carried out at conditions of an accelerating voltage of 4 kV and a beam current of 30 nA by using the electron probe microanalyzer (EPMA) Shimadzu 8705. For EPMA analysis, the surface of DMC was coated with a thin layer of graphite under vacuum to prevent charging of the surface when the electron beam strikes the specimen.

For SEM observation, the surface of DMC, well-rinsed with acetone and coated with a thin layer of Au in vacuum to prevent charging of the surface by the electron beam, was examined using a JEL8600. Photographs were taken with an accelerating voltage of 15 kV and a beam current of 10–12 A.

Figure 6.17 is a SEM picture showing the surface of DMC, which has a microphase-separated structure (average grain size $\sim 0.2 \mu\text{m}$) composed of both a PEC of DEAE-dextran-PMA and PMMA. Figure 6.18 also shows the mapping figure of nitrogen element by EPMA using a probe size of $0.22 \mu\text{m}$ for DMC. From Fig. 6.17 and the imaging by the mapping figure of nitrogen, which shows the PEC of the hydrophilic part of DMC, DMC appears to have a sea-island structure, namely a hydrophilic–hydrophobic microseparated structure having the PEC part as an island and PMMA as a sea.

6.3.3.5 DSC Analysis

Figure 6.19 shows the DSC curve for DMC having ratio of 1:3:16 of DEAE-dextran/MA/MMA, and for the starting material DEAE-dextran and PMMA. The glass transition temperature T_g , which appears as a step or a small kink in the DSC

Fig. 6.17 SEM picture showing the surface of DMC, which has a microphase-separated structure with average microphase grain size of $\sim 0.2 \mu\text{m}$. The grains are composed of the polyelectrolyte complex of DEAE-dextran with PMA and PMMA

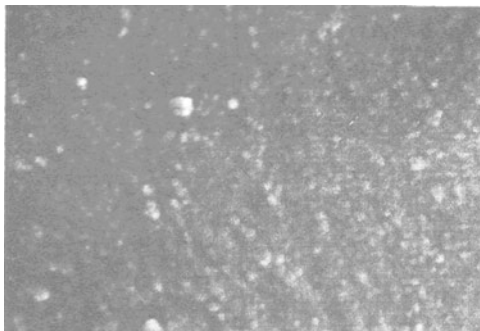
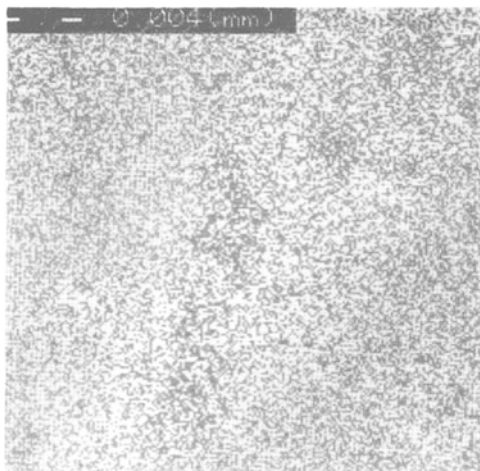


Fig. 6.18 The mapping figure of nitrogen element by EPMA using a probe size of $0.22 \mu\text{m}$ for DMC



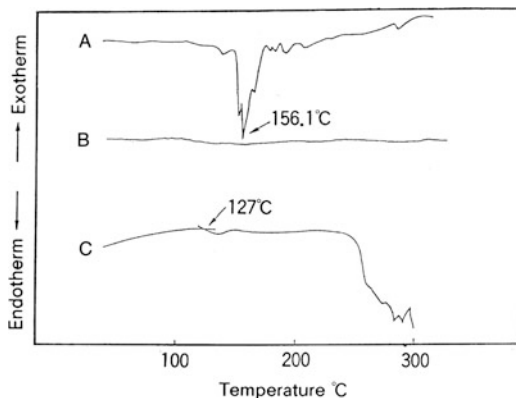
curve, is observed near $199 \text{ }^\circ\text{C}$ for DMC and $127 \text{ }^\circ\text{C}$ for PMMA. For DEAE-dextran, the strong endothermic peak is observed near $144 \text{ }^\circ\text{C}$. For DMC, the endothermic peak relating to the molecular constitution of DEAE-dextran and PMMA does not appear at this region because of its crosslinking in PEC.

It has been shown that DMC has a very stable thermal durability against heat shock.

This DSC analysis indicates that DMC is composed not of a mixture but of an amorphous fraction forming the copolymer between the DEAE-dextran/MA complex and PMMA to give a good transparency and good heat resistance in comparison with PMMA.

This stable property of DMC shown by a good heat resistance is also very important in showing a superior biocompatibility.

Fig. 6.19 DSC curve for DMC having ratio of 1:3:16 of DEAE-dextran/MA/MMA, and for the starting material DEAE-dextran and PMMA. A DEAE-dextran; B DMC; and C PMMA. Temperatures indicate T_g .



6.3.4 Applications for Medical Use

6.3.4.1 DMC as Bioplastic

Figure 6.20 shows the schematic structure of DMC, especially the PEC part of both the polycation of DEAE-dextran and polyanion of PMA, which forms the crosslinking point of the bulk polymerization product of DMC.

Figure 6.21 schematically shows the bulk polymerization product of DMC, which has many crosslinking points due to the formation of a PEC of DEAE-dextran and PMA and has a hydrophilic–hydrophobic microseparated structure. Matrix copolymers having such a hydrophilic–hydrophobic microseparated structure are well known to be biocompatibility materials [6].

As mention above, DMC has been prepared as a model substance of the fluid mosaic model proposed by Singer and Nicolson for a biomembrane such as that composed of a lipid binary molecule membrane having a hydrophilic–hydrophobic microseparated domain, especially containing polysaccharide chains on the surface of the protein [40] (see Fig. 6.15).

When a biomembrane is stimulated from outside, the membrane potential is generated and then a biological electric current flows through an electric path for the conduction of the information to the nervous system.

From this viewpoint, DMC may be a superior biocompatibility material because it not only has a hydrophilic–hydrophobic microseparated structure, but also an electric charge distribution depending on the PEC between DEAE-dextran and PMA, which forms a electric path in this region.

On the other hand, the biomaterials are negatively charged and the negatively charged surfaces usually have a superior biocompatibility.

DMC can be chosen by changing the molar ratio of the cationic dextran/unsaturated acid/olefin compound to obtain suitable properties, especially suitable electric properties, for bioapplications.

Fig. 6.20 Structure of DMC showing its polyelectrolyte complex part of both the polycation DEAE-dextran and polyanion PMA, which forms the crosslinking point of the bulk polymerization product of DMC

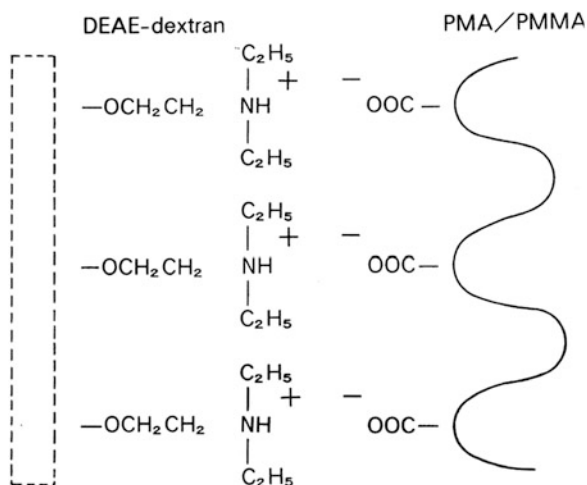


Fig. 6.21 Scheme showing the bulk polymerization product of DMC. DMC has many crosslinking points due to the polyelectrolyte complex of DEAE-dextran and PMA and a hydrophilic–hydrophobic microseparated structure

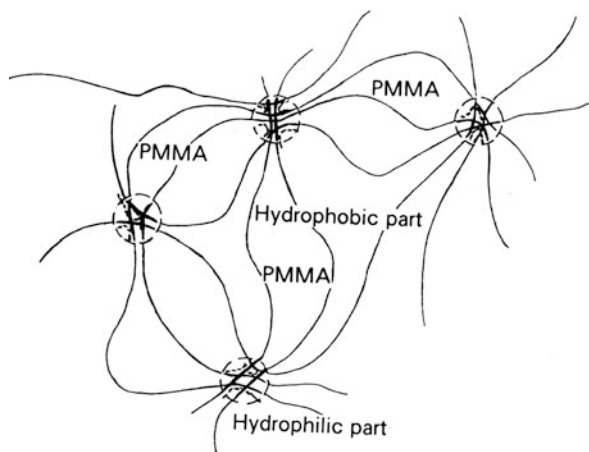


Figure 6.14 shows the surface of a gas-permeable hard contact lens (GPHCL). On its surface, many adhesion antibodies were observed. The adhered matters were easily cleaned using a proteolytic enzyme solution. The protein might be a γ -globulin such as IgE from an antibody reaction by the immune system. This phenomenon is not observed for DMC. For antibody reaction, the recognition of antibody is done by the polysaccharide chains on the surface of the protein. Because of the affinity of dextran for tear liquid, it must play a role in antibody recognition.

Moreover, from this viewpoint, we think that matrix copolymers containing a biocompatible polysaccharide such as dextran do not produce an antibody reaction in vivo.

6.3.4.2 Evaluation of Biocompatibility

The biocompatibility of DMC was evaluated by measuring the contact angle of a human tear on DMC. One drop of human tear was placed on a plate made of DMC, PMMA, silicon rubber or glass. Then, the contact angles on these materials were measured by a contact angle meter and compared with the contact angles on glass.

Figure 6.22 shows the wettability of 0.9 % NaCl solution on plates of glass, PMMA, silicon rubber and DMC. Figure 6.23 shows the wettability of human tears on the same plates of a glass, PMMA, silicon rubber and DMC. From Fig. 6.22, we evaluated the contact angle of each drop of 0.9 % NaCl solution and found that the contact angle for the drop on the glass was the smallest, and that the angles for DMC, PMMA and silicon rubber were larger in that order. From Fig. 6.23, we also measured the contact angle of each drop of human tears to obtain the result that all contact angles were smaller compared with 0.9 % NaCl solution, especially for the drop on DMC, which clearly decreased. From these results, we can guess that the surface of DMC plate is covered with the mucin layer of tear film, which is composed of three layers, namely an oil layer, water layer and mucin layer as shown in Fig. 6.24. This triple layer is why the wettability for tear liquid on DMC is better than that of 0.9 % NaCl solution. The good wettability of DMC by tear liquid may be concluded by its good biocompatibilities. As shown in Fig. 6.15, in the fluid mosaic model, proteins are inserted in a lipid binary molecule and may flow freely in a plane.

Figure 6.24 shows the structure of tear film, which exhibits a similarity with the fluid mosaic model. This similar relationship between the structure for tear film and the fluid mosaic model is very important in obtaining an ideal HCL.

Figure 6.25 expresses the behavior of a DMC lens in the conjunctival sac, inserted and freely moving in a tear film, such as proteins in the fluid mosaic model.

Figure 6.25 also shows that the mucin layer adsorbs the surface of DMC lenses, therefore the three layers of tear film can be kept.

As seen in Fig. 6.26, in order to know more about its biocompatibilities, we observed the drying pattern of 0.2 % human γ -globulin on glass, PMMA, silicon rubber and DMC surfaces using the Sole stagoskopie method [41]. We saw some tree-like patterns similar to the dendrite patterns of NaCl crystals with both glass and DMC although each pattern on the different materials usually showed a different NaCl crystal dendrite pattern. This coincidence between the drying patterns may be useful for a biocompatibility evaluation [42]. The drying pattern of 0.2 % human γ -globulin dissolved in physiological saline on DMC may be useful for its biocompatibility evaluation, because an antibody reaction for a material in vivo is initiated by the adhesion of a γ -globulin such as IgE to the material.

The relationship between drying pattern and biocompatibility for materials is currently being investigated.

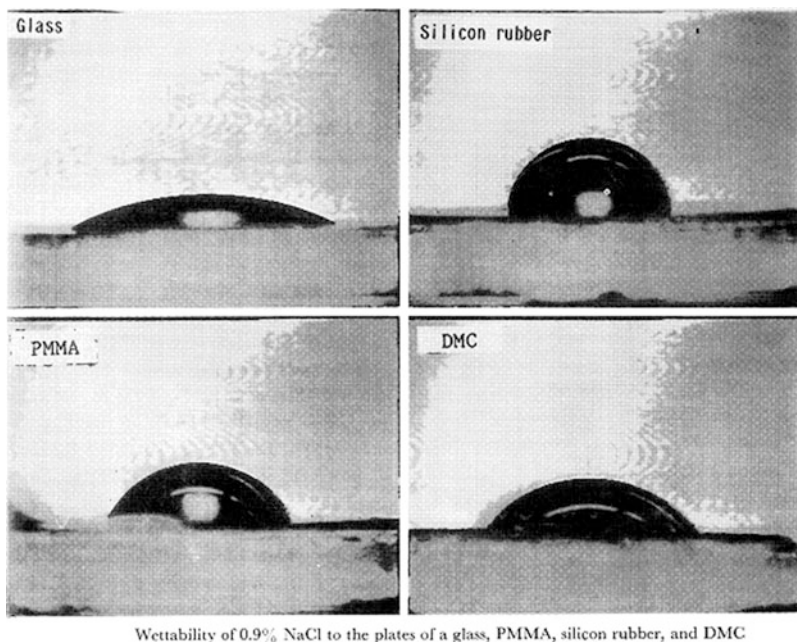


Fig. 6.22 Wettability of 0.9% NaCl solution to plates of glass, PMMA, silicon rubber and DMC

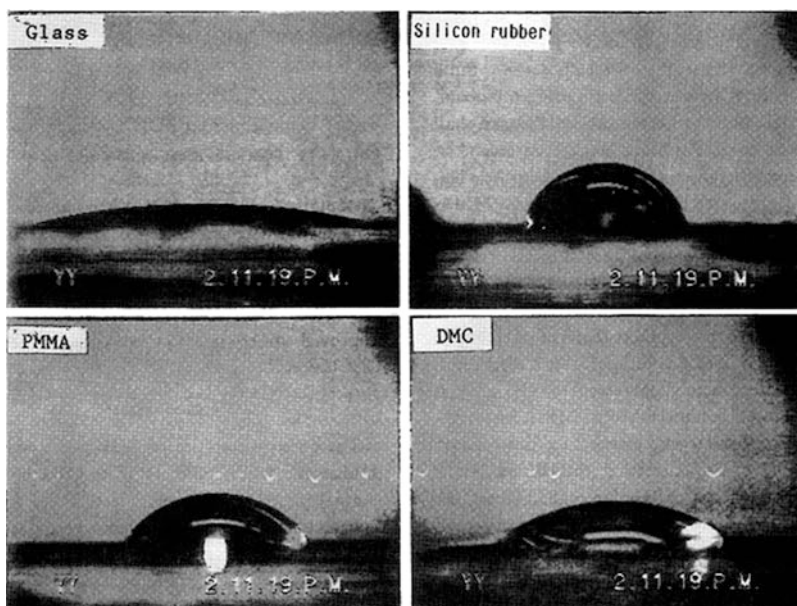


Fig. 6.23 Wettability of human tear to plates of glass, PMMA, silicon rubber and DMC

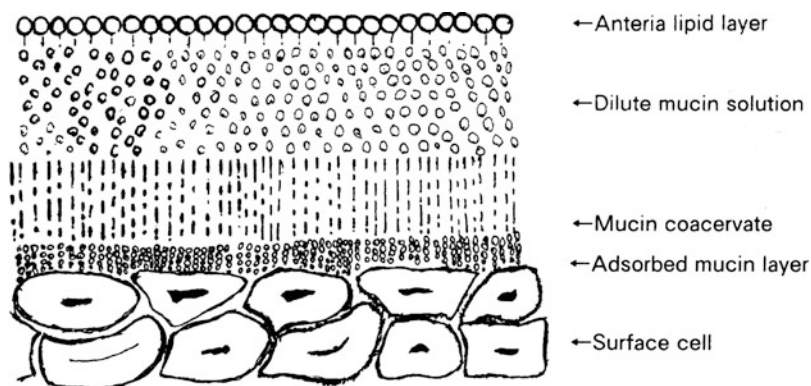


Fig. 6.24 Structure of tear film

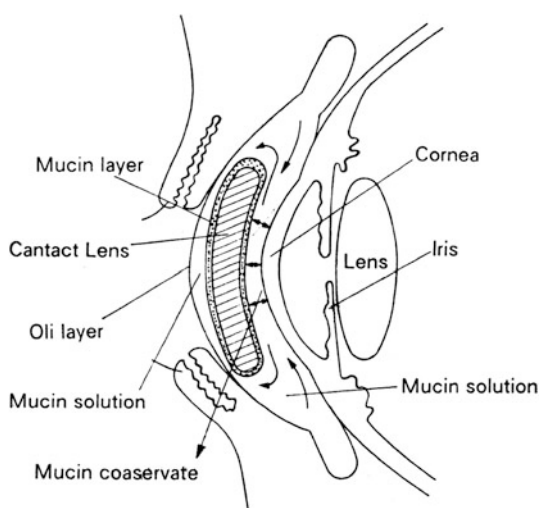


Fig. 6.25 DMC lens in the conjunctival sac

6.4 DEAE-Dextran-MMA Graft Copolymer

MMA graft copolymer (DDMC) has been developed for non-viral gene delivery vectors that are autoclavable at 121 °C for 15 min. Transfection activity was determined using the X-gal staining method and a higher value of 5–10 times or more was confirmed for DDMC samples than for the starting DEAE-dextran hydrochloride. DDMC has been also confirmed as having a high protection facility for DNase degradation. The resulting DDMC has an amphiphilic domain and forms a core-shell polymer micelle and therefore becomes a stable latex with a hydrophilic-hydrophobic microseparated domain. The complex of DDMC and DNA may be

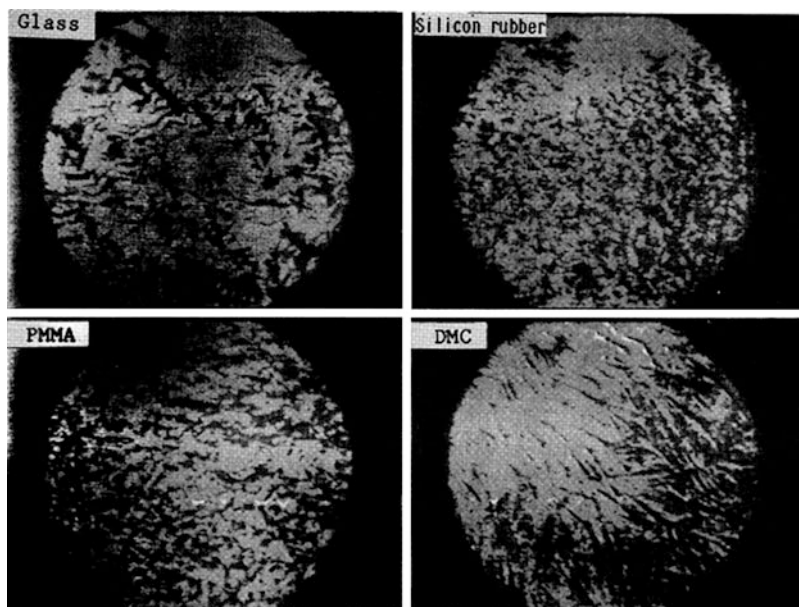


Fig. 6.26 The drying pattern of 0.2% human globulin on glass, PMMA, silicon rubber and DMC surfaces using the Sole method. The coincidence between drying patterns might be useful for a biocompatibility evaluation

formed initially on the stable spherical structure of the amphiphilic microseparated domain of DDMC and has a good affinity to the cell membrane for endocytosis.

The IR absorption spectrum shift to a high-energy direction at around $3,450\text{ cm}^{-1}$ of the complexes between DNA and DDMC indicates the formation of more compact structures, not only by a Coulomb force between the phosphoric acid of DNA and the DEAE group of the DEAE-dextran copolymer but also by a force from multi-intermolecule hydrogen bonding. It indicates that DNA condensation can make possible higher transfection efficiency. The high efficiency of this autoclave-sterilized graft copolymer makes it a valuable tool for safe gene delivery.

6.4.1 Preparation of DDMC

Preparation of DDMC. Samples DDMC1, DDMC2, and DDMC3 in Table 6.7 were prepared as described below: 2 g of DEAE-dextran hydrochloride (nitrogen content 3 %) derived from dextran having molecular weight 500,000 was dissolved in 100 mL of water, and then 4, 3 and 3.5 mL of MMA was added to samples DDMC1, DDMC2 and DDMC3, respectively.

With stirring, the air in the reaction vessel was fully replaced with N_2 gas. To the solution was added 0.1 g of CAN and 15 mL of 0.1 M nitric acid, and the mixture

Table 6.7 Properties of DEAE-dextran-MMA graft copolymers

Copolymer sample	Weight-increase (%) ^a	Precipitation time by DNA (h)
DDMC1	150	2.0
DDMC2	100	1.0
DDMC3	130	1.5
DEAE-dextran	0	96.0

^aSample weight increase (%) =
 (weight of MMA used/weight of DEAE – dextran hydrochloride used) × 100

stirred for 1 h at 30 °C. Then, 3 mL of a 1 % aqueous solution of hydroquinone was added to stop the reaction, and the resulting latex of DDMC was purified by water dialysis using a cellophane tube to remove the unreacted MMA, ceric salts and nitric acid.

6.4.2 Characterization of DDMC

The resulting DDMC precipitated by methanol is insoluble in water and acetone at 25 °C. In view of the fact that DEAE-dextran hydrochloride is soluble in water and PMMA is soluble in acetone, it is evident that the DDMC is not a mixture of DEAE-dextran and PMMA.

The IR absorption spectrum of DDMC as shown in Fig. 6.27 has some characteristic absorption bands at 1,730 cm⁻¹ and at 1,000–1,150 cm⁻¹, which are attributed to the carbonyl group of PMMA and the pyranose ring of DEAE-dextran, respectively. Thus, the resulting DDMC exhibits different solubility to DEAE-dextran and PMMA and shows the above-described characteristic IR absorption spectrum. From this fact, it is judged that the resulting DDMC is a graft-polymerized compound.

6.4.3 Reaction Between DNA and DDMC

For reaction between DDMC and DNA, a solution (10 mg/mL) of the resulting latex of DDMC was added drop-wise to DNA (from Salmon sperm) solution (20 mg/mL) to obtain the complex of DDMC/DNA.

The obtained complex was insoluble in water, which is a good solvent for nucleic acids. These results show that the complex between DNA and DDMC must form a polyion complex. In the case of sample DDMC2, a complex between DNA and DDMC2 having a 100 % weight increase needed 1 h to precipitate.

The complex between DNA and DMC1 having 150 % weight increase needed 2 h to precipitate. However, a complex between DNA and DEAE-dextran hydrochloride needed 96 h to precipitate under the same conditions. Figure 6.27 shows the IR absorption spectra of the resulting complex between DDMC2 and DNA. The spectrum of the complex has some characteristic absorption bands at 1,730 cm⁻¹,

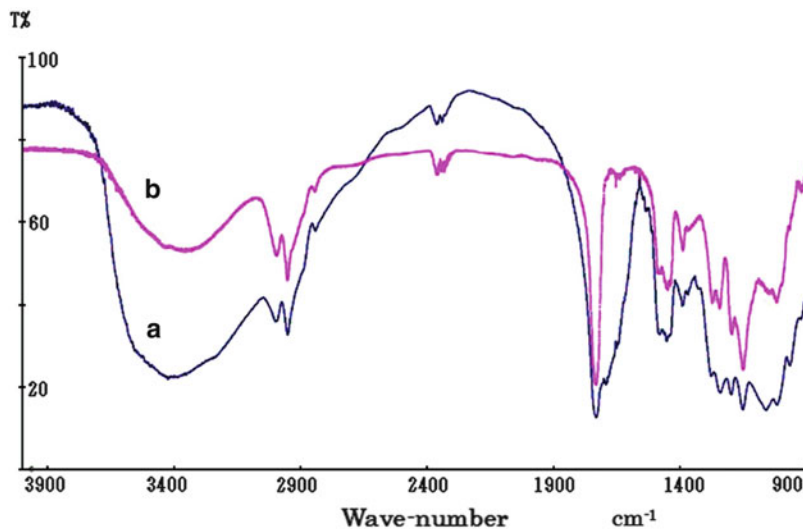


Fig. 6.27 IR absorption spectra of DEAE-dextran-MMA graft copolymer and the complexes between DNA and DEAE-dextran-MMA graft copolymer: *a* complex of DDMC2/DNA and *b* DDMC2

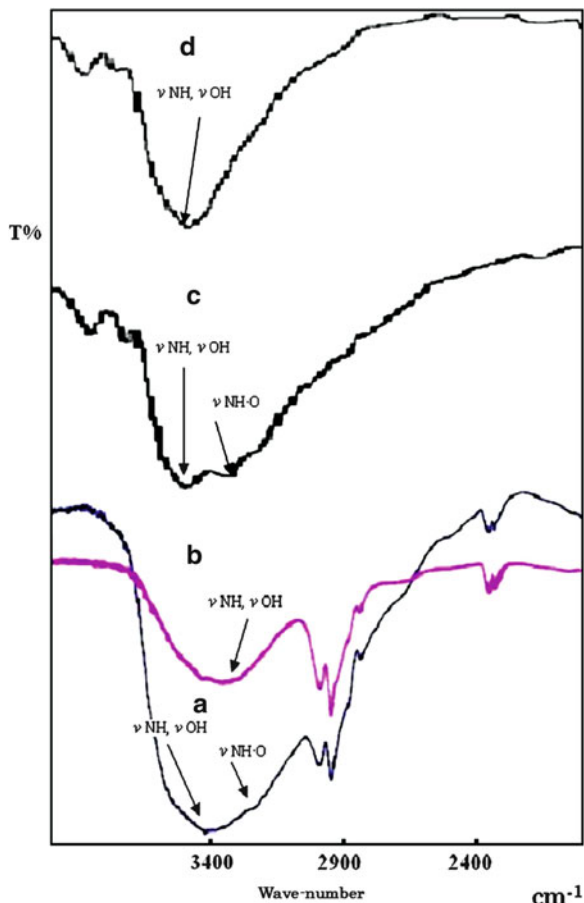
$1,220\text{ cm}^{-1}$, $1,000\text{--}1,150\text{ cm}^{-1}$ and at $3,450\text{ cm}^{-1}$, which are attributed to the carbonyl group of PMMA, the P–O stretching vibration of DNA, the pyranose ring of DEAE-dextran, and the N–H stretching vibration of the DEAE group of DEAE-dextran, respectively.

6.4.4 Measurement of Infrared Absorption Spectra

Figure 6.28 shows the IR spectrum of both the complex of DDMC2/DNA and the complex of DEAE-dextran/DNA in comparison with DDMC2 and DEAE-dextran. The spectrum of the complexes have some characteristic absorption bands owing to hydrogen bonds between the –OH and –NH at around $3,100\text{--}3,800\text{ m}^{-1}$, showing a structure of the complex.

The complex of DDMC/DNA should be a polyion complex formed by a polymer micelle, as shown by the IR absorption spectrum of νOH vibration and νNH vibration at around $3,100\text{--}3,800\text{ m}^{-1}$ (Fig. 6.28). The complex of DDMC/DNA should become more compact, as indicated by the shift of νNH vibration at $3,450\text{ cm}^{-1}$ compared with that of DDMC. There was also a difference between the structures of the complex of DDMC/DNA and the complex of DEAE-dextran/DNA, as shown by the decrease of $\nu\text{NH}\text{--O}$ vibration at around $3,350\text{ cm}^{-1}$ and the shift of νNH vibration from $3,450\text{ cm}^{-1}$ to $3,550\text{ cm}^{-1}$ (Figs. 6.27 and 6.28). This shows that the complex of DDMC/DNA should form more compact polyion complexes due to the multi-intermolecule hydrogen bonds and the hydrophobic force, compared with the complex of DEAE-dextran/DNA.

Fig. 6.28 IR absorption spectra of DDMC: *a* complex of DDMC2/DNA; *b* DDMC2; *c*, complex of DEAE-dextran/DNA; and *d* DEAE-dextran



This may be due not only to a Coulomb force between the phosphoric acid of DNA and the DEAE group of DEAE-dextran copolymer but also to a force from multi-intermolecule hydrogen bonding and a hydrophobic force from the hydrophobic domains of graft PMMA in DDMC. It can be concluded that DNA condensation by a coil-globule transition for DDMC makes possible a high transfection efficiency [43, 44].

6.4.5 DEAE-Dextran-MMA Graft Copolymer as a Non-viral Delivery Carrier

The HEK293 cell line is a permanent line of primary human embryonal kidney cells transformed by sheared human adenovirus type 5 DNA. A pCAGGS/*LacZ*, which expresses β -galactosidase at eukaryotic cells, was inserted under CAG promoter of a plasmid, pCAGGS. Plasmids were amplified in *Escherichia coli* DH5 α and

purified by Qiagen Mega plasmid purification kit. For transfection by DDMC/DNA, HEK293 cells (15×10^4 cells) were seeded onto 35-mm culture dishes and incubated at 37 °C in a humidified atmosphere of 5 % CO₂. In a sterile tube, 10 µg of DNA was dissolved in 270 µL of 1× PBS. Then, 14 µL of the autoclaved DDMC having a concentration of 10 mg/mL was added to the DNA solution and mixed by vortexing briefly. The growth medium (Dulbecco's modified medium with 10 % fetal calf serum) was removed from the cells to be transfected. The cells were washed twice with 1× PBS. DDMC/DNA complex in solution was added to cover the cells. The dish was careened slowly several times to ensure complete coverage of the cells and incubated at 37 °C for 30 min. The dish was slowly careened several times during the incubation and then 1 mL of growth medium was added and the mixture incubated at 37 °C for 48 h. After the incubation, transfection activity was determined using the X-gal staining method. Following the transfection protocol, transfection of HEK293 cells with samples of DDMC1 and DDMC2 was carried out using this plasmid DNA. As shown in Fig. 6.29, a higher value of five times or more was confirmed for samples of DDMC1 and DDMC2 than for the starting DEAE-dextran hydrochloride. From the results, the transfection efficiency and the reaction rate of formation of the complex should increase when using DDMC hydrochloride instead of DEAE-dextran hydrochloride.

6.4.5.1 Charge Ratio of DNA/DDMC

Definition of charge ratio. The ratio of phosphorus content to nitrogen content (P/N) is defined as the charge ratio. With the complex formation reaction between DDMC (N content 1.4 %) and DNA (P content 9.3 %), the compound is formed by ionic bonding (polyion complex), and thus the constituent ratio is expressed as the weight ratio along with the charge ratio as the primary constituent element.

$$P/N(\text{charge ratio}) = (y \times 0.093 \times 14) / (x \times 0.014 \times 31) \quad (6.36)$$

where DNA/DDMC = y/x (weight ratio); P content is 9.3 %; N content is 1.4 %; P atomic weight is 14; N atomic weight is 31; y is the amount of DNA and x is the amount of DDMC.

P/N ratio. When considering transfection efficiency, the charge ratio (P/N) of each sample is an important value as well as the concentration. It is thus necessary to make the P/N values equivalent when comparing RLU (relative luciferase expression) values for DEAE-dextran and DDMC. When investigating related P/N ratios, for example, the percentage of N in DEAE-dextran was 3.3 % and the percentage of P in the DNA was about 9.3 %. The P/N values shown in Table 6.8 were thus obtained.

With regard to dependence of the amount of transferred DNA on P/N ratio shown in Table 6.8, it would appear that a comparison can be made of the RLU values with DEAE-dextran (graft ratio 0 %) and DDMC (graft ratio 130 %) at the respective sample P/N values. In other words, a P/N value of 0.037 is given for DDMC (graft ratio 130 %) at a concentration of 28.6 mg/mL based on the fact that

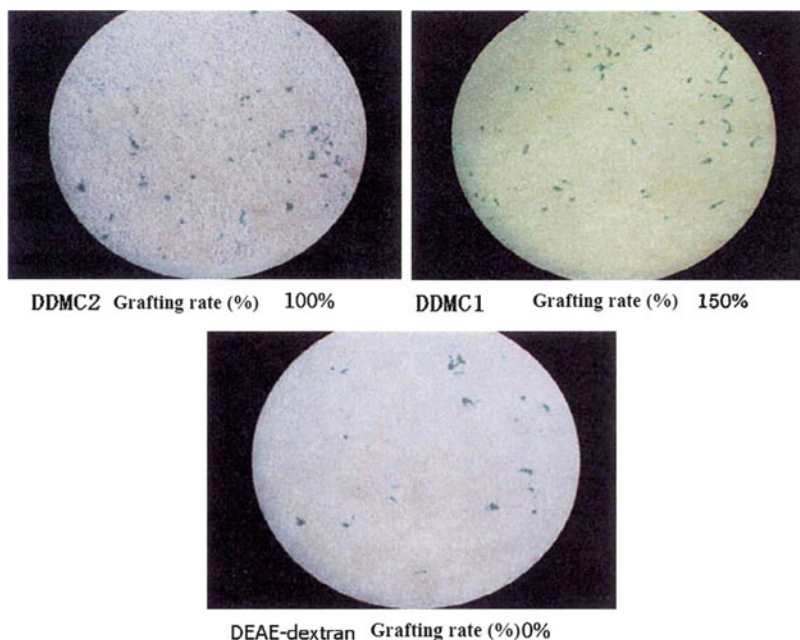


Fig. 6.29 Images showing transfection of a monolayer of HEK293 cells by DEAE-dextran-MMA graft copolymers. DDMC1, weight increase 150%; DDMC2, weight increase 100%; DEAE-dextran, weight increase 0%

the P/N value for DEAE-dextran is nearly at 0.045, and it was concluded that the charge ratios of both DEAE-dextran (graft ratio 0 %) and DDMC (graft ratio 130 %) are nearly equivalent. When actually comparing transfection efficiency (TLU value) based on the two RLU values, the TLU value at a DDMC concentration of 28.6 mg/mL is about $5\times$ higher (see below), and this is thought to be due to micelle microformation resulting from the hydrophilic–hydrophobic microseparated domain of DDMC.

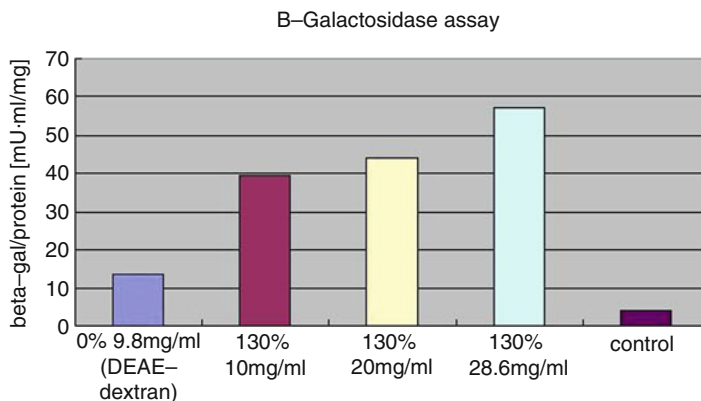
In transfection testing carried out according to the procedure of this report, the transfection efficiency of not only DDMC, but also DEAE-dextran (graft ratio 0 %) gave high RLU values relative to the commercially available product PolyFect (Qiagen) [45], a result that was obtained in preliminary testing using COS-7 cells. This suggests that there is a fairly large variation in efficiency depending on transfection conditions such as reagent amount, etc.

Transfection Efficiency

In Figs. 6.30 and 6.31, the transfection efficiency of DDMC is shown using HEK293 cells by a pCAGGS/LacZ, which expresses β -galactosidase at eukaryotic cells.

Table 6.8 Charge ratios (P/N) of DEAE-dextran-MMA graft copolymer (DDMC) and DEAE-dextran/DNA

Sample	P/N ratio
DEAE-dextran	0.045
DEAE-dextran-MMA graft copolymer (grafting rate 130%)	
DDMC 28.6 mg/mL	0.037
DDMC 20.0 mg/mL	0.052
DDMC 10.0 mg/mL	0.105

**Fig. 6.30** Transfection of HEK293 cells after 49 h with samples of DEAE-dextran and DEAE-dextran-MMA graft copolymers. The grafting rate was 130% for copolymers at concentrations of 10 mg/mL, 20 mg/mL and 28.6 mg/mL

The methods for transfecting a complex by pGL3-Control Vector DNA and carrier DDMC into COS-7 cells were investigated using 96-well microtiter plates. The results are shown in Fig. 6.32. When comparing the transfection efficiencies with DDMC (graft ratio 130 %) and DEAE-dextran (graft ratio 0 %) shown in Fig. 6.32, the TLU values after 72 h for DDMC at a concentration of 10.0 mg/mL were lower than for DEAE-dextran, but the efficiency increased with DDMC concentration and at 28.6 mg/mL were higher than for DEAE-dextran.

Figure 6.30 shows that a higher transfection efficiency is confirmed for samples of DDMC than for the starting DEAE-dextran hydrochloride, with the transfection efficiency and the efficiency increase depending on DDMC concentration.

The results of Fig. 6.30 are very similar to those of Fig. 6.32. The condition of both COS-7 cells and HEK293 cells was common in that a strong shear stress from outside was needed for their transfection solution to completely flow and wet the cell lines.

In Fig. 6.32, the TLU values for DEAE-dextran and DDMC were approximately equivalent at a concentration of 20.0 mg/mL, but the value was $5\times$ higher at a concentration of 28.6 mg/mL after 72 h. The fact that the efficiency increased in a concentration-dependent manner may be due to an increase in transfection

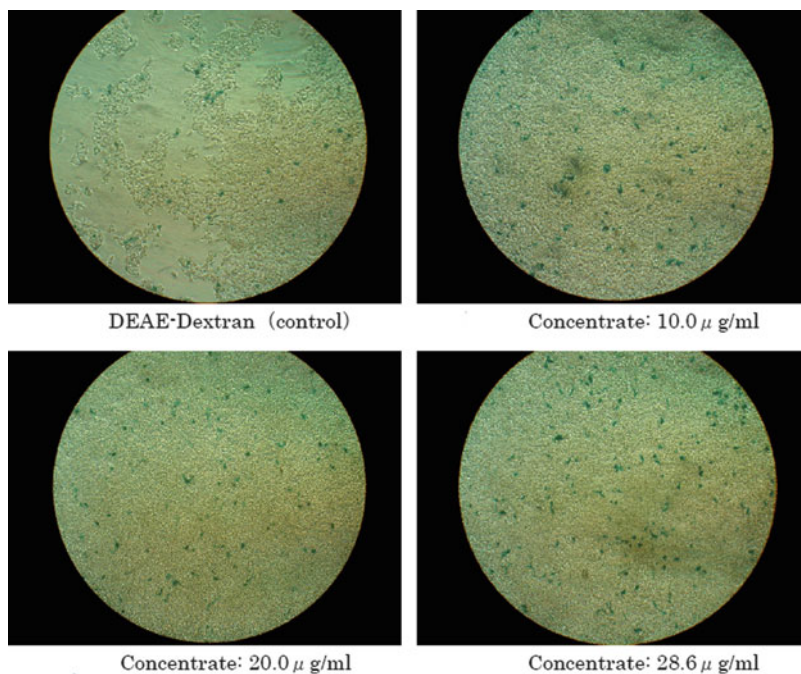


Fig. 6.31 Images showing transfection of HEK293 cells after 49 h with samples of DEAE-dextran and DEAE-dextran-MMA graft copolymers. The grafting rate was 130% for copolymers at concentrations of 10 mg/mL, 20 mg/mL and 28.6 mg/mL

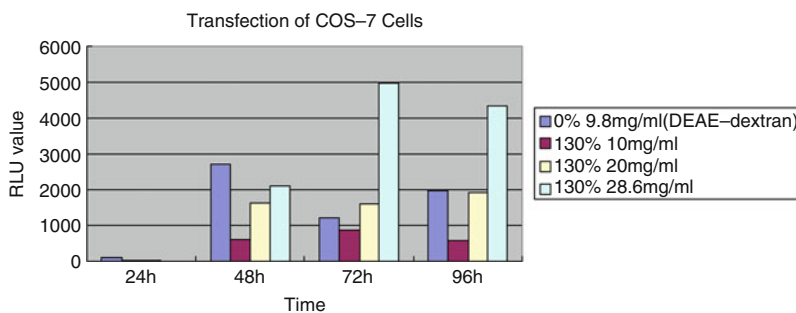
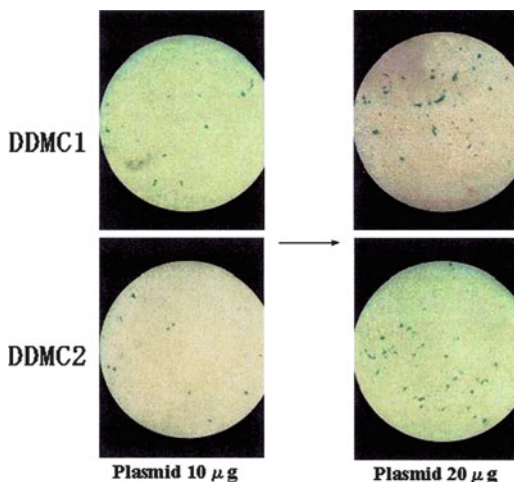


Fig. 6.32 Transfection of HEK293 cells at different time points with samples of DEAE-dextran and DEAE-dextran-MMA graft copolymers. The grafting rate was 130% for copolymers at concentrations of 10 mg/mL, 20 mg/mL and 28.6 mg/mL

efficiency resulting from the low cell toxicity of DDMC associated with its increase in the complex formed with DNA.

The same transfection efficiency increase in a concentration-dependent manner is evident in Fig. 6.30.

Fig. 6.33 Effect of cytotoxicity by DEAE-dextran-MMA graft copolymers at different concentrations on transfection of a monolayer of HEK293 cells



As shown in Figs. 6.29 and 6.31 transfection activity was determined using the X-gal staining method and a higher value of five times or more was confirmed for samples of DDMC1 and DDMC2 than for the starting DEAE-dextran hydrochloride. From the results, the transfection efficiency and the reaction rate of formation of the complex should increase when using DDMC hydrochloride instead of DEAE-dextran hydrochloride.

Cytotoxicity for the Transfection

Figure 6.33 shows the change in transfection efficiency when using twice the protocol quantities of DDMC (for example 20 μg DNA) and of both DNA and DDMC. Transfection of HEK293 by samples DDMC1 and DDMC2 was carried out using twice the protocol quantities of both DNA and DDMC. Transfection efficiency was twice as high than with the protocol amounts, as determined using the X-gal staining method. From these results (impossible for DEAE-dextran), cytotoxicity for the transfection should be confirmed to decrease and improve when using DDMC hydrochloride instead of DEAE-dextran hydrochloride.

6.4.6 Kinetics for the Transfection by DDMC

6.4.6.1 Complex Formation Reaction Mechanisms

The difference in protein expression due to DDMC and DEAE-dextran is thought to be caused by different complex formation reactions, particularly when their concentrations are very low. With the DNA and DDMC complex formation reactions, the hydrophobic bonding force is strongly influenced by the

hydrophobicity of the grafted MMA regions, as well as the Coulomb forces and hydrogen bonding forces, thus giving rise to a reversible equilibrium relationship. The Michaelis–Menten complex formation reaction is thought to occur as follows:

$$\text{Formed complex amount} = K1 (\text{DNA concentration}) (\text{DDMC concentration}) \quad (6.37)$$

The amount of formed complex is proportional to the RLU value. The formation reaction for the complex between DEAE-dextran and DNA is nearly non-reversible because it depends mostly on Coulomb forces, and the reaction is first-order with respect to DEAE-dextran concentration. The reaction is thought to be expressed as follows:

$$\text{Complex formation amount} = K2 (\text{DEAE-dextran concentration}) \quad (6.38)$$

The complex formation capacity is thought to give rise to a reversible equilibrium relationship, which can be expressed as a Michaelis–Menten equation:



Normally, the relationship is between enzyme and substrate, but in this case [E] is used to represent the concentration of DEAE-dextran or DDMC, and [S] is used to represent DNA concentration. Taking the initial DEAE-dextran or DDMC concentration as $[E]_0$, then:

$$[E] = [E]_0 - [ES] \quad (6.40)$$

Inserting these values, the complex concentration becomes:

$$[ES] = [E]_0[S]/(K_m + [S]) \quad (6.41)$$

With DDMC, the Coulomb forces are small (low affinity between E and S, and the fact that [S] is small has a direct influence on the complex formation). As K_m increases, the complex becomes unstable, and [S] is negligible relative to K_m . With this formula, assuming $K_m \gg [S]$, the complex concentration becomes:

$$[ES] = [E]_0[S]/K_m \quad (6.42)$$

This is the case for DDMC, and it is highly likely that the complex is strongly influenced by concentration conditions. In other words, it is thought that a very low DDMC concentration will have a significant influence on complex formation.

Conversely, considering DEAE-dextran, complex formation is stabilized when the Coulomb forces are large (high affinity between E and S, and the fact that [S] is small does not have a direct influence on the complex formation). As K_m is small, K_m thus conversely becomes negligible in comparison to [S]. Assuming that $K_m \ll [S]$, the complex concentration similarly becomes:

$$[ES] = [E]_0 \quad (6.43)$$

This indicates that complex formation is proportional to DEAE-dextran concentration. In other words, it is likely that there is no significant influence on a quantitative complex formation by DEAE-dextran concentration, even when the concentration is very low.

However, the Michaelis–Menten complex formation reaction between DDMC and DNA is thought to be significantly influenced by concentration. The relationship is expressed in Figs. 6.34 and 6.35 using $K1 = 1.055 \times 10^{-7}$ ($\mu\text{g}/\text{well}$) and $K2 = 1.626 \times 10^{-5}$ ($\mu\text{g}/\text{well}$), respectively, as determined at the maximum RLU values, and normalizing the RLU values by taking the maximum experimental values as 100 %. Figures 6.34 and 6.35 show a good correspondence with both DEAE-dextran and DDMC under the conditions of 48 h and 0.075 μg of DNA. For the concentration represented on the horizontal axes of Figs. 6.34 and 6.35, using 0.075 μg DNA and 0.75 μg DDMC, with a total volume of 30 μL for the medium not containing serum, the DNA concentration is 0.075 $\mu\text{g}/30 \mu\text{L}$ or 0.0025 $\mu\text{g}/\text{mL}$. The DDMC concentration is 0.75 $\mu\text{g}/30 \mu\text{L}$ or 0.025 $\mu\text{g}/\mu\text{L}$. Although the vertical axis in Fig. 6.35 should be normalized to the amount of complex, because of this proportion in the amount of complex to RLU, the reaction mechanism may be understood to be analogous if the trend shown in the figure is similar. As shown in Figs. 6.36 and 6.37, transfection of COS-7 cells with samples of DDMC support the Michaelis–Menten complex formation.

Figure 6.36 shows transfection of COS-7 cells with samples of DDMC having a grafting rate of 130 % and including 0.075, 0.150 and 0.30 μg of DNA in comparison with calculation values for 0.075 μg of DNA by Eq. (6.38) at 48 h. The relationship between RLU values and the amount of DDMC with 0.075, 0.150 and 0.30 μg of DNA are also in good accordance with the pattern from calculated values. The degree of transfection of COS-7 cells in Fig. 6.36 are in the order 0.075 > 0.150 > 0.30 μg of DNA, depending on its concentration by diffusion control. The maximum peak of transfection transfer to high concentration of DDMC is in the order 0.075 < 0.150 < 0.30 μg of DNA.

Figure 6.37 shows transfection of COS-7 cells with samples of DDMC having a grafting rate of 130 % and including 0.15 μg of DNA for incubation times of 48, 72 and 96 h.

The relationship between RLU values and the amount of DDMC with incubation times of 48, 72 and 96 h are also in good accordance with the pattern from calculated values in Fig. 6.36.

The degree of transfection of COS-7 cells in Fig. 6.37 are in the order 72 > 96 > 48 h incubation time.

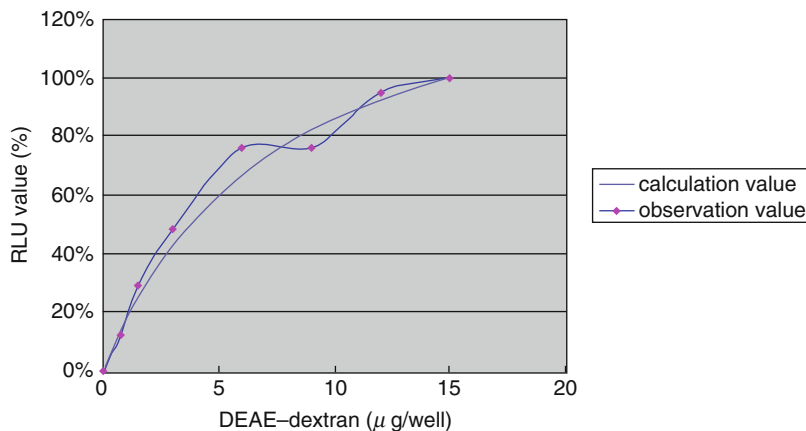


Fig. 6.34 Transfection of COS-7 cells with samples of DEAE-dextran. Maximum luciferase expression within each experiment was set at 100 %

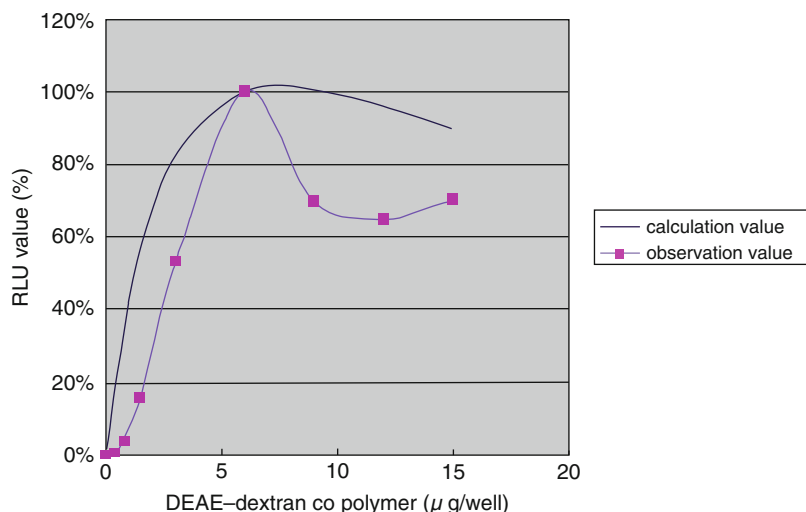


Fig. 6.35 Transfection of COS-7 cells with samples of DEAE-dextran-MMA graft copolymer having a grafting rate of 130 % and including 0.075 μ g of DNA. Maximum luciferase expression within each experiment was set at 100 %

We found that 48 h is the optimal incubation time for DEAE-dextran at very low concentrations. However, the optimal condition for DDMC is 48, 72 and 120 h with 0.075, 0.150 and 0.30 μ g of DNA at very low concentrations, respectively.

These phenomenon can be considered due to not only the diffusion control by viscosity, which is that of a non-Newtonian fluid, but also due to the DNase-protective activity of DDMC because of the hydrophilic-hydrophobic microseparated domain in its structure.

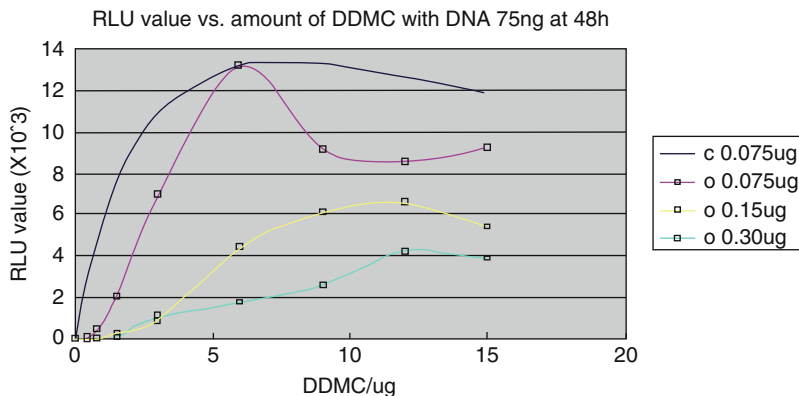


Fig. 6.36 Transfection of COS-7 cells with samples of DEAE-dextran-MMA graft copolymer (grafting rate: 130 %). Results for samples containing 0.075, 0.150 or 0.30 μg of DNA are shown in comparison with the values calculated for DEAE-dextran-MMA copolymer samples containing 0.075 μg of DNA

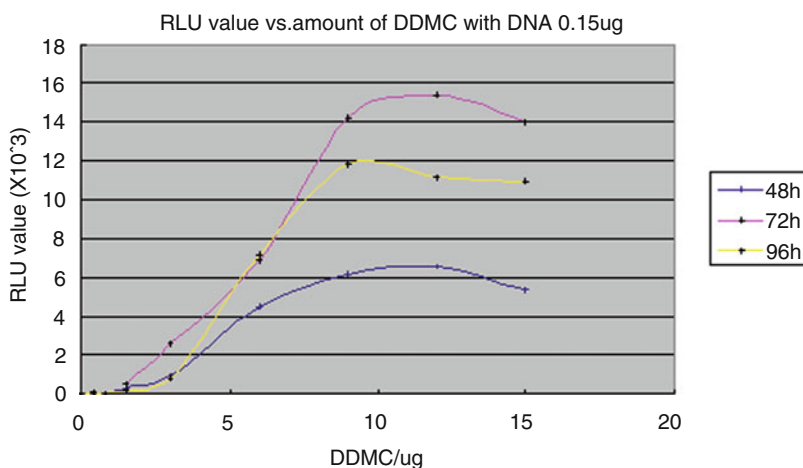


Fig. 6.37 Transfection of COS-7 cells with samples of DEAE-dextran-MMA graft copolymer having a grafting rate of 130 %. Samples include 0.15 μg of DNA for the incubation times of 48, 72 and 96 h

6.4.7 Protection Against DNase Degradation by DDMC

6.4.7.1 Measurement of DNase Degradation

Toluidine Blue (TB) and DNA form a complex by stain reaction [46]. The stain reaction between TB and DNA was carried out by adding 1 mL of 0.005 % TB solution (pH 7.0) to 1 mL of DNA solution (10 mg/mL, from Salmon sperm).

To 2 mL of DNA solution mixed with TB solution, the solution (10 mg/mL as DEAE-dextran) of the latex of DDMC was added in order to obtain the complex of DDMC/DNA stained by TB.

The resulting precipitation of the complex was separated by filtration (Advantec 5A), then 4 mL of distilled water was added, mixed with 0.01 mL (10 μ L) of DNaseI (RQ1 RNase-Free DNase, Promega) and 0.1 mL of 10 \times reaction buffer (400 mM Tris-HCl, 100 mM MgSO₄, 10 mM CaCl₂, pH 8.0) and incubated at 37 °C for 6,600 min. DNase degradation was determined by measuring the absorbance for TB isolated from DNA in the water with a spectrophotometer (Spectronic20, Milton Roy). TB in water absorbs broadly in the red range, with a maximum absorption at 633 nm and a shoulder near 600 nm. The wavelength at which the absorbance was followed was chosen to give a reasonably large initial absorbance; the wavelength used for this experiment was 633 nm.

6.4.7.2 DNase Degradation

DNaseI degrades both double-stranded and single-stranded DNA endonucleolytically, producing 3'-OH oligonucleotides. TB is isolated in water from DNA at the degradation, when DNA is stained by TB. Figure 6.38 shows the absorbance for TB isolated from the DNA of samples in water with a spectrophotometer.

Since Beer's law between the absorbance and concentration of TB applies [46], Fig. 6.38 also shows the rate of DNase degradation, with a slope of both the absorbance and time. The DEAE-dextran/DNA sample shows some degradation by DNase in Fig. 6.38, but the DDMC3/DNA sample shows a very low DNase degradation.

We also found that the DNA was protected against DNase degradation at the colloidal stage of the interaction with DEAE-dextran [15, 47, 48]. As a result, DDMC obviously has a higher protective effect on DNase than DEAE-dextran.

6.4.8 DNA Delivery Pathways to Cytoplasm or Nucleus by DDMC

DDMC transfection of cells has been carried out using the following steps: (a) Formation of a complex between DNA and DDMC. (b) Uptake. (c) Endocytosis (endosome). (d) Escape from endocytic vesicles. (e) DNA release in cytosol. (f) Nuclear entry. (g) DNA release and transcription in the nucleus.

For transfection efficiency, it is very important to examine factors such as uptake (step b), resistance of nuclease (step c), escape from endocytic vesicle (step d), nuclear targeting (step f), and DNA release (step g). The positively charged DEAE-dextran copolymer interacts with the negatively charged phosphate backbone of DNA. The resulting complex (step a) is absorbed into cells by endocytosis. The specifically designed molecular structure of DDMC, having a positive charge and a hydrophilic-hydrophobic microseparated domain, ensures easy entry of DNA into

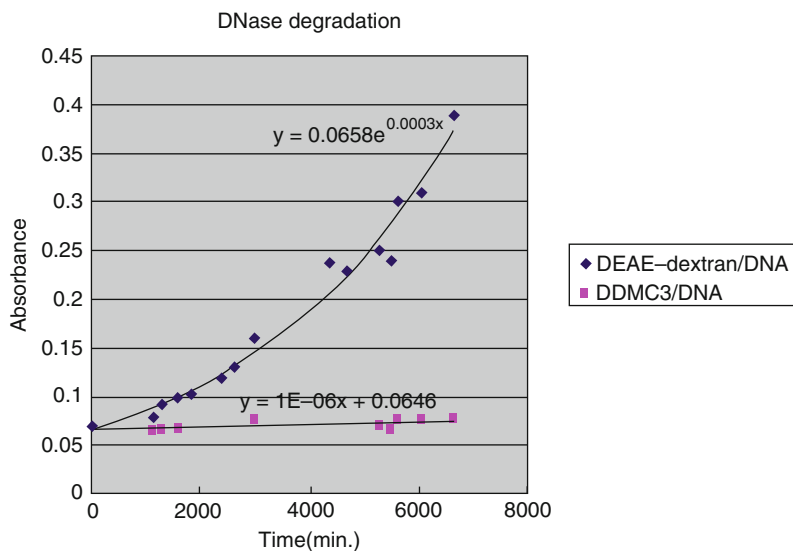


Fig. 6.38 DNase degradation. To the samples were added 4 mL of distilled water, then 10 μm of DNase I (RQ1 RNase-Free DNase, Promega) and 0.1 mL of 10 \times reaction buffer (400 mM Tris-HCl, 100 mM MgSO₄, 10 mM CaCl₂, pH 8) and the mixture incubated at 37 °C. The wavelength used for this experiment was 633 nm for Toluidine Blue isolated from DNA

cells (for steps b,c, d, f and g). The complex of DDMC/DNA in cytoplasm also can be stable (in steps b, c, d, f and g) to be protected from both DNase and Dextranase.

Formation of a complex between nucleic acids (DNA or RNA) and DDMC is accomplished by a Coulomb force between the phosphoric acid of nucleic acids and the DEAE group of DEAE-dextran to ensure easy entry of DNA (for step b) and endosome buffering for osmotic destruction (proton sponge properties) (for step d).

Figure 6.27 shows the IR absorption spectra of the resulting complex between DDMC (sample DDMC2) and DNA. The absorption spectrum shift at around 3,450 cm^{-1} indicates the formation of more compact structures by a Coulomb force between the phosphoric acid of DNA and the DEAE group of DEAE-dextran, leading to DNA condensation [44]. This phenomenon is interesting because DNA is usually tightly packed in native genomes and the manner of this packaging should dominate the mechanism of gene expression.

As shown in Fig. 6.39, DDMC, having an amphiphilic domain, forms a polymer micelle and should become a stable latex with a hydrophilic-hydrophobic microseparated-domain [49]. The complex of DDMC and plasmid may be formed on the spherical structure of the amphiphilic microseparated domain of DDMC and have a good affinity to the cell membrane. The complex of cationic polymers/DNA in cytoplasm can be protected from restriction enzymes that break down DNA. In the case of DEAE-dextran, the complex of DEAE-dextran/DNA in cytoplasm can be weakly protected from DNase, but degraded by Dextranase. However, the complex of DDMC/DNA in cytoplasm can be protected from both DNase and

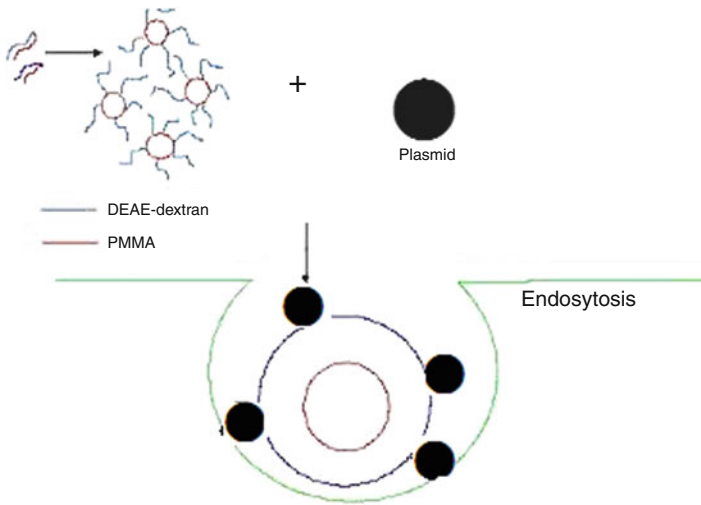


Fig. 6.39 Endocytosis by a complex between DDMC and plasmid

Dextranase. The high efficiency of transfection of DDMC must depend on its stability in cytoplasm and its good affinity to biomembranes, such as cell membrane, owing to its amphiphilic domain.

The high efficiency of this autoclaved graft copolymer can make it a valuable tool for gene delivery *in vivo*.

6.4.9 Protocol

1. Prepare cells by plating the day before the transfection.
2. Prepare the wash solution (not supplied; either 1× PBS or 1× HBSS) Warm wash solution and the cationic graft-copolymer to 37 °C.
3. Using the prepared 10× PBS, dilute it to a 1× solution. Prepare transfection solutions as outlined. Per 35-mm plate: In a sterile tube, dilute 10 μg of DNA to 270 μL in 1× PBS. Add 14 μL of the cationic graft-copolymer having the 10 mg/mL as the starting polycation concentration to the DNA solution (do not reverse the order). Tap the tube to mix.
4. Remove culture medium from the cells. Wash cells twice with 2× PBS 2.0 mL per 35 mm plate.
5. Add the DNA/(cationic graft copolymer) mixture to cells. Swirl plate to distribute.⁵

⁵ An aqueous solution of cationic graft copolymer having a thixotropy property; a strong shear stress is needed for its solution to flow and wet the cell.

6. Incubate plates at 37 °C for 30 min with occasional rocking.
7. Gently add 3.0 mL of growth medium⁶ per 35-mm plate.
Incubate for up to 2.5 h or until cytotoxicity is apparent.
Change medium. Cells are generally ready to harvest 48–72 h post transfection and assayed for transfection activity.

6.4.10 Specification of DDMC Vector

Specifications of DDMC Vector with DEAE-Dextran MMA Copolymer are:

1. Fast and easy procedure
2. Stable for autoclaving sterilization
3. Applicable in high-throughput-screening (HTS)
4. No serum inhibition
5. High efficiency by use of low DNA amounts
6. Excellent reproducibility
7. Low toxicity in comparison with DEAE-dextran.

6.5 DEAE-Dextran-MMA Graft Copolymer for Drug Delivery Systems

A complex of DDMC/PTX obtained by incorporating paclitaxel (PTX) as guest molecule into DEAE-dextran-MMA copolymer (DDMC) as host forms nanoparticles of 200–300 nm in size. It is considered to be very useful for delivery of anticancer agents to malignant melanoma cells because the complex promotes an allosteric supramolecular reaction to tubulin (like an enzyme reaction) that is different to that for paclitaxel alone. The resistance of B16F10 melanoma cells to paclitaxel was confirmed using survival curve analysis. On the other hand, there is no resistance of melanoma cells to DDMC/PTX and the melanoma cells reach apoptosis depending on amount of the paclitaxel in the DDMC/PTX complex.

Of note, the DDMC/PTX complex is not considered to be degraded in cells and represents the efficacy of an intact supramolecule such as artificial enzymes having substrate-selectivity.

These results have not yet been reported and will be very helpful in overcoming cancer diseases.

⁶ Dulbecco's modified Eagle's medium supplemented with 10% fetal calf serum, 0.1 mM nonessential amino acids, 5 mM L-glutamine and antibiotics (100 µg/mL streptomycin, 100 U/mL penicillin).

6.5.1 Drug Delivery Systems

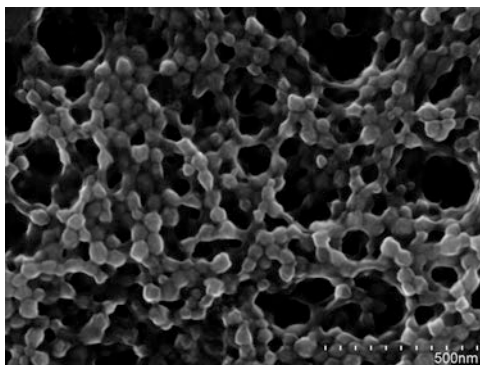
Drug delivery by polymers has been considered for targeted drug delivery because they have an enhanced permeability and retention (EPR) effect [50] and reticuloendothelial system (RES)-avoiding effect [51, 52]. However, new insights have been obtained from recent studies regarding the intracellular distribution and efficacy of drug delivery by polymers. For example, triple-labeling confocal microscopy in live cells revealed the localization of micelles in several cytoplasmic organelles, including mitochondria, but not in the nucleus. Moreover, micelles of the medicinal polymer drug delivery system can change the cellular distribution and increase the amount of agent delivered to the cells [53–55]. A full-scale study of the enzyme was carried out from the purified saccharase by the German chemist Willstätter in 1920. The purified enzyme is thought to consist of active groups of low and high molecular weight carriers, like saccharase [56]. However, it is made possible for catalytic reaction by the large molecules of the enzyme protein. The active site is thought to consist of low molecular weight and high molecular weight carriers, which is the original concept of a supramolecule. DDMC has been obtained by graft-polymerization of MMA onto DEAE-dextran in water [7–9]. The resulting DDMC of hairy nanoparticles have an amphiphilic domain of DEAE-dextran and a hydrophobic domain of PMMA so as to form a polymer micelle [21]. DDMC has a safe transfection efficacy after autoclaving and is superior to other transfectants as a non-viral carrier for gene introduction [23, 57–62]. On the other hand, paclitaxel is well known as a strong anticancer agent that can introduce cancer cells to apoptosis through stabilization of tubulin (i.e., tubulin polymerization).

6.5.2 Preparation of DDMC/PTX Complex

Preparation of DDMC: Two grams of DEAE-dextran hydrochloride (nitrogen content 3 %) derived from dextran (M_w 500,000) was dissolved in 100 mL of water, followed by the addition of 3.5 mL of MMA. While stirring, the air in the reaction vessel was fully replaced with N_2 gas. Next, 0.1 g of CAN and 15 mL of 0.1 N nitric acid was added, and the mixture was stirred for 1 h at 30 °C. Finally, 3 mL of a 1 % aqueous solution of hydroquinone was added to stop the reaction, and the resulting DDMC was purified by water dialysis using a cellophane tube to remove any unreacted MMA, ceric salts and nitric acid.

DDMC–paclitaxel complexation: The DDMC/PTX complex was obtained by adding paclitaxel as a guest to 5 mL of 2 % DDMC. Three samples were prepared, containing 0, 0.385 or 0.709 mg/mL paclitaxel. For all samples, the grafting rate was 102 % and DDMC concentration was 9.6 mg/mL.

Fig. 6.40 SEM image (HITACHI S-4800) of the freeze-dried DDMC/PTX complex. Sample is taken at an accelerating voltage of 5 kV



6.5.3 Characterization of DDMC/PTX Complex

A complex consisting of DDMC and paclitaxel (DDMC/PTX) was generated using paclitaxel as the guest with DDMC as the host. The particle size distribution and ζ -potential of the DDMC/PTX complex were measured in by dynamic light scattering (DLS) and particle electrophoretic mobility. Furthermore, SEM (Fig. 6.40) was used to determine the size and shape of the freeze-dried DDMC/PTX complex and revealed that the complex formed uniform cubic particles with a diameter of 200–300 nm, as measured by DLS (Fig. 6.41). Particle size determined by SEM (Fig. 6.40) was 300–500 nm, similar to that determined by DLS. The ζ -potential of the outer layer of the particles, outside of the electric double layer, was +36 mV, which helps to stabilize the dispersion of the DDMC/PTX complex. Considering that the particle size of DDMC is approximately 100 nm, it seems that the DDMC/PTX complex forms clusters to form stable polymeric micelles [62].

Absorbance of DDMC/PTX in solution was measured at a wavelength of 227 nm (light path, 10 mm), which yielded an absorbance coefficient (ϵ) of $62.4 \times 10^4 \text{ M}^{-1} \text{ cm}^{-1}$ [63]. As shown in Fig. 6.42, this is much larger than that of paclitaxel alone, which was $3.27 \times 10^4 \text{ M}^{-1} \text{ cm}^{-1}$ in acetone/H₂O (50:1), $2.8 \times 10^4 \text{ M}^{-1} \text{ cm}^{-1}$ in CH₃CN:H₂O (4:1) and $2.6 \times 10^4 \text{ M}^{-1} \text{ cm}^{-1}$ in MeOH:H₂O (1:1). This increase in absorbance may be due to the strong photoconductive property of the DDMC/PTX complex by promoting π -electron resonance, which forms a line dependent on the supramolecular π stack structure of paclitaxel self-integrated into DDMC [64]. These properties may also explain why the DDMC/PTX complex showed high reactivity and specificity for its target substrate in melanoma cells, which are known widely as the most lethal cancer cells.

6.5.4 MTT Assay

MTT (WST8) assay. Cell survival was determined using MTT assays with water-soluble tetrazolium salts, a series of water-soluble dyes suitable for MTT assays.

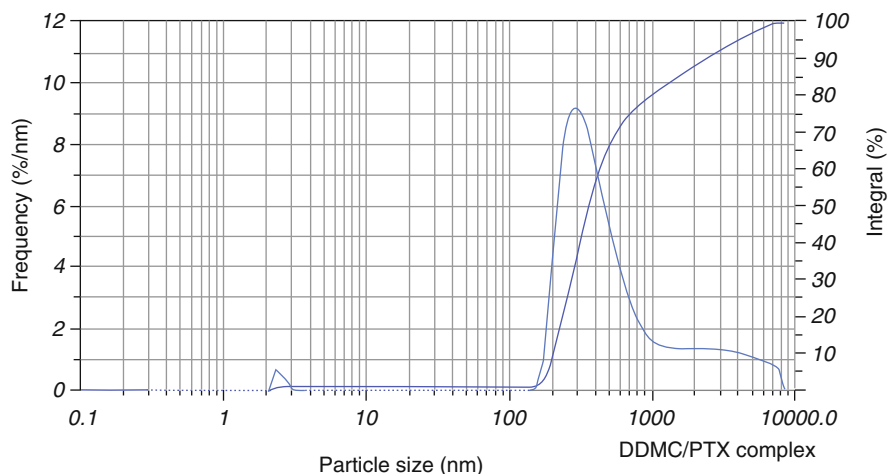


Fig. 6.41 Particle size distribution and zeta potential of a DDMC/PTX complex were measured by using dynamic light scattering and particle electrophoretic mobility (the SZ-100 nanoparticle series instruments from HORIBA, Ltd.)

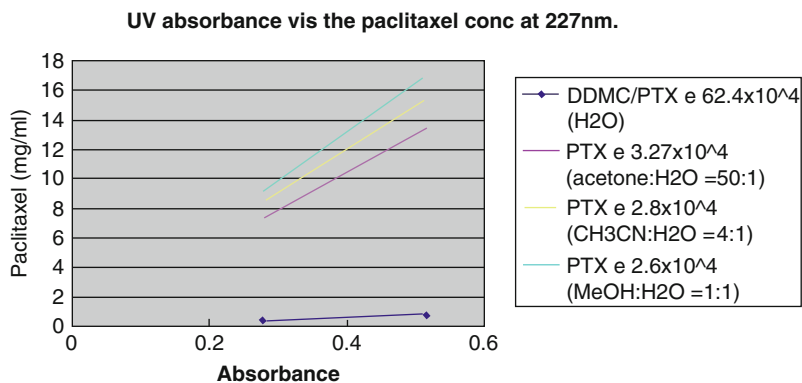


Fig. 6.42 Absorbance of the DDMC/PTX complex. Absorbance of the DDMC/PTX complex solution measured at a wavelength of 227 nm and light path of 10 mm

In this method, cells were plated onto 96-well tissue culture plates at a density of 10,000 cells/well to ensure that the optimal population density was reached within 24–48 h. Next, the indicated concentrations of DDMC/PTX or paclitaxel alone were added to each well, to a final volume of 0.1 mL. The culture medium contained up to 10 % fetal bovine serum. Cell Counting Kit-8 (CCK-8; Dojindo Molecular Technologies, Inc.) solution was added to each well and the plate was incubated under CO₂ at 37 °C for 24 or 48 h. After adding 10 µL of CCK-8 solution to each well, the plate was gently mixed and incubated under CO₂ at 37 °C for 2–4 h. The optical density of each well was measured at 450 nm and cell survival was calculated using the following formula:

$$\text{Cell survival (\%)} = [(A_s - A_b)/(A_c - A_b)] \times 100$$

where A_s = absorbance of the sample, A_c = absorbance of the control well (no cells) and A_b = absorbance of the blank well.

6.5.5 *In Vitro Testing*

The results of a direct MTT assay (WST8) showed a positive correlation between cell number and absorbance (i.e., optical density), and confirm that it is suitable for evaluating the efficacy of paclitaxel on melanoma cells in vitro. Melanoma cells are well known to show resistance to paclitaxel, as indicated in the survival curves shown in Figs. 6.43 and 6.44.

The survival curves, which are inverse to paclitaxel concentration, indicate that gene expression should be taken into account for the concentration-dependent survival at low paclitaxel concentrations (event A) and is a negatively associated with survival at higher concentrations of paclitaxel (event B). In this way, the probability of survival is expressed as the product of the probability of $P(A)$ positively and $P(B)$ negatively, represented as $A \cap B$. The probability of survival is the product of the probability $P(A)$ of gene expression survival that is positively dependent on high paclitaxel concentrations and the probability $P(B)$ of gene expression survival that is negatively dependent on high paclitaxel concentrations. Thus, the probability $A \cap B$ is the phenomenon that events A and B occur in event (A, B). When events A and B are independent of each other, the probability $P(A \cap B)$ is represented by the following formula:

$$P(A \cap B) = P(A) \bullet P(B)$$

where $P(A \cap B)$ = the probability of event A and B ; $P(A)$ = the probability of event A ; and $P(B)$ = the probability of event B . Using this equation, the convex curve used to assume $P(A)$ and $P(B)$ is asymptotic.⁷

Dr. Miyano of The University of Tokyo has conducted extensive research into the resistance of melanoma cells to paclitaxel (here, event A). The survival of melanoma cells resistant to paclitaxel has been extensively analyzed using DNA microarrays and dynamic Bayesian analyses. In such studies, gene expression was measured for 24 h after treatment, which showed gene clustering over time in melanoma cells. These findings obtained from dynamic Bayesian analysis in combination with nonlinear regression were confirmed using data from DNA microarrays [65].

⁷ when $P(A)$: ax and $P(B)$: $b(1 - x)$, $(A \cap B)$ is shown as $y = (ax)(b(1 - x))$. The secondary function (convex curve) of $y = (ax)(b(1 - x))$ makes both $y = ax$ and $y = b(1 - x)$ an asymptote in a range of $a > 0$, $b > 0$ and $1 > x > 0$.

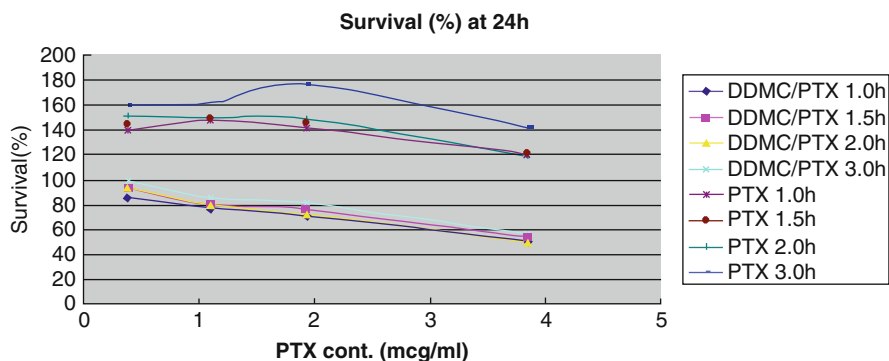


Fig. 6.43 Survival of B16F10 melanoma cells treated with paclitaxel or the DDMC/PTX complex for 24 h. Survival was determined using the MTT (WST8) method

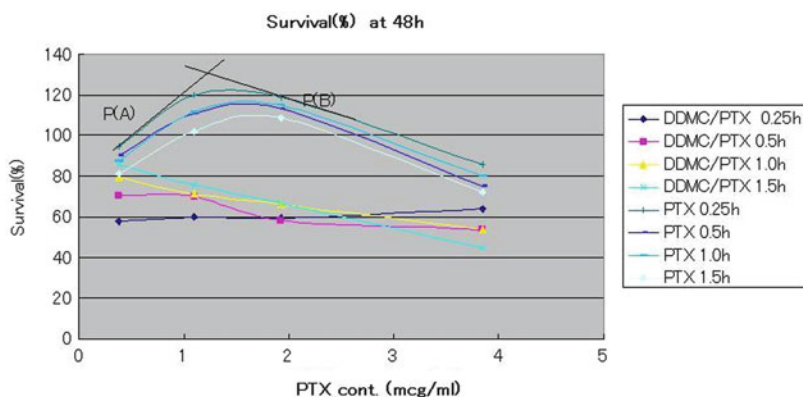


Fig. 6.44 Survival of B16F10 melanoma cells treated with paclitaxel or the DDMC/PTX complex for 48 h. Survival was determined using the MTT (WST8) method. $P(A)$ is the probability of survival that is positively dependent on high paclitaxel concentrations; $P(B)$ is the probability of survival that is negatively dependent on high paclitaxel concentrations

One hour after the administration of paclitaxel, the RBM23 gene, a known target of paclitaxel, acted as a hub and interacted with the TUBA4A gene, which encodes tubulin α -4A chain. Two hours later, TXNIP gene was found to act as a key gene that was not responsive to paclitaxel in the treatment of breast cancer. Four hours later, the DNA microarrays revealed the activation of several genes downstream of EGR1 and TXNIP. Six hours later, CYR61, which is involved in the resistance to paclitaxel in breast cancer, became more active and continued to be influenced by EGR1. In this way, cancer cells exposed to anticancer drugs acquire resistance to the drug over time and show complex cellular behaviors.

In this experiment, we used factor analysis to examine the effects of low paclitaxel concentrations on survival and gene expression of melanoma cells. However, we considered that paclitaxel was unlikely to participate in stabilization

of tubulin (i.e., tubulin polymerization), even at low paclitaxel concentrations. At high concentrations, however, the enhanced tubulin polymerization will be unable to inhibit the responses to paclitaxel. Therefore, the reduced survival dependent on paclitaxel concentrations (i.e., event B) becomes dominant and the efficacy of paclitaxel becomes more apparent.

6.5.6 Response of Melanoma Cells to the DDMC/PTX Complex

By contrast, the responses of melanoma cells to the DDMC/PTX complex are much more specific without event A . Of note, low concentrations of the DDMC/PTX complex markedly inhibited the increase in number of melanoma cells, with a linear negative correlation between paclitaxel concentration $[E]_0$ and survival rate. This means that there is no resistance of melanoma cells to DDMC/PTX complex. In other words, the relationship between the cell death (Cd) rate (Cd/dt) and tubulin polymerization rate (dp/dt) will assume the following equation, as modified from Cheng and Prusoff [66]:

$$Cd/dt = a dp/dt + C_1 \quad (6.44)$$

where a is a constant and C_1 is a device constant corresponding to $a > 0$, $C_1 > 0$. The rate of tubulin polymerization $V = dp/dt$ can also be expressed using a Michaelis–Menten-derived S-shaped curve, as follows:

$$v = \frac{\kappa_{cat}[E]_0[S]_0^n}{[S]_0^n + K_m} \quad (6.45)$$

where K_m = Michaelis constant, $[S]_0$ = initial tubulin concentration and n = Hill coefficient. In this case, because $n > 1$, mutual interactions between numerous points occur, which fit an S-shaped curve. The stability of the enzyme–substrate complex is shown as $1/K_m$, and is larger for DDMC/PTX than for paclitaxel alone, corresponding to $[S]_0^n \gg K_m$.

The equation:

$$V = \kappa_{cat}[E]_0 \quad (6.46)$$

can be substituted with the expression from (6.45), as follows:

$$Cd/dt = a\kappa_{cat}[E]_0 + C_1 \quad (6.47)$$

and integrated into:

$$Cd = a\kappa_{cat}[E]_0 t + C_1 t \quad (6.48)$$

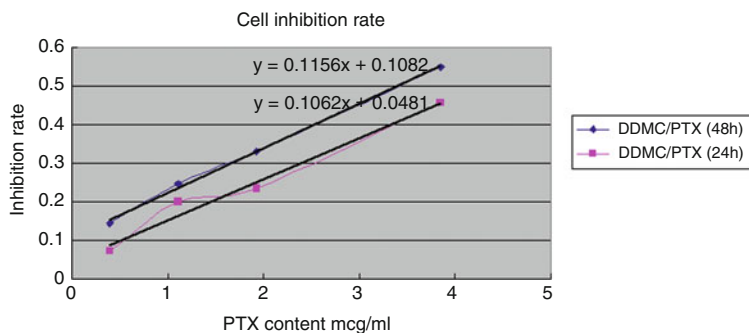


Fig. 6.45 Relationship between Cd and paclitaxel concentration. Tubulin polymerization and cell death (Cd) rates can be expressed by enzymatic kinetic parameters

From this, the rate of tubulin polymerization V can be expressed using enzymatic parameters for Cd. In these equations, $[E]_0$ = initial paclitaxel concentration as an enzyme.

As shown in Fig. 6.45, incubation with MTT for 24 and 48 h yielded the following equation:

$$Cd = 0.1156[E]_0 + 0.1082 \quad (6.49)$$

$$Cd = 0.1062[E]_0 + 0.0481 \quad (6.50)$$

Thus, 0.1082 and 0.0481 represent the constants for $[E]_0$ at 24 and 48 h, respectively.

From Eq. (6.49), the plots of C_1t with time t must be extrapolated to $t = 0$. Accordingly, $C_1t = 0.1082$ at 24 h and 0.0481 at 48 h, when data are extrapolated to $t = 0$ in Fig. 6.46. This confirms the assumption in Eq. (6.49) that the relationship between $[E]_0$ for paclitaxel and the probability of Cd forms a straight line. From these results, and based on $V = dp/dt$, the DDMC/PTX complex promotes tubulin polymerization that can be expressed using Michaelis–Menten kinetics modified with the Hill coefficient [67]. These phenomena also demonstrate the supramolecular properties of the DDMC/PTX complex.

6.5.7 Enzymatic Reactions Allosterically

The results also indicate that these enzymatic reactions allosterically promote tubulin polymerization in cells. Hydrophobic interactions between the polymer and substrate, with paclitaxel located in the hydrophobic pocket, allow paclitaxel to selectively react with tubulin as indicated in Fig. 6.47. This effect is not apparent with paclitaxel alone, and is less susceptible to interference from other signals.

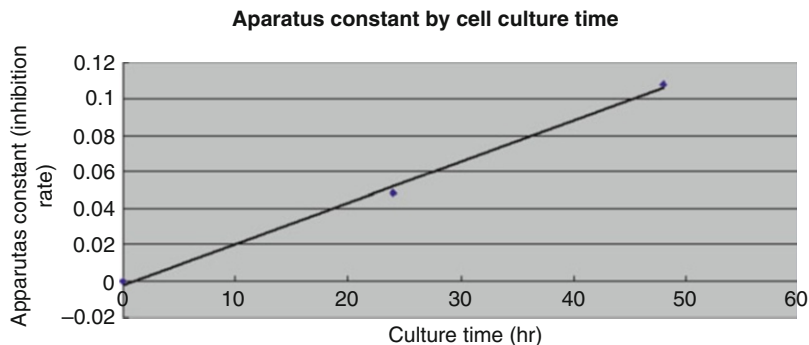


Fig. 6.46 Relationship between the inhibition rate constant $C1$ and paclitaxel concentration

The results also provide evidence that the DMC/PTX complex causes a supramolecular reaction involving allosteric promotion, as in Eq. (6.46). The Hill coefficient included in Eq. (6.46) supports the likelihood of allosteric cooperation as it represents the strength of cooperative molecular joints. These phenomena may depend on the supramolecular characteristics of clathrate compounds as the paclitaxel guest is complexed with DDMC as the host.

This is certified by the strong photoconductive property of DDMC/PTX complex, promoting π -electron resonance as shown in Fig. 6.42. Therefore, the DDMC/PTX complex shows marked substrate specificity, consistent with artificial enzymes. This substrate specificity of the DDMC/PTX complex promotes a reaction between paclitaxel and tubulin, the target of paclitaxel, and avoids potential interference from changes in gene expression that may affect the survival response to paclitaxel, even at low concentrations.

Paclitaxel can be conjugated to a variety of carriers, including polyglutamate and albumin, or encapsulated in cationic liposomes. Using these carriers, paclitaxel is thought to be transported into and released directly in cells, thus improving its efficacy. However, the DDMC/PTX complex is not degraded in the cell, and its efficacy may be enhanced by remaining in supramolecular form.

6.5.8 Thermodynamic Consideration of Supramolecular Allosteric Binding

Promotion of supramolecular allosteric binding of the ligand (as when molecular oxygen binds to hemoglobin) is a phenomenon that increases the reactivity of the active site and other substrate molecule binding sites.

In the case of hemoglobin, the oxygen works efficiently as an effector, and at the same time as the substrate. Allosteric binding to one subunit affects the binding of substrate to the next subunit, enhancing the affinity of binding sites remaining by its

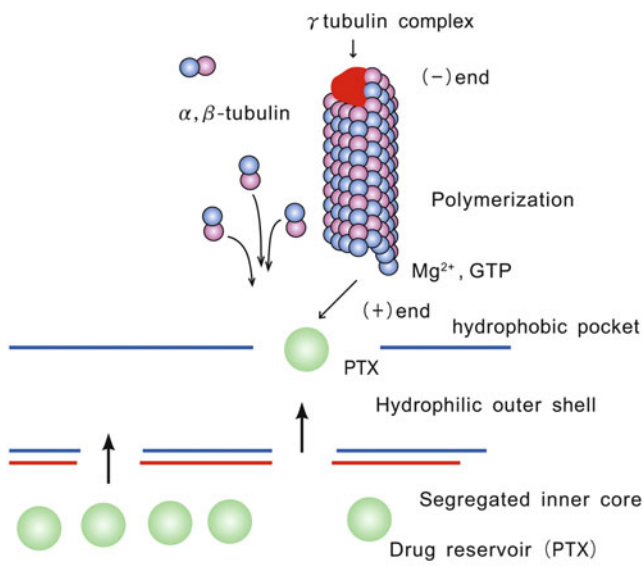


Fig. 6.47 Representation of α,β -tubulin dimer polymerization showing the relationship between the DDMC/PTX complex and α,β -tubulin. The α,β -tubulin dimer orientates with the active site (i.e., paclitaxel) of the DDMC/PTX complex

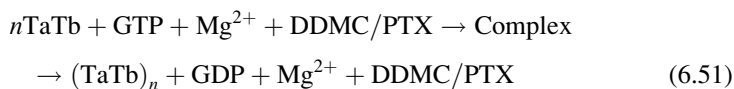
structural change. Supramolecules have allosteric properties like the substrate specificity of enzymes.

In the case of enzyme–substrate interactions of the DDMC/PTX complex with B16F10 melanoma cells, the allosteric properties of supramolecules may yield entropy decreases (entropy trap) depending on the selectivity of the reaction with tubulin and the strain of substrate under its stress from molecular structure, as indicated in Fig. 6.47.

At same time, the enthalpy decrease depends on adhesion of substrate by the supramolecular structure of the DDMC/PTX complex. Paclitaxel is an anti-tumor agent isolated from the bark of the yew and promotes the tubulin polymerization (rescue) to inhibit depolymerization (catastrophes) in β -tubulin.

DDMC/PTX self-assembles, aggregates and the complex eventually becomes close to 270 nm in size. First, there is an electrostatic reaction of cationic DDMC/PTX complex and the substrate α,β -tubulin dimer and also a hydrophobic interaction; then the β -tubulin of the dimer coordinates with the so-called hydrophobic pocket of the DDMC/PTX complex and the substrate α,β -tubulin dimer reacts with the activity point of paclitaxel in DDMC/PTX to form a Michaelis complex. The stability of the enzyme (DDMC/PTX)–substrate (α,β -tubulin dimer) complex is shown with size of $1/K_m$, but in this case is considerably larger, depending on the supramolecular π stack structure in conformational flexibility to make stable for its dynamic instability to stop the treadmill of tubulin protomers.

This α,β -tubulin dimer and DDMC/PTX complex have Mg^{2+} and GTP on the (+) growth edge and the tubulin polymerization (rescue) proceeds as follows:



where TaTb is the α,β -tubulin dimer.

The catalytic power of enzymes to efficiently form transition states has been proposed to involve an equilibrium between the Michaelis complex and a stabilized transition state.

Gibbs free energy in the transition state is considered:

$$\Delta G^\ddagger = \Delta H^\ddagger - T\Delta S^\ddagger \quad (6.52)$$

where ΔG^\ddagger is the free energy of activation, ΔS^\ddagger is the entropy of activation, and ΔH^\ddagger is also the enthalpy of activation.

Figure 6.48 shows the potential energy curve and activation energy E_a , where,

$$E_a \doteq \Delta H^\ddagger.$$

With paclitaxel, many signals from gene expression in melanoma cells yield a huge ΔG^\ddagger owing to large ΔS^\ddagger and large ΔH^\ddagger as in Fig. 6.46.

As $R \propto e^{\Delta H^\ddagger/RT}$ with apoptosis for melanoma cells (R), melanoma cells can overcome paclitaxel at low concentrations.

On the other hand, Fig. 6.48 shows a small activation energy E'_a with the DDMC/PTX complex, and the supramolecular enzyme facility yields a small ΔG^\ddagger owing to low ΔS^\ddagger and low ΔH^\ddagger , which is why apoptosis for melanoma cells (R) should progress.

6.5.9 Supramolecular Template

The α -tubulin side is a negative edge, and the β -tubulin side is a positive edge. Most of the microtubule is polymerized α,β -tubulin dimer bound to GTP.

Many microtubules place a negative edge in the microtubule organizing center (MTOC) (centrosome in animal cells) to extend the (+) growth edge to each place of the cell. Of course, the microtubules are formed outside of centrosome and are searched and transported to it to be associated [68]. In one embodiment, the tubulin-binding agent is a microtubule-stabilizing agent.

Cell division will usually be initiated when polymerization stops forming the complete long hollow tubes to support myosin and actin proteins of the cell surface by gathering the 13 fibers. Nevertheless, although the α,β -tubulin dimer is stabilized extremely by DDMC/PTX, polymerization does not stop and many poor short hollow tubes are formed, leading to apoptosis of the cell.

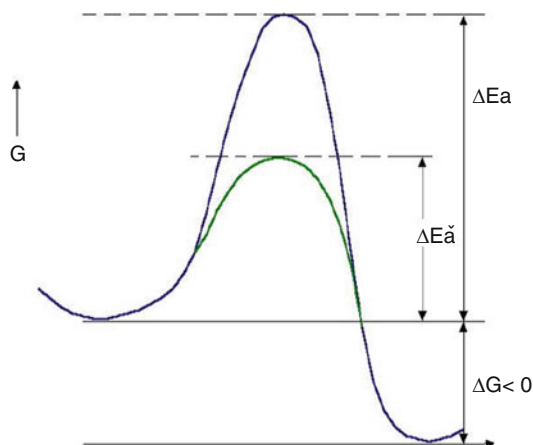


Fig. 6.48 Potential energy curve of paclitaxel (*outer curve*) and DDMC/PTX complex (*inner curve*). E_a is activation energy of paclitaxel, E'_a is activation energy of DDMC/PTX complex

Figure 6.49 shows the diffusion to the outer surface of PTX, the coordination of α,β -tubulin dimer on the DDMC/PTX complex, and the growth reaction of α,β -tubulin dimer on the DDMC/PTX.

At same time, for accelerating the reaction, there is further growth orientation of the PTX part to the surface of the DDMC/PTX complex and the subsequent internal diffusion of α,β -tubulin dimer to a hydrophobic bond (hydrophobic pocket) of DDMC/PTX, and it is promoted for the α,β -tubulin dimer substrate to be polymerized on its active site (PTX).

The characteristic of this polymerization (enzyme–substrate) is that it is coordinated at both the growing end of α,β -tubulin polymer and α,β -tubulin dimer to a supramolecular template, and one-dimensional Brownian movement is also accompanied by a concerted action of the electrostatic force of the DDMC/PTX complex. This coordination polymerization proceeds by Brownian movement [69].

6.6 Conclusion

A graft polymer of MMA on dextran was prepared using ceric ammonium nitrate. The properties of this graft copolymer are very interesting because of its amphiphilic microseparated domain. The solubility, infrared absorption spectrum and thermal behavior of the graft copolymer were investigated. It was found that an extruded film of the copolymer not only shows better water wettability and water absorbing power than PMMA but also exhibits thrombo-resistance and can be formed into a transparent contact lens with an affinity for tears and blood. Electron microscopy shows that the surface of the contact lenses has a microheterogeneous structure, consisting of uniformly distributed phase-separated grains of

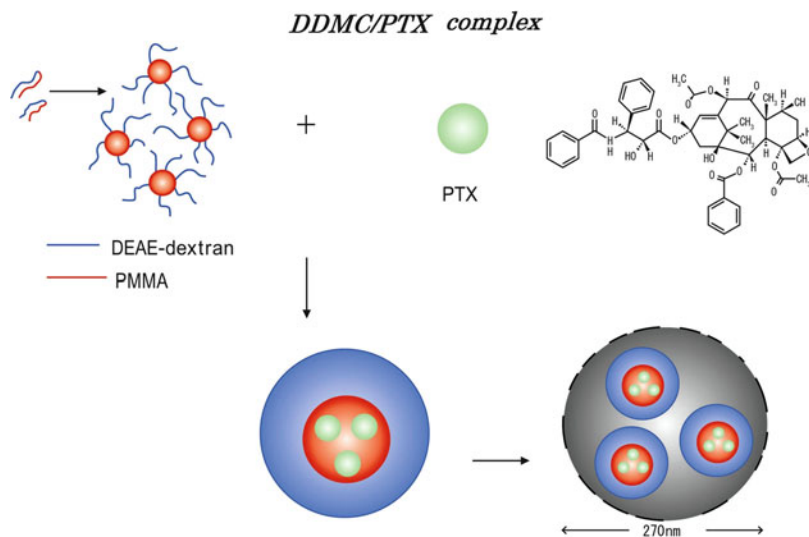


Fig. 6.49 Representation of the DDMC/PTX complex. Simplified structures are shown. The DDMC/PTX complex (~ 270 nm) consists of more than 8.1×10^3 DDMC molecules and 6.7×10^6 paclitaxel molecules

approximately $0.2 \mu\text{m}$ in size. Transparent dextran-matrix copolymers (DMC) have recently been prepared for HCL and IOL applications that consist of the PEC between cationic dextran and unsaturated acids with compounds of vinyl. The PEC is expected to be a biocompatible material having an O_2 transport ability. We have evaluated the biocompatibility of DMC for a human tear by examining the drying pattern of NaCl salt crystals from a 0.2 % solution of human γ -globulin dissolved in physiological saline, as proposed by Sole. We think that the DMC has good biocompatibilities, not only because of its structure containing a hydrophilic–hydrophobic microseparated domain owing to a PEC, but also because of an electric charge distribution that is localized by the polyanion of excess. Moreover, we have clarified the role of dextran in the affinity of DMC to tear liquid.

A stable latex of DEAE-dextran-MMA graft copolymer (DDMC) was developed for non-viral gene delivery vectors that can be autoclaved at 121°C for 15 min. Transfection activity was determined using the X-gal staining method, and a higher value of 5–10 times or more was confirmed for DDMC samples than for the starting DEAE-dextran hydrochloride. DDMC has been also confirmed as having a high protection facility against DNase degradation. The DDMC, having an amphiphilic domain, forms a core–shell polymer micelle that should become a stable latex with a hydrophilic–hydrophobic microseparated domain. The complex of DDMC and DNA can be formed initially on the stable spherical structure of the amphiphilic microseparated domain of DDMC and has a good affinity to the membrane of the cell for endocytosis. The shift in the IR absorption spectrum of the complexes between DNA and DDMC to a high energy direction at around $3,450 \text{ cm}^{-1}$ may

mean that more compact structures are formed, not only by a Coulomb force between the phosphoric acid of DNA and the DEAE group of the DEAE-dextran copolymer but also by a force from multi-intermolecular hydrogen bonding. It indicates that DNA condensation may enable higher transfection efficiency. The high transfection efficiency of this graft copolymer that can be autoclave-sterilized makes it a valuable tool for safe gene delivery. DDMC was also very superior as a drug delivery system. DDMC/PTX complex was obtained using paclitaxel as the guest and DDMC as the host. The resulting nanoparticles were 200–300 nm in diameter and are thought to be useful as an anticancer drug delivery system because they form a stable polymeric micelle in water. The resistance of B16F10 melanoma cells to paclitaxel was confirmed using survival curve analysis. The DDMC/PTX complex showed superior anticancer activity to paclitaxel alone. The rate of mortality of the cell was determined using Michaelis–Menten equations, as the complex promoted an allosteric supramolecular reaction to tubulin. From our results, the DDMC/PTX complex was not extensively degraded in cells and achieved good efficacy as an intact supramolecular anticancer agent.

Dextran graft copolymers offer many opportunities for progress in various fields of medicine.

Acknowledgements This study is very thankful to the late Dr. Sadayoshi Kamia, professor emeritus of Nara Medical University, for his study of the Bio-Plastics and to the late Dr. George Butler, professor emeritus of University of Florida, for his encouragement and the education we received.

References

1. Mino G, Kaizerman K (1958) Polymerization initiated by ceric ion redox systems. *J Polym Sci* 31:242–243
2. Ite F, Takayama Y (1961) Graft polymerization of MMA onto cellulose. *J Chem Soc Jpn Ind Chem Sect [Kogyo Kagaku Zasshi]* 64:213–218
3. Nishiuchi T, Okazaki K (1972) Graft copolymerization of methyl methacrylate onto starch and triethylamino starch. *J Chem Soc Jpn Ind Chem Sect [Nippon Kagaku Zasshi]* 1972:1728–1734
4. Nishiuchi T, Okazaki K (1970) Graft copolymerization of methyl methacrylate onto carboxymethyl-cellulose. *J Chem Soc Jpn Ind Chem Sect [Kogyo Kagaku Zasshi]* 73:2699–2703
5. Wallace RA, Yong DG (1966) Graft polymerization kinetics of acrylamide initiated by ceric nitrate-dextran redox systems. *J Polym Sci Polym Chem Ed A-1* 1:1179–1190
6. Imai Y (1972) Anti-thrombogenic materials—role of heterogeneous surface microstructure. *Kobunshi* 21:569–573
7. Onishi Y, Maruno S, Kamiya S, Hokkoku S, Hasegawa M (1978) Preparation and characteristics of dextran-methyl methacrylate graft copolymer. *Polymer* 19:1325–1328
8. Onishi Y (1980) Effects of dextran molecular weight on graft copolymerization of dextran-methyl methacrylate. *Polymer* 21:819–824
9. Onishi Y, Maruno S, Hokkoku S (1979) Graft copolymerization of methyl methacrylate onto dextran and some properties of copolymer. *Kobunshi Ronbunshu* 36:535–541

10. Otsuka N et al (1972) The molecular-weight distribution of the grafted PMMA chains and molecular-weight of corresponding starch-fractions. *Kobunshi Kagaku* 29:930–935
11. Brckway CE, Seaberg PA (1967) Grafting of polyacrylonitrile to granular corn starch. *J Polym Sci A-1 Polym Chem* 5:1313–1326
12. Murata J, Ohya Y, Ouchi T (1966) Possibility of application of quaternary chitosan having pendant galactose residues as gene delivery tool. *Carbohydr Polym* 29:9–74
13. Sato T (2002) Carbohydrate polymer for gene delivery. *Kobunshi* 51:37–840
14. McCutchan JH, Pagano JS (1968) Enhancement of the infectivity of simian virus 40 deoxyribonucleic acid with diethylaminoethyl-dextran. *J Natl Cancer Inst* 41:51–358
15. Warden D, Thorne HV (1969) Influence of diethylaminoethyl-dextran on uptake and degradation of polyoma virus deoxyribo-nucleic acid by mouse embryo cells. *J Virol* 4:380–387
16. Constantin T, Vendrely C (1969) Effect of DEAE-dextran on the incorporation of tritiated DNA by cultured rat cells. *CR Soc Biol* 163:300–305
17. Mack KD, Wei R, Elbagarri A, Abbey N, McGrath SD (1998) A novel method for DEAE-dextran mediated transfection of adherent primary cultured human macrophages. *Immunol Methods* 211:79–86
18. Onisi Y, Kikuchi Y (2003) Study of the complex between DNA and DEAE-dextran. *Kobunshi Ronbunshu* 60:359–364
19. Onisi Y, Kikuchi Y (2004) Study of the complex between RNA and DEAE-dextran. *Kobunshi Ronbunshu* 61:139–143
20. Onishi Y (1987) US Patent 4816540
21. Onishi Y, Eshita Y, Murashita A, Mizuno M, Yoshida J (2005) Synthesis and characterization of 2-diethylaminoethyl (DEAE)-dextran-MMA graft copolymer for non-viral gene delivery vector. *J Appl Polym Sci* 98:9–14
22. Higashihara J, Onishi Y, Mizuno M, Yoshida J, Tamori, N, Dieng H, Kato K, Okada T, Eshita Y (2005) Transfection of foreign genes into culture cells using novel DEAE-dextran copolymer as a non-viral gene carrier. In: The 55th annual meeting of southern region, the Japan Society of Medical Entomology and Zoology, Miyazaki Prefecture Japan, October 23, Abstract 15
23. Onishi Y, Eshita Y, Murashita A, Mizuno M, Yoshida J (2007) Characteristics of 2-diethylaminoethyl(DEAE)-dextran-MMA graft copolymer as a non-viral gene carrier. *Nanomed Nanotech Biol Med* 3:184–191
24. Chinai S, Matlack JD, Resnic AL, Samuels RJ (1955) Polymethyl methacrylate: dilute solution properties by viscosity and light scattering. *J Polym Sci* 17:391–401
25. Pottenger CR, Johnson DC (1970) Mechanism of cerium (IV) oxidation of glucose and cellulose. *J Polym Sci* 8:01–318
26. Narita H, Okimoto S, Machida S (1969) Polymerization mechanism of methylmethacrylate initiated with ceric ion. *Makromol Chem* 125:5
27. Namikawa R, Okazaki H, Nakanishi K, Matsuno R, Kamikubo T (1977) Diffusion of amino acids and saccharides in solutions of dextran and its derivatives. *Agric Biol Chem* 41:1003–1009
28. Hintz HL, Johnson DC (1967) Mechanism of oxidation of cyclic alcohols by cerium (IV). *J Org Chem* 32:56–564
29. Ardon M (1957) Oxidation of ethanol by ceric perchlorate. *J Chem Soc* 1957:1811–1815
30. Duke FR, Forist AA (1949) The theory and kinetics of specific oxidation. III. The cerate–2,3-butanediol reaction in nitric acid solution. *J Am Chem Soc* 71:790–2792
31. Duke FR, Bremer RF (1951) The theory and kinetics of specific oxidation. IV. The cerate 2,3-butanediol reactions in perchlorate solutions. *J Am Chem Soc* 73:179–5181
32. Morita H (1956) Characterization of starch and related polysaccharides by differential thermal analysis. *Ann Chem* 28:64–67
33. Fox TG, Goode WE, Gratch S, Kincaid JF, Spell A, Stroupe JD (1958) Crystalline polymers of methyl methacrylate. *J Am Chem Soc* 80:1768–1769

34. Elmer TH, Nordberg ME, Carrier GB, Korda FJ (1970) Phase separation in borosilicate glasses as seen by electron microscopy and scanning electron microscopy. *J Am Ceram Soc* 53 (4):171–175
35. Kargina OV, Adorova IV, Kabanov VA, Kargin VA (1960) *Dokl Akad Nauk USSR* 170:1130
36. Bamford CH, Shiki Z (1968) Free-radical template polymerization. *Polymer* 9:595–598
37. Ferguson J, Shah SAO (1968) Further studies on polymerizations in interacting polymer systems. *Eur Polym J* 4:611–619
38. Tsuchida E, Osada Y (1975) Effects of macromolecular matrix on the process of radical polymerization of ionizable monomers. *J Polym Sci Polym Chem Ed* 13:559–569
39. Vogel MK, Cross RA, Bixler HJ (1970) Medical uses for polyelectrolyte complexes. *J Macromol Sci-Chem A4*(3):675–692
40. Singer SJ, Nicolson GL (1972) The fluid mosaic model of the structure of cell membranes. *Science* 175(4023):720–731
41. Sole A (1958) Die Stafoskopie der Tranen. *Klin Monatsbl Augenheilkd* 126:446–451
42. Nishioka K, Hara Y, Kamiya S, Matsuzawa Y, Iguchi M, Yamauchi A (1977) Crystals from vitreous. *F Ophthalm Jpn* 28:579–586
43. Bloomfield VA (1997) DNA condensation by multivalent cations. *Biopolymers* 44:269–282
44. Yoshikawa Y, Emi N, Kanbe T, Yoshikawa K, Saito H (1996) Folding and aggregation of DNA chains induced by complexation with lipospermine formation of a nucleosome-like structure and network assembly. *FEBS Lett* 396:71–76
45. Karak N, Maliti S (1997) Dendritic polymers: a class of novel materials. *J Polym Mater* 14:107–122
46. Schreier JB (1969) Modification of deoxyribonuclease test medium for rapid identification of *Serratia marcescens*. *Am J Clin Pathol* 51:711–716
47. Maes R, Sedwick W, Vaheri A (1967) Interaction between DEAE-dextran and nucleic acids. *Biochim Biophys Acta* 134:269–76
48. Pagano JS, McCutchan JH, Vaheri A (1967) Factors influencing the enhancement of the infectivity of poliovirus ribonucleic acid by diethylaminoethyl-dextran. *J Virol* 1:891–897
49. Price C, Woods DA (1973) Method for studying micellar aggregates in block and graft copolymers. *Eur Polym Sci* 9:827–830
50. Matsumura Y, Maeda H (1986) A new concept for macromolecular therapeutics in cancer chemotherapy: Mechanism of tumorotropic accumulation of proteins and the antitumor agent smancs. *Cancer Res* 46(12 Pt 1):6387–6392
51. Allen TM, Chonn A (1987) Large unilamellar liposomes with low uptake into the reticuloendothelial system. *FEBS Lett* 223:42–46
52. Oku N, Namba Y, Okada S (1992) Tumor accumulation of novel RES-avoiding liposomes. *Biochim Biophys Acta* 1126:255–260
53. Savic R, Luo L, Eisenberg A, Maysinger D (2003) Micellar nanocontainers distribute to defined cytoplasmic organelles. *Science* 300:615–618
54. Hamblin MR et al (2001) Polymer conjugate increases tumor targeting of photosensitizer. *Cancer Res* 61:7155–7162
55. Nishiyama N et al (2003) Free and N-(2-hydroxypropyl)methacrylamide copolymer-bound geldanamycin derivative induce different stress responses in A2780 human ovarian carcinoma cells. *Cancer Res* 63:7876–7882
56. Willstätter R, Pfannenstiel AI (1920) Über Succinyldiessigsäureester. *Justus Liebigs Ann Chem* 422:1–15
57. Eshita Y et al (2009) Mechanism of introducing exogenous genes into cultured cells using DEAE-dextran-MMA graft copolymer as non-viral gene carrier. *Molecules* 14:2669–2683
58. Onishi Y, Eshita Y, Mizuno M (2009) DEAE-dextran-MMA graft copolymer matrices for nonviral delivery of DNA. In: Jorgenson L, Nielson HM (eds) *Delivery technologies for biopharmaceuticals*. Wiley, West Sussex
59. Onishi Y, Eshita Y, Murashita A, Mizuno M, Yoshida J (2008) A novel vector of 2-diethyl aminoethyl(DEAE)-dextran-MMA graft copolymer for non-viral gene delivery. *J Gene Med* 10:472

60. Onishi Y, Eshita Y, Mizuno M (2009) DEAE-dextran and DEAE-dextran-MMA graft copolymer for nonviral delivery of nucleic acids. In: Bartul Z, Trenor J (eds) *Advances in nanotechnology*, vol 3. Nova, New York, NY
61. Onishi Y, Eshita Y, Mizuno M (2010) DEAE-dextran and DEAE-dextran-MMA graft copolymer for nanomedicine. *Polym ResJ* 3:415–453
62. Eshita Y et al (2011) Mechanism of the introduction of exogenous genes into cultured cells using DEAE-Dextran-MMA graft copolymer as a non-viral gene carrier. II. Its thixotropy property. *J Nanomed Nanotechnol* 2:1–8
63. Yguerabide J, Yguerabide EE (1998) Light-scattering submicroscopic particles as highly fluorescent analogs and their use as tracer labels in clinical and biological applications. *Anal Biochem* 262:137–156
64. Nakano TK, YadeT OY (2001) Dibenzofulvene, a 1,1-diphenylethylene analogue, gives a π -stacked polymer by anionic, free-radical, and cationic catalysts. *JACS* 123(37):9182–9183
65. Grants-in-Aid for Scientific Research on Innovative Areas, MEXT, Japan (Project No. 4201), Miyano S (2011) Cancer and supercomputer. *CICSJ Bull* 29:42–48
66. Cheng Y, Prusoff WH (1973) Relationship between the inhibition constant (KI) and the concentration of inhibitor which causes 50 per cent inhibition (I50) of an enzymatic reaction. *Biochem Pharmacol* 22:3099–3108
67. Hill AV (1910) The possible effects of the aggregation of the molecules of hemoglobin on its dissociation curve. *J Physiol* 40(4):iv–vii, Retrieved 18 Mar 2009
68. Wadsworth P, Khodjakov A (2004) E pluribus unum: towards a universal mechanism for spindle assembly. *Trends Cell Biol* 14:413–419
69. Minoura I, Muto E (2006) Dielectric measurement of individual microtubules using the electroorientation method. *Biophys J* 90:3739–3748

Chapter 7

Polysaccharide Hydrogels: Synthesis, Characterization, and Applications

Jaspreet Kaur Bhatia, Balbir Singh Kaith, and Susheel Kalia

Abstract This chapter deals with the review on natural backbone-based superabsorbent hydrogels and their classification based upon method of preparation, monomer type, and ionic charge. The applications of hydrogels in different fields like biomedical, pharmaceuticals, agriculture, metal ion sorption, etc., have been discussed in this chapter. The polysaccharide-based hydrogels are eco-friendly, cost effective, biodegradable, and biocompatible in nature. They can be characterized by different techniques like FTIR, SEM, XRD, AFM, TGA, DTA, DTG, and DSC.

Keywords Polysaccharide • Hydrogels • Control release • Thermal studies • Drug delivery

7.1 Introduction

Hydrogels are three-dimensional network systems which can imbibe large amount of solvent without showing solubility. They are considered as superabsorbent as they can absorb aqueous solvent more than 20 times of their initial weight. The era of hydrogels begins from the late 1950s with the synthesis of biomaterials based upon copolymers of 2-hydroxyethylmethacrylate and ethylene dimethacrylate by Wichterle and Lim [1]. The late 1960s and early 1970s were the era of research on

J.K. Bhatia

Department of Chemistry, Lyallpur Khalsa College, Jalandhar 144001 Punjab, India

B.S. Kaith (✉)

Department of Chemistry, Dr. B.R. Ambedkar National Institute of Technology (NIT),

Jalandhar 144 011, Punjab, India

e-mail: bskaith@yahoo.co.in

S. Kalia

Department of Chemistry, Bahra University, Wahnaghat, Dist. Solan 173234, HP, India

the synthesis of hydrogels by different methods and techniques [2]. The early methods of synthesis of hydrogels were focused on the control of detailed structure of hydrogels, whereas recent scenario has shifted to applicability of hydrogels in diversity fields. They form three-dimensional swollen networks through covalent or ionic linkages between homopolymer and copolymers. Three-dimensional networks can be obtained by different techniques like copolymerization, interpolymer complexes, and semi-interpenetrating polymerization. The hydrophobicity of backbone polymers and density of cross-linking are the governing parameters for different structural properties. The advancement in technology and novel methodologies of genetic engineering diverts the research towards the synthesis of stimuli responsive hydrogels. Hydrogels can respond distinctively towards the external environmental conditions like temperature, pH, magnetic field, electric stimuli, and ionic strength. Such hydrogels are called smart polymers and have widened the area of applicability. Hydrogels with controlled biodegradability, stability towards chemicals and biochemicals, shape stability, biocompatibility, and high permeability of water-soluble nutrients and metabolites are the novel biomaterials of present era. The distinct features make them successful polymeric biomaterials in different fields. Various biomaterials like cellulose, starch, chitosan, and guar gum have been modified for their use in metal ion sorption, controlled drug delivery systems, water treatment processes, pesticides and herbicides delivery, and many other agricultural, biotechnological, and medicinal fields [3–6].

7.2 Classification of Hydrogels

Polysaccharide hydrogels can be classified on the basis of method of synthesis, types of monomer involved, and ionic charges.

7.2.1 On the Basis of Method of Preparation

On the basis of method of synthesis, hydrogels can be physically cross-linked or chemically cross-linked.

7.2.1.1 Physical Hydrogels

These are reversible and unstable hydrogels in which polymer networks are held together by secondary forces. The forces of interactions between polymeric networks may be ionic, hydrogen bonding, or hydrophobic interactions. The stability of these hydrogels depends upon the external conditions. The interactions may get weak by change in environment or by application of stress. Physically cross-linked hydrogels have wide applications in biomedical and pharmaceutical field as

it does not require any cross-linking agent. Blends of starch–carboxymethyl-cellulose, gelatine–agar form physically cross-linked hydrogels [7–9]. Chitosan solution containing glycerol-2-phosphate results in the formation of hydrogel at 37 °C due to hydrophobic interactions [10].

7.2.1.2 Chemical Hydrogels

These are irreversible and stable hydrogels involving chemical cross-linking between polymeric networks. Chemical cross-linking involves reaction of polymeric backbone with cross-linking agent. Polysaccharides have functional groups like hydroxyl or amine group which on reaction with cross-linking agent form gel structure. Cross-linking may occur by different mechanisms like condensation, addition, and vulcanization. These hydrogels having strong covalent bonds can attain equilibrium swelling state which depends upon the polymer–solvent interactions and cross-link density. Polysaccharides like cellulose and its derivatives, chitosan, alginate, dextran, guar gum, and starch, can be cross-linked in the presence of chemical reagents and in the presence of radiations to form chemical hydrogels [11, 12].

7.2.2 *On the Basis of Types of Monomer Units Involved*

Hydrogels can be categorized into three types: homopolymer hydrogels, copolymer hydrogels, and interpenetrating polymeric hydrogels.

7.2.2.1 Homopolymer Hydrogels

Homopolymer hydrogels have single specie as basic unit in the polymer matrix. The single monomer unit cross-links to form three-dimensional network structures. The cross-linked networks are formed in the presence of cross-linking agent or without the presence of cross-linking agent. Cellulose hydrogels were reported through one-step method in which cellulose was dissolved directly in urea/NaOH solutions in the presence of epichlorohydrin as cross-linker. It resulted in fully transparent hydrogel with macroporous inner structure [13]. Irradiation of polysaccharide solutions results in the formation of hydrogels in the absence of gelating agent. Commercial polysaccharides like xanthan, pectin, guar gum, alginate, starch, xanthan, chitin, and chitosan can be modified in the presence of high-energy radiations to form hydrogels [14].

7.2.2.2 Copolymer Hydrogels

Copolymer hydrogel contains two or more monomeric units in which at least one of the monomer is hydrophilic. Copolymer hydrogels have different arrangements of

copolymers like random, block, or alternative with respect to main polymeric chain. The properties of copolymer hydrogels depend upon the varied combination of polymeric units and respective arrangements of these polymeric networks. Polysaccharide copolymer hydrogels may involve two different polysaccharide units or combination of a polysaccharide with synthetic polymer. Blend hydrogels based upon carboxymethylcellulose and carboxymethyl chitosan were reported for metal absorption of Pb and Au [15, 16].

7.2.2.3 Interpenetrating Polymer Network Hydrogels

These hydrogels involve two independent cross-linked networks. These cross-linked networks intermesh into each other in the presence of cross-linker. One polymeric network swells in the network of another polymer results in the formation of interpenetrating polymeric network. These are called semi-IPN when one of the components is cross-linked, while the other component remains uncross-linked. The properties of these interpenetrating polymer network hydrogels (IPNs) depend upon relative hydrophilicity and hydrophobicity of two polymeric networks. IPN hydrogels of alginate and hydrophobically modified ethyl hydroxyl ether cellulose have been studied for gelation behavior [17]. pH and temperature-sensitive semi-interpenetrating polymer network hydrogel based on linear carboxymethyl chitosan and poly(*N*-iso-polyacrylamide) cross-linked with organic clay were reported [18]. IPN hydrogel based on chitosan and *N*-vinylpyrrolidone was prepared with photopolymerization technique [19].

7.2.3 On the Basis of Ionic Charge

On the basis of ionic charge, hydrogels are divided into three categories: neutral, ionic, and amphoteric hydrogels.

7.2.3.1 Neutral Hydrogels

These hydrogels have neutral monomeric units which cross-link to form three-dimensional networks. These nonionic hydrogels may be homopolymeric or copolymeric in nature. The copolymeric polysaccharide hydrogels with monomers like acrylamide, hydroxyalkyl methacrylates, and *N*-vinyl pyrrolidone result in neutral hydrogels. These hydrogels are temperature sensitive resulting in swelling–deswelling behavior with change in temperature. Swelling behavior depends upon the equilibrium between sub-chain stretching and osmotic pressure of solvent. Neutral polysaccharide hydrogels mainly involve covalent cross-linking. These hydrogels have permanent polymer networks as linkages formed are irreversible. This type of linkage allows absorption of water without dissolution and thus allows drug release by diffusion [20].

7.2.3.2 Ionic Hydrogels

Ionic hydrogels contain charged anionic or cationic monomeric species. These may be homopolymeric involving only ionic polymer network or copolymer of ionic and neutral polymer network. These may be formed by modifications in neutral hydrogels by partial hydrolysis or addition of excess of polyelectrolytes. Monomers like acrylic acid derivatives, crotonic acid, and sodium styrene sulphonate result in anionic hydrogels, whereas monomers like aminoethylmethacrylate and 4-vinyl pyridine form cationic hydrogels. Ionic hydrogels are biocompatible and well tolerated. They result in the formation of nonpermanent network due to reversible links. Ionically cross-linked chitosan hydrogels show a higher swelling sensitivity to pH changes compared to covalently cross-linked chitosan hydrogels [21].

7.2.3.3 Ampholytic Hydrogels

Ampholytic hydrogels have polymeric networks having both positively and negatively charged monomeric species. The properties of ampholytic hydrogels depend upon the presence of ionic species along the polymer chain. Oppositely charged solutions have coulombic attractions between them due to which ampholytic hydrogels have interionic as well as intra-ionic attractions. These interactions are weaker than covalent interactions but are stronger than van der Waals forces. Monomeric units like acrylic acid, maleic anhydride, and *N*-vinyl succinimide result in ampholytic hydrogels [22].

7.3 Synthesis of Hydrogels

Hydrogel synthesis involves the linking of macromolecular chains together which progressively results in the development of three-dimensional networks. Formation of network structure involves formation of branched polymer at initial stage which slowly increases in size and results in gel/network structure. This process can be recognized as sol–gel transition or gelation. Cross-linking may be achieved by different techniques depending upon involvement of physical or chemical cross-linking. Various synthesis methods have been reported for the synthesis of polysaccharide-based hydrogels like cellulose, chitin, and alginate.

7.3.1 Physical Cross-Linking

It results in the formation of hydrogels in which networks are held together by secondary forces like ionic interactions, hydrophobic interactions, and hydrogen

bonding. Synthesis of hydrogels involving physical cross-linking does not require any cross-linking agent. Physical cross-linked polysaccharide hydrogels can be synthesized by different techniques like heating/cooling of polymer solution, ionic interactions, H-bonding, heat-induced aggregation, complex coacervation, and freeze drying.

Cooling of hot solution of polysaccharide results in the formation of hydrogel. On cooling of hot solution of polymer, helix formation takes place which results in the formation of junction zones having physical interactions. The stable gels are formed if cooling occurs in the presence of salts like K^+ , Na^+ which further aggregates the helices to form stable gels. Physical cross-linking may also occur by reverse process, i.e., heating of polymer solution. Heating of polymer solution results in block copolymerization. Synthesis of carrageen hydrogels has been reported by cooling of hot solution [23].

Ionic interaction results by mixing of negatively charged polymer with positively charged polymer. This can be achieved by addition of di- or trivalent counter ion polymer solution. Dextran coated with anionic and cationic polymers when mixed together results in the formation of network structure due to formation of ionic complex between oppositely charged polymers. Formation of ionic hydrogels have been reported for chitosan–dextran, chitosan–glycerol phosphate, and chitosan–poly(lysine) hydrogels [24].

Hydrophobic interaction may also result in the formation of physically cross-linked hydrogels. Chitosan–poly(ethylene oxide) hydrogels have hydrophobic interactions which result in the formation of cross-linked network. These hydrogels have been studied for the release of bovine-serum albumin [25].

Hydrogen-bonded hydrogels can be synthesized at low pH. It involves cross-linking of polymeric solution in the presence of acid or polyfunctional monomer. Carboxymethylated chitosan hydrogel can be synthesized in the presence of acid. H-bonding can be achieved by mixing of two polymeric solutions having desirable functional groups for hydrogen bonding. Mixing of alginate and xanthan polysaccharides results in the formation of hydrogels due to intermolecular hydrogen bonding between them [26].

Freeze drying is a simple and effective method to develop physically cross-linked hydrogels. It involves the formation of microcrystals in polymeric structure. Microporous hydroxypropyl cellulose hydrogels were synthesized by freeze drying and subsequent rehydration of gels. This method of synthesis has also been reported for xanthan hydrogels [27].

Self-assembling of polymer to form stereocomplex is a new concept for the formation of physically cross-linked hydrogel. To form hydrogel cross-linked by stereocomplex formation, enantiomeric lactic acid and methylmethacrylate oligomers have been used. These enantiomeric oligomers were coupled to polymer backbone to form hydrogel structure. Self-assembled hydrogels can be obtained by mixing of aqueous solution of each polymeric solution at room temperature. Self-assembled hydrogel has been reported by stereocomplex formation in aqueous solution of enantiomeric lactic acid grafted to dextran [28].

7.3.2 Chemical Cross-Linking

Chemical cross-linking results in permanent or chemical hydrogels having covalent linkages. These hydrogels can attain equilibrium swelling state depending upon the cross-linking density and intensity of interaction of polymer with water. Chemical cross-linking may proceed with polymerization of functional groups present on backbone, polymerization in the presence of cross-linking agent, and polymer–polymer cross-linking. Polysaccharide-based hydrogels involving chemical cross-linking can be synthesized by different techniques.

Chemically cross-linked polysaccharide hydrogels can be synthesized in the presence of cross-linking agent. Different cross-linking agents like glyceraldehydes, formaldehyde, epichlorohydrin, and *N,N'*-methylenebisacrylamide have been reported for the synthesis of polysaccharide-based hydrogels. Cross-linking involves active reaction sites like –OH groups on the polysaccharide backbone. Cross-linking on polysaccharide backbone may proceed via condensation reaction [29], Michael addition [30], hydrazone bonding [31], and enzymatic cross-linking [32]. A carboxymethyl cellulose sodium salt and hydroxyethyl cellulose hydrogels have been prepared using divinyl sulfone as cross-linker to develop novel system for the body water elimination for treatment of edema [33]. Cross-linked carboxymethyl konjac glucomannan was synthesized by reaction of monochloroacetic acid, konjac glucomannan, and monochloroacetic acid. Cross-linked hydrogels were used to absorb Cu^{2+} , Pb^{2+} , and Ca^{2+} ions from aqueous solution [34]. Hyaluronic acid has been cross-linked with α - β -polyacryl hydrazide [35].

Radiation cross-linking is another technique to synthesize hydrogels. It does not involve the use of chemical agents, thereby an important method to develop biocompatible hydrogels. Single-step synthesis and cost-effectiveness are the other advantages of radiation cross-linking. Radiation cross-linking of hydrogels may proceed in the presence of high-energy radiations like gamma radiations, electron beam, or X-rays [36]. The cross-linking may occur in dilute solution, in concentrated solution, or in solid state. In case of radiation-induced cross-linking, in aqueous state, irradiation of dilute solution results in the absorption of radiation by water molecules which generate free radicals to activate polysaccharide backbone. Radiation-induced cross-linking of carboxymethyl cellulose was investigated in aqueous solution at various radiation doses. Cross-linking was observed in 5 % aqueous solution [37]. Blend hydrogels of carboxymethylcellulose and carboxymethyl chitosan were prepared by gamma irradiation of high-concentrated aqueous solution for metal adsorption of Pb and Au [38]. Irradiation of polysaccharides in solid state results in the generation of free radicals directly on polymer chain. The breakdown of glycosidic bond is the primary reaction involved in solid state irradiation. It may result in degradation of polysaccharide which depends upon the concentration of reactants and temperature. Carboxymethyl cellulose, gum arabic, and dextran have been modified in solid state by high-energy radiations to synthesize hydrogels [39].

Graft copolymerization is one of the promising techniques for the synthesis of chemical hydrogels [40]. Grafting involves covalent linkages of a monomer onto polymer backbone. Graft copolymerization in the presence of suitable chemical reagent or high-energy radiations results in the formation of macro-radicals which further cross-link to form gel structure [41]. The presence of initiators and radiations activates the polysaccharide backbone chain which leads to infinite branching and cross-linking [42]. The use of different chemical reagents as initiators has been reported to activate the backbone. Psyllium has been functionalized with acrylamide in the presence of potassium persulfate (KPS)-hexamethylenetetramine (HMTA) as an initiator-cross-linker system. After the initial optimization of different reaction parameters, the resultant hydrogel was used for the absorption of water from different water-oil emulsions [43]. Psyllium hydrogels have also been synthesized under the influence of gamma radiations in the presence of hexamethylenetetramine as cross-linker [44]. Electrosensitive hydrogels based upon gum ghatti were synthesized by graft copolymerization with acrylamide using potassium persulfate-ascorbic acid initiator system and *N,N*-methylenebisacrylamide as cross-linking agent [45]. Thermo- and pH-sensitive hydrogels have been prepared by graft copolymerization of chitosan and *N*-isopropyl acrylamide. Radiation-induced grafting of acrylamide onto chitosan resulted in the synthesis of hydrogels which can act as excellent flocculants [46]. Carboxymethyl cellulose-based hydrogels have been synthesized using electron beam irradiated grafting of acrylic acid onto CMC [47].

7.4 Characterization

The characterization of hydrogels gave idea about their structural as well as physicochemical properties. Techniques employed for characterization depend upon the target application. Different techniques have been developed to study the properties like swelling behavior, release kinetics, and mechanical properties [48].

Macroscopic studies have been done to understand the properties of hydrogels at microscopic and nanoscale. SEM is widely utilized to examine the surface morphology of polysaccharide hydrogels. SEM was used to study the interior morphology of dextran hydrogels and to determine the pore characteristics [49]. SEM analysis of gel networks differentiated between enzymatically and chemically synthesized dextran hydrogels on the basis of pore size. The enzymatically synthesized hydrogels showed more uniform pore size than chemically prepared hydrogels [50]. SEM images have also been utilized to compare acetone-dehydrated versus air-dried cellulose-based hydrogels. Acetone-dehydrated hydrogel showed folding and voids, whereas air-dried cellulose hydrogel showed smooth and dense surface [51]. SEM images provide evidences for the occurrence of chemical modifications like graft copolymerization onto hydrogel surface. The graft copolymerization onto glucomannose with acrylic acid was confirmed by

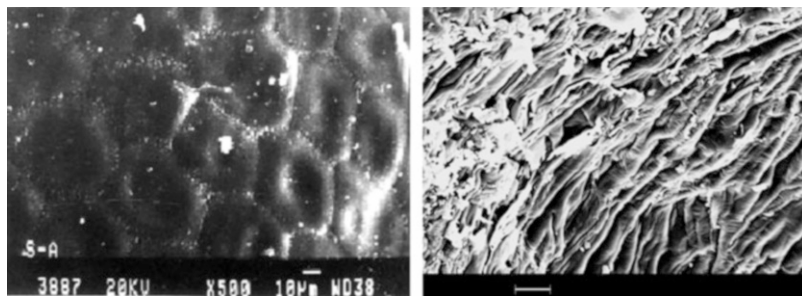


Fig. 7.1 SEM of (a) psyllium and (b) cross-linked Psy-g-poly(AA) [53]

SEM micrograms of before and after graft copolymerization. Surface was found to be less smooth, having caves and holes after graft copolymerization [52]. SEM images of psyllium hydrogel showed marked differences before and after cross-linking (Fig. 7.1). Psyllium has smooth homogeneous surface, while cross-linked psyllium with poly(acrylic acid) showed network structure with cross-linking in the form of overlapped fibrils [53].

AFM is an important technique to study smooth gel surface with nanometer-sized protrusions and provide quantitative information regarding topography. AFM also provides information regarding mechanical properties and local elastic properties of hydrogel surface [54].

Fourier transform infrared spectroscopy is used to determine the nature of modification of hydrogels [55]. Introduction of acrylamide group in psyllium was confirmed by FTIR spectrum which showed emergence of new bands at 1666.7 cm^{-1} (C=O stretch) and 1425.4 cm^{-1} (N-H in plane bending) and 1249.9 cm^{-1} (C-N stretching vibration) besides peaks obtained with that of psyllium (Fig. 7.2) [56]. Gum arabic showed peaks for O-H stretch at 3365.2 cm^{-1} and C-O stretch at 1042.9 cm^{-1} . On the other hand, cross-linked gum arabic revealed peaks at 1725.1 cm^{-1} and 1631.2 cm^{-1} due to C=O stretch which confirms the graft copolymerization onto gum arabic [57].

TGA, DTA, DTG, and DSC are the different techniques to study the thermal behavior and stability of hydrogels. Thermogravimetric analysis of polysaccharide hydrogels is carried out as a function of weight loss versus temperature. Degradation of hydrogels that occurs in different stages corresponds to deacetylation, dehydration, and decarboxylation which may result in single phase or two or more phases of decomposition. TGA of gum ghatti as well as of cross-linked hydrogel showed two stages of decomposition. However, final decomposition temperature of cross-linked hydrogel was found to be higher than that of gum ghatti itself. This could be accounted to the strengthening of amorphous region on cross-linking which increased the stability of hydrogels [58]. Cross-linking of gum arabic with methylmethacrylate enhanced the thermal stability of hydrogel. This is evident from TGA and DTA studies. Cross-linked hydrogel shows high final decomposition

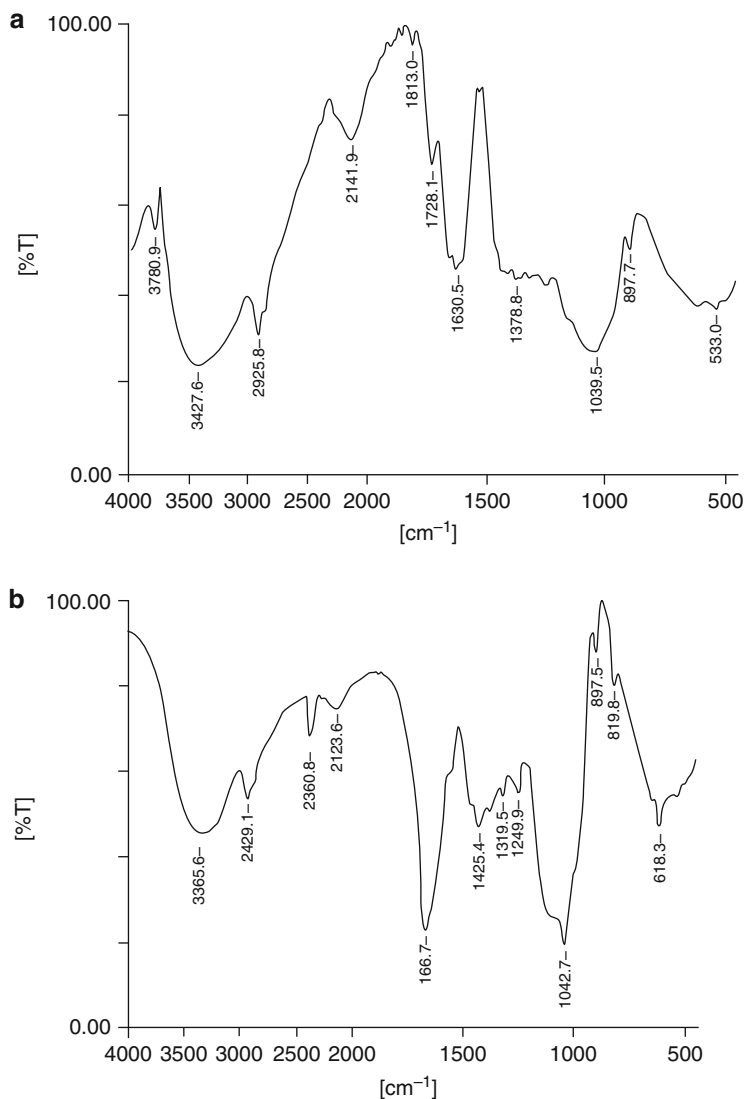


Fig. 7.2 FTIR spectra of (a) psyllium and (b) Psy-cl-poly(AAm) [56]

temperature in TGA studies which were further proved with DTA studied showing high decomposition temperature (Fig. 7.3, [57]).

The knowledge of mechanical properties of hydrogels is required to adequately design and for the efficient use of hydrogels. Polysaccharide hydrogels have been widely studied for tissue engineering applications. Assessment of mechanical properties is useful to design adequate scaffolds for engineering tissues. Modification of polysaccharide hydrogels also affects the mechanical properties of these

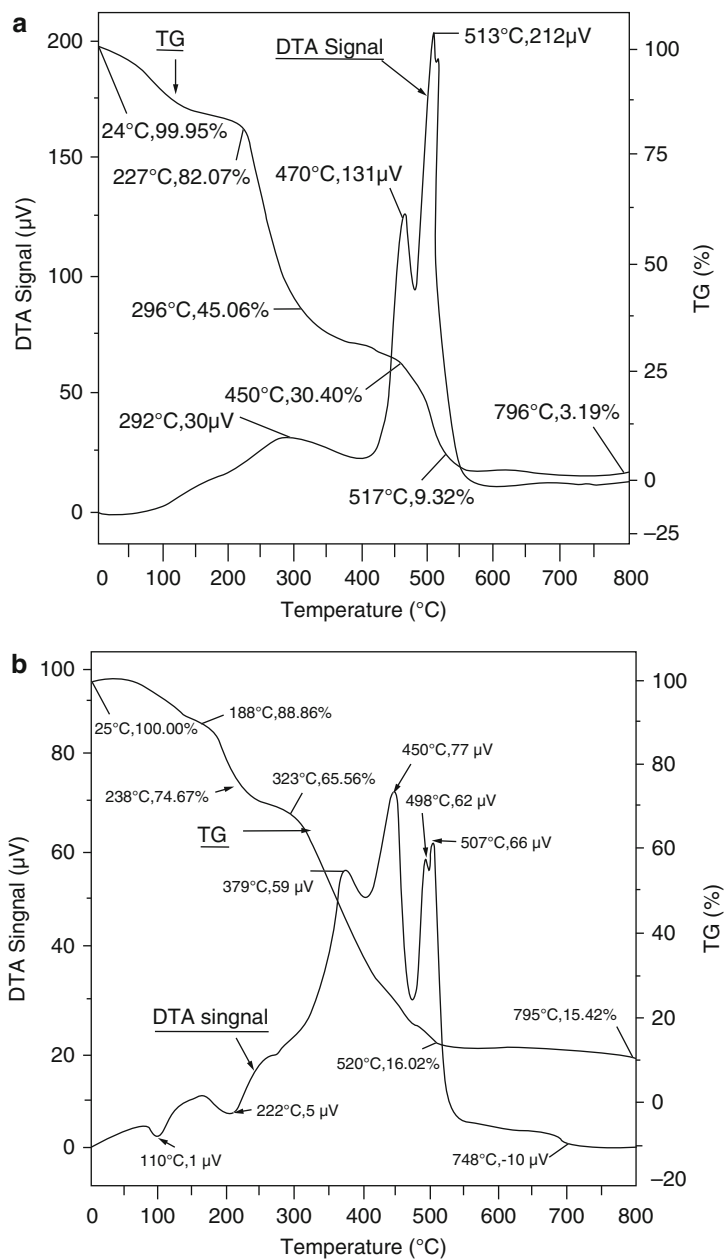


Fig. 7.3 DTA/TGA of (a) gum arabic and (b) GA-cl-poly(MAA) [59]

hydrogels. Many of these properties have been determined for different polysaccharide hydrogels. There is significant data published in regard to mechanical properties of alginate hydrogels. Compressive strength of alginate hydrogels was found to be in the range of less than 1 kPa to more than 1,000 kPa [59, 60]. Shear strength of alginate showed values in the range of 0.02–0.04 kPa [61]. Mechanical properties of hydrogels depend on the cross-linker, storage environment, and gelling environment [62]. Dynamo-mechanical analysis of guar gum hydrogel was performed at three different temperatures to analyze hardness, cohesion, and young modulus which were found to be temperature dependent [63].

7.5 Applications of Polysaccharide Hydrogels

Polysaccharide hydrogels due to their dynamic structural properties have been employed for various potential applications. Polysaccharide-based hydrogels have been commonly utilized in numerous biomedical applications like coatings, as homogeneous materials like contact lenses and devices like sustained drug delivery systems, and as agricultural applications like water storage granules and controlled release of pesticides. These hydrogels are also used in important industrial fields like electrophoresis, chromatography, and protection of technical and electronic instruments, food industry, cosmetic industry, and many more [64, 65].

7.5.1 Biomedical Applications

Polysaccharide hydrogels have been employed for a wide range of biomedical applications. The success of polysaccharide hydrogels as biomaterials is mainly due to their satisfactory performance upon in vivo transplantation and their ability to fabricate into a wide range of morphologies. The use of polysaccharide hydrogels is related to their biocompatibility. Low toxicity, structural similarity to natural materials, and degradation by enzymes are the other properties which make polysaccharide hydrogels a suitable candidate for different biomedical applications.

Among various biomedical applications, hydrogel-based drug delivery devices have become the major area of interest and gained success at the industrial level. A large number of polysaccharide hydrogels have been studied for colon-specific drug carrier systems like chitosan, pectin, dextran, guar gum, and konjac glucomannan [52]. Colon region has been considered as potential adsorption site for proteins and peptides. Carboxymethylcellulose and acrylic acid-based hydrogels have been studied for colon-specific drug carrier for the release of theophylline as a function of time at pH 1 and 7 [66]. Cross-linked hydroxypropyl methyl cellulose hydrogel was found to be a promising drug delivery system for the colon-specific release of antiulcerative colitis drugs [67]. Dextran hydrogels cross-linked with diisocyanate showed potential application for colon-specific drug delivery [68]. Kulkarni and Sa

studied the drug release characteristics of (polyacrylamide-g-xanthan)-carboxymethyl cellulose-based IPN hydrogels [69]. The different cellulose ether-based hydrogels were investigated for swelling behavior, and order of mesh size was found to be the most important parameter for drug diffusion and release [70]. Thermoresponsive acrylic hydrogels having carboxymethylcellulose matrix prepared by emulsion polymerization were employed for transdermal drug release systems at different temperatures [71]. Hydrogel matrix tablet of acarbose was formulated using hydroxypropylmethyl cellulose and guar gum to study the release kinetics and to attain a near-zero release kinetics. These matrix tablets were found suitable for maintenance portion of oral-controlled release tablet [72]. Semi-interpenetrating network hydrogel blends of gelatine and hydroxyethyl cellulose were investigated for the controlled release of antiasthmatic drug theophylline. Drug release profile was investigated in terms of the amount of cross-linker and percentage loading [73].

Chitosan hydrogels have been extensively studied as drug delivery systems. Due to biological properties, it is an attractive material for ophthalmic drug delivery, nasal delivery, intestinal drug delivery, and transdermal delivery [74, 75]. Covalently cross-linked chitosan hydrogels showed pH-controlled drug delivery as the presence of chemical linkages allows drug release by diffusion [76]. *N*-chitosan derivative-based ophthalmic drug delivery system has been developed using supercritical solvent impregnation technique. The tuneable SSI method was found to be an easy and efficient method for desired drug levels according to patient's need [77]. Injectable hydrogels have also been developed as drug carriers, gene carriers, and scaffolds. Injectable chitosan-based hydrogels were investigated as drug delivery matrix to be applied as sealant after ear–nose–throat surgery. These chitosan-based hydrogels showed controlled drug delivery profile for dexamethasone. On cross-linking with oxidized polymer material, chitosan showed more promising results [78].

Polysaccharide hydrogels have been widely studied in the tissue engineering applications. Longer and Vacantie elucidate the ways in which polymer gels are utilized in tissue engineering to repair damage tissues. Hydrogels have been used as scaffolds for cellular organization, as tissue barriers and bioadhesives, and to encapsulate and deliver cells [79]. Hydrogels can be used as scaffold materials as their mechanical properties can be modified to match with natural tissues. Homogeneous alginate hydrogels were formulated as scaffolds for cell culture due to their ability to encapsulate cells under milder conditions. Alginate hydrogels have been employed for the encapsulation of number of cell type like osteoblasts, chondrocytes, neutral stem cells, and mesenchymal cells [80, 81]. Chitosan-based hydrogels have been widely studied for cell transplantation and tissue regeneration. Biodegradable hydrogels based on guar gum methacrylate macromonomer have been studied for in situ fabrication of tissue engineering scaffolds [82]. Methacrylated glycol chitosan hydrogels using blue light initiator riboflavin offer a promising photoinitiator system in tissue engineering application. RF photoinitiated hydrogels supported proliferation of encapsulated chondrocytes and extracellular matrix deposition. The feasibility of these system in situ gelling

hydrogels was further demonstrated in osteochondral and chondral defect models for potential cartilage tissue engineering [83]. Hyaluronic acid grafted with dextran tyramine conjugate was investigated as injectable biomimetic hydrogels for cartilage tissue engineering. The design of these hybrid hydrogels was based on the molecular structure of proteoglycans present in the extracellular matrix of natural cartilage. These hydrogels have enhanced chondrocyte proliferation and matrix production which is an important cartilage tissue engineering application [84].

Wound dressing is one of the important biomedical applications for polysaccharide hydrogels. Their adhesive nature, antifungal and bactericidal characteristics, and permeability to oxygen are the important properties associated with treatment of wound and burns. Chitosan and its derivative-based hydrogels have been widely studied as wound dressing materials [85]. A wound dressing material from alginates was developed by loaded asiaticoside on alginate films by indirect cytotoxicity and direct cell culture [86]. Periodic oxidized alginate cross-linked gelatin in the presence of borax to give in situ forming hydrogels. These hydrogels have hemostatic effect of gelatine, wound healing feature of alginate, and antiseptic property of borax which make it a potential wound dressing material [87]. Synthetic extracellular matrix, implantable devices, biosensors, valve to control permeability across porous membranes, and smart microfluidics are the other applications of polysaccharide hydrogels in biomedical field.

7.5.2 Agriculture Applications

Storage of water in different agriculture fields has remained a challenging task. Hydrogels have been commonly utilized as water storage granules in agriculture fields. Cellulose-based hydrogels are the potential materials to absorb and retain water. Sannino and coworkers develop cellulose-based hydrogels which can absorb 1 l of water per gram of dry material. The hydrogel sorption capacity has been tested at different ionic strengths. The soil with the small amount of hydrogel remains humid for period four times more than without hydrogel. Polysaccharide hydrogels have attracted great deal of attention as potential delivery devices for control release applications [88]. The sodium alginate cross-linked with glutaraldehyde was investigated as a vehicle carrier for the encapsulation and release of natural liquid pesticide neem seed oil. An increase in the degree of cross-linking decreased the release of pesticide [89]. Starch–alginate–clay beads with different compositions were investigated for the release of thiram, a dithiocarbamate fungicide. The maximum release of thiram was of about 10 mg after 30 h [90]. Microsphere of sodium alginate and starch using CaCl_2 as a cross-linker was found to be a promising carrier for the control release of pesticide chlorpyrifos. Optimum fractional release accounts for a bead composition with more alginate and less starch [91]. Starch/ethylene glycol-co-methacrylic acid was designed for controlled delivery of pesticides like fluometuron, thiophanate methyl, and trifluralin. The pesticide release rate was found to decrease as the irradiation was done and pH

was increased and found to increase with MMA content, pesticide concentration, and temperature increase [92].

7.5.3 Metal Ion Sorption

Heavy metal ion sorption is an important application of polysaccharide hydrogels. Psyllium husk and acrylic acid-based polymeric networks using *N,N'*-methylene bis-acrylamide as cross-linker were studied for removal, separation, and enrichment of hazardous metal ions from aqueous solution [93]. Polymer networks based on cellulose and its derivatives like hydroxypropyl cellulose, cyanoethyl cellulose, hydroxyethyl cellulose, hydrazinodeoxy cellulose, cellulose phosphate with acrylamide, and *N,N'*-methylene bis-acrylamide were studied for sorption of Fe^{2+} , Cu^{2+} , and Cr^{2+} ions [94]. Hydrophilic hydrogels based on poly(acrylic acid) and sodium alginate prepared through gamma radiation method showed affinity towards the metal sorption of Cu^{2+} , Co^{2+} , and Ni^{2+} ion [95].

7.6 Conclusion

Polysaccharide-based hydrogels are biodegradable and eco-friendly materials which exhibit promising applications in different fields. Moreover, their availability from natural resources and low cost make them more attractive smart polymeric materials. Innovative hydrogel products have thus been developed as personal hygiene products, underwater devices, water reservoirs for dry soils, and biomedical devices, including soft contact lenses, lubricating surface coatings, phantoms for ultrasound-based imaging, controlled drug release devices, wound healing dressings, and bioactive scaffolds for regenerative medicines.

References

1. Wichterle O, Lim D (1960) Hydrophilic gels for biological use. *Nature* 185:117–118
2. Krejci L, Harrison R, Wichterle O (1970) Hydroxyethyl methacrylate capillary strip animal trials with a new glaucoma drainage device. *Arch Ophthal* 84:76–82
3. Kaith BS, Jindal R, Mittal H (2010) Superabsorbent hydrogels from poly(acrylamide-co-acrylonitrile) grafted Gum ghatti with salt, pH and temperature responsive properties. *Der Chemica Sinica* 1:92–103
4. Kaith BS, Ranjta S (2010) Synthesis of pH—thermosensitive gum arabic based hydrogel and study of its salt-resistant swelling behavior for saline water treatment. *Desalin Water Treat* 24:28–37
5. Jamnongkan T, Kaewpirom S (2010) Controlled-release fertilizer based on chitosan hydrogel: phosphorus release kinetics. *Sci J UBU* 1:43–50

6. Leonardis M, Palange A, Dornelles RF, Hund F (2010) Use of cross-linked carboxymethyl cellulose for soft-tissue augmentation: preliminary clinical studies. *Clin Interv Aging* 5:317–322
7. Liu J, Lin S, Li L, Liu E (2005) Release of theophylline from polymer blend hydrogels. *Int J Pharm* 298:117–125
8. Bajpai AK, Shrivastava J (2005) In vitro enzymatic degradation kinetics of polymeric blends of crosslinked starch and carboxymethyl cellulose. *Polym Int* 54:1524–1536
9. Gupta D, Tator CH, Shoichet MS (2006) Fast-gelling injectable blend of hyaluronan and methylcellulose for intrathecal, localized delivery to the injured spinal cord. *Biomaterials* 27:2370–2379
10. Chenite A, Chaput C, Wang D, Combes C, Buschmann MD, Hoemann CD, Leroux JC, Atkinson BL, Binette F, Selmani A (2000) Novel injectable neutral solutions of chitosan form biodegradable gels in situ. *Biomaterials* 21:2155–2161
11. Gao C, Liu M, Chen J, Zhang X (2009) Preparation and controlled degradation of oxidized sodium alginate hydrogel. *Polym Deg Stab* 94:1405–1410
12. Mittal H, Kaith BS, Jindal R (2010) Microwave radiation induced synthesis of gum ghatti and acrylamide based crosslinked network and evaluation of its thermal and electrical behavior. *Der Chemica Sinica* 1:59–69
13. Zhou J, Chang C, Zhang R, Zhang L (2007) Hydrogels prepared from unsubstituted cellulose in NaOH/urea aqueous solution. *Macromol Biosci* 7:804–809
14. Phillips GO, Du Plessis TA, Al-Assaf S, Williams PA (2005) Biopolymers obtained by solid state irradiation in an unsaturated gaseous atmosphere. US Patent 6841644
15. Hirsch SG, Spontak RJ (2002) Temperature-dependent property development in hydrogels derived from hydroxypropyl cellulose. *Polymer* 43:123–129
16. Mitsumata T, Suemitsu Y, Fujii K, Fujii T, Taniguchi T, Koyama K (2003) pH-Response of chitosan, κ -carrageenan, carboxymethyl cellulose sodium salt complex hydrogels. *Polymer* 44:7103–7111
17. Choudhary S, White JC, Stoppel WL, Roberts SC, Bhatia SR (2011) Gelation behavior of polysaccharide-based interpenetrating polymer network (IPN) hydrogels. *Rheol Acta* 50:39–52
18. Khalid MN, Ho L, Agnely F, Grossiord JL, Couarraze G (1999) Swelling properties and mechanical characterization of a semi-interpenetrating chitosan/polyethylene oxide network—comparison with a chitosan reference gel. *Stp Pharm Sci* 9:359–364
19. Ng LT, Swami S (2005) IPNs based on chitosan with NVP and NVP/HEMA synthesised through photoinitiator-free photopolymerisation technique for biomedical applications. *Carbohydr Polym* 60:523–528
20. Ostroha J, Pong M, Lowman A, Dan N (2004) Controlling the collapse/swelling transition in charged hydrogels. *Biomaterials* 25:4345–4353
21. Hariharan MTA, Peppas NA (1995) Factors influencing drug and protein transport and release from ionic hydrogels. *React Polym* 25:127–137
22. Gupta KC, Kumar MNVR (2000) Semi-interpenetrating polymer network beads of crosslinked chitosan–glycine for controlled release of chlorphenamine maleate. *J Appl Polym Sci* 76:672–683
23. Funami T, Hiroe M, Noda S, Asai I, Ikeda S, Nishimari K (2007) Influence of molecular structure imaged with atomic force microscopy on the rheological behavior of carrageenan aqueous systems in the presence or absence of cations. *Food Hydrocolloids* 21:617–629
24. Bajpai AK, Shukla SK, Bhanu S, Kankane S (2008) Responsive polymers in controlled drug delivery. *Prog Polym Sci* 33:1088–1118
25. Bhattarai N, Ramay HR, Gunn J, Matsen FA, Zhang M (2005) PEG-grafted chitosan as an injectable thermosensitive hydrogel for sustained protein release. *J Control Release* 103:609–624
26. Pongjanyakul T, Puttipipatkachorn S (2007) Xanthan–alginate composite gel beads: molecular interaction and in vitro characterization. *Int J Pharm* 331:61–71

27. Giannouli P, Morris ER (2003) Cryogelation of xanthan. *Food Hydrocolloids* 17:495–501
28. De Jong SJ, De Smedt SC, Wahls MWC, Demeester J, K-van den Bosch JJ, Hennink WE (2000) Novel self-assembled hydrogels by stereocomplex formation in aqueous solution of enantiomeric lactic acid oligomers grafted to dextran. *Macromolecules* 33:3680–3686
29. Eiselt P, Lee KY, Mooney DJ (1999) Rigidity of two-component hydrogels prepared from alginate and poly(ethylene glycol)-diamines. *Macromolecules* 32:5561–5566
30. Cai S, Liu Y, Shu XZ, Prestwich GD (2005) Injectable glycosaminoglycan hydrogels for controlled release of human basic fibroblast growth factor. *Biomaterials* 26:6054–6067
31. Motokawa K, Hahn SK, Nakamura T, Miyamoto H, Shimoboji T (2006) Selectively crosslinked hyaluronic acid hydrogels for sustained release formulation of erythropoietin. *J Biomed Mater Res Part A* 79:459–465
32. Kurisawa M, Chung JE, Yang YY, Gao SJ, Uyama H (2005) Injectable biodegradable hydrogels composed of hyaluronic acid–tyramine conjugates for drug delivery and tissue engineering. *Chem Commun* 34:4312–4314
33. Sannino A, Esposito A, De Rosa A, Cozzolino A, Ambrosio L, Nicolais L (2003) Biomedical application of a superabsorbent hydrogel for body water elimination in the treatment of edemas. *J Biomed Mater Res A* 67:1016–1024
34. Niu C, Wu W, Wang Z, Li S, Wang J (2007) Adsorption of heavy metal ions from aqueous solution by crosslinked carboxymethyl konjac glucomannan. *J Hazard Mater* 141:209–214
35. Pitarresi G, Palumbo FS, Tripodo G, Cavallaro G, Giammona G (2007) Preparation and characterization of new hydrogels based on hyaluronic acid and α,β -polyaspartylhydrazide. *Eur Polym J* 43:3953–3962
36. Kumar K, Kaith BS, Jindal R, Mittal H (2012) Gamma-radiation initiated synthesis of psyllium and acrylic acid based polymeric networks for selective absorption of water from different oil-water emulsions. *J Appl Polym Sci* 124:4969–4977
37. Fei B, Wach RA, Mitomo H, Yoshii F, Kume T (2000) Hydrogel of biodegradable cellulose derivatives I radiation-induced crosslinking of CMC. *J Appl Polym Sci* 78:278–283
38. Hiroki A, Tran HT, Nagasawa N, Yagi T, Tamada M (2009) Metal adsorption of carboxymethyl cellulose/carboxymethyl chitosan blend hydrogels prepared by gamma irradiation. *Radiat Phys Chem* 78:1076–1080
39. Al-Assaf S, Phillips GO, Williams PA, Plessis TA (2007) Application of ionizing radiations to produce new polysaccharides and proteins with enhanced functionality. *Nucl Inst Meth Phys Res B* 265:37–43
40. Kaith BS, Sharma S, Jindal R, Bhatti MS (2011) Screening and RSM optimization for synthesis of gum tragacanth-acrylic acid based device for in-situ controlled cetirizine dihydrochloride release. *Soft Mat* 8:2286–2293
41. Kumari A, Kaith BS, Singha AS, Kalia S (2010) Synthesis, characterization and salt resistant swelling behavior of Psy-g-poly(AA) hydrogel. *Adv Mat Let* 1:123–128
42. Mittal H, Kaith BS, Jindal R (2010) Synthesis, characterization and swelling behaviour of poly (acrylamide-co-methacrylic acid) grafted Gum ghatti based superabsorbent hydrogels. *Adv Appl Sci Res* 1:56–66
43. Kaith BS, Kumar K (2007) Preparation of psyllium based hydrogels and their application in oil sector. *Iran Polym J* 16:529–538
44. Kumar K, Kaith BS, Jindal R, Mittal H (2012) Gamma-radiation initiated synthesis of psyllium and acrylic acid-based polymeric networks for selective absorption of water from different oil-water emulsions. *J Appl Polym Sci* 124:4969–4977
45. Kaith BS, Jindal R, Mittal H, Kumar K (2010) Temperature, pH and electric stimulus responsive hydrogels from Gum ghatti and polyacrylamide-synthesis, characterization and swelling studies. *Der Chemica Sinica* 1:44–54
46. Wang JP, Chen YZ, Zhang SJ, Yu HQ (2008) A chitosan-based flocculant prepared with gamma-irradiation-induced grafting. *Biores Tech* 99:3397–3402

47. Said HM, Alla SGA, El-Naggar AWM (2004) Synthesis and characterization of novel gels based on carboxymethyl cellulose/acrylic acid prepared by electron beam irradiation. *React Funct Polym* 61:397–404
48. Kaith BS, Jindal R, Mittal H, Kumar K (2011) Synthesis, characterization, and swelling behavior evaluation of hydrogels based on gum ghatti and acrylamide for selective absorption of saline from different petroleum fraction–saline emulsions. *J Appl Polym Sci* 124:2037–2047
49. Donald AM (2003) The use of environmental scanning electron microscopy for imaging wet and insulating materials. *Nat Mat* 2:511–516
50. Ferreira L, Gila MH, Cabrita AMS, Dordick JS (2005) Biocatalytic synthesis of highly ordered degradable dextran-based hydrogels. *Biomaterials* 26:4707–4716
51. Sannino A, Demitri C, Madaghiele M (2009) Biodegradable cellulose-based hydrogels: design and applications. *Materials* 2:353–373
52. Chen LG, Liu ZL, Zhuo RX (2005) Synthesis and properties of degradable hydrogels of konjac glucomannan grafted acrylic acid for colon-specific drug delivery. *Polymer* 46:6274–6281
53. Kumar K, Kaith BS, Mittal H (2012) A study on effect of different reaction conditions on grafting of psyllium and acrylic acid-based hydrogels. *J Appl Polym Sci* 123:1874–1883
54. Weisenhorn AL, Khorsandi M, Kasas S, Gotzos V, Butt HJ (1993) Deformation and height anomaly of soft surfaces studied with an AFM. *Nanotechnology* 4:106–113
55. Kaith BS, Kumar K (2007) Selective absorption of water from different oil–water emulsions with Psy-cl-poly(AAm) synthesized using irradiation copolymerization method B. *Bull Mater Sci* 30:387–391
56. Kaith BS, Kumar K (2007) In air synthesis of Psy-cl-poly(AAm) network and its application in water-absorption from oil-water emulsions. *eXPRESS Polym Let* 1:474–480
57. Kaith BS, Ranjita S, Kumar K (2008) In air synthesis of GA-cl-poly(MAA) hydrogel and study of its salt-resistant swelling behavior in different salts. *e-Polymers* 158
58. Kaith BS, Jindal R, Mittal H, Kumar K, Nagla KS (2010) Synthesis and characterization of Gum ghatti based electrosensitive smart networks. *Trends Carbohydr Res* 2:35–44
59. Draget KI, Skjak-Braek G, Smidsrd O (1997) Alginate based new materials. *Int J Biol Macromol* 21:47–55
60. Kuo CK, Ma PX (2001) Ionically crosslinked alginate hydrogels as scaffolds for tissue engineering: Part I Structure, gelation rate and mechanical properties. *Biomaterials* 22:511–21
61. Rowley JA, Mooney DJ (2002) Alginate type and RGD density control myoblast phenotype. *J Biomed Mater Res* 60:217–23
62. Drurya JL, Dennis RG, Mooney DJ (2004) The tensile properties of alginate hydrogels. *Biomaterials* 25:3187–3199
63. Sandolo C, Matricardi P, Alhaique F, Coviello T (2007) Dynamo-mechanical and rheological characterization of guar gum hydrogels. *Eur Polym J* 43:3355–3367
64. Kaith BS, Kiran K (2007) In vacuum preparation of Psy-cl-Poly(AAm) super-absorbent and its applications in oil-industry. *e-Polymers* 002.
65. Kaith BS, Kiran K (2008) In vacuum synthesis of psyllium and acrylic acid based hydrogels for selective water absorption from different oil-water emulsions. *Desalination* 229:331–341
66. El-Hag Ali A, Abd El-Rehim H, Kamal H, Hegazy DES (2008) Synthesis of carboxymethyl cellulose based drug carrier hydrogel using ionizing radiation for possible use as site specific delivery system. *J Macromol Sci A* 45:628–634
67. Davaran S, Rashidi MR, Khani A (2007) Synthesis of chemically cross-linked hydroxypropyl methyl cellulose hydrogels and their application in controlled release of 5-amino salicylic acid. *Drug Dev Ind Pharm* 33:881–887
68. Hovgaard L, Brndsted H (1995) Controlled release dextran hydrogels for colon-specific drug delivery. *J Control Release* 36:159–166
69. Kulkarni RV, Sa B (2008) Evaluation of pH-sensitivity and drug release characteristics of (polyacrylamide-grafted-xanthan)-carboxymethyl cellulose-based pH-sensitive interpenetrating network hydrogel beads. *Drug Dev Ind Pharm* 34:1406–1414

70. Baumgartner S, Kristl J, Peppas NA (2002) Network structure of cellulose ethers used in pharmaceutical applications during swelling and at equilibrium. *Pharm Res* 19:1084–1090
71. Don TM, Huang ML, Chiu AC, Kuo KH, Chiu WY, Chiu LH (2008) Preparation of thermo-responsive acrylic hydrogels useful for the application in transdermal drug delivery systems. *Mater Chem Phys* 107:266–273
72. Kumar G, Juyal V, Badoni PP, Rawat MSM, Semalty A (2009) Formulation and release kinetic study of hydrogel containing acarbose using polymers as hydroxypropylmethyl cellulose and guar gum. *J Pharm Res* 2:370–374
73. Kajjari PB, Manjeshwar LS, Aminabhavi TM (2011) Semi-interpenetrating polymer network hydrogel blend microspheres of gelatin and hydroxyethyl cellulose for controlled release of theophylline. *Ind Eng Chem Res* 150:7833–7840
74. Anders R, Merkle HP (1989) Evaluation of laminated mucoadhesive patches for buccal drug delivery. *Int J Pharm* 49:231–240
75. Cerchiara T, Luppi B, Bigucci F, Zecchi V (2003) Chitosan salts as nasal sustained delivery systems for peptidic drugs. *J Pharm Pharmacol* 55:1623–1627
76. Berger J, Reist M, Mayer JM, Felt O, Peppas NA, Gurny R (2004) Structure and interactions in covalently and ionically crosslinked chitosan hydrogels for biomedical applications. *Eur J Pharm Biopharm* 57:19–34
77. Braga MEM, Pato MTV, Silva HSRC, Ferreira EI, Gil MH, Duarte CMM, de Sousa HC (2008) Supercritical solvent impregnation of ophthalmic drugs on chitosan derivatives. *J Supercrit Fluids* 44:245–257
78. Schaffhausen N, Tijsma E, Hissong B (2008) Injectable chitosan-based hydrogels for drug delivery after ear–nose–throat surgery. *J Control Release* 132:e47–e48
79. Slaughter BV, Khurshid SS, Fisher OZ, Khademhosseini A, Peppas NA (2009) Hydrogels in regenerative medicine. *Adv Mater* 21:3307–3329
80. Augst AD, Kong HJ, Mooney DJ (2006) Alginate hydrogels as biomaterials. *Macromol Biosci* 6:623–633
81. Drury JL, Mooney DJ (2003) Hydrogels for tissue engineering: scaffold design variables and applications. *Biomaterials* 24:4337–4351
82. Tiwari A, Grailler JJ, Pilla S, Steeber DA, Gong S (2009) Biodegradable hydrogels based on novel photopolymerizable guar gum–methacrylate macromonomers for in situ fabrication of tissue engineering scaffolds. *Acta Biomater* 5:3441–3452
83. Hu J, Hou Y, Park H, Choi B, Hou S, Chung A, Lee M (2012) Visible light crosslinkable chitosan hydrogels for tissue engineering. *Acta Biomater* 8:1730–1738
84. Jin R, Teixeira LSM, Dijkstra PJ, Blitterswijk CAV, Karperien M, Feijen J (2010) Enzymatically-crosslinked injectable hydrogels based on biomimetic dextran–hyaluronic acid conjugates for cartilage tissue engineering. *Biomaterials* 31:3103–3113
85. Jayakumar R, Prabakaran M, Kumar PTS, Nair SV, Tamura H (2011) Biomaterials based on chitin and chitosan in wound dressing applications. *Biotech Adv* 29:322–337
86. Sikareepaisan P, Ruktanonchai U, Supaphol P (2011) Preparation and characterization of asiaticoside-loaded alginate films and their potential for use as effectual wound dressings. *Carbohydr Polym* 83:1457–1469
87. Balakrishnan B, Mohanty M, Umashankar PR, Jayakrishnan A (2005) Evaluation of an in situ forming hydrogel wound dressing based on oxidized alginate and gelatine. *Biomaterials* 26:6335–6342
88. Kiran K, Kaith BS (2010) Psyllium and acrylic acid based polymeric networks synthesized under the influence of γ -radiations for sustained release of fungicide. *Fibres Polym* 11:147–152
89. Aouada FA, de Moura MR, Henrique L, Mattoso C (2011) Biodegradable hydrogel as delivery vehicle for the controlled release of pesticide. In: Stoytcheva M (ed) *Pesticides—formulations, effects, fate*. CC BY-NC-SA
90. Singh B, Sharma DK, Kumar R, Gupta A (2009) Controlled release of the fungicide thiram from starch–alginate–clay based formulation. *Appl Clay Sci* 45:76–82

91. Roy A, Bajpai J, Bajpai AK (2009) Dynamics of controlled release of chlorpyrifos from swelling and eroding biopolymeric microspheres of calcium alginate and starch. *Carbohydr Polym* 76:222–231
92. Abd El-Mohdy HL, Hegazy EA, El-Nesr EM, El-Wahab MA (2011) Control release of some pesticides from starch/(ethylene glycol-*co*-methacrylic acid) copolymers prepared by γ -irradiation. *J Appl Polym Sci* 122:1500–1509
93. Singh B, Chauhan GS, Bhatt SS, Kumar K (2006) Metal ion sorption and swelling studies of psyllium and acrylic acid based hydrogels. *Carbohydr Polym* 64:50–56
94. Chauhan GS, Singh BS, Chauhan S, Verma M, Mahajan S (2005) Sorption of some metal ions on cellulosic-based hydrogels. *Desalination* 181:217–224
95. Nizam El-Din HM, Abou Taleb MF, Abdel Wahab AM, El-Naggar AM (2008) Metal sorption and swelling characters of acrylic acid and sodium alginate based hydrogels synthesized by gamma irradiation. *Nucl Inst Meth Phys Res B Beam* 266:2607–2613

Chapter 8

Hyaluronic Acid-g-Copolymers: Synthesis, Properties, and Applications

Fabio Salvatore Palumbo, Giovanna Pitarresi, Calogero Fiorica,
and Gaetano Giammona

Abstract The aim of this chapter is to review hyaluronic acid (HA) graft copolymers focusing in the description of chemical strategies employed for their synthesis, characterization procedures, and applications in biomedical and pharmaceutical field. Usually biocompatible synthetic polymers and peptides with therapeutic activity are grafted to HA to modify in appropriate way the physicochemical properties of the starting polysaccharide for a specific purpose and at the same time to exploit its biological role, biocompatibility, and targeting ability toward cells with receptors for HA. The use of such HA graft copolymers in the production of nanocarriers or hydrogels for modified drug release and scaffolds for regenerative medicine will be outlined.

Keywords Hyaluronic acid • Chemical grafting • Nanomedicine • Tissue engineering • Protein therapeutics

F.S. Palumbo • C. Fiorica

Dipartimento di Scienze e Tecnologie Molecolari e Biomolecolari, Sezione di Chimica e Tecnologie Farmaceutiche, Università degli Studi di Palermo, Via Archirafi 32, 90123, Palermo, Italy

G. Pitarresi

Dipartimento di Scienze e Tecnologie Molecolari e Biomolecolari, Sezione di Chimica e Tecnologie Farmaceutiche, Università degli Studi di Palermo, Via Archirafi 32, 90123, Palermo, Italy

IBIM-CNR, Via Ugo La Malfa 153, 90146, Palermo, Italy

G. Giammona (✉)

Dipartimento di Scienze e Tecnologie Molecolari e Biomolecolari, Sezione di Chimica e Tecnologie Farmaceutiche, Università degli Studi di Palermo, Via Archirafi 32, 90123, Palermo, Italy

Institute of Biophysics at Palermo, Italian National Research Council, Via Ugo La Malfa 153, 90146, Palermo, Italy

e-mail: gaetano.giammona@unipa.it

8.1 Introduction

Hyaluronic acid (HA) is a glycosaminoglycan (GAG) of the extracellular matrix (ECM), where it plays fundamental biological and structural roles, being, for example, involved in the wound repair processes, in the cartilage and synovial fluid as well as in the ocular homeostasis [1, 2]. HA is a linear polysaccharide composed of repeating D-glucuronic acid and N-acetyl-D-glucosamine units and in the ECM exists with a molecular weight ranging from 10^3 to 10^7 Da [3, 4]. The HA molecular weight influences its specific activity being high molecular weight HA mainly involved for maintaining tissue tones because of its osmotic activity, while low molecular weight HA exploits signaling and cell recognition activity [5]. The biological role of the HA is exploited through the recognition of specific binding receptors involved in cell proliferation, morphogenesis, and inflammation. Several tumoral cells and organs overexpress HA-binding receptors like cluster determinant 44 (CD-44) [6–9] that drives numerous tumor-promoting signaling pathways and transporter activities. The receptor for hyaluronate-mediated motility (RHAMM) and the HA receptor for endocytosis (HARE) are involved in the specific uptake into the liver, and the lymphatic vessel endothelial hyaluronan receptor-1 (LYVE-1) plays a role in the autocrine regulation of cell growth [10–13]. HA has found a wide application in pharmaceuticals as viscosupplement for treating osteoarthritis or for ophthalmic surgery, and it has been employed to produce chemically cross-linked biomaterials [14, 15]. HA has been employed to regulate cell homeostasis in wound healing and cartilage regeneration, and it has been also functionalized to introduce pendant chemical moieties suitable to obtain in situ-forming hydrogels [16, 17]. Since the late 1990s, HA has been also considered as a water-soluble backbone for the production of macromolecular prodrugs to obtain tumor or tissue targeting exploiting the selective recognition for HA-binding receptors [18]. In this chapter, the design, production, and characterization of HA-g-copolymers will be focused. The rationale for the production of HA-g-copolymers can be summarized in the following points: (a) to improve HA physicochemical properties, changing water solubility and affinity, tuning viscoelastic behavior and hydrolytical resistance, and producing HA-g-derivatives better suitable for pharmaceutical processing; (b) to exploit targeting properties of HA obtaining water-soluble HA-g-copolymers or nanometric aggregates; and (c) to develop HA-g-therapeutic proteins where hyaluronic acid can act as hydrophilic carrier to increase protein circulation time, reducing recognition by immune system or as targeting toward hyaluronan receptors rich organs and tissues and improving protein therapeutic effect. Two main classes of polymers can be selected for the design of such graft copolymers: (a) synthetic polymers having a not specific biological activity such as polyesters that are grafted to the HA backbone to exploit their structural properties and (b) bioactive polypeptides grafted to the HA to obtain a targeted delivery and to improve their pharmacokinetic behavior. In this chapter, several examples of both classes will be described focusing in the adopted chemical procedures, characterizations, and applications of these HA-g-copolymers.

8.2 Chemical Strategies for the Synthesis of HA Graft Copolymers

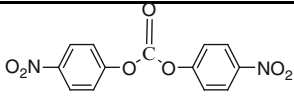
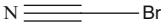
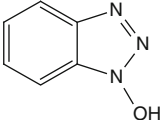
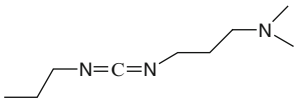
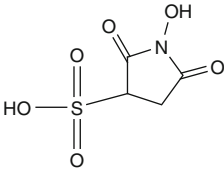
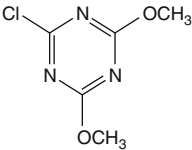
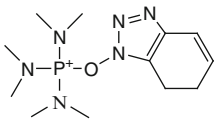
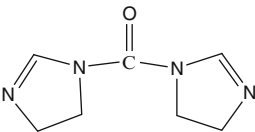
The most exploited HA functional portions for grafting procedures are the carboxyl group on the D-glucuronic acid and the primary hydroxyl group on the *N*-acetylglucosamine; less employed procedures consist in the oxidation of HA backbone to produce aldehyde groups or in the breaking of *N*-acetylic portions. Reactions involving COOH or OH functionalities can be performed both in water and in polar aprotic solvents (dimethylsulfoxide, dimethylformamide, tetrahydrofuran, etc.). In this second case to reach solubility, HA should be transformed in its tetrabutylammonium (TBA) or cetyltrimethylammonium (CTA) salt, or at least it should be used with a very low molecular weight [19]. Selection of the chemical functionality to perform grafting reactions should be made taking into account not only the chemical convenience but also the pursued physicochemical or biological modification. As example, the functionalization of D-glucuronic carboxyl group can be chosen to obtain a modulation of water affinity or a reduction of pH sensibility. Moreover, free COOH glucuronic groups are recognized as fundamental for binding hyaluronan receptors, and then regulating their degree of functionalization, it is possible to control HA-receptor affinity. Here it will be described only main functionalization strategies employed to graft polymers to HA backbone. In Table 8.1, principal activants used for hydroxyl and carboxyl groups of HA during grafting reactions are listed.

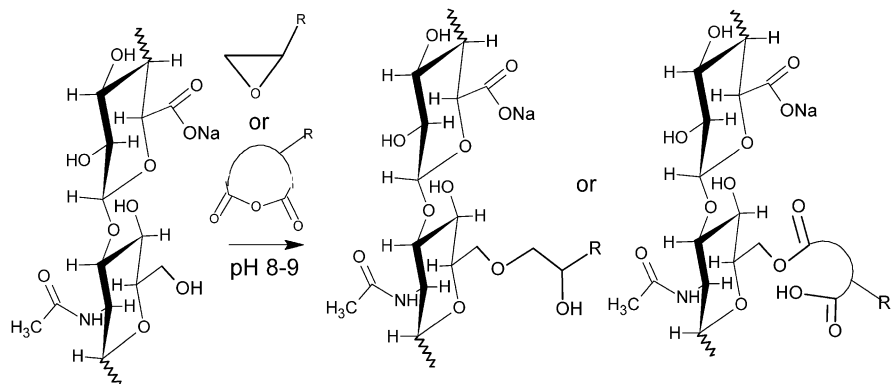
8.2.1 Grafting on HA Hydroxyl Groups

Reactivity of primary hydroxyl groups of *N*-acetylglucosamine portions in aqueous environment is very low; reaction is possible at high pH toward epoxides or anhydrides to form the corresponding ether or ester linkages, and most of these reactions have been employed to obtain cross-linked materials [20, 21]. Few examples are present in the literature showing such kind of chemistry to obtain HA-graft-copolymers as the production of HA-octenyl derivatives [22]. In these cases, water-soluble polymers with epoxide or anhydride functionalities react at basic pH (8–10) with HA sodium salt in the presence of the opportune catalyst (Scheme 8.1). However, hydroxyl reactivity is low in such condition, and often a great excess of reacting polymer is necessary to obtain a significant functionalization.

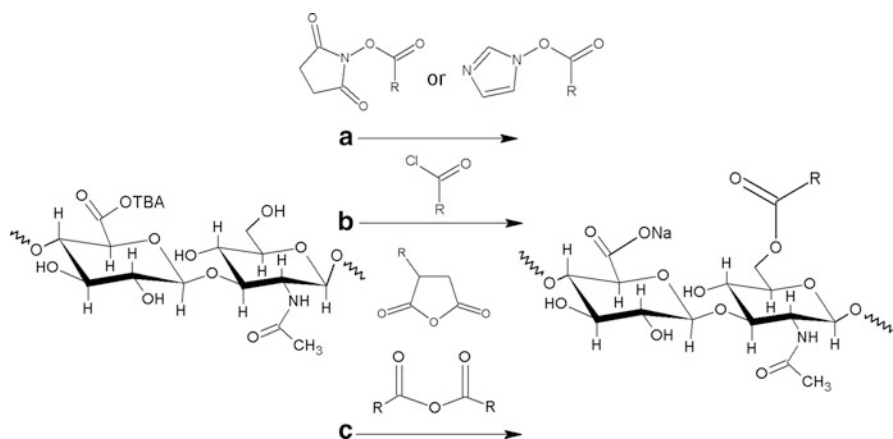
Direct functionalization of the HA primary hydroxyl groups could be performed also in polar aprotic solvents working with TBA or CTA HA salts. In this case, reactivity of hydroxyl groups is hampered if compared to the reactions performed in water. Polymers need to be opportunely activated before to react with the HA salt, and reaction may be performed in the presence of a base employed as proton trap. As an example, carboxyl-terminated polymers could be easily activated employing

Table 8.1 Principal activants used for hydroxyl and carboxyl groups of hyaluronic acid during grafting reactions

Name	Chemical structure	Function	Text
Bis(4-nitrophenyl)carbonate		Hydroxyl groups activant	Scheme 3
Cyanogen bromide		Hydroxyl groups activant	Scheme 3
1-Hydroxybenzotriazole (HOBT)		Carboxyl groups activant	Scheme 4
<i>N</i> -(3-dimethylaminopropyl)- <i>N'</i> -ethylcarbodiimide hydrochloride (EDC)		Carboxyl groups activant	Scheme 4
<i>N</i> -Hydroxysulfosuccinimide (NHS)		Carboxyl groups activant	Scheme 4
2-Chloro-dimethoxy-1,3,5-triazine (CMDT)		Carboxyl groups activant	Scheme 5
Benzotriazol-1-yloxy-tris(dimethyl-amino)phosphonium hexafluorophosphate (BOP)		Carboxyl groups activant	Scheme 5
Carbonyldiimidazole (CDI)		Carboxyl groups activant	Scheme 5

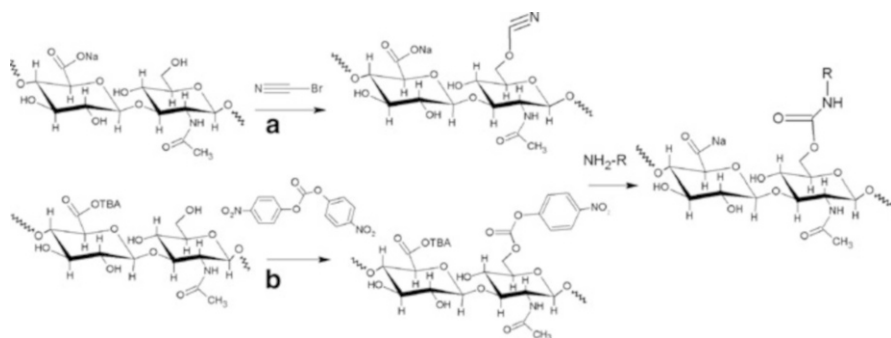


Scheme 8.1 Grafting procedures with epoxide- or anhydride-terminated polymers (R=polymeric chain) [22]



Scheme 8.2 Grafting procedure on the *N*-acetylglucosamine primary hydroxyl groups performed in aprotic polar solvents employing HA-TBA; in particular a direct coupling strategy on activated polymers is described. (a) Reaction with *N*-hydroxysuccinimide or imidazole-activated carboxyl-terminated polymers [23]. (b) Reaction with acyl-chloride-activated carboxyl-terminated derivatives [24]. (c) Reaction with cyclic or linear anhydride-functionalized polymers [50] (R=polymeric chain)

N-hydroxysuccinimides or carbonyldiimidazoles (Scheme 8.2a) [23]. Such kind of activators has the advantage to be suitable for a wide range of polymers both synthetic and natural including short polypeptides. Carboxyl-terminated polymers could be also activated as acyl-chloride derivatives, thus allowing faster reactions [24]. However, some concerns can be issued considering the reactivity and toxicity of thionyl chloride employed to perform the activation and about the release of HCl during the coupling reaction (Scheme 8.2b). Ester linkages can be also obtained performing the reaction with polymers having anhydride functionalities (Scheme 8.2c) [25].

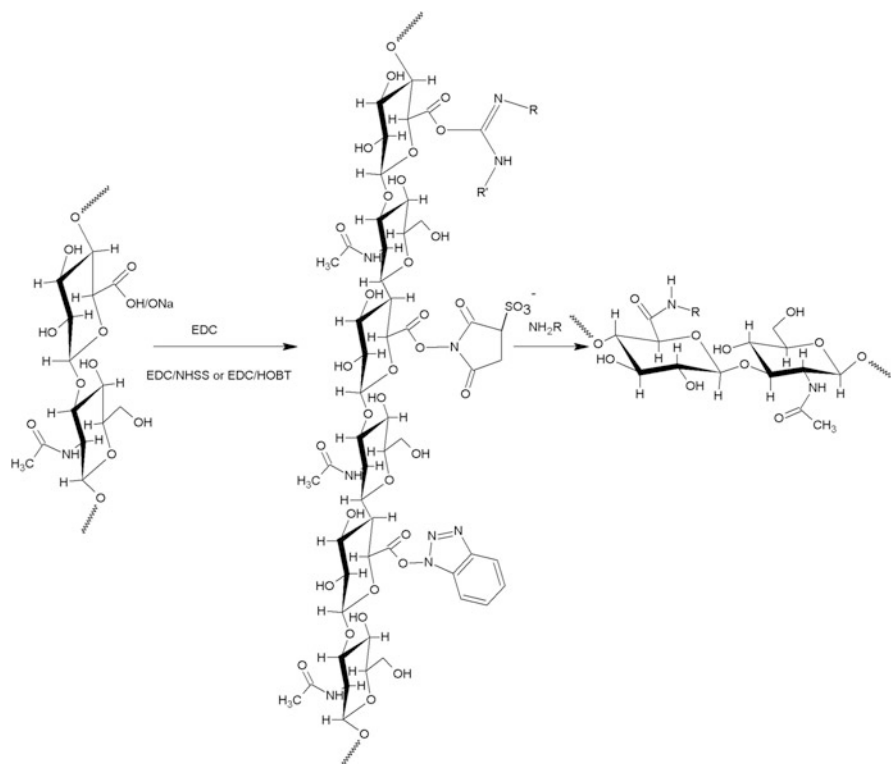


Scheme 8.3 Grafting procedure on the *N*-acetylglucosamine primary hydroxyl groups performed in aprotic polar solvents employing HA-TBA. In this case, opportune agent is employed to activate the hydroxyl group, and then an amino-terminated polymer is employed for coupling. (a) Activation of the *N*-acetylglucosamine hydroxyl group in water by using cyanogen bromide [26]. (b) Activation of the *N*-acetylglucosamine hydroxyl group in DMSO using Bis(4-nitrophenyl) carbonate condensing agents [27, 28] (R=polymeric chain)

An alternative functionalization strategy consists in the activation of HA primary hydroxyl groups by using a proper condensing agent. This activation can be performed in aqueous or organic medium, and it has often the advantage of high chemical selectivity and efficiency. Moreover, in some cases, it is possible to isolate the activated HA intermediate that can be employed, on the occurrence, with the opportune polymer to perform the coupling reaction. As an example, Mlčochová described the activation of the *N*-acetylglucosamine hydroxyl group in water by using cyanogen bromide; the intermediate HA-cyanate reacts efficiently with an amino-substituted polymer forming a stable carbamate linkage (Scheme 8.3a) [26]. A similar carbamate linkage can be also formed in a polar aprotic solvent employing as HA activator a *p*-nitrophenyl carbonate condensing agent such as bis(4-nitrophenyl) carbonate (4-NPBC) or chloro-4-nitrophenylcarbonate. The activation strategy is fast and quantitative and allows grafting procedures with amino-terminated polymers (see Scheme 8.3b) [27, 28].

8.2.2 Grafting on HA Carboxyl Groups

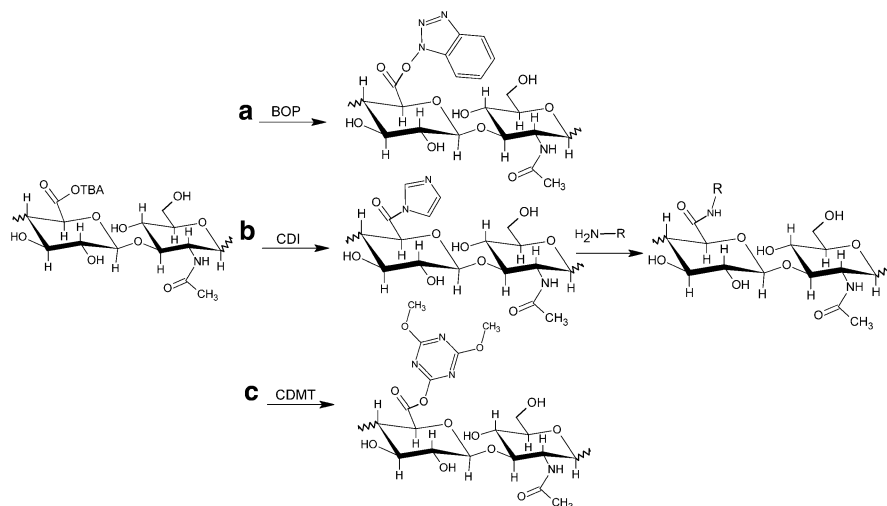
Several chemical procedures performed with condensing agents reactive toward glucuronic carboxyl groups can be performed in water. To avoid the employ of organic solvents is a good strategy for an easier industrial manufacturing and scaling-up of all pharmaceutical polymers if higher costs and risks linked to the treatment of organic wastes are considered; however, when water solubility of grafting molecules (polymers, active agents, etc.) is poor, the use of organic solvents cannot be avoided. Water-soluble carbodiimides, in pH-controlled



Scheme 8.4 Grafting procedures on the glucuronic COOH group performed in water. Water-soluble condensing agents are employed to make pH-controlled coupling reactions with amino-terminated polymers [30, 31] (R=polymeric chain)

reactions, are employed to activate the COOH functionality for coupling amino-terminated water-soluble polymers (Scheme 8.4). The water-soluble condensing agent 1-ethyl-3-[3-(dimethyl-amino)-propyl]-carbodiimide (EDC) is more efficient at pH comprised between 3 and 5 even if amine is more reactive at basic pH [29, 30]. However, at higher pH, the activated O-acyl ureic intermediate can easily rearrange in the stable intermediate *N*-acyl urea, and then the amidation reaction can be impeded [31]. Better reactivity at lower pH can be obtained using Hydrazide-terminated polymers reducing the possibility of EDC rearrangement. Bulpitt and Aelschiman proposed to couple to the EDC a second activating agent such as 1-hydroxybenzotriazole (HOBt) or *N*-hydroxysulfosuccinimide (NHSS) obtaining in such way the formation of more stable intermediate O-NHS or O-benzotriazole that avoids the possible rearrangement into *N*-acyl urea and make more efficient coupling with amine at pH 6–8 (see Scheme 8.4) [32].

The same reaction can be performed also in dimethylsulfoxide (DMSO) employing HA-TBA; in this case, the rearrangement of the O-acyl adducts is not possible, and the activation reaction is more efficient. Both strategies employing



Scheme 8.5 Examples of condensing agents suitable for coupling reaction with HA-TBA in polar aprotic solvents. (a) Benzotriazol-1-yloxy-tris(dimethyl-amino) phosphonium hexafluorophosphate (BOP) [33]; (b) carbonyldiimidazole (CDI) [34], and (c) 2-chloro-dimethoxy-1,3,5 triazine (CDMT) [35] (R=polymeric chain)

EDC or EDC with HOBt or NHSS are commonly used to graft molecules or chains to the HA backbone.

Activation of the D-glucuronic carboxyl groups can be performed also in polar aprotic solvents such as DMSO, dimethylformamide (DMF), *N*-methylpyrrolidone (NMP), etc., employing HA-TBA or HA-CTA and an appropriate condensing agent such as benzotriazol-1-yloxy-tris (dimethyl-amino) phosphonium hexafluorophosphate (BOP), carbonyldiimidazole (CDI), chloro dimethoxytriazine (CDMT), etc. BOP activates HA-TBA with a good efficiency, and a proton trap, like diisopropylethylamine (DIPEA) or similar, is necessary to allow the grafting of amino-terminated polymers (see Scheme 8.5a) [33].

CDI condensing agent reacts very efficiently with the COOTBA in organic solvent, producing, after a spontaneous molecular rearrangement with the release of CO₂, a stable HA-imidazole derivative, and then the addition of the amine completes the functionalization (see Scheme 8.5b) [34]. The activation with 2-chloro-dimethoxy-1,3,5 triazine (CDMT) can be performed with HA-TBA in a mixed solvent acetonitrile/water (see Scheme 8.5c) [35]. However with the same COOH activation strategies ester linkages could be obtained using hydroxyl terminated polymers, even if their reactivity is lower if compared to the amino terminated one. Very efficient is instead reaction proposed by Della Valle and Romeo exploited by Fidia Advanced Biopolymers for the production of HA derivatives (employed for the fabrication of HYAFF fibrillar scaffolds) and easily exploitable to obtain the formation of HA graft copolymers. HA-TBA reacts in organic solvents with preformed alkyl halogens [36].

8.2.3 Grafting Employing HA-Functionalized Derivatives

Several HA functional derivatives have been proposed as key reactive to afford simple grafting procedures both in aqueous and aprotic polar medium. Nucleophilic and electrophilic groups have been introduced in the HA backbone, such as amino or hydrazide and aldehyde or haloacetate groups, respectively.

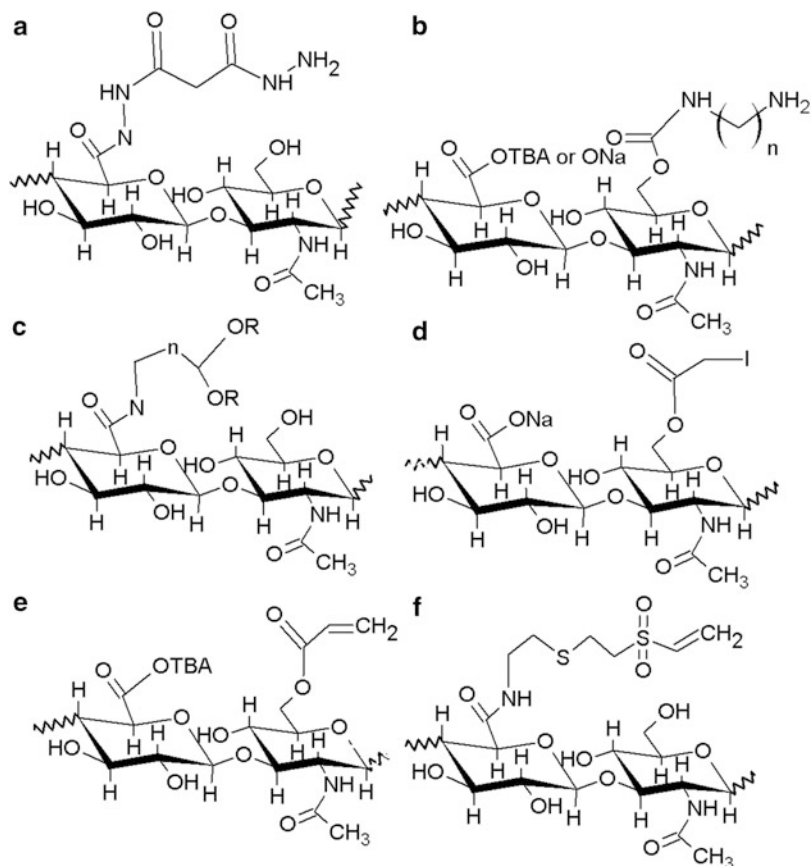
Such HA functional derivatives are finding wide application for the production of HA-g copolymers with synthetic polymers as well as with polypeptides. One of this HA derivative has been proposed by Prestwich et al. consisting in an adipic hydrazide-functionalized hyaluronic acid derivative (HA-ADH) obtained by a carbodiimide activation of the COOH group in the presence of adipic dihydrazide in water at pH 3–4 [37]. The inserted pendant hydrazide groups can react in aqueous environment at low pH with carbodiimide-activated carboxyl-terminated polymers (see Scheme 8.6a) [38].

Similar hyaluronic acid amino derivatives have been proposed also by Giammona et al. in a recent patent; such derivatives can be obtained after the activation of the primary hydroxyl groups with *p*-nitrophenyl carbonate and subsequent reaction with hydrazine or an appropriate diamine derivative. The HA-amino derivatives can be isolated as TBA salt and employed for reactions in organic solvent or as sodium salt in water (Scheme 8.6b) [27].

Bulpitt and Aeshilmann proposed the production of a hemiacetal HA derivative obtained by carbodiimide/benzotriazole chemistry performed in water at pH 6–7 (Scheme 8.6c).

After the opportune deprotection, the HA-aldehyde can be employed to perform coupling with polymers bearing reactive amino functionalities. Recently Fidia Advanced Biopolymer proposed a similar strategy to couple bioactive polypeptides; in this case, the reaction was performed in organic solvent employing HA-TBA salt and carbonyldiimidazole (CDI) as an activator of the glucuronic COOH. Deprotection of the hemiacetals is obtained by an acidic treatment at 60 °C; then the addition of the amino-terminated polymer or protein after deprotection allows the coupling. Serban et al. proposed HA haloacetate derivatives at the hydroxyl group of the *N*-acetylglucosamine portion suitable for cross-linking reactions or as an electrophilic reactive toward nucleophilic polymers. HA haloacetate, for example, can be potentially employed for selective reactions with polymers or peptides bearing thiol groups (see Scheme 8.6d) [39].

Acrylate or vinyl sulfonic derivatives have been proposed as reactive to perform grafting of biological peptides bearing free thiol groups through a Michael-type reaction; such grafting procedures are affordable in water at physiological pH, and they have the advantage of chemical selectivity (see Scheme 8.6e, f) [40].



Scheme 8.6 Examples of HA-functionalized derivatives employed as nucleophiles or electrophiles for grafting reaction with suitable polymers. (a) HA hydrazide derivative (HA-ADH) [38]; (b) HA-amino-functionalized derivatives as TBA or Na salts [27]; (c) HA-hemiacetal that after treatment in acidic environment can be transformed in the corresponding HA-aldehyde [32]; (d) HA-haloacetates [39]; (e) HA-acrylate, and (f) HA-vinyl sulfone affordable for Michael-type reaction [40] (R=polymeric chain)

8.3 HA-Graft-Synthetic Polymers: Characterization and Properties

The production of HA-g-copolymers using synthetic polymers allows to modify in appropriate way physicochemical properties of HA. Synthetic biocompatible polymers have been selected, taking into account hydrophilic or lipophilic character or peculiar physical properties such as thermoresponsiveness or rheological behavior. For example, grafting hydrophobic chains into HA backbone allows the production of amphiphilic polymeric derivatives that may self-assemble in aqueous medium forming nano- or microaggregates potentially employable as drug carriers or, if dispersed at specified concentration in water, could form physical hydrogels

with potential application for drug delivery or as scaffolds for tissue engineering. Synthetic polymeric chains, having peculiar properties such as thermoresponsiveness, can be linked to obtain HA graft derivatives with *in vivo* gel-forming ability. Polymers such as polyesters [polylactic acid, poly(lactic-co-glycolic) acid, polycaprolactone] have been exhaustively employed, and related derivatives have been described for the production of drug-loaded nanoparticles for drug targeting or scaffolds for tissue engineering. In this section, representative examples of these HA-graft derivatives will be reported describing synthetic procedures, characterization, and applications.

8.3.1 HA-Graft Synthetic Polymers to Produce Nanostructures and Hydrogels for Drug Delivery

The potential utility of nanometric aggregates such as nanoparticles, nanogels, or micelles constituted by HA is mainly related to the targeting ability toward specific receptors expressed in tumors or tissues. High molecular weight HA binds multiple receptors, and if a drug is linked to the HA backbone, a specific endocytosis can occur; for certain drugs, this can offer the opportunity to escape multidrug resistance efflux pumps [41]. However, applicability of HA as targeting moiety may be hindered by the difficulty to escape hepatic accumulation [42, 43]. As example ONCOFID, a prodrug of taxol proposed by Fidia Advanced Biopolymers is finding application more for the treatment of locoregional therapies than for the treatment of tumors by systemic delivery because of a preferential hepatic accumulation [44]. Therefore, to improve potential application of HA as suitable targeting carrier, strategies must be developed to reduce hepatic clearance. HA binds CD44, HARE, or LYVE-1 receptors with a minimum length of 6–8 HA disaccharides [45]. As recently studied, analyzing the binding of both free HA and HA linked to liposomes, high molecular weight HA-binding affinity seems to increase increasing HA molecular weight, being HA with low molecular weight faster dissociated from the CD44 interaction. Longer HA chains better interact with CD44 receptors because of the instauration of a multivalent interaction with the binding receptors. Considering such properties and selecting HA with dimension suitable to interact with CD44 but not with receptor HARE into the liver, it could be theoretically possible to tailor the biodistribution of HA or HA-coated nanocarriers avoiding hepatic accumulation [46, 47]. However, the employ of short oligosaccharides of HA limits the possibility to produce nanocarriers or polymeric prodrugs. Recently, Hanh and colleagues described the influence of glucuronic COOH degree of functionalization on tissue biodistribution of HA derivatives. In particular by linking HA hydrazide derivatives to QDots photoluminescent nanocrystals, these authors investigated relationships between HA dimension, chemical functionalization, and biodistribution [48].

Obtained results demonstrated that increasing glucuronic functionalization, HA derivatives accumulated in less extent into HA receptor-rich tissues such as liver

and lymphatic vessels, producing longer circulation time and increased $t_{1/2}$ in plasma and then increasing the possibility to use HA to conjugate drugs or therapeutic proteins. Obviously reducing COOH interaction with specific receptors improves circulation time of HA conjugates, but this can potentially reduce the targeting ability toward other tissues or organs expressing hyaluronic acid receptors. Therefore, a proper degree of COOH functionalization, to reduce HARE recognition and to maintain a sufficient interaction with CD44, could be properly tuned to improve targeting efficiency.

The presence of hydrophobic chains linked to the HA backbone allows the formation of aggregates in aqueous medium. If the amount of hydrophobic chains linked to the HA is opportunely regulated to obtain a water-insoluble derivative, it is possible to produce nanoparticles constituted by HA with hydrophobic cores. Pelletier and colleagues [49] proposed amphiphilic HA graft derivatives obtained by linking to the HA backbone short alkyl chains constituted by 12–18 CH_2 . In particular, employing the synthetic procedure proposed by Della Valle and Romeo, consisting in the reaction of the HA-TBA salt with the alkyl bromide derivatives, HA-alkyl derivatives have been obtained where alkyl chains were linked through an ester bond to the glucuronic COOH functionality. Derivatives HA-C12 and HA-C18 obtained with a derivatization degree equal to 1.5–8 mol% (alkyl chains for 100 HA repetitive units) showed a strong associative behavior in aqueous diluted solutions as demonstrated by rheological studies performed employing an Ostwald-type automatic capillary viscometer. In particular, hydrophobized HA derivatives showed lower intrinsic viscosity and higher Huggins coefficient compared to the not functionalized HA. The presence of hydrophobic aggregates was confirmed by fluorescence spectroscopy performed in the presence of the fluorescent dye 1,1-dicyano-(40-*N,N*-dimethylaminophenyl)-1,3-butadiene (DMAC). The formation of such hydrophobic microdomains suggested the possibility to obtain nanoaggregates for drug delivery purposes. Other researchers later proposed similar HA-aliphatic chains copolymers and demonstrated their potentiality as drug carriers. For example, Novozymes patented a chemical procedure concerning the grafting of HA sodium salt with alkyl succinate anhydrides in alkaline water (pH 8.5) (see Scheme 8.2c) [50].

In this case, the obvious advantage was to perform the reaction in water avoiding organic solvents. In particular, following this patented procedure, Eenschooten and colleagues optimized the reaction between HA and octenyl succinic anhydride (OSA) demonstrating how it is possible to produce different derivatives having functionalization degrees ranging from 2 to 43 mol%. In a subsequent study, such octenyl derivatives were successfully employed for the production of micelles, and the potentiality to entrap hydrophobic drugs was demonstrated [51]. The self-associative properties of HA-OSA derivatives were studied by fluorescence spectroscopy using Nile red as chromophore, and critical aggregation concentrations (CAC) ranging from 0.015 to 0.1 g/l were obtained. In particular, more functionalized derivatives were able to form more stable aggregates at lower concentration. TEM analysis captured micelles having dimensions comprised between 10 and 120 nm. Interestingly the authors, considering the degree of

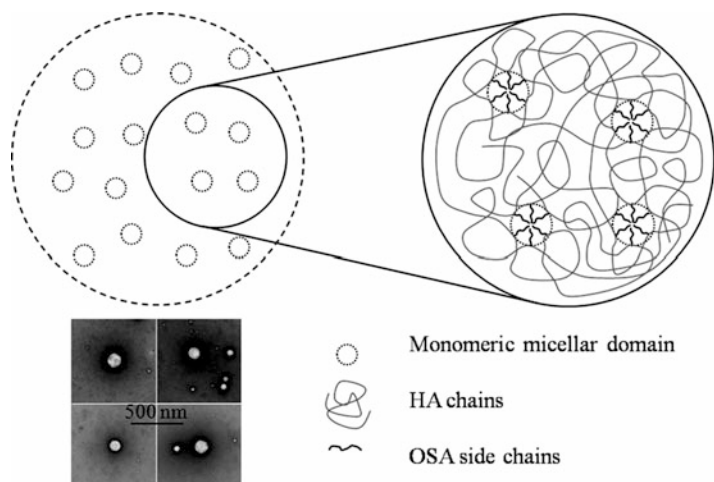


Fig. 8.1 Representation of the supposed structure of HA-OSA aggregates showed as multi microdomains of OSA aggregation points inside the HA entanglements (Reproduced with permission, copyright 2012 Elsevier [51])

substitution and the short length of the hydrophobic chains grafted, proposed the formation of a multiphase nanoaggregate composed of entangled HA chains and a dispersion of hydrophobic domains (Fig. 8.1).

Recently Liu and colleagues have investigated micelles made by HA grafted with octadecylamine (C18) and loaded with paclitaxel (PTX) [52]. This work demonstrated how, introducing into the HA graft copolymer a folic acid portion, micelles were capable of a dual specific targeting toward CD44 and folate receptor overexpressing tumor cells. In particular, these authors employed a low molecular weight HA (11 kDa) that was processed in DMF, reacting with the octadecylamine at 60 °C in the presence of EDCI and NHS as activators of the glucuronic COOH. Folic acid (FA) was activated with DCC/NHS, and the obtained derivative was linked to the *N*-acetylglucosaminic OH group. Changing opportunely reaction conditions, a C18 functionalization ranging from 12.7 to 19.3 mol% and an FA functionalization of 6.8 mol% were obtained. Also in this case, increased amounts of hydrophobic chains linked produce more stable micelles with lower CMC values. Derivatives HA-C18 and HA-FA-C18 bearing 19 % of C18 and 9.3 % of FA produced micelles with a dimension of 175 and 191 nm, respectively, and a negative zeta potential value. Micelles were efficiently loaded with paclitaxel indeed employing a drug/carrier weight ratio ranging from 10 to 30; encapsulation efficiencies of 80–90 % were obtained. In vitro cytotoxicity studies confirmed higher activity toward CD44-overexpressing cells A549 (non-small cell lung cancer) and MCF-7 (breast cancer cells), and moreover HA-C18 bearing FA moieties was more active toward MCF-7 cell lines expressing FA receptors (see Fig. 8.2).

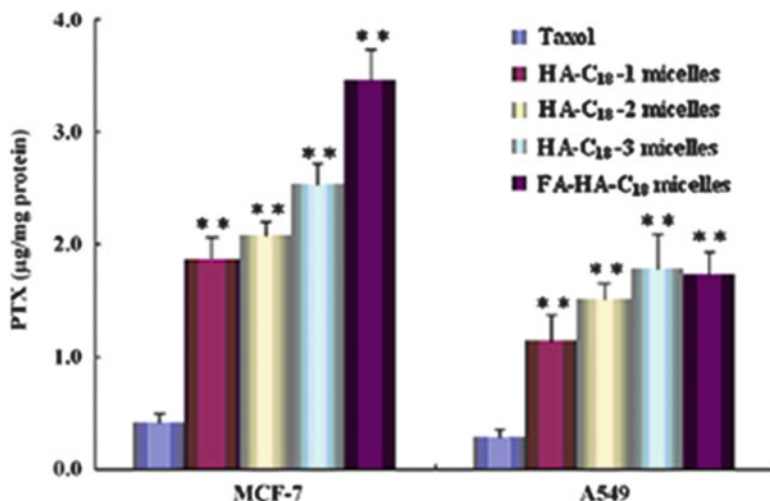


Fig. 8.2 Cellular uptake of paclitaxel (PTX) in breast cancer cells (MCF-7) (cell expressing both CD44 and Folate receptors) and non-small cell lung cancer (A549) (expressing CD44 receptors) (Reproduced with permission, copyright 2011 Elsevier [52])

Other suitable hydrophobic synthetic polymers exploitable to produce HA-based nanoaggregates are polyesters. Several examples of HA-g-polyesters have been proposed using preformed polymers such as PLA, PLGA, or PCL. Choosing appropriate polyester chain length, and regulating the derivatization degree, it is possible to obtain HA-g derivatives able to form hydrogels or nanoaggregates. The first example of HA-g-polyester obtained with the “grafting into” technique was made by Giammona research group, where a HA-g-PLA derivative was synthesized employing the chemistry described in the Scheme 8.2a. It was demonstrated how employing low molecular weight HA (200 kDa) and short molecular weight PLA (8 kDa) and changing derivatization degree (DD) in PLA from 1.4 to 8 mol% were possible to obtain at concentrations ranging from 0.125 to 1 % w/v colloidal aggregates or viscous physical hydrogels [23]. HA-g-PLA derivatives having a DD in PLA of 1.8 mol% and similar derivatives obtained by grafting PLA and PEG chains named PEG-g-HA-g-PLA (Mw of PEG 2 kDa) were successfully employed to produce doxorubicin-loaded micelles [53]. CAC of such HA-g derivatives was comprised between 0.04 and 0.06 g/l, and micelles formed had a diameter of 30 and 37 nm in the absence and in the presence of PEG, respectively, as demonstrated by light scattering and TEM measurements. The presence of PEG increased stability and drug-loading capacity of micelles. In vitro studies demonstrated how HA targeted selective uptake of micelles in CD44 expressing human colon tumoral cells (HCT-116). Lee and colleagues proposed HA-g-PLGA derivatives obtained through a reaction between the DCC-activated glucuronic HA carboxyl groups and PLGA [54]. In particular, graft copolymers obtained employing HA molecular weights ranging from 17 to 64 kDa and PLGA from 5 to 26 kDa were studied.

Selected HA-g-PLGA derivatives were successfully employed to produce doxorubicin-loaded micelles having a dimension of 200–300 nm. Number of PLGA chains linked, HA, and PLGA molecular weights influenced micelles properties. In particular, increasing the grafting percent in PLGA, CAC decreased, and increasing the length of linked PLGA compared to the length of HA backbone, micelles drug-loading efficiency increased. In vitro cytotoxicity studies performed on HCT CD44-overexpressing cells demonstrated how micelles were about six times more efficient compared to free doxorubicin.

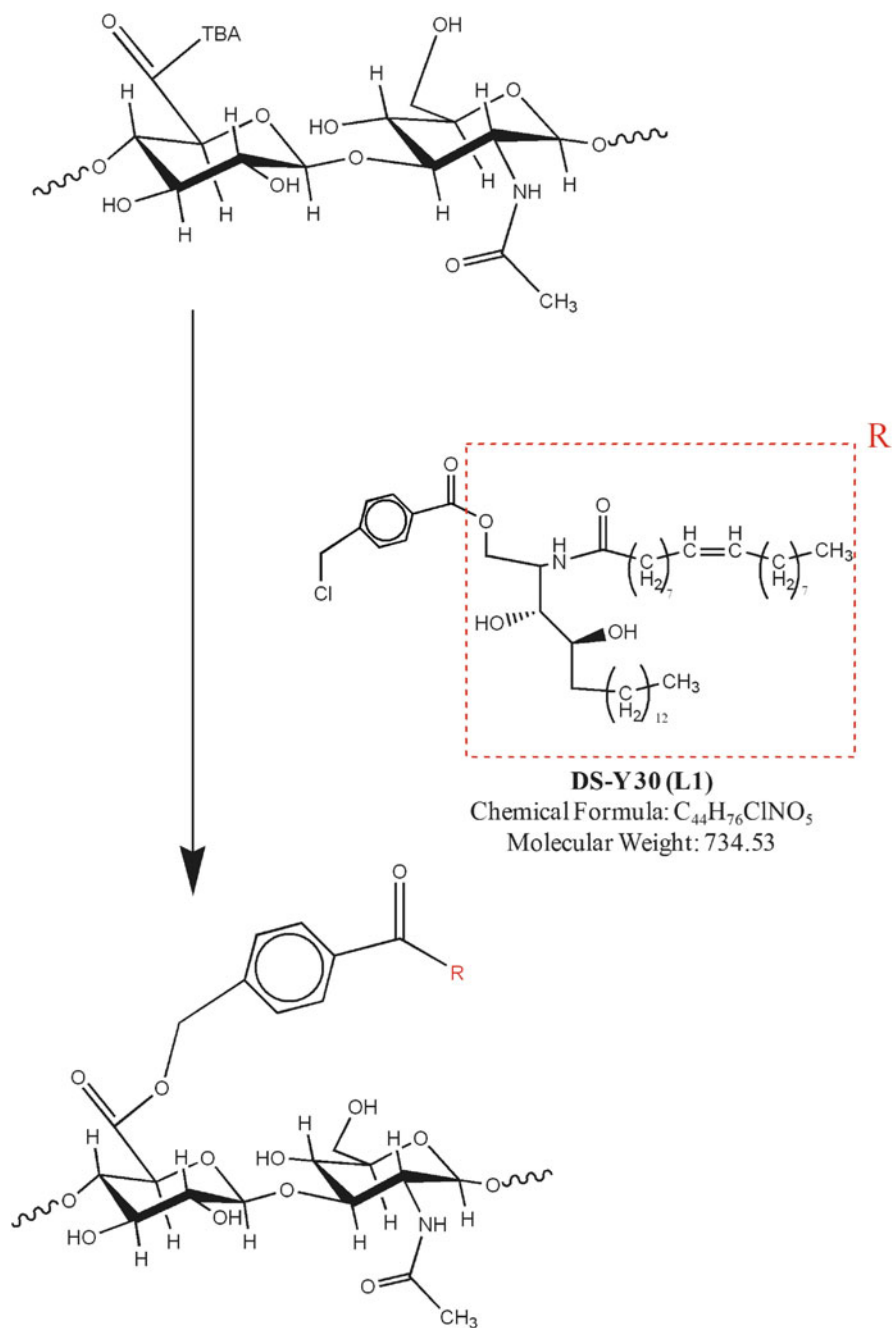
As example of potential clinical application, similar micelles loading 4.4 % in weight of PTX were employed to coat heparinized cobalt stents exploiting the antiproliferative activity for the treatment of restenosis [55].

By a coating technique named layer-by-layer assembly, metal stents were coated with heparin, and HA-g-PLGA micelles were embedded, obtaining a multilayer deposition. Negative charged HA-g-PLGA micelles loading PTX well fitted for the layer-by-layer coating technique; moreover, a control of the dose of drug released was possible regulating the number of micelles layers coated on the stent surface. The micelle-loaded multilayer without heparin arrested the proliferation of smooth muscle cells much more significantly up to about 95.7 % after 5 days compared to the system not loaded, and no significant difference was showed by the system coated with heparin.

Low molecular weight hyaluronic acid has been recently employed for the production of HA-ceramide-based nanoparticles proposed for the targeted delivery of docetaxel on CD44-overexpressing tumors. In this case, the hydrophobic portion driving the self-assembling was ceramide, a natural component of cellular membranes already known for its properties of control on cell apoptosis (see in Scheme 8.7 the structure of ceramide and grafting into HA). The procedure of Della Valle and Romeo was employed starting from the halogen ceramide derivative, and the graft was performed in DMSO on the glucuronic COOH [56]. In particular, ceramide was activated using 4-chloromethylbenzoyl-chloride and then employed for the reaction with HA-TBA.

HA-ceramide derivative obtained with a derivatization degree of 2.8 mol% showed a significant alteration of the HA solubility being it soluble in methanol. Exploiting this improved solubility in organic medium, nanoparticles with a diameter of 111 nm and a drug loading of 11 % were obtained by a technique of solvent evaporation of the polymeric dispersion and subsequent hydration of the polymeric film in the presence of docetaxel. In vivo imaging biodistribution study performed in mice bearing subcutaneous xenografted human breast adenocarcinoma cells (MCF-7/ADR) demonstrated how nanoparticles targeted the tumor because of the specific recognition of the CD44 receptor; indeed the pretreatment with an excess of HA saturated the receptor reducing the uptake of HA-ceramide nanoparticles containing cyanine 5.5 dye (see Fig. 8.3).

Exploiting its specific recognition by HARE receptors, HA can be successfully employed for the targeted delivery to the liver. Park and colleagues described the production of TGF- α siRNA/(PEISS)-g-HA complexes to treat liver fibrosis associated to cirrhosis [57]. TGF- α silencing RNA has great potentiality to reduce



Scheme 8.7 Reaction between benzoyl-chloride-activated ceramide and HA-TBA to give HA-g-ceramide copolymer [56]

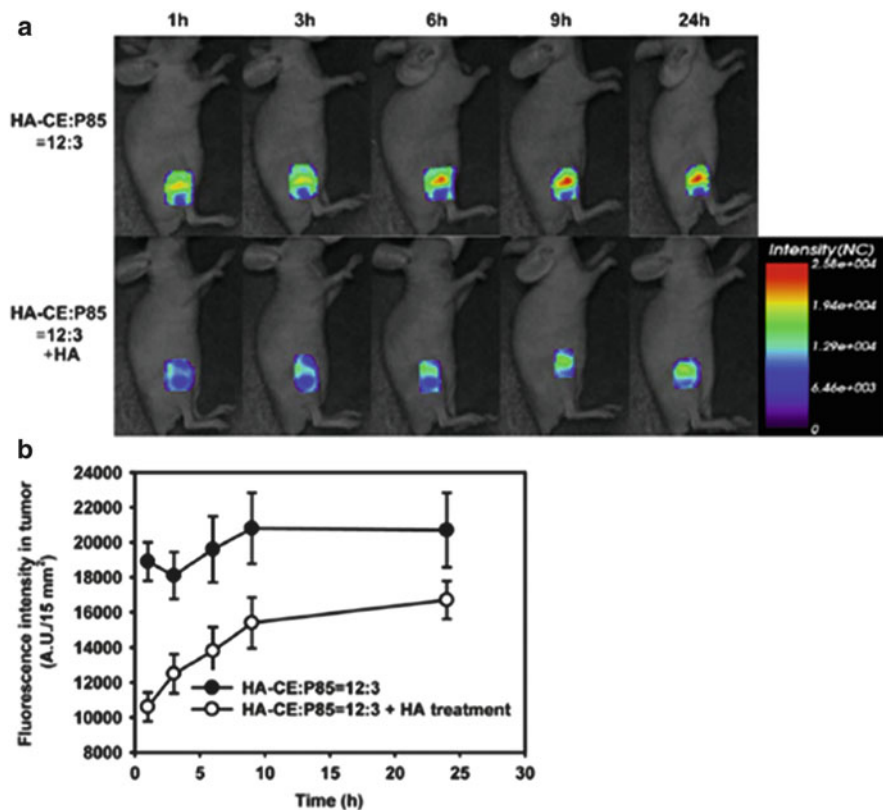


Fig. 8.3 (a) Real-time images of fluorescent dye-loaded HA-ceramide nanoparticles accumulated into the MCF-7/ADR xenograft tumor. Pictures in the superior part of the panel are mice treated only with nanoparticles. Pictures in the inferior part of the panel are animals treated with HA before the injection of HA-ceramide nanoparticles. (b) Quantitative evaluation of fluorescence until 24 h (Reproduced with permission, copyright 2011 Elsevier [56])

tissue fibrosis in general and in particular liver fibrosis. Successful targeting of siRNA needs the development of an appropriate carrier, which should complex plasmid and allow accumulation into the target organ. Complexes plasmids/polymers are an advantageous alternative to the employ of attenuated viruses. Polyethyleneimine (PEI) is still the more efficient polymer in terms of complex formation and transfection efficiency even if the toxicity limits its employ. Grafting of PEI into HA can mask PEI toxicity, improving polyplex plasma half-life. Thiol cross-linked PEI derivative (PEISS) was grafted into HA through an EDC/HOBT activation of the glucuronic COOH groups (see Scheme 8.4 for general reaction procedure). Copolymer HA-g-PEISS complexed siRNA with a weight ratio polymer/RNA equal to 10 forming aggregates with a mean diameter of 140 nm and a slightly positive zeta potential. First, *in vitro* silencing effect was tested using luciferase siRNA, and testing transfection efficiency in CD44-expressing cells

like melanoma cell line (B16F1) and hepatic stellate cells (HSCs-16) and PEISS-g-HA showed efficiency higher than PEI. Targeting to the liver was assessed by injection of polyplexes with siRNA anti-ApoB lipoprotein in Balb/c mice and finally with TGF- α siRNA on cirrhotic mice. Results demonstrated how HA-g-PEISS was more efficient if compared to PEISS, reducing nonspecific interactions with plasma and producing a receptor-mediated targeting. Moreover, treatment with the same dose of PEISS resulted in the death of mice because of pulmonary embolism, thus demonstrating the ability of HA to reduce PEI toxicity. The reduced TGF- α expression effectively resulted in a positive therapeutic effect on cirrhotic mice.

Since the vitreous humor is naturally composed of HA and collagen, hyaluronic acid hydrogels represent a good choice for the design of retinal drug delivery devices. To be administered into the posterior eye segment, hydrogels should flow if injected and then inside of the eye should form, owing to a specific stimulus such as temperature, light, UV, or pH, a stable cross-linked hydrogel suitable to control therapeutic release. An interesting example of HA-g-copolymer applied for intraretinal drug delivery has been proposed by Wells and colleagues that designed a smart derivative obtained by linking a UV sensible PEG-anthracene to the HA backbone [58].

Anthracene forms reversible dimers or dissociates at wavelengths higher and lower than 300 nm, respectively; as a consequence, HA-g-PEG-anthracene solutions cross-linked and de-cross-linked reversibly. Radiations with wavelength higher than 300 nm penetrate the eye and can be employed to induce gel formation of the polymeric solution after injection. Upon stimulation with wavelengths lower than 300 nm (e.g., by means of two photons absorption technique), it is possible for a de-cross-linking of the hydrogel. The suitability of the hydrogel to control the drug release was proved using various protein models such as myoglobine, lysozyme, and BSA. PEG-anthracene alone showed a dose-dependent cytotoxicity toward retinal cells, while HA-g-PEG-anthracene derivative demonstrated both short-term and long-term *in vitro* biocompatibility; however, it remains to evaluate, by proper *in vivo* study, short-term and long-term potential toxicity of fragments bearing PEG-anthracene moieties.

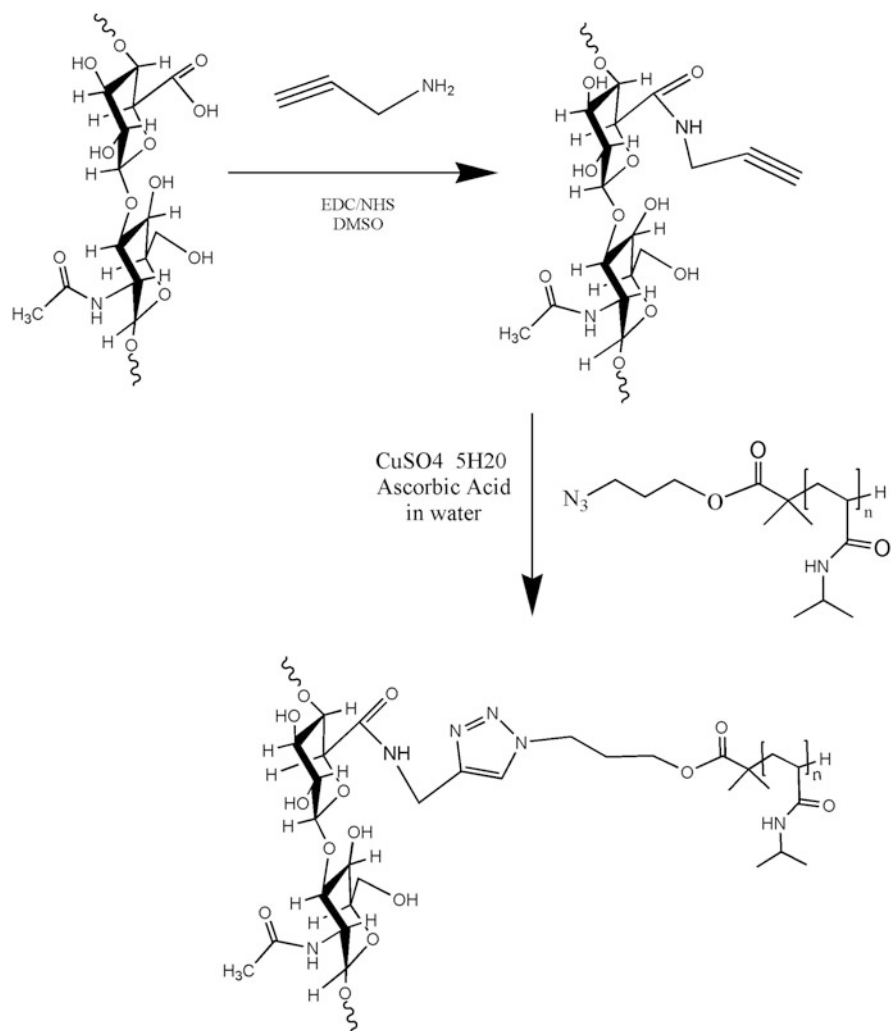
Thermosensitive HA hydrogels have been obtained grafting poly-*N*-isopropylacrylamide (pNIPAM) chains. pNIPAM polymers are known to undergo change in solubility because of the aggregation of the isopropylacrylamide portion by an increase of the temperature up to the critical transition point that is around 30 °C. Grafting pNIPAM into biopolymers allows the formation of thermoresponsive dispersions able to form physical hydrogels at the body temperature.

Several strategies have been adopted to obtain HA-grafted pNIPAM derivatives starting from the work of Matsuda and colleagues that proposed to graft *N*-isopropylacrylamide (NIPAM) monomers directly on HA backbone by radical polymerization technique [59]. HA was first activated with *N,N* diethyldithiocarbamate (DCB) by a chemical procedure in DMF using HA-TBA and DCB activated with DCC/DMAP. Then the activated HA-DBC derivative was employed as polymeric initiator for a UV-induced polymerization of the monomer NIPAM

directly on the HA backbone. The mol% of functionalization of DCB on HA, the amount of NIPAM, and the polymerization time influenced pNIPAM grafting degree on HA and its final molecular weight. In this way, it was possible to prepare HA-g-pNIPAM derivatives having from 0.4 to 11 mol% of grafting degree and a molecular weight of grafted pNIPAM ranging from 5 to 840 kDa. Derivatives with increased grafting degree and higher pNIPAM molecular weight produced sharper sol-gel transitions (32–34 °C). However, in this work, no mechanical or rheological characterization was made; moreover, the use of DCC to activate DCB could cause HA cross-linking due to a possible activation of glucuronic carboxyl group. More recently, Ha and colleagues proposed an alternative way to produce HA-g-pNIPAM derivatives linking pNIPAM-preformed chains to HA [60]. Amino-terminated pNIPAM was first synthesized by radical polymerization technique and then linked to hyaluronic acid COOH groups via EDCI chemistry in water. HA derivatives bearing pNIPAM chains of 6,000 Da and with a functionalization degree comprised between 51 and 70 mol% were tested as injectable depot delivery systems to control protein release, using fluorescent BSA as a model. In particular, fluorescent BSA alone and fluorescent BSA loaded in the HA-g-pNIPAM dispersion were injected subcutaneously to rabbits, and plasma concentration was monitored. The depot was able to sustain protein delivery maintaining higher BSA concentration for more than 60 h. However, such HA-g-pNIPAM derivatives showed only a slight increase in viscosity at 37 °C and below 35 °C; most of the derivatives were too viscous to suppose a suitable application by injection with common syringe gauges.

Recently Mortinsen and colleagues produced a HA-g-pNIPAM derivative by click chemistry grafting into a HA-propargilamine (HApA) (formed by reacting the propargilamine with the glucuronic COOH using EDC/NHS in DMSO), an azido-terminated poly(*N*-isopropylacrylamide) (obtained by reversible addition–fragmentation chain transfer polymerization-RAFT) [61]. Click grafting is performed in water in the presence of ascorbic acid and CuSO₄, stopping the reaction with EDTA to chelate Cu²⁺ ions (see Scheme 8.8).

RAFT allows the production of pNIPAM with controlled molecular weight and a very narrow polydispersity index (PDI). Authors described the possibility to control the viscosity of the copolymer solution before gelling. For example, at 25 °C HA-g-pNIPAM copolymers (10 % w/v solution), having a degree of functionalization ranging from 25 to 30 mol% and a length of pNIPAM of 10,000; 25,000; or 30,000 Da, have a viscosity suitable for injection being comprised between 3.1 and 23 Pa s⁻¹. Even if gel formation was not very quick if compared to gelling properties of pNIPAM solution at 30 °C, it was suitable for an efficient gel forming for an *in vivo* application (about 10 min). Functionalization degree does not influence the gel-forming properties, while better gelling performances were observed for derivatives bearing pNIPAM with higher molecular weight. Mechanical tests performed at different temperatures confirmed the best behavior of hydrogels and obtained grafting pNIPAM with 25 and 30 kDa to HA where at 30 °C a pronounced increase in *G'* modulus was observed with values at 37 °C of 0.14 and 16.1 kPa, respectively. Interestingly HA-g-pNIPAM showed better reversibility upon decrease in temperature if compared to pNIPAM alone. The chemical



Scheme 8.8 Grafting of azido-terminated pNIPAM onto HA-propargilamine by click chemistry [61]

strategy proposed by Mortinsen is potentially exploitable to link drugs previously activated with azido functionalities as demonstrated by linking the hydrophobic dye fluorescein.

Physical hydrogels obtained starting from HA-g-hydrophobic chains can have potential utility as drug delivery systems. Recently Novagenit s.r.l. patented an application of HA graft copolymers with polyesters as biomaterials to coat orthopedic prosthesis. Medicated hydrogels based on these copolymers can be employed during prosthesis implantation to release antibiotics, thus protecting against

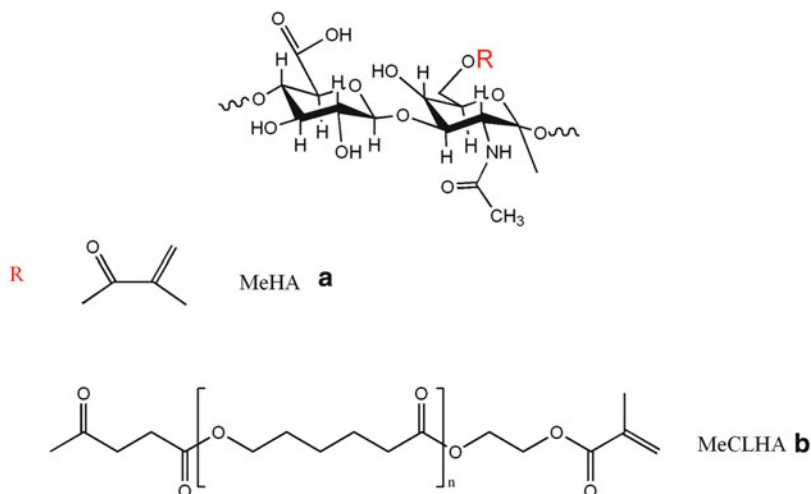
possible formation of bacterial colonies, or to maintain the action of analgesics for controlled period of time. HA can have, if compared to other polymers already employed as coating films, the potentiality of antifouling properties, thanks to its poor ability to allow bacteria adhesion. In this patent, in particular, HA-g polyesters are proposed to form, at the opportune concentration in aqueous environment, physical hydrogels with proper rheological behavior to be, just before the surgical intervention, mixed with drug solution and then applied on prosthesis surface [62, 63].

8.3.2 HA-Graft-Synthetic Polymers to Obtain Scaffolds for Tissue Engineering

Thanks to its structural and bio-inductive role in the ECM, HA finds a wide application for the production of scaffolds to support cell growth or to obtain their delivery to a damaged tissue or organ. Most of the examples employ HA graft copolymers to change physicochemical properties of starting HA, with the aim to improve hydrolytic and mechanic resistance or to produce self-assembled physical hydrogels or to obtain copolymers with peculiar solubility in organic solvents better suitable for processing strategies.

Examples in regenerative medicine include the induction of chondrocytes expansion and differentiation or [64] the employ of in situ implantable HA-based biomaterials to delivery mesenchymal stem cells for the treatment of full-thickness defects [65]. Physical hydrogels, obtained by aqueous dispersion of HA-alkyl chain derivatives, for instance, HA-C12 and HA-C18, were proposed as biomaterials to delivery primary chondrocytes into full-thickness articular defects [66]. Dispersions of such copolymers in physiological solution at concentration equal to 1 % w/v produced viscoelastic injectable hydrogels that were loaded into rat articular cartilage defects and tested for their property to improve cartilage repair in comparison with hybrid sponges made of Alginate/HA and Alginate/HAC18. Authors demonstrated that physical hydrogels made of HA-C18 copolymer were suitable to stimulate bone regeneration; however, better results, in terms of GAG and collagen neosynthesis, were obtained with implants made of HA-C18 and Alginate. Major concerns about the use of physical HA hydrogels are however related to the lower stability due to a possible dissolution in the aqueous fluids if compared with chemically cross-linked HA-based materials. Burdick and colleagues designed HA photocrosslinkable hydrogels for cartilage regeneration obtained mixing in different ratio-methacrylated HA (HA-MA) derivatives and HA-g-polycaprolactone-methacrylated (HA-g-PCL-MA) derivatives (see Scheme 8.9) [67].

Compared to the photocrosslinked HA-MA derivatives, HA-g-PCL-MA cross-linked derivatives allow a faster degradation due to the hydrolysis of the grafted polyester. Indeed HA-methacrylated cross-linked hydrogels are characterized by a



Scheme 8.9 HA modifications with methacrylic (MA) (a) and polycaprolactone-MA (PCL-MA) and (b) moieties proposed by Burdick et al. [69, 70]

long-term hydrolytic resistance, thanks to a reduced recognition of the cross-linked material by hyaluronidase [68]. However, to facilitate chondrocyte growth, an appropriate temporal degradation of the scaffold should occur, because cells need more space to receive nutrients and to clear wastes. The introduction of hydrolytically degradable polyester chains, such as PCL, has been successfully designed to improve scaffold hydrolysis rate with time [69, 70].

Mixing different weight ratios of not grafted and PCL-grafted HA-MA derivatives, it was possible to properly control the rate of hydrolysis of chondrocyte or mesenchymal stem cell-loaded scaffolds. In particular, hydrogel obtained by cross-linking HA-MA and HA-g-PCL-MA in a ratio 1:1 with a concentration of 2 % w/v had the best rate of hydrolysis, enough to allow a uniform deposition of collagen II and GAG inside the hydrogel. Chemically cross-linked hydrogels based on HA-MA alone have instead a rate of hydrolysis too slow, and they do not permit a uniform deposition of ECM matrix, thus producing a neocartilage with lower mechanical properties.

A HA-g-PLGA was proposed recently by Park and colleagues as suitable derivative for the production of scaffolds by solid free-form fabrication technique (SSFF). The SSFF allows the production of micro-engineered scaffolds with ordered morphologies. The core of the system is a computerized multihead deposition system that controls the injection of thin layers of the polymeric solution in a hot air-conditioned box. Upon evaporation of the solvent, the polymeric solution solidifies producing the scaffold. The HA-g-PLGA copolymer was produced starting from a HA with a molecular weight of 20,000 Da through the formation of the hydrazide-functionalized HA-ADH derivative (see Scheme 8.6a). This hydrazide-terminated HA derivative was then employed for the grafting with

PLGA-NHS derivative (PLGA Mw was 80,000 Da) [19]. Interestingly the obtained HA-g-PLGA (bearing 30 mol% of PLGA) was soluble in dichloromethane at 12.5 % w/v and employed for the SSFF technique. In this way, it was possible to obtain HA-g-PLGA scaffolds having an ordered structure with lines of 250 μm and pores of 200–400 μm ; the trabecular morphology was designed to better mimic the bone micromorphology.

HA-g-PLGA scaffolds empty or loaded with bone morphogenetic protein-2 (BMP2) were tested *in vivo* for the regeneration of calvarial bone defects after 4 weeks of implantation in a rat model. Results demonstrated how both kinds of scaffolds were useful to improve bone regeneration if compared to the non-treated animals, and in particular, the BMP-loaded scaffold was able to induce the formation of osteoid tissue composed of type I collagen, chondroitin sulfate, and osteocalcin in its surface as well as inside.

HA-g-copolymer-based biomaterials with thermoresponsiveness can find application in regenerative medicine as *in situ*-forming hydrogels or as reversible scaffolds for cell culture recovery. For example, HA-g-pNIPAM derivatives previously reported (see Sect. 8.3.1) obtained by click chemistry have been applied to encapsulate nucleus pulposus (NP) cells and evaluated for spinal NP regeneration [71].

This study demonstrated how cell viability was dependent on molecular weight of pNIPAM linked to the HA backbone; indeed derivatives bearing pNIPAM of 30 kDa, which showed the best mechanical performances, produced a sensible decrease in NP viability, while derivatives bearing pNIPAM with 20 kDa, even if softer, allowed a good viability of NP. Probably longer pNIPAM chains produced, upon temperature increase, greater volume contraction that caused cell death. HA-g-pNIPAM 20 kDa having lower mechanical resistance allowed cell survival for 7 days and the maintenance of correct phenotype.

HA-g-pNIPAM was also proposed to give *in situ*-forming hydrogels for the growth of adipose-derived stem cells [72]. Grafting of preformed carboxyl-terminated pNIPAM was accomplished using hydrazide-functionalized HA-ADH derivative. In particular pNIPAM was activated with EDC and added to HA-ADH dispersed in water at pH 5.6. The derivative bearing the 53 % w/w in pNIPAM without cells was injected in the dorsal subcutaneous region of athymic nude mice to test scaffold biocompatibility. Scaffold maintained a good consistence for more than 5 days and no cellular infiltrate was observed. No longer studies were performed to see mechanical performances of this scaffold. *In vitro* tests confirmed the possibility to encapsulate human adipose-derived stem cells (ASCs) during 28 days of culture. The encapsulated ASCs were better retained in the hydrogel bearing higher amount of pNIPAM probably because of optimal scaffold porosity, and maintenance of round shape suggested preservation of correct phenotype.

To avoid possible scaffold dissolution, a chemical cross-linking, better if induced by an external stimulation, is often coupled to physical gel-forming strategies. Park proposed a thermosensible gel-forming material obtained grafting into HA backbone, Pluronic F127 chains. Pluronic triblock copolymers, like pNIPAM, show thermo-induced assembling because of the formation of

hydrophobic coils upon temperature increase. Like pNIPAM, pluronic solutions give this transition at temperature comprised between 20 and 30 °C, and then they are exploitable to produce injectable in situ-forming hydrogels for body injection. An amino-terminated Pluronic F127 was employed to perform the grafting reaction with the glucuronic COOH groups in water using EDC/HOBt as coupling reactants [73].

Moreover, a photo-sensible methacrylic moiety was inserted as pendant group of HA backbone. Such methacrylated HA-g-pluronic solutions produced physical hydrogels at 37 °C, and then they were transformed into chemically cross-linked scaffolds upon UV irradiation at 365 nm. Bovine chondrocytes were safely encapsulated being viable after both physical gel formation and UV cross-linking. Chondrocytes proliferate inside the scaffold producing specific cartilage components as collagen type II and aggrecan.

8.4 HA-Graft-Peptides with Pharmacological Activity: Characterization and Properties

HA has been proposed as a suitable biopolymer to prolong and improve therapeutic protein activity. As PEG, HA can shield proteins, thus protecting them from a specific recognition by complement system against specific enzymatic hydrolysis or immunologic adverse responses; moreover, unlike PEG that has been found to accumulate into the body [74, 75], HA has the advantage of complete biodegradability. Moreover, even for the delivery of therapeutic proteins, the specific targeting ability toward a series of receptors implicated in several biological processes represents a great potentiality. Finally from a chemical point of view, HA offers several anchorage points for grafting procedure compared to PEG that has only terminal functionalities available for grafting. The potential application of a polymer for the development of protein therapeutic systems has been extensively theorized by Duncan that introduced the concept of polymer masked-unmasked protein therapy (PUMPT) which postulates the employ of a suitable polymer able to first mask protein from the adverse enzymatic recognition and then to unmask protein activity at the specific action site [76, 77].

Application suitability of HA polymeric prodrugs, both for local organ or tissue delivery and for systemic administration, has been proved by the production of several HA-g-therapeutic protein derivatives. One of the first examples of HA-g-therapeutic proteins exploited the known property of high molecular weight HA as anti-inflammatory and scavenger in tissue injuries associated with inflammatory reactions [78]. Superoxide dismutase (SOD) is a protein that catalyzes the dismutation of reactive superoxide anion to molecular oxygen and for this activity has potential therapeutic effects for the treatment of allergic reactions and Crohn's disease. In addition to improve plasma half-life, pegylated SOD derivatives have been proposed for the treatment of ischemia or pleurisy [79–81]. Sakurai and

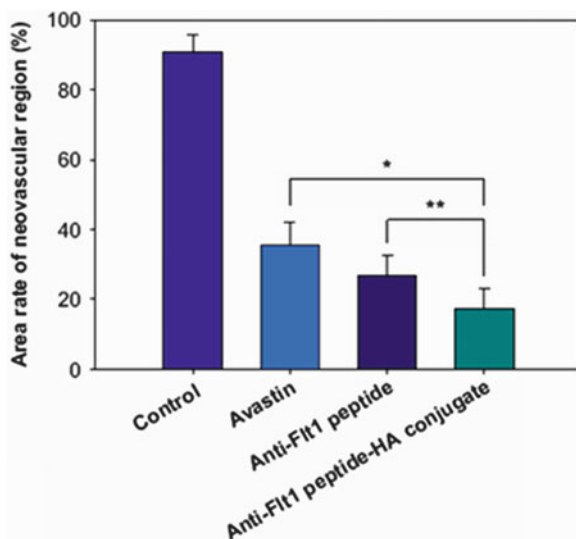
colleagues described the potentiality of the HA-g-SOD derivative testing its immunological and suppressive activity toward ischemic paw edema, pleurisy, and arthritis in experiment animals. Grafting of SOD into HA was performed by EDC chemistry in aqueous environment linking amino-functionalized amino acids of SOD to the glucuronic COOH and obtaining a grafting degree of protein equal to 4.6 % w/w. Compared to the bovine SOD, the HA-g-SOD was very less immunoreponsive. Moreover, HA-g-SOD derivatives exhibited much higher activity than SOD and SOD-PEG in all the simulated inflammation conditions, probably because of the cooperative action of HA as radical scavenger. When employed as a polymeric prodrug, exploiting both structural and biological functions, HA offers the best opportunity as a carrier for therapeutic protein. For example, it is known the good suitability of HA as biomaterial for ocular application [82, 83] since it binds to the layer of mucin on the corneal epithelium, prolonging the residence time in the conjunctive sac [84]. HA is abundantly produced in the vitreous of the eye, and low molecular weight HA recognizes receptors CD44 and RHAMM expressed also in the vascular endothelial layer of the retina [85]. Recently Oh and colleagues described the production and the activity of a graft copolymer of HA with the antiangiogenic peptide anti-Flt1, a potent inhibitor of the vascular endothelial growth factor receptor 1 (VEGFR-1) that has been proposed for the treatment of the corneal and the retinal neovascularization [33]. The anti-Flt1 peptide (6 amino acids) was linked to the HA through its terminal amino group employing benzotriazol-1-yloxy-tris(dimethyl-amino)phosphonium hexafluorophosphate (BOP) as an activator of glucuronic COOH groups, performing the reaction in DMSO in the presence of diisopropyl ethylenamine as a proton trap (see Scheme 8.5a).

The derivative was then characterized in terms of number of peptide linked for HA chain through a fluorimetric analysis exploiting peptide photoluminescence. In particular following the chemical procedure showed before, and using an amount of peptide from 4 to 55 molecules respect to a single HA chain, it was possible to obtain a functionalization ranging from 3 to 30 molecules for HA chain. When low molecular weight HA was employed, the derivative self-assembled into micelles because of peptide hydrophobicity. The first beneficial effect was to improve protein solubility, as reflected also by the increased ability of the HA graft copolymer to interact with the VEGF receptor in comparison with free peptide. The inhibitory effect on corneal neovascularization was detected comparing the activity of the HA graft copolymer with that of free peptide and Avastin[®], and as showed in Fig. 8.4, HA-g-Anti-Flt1 was statistically more efficient in reducing neovascularization area.

The system was tested also for the retina vascularization by evaluating its activity after intravitreous injection to diabetic rats. Results confirmed the increased activity of the HA-g-Anti-Ftl1 compared to free peptide. Moreover, pharmacokinetic studies confirmed the lower clearance of the HA-g-Anti-Ftl1 from the vitreous body.

Natural HA has a half-life in plasma of 5 min; moreover, more than 90 % of not functionalized HA is known to accumulate into the liver, mainly because of the

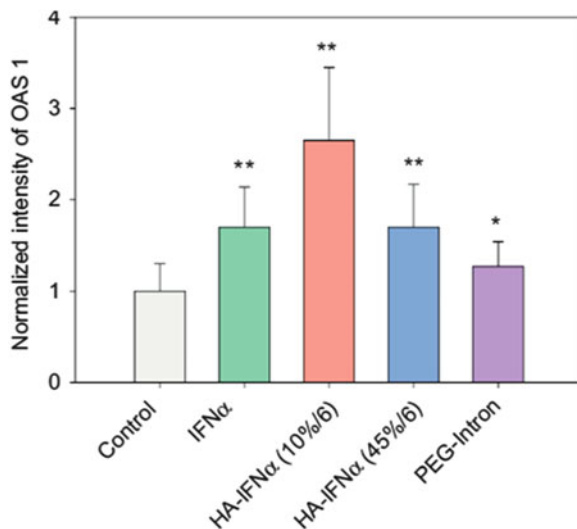
Fig. 8.4 Antiangiogenic activity of anti-Flt1 peptide, HA-g-Anti-Flt1, and Avastin measured by inhibition of neovascularization in silver nitrate cauterized corneas of rats in 2 weeks (Reproduced with permission, copyright 2009 Elsevier [33])



recognition by hepatic receptors including LYVE-1 and HARE [86, 87]. As described in Sect. 8.3.1, Hahn's research group demonstrated that biodistribution and pharmacokinetic of HA can be affected by the degree of substitution of the glucuronic COOH groups [88].

In particular using HA-ADH tethered to Qdots having a COOH functionalization with ADH lower than 30 mol%, the interaction with HARE hepatic receptors was not masked, and HA-ADH-g-Qdots accumulated mainly into liver. Starting from these findings, Yang and colleagues [89] described the production and the *in vivo* efficacy of a HA-g-interferon- α derivative. Interferon- α (IFN- α) is extensively employed for the treatment of hepatitis C, even if the employ of free peptide is limited by its side effects related to the not optimal pharmacokinetic. PEGylation has been employed to obtain long-acting derivatives through the production and commercialization of PEGASYS or PEG-Intron [90, 91]. However, even if these pegylated derivatives improved interferon- α activity, only the 39 % of patients affected by hepatitis C respond completely to the treatment. To test the potentiality of HA as PEG substitute, a HA-aldehyde derivative, obtained by periodate oxidation, was employed to conjugate the INF- α via the formation of imidic linkage with the primary amine of a lysine portion. This reaction was very efficient in aqueous environment at pH 5.5. However, the aldehyde functionalization performed by periodate oxidation offers several concerns, related to the HA stability during the oxidative reaction and to the stability of the HA-aldehyde derivative during the storage. Starting from HA-aldehyde derivatives with a molar functionalization in aldehyde groups ranging from 10 to 45 % and using a molar ratio INF- α /aldehyde from 2 to 9, HA-g-INF- α derivatives, with a bioconjugation efficiency near to the 95 %, were obtained. The unreacted free aldehyde can be blocked by treatment with an excess of ethylcarbазate. HA-g-INF α shows a stability three times longer in

Fig. 8.5 Levels of OAS 1 detected by densitometric analysis in mouse liver tissues treated with interferon- α (IFN- α), two kinds of HA-g-IFN α derivatives prepared with 10 mol% and 45 mol% aldehyde modified HA, and PEG-Intron (Reproduced with permission, copyright 2011 Elsevier [89])



serum and an in vitro efficacy lower than free INF- α but comparable to that of commercial available PEG-Intron. In animals, dye-labeled INF- α rapidly distributed to all body compartments and was completely eliminated after 24 h, while dye-labeled HA-g-INF- α accumulated just after 60 min mostly into the liver and prolonged its circulation time for more than 96 h. The detection of protein OAS1 (enzyme involved in the activation of a RNase that inhibits viral replication) was considered as a marker of the INF- α activity in the animals treated with INF- α , PEG-Intron, and two batches of HA-g-INF- α bearing the same amount of interferon (6 mol%) but obtained starting from a HA bearing 10 and 45 mol% of aldehyde, respectively.

As shown in Fig. 8.5, 10 mol% functionalized HA-g-INF- α resulted much more efficient if compared to PEG-Intron and the more functionalized HA-g-INF- α derivative, confirming that a HA glucuronic functionalization lower than 30 mol% does not reduce hepatic accumulation while more functionalized derivatives escape hepatic targeting.

Similar HA-g-INF- α copolymers were proposed also by Fidia Advanced Biopolymers that employed for the grafting procedure hemiacetalic HA derivatives generating HA-aldehyde with a chemical structure similar to that showed in Scheme 8.6c [92]. In this procedure, aldehyde is deprotected just before the protein conjugation with an acidic treatment. Moreover, the functionalization of HA with the masked aldehyde can be performed with EDC/NHS or CDI chemistry employing HA-TBA and hemiacetal amines.

An example of HA-g-peptide copolymer applied for a non-hepatic targeting has been presented recently by Hahn research group that tested the antidiabetic effect of the short peptide exendin 4. The exendin 4 is an incretin mimetic with gluco-regulatory activity commercialized as Byetta[®] for the treatment of type 2 diabetes that however has found a limited clinical application because of a very short

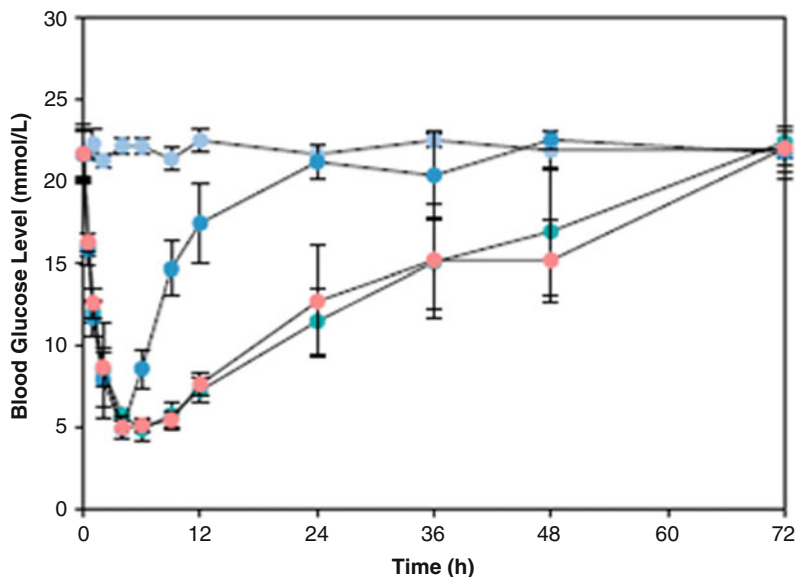


Fig. 8.6 Glucose-lowering profile in type 2 db/db mice after subcutaneous injection of (*gray diamond*) PBS, (*blue diamond*) exendin 4, (*red circle*) HA-g-exendin 4 derivative (30/10), and (*green circle*) HA-g-exendin 4 derivative (70/10) at a dose of 50 nmol/kg (Reproduced with permission, copyright 2010 Elsevier [40])

$t_{1/2}$ (90 min). PEGylation was tested to improve pharmacokinetic of the exendin but produced a significant decrease in peptide activity. An elegant functionalization strategy was proposed to graft exendin 4 to the HA backbone by the production of a vinyl sulfone HA intermediate (see Scheme 8.6f) easily exploitable to graft thiol-bearing peptides through a Michael addition performed at pH 9 [40]. Stability of HA-g-exendin-4 enhanced, reaching in human plasma a $t_{1/2}$ of 96 h, and more functionalized derivatives showed better results probably because of the reduction of free glucuronic COOH. Glucose-lowering ability of these derivatives was assessed on diabetic mice showing how they were able to prolong peptide activity (Fig. 8.6).

8.5 Conclusions

A review of chemical modifications, carried out to graft polymers or peptides to hyaluronic acid, has been reported, by underlining the reasons that justify the production of a specific HA graft derivative. In general the production of HA graft derivatives allows to obtain copolymers with physicochemical properties suitable for a specific aim, for instance, to prepare a drug delivery system or a three-dimensional scaffold for tissue engineering. However, despite of many works

performed by various research groups throughout the world, only few HA graft copolymers have reached the clinical phase and even less the market. While from the chemical point of view, great levels of knowledge have been obtained, in the biochemical and pharmacological field, a lot more still needs to be done. This is the main reason why still nowadays several research groups are involved in the production of HA graft derivatives that could be able to overcome the clinical phase and to reach the market. Among HA graft copolymers, derivatives containing peptides with pharmacological activity seem very interesting, thanks to the possibility to control their hepatic accumulation, by exploiting HA targeting toward specific cell receptors and preparing long circulating blood systems. Thanks to the remarkable progress made by molecular biology, that explains the role that several bioactive peptides play in pathological processes (e.g., in the cancer) and being known problems related to peptide administration in humans, in the near future, HA graft peptides could represent an effective tool for the administration and release of a variety of peptides with biological activity.

References

1. Kuo JW (2006) Practical aspects of hyaluronan-based medical products. CRC Press, New York, NY
2. Kogan G, Soltés L, Stern R, Gemeiner P (2007) Hyaluronic acid: a natural biopolymer with a broad range of biomedical and industrial applications. *Biotechnol Lett* 29:17–25
3. Toole BP (2001) Hyaluronan in morphogenesis. *Semin Cell Dev Biol* 12:79–87
4. Toole BP (2004) Hyaluronan: from extracellular glue to pericellular cue. *Nat Rev Cancer* 4:528–539
5. Stern R, Asari AA, Sugahara KN (2006) Hyaluronan fragments: an information-rich system. *Eur J Cell Biol* 85:699–715
6. Aruffo A, Stamenkovic I, Melnick M, Underhill CB (1990) Seed B CD44 is the principal cell surface receptor for hyaluronate. *Cell* 61:1303–1313
7. Toole BP (2009) Hyaluronan-CD44 interactions in cancer: paradoxes and possibilities. *Clin Cancer Res* 15:7462–7468
8. Entwistle J, Hall CL, Turley EA (1996) HA receptors: regulators of signalling to the cytoskeleton. *J Cell Biochem* 61:569–577
9. Toole BP (1998) Hyaluronan-cell interactions in morphogenesis. Portland Press, London
10. Asayama S, Nogawa M, Takei Y, Akaike T, Maruyama A (1998) Synthesis of novel polyampholyte comb-type copolymers consisting of a poly(L-lysine) backbone and hyaluronic acid side chains for a DNA carrier. *Bioconjugate Chem* 9:476–481
11. Takei Y, Maruyama A, Ferdous A, Nishimura Y, Kawano S, Ikejima K, Okumura S, Asayama S, Nogawa M, Hashimoto M, Makino Y, Kinoshita M, Watanabe S, Akaike T, Lemasters JJ, Sato N (2004) Targeted gene delivery to sinusoidal endothelial cells: DNA nanoassociate bearing hyaluronan-glycocalyx. *FASEB J* 18:699–701
12. Schledzewski K, Falkowski M, Moldenhauer G, Metharom P, Kzhyshkowska J, Ganss R, Demory A, Falkowska-Hansen B, Kurzen H, Ugurel S, Geginat G, Arnold B, Goerdts S (2006) Lymphatic endothelium-specific hyaluronan receptor LYVE-1 is expressed by stabilin-1+, F4/80+, CD11b+ macrophages in malignant tumours and wound healing tissue. In vivo and in bone marrow cultures in vitro: implications for the assessment of lymphangiogenesis. *J Pathol* 209:67–77

13. Eriksson S, Fraser JR, Laurent TC, Pertoft H, Smedsrod B (1983) Endothelial cells are a site of uptake and degradation of hyaluronic acid in the liver. *Exp Cell Res* 144:223–228
14. Balazs EA (2009) Therapeutic use of hyaluronan. *Struct Chem* 20:341–349
15. Prestwich GD (2011) Hyaluronic acid-based clinical biomaterials derived for cell and molecule delivery in regenerative medicine. *J Control Release* 155:193–199
16. Elisseeff J (2004) Injectable cartilage tissue engineering. *Expert Opin Biol Ther* 4:1849–1859
17. Mori M, Yamaguchi SS, Takai Y (2004) Hyaluronan-based biomaterials in tissue engineering. *Acta Histochem Cytochem* 37:1–5
18. Misra S, Heldin P, Hascall VC, Karamanos NK, Skandalis SS, Markwald RR, Ghatak S (2010) Hyaluronan–CD44 interactions as potential targets for cancer therapy. *Expert Opin Drug Deliv* 7:681–703
19. Park H, Yeom J, Oh EJ, Reddy M, Kim JY, Cho DW, Lim HP, Kim NS, Park SW, Shin HI, Yang DJ, Park KB, Hahn SK (2009) Guided bone regeneration by poly(lactic-co-glycolic acid) grafted hyaluronic acid bi-layer films for periodontal barrier applications. *Acta Biomater* 5:3394–3403
20. Malson T, Lindqvist B (1986) Gels of crosslinked hyaluronic acid for use as a vitreous humor substitute. IWO Patent Application 000079
21. Yui N, Okano T, Sakurai Y (1992) Inflammation responsive degradation of crosslinked hyaluronic acid gels. *J Control Release* 22:105–116
22. Toemmeras K, Eenschooten C (2007) Aryl/alkyl succinic anhydride hyaluronan derivatives. IWO Patent Application 033677
23. Palumbo FS, Pitarresi G, Mandracchia D, Tripodo G, Giammona G (2006) New graft copolymers of hyaluronic acid and polylactic acid: synthesis and characterization. *Carbohydr Polym* 66:379–385
24. Pravata L, Braud C, Boustta M, El Ghzaoui A, Tømmeras K, Guillaumie F, Schwach-Abdellaoui K, Vert M (2008) New amphiphilic lactic acid oligomer–hyaluronan conjugates: synthesis and physicochemical characterization. *Biomacromolecules* 9:340–348
25. Eenschooten C, Guillaumie F, Kontogeorgis G, Stenby E, Schwach-Abdellaoui K (2010) Preparation and structural characterisation of novel and versatile amphiphilic octenyl succinic anhydride-modified hyaluronic acid derivatives. *Carbohydr Polym* 79:597–605
26. Mlčochová P, Bystrický S, Steiner B, Machová E, Kooš M, Velebný V, Krcmár M (2006) Synthesis and characterization of new biodegradable hyaluronan alkyl derivatives. *Biopolymers* 82:74–79
27. Giammona G, Palumbo FS, Pitarresi G (2010) Method to produce hyaluronic acid functionalized derivatives and formation of hydrogels thereof. IWO Patent Application 061005A
28. Palumbo FS, Pitarresi G, Fiorica C, Matricardi P, Albanese A, Giammona G (2012) In situ forming hydrogels of new amino hyaluronic acid/benzoyl-cysteine derivatives as potential scaffolds for cartilage regeneration. *Soft Matter* 8:4918–4927
29. Danishefsky I, Siskovic E (1971) Conversion of carboxyl groups of mucopolysaccharides into amides of amino acid esters. *Carbohydr Res* 16:199–205
30. Nakajima N, Ikada Y (1995) Mechanism of amide formation by carbodiimide for bioconjugation in aqueous media. *Bioconjugate Chem* 6:123–130
31. Pouyani T, Prestwich GD (1994) Functionalized derivatives of hyaluronic acid oligosaccharides: drug carriers and novel biomaterials. *Bioconjugate Chem* 5:339–347
32. Bulpitt P, Aeschlimann D (1999) New strategy for chemical modification of hyaluronic acid: preparation of functionalized derivatives and their use in the formation of novel biocompatible hydrogels. *J Biomed Mater Res* 47:152–169
33. Oha EJ, Park K, Choi CK, Joo CK, Hahn SK (2009) Synthesis, characterization, and preliminary assessment of anti-Flt1 peptide–hyaluronate conjugate for the treatment of corneal neovascularisation. *Biomaterials* 30:6026–6034
34. Bellini D, Topai A (2001) Amides of hyaluronic acid and the derivatives thereof and a process for their preparation. EP 1095064

35. Bergman K, Elvingson C, Hilborn J, Svensk G, Bowden T (2007) Hyaluronic acid derivatives prepared in aqueous media by triazine-activated amidation. *Biomacromolecules* 8:2190–2195
36. Della Valle F, Romeo A (1990) Cross-linked esters of hyaluronic acid. US 4957744
37. Prestwich G, Marecak D, Marecek J, Vercruyse K, Ziebell M (1998) Controlled chemical modification of hyaluronic acid: synthesis, applications, and biodegradation of hydrazide derivatives. *J Control Release* 53:93–103
38. Park JK, Shim JH, Kang HS, Yeom J, Jung HS, Kim JY, Lee KH, Kim TH, Kim SY, Cho DW, Hahn SK (2011) Solid free-form fabrication of tissue engineering scaffolds with a poly(lactic-co-glycolic acid) grafted hyaluronic acid conjugate encapsulating an intact bone morphogenetic protein–2/poly(ethylene glycol) complex. *Adv Funct Mater* 2011:2906–2912
39. Serban MA, Prestwich GD (2007) Synthesis of hyaluronan haloacetates and biology of novel cross-linker-free synthetic extracellular matrix hydrogels. *Biomacromolecules* 8:2821–2828
40. Kong JH, Oh EJ, Chae SY, Lee KC, Hahn SK (2010) Long acting hyaluronate—exendin 4 conjugate for the treatment of type 2 diabetes. *Biomaterials* 31:4121–4128
41. Brigger I, Dubernet C, Couvreur P (2002) Nanoparticles in cancer therapy and diagnosis. *Adv Drug Deliv Rev* 54:631–651
42. Katoh S, Zheng Z, Oritani K, Shimozato T, Kincade PW (1995) Glycosylation of CD44 negatively regulates its recognition of hyaluronan. *J Exp Med* 182:419–429
43. Harris EN, Kyosseva SV, Weigel JA, Weigel PH (2007) Expression, processing, and glycosaminoglycan binding activity of the recombinant human 315-kDa hyaluronic acid receptor for endocytosis (HARE). *J Biol Chem* 282:2785–2797
44. Tringali G, Lisi L, Bettella F, Renier D, Di Stasi SM, Navarra P (2008) The in vitro rabbit whole bladder as a model to investigate the urothelial transport of anticancer agents The ONCOFID-P[®] paradigm. *Pharmacol Res* 58:340–343
45. Lesley J, Hascall VC, Tammi M, Hyman R (2000) Hyaluronan binding by cell surface CD44. *J Biol Chem* 275:26967–26975
46. Platt MV, Szoka FC (2008) Anticancer therapeutics: targeting macromolecules and nanocarriers to hyaluronan or CD44, a hyaluronan receptor. *Mol Pharmacol* 5:474–486
47. Kim J, Kim KS, Jiang G, Kang H, Kim S, Kim BS, Park MH, Hahn SK (2008) In vivo real-time bioimaging of hyaluronic acid derivatives using quantum dots. *Biopolymers* 89:1144–1153
48. Kim J, Park K, Hahn SK (2008) Effect of hyaluronic acid molecular weight on the morphology of quantum dot–hyaluronic acid conjugates. *Int J Biol Macromol* 42:41–45
49. Pelletier S, Hubert P, Lapique F, Payan E, Dellacherie E (2000) Amphiphilic derivatives of sodium alginate and hyaluronate: synthesis and physico-chemical properties of aqueous dilute solutions. *Carbohydr Polym* 43:343–349
50. Eenschooten C, Christensen MW (2007) Aryl/alkyl vinyl sulfone hyaluronic acid derivatives. IWO Patent Application 098770A1
51. Eenschooten C, Vaccaro A, Delie F, Guillaumie F, Tømmeraaas K, Kontogeorgis GM, Schwach-Abdellaoui K, Borkovec M, Gurny R (2012) Novel self-associative and multiphasic nanostructured soft carriers based on amphiphilic hyaluronic acid derivatives. *Carbohydr Polym* 87:444–451
52. Liu Y, Sun J, Cao W, Yang J, Lian H, Li X, Sun Y, Wang Y, Wang S, He Z (2011) Dual targeting folate-conjugated hyaluronic acid polymeric micelles for paclitaxel delivery. *Int J Pharm* 421:160–169
53. Pitarresi G, Palumbo FS, Albanese A, Fiorica C, Picone P, Giammona G (2010) Self-assembled amphiphilic hyaluronic acid graft copolymers for targeted release of antitumoral drug. *J Drug Target* 18:264–276
54. Lee H, Ahn CH, Park TG (2009) Poly[lactic-co-(glycolic acid)]-grafted hyaluronic acid copolymer micelle nanoparticles for target-specific delivery of doxorubicin. *Macromol Biosci* 2009:336–342
55. Kim TG, Lee H, Jang Y, Park TG (2009) Controlled release of paclitaxel from heparinized metal stent fabricated by layer-by-layer assembly of polylysine and hyaluronic acid-g-poly

- (lactic-co-glycolic acid) micelles encapsulating paclitaxel. *Biomacromolecules* 2009:1532–1539
56. Cho HJ, Yoon HY, Koo H, Ko SH, Shim JS, Lee JH, Kim K, Kwon IC, Kim DD (2011) Self-assembled nanoparticles based on hyaluronic acid-ceramide (HA-CE) and Pluronic[®] for tumor-targeted delivery of docetaxel. *Biomaterials* 32:7181–7190
 57. Park K, Hong SW, Hur W, Lee MY, Yang JA, Kim SW, Yoon SK, Hahn SK (2011) Target specific systemic delivery of TGF- β siRNA/(PEI-SS)-g-HA complex for the treatment of liver cirrhosis. *Biomaterials* 32:4951–4958
 58. Wells LA, Furukawa S, Sheardown H (2011) Photoresponsive PEG-anthracene grafted hyaluronan as a controlled-delivery biomaterial. *Biomacromolecules* 12:923–932
 59. Ohya S, Nakayama Y, Matsuda T (2001) Thermoresponsive artificial extracellular matrix for tissue engineering: hyaluronic acid bioconjugated with poly(N-isopropylacrylamide) grafts. *Biomacromolecules* 2:856–863
 60. Ha DI, Lee SB, Chong MS, Lee YM (2006) Preparation of thermo-responsive and injectable hydrogels based on hyaluronic acid and poly(N-isopropylacrylamide) and their drug release behaviors. *Macromol Res* 14:87–93
 61. Mortisen D, Peroglio M, Alini M, Eglin D (2010) Tailoring thermoreversible hyaluronan hydrogels by “Click” chemistry and RAFT polymerization for cell and drug therapy. *Biomacromolecules* 11:1261–1272
 62. Giammona G, Pitarresi G, Palumbo FS, Romanò CL, Meani E, Cremascoli E (2010) Antibacterial hydrogel and use thereof in orthopaedics. EPO 09151755.7
 63. Giammona G, Pitarresi G, Palumbo FS, Romanò CL, Meani E, Cremascoli E (2010) Idrogelo a base di acido ialuronico e suo uso in ortopedia. Italian Patent MIA001451
 64. Bedi A, Feeley BT, Williams RJ (2010) Management of articular cartilage defects of the knee. *J Bone Joint Surg Am* 92:994–1009
 65. Galle J, Bader A, Hepp P, Grill W, Fuchs B, Käs JA, Krinner A, Marquass B, Müller K, Schiller J, Schulz RM, von Buttler M, von der Burg E, Zscharnack M, Löffler M (2010) Mesenchymal stem cells in cartilage repair: state of the art and methods to monitor cell growth, differentiation and cartilage regeneration. *Curr Med Chem* 17:2274–2291
 66. Dausse Y, Grossi L, Miralles G, Pelletier S, Mainard D, Hubert P, Baptiste D, Gillet P, Dellacherie E, Netter P, Payan E (2003) Cartilage repair using new polysaccharidic biomaterials: macroscopic, histological and biochemical approaches in a rat model of cartilage defect. *Osteoarthr Cartil* 11:16–28
 67. Kim IL, Mauck RL, Burdick JA (2011) Hydrogel design for cartilage tissue engineering: a case study with hyaluronic acid. *Biomaterials* 32:8771–8782
 68. Smeds KA, Pfister-Serres A, Miki D, Dastgheib K, Inoue M, Hatchell DL, Grinstaff MW (2001) Photocrosslinkable polysaccharides for in situ hydrogel formation. *J Biomed Mater Res* 54:115–121
 69. Burdick JA, Chung C, Jia XQ, Randolph MA, Langer R (2005) Controlled degradation and mechanical behavior of photopolymerized hyaluronic acid networks. *Biomacromolecules* 6:386–391
 70. Bryant SJ, Nuttelman CR, Anseth KS (1999) The effects of crosslinking density on cartilage formation in photocrosslinkable hydrogels. *Biomed Sci Instrum* 35:309–314
 71. Peroglio M, Grad S, Mortisen D, Sprecher CM, Illien-Jünger S, Alini M, Eglin D (2011) Injectable thermoreversible hyaluronan-based hydrogels for nucleus pulposus cell encapsulation. *Eur Spine J*. doi:10.1007/s00586-011-1976-2
 72. Tan H, Ramirez CM, Miljkovic N, Li H, Rubin JP, Marra KG (2009) Thermosensitive injectable hyaluronic acid hydrogel for adipose tissue engineering. *Biomaterials* 30:6844–6853
 73. Lee H, Tae TG (2009) Photo-crosslinkable, biomimetic, and thermo-sensitive pluronic grafted hyaluronic acid copolymers for injectable delivery of chondrocytes. *J Biomed Mater Res A* 88:797–806

74. Bendele A, Seely J, Richey C, Sennello G, Shopp G (1998) Renal tubular vacuolation in animals treated with polyethylene-glycolconjugated proteins. *Toxicol Sci* 42:152–157
75. Veronese FM, Harris JM (2002) Introduction and overview of peptide and protein pegylation. *Adv Drug Deliv Rev* 54:453–456
76. Duncan R (2006) Polymer conjugates as anticancer nanomedicines. *Nat Rev Cancer* 6:688–701
77. Duncan R, Gilbert HRP, Carbajo RJ, Vicent MJ (2008) Polymer masked–unmasked protein therapy (PUMPT) 1. Bioresponsive dextrin–trypsin and –MSH conjugates designed for α -amylase activation. *Biomacromolecules* 9:1146–1154
78. Sakurai K, Miyazaki K, Kodera Y, Nishimura H, Shingu M, Inada Y (1997) Anti-inflammatory activity of superoxide dismutase conjugated with sodium hyaluronate. *Glycoconj J* 14:723–728
79. Pyatak PS, Abuchowski A, Davis SS (1980) Preparation of a polyethylene glycol: superoxide dismutase adduct, and an examination of its blood circulating life and anti-inflammatory activity. *Res Commun Chem Pathol Pharmacol* 29:113–127
80. White CW, Jackson JH, Abuchowski A, Kazo GM, Mimmack RF, Berger EM, Freeman BA, McCord JM, Repine JE (1989) Polyethylene glycol-attached antioxidant enzymes decrease pulmonary oxygen toxicity in rats. *J Appl Physiol* 66:584–590
81. Walther FJ, Nunez FL, David-Cu R, Hill KE (1993) Mitigation of pulmonary oxygen toxicity in instillation of polyethylene glycol-conjugated antioxidant en-zymes. *Pediatr Res* 33:332–335
82. Lapcik JL, Lapcik L, De Smedt S, Demeesters J, Chabreck P (1998) Hyaluronan: preparation, structure, properties, and applications. *Chem Rev* 98:2663–2684
83. Kaur I, Smitha R (2002) Penetration enhancers and ocular bioadhesives: two new avenues for ophthalmic drug delivery. *Drug Dev Ind Pharm* 28:353–369
84. Saettone M, Chetoni P, Torracca M, Burgalassi S, Giannaccini B (1989) Evaluation of muco-adhesive properties and in vivo activity of ophthalmic vehicles based on hyaluronic acid. *Int J Pharm* 51:203–212
85. Liao YH, Jones SA, Forbes B, Martin GP, Brown MB (2005) Hyaluronan: pharmaceutical characterization and drug delivery. *Drug Deliv* 12:327–342
86. Zhou B, Weigel JA, Fauss LA, Weigel PH (2000) Identification of the hyaluronan receptor for endocytosis (HARE). *J Biol Chem* 275:37733–37741
87. Banerji S, Ni J, Wang SX, Clasper S, Su J, Tammi R, Jones M, Jackson DG (1999) LYVE-1 a new homologue of the CD44 glycoprotein, is a lymph-specific receptor for hyaluronan. *J Cell Biol* 144:789–801
88. Kim KS, Hur W, Park SJ, Hong SW, Choi JE, Goh EJ, Yoon SK, Hahn SK (2010) Bioimaging for targeted delivery of hyaluronic acid derivatives to the livers in cirrhotic mice using quantum dots. *ACS Nano* 4:3005–30014
89. Yang JA, Park K, Jung H, Kim H, Hong SW, Yoon SK, Hahn SK (2011) Target specific hyaluronic acideinterferon alpha conjugate for the treatment of hepatitis C virus infection. *Biomaterials* 32:8722–8729
90. Bailon P, Palleroni A, Schaffer CA, Spence CL, Fung WJ, Porter JE, Ehrlich GK, Pan W, Xu ZX, Modi MW, Farid A, Berthold W (2001) Rational design of a potent, long-lasting form of interferon: a 40 kDa branched polyethylene glycol-conjugated interferon alpha-2a for the treatment of hepatitis C. *Bioconj Chem* 12:195–202
91. Foser S, Schacher A, Weyer KA, Brugger D, Dietel E, Marti S, Schreitmüller T (2003) Isolation, structural characterization, and antiviral activity of positional isomers of monopegylated interferon alpha-2a (PEGASYS). *Protein Expr Purif* 30:78–87
92. D'Este M, Renier D, Pasut G, Rosato A (2010) Process for the synthesis of conjugates of glycosaminoglycanes (GAG) with biologically active molecules polymeric conjugates and relative uses thereof. IWO Patent Application 145821A1

Chapter 9

Polysaccharide-Based Graft Copolymers for Biomedical Applications

Sagar Pal and Raghunath Das

Abstract Polysaccharides play an important role in the field of science and technology because of their unique properties. The polysaccharides are available from natural and microbial resources. They are biodegradable as well as nontoxic. Water soluble polymers based on grafted polysaccharides have drawn much attention in recent decades because of their controlled biodegradability, shear stability, and high efficiency in various applications. One of the important applications of polysaccharide-based graft copolymers is in biomedical science—as matrix for controlled/targeted drug delivery. It is observed in authors' laboratory that rate of release of enclosed drug can be precisely controlled by controlling the grafting/cross-linking efficiency. Thus tailor-made grafted polysaccharides have potential application in drug delivery research. This chapter deals with the techniques employed for the synthesis of grafted polysaccharides, and recent developments took place in author's laboratory based on application of grafted polysaccharides in controlled/targeted drug delivery.

Keywords Ciprofloxacin • Controlled drug release • Graft copolymer • Guar gum • Polysaccharide

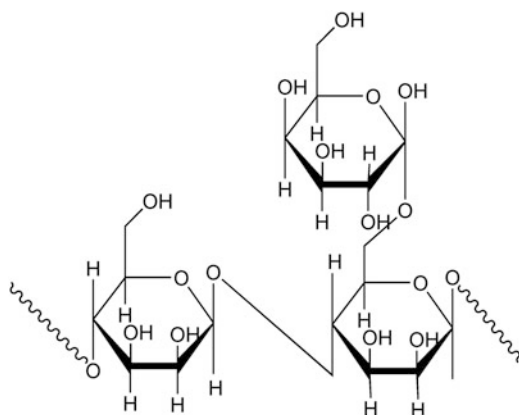
9.1 Polysaccharide and Its Importance

Polysaccharides are most abundant organic compounds on this planet. They are renewable as well as biodegradable. Polysaccharides are the vital component of our food, as an energy source (e.g., starch) and also as roughage (e.g., cellulose fibers) which aids digestion. They are the earliest known structural materials, which still

S. Pal (✉) • R. Das

Polymer Chemistry Laboratory, Department of Applied Chemistry, Indian School of Mines, Dhanbad, Jharkhand 826004, India
e-mail: sagarpal1@hotmail.com

Fig. 9.1 Structure of guar gum



hold a prominent place as an engineering material. They constituted the first fuel used by man. The role of polysaccharides in human civilization is vast, and they surround us all the time, even in this era of synthetic materials/plastics, in the form of textiles, paper, glue, etc., and that too, without causing any major environmental disposal problems.

Natural polysaccharides and their derivatives represent a group of polymers widely used in the pharmaceutical and biomedical fields for controlled release application [1]. Several polysaccharides like chitosan, starch, guar gum, xanthan gum, sodium alginate, pectin, gellan gum, and tamarind kernel polysaccharide have been extensively used either alone or in combination with their modified forms to control the drug release from various drug delivery systems [2–10]. The polysaccharides have advantages over the synthetic polymers, generally because they are non-toxic, less expensive, biodegradable, and freely available. However, natural polymers also possess some drawbacks, such as uncontrolled rate of hydration, microbial contamination, and drop in viscosity in storing. Fortunately, there are strategies to overcome these drawbacks by suitable chemical modification. Hence, it is not surprising that hydrogel of several modified natural polymers already find application in sustained drug delivery and other fields [5–10]. The conjugation of natural polymers with synthetic polymers is of great interest because of its wide range of potentially new applications. In the last few years, an expanding interest has been devoted to the synthesis of chemically modified polysaccharides through grafting which combine the advantages of both synthetic and natural polymers. Graft copolymerization of vinyl monomers onto natural polysaccharides is the most promising technique as it functionalizes these biopolymers to their potential by imparting desirable properties onto them.

One of the important modified polysaccharide, which is having wide applications in various fields, is guar gum [11–14]. Guar gum (GG) is one of the most important industrial gums. It has been extracted from the seeds of *Cyamopsis tetragonoloba*, which belongs to the *Leguminosae* family. GG is a linear polymannose with pendent galactose sugars on alternating mannose units (Fig. 9.1). On the average, there are

between 1.5 and 2 mannose residues for every galactose residue, with few, if any, non-substituted regions. Carboxymethyl guar gum (CMG) is a derivative of guar gum, synthesized by inserting carboxymethyl groups onto the backbone of guar gum [15].

9.2 Polysaccharide-Based Graft Copolymers

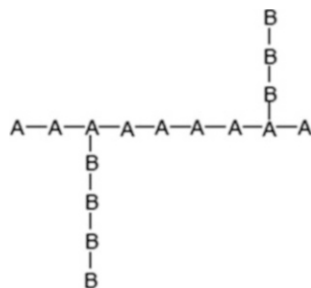
The graft copolymerization provides a unique technique for modifying polymers to meet desired end user requirements. The graft copolymers of polysaccharides are of additional interest because of their potential use as viscosifiers in enhanced oil recovery operations, as flocculants in wastewater treatment, as drug reducing agents, etc. [11, 16–20]. An important advantage of graft copolymerization is that the polymeric substrate or backbone polymer and grafted polymer chains are held together by chemical bonding, which allow two polymers to be intimately associated rather than as mere physical mixtures. The method of graft copolymerization has been utilized as a special technique in the recent decades for synthesizing new class of polymeric materials by modifying the physical and chemical properties of synthetic and natural polymers. A graft copolymer is consisting of a primary backbone chain to which side chains having different atomic constituents are attached at various points [21]. The graft copolymer chain contains a mixture of monomer units, and the proportions are different from that of a mixture of the two equivalent homopolymers. Figure 9.2 represents the simple structure of a graft copolymer, where a sequential arrangement of the monomer units A is referred to as the main chain or backbone. The sequence of B units is the side chain or graft which is attached onto main chain.

Out of various polymers onto which the grafting of synthetic polymers can be done, polysaccharides are found to be the most interesting and promising. It is because of their abundance and cheap cost. The actual properties of a graft copolymer will vary according to the number and length of the grafted side chains. Therefore, it is most important to control the grafting frequency and grafted chain length in order to achieve particular characteristics. The graft copolymers based on polysaccharides have been synthesized by generating free radical sites on the polysaccharide backbone and allowing these free radicals to act as micro-initiators for acrylic and vinyl monomers. Generally, two methods have been proposed for initiating free radicals on the polysaccharide backbone, such as, chemical initiation and initiation by irradiation. However, in some cases, free radicals are developed by mastication of polysaccharides as a result of rupture of the backbone.

9.2.1 *Initiation by Ceric Ion*

The ceric ion initiation method has been used extensively for graft copolymerization of several polysaccharides. Most commonly used are ceric ammonium nitrate

Fig. 9.2 Structure of graft copolymer



(CAN) and ceric ammonium sulfate (CAS). At low temperatures, CAN is more efficient than CAS. However, at high temperature, CAS is found to be more efficient because of the instability of CAN at elevated temperature [22]. Although several techniques [23, 24] have been reported for generation of free radicals using oxidation of 1,2-diols with ceric ions, Mino and Kaizerman [25] for the first time showed the formation of graft and block copolymers on these reaction sites. Since then, the ceric ion initiation method has been used most widely for initiating graft copolymerization of monomers onto polysaccharides. The mechanism by which Ce (IV) ion generates free radical sites on polysaccharide backbone is believed to involve the formation of a complex between the hydroxyl group of the polysaccharide and the oxidant. The formed complex then disproportionates and forms free radicals on the polysaccharide backbone. Evidence of the complex formation between Ce (IV) and polysaccharide has been proposed by several investigations [26–33]. Model compound studies of Ce (IV) oxidation of polysaccharides and 1,2 glycols support the postulated mechanism and suggested that the C2–C3 glycol and the C5 hydroxyl groups of D-anhydroglucose unit of polysaccharides may be the preferred sites for free radical generation [34, 35].

9.2.2 Initiation by Trivalent Manganese

Duke [36] pointed out that 1,2 glycols can also be oxidized by Mn^{3+} . The oxidation reaction proceeds by electron transfer reaction via free radical mechanism. Singh et al. [37] followed the same mechanism, using a manganese sulfate–sulfuric acid system, for initiating graft copolymerization onto polysaccharides. The formation of sulfate complex of Mn^{3+} introduces a problem in the sense that the Mn^{3+} ions in sulfuric acid media are unstable and disproportionate as follows:



However, disproportionation reaction can be stopped at highly acidic condition. But this leads to acidic hydrolysis and consequent degradation of the polysaccharide backbone during grafting reaction. Mehrotra and Ranby [38–41] for the first

time solved the problem by using pyrophosphate complex of Mn^{3+} ions, which exists as $[\text{Mn}(\text{H}_2\text{P}_2\text{O}_7)]^{3-}$ and undergoes no disproportionation in acidic medium. They have studied the grafting of monomers like methyl methacrylate (MMA), acrylonitrile, and acrylamide onto starch by the use of pyrophosphate complex of Mn^{3+} as an initiator.

9.2.3 Initiation by Hydrogen Peroxide/ Fe^{2+} System (Fenton's Reagent)

The chemical initiation for graft copolymerization onto polysaccharides has also been reported using Fenton's reagent. Brockway and Moser [42, 43] have studied the initiation of grafting of methyl methacrylate (MMA) onto starch by use of hydrogen peroxide and ferrous ammonium sulfate. This process also involves the formation of free radical sites on the backbone of polymer as studied in other cases.

9.2.4 Initiation by Cu (II) Ion

Kimura et al. [44] reported the grafting reaction of MMA onto starch using Cu (II) as initiator. Imoto et al. [45] have concluded that the polymerization proceeds in water phase, particularly at the hydrophobic ends (or micelles) formed by starch. Ozone–oxygen-initiated graft copolymerization onto starch has been studied by Katai and Schuech [46]. This process involves the formation of hydroxyperoxy groups onto starch backbone, which is then decomposed by heat or any reducing agents in the presence of monomer, forming free radicals and initiates graft copolymerization.

9.2.5 Initiation by Chromium (VI) Ion

Chromium (VI)-initiated graft copolymerization of vinyl monomers onto polysaccharide backbone was investigated by many researchers. Nayak et al. [47, 48] used Cr (VI) as an initiator for graft copolymerization as well as homopolymerization [49]. Mishra et al. [50] reported the feasibility of Cr (VI) to induce graft copolymerization of MMA onto cellulose. It was also reported that in a system of potassium dichromate, perchloric acid, MMA, and cellulose, Cr (VI) reacts with cellulose to form cellulose macro-radicals, which then react with vinyl monomers to form graft copolymer.

9.2.6 Initiation by V^{5+}

Lenka et al. [51] carried out graft copolymerization of MMA on cellulosic materials with the use of V^{5+} as an initiator. Increase of V^{5+} ion concentration up to 0.0025 mol/l increases grafting yield and then decreases with further increase of initiator concentration. Grafting of acrylonitrile onto chemically modified jute was carried out in the temperature range of 40–60 °C using V^{5+} cyclohexanone redox initiator system [52].

9.2.7 Initiation by Irradiation

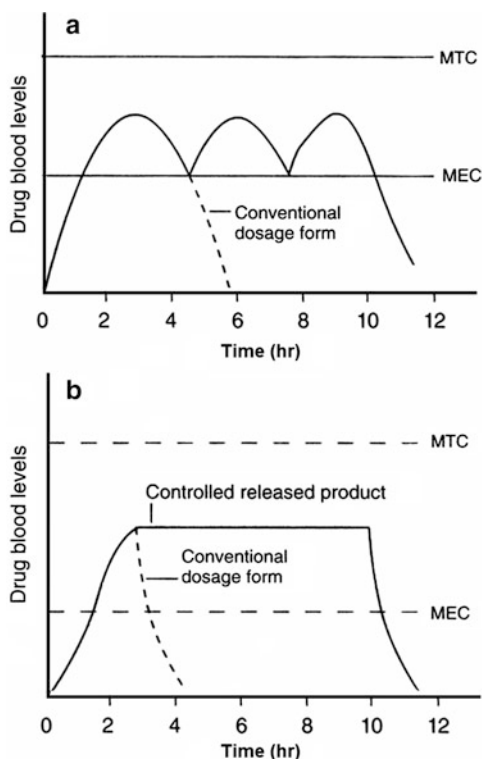
Another important method, which is also used to create free radical sites on polysaccharide backbone, is by using high-energy radiations like γ -rays or electron beam [53–60]. Although high-energy radiation-induced grafting is very much suitable for commercial/bulk production of the graft copolymer, they also cause unpredictable damage (radiolysis) of the backbone polymer (especially if the backbone polymer is polysaccharide). This makes the graft copolymer prone to failure [61–66]. The processes of high-energy radiation-induced graft copolymerization are especially suitable for fluoropolymers, because of their exceptional stability [67–75].

Radiation-induced grafting can also be carried out using UV radiation [76–82] in the presence of a photo initiator like benzophenone [83]. However, low penetration ability of UV rays leads to nonuniform grafting and low grafting yield. The most recent method of graft copolymer synthesis is by the use of microwave irradiation. Microwave-based synthesis of graft copolymers is expected to result in much greater control on percentage grafting—as here one can electronically (hence precisely) control this reaction parameter (percentage grafting) in terms of exposure time of irradiation [84].

9.3 Grafted Polysaccharide as Matrix for Controlled Drug Release

One major challenge in the field of pharmacokinetics is to sustain the therapeutic level of a drug in body tissue as long as possible, during the entire length of treatment. Traditional delivery systems (TDS) (Fig. 9.3a) are characterized by immediate and uncontrolled drug release kinetics. Here drug absorption is essentially controlled by the body's ability to assimilate the therapeutic molecule, and hence, drug concentration in different body tissues undergoes an abrupt increase on administration of the dosage, followed by a similar decrease. This may create side effects in our body since drug concentration dangerously approaches the toxic

Fig. 9.3 Drug level in body tissue (e.g., blood) in case of (a) traditional drug delivery system (TDS) and (b) controlled drug delivery system (CDS)



threshold and, after sometime, falls down below the effective therapeutic level [85, 86]. On the contrary, the purpose of controlled release systems (CRS) is to maintain drug concentration in the target tissues at the therapeutic level as long as possible (Fig. 9.3b). Thus, both the high concentrations (peaks) and the subsequent subtherapeutic levels (troughs) of the drug, associated with TDS, get avoided. As a result, this minimizes the side effects and also reduces the chances of drug resistance [85, 86]. Further, the low frequency of dosage leads to patient convenience.

The most convenient controlled release system (CRS) consists of the drug enclosed in a customized matrix, which releases the drug at a predetermined rate. This maintained the therapeutic level of the drug in blood plasma or in the area of the intended tissue.

9.3.1 The Concept of Drug Delivery Matrix

Because of low cost and ease of fabrication, one common way of obtaining controlled release of a drug is by enclosing it in a hydrophobic matrix (such as wax, polyethylene, polypropylene, ethyl cellulose, etc.) or in a hydrophilic matrix

(such as carboxymethyl tamarind, hydroxypropyl cellulose, hydroxypropyl methylcellulose, methylcellulose, sodium carboxymethyl cellulose, alginates and scleroglucan, etc.) [87–118]. Various techniques of drug loading into the matrix are in practice. Most commonly used are:

1. Solvent swelling technique: The matrix can be left to swell in the highly concentrated drug solution. Afterwards, the solvent is removed by suitable physical treatment (e.g., evaporation) [119].

2. Supercritical fluid technique: Supercritical fluids are dense as liquids but have viscosity as low as that of gas. In this technique, a solution of the drug in a supercritical fluid easily and efficiently swells the matrix, and the solvent (supercritical fluid) is then easily removed by decreasing the pressure (leaving the drug behind, in the matrix) [120, 121].

3. Direct compression method: In this method, the drug is grounded and mixed with the matrix and a binder in a definite proportion, in the presence of a volatile solvent. Afterwards, they are compressed into tablets under high pressure (2–3 tons/cm²) [122, 123]. It is noted that direct compression method is the simplest and most economically viable method of tablet preparation.

9.3.2 Mechanism of Drug Release

The mechanism of drug release depends on the nature of the matrix as well as on the mode of drug delivery. For example, diffusion of drug through skin is the mechanism involved in case of transdermal drug release. Generally, for polymeric drug delivery matrix, the mechanism is either one or a combination of (1) diffusion, (2) erosion, and (3) osmosis. The drug delivery studies, which are reported here, follow the underlying mechanism of release, from its cumulative drug release profile, by applying the power law equation:

$$M_t/M_\infty = Kt^n \quad (9.1)$$

The value of exponential component “*n*” indicates the mechanism of drug transport from the tablet.

9.3.3 Oral Mode of Drug Delivery

Among various modes of drug delivery (Fig. 9.4), the oral mode is the most convenient and acceptable option. However, still the current knowledge on mechanism of drug absorption, transit, and microenvironment of human gastrointestinal tract is incomplete and poorly understood. The physiology of the gastrointestinal tract is beset with constraints like chemical degradation in the stomach, gastric emptying, intestinal motility, mucosal surface area, specific absorption sites, and

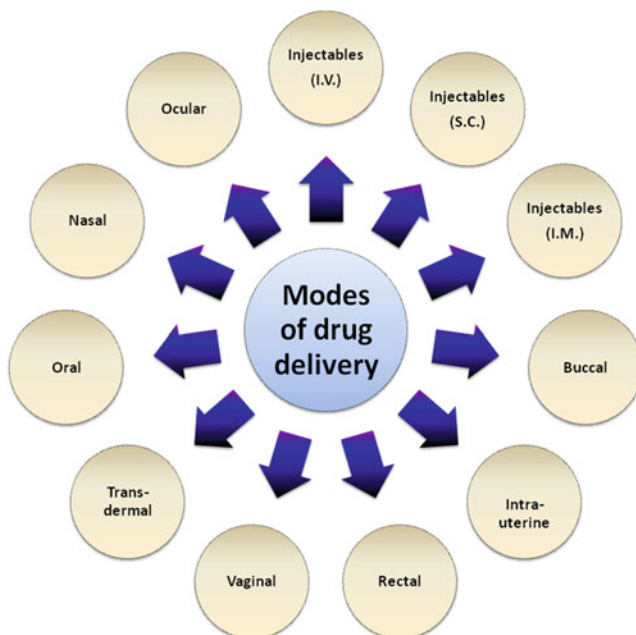


Fig. 9.4 Various modes of drug delivery

metabolic degradation during passage through mucosa and subsequently the liver. The most prominent among these challenges is the harsh environment of the stomach, where enzymatic degradation of many drugs like the polypeptides (e.g., insulin) takes place. Further, certain drugs like the salicylates can damage the stomach lining, leading to gastric ulcer. The only solution to this problem is to enclose the drug in a matrix that protects it during passage through the harsh environment of the stomach and releases it in the lower gastrointestinal tract. This gastric bypass can be achieved through the following strategies:

- (a) Delayed release formulation:** In this case, the matrix releases the drug after a time delay. This time delay can be adjusted to cover the gastric region transit time. The matrix in this case essentially consists of cross-linked/grafted polymers, and the extent of cross-linking/grafting controls the time delay.
- (b) pH-triggered drug release:** pH of stomach is acidic, while that of lower gastrointestinal tract is neutral/alkaline. This difference in pH can act as a trigger for drug release into the lower gastrointestinal tract (bypassing the gastric region). Evidently, this involves a drug delivery matrix which does not significantly release the drug in acidic pH (of stomach) and release it at a much faster rate in the neutral/alkaline pH (of lower gastrointestinal tract).
- (c) Drug release from matrix degradable by colonic micro flora:** The drug can be enclosed in a matrix that is not affected (and can protect the drug) by the stomach environment, but undergoes biodegradation by colonic micro flora.

As a result, the drug remains protected during the gastric transit, and as the matrix gets degraded in the colonic region, the enclosed drug gets released for subsequent absorption.

9.3.4 Targeted Drug Delivery

In case of traditional drug delivery, the spatial distribution of the drug throughout the body is controlled by its pharmacokinetic factors rather than any specific control factor within the system. This has two main disadvantages:

1. Even if one administers substantial dose of the drug, its actual concentration at the targeted tissue may remain low, thus resulting less than optimal response.
2. The indiscriminate delivery of the drug to all parts of the body may lead to undesired side effects.

9.3.5 “In Vitro” Drug Release Study

Assessment of drug dissolution from solid oral dosage formulations (e.g., tablets) is an established practice in study of controlled drug release. The rationale for conducting drug dissolution tests is based on the fact that for a drug to be delivered via the gastrointestinal tract, it should at first be released from the tablet and get dissolved in aqueous-based gastrointestinal tract fluid. Being a critical part of drug formulation development, all aspects of in vitro drug dissolution studies have been extensively standardized by USP guidelines (general chapter <711 > dissolution) [124].

In fact, dissolution testing is basically a specific form of solubility testing. However, it differs from the later by the fact that the measurements are taken multiple times, usually below saturation and at 37 °C (physiological temperature) in water or aqueous-based buffers, whereas solubility is determined in pure solvent at a single point, i.e., at the point of saturation and usually at 20 °C, if otherwise stated.

Drug dissolution testing for oral mode formulations is performed in various buffers representing the pH of various regions of the gastrointestinal tract. The tests are conducted in basket-/paddle-type standard USP drug dissolution rate test apparatus (Fig. 9.5), in 900 mL of the buffer solution maintained at the physiological temperature of 37 °C (using isothermal bath). The spindle rotation is maintained in between 50 and 150 rpm. Aliquots are drawn at equal interval of time; drug content assayed spectrophotometrically and is graphically expressed as drug release profile (plot of cumulative drug release (%) vs. time).

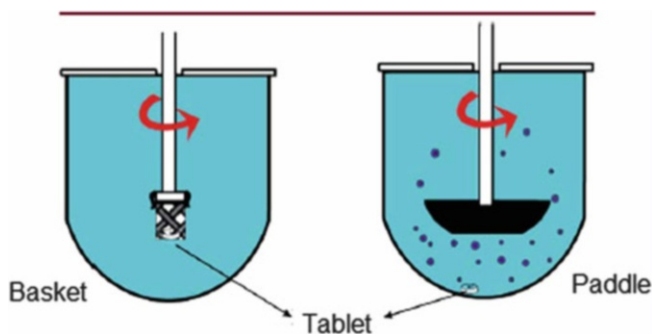


Fig. 9.5 Basket- and paddle-type standard USP drug dissolution rate test apparatus

9.4 Application of Polyacrylamide-Grafted Carboxymethyl Guar Gum (CMG-g-PAM) as Matrix for Colon-Targeted Drug Release of 5-Amino Salicylic Acid

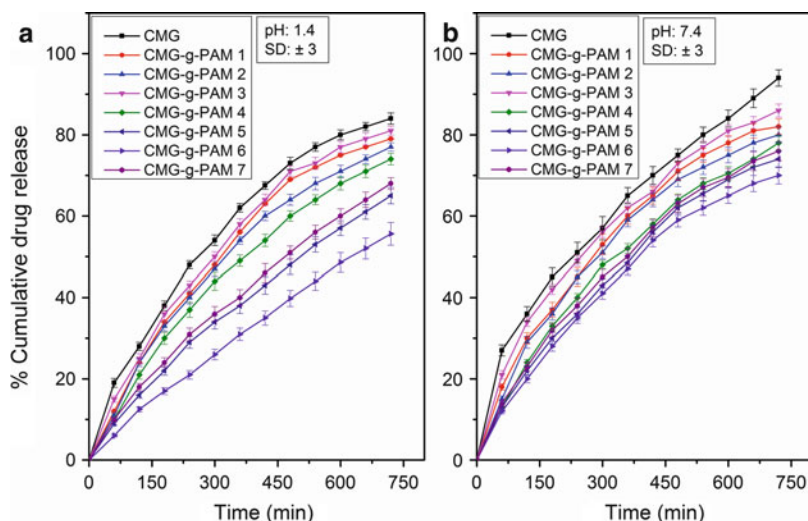
The gastrointestinal tract is divided into stomach, small intestine, and large intestine. The pH varies widely along the gastrointestinal tract. It varies from low pH 1.2–1.4 (fasting condition) in stomach to up to 7.4 in colon region (Table 9.1). The acidic environment coupled with the various enzymes in stomach offers an environment harsh enough for degradation of the peptides and many other drugs [114, 125]. An ideal drug delivery matrix for oral delivery should protect the drug from the low-pH harsh environment of the stomach and should preferably release the drug in lower gastrointestinal tract. Consequently, the matrix should have lower rate of drug release in acidic pH and higher in alkaline pH conditions.

In authors' laboratory, a novel polymeric material has been developed based on polyacrylamide-grafted carboxymethyl guar gum using conventional method as well as microwave-assisted method [126]. It has explained in earlier reported article that microwave-assisted graft copolymer is having higher % grafting efficiency (% GE) in comparison with conventional method [126]. The mechanism of formation of graft copolymer is based on the fact that the microwave irradiation as well as initiator generates free radical sites on polysaccharide backbone, and grafting of polyacrylamide took place onto these free radicals, which are generated. The detailed mechanism has been explained in our earlier report [126]. It is also to be mentioned that the reaction was terminated using hydroquinone as inhibitor. By varying reaction parameters several grades of graft copolymers were prepared and optimized based on higher % GE [126]. Various characterizations confirm that graft copolymerization does take place.

Drug delivery potential of neat CMG and all the graft copolymers are compared in Fig. 9.6. From these drug release profiles, their corresponding t_{50} value (time taken for release of 50 % of the enclosed drug) has been reported in Table 9.2. For all the matrices except CMG, the tablet integrity remained intact, albeit swelling. In case of CMG-based tablets, the rate of erosion (Table 9.2) was so high that the

Table 9.1 pH in various parts of G.I. tract

Location	pH
Oral cavity	6.2–7.4
Esophagus	5.0–6.0
Stomach	Fast condition 1.4–2.0 Fed condition 3.5–5.0
Small intestine	Jejunum 5.0–6.5 Ileum 6.0–7.5
Large intestine	Right colon 6.4 Mild colon and left colon 6.0–7.4

**Fig. 9.6** Cumulative drug release profile of CMG and various graft copolymers for 5-amino salicylic acid at (a) pH=1.4 and (b) pH=7.4. The results are mean \pm SD ($n = 3$)

tablet disintegrated rapidly in the colon region, releasing the enclosed drug very fast. This trend for CMG matrix got reflected in its drug release profile (Fig. 9.6) and also its corresponding low “ t_{50} value” (Table 9.2). Thus, the native polysaccharide was not found to be suitable as matrix for controlled/sustained drug release of 5-ASA. It is well known that cross-linking/grafting tends to lower solubility of hydrogels, mainly because of the increase in molecular weight and branching (grafts) which leads to chain entanglements. Eventually, grafting of PAM chains onto CMG leads to considerable decrease in solubility. Their drug release profiles are more sustained compared to CMG as obvious from the figure. Also it is noted that the higher is the % GE (i.e., lower equilibrium swelling for CMG-g-PAM 6—Table 9.3), the more sustained is the rate of drug release, i.e., CMG-g-PAM 6 is the most ideal matrix for controlled release of 5-ASA. From the drug release profile (Fig. 9.6) and their corresponding t_{50} value (Table 9.2), it is obvious that higher is the percentage grafting, lower (hence more sustained) is the rate of drug release. This trend can be explained by the fact that with increase in percentage grafting, the

Table 9.2 % Erosion and t_{50} values of various hydrogel based tablets for model drug 5-amino salicylic acid

Polymer grade	% Erosion ^a		t_{50} (min)	
	pH 1.4	pH 7.4	pH 1.4	pH 7.4
CMG-g-PAM 1	60.0	69.3	327	309
CMG-g-PAM 2	59.0	72.0	356	332
CMG-g-PAM 3	62.2	79.2	298	260
CMG-g-PAM 4	54.6	63.5	370	305
CMG-g-PAM 5	48.0	62.2	565	410
CMG-g-PAM 6	41.7	59.6	632	405
CMG-g-PAM 7	52.2	60.2	388	332
CMG	70.1	88.0	262	224

$${}^a\% \text{Erosion} = \frac{W_i - W_d(t) - W_{\text{drug}} \left(1 - \frac{M_t}{M_\alpha}\right)}{W_i} \times 100$$

where W_i is the initial dry weight of the tablet, W_d is the dry weight of the tablet at time t , considering drug release at time t (M_t/M_α), M_t is the amount of drug release at time t , M_α is the total amount of drug released after infinite time, and W_{drug} is the initial weight of drug (i.e., 5-ASA)

Table 9.3 % Grafting efficiency (GE) and equilibrium swelling of various graft copolymers

Polymer grade	% GE ^a	% Equilibrium swelling ^b (12 h)	
		pH: 1.4	pH: 7.4
CMG-g-PAM 1	84	312 ± 11.60	452 ± 8.56
CMG-g-PAM 2	89	296 ± 10.25	440 ± 9.21
CMG-g-PAM 3	81	330 ± 9.66	463 ± 9.09
CMG-g-PAM 4	90	284 ± 9.47	428 ± 9.83
CMG-g-PAM 5	93	259 ± 8.43	394 ± 9.31
CMG-g-PAM 6	96	250 ± 12.50	381 ± 10.05
CMG-g-PAM 7	91	274 ± 7.71	410 ± 9.65
CMG	0	360 ± 11.23	483 ± 7.33

$${}^a\% \text{Grafting efficiency} = \frac{\text{Wt. of graft copolymer} - \text{Wt. of polysaccharide}}{\text{Wt. of monomer}} \times 100$$

$${}^b\% \text{Equilibrium swelling} = \frac{\text{Wt. of swollen gel} - \text{Wt. of dried gel}}{\text{Wt. of dried gel}} \times 100$$

solubility of the graft copolymer decreases. The decreasing trend of solubility in turn results in lower erosion rate of the tablet (made using the graft copolymer as matrix), leading to slower rate of release of the enclosed drug. This in turn results in higher t_{50} value.

Also it is observed that the t_{50} values (Table 9.2) for all the matrices are lower in alkaline pH compared to acidic pH, i.e., the enclosed drug is released at a faster rate in SIF. This property (pH-triggered drug release) coupled with the most sustained release behavior of CMG-g-PAM 6 makes it an ideal candidate as matrix for lower G.I. tract targeted drug delivery. Also from release kinetics, it is observed that diffusion exponent “ n ” value remains between 0.5 and 1.0. This confirms “non-Fickian” release behavior, i.e., the drug release was due to a combination of swelling and erosion of the matrix.

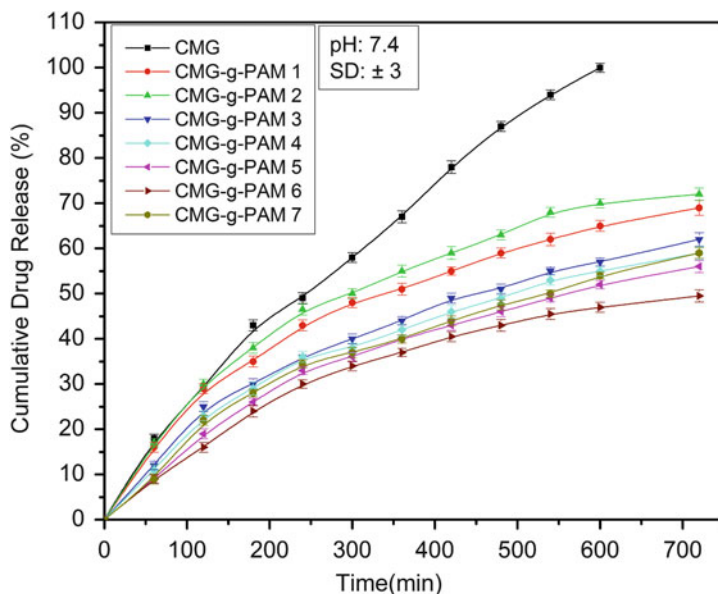


Fig. 9.7 Cumulative drug release profile of CMG and various graft copolymers for ciprofloxacin at pH-7.4. The results are mean \pm SD ($n = 3$)

9.5 Application of Polyacrylamide-Grafted Carboxymethyl Guar Gum (CMG-g-PAM) as Matrix for Controlled Release of Ciprofloxacin

An attempt had been made to find out the suitability of the synthesized graft copolymer as matrix for controlled release of model drug ciprofloxacin. The study was done for dissolution media having pH 7.4. Drug release profiles are reported for the drug ciprofloxacin, in Fig. 9.7. From these drug release profiles, their corresponding t_{50} value (time taken for release of 50 % of the enclosed drug) has been reported in Table 9.4.

For all the matrices the tablet integrity remained intact. However, CMG-based tablets disintegrate in faster rate compared to others because of its higher rate of erosion. This trend gets reflected in the corresponding t_{50} value (Table 9.4). Thus, the raw material CMG was not found to be a good matrix for controlled release of ciprofloxacin. In case of CMG-g-PAM-based matrices, although the swelling was slightly high, the much lower solubility overcomes its effect by drastically reducing the tablet erosion rate. This is evident in the drug release profile. Out of all the hydrogels, CMG-g-PAM 6 has the highest % conversion and lowest swelling, which shows the most sustained drug release profile. Further, the high t_{50} value (Table 9.4) corresponding to the drug release profile confirms this finding. Figure 9.7 has proved that out of various hydrogels, CMG-g-PAM 6 releases the

Table 9.4 % Erosion and t_{50} values of CMG and various graft copolymer based tablets for model drug ciprofloxacin

Polymer grade	% Erosion ^a pH: 7.4	t_{50} (min) pH: 7.4
CMG-g-PAM 1	58.2	351
CMG-g-PAM 2	64.5	309
CMG-g-PAM 3	57.0	483
CMG-g-PAM 4	52.8	514
CMG-g-PAM 5	48.3	567
CMG-g-PAM 6	42.7	716
CMG-g-PAM 7	50.3	542
CMG	81.6	248

$${}^a\% \text{Erosion} = \frac{W_i - W_d(t) - W_{\text{drug}} \left(1 - \frac{M_t}{M_\infty}\right)}{W_i} \times 100$$

where W_i is the initial dry weight of the tablet, W_d is the dry weight of the tablet at time t , considering drug release at time t (M_t/M_∞), M_t is the amount of drug release at time t , M_∞ is the total amount of drug released after infinite time, and W_{drug} is the initial weight of drug (i.e., 5-ASA)

enclosed drug at the most sustained rate; hence, it is the most ideal matrix developed in this study, for controlled release of ciprofloxacin. Also the diffusion exponent “ n ” remained between 0.5 and 1.0 (Table 9.4). This explained that the developed hydrogel-based matrix follows “non-Fickian” release behavior.

9.6 Summary

From the above theoretical and experimental observation, it is evident that by grafting synthetic polymer on polysaccharide backbone, it is possible to develop novel polymeric matrices, which are having wide application in the field of biomedical science.

Acknowledgment The authors are grateful to Indian School of Mines, Dhanbad, India, for providing necessary facilities to carry out the reported drug delivery study. The authors also earnestly acknowledge the financial support from University Grants Commissions, New Delhi, India, in form of a research grant [No. 36-59/2008 (SR)].

References

1. Maity S, Ranjit S, Sa B (2010) Polysaccharide-based graft copolymers in controlled drug delivery. *Int J Pharm Tech Res* 2:1350–1358
2. Kumar A, Singh K, Ahuja M (2009) Xanthan-g-poly (acrylamide): microwave-assisted synthesis, characterization and in vitro release behaviour. *Carbohydr Polym* 76:261–267
3. Sinha VR, Kumria R (2001) Polysaccharides in colon-specific drug delivery. *Int J Pharm* 224:19–38

4. Dey RK, Tiwary GS, Patnaik T, Jha U (2011) Controlled release of 5-aminosalicylic acid from a new pH responsive polymer derived from tamarind seed polysaccharide, acrylic acid, and polyamidoamine. *Polym Bull* 66:583–598
5. Coviello T, Matricardi P, Marianecci C, Alhaique F (2007) Polysaccharide hydrogels for modified release formulations. *J Control Release* 119:5–24
6. Sen G, Pal S (2009) Microwave initiated synthesis of polyacrylamide grafted carboxymethylstarch (CMG-g-PAM): application as a novel matrix for sustained drug release. *Int J Biol Macromol* 45:48–55
7. Giri A, Ghosh T, Panda AB, Pal S, Bandyopadhyay A (2012) Tailoring carboxymethyl guar gum hydrogel with nanosilica for sustained transdermal release of diclofenac sodium. *Carbohydr Polym* 87:1532–1538
8. Vijan V, Kaity S, Biswas S, Isaac J, Ghosh A (2012) Microwave assisted synthesis and characterization of acrylamide grafted gellan, application in drug delivery. *Carbohydr Polym* 90:496–506
9. Rana V, Rai P, Tiwari AK, Singh RS, Kennedy JF, Knill CJ (2011) Modified gums: approaches and applications in drug delivery. *Carbohydr Polym* 83:1031–1047
10. Mundargi RC, Patil SA, Aminabhavi TM (2007) Evaluation of acrylamide-grafted-xanthan gum copolymer matrix tablets for oral controlled delivery of antihypertensive drugs. *Carbohydr Polym* 69:130–141
11. Deshmukh SR, Singh RP (1987) Drag reduction effectiveness, shear stability and biodegradation resistance on guar gum-based graft copolymers. *J Appl Polym Sci* 33:1963–1975
12. Pal S, Mal D, Singh RP (2007) Synthesis and characterization of cationic guar gum: a high performance flocculating agent. *J Appl Polym Sci* 105:3240–3245
13. Singh RP, Pal S, Mal D (2006) A high performance flocculating agent and viscosifier based on cationic guar gum. *Macromol Symp* 242:227–234
14. Singh V, Tiwari A, Tripathy DN, Sanghi R (2004) Microwave assisted synthesis of guar-g-polyacrylamide. *Carbohydr Polym* 58:1–6
15. Pal S (2009) Carboxymethyl guar: its synthesis and macromolecular characterization. *J Appl Polym Sci* 111:2630–2636
16. Brostow W, Lobland HEL, Reddy T, Singh RP (2007) Lowering mechanical degradation of drag reducers in turbulent flow. *J Mater Res* 22:56–60
17. Wang L, Zhang LM (2009) Viscoelastic characterization of a new guar gum derivative containing anionic carboxymethyl and cationic 2-hydroxy-3-(trimethylammonio) propyl substituents. *Ind Crops Prod* 29:524–529
18. Singh RP, Nayak BR, Biswal DR, Tripathy T, Banik K (2003) Biobased polymeric flocculants for industrial effluent treatment. *Mater Res Innovat* 7:331–340
19. Ghosh S, Sen G, Jha U, Pal S (2010) Novel biodegradable polymeric flocculant based on polyacrylamide grafted tamarind kernel polysaccharide. *Biores Tech* 101:9638–9644
20. Singh RP, Pal S, Krishnamoorthy S, Adhikary P, Ali SK (2009) High-technology materials based on modified polysaccharides. *Pure Appl Chem* 81:525–547
21. Stannett SV (1981) Grafting. *Radiat Phys Chem* 18:215–222
22. Schwab E, Stannett V, Rakowitz DH, Magrane JK (1962) Paper grafted with vinyl monomers using the ceric ion method. *Tappi* 45:390–400
23. Duke FR, Forist AA (1949) The theory and kinetics of specific oxidation III. The cerate-2-3-butanediol reaction in nitric acid solution. *J Am Chem Soc* 71:2790–2792
24. Duke FR, Bremer RF (1951) The theory and kinetics of specific oxidation IV. The cerate 2, s-butanediol reactions in perchlorate solutions. *J Am Chem Soc* 73:5179–5181
25. Mino G, Kaizarman S (1958) A new method for the preparation of graft copolymers. Polymerization initiated by ceric ion redox systems. *J Polym Sci Part A: Polym Chem* 31:242–243
26. Iwakura Y, Kurosaki T, Imai Y (1965) Graft copolymerization onto cellulose by the ceric ion method. *J Polym Sci Part A: Polym Chem* 3:1185–1193

27. Kurlyankina VI, Molotkov VA, Koz'mina PO, Khripunov AK, Shtennikova IN (1969) On the mechanism of grafting chains of synthetic polymers to cellulose using salts of transition metals. *Eur Polym J* 5:441–445
28. Kurlyankina VI, Koz'mina PO, Khripunov AK, Molotkov VA, Novoselova TD (1967) Complexing of cerium with cellulose and other hydroxyl containing compounds. *Dokl Akad Nauk USSR* 172:344–350
29. Kulkarni AY, Meheta PC (1967) Oxidation of cellulose by ceric ions. *J Appl Polym Sci B Polym Lett* 5:209–215
30. Kulkarni AY, Meheta PC (1968) Ceric ion-induced redox polymerization of acrylonitrile on cellulose. *J Appl Polym Sci* 12:1321–1342
31. Ogiwara YO, Ogiwara YV, Kubota H (1968) The mechanism of consumption of ceric salt with cellulosic materials. *J Polym Sci Part A: Polym Chem* 6:1489–1499
32. Nayak BR, Singh RP (2001) Development of graft copolymer flocculating agents based on hydroxypropyl guar gum and acrylamide. *Eur Polym J* 37:1776–1785
33. Gupta KC, Sahoo S (2001) Grafting of acrylonitrile and methyl methacrylate from their binary mixtures on cellulose using ceric ions. *J Appl Polym Sci* 79:767–778
34. Mino G, Kaizerman S, Rasmussen E (1959) The oxidation of pinacol by ceric sulfate. *J Am Chem Soc* 81:1494–1496
35. Hinz HL, Johnson DC (1967) The mechanism of oxidation of cyclic alcohols. *J Org Chem* 32:556–564
36. Duke R (1947) The theory and kinetics of specific oxidation I. The trivalent manganese-oxalate reaction. *J Am Chem Soc* 69:2885–2888
37. Singh H, Thampy RT, Chipalkatti VB (1965) Graft copolymerization of vinyl monomers initiated by manganese sulfate–sulfuric acid. *J Polym Sci Part A: Polym Chem* 3:4289–4293
38. Mehrotra R, Ranby B (1977) Graft copolymerization onto starch. I. Complexes of Mn^{3+} as initiators. *J Appl Polym Sci* 21:1647–1654
39. Mehrotra R, Ranby B (1977) Graft copolymerization onto starch. II. Grafting of acrylonitrile to granular native potato starch by manganese pyrophosphate initiation. Effect of reaction conditions on grafting parameters. *J Appl Polym Sci* 21:3407–3415
40. Mehrotra R, Ranby B (1978) Graft copolymerization onto starch. III. Grafting of acrylonitrile to gelatinized potato starch by manganese pyrophosphate initiation. *J Appl Polym Sci* 22:2991–3001
41. Mehrotra R, Ranby B (1978) Graft copolymerization onto starch. IV. Grafting of methyl methacrylate to granular native potato starch by manganese pyrophosphate initiation. *J Appl Polym Sci* 22:3003–3010
42. Brockway CE, Moser KB (1963) Grafting of poly (methyl methacrylate) to granular corn starch. *J Polym Sci Part A: Polym Chem* 1:1025–1039
43. Brockway CE (1964) Efficiency and frequency of grafting of methyl methacrylate to granular corn starch. *J Polym Sci Part A: Polym Chem* 2:3721–3731
44. Kimura S, Takitani T, Imoto M (1962) Vinyl polymerization (LXIV) graft copolymerization of vinyl monomers to starch. *Bull Chem Soc Jpn* 35:2012–2019
45. Imoto M, Morita E, Ouchi T (1980) Vinyl polymerisation (CCCLXXVIII) radical polymerization of methyl methacrylate with starch in aqueous solution of Cu (II) ion. *J Polym Sci Polym Symp* 68:1–11
46. Katai AA, Schuech C (1966) Mechanism of ozone attack on α -methyl glucoside and cellulosic materials. *J Polym Sci part A: Polym Chem* 4:2683–2703
47. Nayak PL, Lenka S, Pati NC (1979) Grafting vinyl monomers onto silk fibers. II. Graft copolymerization of methyl methacrylate onto silk by hexavalent chromium ion. *J Appl Polym Sci* 23:1345–1354
48. Nayak PL, Lenka S, Pati NC (1979) *J Polym Sci Polym Chem Ed* 17:3425–3430
49. Samal RK, Mohanty TR, Nayak PL (1967) *J Macromol Sci Chem A* 10:1239–1245

50. Mishra MK, Tripathy AK, Lenka S, Nayak PL (1981) Grafting vinyl monomers onto cellulose. V. Graft copolymerization of methyl methacrylate onto cellulose using a hexavalent chromium ion. *J Appl Polym Sci* 26:2769–2771
51. Lenka S, Nayak PL, Mishra MK (1980) Grafting vinyl monomers onto cellulose. I. Graft copolymerization of methyl methacrylate onto cellulose using quinquevalent vanadium ion. *J Appl Polym Sci* 25:1323–1333
52. Mohanty AK, Patnaik S, Singh BC, Misra M (1989) Graft copolymerization of acrylonitrile onto acetylated jute fibers. *J Appl Polym Sci* 37:1171–1181
53. Huang RYM, Immergut B, Immergut EH, Rapson WH (1963) Grafting vinyl polymers onto cellulose by high energy radiation. I. High energy radiation-induced graft copolymerization of styrene onto cellulose. *J Polym Sci Part A: Polym Chem* 1:1257–1270
54. Hebeish A, Mehta PC (1968) Grafting of acrylonitrile to different cellulosic materials by high-energy radiation. *Textile Res J* 38:1070–1075
55. Geresh S, Gdalevsky GY, Gilboa I, Voorspoels J, Remon JP, Kost J (2004) Bioadhesive grafted starch copolymers as platforms for peroral drug delivery: a study of theophylline release. *J Control Release* 94:391–399
56. Shiraishi N, Williams JL, Stannett V (1982) The radiation grafting of vinyl monomers to cotton fabrics—I. Methacrylic acid to terry cloth towelling. *Radiat Phys Chem* 19:73–78
57. Sharma RK, Misra BN (1981) Grafting onto wool 22. Radiation induced grafted copolymerization of methyl methacrylate in water-methanol system. *Polym Bull* 6:183–188
58. Carezza M (1992) Recent achievements in the use of radiation polymerization and grafting for biomedical applications. *Radiat Phys Chem* 39:485–493
59. Wang JP, Chen YZ, Zhang SJ, Yu HQ (2008) A chitosan-based flocculant prepared with gamma-irradiation-induced grafting. *Biores Tech* 99:3397–3402
60. Madani M (2011) Structure, optical and thermal decomposition characters of LDPE graft copolymers synthesized by gamma irradiation. *Curr Appl Phys* 11:70–76
61. Adams S (1983) Recent advances in radiation chemistry of carbohydrates. In: Elias PS, Cohen AJ (eds) *Recent advances in food irradiation*. Elsevier Biomedical Press, Amsterdam, p 149
62. Edimecheva IP, Kisel RM, Shadyro OI, Kazem K, Murase H, Kagiya T (2005) Homolytic cleavage of the O-glycoside bond in carbohydrates: a steady-state radiolysis study. *J Radiat Res (Tokyo)* 46:319–324
63. Grubb DT (1974) Radiation damage and electron microscopy of organic polymers. *J Mater Sci* 9:1715–1736
64. Fink D (2004) *Fundamentals of ion-irradiated polymers*, vol 66. Springer, New York, NY
65. Pietraner MSA, Narvaiz P (2001) Examination of some protective conditions on technological properties of irradiated food grade polysaccharides. *Radiat Phys Chem* 60:195–201
66. Kim BN, Lee DH, Han DH (2008) Thermal, mechanical and electrical properties on the styrene-grafted and subsequently sulfonated FEP film induced by electron beam. *Polym Degr Stab* 93:1214–1221
67. Dargaville TR, George GA, Hill DJT, Whittaker AK (2003) High energy radiation grafting of fluoropolymers. *Prog Polym Sci* 28:1355–1376
68. Farquet P, Padeste C, Solak HH, Gürsel SA, Scherer GG, Wokaun A (2008) Extreme UV radiation grafting of glycidyl methacrylate nanostructures onto fluoropolymer foils by RAFT-mediated polymerization. *Macromolecules* 41:6309–6316
69. Guilmeau I, Esnouf S, Betz N, Le MA (1997) Kinetics and characterization of radiation-induced grafting of styrene on fluoropolymers. *Nucl Instr Meth Phys Res Sec B: Beam Interact Mater Atoms* 131:270–275
70. Kimura Y, Asano M, Chen J, Maekawa Y, Katakai R, Yoshida M (2008) Influence of grafting solvents on the properties of polymer electrolyte membranes prepared by γ -ray pre irradiation method. *Radiat Phys Chem* 77:864–870
71. Ameduri B, Boutevin B (2004) *Well-architected fluoropolymers*. Elsevier, Amsterdam

72. Gubler L, Slaski M, Wallasch F, Wokaun A, Scherer GG (2009) Radiation grafted fuel cell membranes based on co-grafting of α -methylstyrene and methacrylonitrile into a fluoropolymer base film. *J Mem Sci* 339:68–77
73. Lappan U, Geißler U, Uhlmann S (2005) Radiation-induced grafting of styrene into radiation-modified fluoropolymer films. *Nucl Instr Meth Phys Res Sec B: Beam Interact Mater Atoms* 236:413–419
74. Chen J, Asano M, Maekawa Y, Yoshida M (2007) Polymer electrolyte hybrid membranes prepared by radiation grafting of p-styryltrimethoxysilane into poly(ethylene-co-tetrafluoroethylene) films. *J Mem Sci* 296:77–82
75. Tzanetakis N, Varcoe JR, Slade RCT, Scott K (2005) Radiation-grafted PVDF anion exchange membrane for salt splitting. *Desalination* 174:257–265
76. Deng J, Wang L, Liu L, Yang W (2009) Developments and new applications of UV-induced surface graft polymerizations. *Prog Polym Sci* 34:156–193
77. Deng H, Xu Y, Chen Q, Wei X, Zhu B (2011) High flux positively charged nanofiltration membranes prepared by UV-initiated graft polymerization of methacryloethyl trimethyl ammonium chloride (DMC) onto polysulfone membranes. *J Mem Sci* 366:363–372
78. Hua H, Li N, Wu L, Zhong H, Wu G, Yuan Z, Lin X, Tang L (2008) Anti-fouling ultrafiltration membrane prepared from polysulfone-graft-methyl acrylate copolymers by UV-induced grafting method. *J Envir Sci* 20:565–570
79. Shanmugaraj AM, Kim JK, Ryu SH (2006) Modification of rubber surface by UV surface grafting. *Appl Surf Sci* 252:5714–5722
80. Zhu Z, Kelley MJ (2005) Grafting onto poly (ethylene terephthalate) driven by 172 nm UV light. *Appl Surf Sci* 252:303–310
81. Deng J, Yang W (2005) Grafting copolymerization of styrene and maleic anhydride binary monomer systems induced by UV irradiation. *Eur Polym J* 41:2685–2629
82. Thaker MD, Trivedi HC (2005) Ultraviolet-radiation-induced graft copolymerization of methyl acrylate onto the sodium salt of partially carboxymethylated guar gum. *J Appl Polym Sci* 97:1977–1986
83. Odian G (2002) principles of polymerization, 3rd edn. Wiley, New York, NY
84. Sen G, Kumar R, Ghosh S, Pal S (2009) A novel polymeric flocculant based on polyacrylamide grafted carboxymethylstarch. *Carbohydr Polym* 77:822–831
85. Grassi M, Grassi G (2005) Mathematical modelling and controlled drug delivery: matrix systems. *Curr Drug Deliv* 2:97–116
86. Langer RS, Wise DL (eds) (1984) Medical applications of controlled release, applications and evaluation, vol I and II. CRC Press, Boca Raton, FL
87. Al-Saidan SM, Krishnaiah YSR, Satyanarayana V, Rao GS (2005) In vitro and in vivo evaluation of guar gum-based matrix tablets of rofecoxib for colonic drug delivery. *Curr Drug Deliv* 2:155–163
88. Krishnaiah YSR, Muzib YI, Bhaskar P, Satyanarayana V, Latha K (2003) Pharmacokinetic evaluation of guar gum-based colon-targeted drug delivery systems of tinidazole in healthy human volunteers. *Drug Deliv* 10:263–268
89. Krishnaiah YS, Satyanarayana V, Dinesh Kumar B, Karthikeyan RS (2002) In vitro drug release studies on guar gum-based colon targeted oral drug delivery systems of 5-fluorouracil. *Eur J Pharm Sci* 16:185–192
90. Tuğcu-Demiröz F, Acartürk F, Takka S, Konuş-Boyunağa K (2004) In-vitro and in-vivo evaluation of mesalazine-guar gum matrix tablets for colonic drug delivery. *J Drug Target* 12:105–112
91. Rama Prasad YV, Krishnaiah YSR, Satyanarayana S (1998) In vitro evaluation of guar gum as a carrier for colon-specific drug delivery. *J Control Release* 51:281–287
92. Krishnaiah YSR, Indira MY, Bhaskar P (2003) In vivo evaluation of guar gum-based colon-targeted drug delivery systems of ornidazole in healthy human volunteers. *J Drug Target* 11:109–115

93. Krishnaiah YSR, Raju PV, Kumar BD, Satyanarayana V, Karthikeyan RS, Bhaskar P (2003) Pharmacokinetic evaluation of guar gum-based colon-targeted drug delivery systems of mebendazole in healthy volunteers. *J Control Release* 88:95–103
94. Krishnaiah YSR, Satyanarayana S, Rama Prasad YV, Narasimha RS (1998) Gamma scintigraphic studies on guar gum matrix tablets for colonic drug delivery in healthy human volunteers. *J Control Release* 55:245–252
95. Tuğcu-Demiröz F, Acartürk F, Takka S, Konuş-Boyunağa Ö (2007) Evaluation of alginate based mesalazine tablets for intestinal drug delivery. *Eur J Pharm Biopharm* 67:491–497
96. Miyazaki S, Nakayama A, Oda M, Takada M, Attwood D (1994) Chitosan and sodium alginate based bioadhesive tablets for intraoral drug delivery. *Biol Pharm Bull* 17:745–747
97. Kim MS, Kim JS, Hwang SJ (2007) The effect of sodium alginate on physical and dissolution properties of Surelease-matrix pellets prepared by a novel pelletizer. *Chem Pharm Bull (Tokyo)* 55:1631–1634
98. Al-Saidan SM, Krishnaiah YSR, Satyanarayana V, Bhaskar P, Karthikeyan RS (2004) Pharmacokinetic evaluation of guar gum-based three-layer matrix tablets for oral controlled delivery of highly soluble metoprolol tartrate as a model drug. *Eur J Pharm Biopharm* 58:697–703
99. Krishnaiah YSR, Satyanarayana S, Rama Prasad YV (1999) Studies of guar gum compression-coated 5-aminosalicylic acid tablets for colon-specific drug delivery. *Drug Dev Ind Pharm* 25:651–657
100. Krishnaiah YSR, Karthikeyan RS, GouriSankar V, Satyanarayana V (2002) Three-layer guar gum matrix tablet formulations for oral controlled delivery of highly soluble trimetazidine dihydrochloride. *J Control Release* 81:45–56
101. Momin M, Pundarikakshudu K (2004) In vitro studies on guar gum based formulation for the colon targeted delivery of Sennosides. *J Pharm Sci* 7:325–331
102. Alvarez-Manceño F, Landin M, Martínez-Pacheco R (2008) Konjac glucomannan/xanthan gum enzyme sensitive binary mixtures for colonic drug delivery. *Eur J Pharm Biopharm* 69:573–581
103. Wang W, Wang A (2009) Preparation, characterization and properties of superabsorbent nanocomposites based on natural guar gum and modified rectorite. *Carbohydr Polym* 77:891–897
104. Rodrigues A, Emeje M (2012) Recent applications of starch derivatives in nanodrug delivery. *Carbohydr Polym* 87:987–994
105. Prabakaran M, Gong S (2008) Novel thiolated carboxymethyl chitosan-g-b-cyclodextrin as mucoadhesive hydrophobic drug delivery carriers. *Carbohydr Polym* 73:117–125
106. Wang LC, Chen XG, Zhong DY, Xu QC (2007) Study on poly (vinyl alcohol)/carboxymethyl-chitosan blend film as local drug delivery system. *J Mater Sci Mater Med* 18:1125–1133
107. Reddy T, Tammishetti S (2002) Gastric resistant microbeads of metal ion cross-linked carboxymethyl guar gum for oral drug delivery. *J Microencaps* 19:311–318
108. Du J, Zhang S, Sun R, Zhang LF, Xiong CD, Peng YX (2005) Novel polyelectrolyte carboxymethyl konjac glucomannan-chitosan nanoparticles for drug delivery. II. Release of albumin in vitro. *J Biomed Mater Res B: Appl Biomater* 72:299–304
109. Du J, Sun R, Zhang S, Zhang LF, Xiong CD, Peng YX (2005) Novel polyelectrolyte carboxymethyl konjac glucomannan-chitosan nanoparticles for drug delivery. I. Physico-chemical characterization of the carboxymethyl konjac glucomannan-chitosan nanoparticles. *Biopolymers* 78:1–8
110. Efentakis M, Koligliati S, Vlachou M (2006) Design and evaluation of a dry coated drug delivery system with an impermeable cup, swellable top layer and pulsatile release. *Int J Pharm* 311:147–156
111. Liang XF, Wang HJ, Luo H, Tian H, Zhang BB, Hao LJ, Teng JI, Chang J (2008) Characterization of novel multifunctional cationic polymeric liposomes formed from octadecyl

- quaternized carboxymethyl chitosan/cholesterol and drug encapsulation. *Langmuir* 24:7147–7153
112. Pal K, Banthia AK, Majumdar DK (2006) Development of carboxymethyl cellulose acrylate for various biomedical applications. *Biomed Mater* 1:85–91
 113. Bajpai AK, Mishra A (2008) Carboxymethyl cellulose (CMC) based semi-IPNs as carriers for controlled release of ciprofloxacin: an in-vitro dynamic study. *J Mater Sci Mater Med* 19:2121–2130
 114. Sen G, Pal S (2009) A novel polymeric biomaterial based on carboxymethylstarch 2130. and its application in controlled drug release. *J Appl Polym Sci* 114:2798–2805
 115. Wise LD (2000) *Handbook of pharmaceutical controlled release technology*. Dekker, New York, NY
 116. Kydonieus A (1992) *Treatise on controlled drug delivery*. Dekker, New York, NY
 117. Sumathi S, Roy AK (2002) Release behaviour of drugs from tamarind seed polysaccharide tablets. *J Pharm Sci* 5:12–18
 118. Singh B, Chauhan N (2009) Modification of psyllium polysaccharide for use in oral insulin delivery. *Food Hydrocolloids* 23:928–935
 119. Hsieh DS (ed) (1987) *Controlled release systems: fabrication technology*, vol I. CRC Press, Inc., Boca Raton, FL
 120. Ghaderi R, Artusson P, Carlfors J (2000) A new method for preparing biodegradable microparticles and entrapment of hydrocortisone in -PLG microparticles using supercritical fluids. *Eur J Pharm Sci* 10:1–9
 121. Falk R, Randolph TW, Meyer JD, Kelly RM, Manning MC (1997) Controlled release of ionic compounds from poly (L-lactide) microspheres produced by precipitation with a compressed antisolvent. *J Control Release* 44:77–85
 122. Pal S, Sen G, Mishra S, Dey RK, Jha U (2008) Carboxymethyl tamarind: synthesis, characterization and its application as novel drug-delivery agent. *J Appl Polym Sci* 110:392–400
 123. Sen G, Pal S (2009) Microwave initiated synthesis of polyacrylamide grafted carboxymethylstarch (CMS-g-PAM): application as a novel matrix for sustained drug release. *Int J Bio Macromol* 45:48–55
 124. USP (2003) General chapter <711 > Dissolution, USP 27—The United States Pharmacopeia Convention, Inc., Rockville, MD, p 2303.
 125. Friend DR (1991) Colon-specific drug delivery. *Adv Drug Deliv Rev* 7:149–199
 126. Pal S, Ghorai S, Dash MK, Ghosh S, Udayabhanu G (2011) Flocculation properties of polyacrylamide grafted carboxymethyl guar gum (CMG-g-PAM) synthesised by conventional and microwave assisted method. *J Hazard Mat* 192:1580–1588

Index

A

- Acacia gum (AG), 159
- Acid–base titration method, 113–114
- Acrylamide/acrylic acid content, starch-graft-copolymers, 71
- Alginate, 158–159
- 5-Amino salicylic acid (5-ASA)
 - cumulative drug release profile, 336
 - % erosion and t_{50} values, 337
 - grafting efficiency and equilibrium swelling, 337
 - pH, gastrointestinal tract, 336
- Ampholytic hydrogels, 275
- Amylopectin, 60
- Anhydroglucose units (AGU) per graft, 72
- Antlers gum, 157–158
- 5-ASA. *See* 5-Amino salicylic acid (5-ASA)
- Atomic force microscopy (AFM), 279
- Atom transfer radical polymerization (ATRP), 6
 - advantages, 20
 - gum-graft-copolymers, 175–176

B

- Biodegradability
 - cellulose graft polymers, 31–32
 - starch-g-copolymers, 90–91
- Biodegradable plastics and films, 94–96
- Block copolymer, 4
- Bromate/cyclohexanone redox system, 67–68

C

- CAN-HNO₃, 44
- Carboxymethyl chitosan (CMCh)
 - O*-CMCh
 - degree of substitution, 120
 - microwave technique, 119
 - thermal technique, 120
 - potentiometric titration method, 120–121
 - types, 118–119
- Cassava starch-g-poly(acrylic acid) copolymers, 68
- Cassia gum, 155
- ¹³C cross-polarisation/magic-angle-spinning spectra,
 - starch-g-copolymers, 81–83
- Cellulose graft polymers
 - characterization
 - biodegradability, 31–32
 - DSC, 32
 - FTIR, 32–35
 - grafting efficiency, 29–30
 - grafting percentage, 29
 - mechanical properties, 31
 - number of grafts per cellulose chain, 30–31
 - SEM, 36, 37
 - water absorption capacity, 31
 - XRD, 35, 36
 - degree of crystallinity, 16
 - forms of, 16
 - grafting conditions, 38–39
 - applications, 49–50
 - kind and concentration, initiator, 43–47

- kind and concentration, monomer, 42–43
 - pretreatment of cellulose, 36–37, 40–41
 - solvent effect, 47–48
 - temperature effect, 49
 - grafting reactions, 21–23
 - hydrogen bondings, 16
 - initiators
 - ceric ion, 25–28
 - iron (II)-hydrogen peroxide system, 24–25
 - persulfates, 28, 29
 - structure, 16
 - Ceric ion
 - cellulose graft polymers, 25–28
 - initiation, graft copolymer, 327–328
 - starch-g-copolymers, 61–63
 - Cerium ammonium nitrate (CAN), 25–28
 - Chitosan
 - amino group determination
 - acid–base titration method, 113–114
 - colloidal titration method, 114
 - applications
 - biomedical field, 135–139
 - metals ion adsorption and ion exchangers, 132–134
 - pharmaceutical field, 135–139
 - superabsorbent materials, 132
 - characterization
 - SEM, 129, 130
 - spectral analyses, 127–128
 - thermal analyses, 129–131
 - XRD, 128–129
 - chemical modifications
 - grafting technique, 121–126
 - inorganic esters, 115–116
 - organic esters, 116–121
 - chemical structure, 112
 - description, 111
 - solubility, 113
 - synthesis, 112
 - Chitosan nitrate, 115
 - Chitosan phosphate, 115–116
 - Chitosan sulfate, 116
 - Ciprofloxacin, graft copolymer
 - cumulative drug release profile, 338
 - % erosion and t_{50} value, 339
 - CMCh. *See* Carboxymethyl chitosan (CMCh)
 - Co(acac)₃-HClO₄ initiator, 43–44
 - Colloidal titration method, 114
 - Continuous reactive twin-screw extrusion, 61
- D**
- Destructurised starch, 95
 - Dextran-matrix copolymer (DMC)
 - applications
 - biocompatibility, 234–236
 - bioplastic material, 232–233
 - characterization
 - DSC, 230–232
 - electron probe microanalysis, 230
 - IR absorption spectra, 228
 - material tests and physical properties, 229–230
 - SEM, 230, 231
 - solubility and material tests, 228
 - thermal analysis, 228
 - intraocular lenses and hard contact lenses, 226
 - preparation, 226–227
 - Dextran-MMA graft copolymers
 - Ce⁴⁺ consumption rate, 210–212
 - characterization
 - contact angle, 220
 - DSC, 222–223
 - glass transition temperature, 223, 224
 - hydrolysis, 219
 - IR absorption spectra, 222, 223
 - material tests, 220, 221
 - solubilities, 220, 221
 - tensile strength, 219
 - thrombus formation curves, 224, 225
 - water absorption, 220
 - polymerization kinetics
 - molecular weight effect, 216–218
 - theory, 212–216
 - polymerization procedure, 208–210
 - SEM, 207, 208
 - uses, 207
 - 2-Diethylaminoethyl (DEAE)-dextran-MMA graft copolymer (DDMC)
 - characterization, 238
 - complex formation reaction mechanisms, 245–248
 - DDMC/PTX complex
 - characterization, 255, 256
 - enzymatic reactions, 260–261
 - in vitro testing, 257–259
 - melanoma cell response, 259–260
 - MTT assay, 255–257
 - preparation, 254
 - supramolecular allosteric binding, 261–263
 - supramolecular template, 263–264
 - and DNA, 238–239

- DNA delivery pathways, 250–252
- drug delivery systems, 254
- IR spectrum, 239–240
- non-viral delivery carrier
 - charge ratio, 241–242
 - cytotoxicity, transfection, 245
 - transfection efficiency, 242–245
- preparation, 237–238
- protection against DNase degradation, 249–250
- protocol, 252–253
- vector, 253
- Differential scanning calorimetry (DSC)
 - cellulose graft polymers, 32
 - dextran-MMA graft copolymers, 222–223
- DMC, 230–232
- N,N*-Dimethylacrylamide (DMAAm), 42
- Direct compression method, 332
- DMSO/PF system, 47
- Dynamic combinatorial chemistry, 174–175

- E**
- Electron beam-initiated grafting
 - copolymerization, 173
- Electron probe microanalysis, DMC, 230
- Enzymatic grafting, 8
- Enzymatic reactions, DDMC/PTX complex, 260–261
- 1-Ethyl-3-[3-(dimethylamino)-propyl]-carbodiimide (EDC), 297
- Ethylenediamine (EDA), 41

- F**
- Fenton reagent, 24–25
- Flocculating agents, wastewater treatment, 91–92
- Fourier transform infrared (FTIR) spectra
 - cellulose graft polymers, 32–35
 - chitosan-g-copolymers, 127, 128
 - hydrogels, 279, 280
 - starch-g-copolymers, 73–75
- Free radical initiating systems, 60–61

- G**
- Gas-permeable hard contact lens (GPHCL), 233
- Glass transition temperature (T_g)
 - dextran-MMA graft copolymers, 223, 224
 - starch-g-copolymers, 85
- Graft copolymer
 - advantages, 327
 - ceric ion initiation, 327–328
 - chromium (VI) ion initiation, 329
 - CMG-g-PAM application
 - 5-amino salicylic acid, 335–337
 - (*see also* 5-Amino salicylic acid (5-ASA))
 - ciprofloxacin, 338–339
 - controlled drug release
 - concept of, 331–332
 - in vitro study, 334
 - mechanism, 332
 - oral mode, 332–334
 - targeted, 334
 - USP drug dissolution rate test, 335
 - Cu (II) ion initiation, 329
 - guar gum structure, 326
 - hydrogen peroxide/ Fe^{2+} initiation, 329
 - irradiation initiation, 330
 - trivalent manganese initiation, 328–329
 - V^{5+} initiation, 330
- Graft copolymerization, 278
- Graft copolymers
 - applications, 9
 - cellulose (*see* Cellulose graft polymers)
 - definition, 3
 - description, 4–5
 - structure, 3
 - synthesis methods (*see also* Polymer grafting)
 - chemical method, 5–6
 - enzymatic grafting, 8
 - plasma-initiated grafting, 8–9
 - radiation-induced grafting, 6–8
- Grafting method
 - chitosan modification
 - ceric ion-induced grafting, 122–123
 - Fenton's reagent, 123–124
 - novel redox initiators, 125–127
 - persulfate-induced grafting, 124–125
 - radical induced methods, 122
 - gum-g-copolymers
 - conventional radical, 164–167
 - electron beam-initiated grafting
 - copolymerization, 173
 - macromonomer radical methods, 167
 - microwave-assisted grafting
 - copolymerization, 170–171
 - radiation-initiated grafting
 - copolymerization, 171–174
 - UV radiation-initiated grafting
 - copolymerization, 173

- Guar gum
 description, 153–154
 structure of, 326
- Gum-g-copolymers
 advantages, 151
 amphoteric derivatives, 163
 anionic gums
 acacia gum, 159
 alginate, 158–159
k-Carrageenan, 157–158
 XG, 157
 applications
 drilling additives, 184
 drug delivery carriers, 188–189
 electrical biomaterials, 187–188
 flocculating agent, 186
 macromolecular surfactants, 187
 micro-reactor, nanomaterial
 preparation, 190–191
 papermaking industry, 186–187
 sand-binding materials, 190
 superabsorbent materials, 189–190
 thickener, 184
 toxic heavy metal adsorption, 184–186
- ATRP, 175–176
 carboxyl derivatives, 160, 161
 cationic derivatives, 161–163
 characterization
 DSC, 177–178
 elemental analysis, 179
 infrared spectroscopy, 177
 NMR analysis, 179–180
 thermogravimetric analysis, 177–178
 UV-vis spectra, 179
- click chemistry, 174–175
 conventional grafting method, 164–167
 high-energy initiation grafting method
 electron beam-initiated grafting
 copolymerization, 173
 microwave-assisted grafting
 copolymerization, 170–171
 radiation-initiated grafting
 copolymerization, 171–174
 UV radiation-initiated grafting
 copolymerization, 173
- hydrophobic derivatives, 164
 hydroxyethyl derivatives, 160
 macromonomer radical methods, 167
 nonionic gums
 cassia, 155
 guar gum, 153–154
 ipomoea seed, 156–157
 konjac glucomannan, 155–156
 LBG, 154, 155
 properties, 152
 amphiphilic properties, 182
 complexing capacity, 181
 electrical property, 182–183
 flocculating and decoloring, 182
 mechanical property, 181
 stimuli-responsive, 183
 thermo- and degradation-resistance, 180
 viscous and rheological, 180–181
 redox initiation, 165, 166
 vinyl-functionalized derivatives, 161
- H**
- Heterogeneous media, grafting reactions in,
 18, 21–23
- High-energy radiation-induced grafting,
 6–7
- ¹H-NMR spectra, chitosan-g-copolymer,
 127–129
- Homogeneous media, grafting reactions in,
 19–23
- Homopolymer hydrogels, 273
- Horseradish peroxidase (HRP), 69
- Hyaluronic acid-g-copolymers
 carboxyl groups
 D-glucuronic activation, 298
 dimethylsulfoxide, 297–298
 EDC, 297
 glucuronic COOH group, 297
 HA-TBA, 298
 description, 292
 HA-functionalized derivatives, 299–300
 hydroxyl groups
 direct functionalization, 293
 epoxide- or anhydride-terminated
 polymers, 295
N-acetylglucosamine, 293, 295, 296
 principal activants, 294
 lymphatic vessel endothelial hyaluronan
 receptor-1, 292
 nanostructures and hydrogels, drug
 delivery, 301–311
 pharmacological activity
 anti-Flt1 peptide, 315, 316
 glucose-lowering ability, 318
 HA-g-INF- α derivatives, 316–317
 HA-g-SOD derivatives, 315
 OAS 1 detection levels, 317
 PEG, 314
 VEGFR-1, 315
 tissue engineering, 311–314

Hydrogels

- agriculture applications, 284–285
 - ampholytic, 275
 - biomedical applications
 - drug delivery, 282–283
 - tissue engineering, 283
 - wound dressing, 284
 - characterization
 - AFM, 279
 - DTA/TGA, 279–281
 - dynamo-mechanical analysis, 282
 - FTIR spectra, 279, 280
 - SEM, 278–279
 - chemical, 273
 - copolymer, 273–274
 - description, 271
 - drug delivery
 - clinical application, 305
 - COOH functionalization, 301–302
 - HA-ceramide derivative, 305, 306
 - HA-g-PLGA derivatives, 305
 - HA-g-pNIPAM derivatives, 308–309
 - HA-g-polyesters, 304
 - HA-OSA derivatives, 302–303
 - hydrophobic chains, 302
 - layer-by-layer coating technique, 305
 - octadecylamine, 303
 - ONCOFID, 301
 - PEG-anthracene, 308
 - polyethyleneimine, 307–308
 - PTX cellular uptake, 304
 - homopolymer, 273
 - interpenetrating polymer network hydrogels, 274
 - ionic, 275
 - metal ion sorption, 285
 - neutral, 274
 - physical, 272–273
 - synthesis
 - chemical cross-linking, 277–278
 - physical cross-linking, 275–276
- Hydrolysed starch-graft-poly acrylonitrile (HSPAN), 92–93
- dehydrating agent, 102
- I**
- Infrared (IR) spectra
- DDMC, 239–240
 - dextran-MMA graft copolymers, 222, 223
 - DMC, 228
 - starch-g-copolymers, 73, 74

Interpenetrating polymer network hydrogels (IPNs), 274

- Intramolecular hydrogen bondings, 16
- In vitro testing, DDMC/PTX complex, 257–259
- In vivo gene delivery, 206–207
- Ion-exchange resins, 92–94
- Ionic hydrogels, 275
- Ipomoea seed gums, 156–157
- Iron (II)-hydrogen peroxide system
 - cellulose graft polymers, 24–25
 - starch-g-copolymers, 64–65

K

- k*-Carrageenan. *See* Antlers gum
- Konjac glucomannan (KGM), 155–156

L

- Locust bean gum (LBG), 154–155
- Low-energy radiation-induced grafting, 6

M

- Macromonomer radical methods, 167
- Manganic pyrophosphate, 65, 66
- Mechanical properties, cellulose graft polymers, 31
- Methylacrylamide (MAAm), 42
- Michaelis–Menten complex formation, 247
- Microwave-assisted grafting copolymerization, 170–171
- Microwave radiation-induced grafting, 7, 8
- Mosaic grafting, 17

N

- N*-acyl derivatives, chitosan, 116–117
- Neutral hydrogels, 274
- N*-isopropylacrylamide (NIPAM), 47–48
- Nonionic gums
 - cassia, 155
 - guar gum, 153–154
 - ipomoea seed, 156–157
 - konjac glucomannan, 155–156
 - LBG, 154, 155
- Non-viral delivery carrier, DDMC charge ratio, 241–242
- cytotoxicity, transfection, 245
- transfection efficiency, 242–245
- N*-tert-butyl acrylamide (BAM), 62

O

- O*-acyl derivatives, chitosan, 117–118
- Oilfield applications, starch-g-copolymers, 98–99

P

- Persulfates
 - cellulose graft polymers, 28, 29
 - starch-g-copolymers, 63–64
- Physical hydrogels, 272–273
- Plasma-initiated grafting, 8–9
- Polymer grafting
 - chemical method, 5–6
 - description, 4–5
 - enzymatic grafting, 8
 - plasma-initiated grafting, 8–9
 - radiation method
 - high-energy radiation-induced grafting, 6–7
 - low-energy radiation-induced grafting, 6
 - microwave radiation-induced grafting, 7, 8
- Polysaccharides, 2–3
- Potassium permanganate-acid system, 65, 66
- Potassium persulfate (KPS), 28, 29
- Potato starch-graft-poly(acrylonitrile), 68

R

- Radiation cross-linking, 277
- Radiation-initiated grafting copolymerization, 171–173
- Random copolymer, 4

S

- Scanning electron microscopy (SEM)
 - cellulose graft polymers, 36, 37
 - chitosan-g-copolymers, 129, 130
 - dextran-MMA graft copolymers, 207, 208
 - DMC, 230, 231
 - hydrogels, 278–279
- Semi-interpenetrating polymer network (IPN) hydrogels, 64
- Solubility
 - chitosan, 113
 - DMC, 228
- Solvent swelling technique, 332
- Starch-g-copolymers
 - applications
 - adhesives, 102
 - biodegradable plastics and films, 94–96
 - compatibiliser, 102–103

- dehydrating agent, 102
- flocculating agents, wastewater treatment, 91–92
- ion-exchange resins, 92–94
- non-irritant bioadhesive drug release systems, 101–102
- oilfield applications, 98–99
- superabsorbent polymers, 96–98
- textile sizing agents and thickeners, 100
- wound dressing, 100

- biodegradability, 90–91
- characterisation
 - acrylamide/acrylic acid content, 71
 - add-on/grafting, 70
 - FTIR spectroscopy, 73–75
 - grafting efficiency, 70, 71
 - homopolymer, 70
 - molecular weight and frequency of grafts, 71–72
 - monomer conversion, 70
 - NMR spectra, 80–83
 - percent grafting ratio, 70
 - SEM, 76, 77
 - XRD, 77–80
- synthesis, initiating systems
 - bromate/cyclohexanone redox system, 67–68
 - ceric ion, 61–63
 - gamma-ray irradiation, 68
 - iron (II)-hydrogen peroxide, 64–65
 - manganese, 65–67
 - microwave irradiation, 68–69
 - persulphates, 63–64
 - starch, 69
- thermal properties
 - melting and glass transition temperature, 85–86
 - thermogravimetric analysis, 86–90
 - water-absorbing property, 83–85
- Starch-g-ethyl methacrylate/sodium silicate, 91
- Superabsorbent polymers (SAPs), 96–98, 132
- Supercritical fluid technique, 332
- Superslurpers. *See* Superabsorbent polymers (SAPs)
- Surface morphology, starch-g-copolymers, 76–77

T

- Thermogravimetric analysis (TGA)
 - chitosan, 129–131
 - hydrogels, 279–281
 - starch-g-copolymers, 86–90

Tissue engineering

HA-g-PLGA scaffolds

BMP2, 313

SSFF, 312

HA-g-pNIPAM, 313

photo-sensible methacrylic moiety, 314

physicochemical properties, 311

regenerative medicine, 311, 313

Toluidine Blue (TB), 249–250

U

UV radiation-initiated grafting

copolymerization, 173

W

Water absorption

cellulose graft polymers, 31

starch-g-copolymers, 83–85

Wood pulp and CAN, 40, 41

X

Xanthan gum (XG), 157, 158

X-ray diffraction analysis (XRD)

cellulose graft polymers, 35, 36

chitosan-g-copolymers, 128–129

starch-g-copolymers, 77–81